UNIVERSITY OF SOUTHAMPTON

DYNAMIC RESPONSE OF STANDING AND SEATED PERSONS TO WHOLE-BODY VIBRATION: PRINCIPAL RESONANCE OF THE BODY

YASUNAO MATSUMOTO, B.Eng, M.Eng

DOCTOR OF PHILOSOPHY

FACULTY OF ENGINEERING AND APPLIED SCIENCE
INSTITUTE OF SOUND AND VIBRATION RESEARCH

JUNE 1999

UNIVERSITY OF SOUTHAMPTON

ABSTRACT

FACULTY OF ENGINEERING AND APPLIED SCIENCE
INSTITUTE OF SOUND AND VIBRATION RESEARCH

Doctor of Philosophy

DYNAMIC RESPONSE OF STANDING AND SEATED PERSONS TO WHOLE-BODY VIBRATION: PRINCIPAL RESONANCE OF THE BODY

by Yasunao Matsumoto

A review of literature shows that the driving-point mechanical impedance and apparent mass have been well established experimentally for the seated body and show a principal resonance at about 5 Hz. However, the causes of the principal resonance have not been fully understood. The standing body driving-point response has been determined in a few studies and the findings have varied. This thesis presents a study of the principal resonance of standing and seated bodies by inspection of experimental data and development of mathematical models.

The driving-point apparent masses of standing subjects were obtained in three experiments. Thirty two subjects were exposed to random vibration between 0.5 and 50 Hz at vibration magnitudes from 0.125 to 2.0 ms^{-2} r.m.s. A principal peak of the apparent mass of subjects standing normally was found in the 4 to 6 Hz frequency range. The resonance frequency tended to be higher in a normal standing posture than in a normal sitting posture, although the difference was generally within 1 Hz. The resonance frequency of the apparent mass decreased by about 1.5 Hz with increases in the vibration magnitude from 0.125 to 2.0 ms^{-2} r.m.s. in both the standing posture and the sitting posture. It was thought likely that common dynamic mechanisms in the upper-body contributed to the principal resonances of both standing and seated bodies.

The transmission of vibration to nine body locations was determined in the 0.5 to 20 Hz frequency range with twenty subjects in two experiments. A multi-axis measurement method was developed to determine the effect of pitch motion on translational motions along the spine in the sagittal plane. The movement of the upper-bodies of standing and seated subjects at the principal resonance consisted of bending of the spine, particularly in the lumbar region, pitching of the thoracic spine and rib cage and pitching of the pelvis. These motions might be coupled with each other due to the heavy damping of the human body. For the seated body, deformation of the buttocks tissue was also involved in the movement at the resonance. For the standing body, axial motion might be coupled with bending motion in the lower spine. A combination of rotational motions at the leg joints and deformation of the tissue at the sole of the foot occurred at the principal resonance.

Lumped parameter models were developed to interpret the experimental results and investigate dynamic mechanisms involved in the principal resonance. The inclusion of rotational degrees of freedom improved the representation of the transmissibilities. It is concluded from the experiments and the models that the principal resonance in the apparent mass of the seated body is mainly caused by deformation of the tissue beneath the pelvis in phase with vertical motion of the viscera. The deformation of the buttocks tissue causes vertical, fore-and-aft and pitch motions of the pelvis. The principal resonance of the standing body is most influenced by the dynamic response of the viscera and also influenced by rotational motions at the leg joints and deformation of the tissue of the foot sole. Bending motion of the spine, significant in the lumbar spine, occur at the principal resonance frequency but makes a minor contribution to the apparent mass resonance in both standing and seated postures.

ACKNOWLEDGEMENTS

I would like to express my deepest gratitude to Professor Mike Griffin for his advice and encouragement during the course of the research. Useful technical advice from Dr Mike Brennan and Dr Roger Pinnington, the members of my review board, are also acknowledged. I would also like to acknowledge Professor Yozo Fujino, University of Tokyo, Japan, who gave me the opportunity to conduct this research in Southampton. The contributions from all of the subjects who participated in the experiments are very much appreciated. All the members of the Human Factors Research Unit have provided a pleasant working environment. I would like to thank particularly Dr Gurmail Paddan and Dr Chris Lewis for their interesting questions about the research and Mr Gary Parker for his technical support. I would also like to thank Dr Neil Mansfield and Mr Paul Woodman, former unit members, who kindly helped me at the early stage of my life in the unit. My friends from Japan and many other countries have contributed to my precious experiences in England. Finally, I would like to thank my family, Yasutoshi, Satoko and Mari Matsumoto, and Hirotaro and Reiko Kato, for their constant support and encouragement.

CONTENTS

CHAPTER 1 GENERAL INTRODUCTION 1

CHAPTER 2 LITERATURE REVIEW 4

2.1 INTRODUCTION 4
2.2 METHODS FOR REPRESENTING THE DYNAMIC RESPONSE OF THE HUMAN BODY TO VERTICAL WHOLE-BODY VIBRATION 5
2.2.1 Introduction 5
2.2.2 Driving-point dynamic response of the body 6
2.2.3 Transmissibility of the body 8
2.3 DRIVING-POINT DYNAMIC RESPONSE OF THE HUMAN BODY TO VERTICAL WHOLE BODY VIBRATION 9
2.3.1 Standing subjects 9
2.3.1.1 Driving-point dynamic response in normal standing posture 9
2.3.1.2 Effect of posture of subjects on driving-point dynamic response 13
2.3.1.2 Effect of vibration magnitude on driving-point dynamic response 15
2.3.2 Seated subjects 16
2.4 DYNAMIC RESPONSE OF VARIOUS BODY PARTS TO VERTICAL WHOLE-BODY VIBRATION 22
2.4.1 Dynamic response of the spine 22
2.4.1.1 Basic musculoskeletal anatomy of the spine 22
2.4.1.2 Methods to measure the spinal motion *in situ* 25
2.4.1.3 Transmissibility to the spine in a normal standing posture 31
2.4.1.4 Transmissibility to the spine in a normal sitting posture 38
2.4.1.5 Effects of posture and muscle tension on transmissibility to the spine 47
2.4.1.6 Effect of excitation magnitude on transmissibility to the spine 51
2.4.2 Dynamic response of the head 52
2.4.2.1 Methods of the head motion measurement 52
2.4.2.2 Transmissibility to the head in a normal standing posture 55
2.4.2.3 Transmissibility to the head in a normal sitting posture 62
2.4.2.4 Effects of posture and muscle tension on transmissibility to the head 70
2.4.2.5 Effect of excitation magnitude on transmissibility to the head 77

2.4.3 Dynamic response of the pelvis 78
2.4.3.1 Basic musculoskeletal anatomy of the pelvis 78
2.4.3.2 Results from previous studies 79
2.4.4 Dynamic response of the viscera 81
2.4.4.1 Basic anatomy of the viscera and trunk cavities 81
2.4.4.2 Results from previous studies 82
2.4.5 Dynamic response of the whole upper-body - modal analysis 84
2.5 MATHEMATICAL MODELS OF THE BIODYNAMIC RESPONSE TO VERTICAL WHOLE-BODY VIBRATION 86
2.5.1 Mathematical models correlated with the driving-point response 93
2.5.2 Mathematical models correlated with the vibration transmission to the head or other location 99
2.5.3 Comprehensive mathematical models 102
2.6 DISCUSSION AND CONCLUSIONS 109

CHAPTER 3 EXPERIMENTAL APPARATUS AND DESIGN, AND DATA ANALYSIS 114

3.1 INTRODUCTION 114
3.2 APPARATUS 114
3.2.1 Vibrators 114
3.2.1.1 Electro-magnetic vibrator 114
3.2.1.2 Electro-hydraulic vibrator 115
3.2.2 Transducers 115
3.2.2.1 Accelerometers 115
3.2.2.2 Force transducers 116
3.2.3 Data acquisition 117
3.3 SUMMARY OF DESIGNS OF EXPERIMENTS 118
3.4 DATA ANALYSIS 119
3.4.1 Frequency response functions 119
3.4.1.1 Apparent mass 119
3.4.1.2 Transmissibility 121
3.4.2 Statistical analysis 122
3.4.2.1 Wilcoxon matched-pairs signed ranks test 122
3.4.2.2 Friedman two-way analysis of variance 124
3.4.2.3 Kendall rank-order correlation coefficient 126

CHAPTER 4 APPARENT MASS OF THE HUMAN BODY IN STANDING POSITION EXPOSED TO VERTICAL WHOLE-BODY VIBRATION: INFLUENCE OF POSTURE 129

4.1 INTRODUCTION 129
4.2 EXPERIMENTAL METHOD 130
4.2.1 Apparatus and procedure 130
4.2.2 Analysis 132
4.3 EXPERIMENTAL RESULTS 133
4.3.1 Standing and sitting 133
4.3.1.1 Repeatability - intra-subject variability 133
4.3.1.2 Variability across subjects - inter-subject variability 135
4.3.2 Effect of posture and muscle tension in standing position 139
4.3.2.1 Effect of upper-body posture in standing position 139
4.3.2.2 Effect of muscle tension 141
4.3.2.3 Effect of leg posture 143
4.4 MATHEMATICAL MODELS OF APPARENT MASS 146
4.4.1 Single degree-of-freedom models 146
4.4.2 Two degree-of-freedom models 148
4.4.2.1 Standing and sitting 149
4.4.2.2 Standing with different leg postures 154
4.5 DISCUSSION 158
4.5.1 Discussion of experimental results 158
4.5.2 Discussion of mathematical modelling 161
4.6 CONCLUSIONS 164

CHAPTER 5 INFLUENCE OF LEG POSTURE AND VIBRATION MAGNITUDE ON DYNAMIC RESPONSE OF THE STANDING HUMAN BODY EXPOSED TO VERTICAL WHOLE-BODY VIBRATION 166

5.1 INTRODUCTION 166
5.2 METHOD 168
5.3 ANALYSIS 170
5.4 RESULTS 172

5.4.1 Influence of leg posture on apparent mass 172
5.4.2 Transmissibility in normal standing posture 177
5.4.3 Influence of leg posture on transmissibility 181
5.4.3.1 Transmissibility to the pelvis region 181
5.4.3.2 Transmissibility to the spine 183
5.4.3.3 Transmissibility to the knee 184
5.4.4 Influence of vibration magnitude 185
5.4.4.1 Apparent mass in normal standing posture 185
5.4.4.2 Apparent mass in legs bent and one leg postures 190
5.4.4.3 Influence of vibration magnitude on transmissibility 193
5.5 DISCUSSION 195
5.6 CONCLUSIONS 200

CHAPTER 6 DIFFERENCES IN DYNAMIC RESPONSES BETWEEN STANDING AND SEATED BODIES AND THE NONLINEARITY IN BIODYNAMIC RESPONSES 202

6.1 INTRODUCTION 202
6.2 METHOD 204
6.3 ANALYSIS 206
6.4 RESULTS 210
6.4.1 Effect of data correction method on transmissibility 210
6.4.2 Dynamic responses of the body in standing and sitting positions 214
6.4.3 Nonlinearity in dynamic responses 218
6.4.3.1 Nonlinearity in apparent mass 218
6.4.3.2 Nonlinearity in transmissibility 223
6.5 DISCUSSION 231
6.6 CONCLUSIONS 242

CHAPTER 7 MOVEMENT OF THE BODY OF SEATED AND STANDING SUBJECTS EXPOSED TO VERTICAL WHOLE-BODY VIBRATION AT THE PRINCIPAL RESONANCE FREQUENCY 244

7.1 INTRODUCTION 244

7.2 METHOD AND ANALYSIS 246
7.3 RESULTS 249
7.3.1 Seated position 249
7.3.2 Standing position 259
7.4 DISCUSSION 270
7.4.1 Discussion of seated position 270
7.4.2 Discussion of standing position 276
7.5 CONCLUSIONS 280

CHAPTER 8 MODELLING DYNAMIC RESPONSES OF THE HUMAN BODY IN STANDING AND SEATED POSITIONS TO VERTICAL WHOLE-BODY VIBRATION 282

8.1 INTRODUCTION 282
8.2 MODEL DESCRIPTION 284
8.2.1 Equations of motion 285
8.2.2 Model parameters 287
8.3 RESULTS AND DISCUSSION 289
8.3.1 Seated body model 289
8.3.1.1 Effect of model structure for the pelvis region 289
8.3.1.2 Effect of visceral mass 293
8.3.1.3 Effect of model structure for the spine 295
8.3.1.4 Parameter sensitivity in seated body models 302
8.3.1.5 Discussion of model parameters in seated body models 306
8.3.2 Standing body model 309
8.3.2.1 Effect of model structure for the legs of the standing body 309
8.3.2.2 Parameter sensitivity in standing body models 316
8.3.2.3 Discussion of model parameters in standing body models 319
8.4 CONCLUSIONS 321

CHAPTER 9 GENERAL DISCUSSION, GENERAL CONCLUSIONS, AND RECOMMENDATIONS 323

9.1 General discussion 323
9.1.1 Principal resonance of the apparent mass 323

9.1.2 Dynamic mechanisms of the seated body 323
9.1.3 Dynamic mechanisms of the standing body 326
9.2 General conclusions 327
9.3 Recommendations 328

APPENDICES 332

APPENDIX A RELATION BETWEEN APPARENT MASS, NORMALISED APPARENT MASS AND TRANSMISSIBILITY IN LUMPED PARAMETER MODELS 332

APPENDIX B DATA FROM EXPERIMENT 1 336

APPENDIX C DATA FROM EXPERIMENT 2 338

APPENDIX D DATA FROM EXPERIMENT 3 342

APPENDIX E M-FILES TO ANIMATE THE MOVEMENT OF THE UPPER-BODY OF STANDING AND SEATED SUBJECTS AT THE PRINCIPAL RESONANCE FREQUENCY 347

REFERENCES 352

CHAPTER 1

GENERAL INTRODUCTION

People experience various types of whole-body vibration in daily life: most commonly through a seat of a vehicle or while walking. In public transportation, industrial vehicles or buildings, people are exposed to vibration when standing. Such whole-body vibrations could have adverse effects on health, activities and feelings of occupants. An excessive magnitude of vibration or shock could result in fractures of some body structures, such as bones or connective tissues. Long term exposures to vibration have been suggested as a cause of low back pain or pathological changes to the spine in occupational vehicle drivers, according to epidemiological studies (e.g. Dupuis and Zerlett, 1987; Wilder and Pope, 1996). Activities in vibrating environments, such as control of a vehicle, writing in a train or walking on a vibrating bridge, might be interfered by unwanted body movements, degraded visual acuity and decreased concentration due to vibration. Movements of some parts of the body induced by an input vibration might cause discomfort.

In order to minimise undesirable influences of vibration on people, the reduction of magnitude of vibration by modifying the supporting structure, for example, suspensions in a vehicle, has been a main issue both in research and in industrial development. An understanding of human responses to vibration has also been needed so as to reduce adverse effects of vibration on people.

Human responses to vibration have various characteristics, such as psychological, physiological, and mechanical responses. Understanding of each response, and the interaction between these responses, is required so as to understand the human response to vibration comprehensively and reduce undesirable influences caused by vibration. However, each response has not yet been fully understood, despite previous studies in each area. This is partly because each response itself is complicated and partly because one response is related to other responses in a complex manner. Therefore, studies of a particular response, followed by studies of the interaction between responses, are still needed.

One response of the human body to whole-body vibration is the mechanical, or dynamic, movement of the body caused by vibration. This was investigated in this thesis. The

dynamic response of the human body is an objective measure of how people respond to vibration.

Understanding of the dynamic responses of the body to whole-body vibration is not only needed to understand the effects of vibration on health, activities and comfort, but also to consider the dynamic interaction between the human body and structures supporting the human body. For example, the dynamic performance of a vehicle seat is affected by the dynamic response of the occupant, the dynamic behaviour of a pedestrian bridge is affected by the existence and locomotion of pedestrians on the bridge.

The dynamic responses of the human body (i.e., the biodynamic responses) exposed to vertical whole-body vibration or shock have been investigated experimentally for more than four decades. An initial interest seemed to be placed on the behaviour of military aircraft pilots during emergency ejection, in which the pilot would experience a severe shock-type acceleration in the longitudinal direction. The research interest has been widened since then from health to the comfort and the activities of people in various vibrating environments. The range of magnitudes of vibration and shock investigated has, therefore, varied from high extremes to the lower ranges of conditions which people experience in their daily lives, such as in cars.

Mathematical models of the biodynamic responses to whole-body vibration have been developed so as to predict the responses, replace experimental studies involving human subjects, and provide insights into the dynamic characteristics of the body. However, the validation of such models, particularly complex models, has been difficult because of insufficient experimental data on the dynamic responses of the human body and uncertainty in the mechanical properties and functions of body elements.

The general objective of the research described in this thesis was to contribute to understanding of the dynamic response of the human body exposed to vertical whole-body vibration. Standing and seated positions were investigated. Experiments with human subjects were conducted so as to obtain experimental data which were needed to understand the dynamic characteristics of the body. Mathematical models were developed so as to interpret the experimental data.

The thesis is divided into 9 chapters, including this introductory chapter.

Chapter 2 reviews principal literature on the dynamic response of the human body in standing and seated positions. Experimental studies and mathematical models are discussed. Some fundamental information on the human anatomy is also documented.

Chapter 3 summarises the apparatus and design of experiments and the methods of data analysis.

Chapter 4 documents measurements of the driving-point apparent mass of standing subjects. The influence of posture in a standing position is also investigated.

Chapter 5 describes an investigation of the nature of the vibration transmission through the standing body. The influences of posture and vibration magnitude are investigated.

Chapter 6 documents the differences in the dynamic responses between standing and seated bodies. The influence of vibration magnitude is also discussed.

Chapter 7 presents illustrations of the movement of the upper-body in seated and standing positions exposed to vertical whole-body vibration based on the results presented in Chapter 6.

Chapter 8 describes the development of lumped parameter models with rotational degrees of freedom so as to interpret experimental data obtained in earlier chapters.

Chapter 9 presents a general discussion and the conclusions of the thesis and provides some recommendations for future work.

CHAPTER 2

LITERATURE REVIEW

2.1 INTRODUCTION

The dynamic responses of the human body exposed to vertical whole-body vibration or shock have been investigated for some decades. Various experimental studies involving living human subjects have been conducted so as to obtain data representing the dynamic characteristics of the living human body during exposure to vibration or shock. The effects of posture, muscle tension and nature of input stimulus on the biodynamic response have been investigated. The development of mathematical models has also been presented in previous studies. The complexity of the human body structure has required some simplifications, or assumptions, in the models. The extent of simplification in the models has been dependent on various matters, such as the aims of the modelling, the availability of reliable data on the properties of the living human body, and the capability of computing. The majority of previous studies of the biodynamic responses to vertical whole-body vibration have focused on the seated body, although some have investigated the dynamic responses of the standing body.

This literature review first introduces the methods for representing the dynamic response of the human body used in previous studies. It is then divided into sections concerned with the dynamic response of the human body as a whole, the dynamic responses of various parts of the body, mathematical models of the biodynamic response, and conclusions.

2.2 METHODS FOR REPRESENTING THE DYNAMIC RESPONSE OF THE HUMAN BODY TO VERTICAL WHOLE-BODY VIBRATION

2.2.1 Introduction

The dynamic response of the body is usually represented by frequency response functions based on spectral analysis. These frequency response functions are

normally complex functions and presented with magnitude and phase. In using these functions it is assumed that the behaviour of the human body during exposure to whole-body vibration can be represented by a linear system.

At least two measurements of motion or force are required to determine a frequency response function representing the biodynamic response. These measurements may be obtained either at the same point or at different points.

In the case of using two measurements at a point, the ratio of the force to the motion at the driving point (either at the seat-person interface or at the floor-person interface, depending on the position of the subjects) has been measured in previous studies. This ratio is generally called the ‘driving-point frequency response function’:

$$T_D(f) = \frac{F(f)}{X(f)} \tag{2.1}$$

where $X(f)$ is the Fourier transform of the driving motion acting on the body and $F(f)$ is the Fourier transform of the force measured at the driving point. The term ‘mechanical impedance’ is often used for this function, although this has the specific meaning of the ratio between the force and velocity measured at the same point.

Based on two measurements at different points, the ratio of the motions measured at two distant parts of the body is used:

$$T_T(f) = \frac{X_2(f)}{X_1(f)} \tag{2.2}$$

which is usually called the ‘transmissibility’. The term $X_1(f)$ is the Fourier transform of the motion at a point, usually the driving point, and $X_2(f)$ is the motion at a distant point of interest. Both of these functions are required to establish a comprehensive understanding of the dynamic response of the human body to vibration.

2.2.2 Driving-point dynamic response of the body

In the measurement of the driving-point dynamic response, acceleration, velocity or displacement at the driving point can be taken as the input motion to the body. Some common measures used to represent the dynamic responses of a linear system are shown in Table 2.1. The measure depends on the type of motion used in the calculation. In previous studies investigating the dynamic response of the human body, either the mechanical impedance or the apparent mass has usually been used.

The mechanical impedance, $Z(f)$, is the ratio of the force to the velocity measured at the driving point:

$$Z(f) = \frac{F(f)}{V(f)} \tag{2.3}$$

where $V(f)$ is the Fourier transform of the input velocity at the driving point and $F(f)$ is that of the force. The mechanical impedance has been used by analogy with the impedance of an electrical circuit, which is a complex resistance. This has been used in the early studies.

The apparent mass, $M(f)$, is defined as the ratio between the force and the acceleration at the driving point:

$$M(f) = \frac{F(f)}{A(f)} \tag{2.4}$$

where $F(f)$ and $A(f)$ are the Fourier transforms of the force and acceleration,

Table 2.1 Some common measures used to represent the dynamic response of a linear system.

Motion	Force / Motion	Motion / Force
Acceleration	Apparent mass	Accelerance
Velocity	Mechanical impedance	Mobility
Displacement	Dynamic stiffness	Receptance

respectively. The advantages in the use of the apparent mass are as follows: 1) the apparent mass can be obtained directly from the measurements by accelerometers and force transducers, which are normally used for this type of measurement, 2) the concept of the apparent mass is intuitively related to Newton's second law of motion: 'the rate of the change of momentum of a mass is equal to the force acting on it', that is, if a mass does not vary with time, the acceleration of a body is proportional to the force and the constant of proportionality is the mass of the body, and 3) with respect to the advantage mentioned above, if the human body behaves like a rigid mass during exposure to vibration, the apparent mass is equal to its static mass.

The apparent mass can be easily obtained from the mechanical impedance using the relationship between the Fourier transform of the velocity and that of the acceleration:

$$M(f) = \frac{Z(f)}{i2\pi f} \tag{2.5}$$

where $i^2 = -1$.

The magnitudes and phases of these frequency response functions can indicate the similarity between the dynamic response of the human body and that of some system whose dynamic response is already known, such as a mass, a damper, a spring or a combination of these. The measurement of the mechanical impedance, or apparent mass, therefore, may be suited to help understand a general trend in the dynamic response of the human body to vibration. The driving-point dynamic response may not be affected much by motions of body parts far from the driving point.

2.2.3 Transmissibility of the body

The transmissibility represents the ratio between the motion at one measurement point in the body and the motion at another point. The motion at the driving point is usually chosen as a reference motion. In previous studies, the ratios of the motions at various locations in the body, for example, the head, to the driving point motion, which is the seat motion for seated subjects and the floor motion for standing subjects, have been investigated. The transmissibility to various levels of the spine has also been

measured in view of the occurrence of spinal disorders due to exposure to vibration or impact.

The transmissibility, $T(f)$, is calculated as Equation (2.2):

$$T(f) = \frac{X_2(f)}{X_1(f)} \tag{2.6}$$

where $X_1(f)$ and $X_2(f)$ are the Fourier transforms of the motions at two different measurement points. Acceleration signals are usually obtained from the transducers and used in the calculation in most studies. The transmissibility is also a complex function from which the magnitude and phase can be derived. The magnitude of the transmissibility may indicate the ratio between two motions at distant points at each frequency. The phase value may represent the time delay in the transmission of the oscillatory motion at a particular frequency between two positions.

The measurement of the transmissibility could be used to understand both the dynamic response of a particular part of the body to a whole-body vibration input and the relative movement between two particular parts of the body. This may also be useful to identify the mechanisms contributing to the characteristics of the driving-point response.

2.3 DRIVING-POINT DYNAMIC RESPONSE OF THE HUMAN BODY TO VERTICAL WHOLE-BODY VIBRATION

The dynamic response of the human body to whole-body vibration at the driving point has been measured so as to obtain an objective representation of the biodynamic response in previous studies. For the seated body, measurements of the driving point response have been conducted and some consistent trends can be found. Several factors, such as changes in the posture of the subjects and changes in the magnitude of the stimuli, have been investigated in order to identify their effects on mechanical impedance, or apparent mass. The driving point response of the standing body, however, has been reported in fewer studies. In this section, the studies conducted on the driving-point response of the body in standing and sitting positions are reviewed.

2.3.1 Standing subjects

2.3.1.1 Driving-point dynamic response in normal standing posture

Previous studies concerned with the driving-point response of standing subjects are summarised in Table 2.2, together with the experimental conditions used. Coermann (1962) measured the mechanical impedance of eight male subjects in a standing position. Vertical sinusoidal vibration in the frequency range 1 to 20 Hz with the frequency interval of either 0.5 Hz for the frequencies below 14 Hz or 1.0 Hz for those above 14 Hz was used. A vibration magnitude of 0.5 g and a duration of one minute were used. When in a ‘standing erect with stiff knees’ posture, a resonance was found at 5.9 Hz which was in between the resonance frequencies of two sitting postures measured in the study: ‘sitting erect’ and ‘sitting relaxed’. A local peak can be seen in the frequency region of 11 Hz in the presented figure showing the mechanical impedance of one subject, although this is not mentioned by the author.

Table 2.2 Summary of experimental conditions used in previous studies of the driving point response of standing subjects.

Authors (year)	Subjects	Postures, Controls	Stimuli (vertical)	Analyses
Coermann (1962)	8 male subjects Age: 29 to 47 yrs Height: 1.70 to 1.93 m (median: 1.82 m) Weight: 70 to 99 kg (median: 86.9 kg)	'Erect with stiff knees' 'Bending legs'	Sinusoidal Frequency: 1 to 20 Hz Interval: 0.5 Hz (1 to 14 Hz), 1.0 Hz (14 to 20 Hz) Magnitude: up to 0.5 g Duration: 1 min	Mechanical impedance (calculated from peak values of band-pass filtered wave forms)
Edwards and Lange (1964)	2 male subjects Age: 23, 26 yrs Height: 1.91, 1.80 m Weight: 84, 78 kg	Standing	Sinusoidal Frequency: 1 to 20 Hz Magnitude: 0.2, 0.35, 0.5 g Duration: 10 sec	Mechanical impedance (calculated from maximum values per cycle)
Fairley (1981)	10 male subjects Age: 20 to 28 yrs Height: 1.69 to 1.83 m (median: 1.78 m) Weight: 65 to 75 kg (median: 68 kg)	'Standing normally' (normal upright posture, normal muscle tension, knees locked, arms hanging by sides, stocking feet) 'Legs slightly bent' (knees not locked)	Random Frequency: 2.5 to 50 Hz Magnitude: 3.5 ms^{-2} rms Duration: 40 sec	Apparent mass (calculated from cross and power spectral densities)
Fairley (1986)	8 male subjects Age: 24 to 30 yrs Height: 1.66 to 1.93 m (median: 1.79 m) Weight: 57 to 80 kg (median: 75 kg)	'Knees locked' 'Knees bent' (upper and lower legs made an angle of approximately 15 degrees)	Random Frequency: 0.5 to 20 Hz Magnitude: 1.0 ms^{-2} rms Duration: 64 sec	Apparent mass (calculated from cross and power spectral densities)
Miwa (1975)	20 subjects Weight: 50 to 76 kg (from 12 subjects)	'Erect with erect legs' 'Relaxed with erect legs' 'Knee-bending' 'Standing on heels' 'Standing on tiptoes' 'Standing on one leg' 'Standing on knees'	Frequency sweep Frequency: 3 to 200 Hz Magnitude: 0.1 g Duration: 90 sec	Mechanical impedance (calculated with analogue computer)

Edwards and Lange (1964) conducted measurements of the mechanical impedance of the standing body with three different magnitudes of vertical sinusoidal vibration, 0.2, 0.35 and 0.5 g, in the frequency range from 1 to 20 Hz. Two male subjects took part in the experiment. A prominent resonance was found to occur at a frequency between 4 and 5 Hz and a second resonance was located in the range 11 to 15 Hz with a 'relaxed standing attitude' with all magnitudes of vibration.

The mechanical impedances of standing subjects in various postures were also investigated by Miwa (1975). Twenty subjects whose gender was not mentioned were exposed to vertical swept sinusoidal vibration in a wide frequency range with an acceleration amplitude of 0.1 g. The frequency sweep time from 3 to 300 Hz was 90 seconds. There was found to be a main peak in the average mechanical impedance of twenty subjects in a 'standing posture' at 7 Hz, although a clear definition of the posture was not presented. Two local peaks were also found at 20 and 55 Hz.

A range for the mechanical impedance values of standing subjects in the vertical direction, which is based on the results of the early studies, is presented in International Standard (ISO) 5982 (1981). The frequency range is between 0.5 and 31.5 Hz, with extrapolation at the lowest frequencies. It is stated that the range covers approximately 80% of the experimental data in available literature. However, these data are said to be from only five subjects which have been obtained with sinusoidal floor vibration and a loosely defined subject posture.

Figure 2.1 shows the mechanical impedances of subjects in an upright standing posture derived from the studies and the standard mentioned above.

There is an unpublished study of the apparent mass of the standing subjects conducted by Fairley (1981). Ten male subjects were exposed to vertical random vibration in the frequency range of 2.5 to 30 Hz. The vibration magnitude and duration were 3.5 ms^{-2} r.m.s. and 40 seconds, respectively. In a 'standing normally' posture in which the knees were held locked with normal muscle tension, a resonance was found at about 5.5 Hz with a magnitude of 1.5 to 2.0 times the static weight of the subjects in the mean apparent mass of the ten subjects. A small peak was also seen at around 11 Hz.

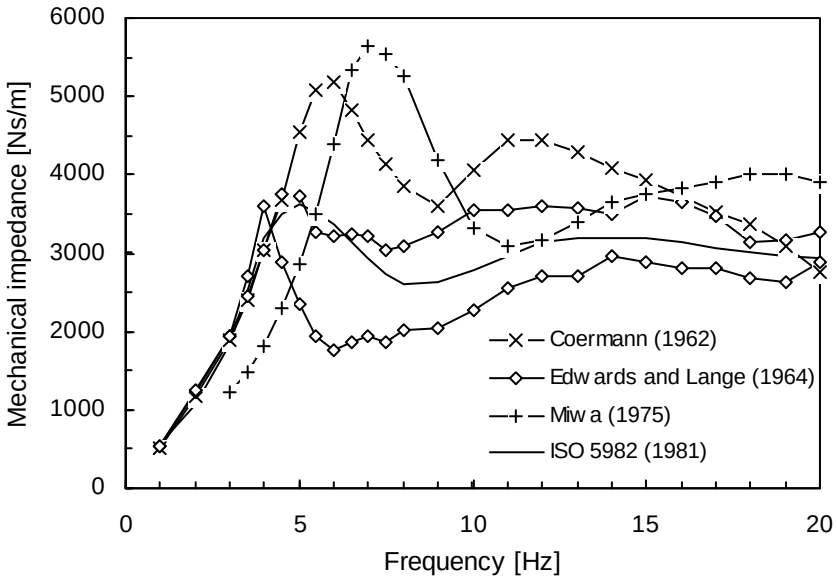

Figure 2.1 Mechanical impedances of standing subjects in previous studies and standard. Individual data from Coermann (1962, 'erect with stiff knee' with sinusoidal vibrations at 0.5 g) and Edwards and Lange (1964, 'relaxed standing attitude' with sinusoidal vibrations at 0.5 g). Mean from 20 subjects by Miwa (1975, 'standing posture' with frequency swept vibrations at 0.1g).

The same author measured the apparent mass of eight male subjects in another study (Fairley, 1986) (Figure 2.2). There was a main resonance at around 5 Hz in the results of all the subjects in a 'knees locked' posture, although a second resonance which can

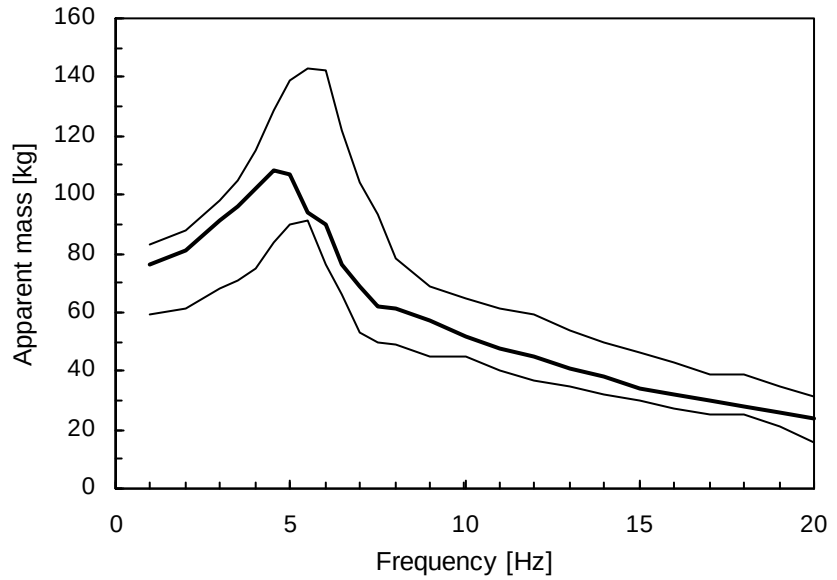

Figure 2.2 Median, maximum and minimum apparent mass from eight standing subjects in 'knee locked' posture by Fairley (1986). With random vibration at 1.0 ms^{-2} r.m.s.

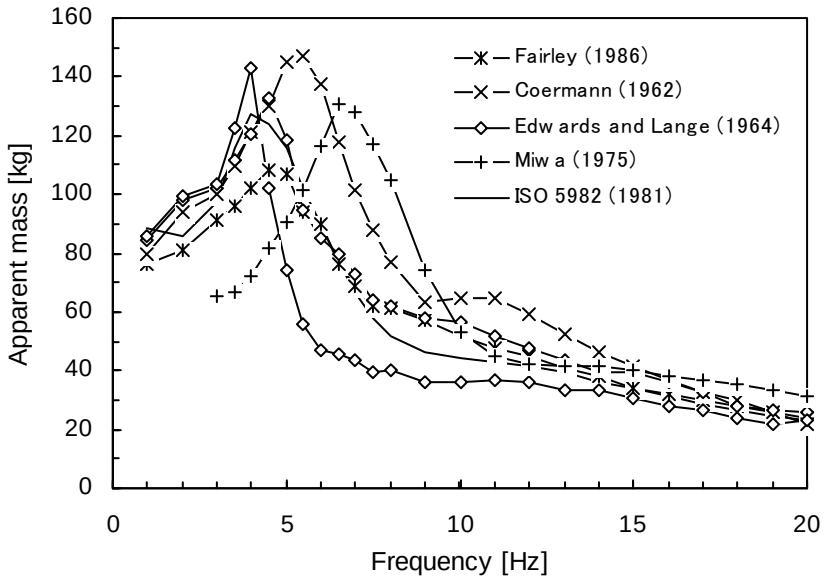

Figure 2.3 Data in previous studies in terms of apparent mass. Individual data from Coermann (1962) and Edwards and Lange (1964). Mean from twenty subjects by Miwa (1975). Median from eight subjects by Fairley (1986).

be seen in the other studies were not clearly found in some subjects.

Using Equation (2.5), the mechanical impedance data presented in Figure 2.1 are easily transformed in the apparent mass. Figure 2.3 shows all the data mentioned above in terms of the apparent mass.

2.3.1.2 Effect of posture of subjects on driving-point dynamic response

There have been a few studies in which the effects of postural changes on the mechanical impedance or apparent mass in a standing position were investigated.

The effects of bending the legs were investigated by Coermann (1962), Miwa (1975) and Fairley (1981, 1986). In these studies, the first resonance frequency, which was seen at around 5 Hz in a standing posture with the legs straight, was found to decrease to the range from 2 to 3 Hz when the legs were bent to a certain extent during exposure to vertical floor vibration.

A low natural frequency below 2 Hz with the legs bent was stated by Coermann (1962), although the extent of bending was not clear and any data showing this effect

were not presented. Miwa (1975) also did not describe the definition of the 'knee-bending' posture. In his results, three peaks with similar magnitudes of the mechanical impedance were located at 3, 20 and 60 Hz. The frequency of the first peak could be lower, that is, less than 3 Hz, as 3 Hz was the lowest frequency of the frequency range used in the study.

Fairley (1981, 1986) used two different legs bent postures in his separate studies: a 'standing legs slightly bent' posture in which 'the legs were bent slightly so that the change was hardly noticeable to an observer' and a 'knees bent' posture in which 'the knees were bent so that the upper and lower legs made an angle of approximately fifteen degrees'. It was stated that the 'legs slightly bent' posture caused a decrease in the first resonance frequency to 3 Hz while the 'knees bent' posture caused a main resonance at 2.5 Hz, although there can be an inter-subject variability in those data (Figure 2.4).

Some other changes in leg posture were investigated by Miwa (1975). Five subjects adopted the following five postures: 'standing on the heels', 'on the tiptoes', 'on one leg', 'on the knee' and 'squatting'. A similarity in the impedance versus frequency curves was found in the 'standing on the tiptoes' and 'squatting' postures. The first resonance existed at about 4 Hz which was lower than that in the 'standing erect' posture which was 7 Hz in the study. There was also found to be a lower resonance

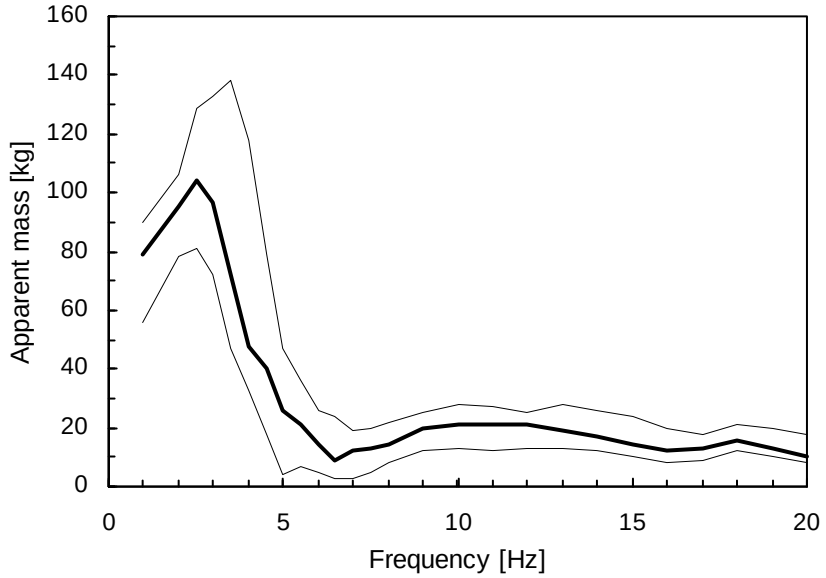

Figure 2.4 Median, maximum and minimum apparent mass from eight standing subjects in 'knee bent' posture by Fairley (1986). With random vibration at 1.0 ms^{-2} r.m.s.

frequency, about 5 Hz, in the ‘standing on one leg’ posture. The result in the ‘standing on the knees’ posture, which had a resonance at 6.5 Hz, and the results of some subjects in the ‘standing on the heels’ posture showed a similar trend to that in the ‘standing erect’ posture, while some in the ‘standing on the heels’ posture had no clear peak.

The effect of postural change in the upper body was also investigated by Miwa (1975). It was stated that there was not an obvious difference in the impedance curves between two different upper-body postures, ‘erect’ and ‘relaxed’, when the posture of the legs was in an ‘erect state’. Data to support this conclusion were not presented.

2.3.1.3 Effect of vibration magnitude on driving-point dynamic response

There have been several previous studies of the effect of the magnitude of the input on the mechanical impedance or apparent mass of seated subjects and it has been understood that the change in the input magnitude affects the dynamic response of the body (e.g. Hinz and Seidel, 1987; Mansfield, 1998; Mansfield and Griffin, 1999). That is, the dynamic response of the human body has nonlinear characteristics. However, the number of studies which have investigated the effect of the input magnitude on the driving-point response of the standing body is very limited.

Edwards and Lange (1964) used three different magnitudes of vertical sinusoidal vibration, 0.2, 0.35 and 0.5 g, in order to identify the effect of the vibration magnitude on the mechanical impedance of two standing subjects. There was an effect observed in one subject: both the resonance frequency and the magnitude of the impedance shifted downward with an increase in the magnitude of vibration. The mechanical impedance of the other subject, however, did not show a significant effect of a change of the acceleration level.

2.3.2 Seated Subjects

There have been more studies of the driving-point dynamic response of seated subjects than standing subjects. Table 2.3 presents a summary of some relevant studies on seated subjects. A rigid flat seat was used in these studies to eliminate any effects of compliance on the response of the body.

Most studies have reported a resonance of the mechanical impedance or apparent mass in the region of 5 Hz, which was consistently found by Fairley and Griffin (1989) using a group of 60 people, including male and female adults and children (Figure 2.5). Some studies have detected a second peak at 8 to 17 Hz which was not distinct. The influence of postural changes has been investigated in a few studies and it is reported that the main resonance frequency tends to increase when the posture of subjects changes from ‘relaxed’ to ‘erect’ (Coermann, 1962; Fairley and Griffin, 1989; Figure 2.6). Nonlinear characteristics of the dynamic response of the body were found by using different input vibration magnitudes or different magnitudes of static acceleration and by looking at time histories of the output signal caused by sinusoidal input. It was found that the main resonance frequency decreased with increasing vibration magnitude (Hinz and Seidel, 1987; Mansfield, 1998; Mansfield and Griffin, 1999; Figure 2.7). However, the resonance frequency increased with increasing static acceleration (Mertens, 1978; Vogt *et al*. 1968; Figure 2.8). When an input motion was sinusoidal, a time history of the force measured was found not to be sinusoidal (Hinz and Seidel, 1987; Wittmann and Phillips, 1969).

Table 2.3 Summary of some principal previous studies of the driving point response of sitting subjects.

Authors, Keywords	Subjects, Conditions, Stimuli	Findings
Coermann (1962) mechanical impedance posture vibration magnitude constraint	8 male subjects (29 to 47 yrs) Posture: erect, relaxed Constraint: pelvis and abdomen, whole-body Vibration: vertical sinusoidal, 1 to 20 Hz, up to 0.5 g	• Peak at 6.3 Hz in erect posture and 5.2 Hz in relaxed posture for 1 subject • First peak at 5 Hz and second peak at 9 Hz from median mechanical impedance in erect posture • Constraints for upper body suppressed first peak and enhanced second peak • Effect of change in vibration magnitude was small: within 10% for 0.1, 0.3 and 0.5 g
Donati and Bonthoux (1983) mechanical impedance	15 male subjects (18 to 25 yrs) Posture: erect but not stiff Vibration: vertical sweep and broad band random, 1 to 10 Hz, 1.6 ms^{-2} r.m.s.	• Marked resonance at around 4 Hz for some subjects • Damping force was prominent for other subjects • Effect of input waveform was not significant, except values at resonance frequency
Fairley (1986) Fairley and Griffin (1989) apparent mass posture vibration magnitude gender body size	60 subjects (24 male, 24 female, 12 children) Posture: normal (comfortable upright) 8 male subjects for investigation into effect of posture and vibration magnitude Posture: normal, erect, tense (muscle), backrest, footrest Vibration: vertical random, 0.25 to 20 Hz, 1.0 ms^{-2} r.m.s. (0.25, 0.5, 1.0, 2.0 ms^{-2} r.m.s.)	• Main resonance at about 5 Hz • Second mode in the region of 10 Hz (never distinct) • Variability between subjects arose from different static weight • Variability in normalised apparent masses was small • Mean normalised apparent masses for men, women and children were similar • Relative movement between feet and platform had an effect on the response • Resonance frequency was larger for 'backrest', 'erect' and 'tense' (largest change) postures compared to 'normal' posture. • Resonance frequency decreased with increasing vibration magnitude
Hinz and Seidel (1987) apparent mass vibration magnitude waveform	4 male subjects (23 to 25 yrs) Posture: moderately erect Vibration: vertical sinusoidal, 2 to 12 Hz, 1.5 and 3.0 ms^{-2} r.m.s.	• Resonance frequency: 4.5 Hz at 1.5 ms^{-2} r.m.s. and 4 Hz at 3.0 ms^{-2} r.m.s. • Great inter-individual differences • Clear transformation of the sinusoidal input into non-sinusoidal output
Mansfield (1998) Mansfield and Griffin (1999) apparent mass vibration magnitude	12 male subjects (mean 26.3 yrs) Posture: comfortable upright Vibration: vertical random, 0.2 to 20 Hz, 0.25, 0.5, 1.0, 1.5, 2.0, 2.5 ms^{-2} r.m.s.	• First resonance frequency decreased with increase in vibration magnitude: 5.4 Hz at 0.25 ms^{-2} r.m.s. to 4.2 Hz at 2.5 ms^{-2} r.m.s. • Magnitude at resonance tended to increase slightly with increasing vibration magnitude • Second resonance in 8 to 12 Hz was affected by vibration magnitude • Non-linearity over 3 to 16 Hz • Greatest change over the four lowest acceleration magnitudes

Table 2.3 (continued) Summary of some principal previous studies of the driving point response of sitting subjects.

Authors, Keywords	Subjects, Conditions, Stimuli	Findings
Mertens (1978) mechanical impedance static acceleration gender	9 subjects (6 male and 3 female, 24 to 44 yrs) Posture: upright Vibration: vertical sinusoidal, 2 to 20 Hz, 0.4 g r.m.s. Static acceleration: vertical, 1, 2, 3, 4 g	• Main resonance in mechanical impedance was stiffened with increasing static acceleration: 5 Hz at 1 g, 11 Hz at 2 g, 12 Hz at 3 g, 13 Hz at 4 g • At 2 g, first peak at 7 Hz • No significant difference between male and female
Miwa (1975) mechanical impedance posture vibration magnitude	20 subjects Posture: erect, relaxed, leaned-back, stooping Vibration: vertical sweep, 3 to 200 Hz, 0.1 and 0.3 g	• No obvious difference between erect and relaxed • Peak at 6 to 7 Hz and 17 Hz in mean mechanical impedance • Several peaks below 5 Hz in leaned-back posture • Mechanical impedance in stooping posture was equal to that in erect posture • Softening effect with increase in vibration magnitude
Sandover (1978) apparent mass vibration magnitude constraint	Data from 2 subjects were reported Posture: erect but not stiff Constraint: wooden blocks under ischial tuberosities, visceral support Vibration: vertical random, up to 25 Hz, 1 and 2 ms^{-2} r.m.s.	• Any non-linear effects were small • Resonance frequency shifted from 4 Hz in sitting erect posture to 5.5 Hz with 'short-circuit' buttocks for 1 subject • Clear second resonance at 7 to 8 Hz with visceral support (1 subject)
Vogt et al. (1968) mechanical impedance static acceleration	10 male subjects Posture: slightly erect with backrest Vibration: vertical sinusoidal, 2 to 15 Hz, 0.5 g Static acceleration: vertical, 1, 2, 3 g	• Fundamental resonance: 5 Hz at 1 g, 7 Hz at 2 g, 8 Hz at 3 g
Vykukal (1968) mechanical impedance static acceleration	4 subjects Posture: semisupine position Vibration: vertical sinusoidal, 2.5 to 20 Hz, 0.4 g (peak) Static acceleration: vertical, 1, 2.5, 4 g	• Stiffness increased and damping reduced with increasing bias linear acceleration • Resonances at 1 g: 7, 11, 13, 15, 18 Hz
Wittmann and Phillips (1969) mechanical impedance impact magnitude impact duration waveform	More than 4 subjects Posture: erect Impact: vertical, peak acceleration, 6 to 7 and 12 to 14 g, duration, 55 and 120 msec Vibration: vertical sinusoidal, low level acceleration	• Impedance curve depended on duration of impact • Greater impedance with high acceleration below some frequency, smaller impedance with short duration above some frequency (1 subject) • Waveform of transmitted force was not sinusoidal with steady state sinusoidal input: magnitude in loading phase was larger than that in unloading phase

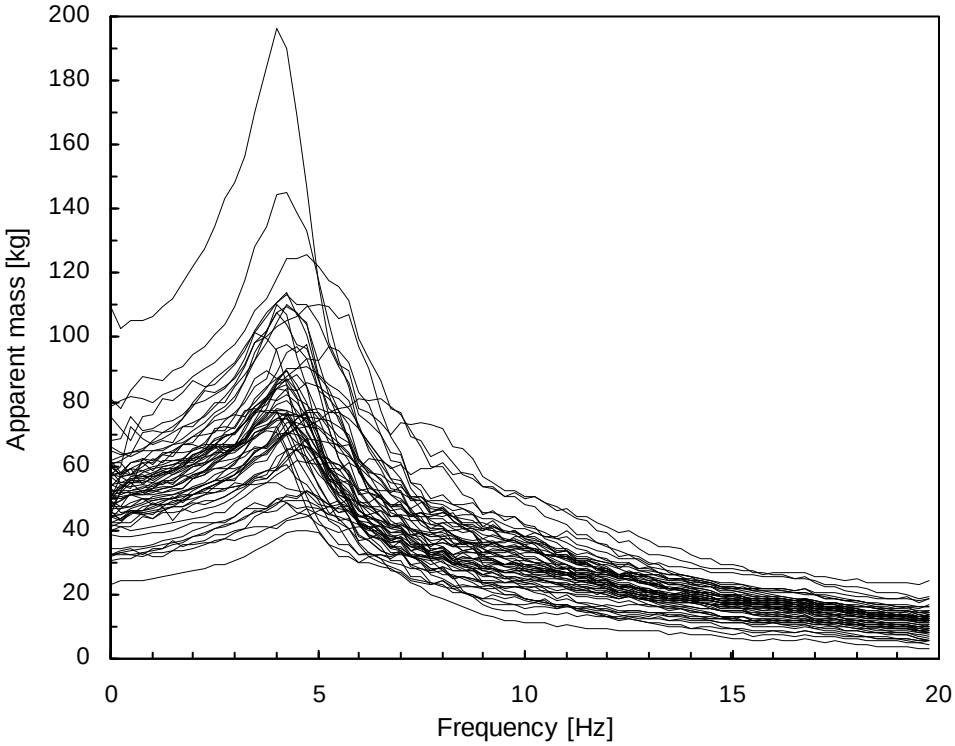

Figure 2.5 Apparent mass of 60 subjects from Fairley and Griffin (1989). Stimulus: vertical random vibration at 1.0 ms^{-2} r.m.s. Posture: normal comfortable upright.

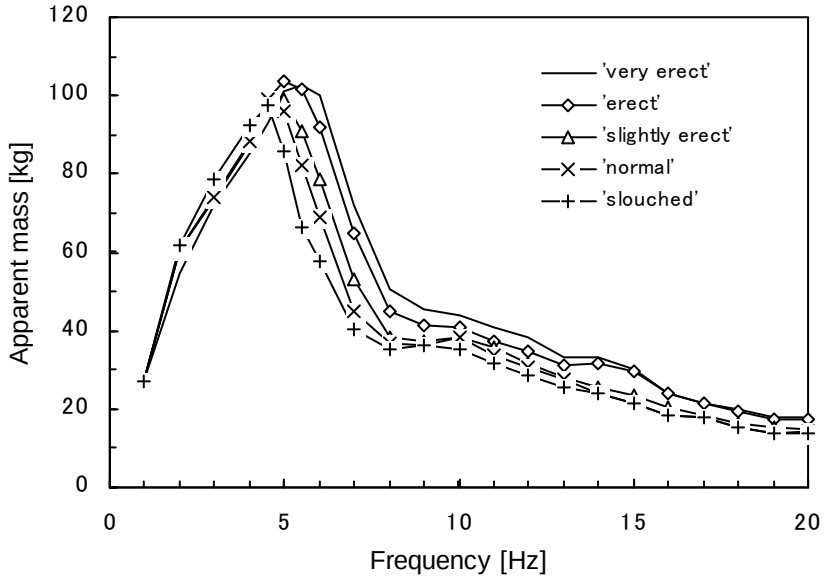

Figure 2.6 Effect of postural change on the apparent mass by Fairley and Griffin (1989). Data from one subject.

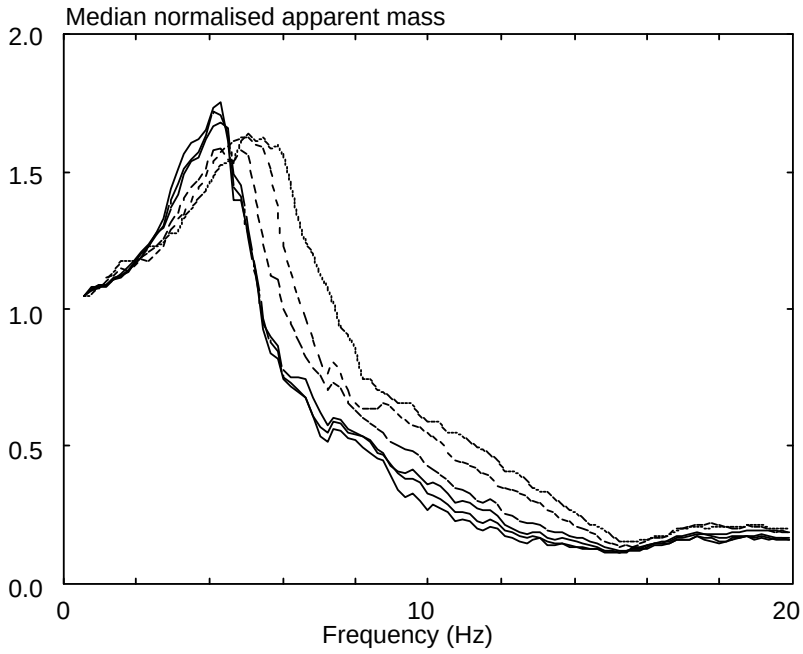

Figure 2.7 Effect of vibration magnitude on the apparent mass. After Mansfield (1998) and Mansfield and Griffin (1999). Median of twelve subjects measured at 0.25, 0.5, 1.0, 1.5, 2.0 and 2.5 ms^{-2} r.m.s.

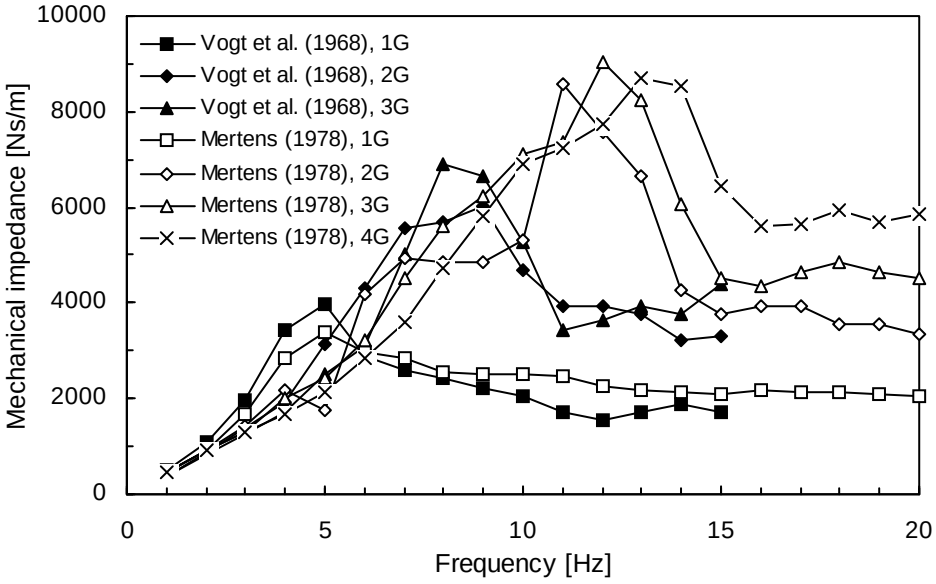

Figure 2.8 Effect of static acceleration on the mechanical impedance. Data from one subject by Vogt *et al*. (1968, 'sitting slightly erect' with sinusoidal vibration at 0.5 g). Mean of nine subjects by Mertens (1978, 'sitting upright' with sinusoidal vibration at 0.4 g r.m.s.).

In previous studies, the variability of the static mass of subjects could contribute to the variability in the mechanical impedance or apparent mass between individuals. Fairley and Griffin (1989) suggested a method to eliminate the effect of the static weight by dividing the apparent mass by the apparent mass at the lowest frequency which is approximately identical to the static weight. Small variability in the 'normalised apparent masses' was reported (Figure 2.9).

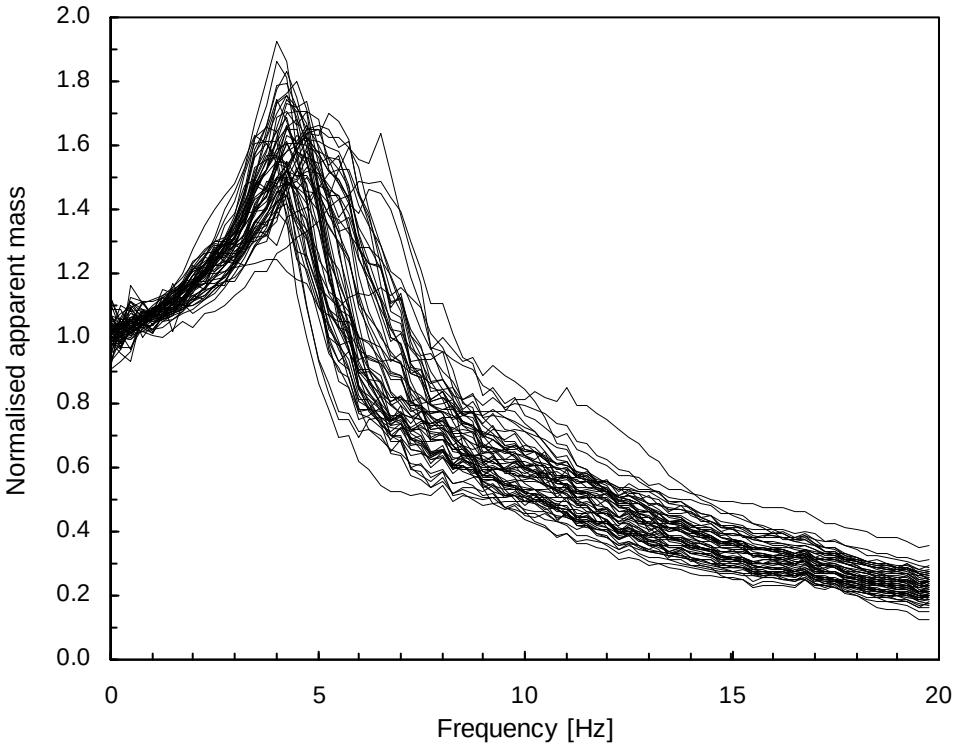

Figure 2.9 Normalised apparent mass of 60 subjects from Fairley and Griffin (1989). Stimulus: vertical random vibration at 1.0 ms^{-2} r.m.s. Posture: normal comfortable upright.

2.4 DYNAMIC RESPONSES OF VARIOUS BODY PARTS TO VERTICAL WHOLE-BODY VIBRATION

The transmission of whole-body vibration to various locations in the body has been investigated so as to understand how much motion at a point of interest is produced by whole-body vibration. The dynamic response of the spine has been of interest in many studies so as to investigate the mechanism of spinal disorders. A possible relation between risk of low back pain or spinal disorders and both vibration and impact exposures has been reported from epidemiological studies (for example, reviewed by Wilder and Pope, 1996). The interest in spinal motion has also been based on the assumption that it could be a vital part in the vibration transmission through the body. The head motion has also been measured, probably so as to investigate principally the effect of vibration on vision. The transmissibility has mainly been used to represent the vibration transmission from the floor, or the seat, to various locations in the body. As in the case of the driving-point response, factors affecting the vibration transmission through the body have been investigated.

2.4.1 Dynamic response of the spine

2.4.1.1 Basic musculoskeletal anatomy of the spine (extracted from Dean and Pegington, 1996a)

The spine (i.e., the vertebral column), rib cage, and skull form the axial skeleton of the human body. The vertebral column supports the skull above and provides anchorage for the ribs. Each bone in the vertebral column is called a vertebra. The vertebral column consists of seven vertebrae in the cervical region, twelve vertebrae in the thoracic region and five vertebrae in the lumbar region (Figure 2.10). There are five fused sacral vertebral segments which are wedged between the two sides of the pelvis. The lower extremity of the column is composed of several small fused bones called the coccyx. The vertebral column is held together by a series of strong ligaments and muscles which move and support the vertebrae. The vertebral column has a curved shape. Lordosis is an increased anterior convexity of the vertebral column and is commonly seen in the lumbar region. Kyphosis means the opposite, an increase in the posterior convexity of the spine.

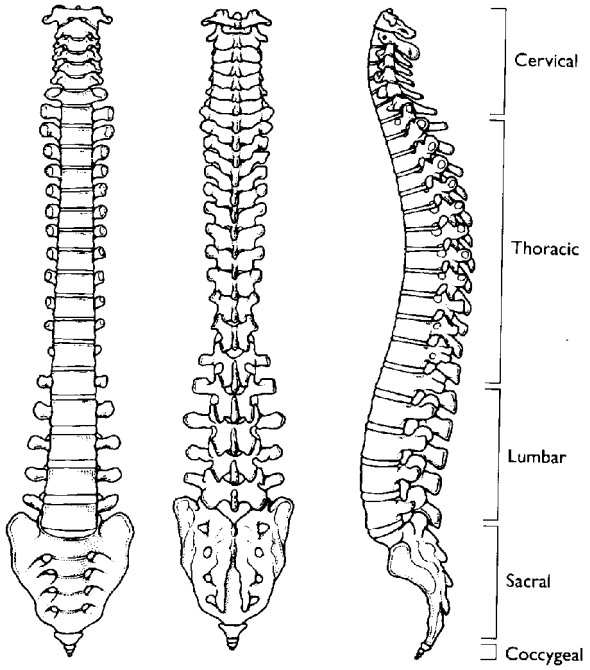

Figure 2.10 Vertebral column. Made up of cervical, thoracic, lumbar, sacral and coccygeal regions. After Dean and Pegington (1996a).

Vertebrae differ in shape from region to region. However, each vertebra is generally composed of two basic parts: anteriorly there is a mass of bone called the body and posteriorly there is a crescent of bone called the vertebral arch (Figure 2.11). Three bony processes, the spinous process and the right and left transverse processes, arise from the vertebral arch, which give attachment to muscles and ligaments. The lumbar vertebrae are more massive and stronger then either the cervical or thoracic vertebrae and their processes are short and strong. Vertebrae articulate with one another by means of joints. They are further joined by ligaments. Basically there are two articulations between any pair of vertebrae, body to body and vertebral arch to vertebral arch.

The body of one vertebra articulates with the body of another by an intervertebral disc. A mesh of strong fibrous tissue unites the cartilages which cover the surface of each vertebral body in the region

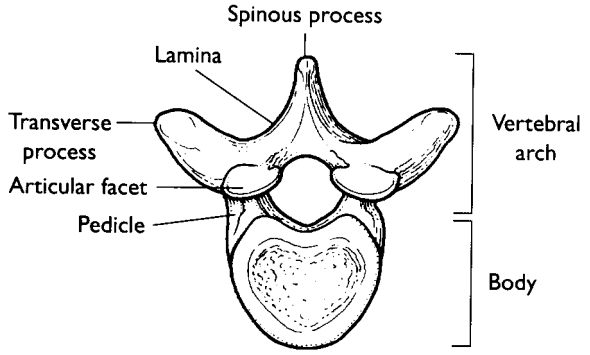

Figure 2.11 Typical vertebra. After Dean and Pegington (1996a).

of the disc. The fibrous tissue exists only around the periphery of the disc, it is called the annulus fibrosus. The centre of the disc consists of a gelatinous ‘ball’ called the nucleus pulposus. Vertebral bodies are also held together by the anterior and posterior longitudinal ligaments. The vertebral arches also articulate one with the other. These articulations are synovial joints. Each vertebral arch bears four articular facets: two are for the articulation with the vertebra above and two for the vertebra below. Several ligaments, the ligamenta flava, supraspinous and interspinous ligaments, and intertransverse ligaments, also attach the vertebral arches together. The characteristics of the connection between vertebrae described here are generally common in the column. However, the first and second cervical vertebrae, the altas and axis, are special, being adapted to support the skull and to allow the movements of nodding and rotation of the head respectively.

Each thoracic vertebra articulates with a pair of ribs at the lateral aspects of the body. Each rib articulates with the vertebra of its own number and also with the one above. Ribs at the first (T1) and last two (T11 and T12) thoracic vertebrae, however, articulate only with the thoracic vertebra of their own number. Ribs also articulate with the transverse processes of their own thoracic vertebrae at another synovial joint.

The vertebral column is surrounded by muscles. The musculature of the body wall is generally composed of three layers: the internal layer, which lies inside the ribs or costal elements of the vertebrae, the middle layer, which lies between costal elements or ribs, and the outer layer, which lies outside ribs. An example of muscle derived from the inner layer that is closely associated with the vertebral column is the psoas major in the lumbar region (Figure 2.12(a)). The origin and insertion of this muscle is from vertebral bodies and discs. An example of muscle derived from the middle layer in the region of the vertebral column is the quadratus lumborum in the lumbar region (Figure 2.12(b)). The quadratus lumborum arises from the ilium and inserts into transverse processes of the lumbar vertebrae and into the twelfth ribs. The external group of muscles associated with the vertebral column is very strong and extends on either side from the sacrum up to the base of the skull (Figure 2.12(c)). They may be collectively called the erector spinae mass. The erector spinae group extends the vertebral column. The movements are marked in the lumbar and cervical regions. The smaller deeper group of the muscle mass is also able to make fine adjusting movements which include rotation of one vertebra on another. Flexion of the vertebral column is

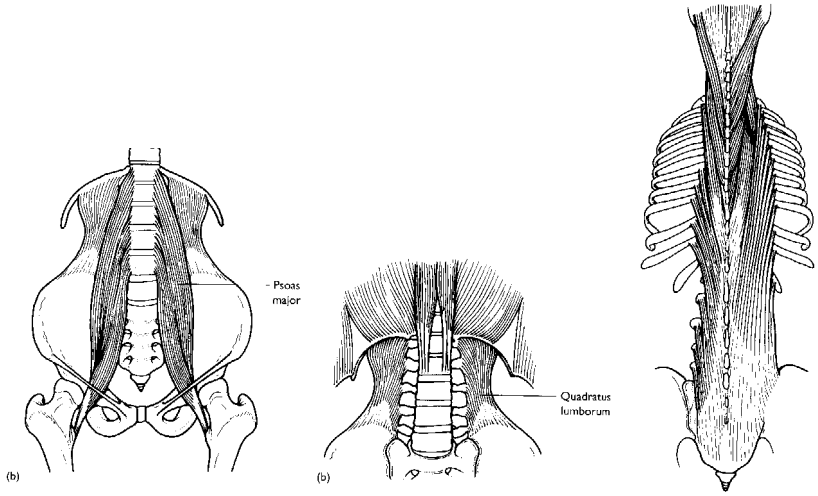

(a) (b) (c)

Figure 2.12 Three layers of muscles associated with the vertebral column. (a) the psoas muscle, (b) the quadratus lumborum, and (c) the sacrospinails group of muscles that is one of two main muscle group in the erector spinae mass. The sacrospinails group of muscles all run vertically while the transverse spinails group of muscles in the erector spinae mass run obliquely. After Dean and Pegington (1996a).

produced by such muscles as the prevertebral and psoas muscles. Lateral flexion in the lumbar region is effected by the quadratus lumborum muscle.

2.4.1.2 Methods to measure the spinal motion in situ

Although the motion of interest is that of the vertebral body, it is not straightforward to mount a transducer directly to the skeleton *in vivo*. It has been found that, in measuring the motion of the body by a transducer mounted on to the body surface, the tissue and the skin lying between the skeleton and the transducer have effects on the measurement (i.e., the motion measured at the body surface would be different from that of the skeleton underneath the transducer, e.g. Pope *et al*., 1986). In early studies of the dynamic response of the spine using human subjects, this effect was not taken into account and the results did not necessarily represent the motion of the skeleton. There have been mainly two methods developed for measurements of the spinal motion to eliminate the effect of the tissue and the skin: ‘direct measurement’ and ‘surface measurement’.

Direct measurement

Direct measurement is an invasive method: some transducers are mounted to a thin pin (e.g. Kirschner-wire) inserted into the spinous processes under local anaesthesia. To measure the vertical motions at five points over the spine, Hagena *et al*. (1985, 1986) used pairs of an accelerometer and a Kirschner-wire (K-wire) with a diameter of 1.8 mm and insertion depth between 1 and 2 cm which produced a distance between the bone and the accelerometer of 2 to 3 cm. It was stated that a direct linear transmission of the acceleration was proved by pre-tests using preloaded spinal segments taken from cadavers: the accelerations measured by the rig corresponded to stimuli directly applied to the vertebral body.

Panjabi *et al*. (1986) used thicker K-wires, 2.4 mm in diameter, placed 10 mm into the spinous processes of the first and third lumbar vertebrae (Figure 2.13). Three accelerometers mounted on an aluminium fixture were attached to each wire so that the weight of the complete transducer was 32.0 g so as to measure two linear accelerations and a rotational acceleration in the mid-sagittal plane. Several spinal units consisting of two adjacent vertebrae with interconnecting disc and ligaments were used to validate the measurement method by comparing the vertical acceleration measured by the system to that measured with an accelerometer rigidly attached to the top of the upper vertebral body. It was stated that 'except for some overlying high frequency noise, the two signals were nearly identical'. They concluded that the diameter and the 'free length' of the K-wire should be at least 2 mm and less than 6 mm, respectively, so as to 'produce a resonance frequency of more than 80 Hz for the measurement system' which would not affect the acceleration measured. A similar system was used by Pope *et al*. (1986) who detected 'substantial differences in measured displacements' between 'surface mounted' transducers and 'those mounted on pins rigidly attached to the skeleton' at the level of the third lumbar vertebra (Table 2.4).

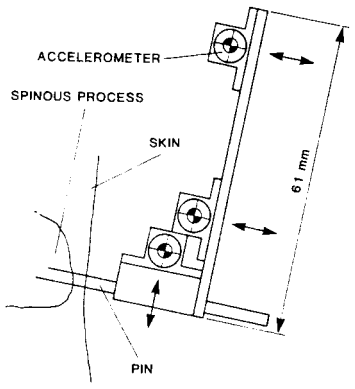

Figure 2.13 Schematic diagram of the accelerometer mounting used by Panjabi *et al*. (1986).

Table 2.4 Average peak displacement relative to adjacent pins [mm/g] from Pope *et al*. (1986). PSIS: the posterior superior iliac spine. LEDs: Light Emitting Diodes. LEDs were mounted to the pins inserted into PSIS and L3 and to the skin at 20 and 40 mm away from the pins at the same height. 0.2 g vertical sinusoidal motion at frequencies of 2, 4, 5 and 6 Hz.

	Surface LEDs	
Pin LEDs	20 mm away	40 mm away
PSIS	1.97	5.53
L3	4.68	4.46

A measurement system consisting of 2 accelerometers mounted on aluminium fixtures and attached to a 2 mm K-wire was used by Magnusson *et al*. (1993) so as to obtain the motion of the fourth lumbar vertebra in *x*- (ventral) and *z*- (cranial) axes. The wire 'was 'plucked' to establish pin resonance' and 'the integrity of the pin placement' was checked. It was stated that the resonance of the pin was 'generally about 50 Hz, well above the range of interest'.

Kaigle *et al*. (1992) measured the relative motion between adjacent vertebrae using 'an instrumented linkage transducer system' called 'the intervertebral motion device (IMD)' (Figure 2.14). 'This trapezoidal linkage system consisted of two columns (11-gage tubing), which slid onto the pins and were secured at both ends with lock nuts'. The two pins (intraosseous Steinman pins, 2.38 mm diameter, 110 mm length) were 'inserted approximately 10 mm into the spinous process of the vertebra'. 'Three sliding rods (20-gage tubing), were allowed to rotate sagittally at their respective origins on the columns'. Three 'custom-built omega-shaped extensiometers' with the average compliance of 0.0183 $m \cdot N^{-1}$ were 'attached to the IMD at ball-and-socket junctions' so that they would 'either compress or extend only'. The weight of the IMD was 20.26 g. With the IMD, the relative motion between the vertebral bodies could be 'resolved into sagittal rotation, axial translation, and anterior-posterior shear translation'. 'Static calibrations' 'in the range ± 4° rotation and ± 4 mm translation determined the absolute maximum errors to be 0.2° and 0.07 mm for rotation and translation measurements, respectively, with corresponding variances of 0.1° and 0.03 mm'. Dynamic calibrations were also conducted using 'a continuous sine sweep from 1 to 80 Hz, with a constant amplitude of 0.3 mm peak to peak'. It was stated that, within the frequency range from 1 to 10 Hz, 'the maximum 'noise' voltage for all three extensiometers was negligible at 0.1%'. 'The first natural frequency' of the system was identified 'at approximately 16.25

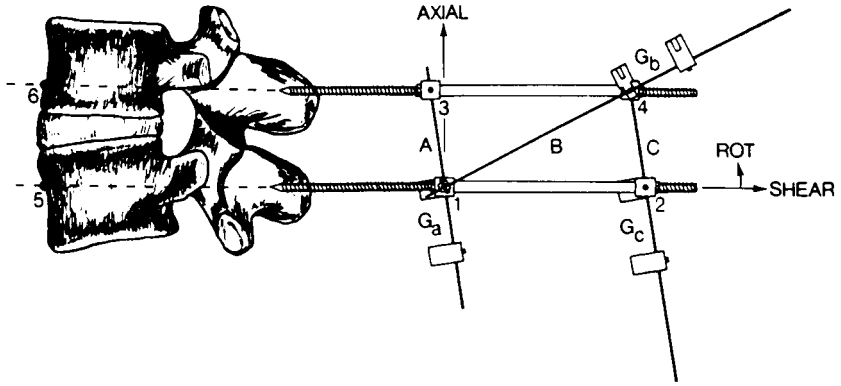

Figure 2.14 Schematic diagram of the intervertebral motion device (IMD) used by Kaigle *et al*. (1992).

Hz'. For the other dynamic test, the relative movement of two adjacent vertebrae taken from the body was measured by the IMD when 'the superior vertebra was sinusoidally vibrated' while 'the inferior vertebra was fixed to the table'. The excitations of both 1 mm peak-to-peak amplitude from 1 to 20 Hz and 2 mm peak-to-peak amplitude from 1 to 10 Hz were used. A mean discrepancy between the axial translation output from the system and that from the shaker was 12.4% (a standard deviation of 3.5%), which was greatest at 8 and 16 Hz, with 'a slight phase difference at half cycle'. It was stated that the measurement accuracy was improved with increased stiffness of the pins.

Surface measurement

It must be the most natural attempt to mount transducers rigidly to the bone, such as those mentioned above, when the motion of the skeletal system is of interest. However, in using those measurement methods, appropriate medical treatments are required and the number of participants is limited for ethical reasons. An alternative to obtain the motion of the skeleton beneath the surface of the body is to minimise the effect of the tissues between the transducer and the bone when the transducers are mounted to the skin. There have been two approaches: (1) an application of preload to a transducer and tissues and (2) a mathematical model of a tissue-transducer system to correct signals measured at the skin.

Preload methods are based on the idea that application of a preload makes the tissue beneath the transducer stiffer so that the resonance of the local tissue-transducer system would occur at a higher frequency than the frequency range of interest. Nokes *et al*. (1984), for example, measured the impulse response of tibias taken from

cadavers with both the accelerometer mounted to the skin with several levels of preloads and that mounted directly to the bone through a pin. They concluded that 'the vibration response of the bone could be recorded from a skin-mounted accelerometer' 'only if it is sufficiently preloaded'. The appropriate amount of preload depended on the thickness of the soft tissue. Saha and Lakes (1977) examined two different methods in applying preload and found that measurement errors related to soft-tissue were 'reduced if the accelerometer was spring-loaded rather than mass-loaded'. However, there was found 'no saturation of soft-tissue related effects at any preload level below the pain threshold' in measurements of the impulse response of the tibias of human volunteers. Ziegert and Lewis (1979) compared signals from two accelerometers, with different weights mounted to the skin of the antero-medial tibia with an elastic strap, to those from a light weight bone-mounted accelerometer when the medial malleolus was struck with an impacting device. It was found that a light weight (1.5 g) skin-mounted accelerometer 'showed nearly identical output' to that from the bone accelerometer. They concluded that 'a condition of preload and accelerometer mass was found for which the soft tissue effects were negligible, and the skin-mounted accelerometer response was an adequate reproduction of the input signal'. However, all of these studies were concerned with measurements of the motion at the lower limbs and the methods for preloading are not appropriate for measurements of the spinal motion.

Mathematical correction methods are such that a correction function is formed to obtain the skeletal motion from signals measured at the body surface. It is assumed that a local tissue-transducer system which modifies the motion of the bone is represented by a simple linear system. Collier and Donarski (1987) measured the driving-point mechanical impedance of a local system consisting of a 1.8 g accelerometer and the tissue between the accelerometer and the tibia in the direction perpendicular to the bone, using locally forced vibration. Based on the assumption that the mass of the tissue involved in the local vibration could be neglected, the ratio between the velocity of the bone and the velocity measured at the skin could be calculated using the mechanical impedance of the local system. The correction method was not validated by the authors.

Hinz *et al*. (1988a) assumed that the dynamic behaviour of the local tissue-accelerometer system over the spine in the vertical direction could be represented by a single degree of freedom (SDOF) system. Accelerometers weighing 0.5 g were stuck to the skin at the level of the fifth thoracic vertebra (T5) and the third lumbar vertebra

(L3) ‘by means of a special epoxide compound’. The natural frequency and the damping ratio of the assumed SDOF system were derived from the logarithmic decrements and the period of free damped vibration when ‘the skin was gently pulled upwards or downwards and released suddenly’. The significant differences in the parameters of the system were found across subjects and levels of the spine, although ‘the direction of releasing the skin did not affect the parameters’ determined at each measurement point. They stated that the calculated r.m.s. accelerations of the bone when a seated subject was exposed to sinusoidal whole-body vibration agreed well with the transmissibility to the vertebral body obtained by invasive measurements, for example, by Panjabi *et al*. (1986). Almost the same method was used by Smeathers (1989) to measure the motion at the spine caused by the heel strike using accelerometers, weighing 2.4 g, attached to the skin by adhesive tape over an area of approximately 6 cm^2.

Kitazaki and Griffin (1995) developed a mathematical correction method for surface measurement over the spine in both the vertical and the fore-and-aft directions based on the same assumption as that used by, for example, Hinz *et al*. (1988a). The parameters of the SDOF system were obtained from the principal peak and the band width of the spectrum of the free damped vibration of the local tissue-accelerometer system. Acceleration frequency response functions from the seat to L3 were calculated when seated subjects were exposed to vertical random vibration. Although different frequency response functions were obtained from accelerations measured at the skin with four different additional masses, the differences were eliminated by the correction method. The acceleration frequency response function obtained for L3 in both the vertical and fore-and-aft directions showed good agreement with the results from direct measurement by Panjabi *et al*. (1986) and Magnusson *et al*. (1993) (Figure 2.15). They concluded that ‘for vertical responses, the correction method was effective at frequencies below the estimated natural frequencies of the local system’, whereas ‘fore-and-aft responses over the spine did not require correction at frequencies below 35 Hz’. This limitation for vertical measurements coincides with that reported by Kim *et al*. (1993) who validated the correction method based on the same assumption for measurements of the longitudinal motion of the tibia by comparing the surface measurement to the direct measurement.

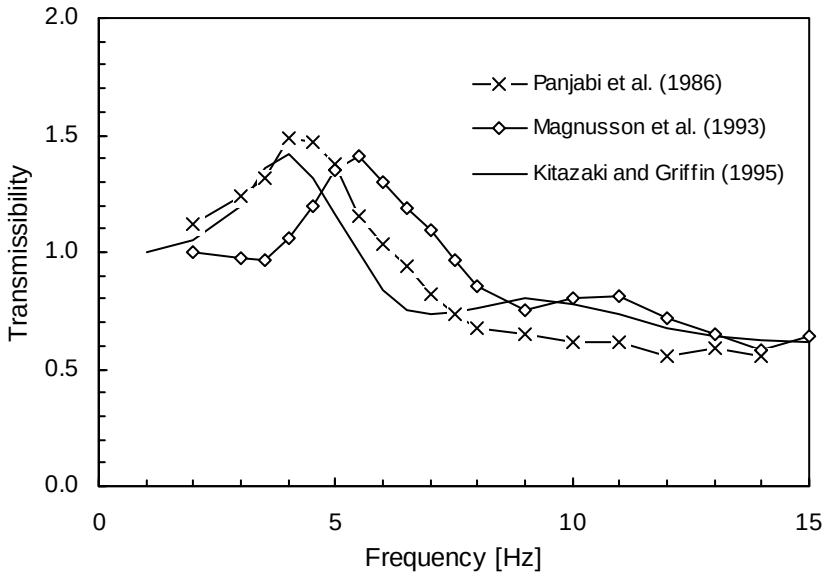

Figure 2.15 Vertical transmissibilities of seat vibration to the lumbar vertebra measured in previous studies. Median from five subjects and three subjects from Panjabi *et al*. (1986) and Magnusson *et al*. (1993), respectively. Mean of eight subjects from Kitazaki and Griffin (1995). Experimental conditions: Panjabi *et al*.: direct measurement at L3, sinusoidal vibration at 0.98 and 2.94 ms^{-2} r.m.s., sitting upright unsupported; Magnusson *et al*.: direct measurement at L4, impact, sitting upright ; Kitazaki and Griffin: surface measurement at L3, random vibration at 2.0 ms^{-2} r.m.s., sitting normal relaxed.

2.4.1.3 Transmissibility to the spine in a normal standing posture

Some principal previous studies of the dynamic response of the spine to whole-body vibration or impact are summarised in Table 2.5. These include the studies of both standing and seated bodies: Hagena *et al*. (1985, 1986), Pope *et al*. (1989) and Herterich and Schnauber (1992) investigated standing subjects, whereas all the other studies were concerned with seated subjects. Whichever the position of subjects, the motion of the lumbar spine has been investigated in all the studies in Table 2.5, possibly because of the expected relation between that motion and low back pain.

Table 2.5 Summary of experimental conditions used in some principal previous studies of the transmissibility to the spine.

Authors (year)	Subjects	Postures, Controls	Measurements	Stimuli (vertical)	Analysis
Hagena *et al*. (1985, 1986)	9 male and 2 female Age: 26 yrs (mean) Height: 1.75 m (mean) Weight: 69 kg (mean)	Standing Sitting	Direct measurement Locations: head, C7, T6, L1, L4, L5, sacrum Direction: vertical	Frequency sweep Frequency: 3 to 40 Hz Magnitude: 0.2 g	Transmissibility (amplitude ratio)
Herterich and Schnauber (1992)	14 subjects	Standing	Surface measurement Locations: head, cervical spine, lumbar spine Directions: vertical (and fore-and-aft for head)	Sinusoidal Frequency: 0.5 to 200 Hz Magnitude: 0.4 to 2.2 ms^{-2} rms	Transmissibility
Hinz *et al*. (1988a)	1 male subject Age: between 23 and 25 yrs Height: 1.72 m Weight: 68 kg	Sitting	Surface measurement Locations: C7, T1, T3, T5, T7, T9, T12, L1, L3, L5, S1 Direction: vertical	Sinusoidal Frequency: 4.5, 8.0 Hz Magnitude: 1.5 ms^{-2} rms Duration: 1 min	Transmissibility (calculated from extreme values and rms values)
Hinz *et al*. (1988b)	3 male subjects 1 subject for detailed analysis Height: 1.72 m Weight: 68 kg	Sitting without backrest	Surface measurement Locations: head, acromion, T5, L3, L4, Directions: vertical and fore-and-aft	Sinusoidal Frequency: 4.5, 8.0 Hz Magnitude: 1.5 ms^{-2} rms Duration: 1 min	Time series (motion measured on skin, estimated bone motion, relative motion between L3 and L4)

Table 2.5 (continued) Summary of experimental conditions used in some principal previous studies of the transmissibility to the spine.

Authors (year)	Subjects	Postures, Controls	Measurements	Stimuli (vertical)	Analysis
Kitazaki (1994) Kitazaki and Griffin (1998)	8 male subjects	Sitting without backrest, moving footrest 'Erect: pelvis rotate maximally forward, upright thoracic and cervical spine' 'Normal: straight lumbar spine, upright thoracic and cervical spine' 'Slouched: thoracic and cervical spine incline forward 25º'	Surface measurement Locations: head, T1, T6, T11, L3, S2, iliac crest, abdominal wall at L2 level Directions: vertical and fore-and-aft	Random Frequency: 0.5 to 35 Hz Magnitude: 1.7 ms^{-2} rms Duration: 1 min	Transmissibility Experimental modal analysis
Magnusson *et al*. (1993)	3 female subjects Age: 27, 23, 24 yrs Height: 1.60, 1.61, 1.63 m Weight: 49, 54, 62 kg	Sitting with feet supported 'Forward flexion 80º' 'Upright 90º' 'Leaning backwards against backrest of 110º and 120º'	Direct measurement Location: L4 Directions: vertical and fore-and-aft	Impact (with adequate duration to excite frequencies of 0 to 32 Hz) 5 impacts with irregular intervals	Transmissibility (calculated from cross and power spectral density after smoothing, average of five repetition)
Mansfield (1998) Mansfield and Griffin (1999)	12 male subjects Age: 26.3 yrs (mean) Height: 1.79 m (mean) Weight: 68.3 kg (mean)	Sitting 'Comfortable upright'	Surface measurement Locations: L3, abdominal wall, iliac crest, posterior superior iliac spine Directions: vertical and fore-and-aft	Random Frequency: 0.2 to 20 Hz Magnitude: 0.25, 0.5, 1.0, 1.5, 2.0, 2.5 ms^{-2} rms Duration: 1 min	Transmissibility
Panjabi *et al*. (1986)	5 subjects Age: 29 to 37 yrs (mean: 33 yrs) Height: 1.56 to 1.72 m (mean: 1.67 m) Weight: 55 to 63 kg (mean: 59 kg)	Sitting on plywood seat 'Upright unsupported posture with feet resting on footboard, in relaxed manner with knees flexed to 90º'	Direct measurement Locations: L1, L3 sacrum Directions: vertical and fore-and-aft	Sinusoidal Frequency: 2 to 15 Hz (approximately 10 steps) Magnitude: 0.98, 2.94 ms^{-2} rms Duration: 30 sec	Transmissibility (calculated from rms values) Phase (shift between 2 signals at zero cross-over point)

Table 2.5 (continued) Summary of experimental conditions used in some principal previous studies of the transmissibility to the spine.

Authors (year)	Subjects	Postures, Controls	Measurements	Stimuli (vertical)	Analysis
Pope *et al*. (1989)	1 female subject Age: 29 yrs Weight: 63 kg	Standing in 20 conditions 'Erect' 'Relaxed' 'Valsalva' 'Knee bending' 'Pelvic tilt' etc.	Direct measurement Locations: L3, posterior superior iliac spine Directions: vertical	Impact Magnitude: 1.9 Joules (the same as Magnusson *et al*. 1993)	Transmissibility (average of five repetition)
Pope *et al*. (1990) Broman *et al*. (1991)	3 female subjects Age: 31 to 37 yrs Height: 1.73, 1.69, 1.74 m Weight: 65, 70, 61 kg	Sitting 'Relaxed' 'Erect' 'Valsalva' 'Pelvis support' etc.	Direct measurement Location: L3 Direction: vertical	Impact (the same as Magnusson *et al*. 1993)	Transmissibility
Pope *et al*. (1991)	3 female subjects Age: 29.7 yrs (mean) Height: 1.73 m (mean) Weight: 61.7 kg (mean)	Sitting with feet supported 'Upright' 'Flexion 20º' '10 kg load' etc.	Direct measurement (intervertebral motion device) Locations: L3-L4, L4-L5 Directions: relative sagittal plane rotation, axial translation, anterior-posterior shear translation	Sinusoidal Frequency: 5, 8 Hz Magnitude: about 0.49, 0.98, 1.47 ms^{-2} rms Duration: 10 sec	Relative displacement between adjacent vertebrae (peak-to-peak amplitude)
Sandover and Dupuis (1987)	1 subject	Sitting	Filmed pin motion (Christ and Dupuis, 1966) Locations: T12, L2, L4	Sinusoidal Frequency: 2, 3, 3.5, 4, 4.5, 5, 6, 7 Hz Magnitude: 10 mm peak-to-peak	Transmissibility Relative displacement between vertebrae

Hagena *et al*. (1985, 1986) measured the spinal motion of standing subjects exposed to vertical swept sinusoidal vibration from 3 to 40 Hz at the constant magnitude of 0.2 g. Nine male and two female subjects were involved in the experiment. The vertical motions at six points over the spine were measured with accelerometers mounted on K-wires: the seventh cervical vertebra (C7), the sixth thoracic vertebra (T6), the first, fourth and fifth lumbar vertebrae (L1, L4 and L5), and the sacrum. The transmissibilities from the floor to each measurement point of a subject show a peak at 4 Hz, which is the most remarkable at the sacrum. There were some other small broad peaks in the frequency range between 8 and 13 Hz and at 18 Hz for all positions. They also calculated the spine transmissibility with reference to the motion at the sacrum at seven frequencies: at 4, 5.4, 8.8, 14.3, 18, 20 and 40 Hz (Figure 2.16). The mean values from eleven subjects show that the spine amplifies an 'input' motion at the sacrum at 4 and 8.8 Hz and attenuates at 5.4 and 14.3 Hz. The transmissibility from the sacrum at 4 Hz was greater at L5, L1 and C7, whereas that at 8 Hz was almost the same at all the measurement points except for L4 where the transmissibility from the sacrum tended to be smaller than those at the other points at all frequencies. The transmissibilities from the sacrum to all measurement points were almost identical, a magnitude of about 0.7, at 5.4 Hz.

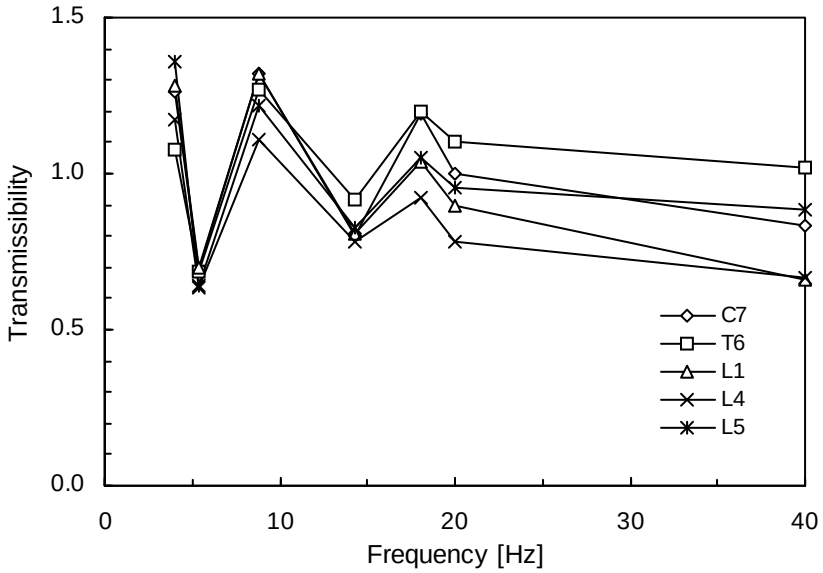

Figure 2.16 Vertical transmissibilities from the sacrum to the spine of subjects standing erect from Hagena *et al*. (1985, 1986). Average of eleven subjects.

Pope *et al*. (1989) investigated the dynamic response of the spine at the level of the third lumbar vertebra (L3) of a female subject using an impact platform. A direct measurement method, with an accelerometer mounted on a K-wire, was used to obtain the vertical motion of the spinous process of L3. In a 'relaxed erect ('at ease') posture', 'with the only constraint being that the subject's eyes looked forward at a local horizon', the vertical transmissibility to L3 had a single peak of about 3.5 dB (1.5 in the linear scale) at about 5.5 Hz.

Herterich and Schnauber (1992) measured the dynamic response of the lumbar and the cervical spines of fourteen subjects in a standing position as a part of their larger study. The stimuli used in their laboratory study were vertical sinusoidal vibrations in the frequency range of 0.5 to 200 Hz whose magnitudes were between 0.4 and 2.0 ms^{-2} r.m.s. The vertical motions at the spine were measured at the skin surface with 'vibration pickups' 'attached to light Pertinax-boards'. Peaks in the transmissibility curves to the lumbar and cervical spine were located at about 8 Hz, with a magnitude of about 1.9, and at about 16 Hz, with a magnitude of about 1.9, respectively. However, the experimental conditions that were used to produce the transmissibility curves, that is, the subjects' posture, the measurement locations, the vibration magnitude, and so on, were not clear.

Figure 2.17 shows the transmissibilities to the spine of standing subjects in the previous studies mentioned above.

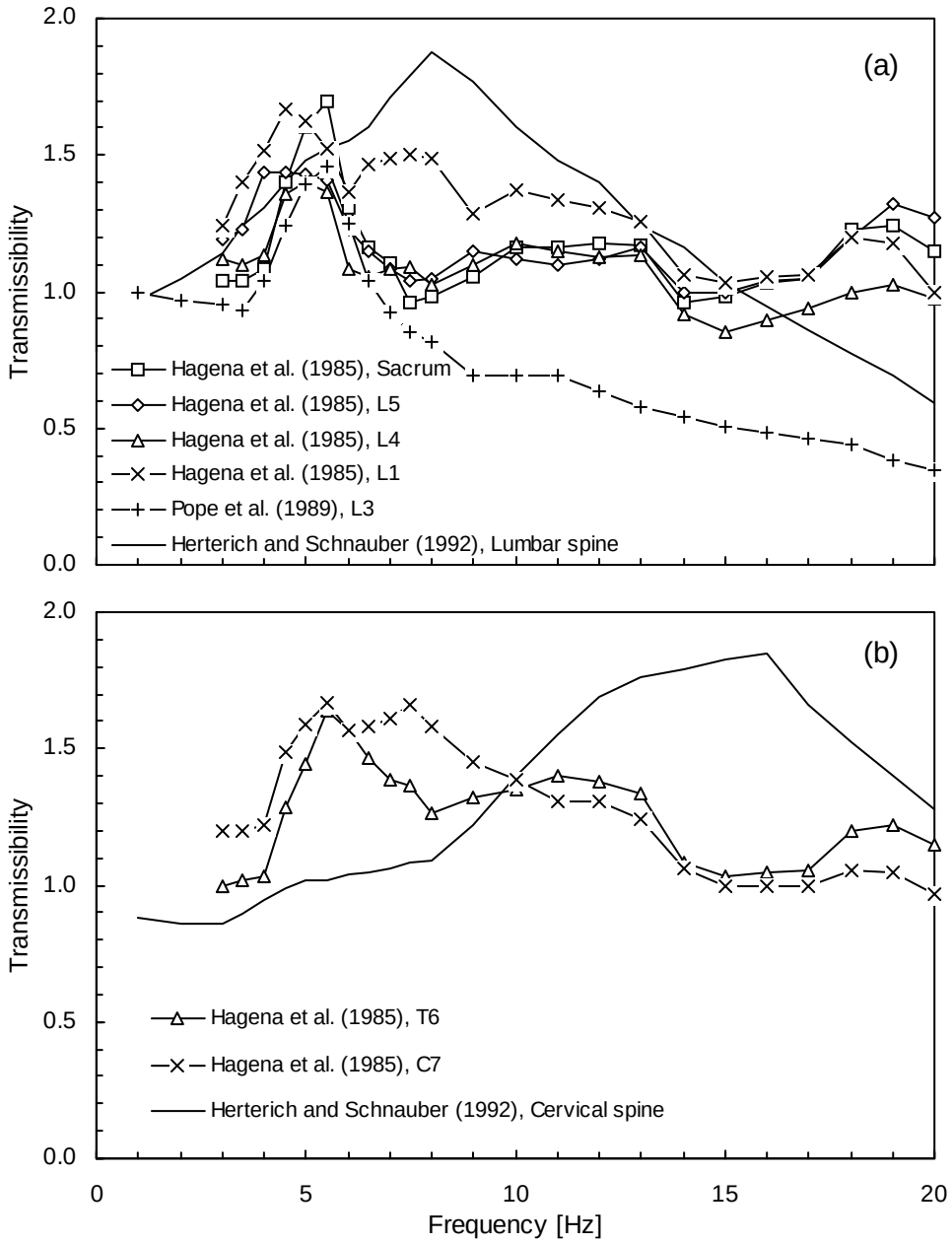

Figure 2.17 Vertical transmissibilities to the spine of standing subjects: (a) to the sacrum and the lumbar spine, (b) to the thoracic and cervical spines. Data from one subject by Hagena *et al*. (1985, with frequency swept vibrations at 0.2 g) and by Pope (1989, 'at ease' posture with impacts). Mean from fourteen subjects by Herterich and Schnauber (1992, with sinusoidal vibrations at between 0.2 and 2.2 ms^{-2} r.m.s.).

2.4.1.4 Transmissibility to the spine in a normal sitting posture

Some principal previous studies of the dynamic response of the spine to whole-body vibration or impact of seated subjects are summarised in Table 2.5, together with those of standing subjects. The data, which were obtained with a hard seat without backrest, are discussed in the following sections.

The vertebral motions in three axes in the sagittal plane were measured by Panjabi *et al*. (1986), using accelerometers mounted rigidly to the vertebral bodies, as mentioned in the previous section (see Figure 2.13). The vertical, fore-and-aft and pitch motions at the first and third lumbar vertebrae (L1 and L3) and the vertical motion at the sacrum were obtained. Five subjects were exposed to vertical sinusoidal vibrations in the frequency range from 2 to 15 Hz increased in approximately ten steps. The vibration magnitudes were 0.98 and 2.94 ms^{-2} r.m.s. The subjects were seated on a plywood seat in an 'upright unsupported sitting posture, in a relaxed manner, with the feet resting on the footboard'. They found that there was no difference between the calculated vertical and fore-and-aft accelerations at L1 and L3. The vertical transmissibilities to the lumbar vertebrae of five subjects were similar and had a peak of about 1.6 at about 4.4 Hz. The horizontal transmissibilities to the lumbar vertebrae increased from about 0.2 at the lowest frequency to the maximum of 0.8 with increasing frequency without any peaks. For the pitch motion of the vertebral bodies, the variability between subjects was large and it was not possible to characterise a general trend. The vertical transmissibility to the sacrum had a peak at 4.76 Hz with a magnitude of 1.92 for the average of five subjects. The differences between the peak frequency and peak magnitude of the lumbar vertebrae and the sacrum were statistically significant ($p < 0.05$). They concluded, therefore, that 'the spinal connection between the sacrum and the third lumbar vertebra was sufficiently flexible to decrease the resonance frequency of that vertebra, in spite of the smaller mass associated with L3 as compared with the sacrum'.

Sandover and Dupuis (1987) reanalysed 'calibrated film of the motion of the lumbar spine' investigated by Christ and Dupuis (1966). In the original study using a subject, the motion of small pins driven into the spinous processes of the twelfth thoracic vertebra (T12), the first, second, third and fourth lumbar vertebrae (L1, L2, L3, L4) were recorded by 'cinematographic and radiographic techniques'. The motions at T12, L2 and L4 where small visible targets were attached were reanalysed and the vertical,

fore-and-aft and angular motions were resolved. Vertical sinusoidal vibrations at 2, 3, 3.5, 4, 4.5, 5, 6, 7 Hz with a 10 mm peak-to-peak displacement were used. The motions at all points in all three directions, except for the angular motion at L2, showed a peak at 4 Hz. Very similar vertical displacements at T12, L2 and L4 accompanied by small phase angles at all frequencies suggested that 'compression along the spinal axis was small'. However, the films were found not to be sufficiently accurate to obtain reliable spinal compression because of very small relative displacement between two adjacent vertebrae. For the fore-and-aft and angular motions, large phase differences between T12, L2 and L4 suggested 'more significant relative motion'. Calculated 'relative bending between adjacent vertebrae', which was greatest in the lower spine, had 'a maximum of about 1º per ms^{-2} r.m.s. seat vibration at 3 and 4 Hz with a very sharp roll-off at higher frequencies'. They suggested that 'the resonances observed during human response to vibration' were 'related to bending in the lumbar spine which arose from a rocking of the pelvis'.

Hinz *et al*. (1988a) investigated the dynamic response of the spine at eleven locations: the seventh cervical vertebra (C7), the first, third, fifth, seventh, ninth and twelfth thoracic vertebrae (T1, T3, T5, T7, T9, T12), the first, third and fifth lumbar vertebrae (L1, L3, L5) and the first sacrum (S1). A male subject was exposed to vertical sinusoidal vibrations at 4.5 and 8.0 Hz with a magnitude of 1.5 ms^{-2} r.m.s. The vertical motions at each location were measured with an accelerometer mounted to the body surface and corrected so as to minimise the effect of the tissue and skin situated between the skeleton and the accelerometer, as mentioned in the previous section. The transmissibilities to each measurement point were obtained, although they presented r.m.s. accelerations corrected for the bone (Figure 2.18). It was clear that, at all the measurement points, the transmissibility at 4.5 Hz was greater than that at 8 Hz. The trends of the transmissibility over the spine at both frequencies seem to be similar, except for a greater motion at C7 at 4.5 Hz. Local maximum transmissibilities over the spine were found at T7, L1 and S1 at both frequencies used. No data of phase between measurement points were presented.

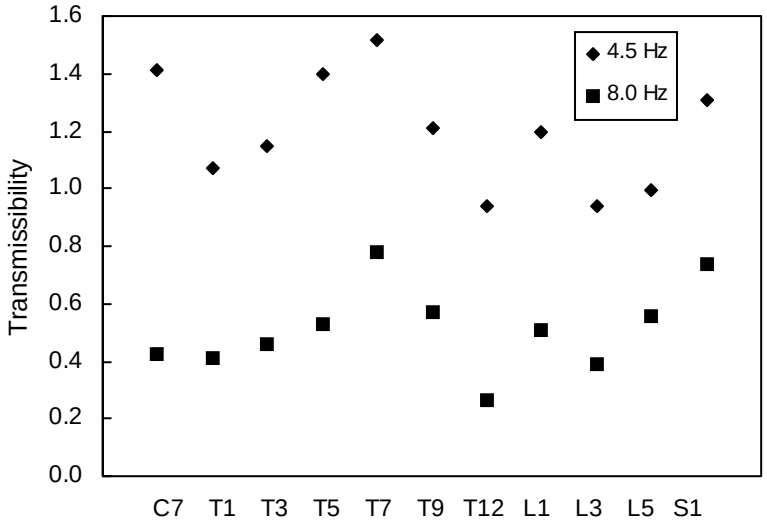

Figure 2.18 Vertical transmissibilities to the spine of a seated subject calculated from the data by Hinz *et al*. (1988a).

In the other study by Hinz *et al*. (1988b), the relative motion between the third and fourth lumbar vertebrae was investigated. The vertical and fore-and-aft accelerations at the body surface over the spinous processes of L3 and L4 were measured during exposure to vertical sinusoidal vibrations at 4.5 and 8.0 Hz with magnitudes of 1.5 and 3.0 ms^{-2} r.m.s. The data correction method was applied so as to minimise the effect of the tissue and the skin beneath the accelerometer (Hinz *et al*. 1988a). One of three subjects was involved in a detailed study including an additional measurement of the vertical motions at the head, the acromion and the fifth thoracic vertebra, T5. The acceleration time histories were investigated. It was stated that the relative motions between two adjacent lumbar vertebrae in the sagittal plane were 'combined with angular motions'. In their conclusions, a flexion of the lumbar spine during 'upwards acceleration of the seat' and an extension during 'downwards acceleration of the seat' were suggested. From the detailed study, they found that the downwards accelerations at the points above the lumbar spine were in phase with a probable flexion of the lumbar spine, while the upwards accelerations were in phase with a probable extension. It was assumed that bending motion of the lumbar spine accompanied by rocking motion of the pelvis was mainly caused by the vertical motion of the body above the lumbar spine.

Pope *et al*. (1990) and Broman *et al*. (1991) measured the vertical motion of the third lumbar vertebra (L3) with an accelerometer rigidly mounted to the spinous process by

means of a K-wire. They used the same impact device as Pope *et al*. (1989) used. Three female subjects took part in the experiment. A 'relaxed posture, with the only constraint being that the subject looked straight out at a local horizon' was used as a reference position. 'A marked peak' at 5 Hz and 'a maximum attenuation (transmissibility valley)' at 7 to 8.5 Hz were found in the transmissibility from the platform to L3 of one subject. It was stated that 'the data were fairly similar between subjects', except one subject showed 'a greater maximum attenuation at 8.5 Hz'.

Pope *et al*. (1991) investigated the relative motion between two vertebrae using a special measurement device which could be mounted directly to adjacent spinous processes such that the relative displacements in the vertical, fore-and-aft and pitch directions were measurable (see Figure 2.14). Three female subjects in an 'upright' sitting posture with feet supported were exposed to vertical sinusoidal vibrations at 5 and 8 Hz with a magnitude of about 1.0 ms^{-2} r.m.s. The relative motion between the fourth and fifth lumbar vertebrae (L4 and L5) was measured for two subjects, while that between the third and fourth lumbar vertebrae (L3 and L4) was measured for one subject. It was found that 'the motion segments generally displayed coupled oscillatory behaviour in response to pure sinusoidal vertical vibration'. It was stated that 'for all subjects, both translations and rotations were greater at 5 Hz than at 8 Hz, with the greatest differences occurring between axial translation values' (Table 2.6). However, this turned out not to be true if the corresponded accelerations were considered on the assumption that the relative motion between adjacent vertebra was almost sinusoidal at the same frequency as the excitation. The calculated translational accelerations were greater at 5 Hz than at 8 Hz for the subject 3, almost the same at both frequencies for the subject 1, and smaller at 5 Hz than at 8 Hz for subject 2.

Table 2.6 Relative displacements between two adjacent vertebrae in the sagittal plane from Pope *et al*. (1991). Peak-to-peak amplitudes.

Subject	5 Hz			8 Hz		
	Axial [mm]	Shear [mm]	Rotation [deg]	Axial [mm]	Shear [mm]	Rotation [deg]
1	0.18	0.08	0.1	0.07	0.04	0.0
2	0.52	0.04	0.2	0.29	0.03	0.1
3	0.78	0.11	0.2	0.08	0.03	0.0

Magnusson *et al*. (1993) investigated the response of the fourth lumbar vertebra (L4) to impact with the same method used by Pope *et al*. (1989, 1990) and Broman *et al*. (1991), except that measurements were conducted in two directions: vertical and fore-and-aft. Three female subjects took part in the experiment. The vertical transmissibilities to L3 when subjects were in an 'upright sitting 90º' posture showed a marked peak in the frequency range between 4.5 and 7 Hz with a magnitude of between 2.5 to 4.9 dB (1.3 to 1.8 in the linear scale). The phase remained about 0º at frequencies below 4 Hz. A 'valley' in the frequency range from 8 to 10 Hz was also found in the vertical transmissibility. In the fore-and-aft direction, the transmissibilities were less than 0 dB (1.0, linear) at all frequencies. A variability between subjects was larger in the fore-and-aft transmissibility compared to the vertical transmissibility. The fore-and-aft transmissibilities of two subjects showed a small peak just below 5 Hz, while that of the other subject had a peak at about 8 Hz.

Kitazaki (1994) measured the vertical and fore-and-aft motions at five points over the spine at the body surface: the first, sixth and eleventh thoracic vertebrae, the third lumbar vertebra and the second sacrum (T1, T6, T11, L3, S2). Eight male subjects were exposed to random vibration in the frequency range from 0.5 to 35 Hz at a magnitude of 1.7 ms^{-2} r.m.s. A posture with 'a straightened lumbar spine and an upright thoracic and cervical spine' was defined as a 'normal posture'. The mean vertical transmissibilities at all measurement points had a peak at about 5 Hz with a greater magnitude at lower spine. The vertical transmissibility to S2 showed a peak at about 8 Hz which was greater than that at 5 Hz. A peak at about 8 Hz was also found in the vertical transmissibility to L3, although the magnitude was much smaller than that at 5 Hz. The vertical transmissibility to T1 had a second peak at about 10 Hz which might differ from those found in the transmissibility to the lower spine at 8 Hz. For the fore-and-aft direction, the transmissibilities to T1 and T6 showed clear peaks at about 5 Hz, which were not able to be found in those to T11 and L3. The fore-and-aft transmissibility to T1 at 5 Hz was almost equal to that in the vertical direction. The fore-and-aft transmissibility to S2 showed two peaks at the frequencies where those in the vertical direction had peaks. Over the frequency range below 20 Hz, the fore-and-aft transmissibilities at all points except at T1 remained less than unity while those to T11 and L3 increased with increasing frequency.

The vertical and fore-and-aft motions on the skin over the spinous process of the third lumbar vertebra (L3) were measured with twelve male subjects by Mansfield (1998)

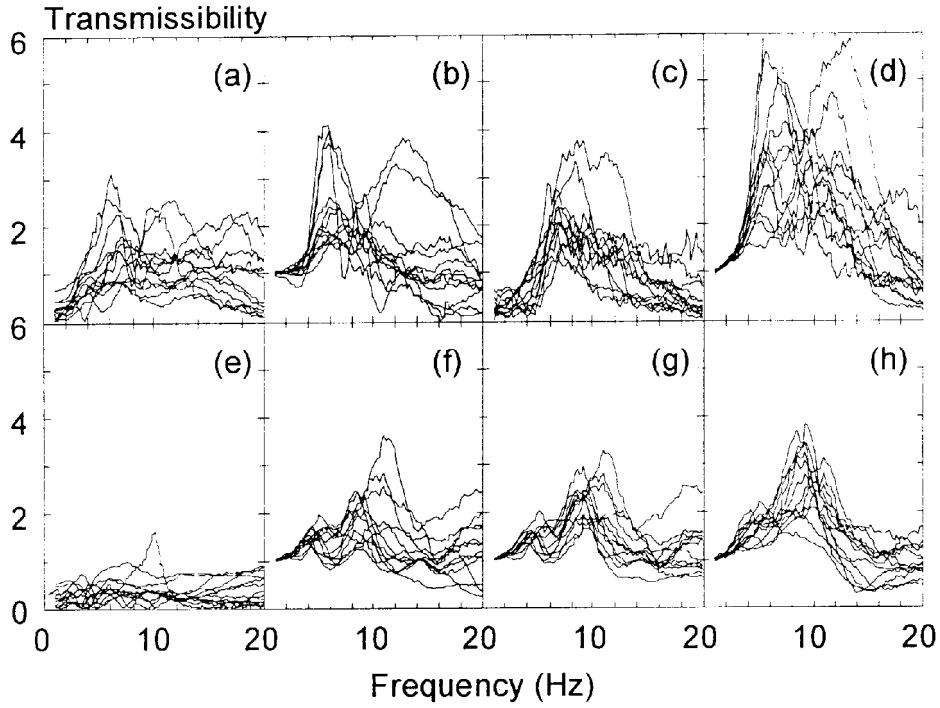

Figure 2.19 Seat to abdomen transmissibilities of twelve subjects measured at 1.0 ms^{-2} r.m.s. After Mansfield (1998). (a and b) seat to lower abdominal wall in fore-and-aft and vertical axes, (c and d) seat to upper abdominal wall in fore-and-aft and vertical axes, (e and f) seat to L3 in fore-and-aft and vertical, (g) seat to posterior superior iliac spine, (h) seat to iliac crest.

and Mansfield and Griffin (1999), together with several other locations, such as the pelvis. The measurements were made with vertical random vibration in the frequency range between 0.2 and 20 Hz at six magnitudes from 0.25 to 2.5 ms^{-2} r.m.s. The median transmissibility to vertical L3 motion showed 'the first resonance' 'at around 4 Hz' with 'a magnitude in the range of approximately 1.5 to 1.8'. 'The second, larger resonance' was found 'at approximately 8 to 10 Hz'. The transmissibility to fore-and-aft motion at L3 showed 'a transmissibility of less than 0.5' and 'no clear resonance' both in individual and median data. Figure 2.19 shows the individual transmissibilities to the vertical and fore-and-aft motions at L3, together with the transmissibilities measured at other locations by the authors which are discussed in later sections.

The transmissibility to the spine of seated subjects in previous studies are presented in Figures 2.20 to 2.22.

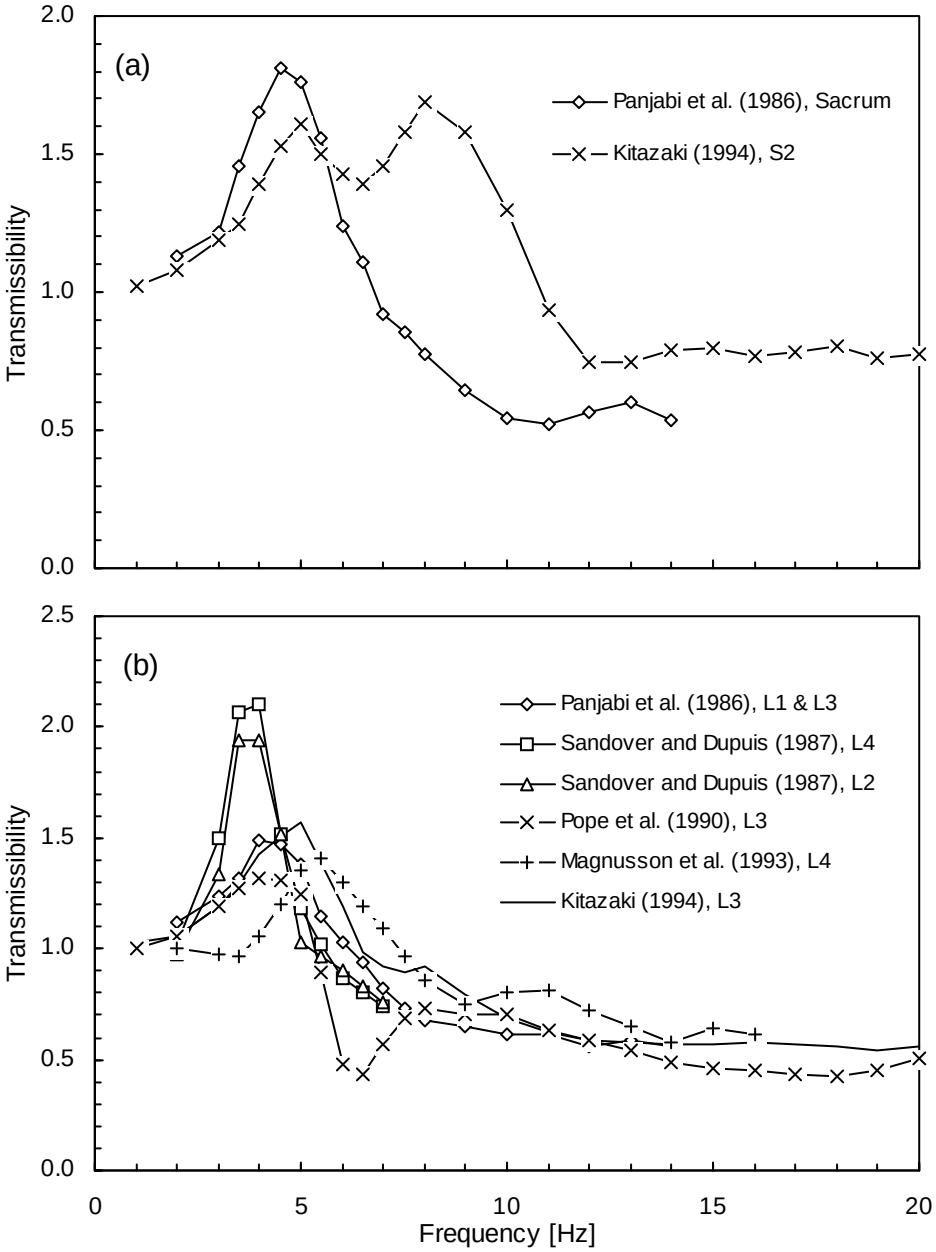

Figure 2.20 Transmissibilities to (a) the sacrum, (b) the lumbar spine, and (c) the thoracic spine of seated subjects in the vertical direction measured in previous studies. Median of five subjects and three subjects from Panjabi *et al*. (1986) and Magnusson *et al*. (1993), respectively. Data from one subject from Sandover and Dupuis (1987) and Pope *et al*. (1990). Mean of eight subjects from Kitazaki (1994). Experimental conditions: Panjabi *et al*.: direct measurement, sinusoidal vibration at 0.98 and 2.94 ms^{-2} r.m.s., sitting upright in relaxed manner; Sandover and Dupuis: film, sinusoidal vibration with 10 mm peak-to-peak, sitting; Pope *et al*.: direct measurement, impact, sitting relaxed; Magnusson *et al*.: direct measurement, impact, sitting upright; Kitazaki: surface measurement, random vibration at 1.7 ms^{-2} r.m.s., normal sitting. -cont.

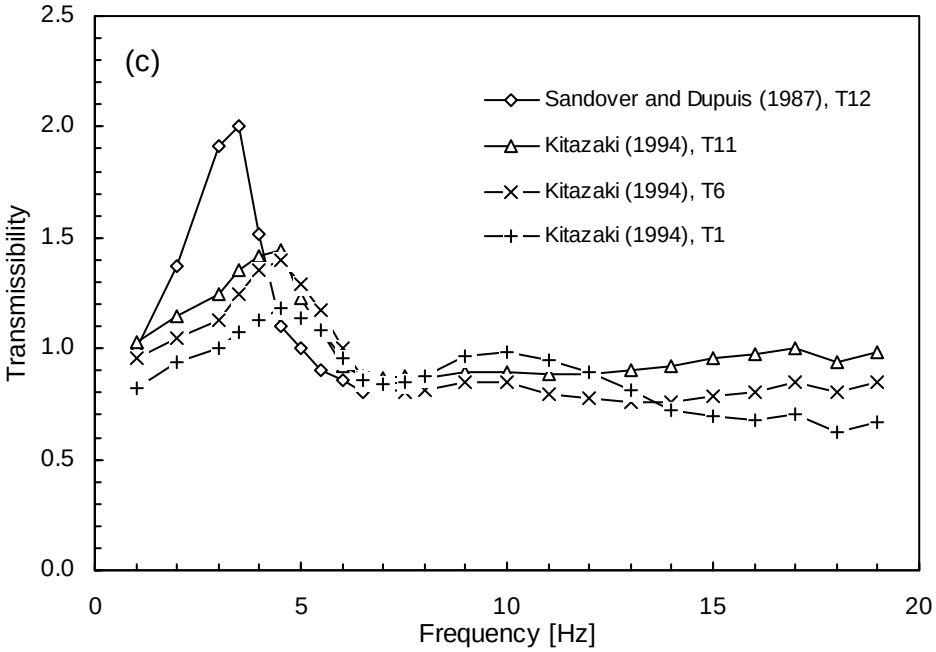

Figure 2.20 (continued) Transmissibilities to (a) the sacrum, (b) the lumbar spine, and (c) the thoracic spine of seated subjects in the vertical direction measured in previous studies.

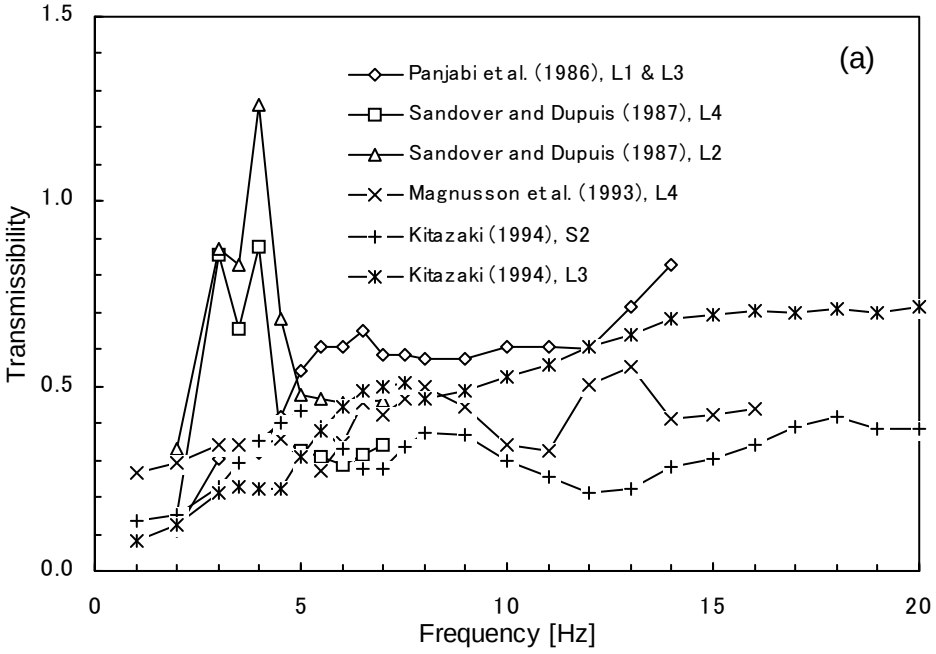

Figure 2.21 Transmissibilities to (a) the sacrum and the lumbar spine, and (b) the thoracic spine of seated subjects in the fore-and-aft direction measured in previous studies. Median of five subjects and three subjects from Panjabi *et al*. (1986) and Magnusson *et al*. (1993), respectively. Data from one subject from Sandover and Dupuis (1987). Mean of eight subjects from Kitazaki (1994). See the caption of Figure 2.20, or Table 2.5, for the experimental conditions. -cont.

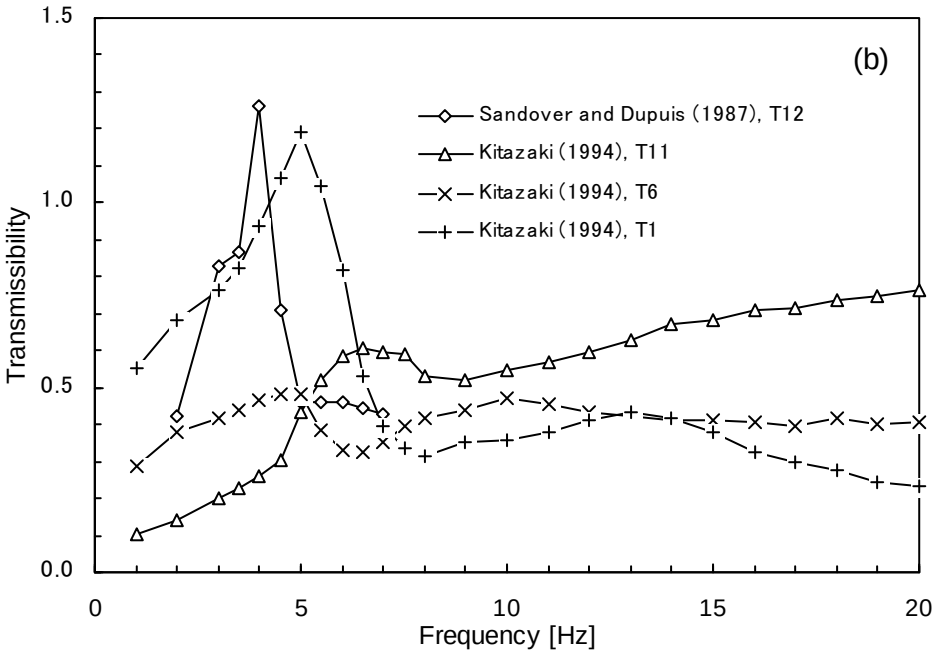

Figure 2.21 (continued) Transmissibilities to (a) the sacrum and the lumbar spine, and (b) the thoracic spine of seated subjects in the fore-and-aft direction measured in previous studies.

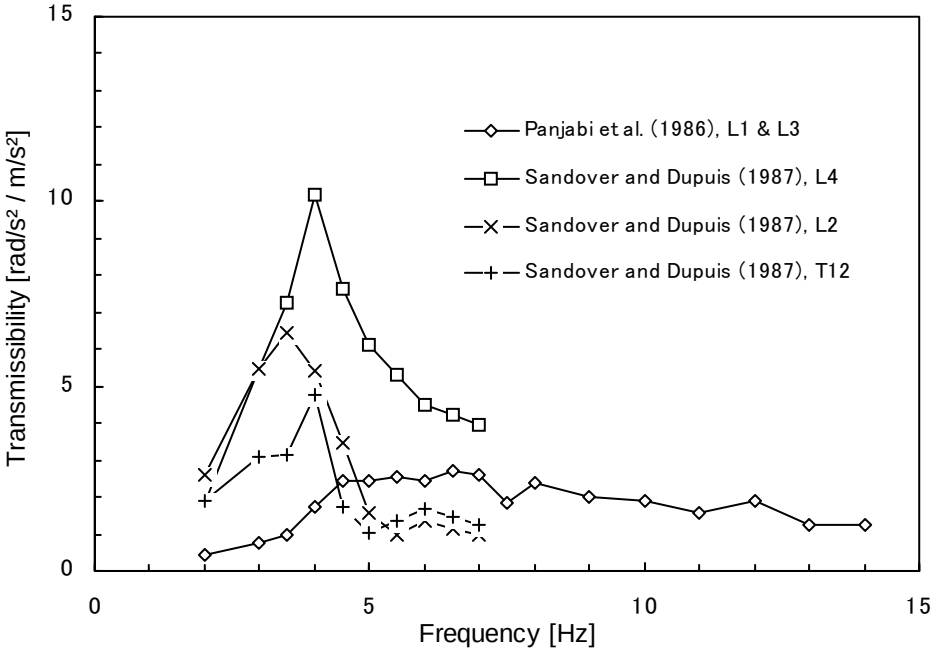

Figure 2.22 Transmissibilities to the spine of seated subjects in the pitch direction measured in previous studies. Median of five subjects from Panjabi *et al*. (1986). Data from one subject from Sandover and Dupuis (1987). See the caption of Figure 2.20, or Table 2.5, for the experimental conditions.

2.4.1.5 Effects of posture and muscle tension on transmissibility to the spine

There has been one study investigating the effects of subject's posture and muscle tension on the dynamic response of the spine of a standing subject. Pope *et al*. (1989) used several postures including a 'Valsalva', that is, pressurising the abdomen voluntarily. 'An erect posture where the back of the head, the peak of the thoracic spine and the midpoint between the posterior superior iliac spines were colinear' and 'this line was oriented normal to the platform' was used as a reference posture. In a 'rigid erect ('at attention') posture', the vertical transmissibility to L3 with a peak at 5.5 Hz was similar to that in a 'relaxed erect ('at ease') posture', although the magnitudes slightly decreased in the 'relaxed erect posture' (Figure 2.23). A 'knee bend posture', 'with an erect spine' and 'with the knees slightly flexed (at 30º)', 'markedly attenuated' the transmissibility at frequencies above 3 Hz and slightly amplified at around 2 Hz, compared to that in an 'at attention' posture (Figure 2.23). In an 'at attention' posture with a 'Valsalva', the peak frequency increased to 7 Hz without any other effects (Figure 2.23). Some other postures, such as a 'pelvic tilt', 'hip flexion' or 'forward leaning', were also investigated, although the definitions of the postures were not clear.

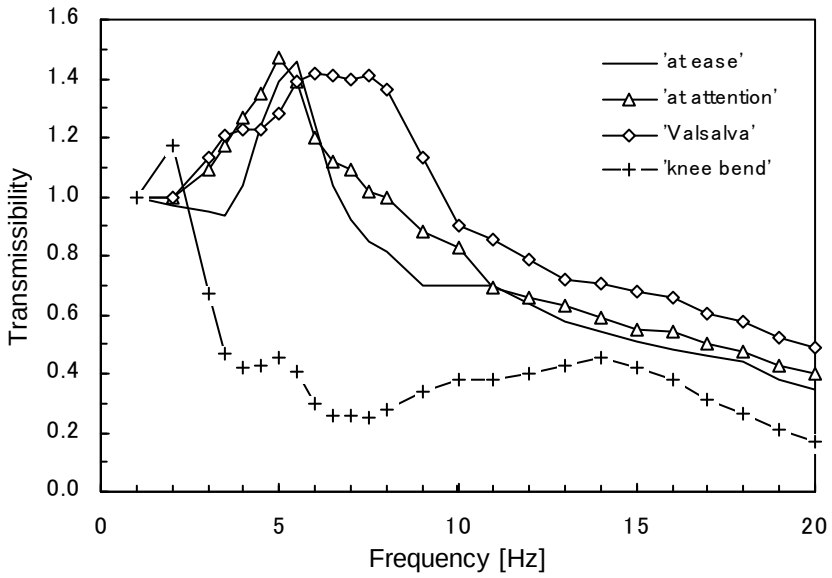

Figure 2.23 Effect of posture on the transmissibility to L3 of standing subject from Pope et al. (1989). Data from one subject.

For the seated body, the effects of posture and muscle tension on the response of the spine have been investigated in some studies. With seated subjects, Pope *et al*. (1990) and Broman *et al*. (1991) investigated the same conditions as they used in their previous study of the standing body (Pope *et al*. 1989). The vertical transmissibilities to L3 in a 'relaxed' posture and an 'erect' posture were similar except for a 'much more marked' peak at 5 Hz in the 'erect' posture, which was consistent with their finding with the standing body (Figure 2.24(a)). A 'Valsalva' manoeuvre increased the transmissibility at 5 Hz and altered the trend of the transmissibility above 6 Hz, decreasing with increasing frequency (Figure 2.24(a)). The effect of a 'contraction of the gluteal muscles' was also examined as 'an attempt to influence pelvic support'.

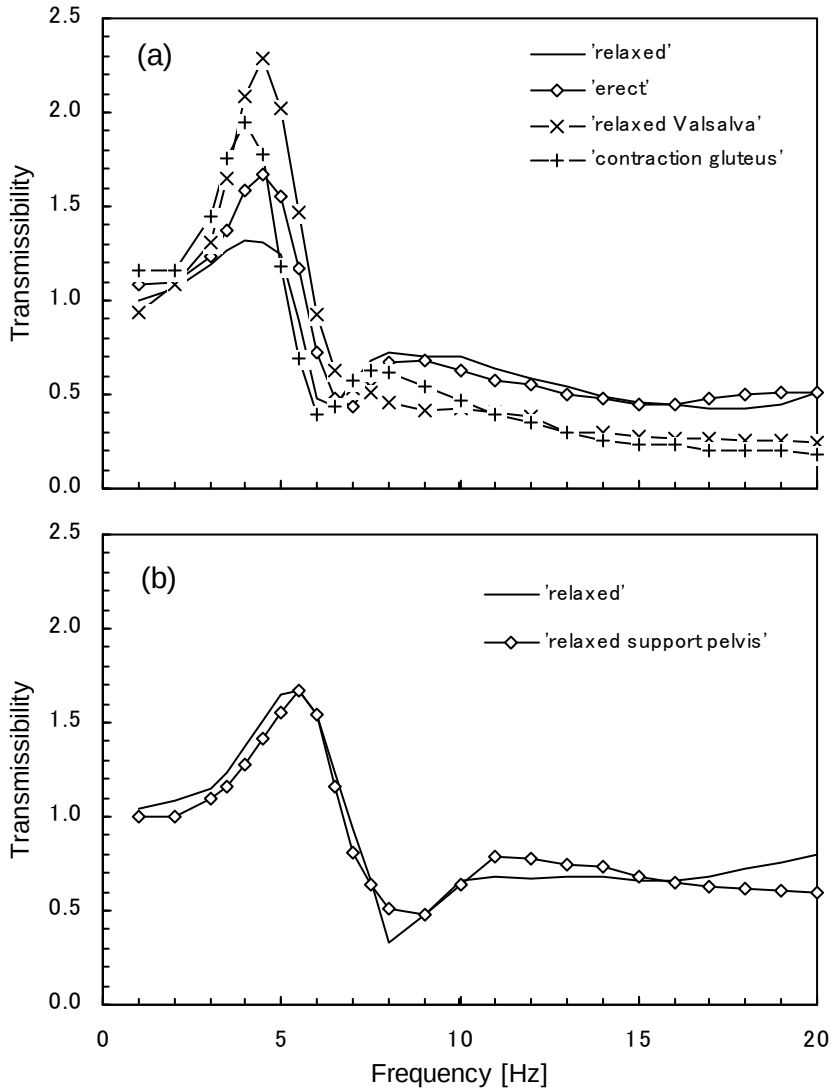

Figure 2.24 Effects of (a) posture and (b) pelvis support on the transmissibility to L3 of seated subject from Pope *et al*. (1990). Data from one subject. Subjects shown in (a) and (b) are different.

The transmissibility curve in this condition lay between those in the ‘relaxed’ posture and in the ‘relaxed plus Valsalva’ posture (Figure 2.24(a)). In addition, when ‘the pelvis was supported anteriorly with a wooden block to minimise pelvis rotation’, the transmissibility at 8 Hz, which was a local minimum in the relaxed posture, increased (Figure 2.24(b)). It was stated that the rotational motion of the pelvis is ‘active at the higher frequencies’.

Magnusson *et al*. (1993) investigated the effect of the inclination of the subjects’ back on the transmissibility to L4. The difference between two postures without contact between subjects’ back and the backrest of the seat, a ‘forward flexion 80º’ and an ‘upright sitting 90º’, was not significant.

Kitazaki (1994) used two sitting postures in addition to the ‘normal’ posture mentioned above: an ‘erect’ posture where the pelvis was ‘rotated most forward with a maximally forward bent lumbar spine and an upright thoracic and cervical spine’, and a ‘slouched’ posture where the thoracic and cervical spine and the head ‘inclined forward about 25 degrees from the normal position with the same position of the pelvis and the lumbar spine as for the normal posture’. The peak frequency of the vertical transmissibilities at about 5 Hz was found to decrease with the postural change from the ‘erect’ to the ‘slouched’ at all measurement points, while the peak magnitude tended to decrease. This postural change also caused a decrease in the vertical transmissibilities to thoracic vertebrae at high frequencies. The peak magnitude of the transmissibilities to T1 and, in particular, T6 increased with the same change in posture. The second peak of the transmissibility to S2 at about 8 Hz was not significantly affected by posture (Figure 2.25).

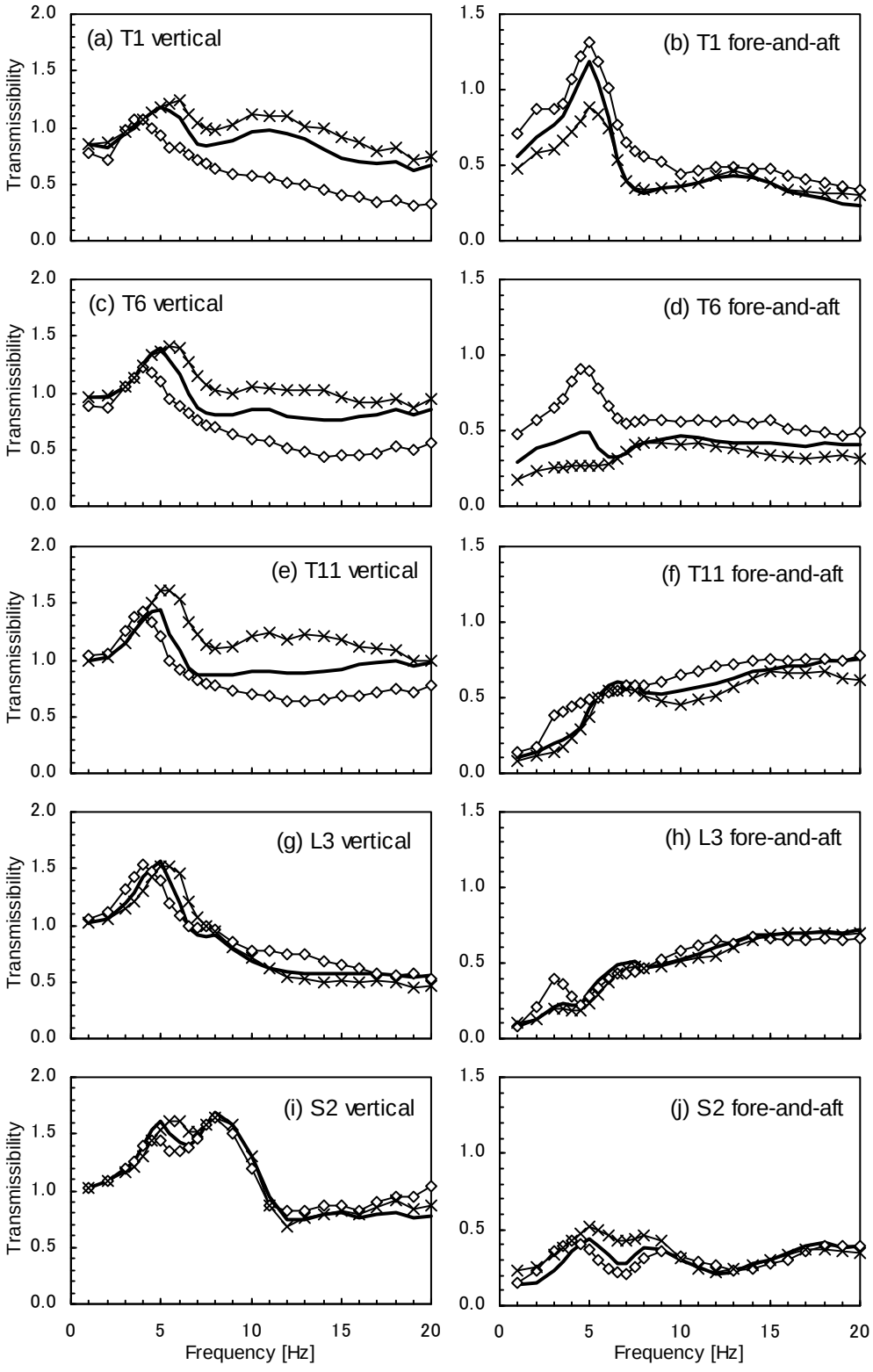

Figure 2.25 Effect of posture on the transmissibilities to the spine of seated subjects from Kitazaki (1994). Mean of eight subjects. ——, normal posture; —×—, erect posture; —◇—, slouched posture.

2.4.1.6 Effect of excitation magnitude on transmissibility to the spine

In some studies mentioned above (see Table 2.5), the effect of the magnitude of the input stimuli has been investigated, although any significant effects on the transmissibility to the spine have not been found. Panjabi *et al*. (1986) used sinusoidal vibrations with two different magnitudes, 0.98 and 2.94 ms^{-2} r.m.s., however, no statistically significant differences in the transmissibilities to L1, L3 and the sacrum were shown. Pope *et al*. (1989) and Broman *et al*. (1991) found that only minor differences in the vertical transmissibilities to L3 in both the standing and seated body were caused by two different energies of impact. Mansfield (1998) and Mansfield and Griffin (1999), however, reported reduction in two peak frequencies in the median transmissibility to L3 of twelve subjects, from 6 to 4 Hz for the first peak and from 10 to 7 Hz for the second peak, with increases in the vibration magnitude from 0.25 to 2.5 ms^{-2} r.m.s. (Figure 2.26).

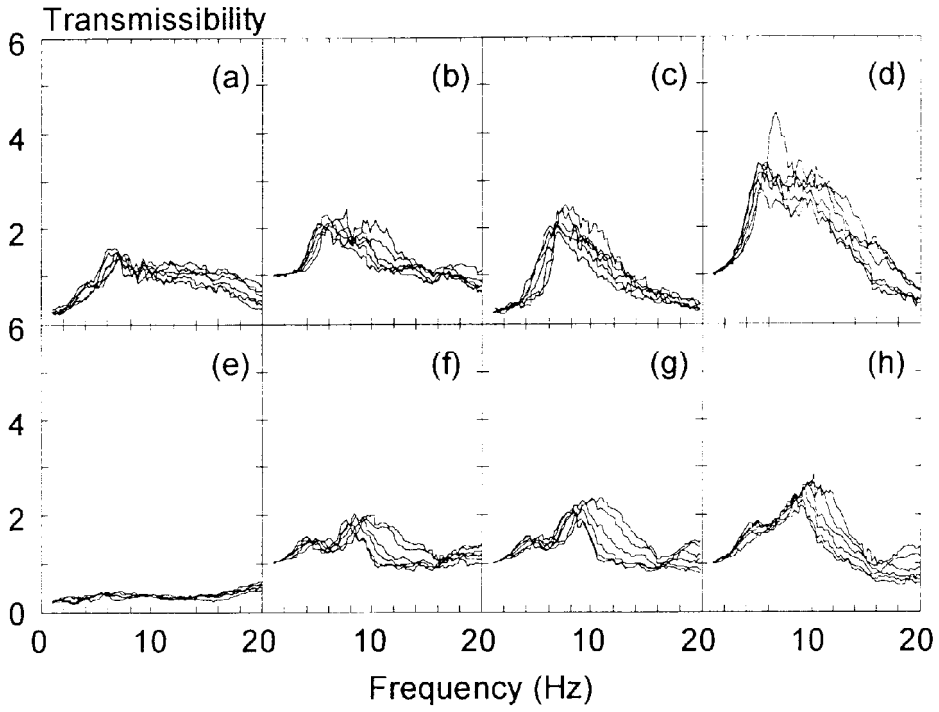

Figure 2.26 Median seat to abdomen transmissibilities of twelve subjects measured at 0.25, 0.5, 1.0, 1.5, 2.0 and 2.5 ms^{-2} r.m.s. After Mansfield (1998). (a and b) seat to lower abdominal wall in fore-and-aft and vertical axes, (c and d) seat to upper abdominal wall in fore-and-aft and vertical axes, (e and f) seat to L3 in fore-and-aft and vertical, (g) seat to posterior superior iliac spine, (h) seat to iliac crest. Resonance frequencies decrease with increases in vibration magnitude.

2.4.2 Dynamic response of the head

2.4.2.1 Methods to measure the head motion

The method to determine the head motion has varied among previous studies in which the motion of the head during exposure to the vertical floor or seat vibration was measured: the measurement location on the head and the method to mount transducers to the head have been different. The measurement location has varied from the top of the head (e.g. Coermann, 1962; Hagena *et al*., 1985, 1986), the forehead (e.g. Herterich and Schnaubar, 1992), to the mouth (e.g. Griffin, 1975; Paddan and Griffin, 1988; Pope *et al*., 1987).

For the measurements at the top of the head, a transducer has been generally mounted to the head by using a head harness (e.g. Coermann 1962). It is difficult to understand how rigidly the transducer was secured to the head by the harness. Possible local motions between the transducer and the skeleton due to the tissue, skin, hair and harness have not been taken into account. A transducer secured to a helmet was used to measure the head motion in some studies (e.g. Garg and Ross, 1976; Wilder *et al*., 1982). However, the relative motions between the head and the helmet have been reported in previous studies (e.g. Woodman, 1995). It is not, therefore, appropriate to measure the head motion with a transducer mounted to a helmet.

The measurements at the forehead have been made with a transducer attached to ‘light Pertinax-board’ which is stuck to the skin by adhesive tape by Herterich and Schnaubar (1992). The effect of local motions between the transducer and the skeleton due to the tissue and skin, as described in the previous section about the spine, has not been considered in the study.

The head motion measurements at the mouth may have an advantage over the others mentioned above because the teeth can be thought to be rigidly connected to the skull in the frequency range interested in studies of the effect of whole-body vibration to the human body. Some different methods of mounting transducers to the mouth have been used in previous studies: for example, an accelerometer directly ‘clenched’ by subjects by Rao *et al*. (1975) and Rao (1982), accelerometers mounted to a ‘tooth

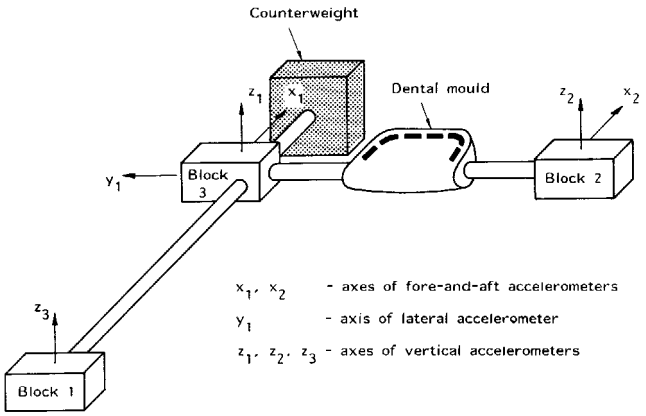

Figure 2.27 Bite-bar with relative positions of the accelerometers, mounting blocks and a conterweight from Paddan and Griffin (1988).

impression' by Kobayashi *et al*. (1981), an accelerometer mounted to a wooden bite-block by Pope *et al*. (1987), and accelerometers mounted to a 'bite-bar' made from aluminium alloy by Messenger (1987, 1989) and Paddan and Griffin (1988, 1993). The bite-bar used by Paddan and Griffin (1988, 1993) is shown in Figure 2.27. Six translational accelerometers implemented in the bite-bar provides accelerations in three translational (i.e., fore-and-aft, lateral, and vertical) and three rotational (i.e., roll, pitch, and yaw) axes.

Kobayashi *et al*. (1981) compared three methods to mount accelerometers to the head in the measurement of the head motion of three subjects exposed to vertical floor vibration: a 'rigid tooth impression' which was 'closely fitted to the upper incisors of subjects', an 'iron plate' which was 'fixed to the forehead with an elastic band', and direct attachment to the forehead with adhesive tape. They concluded that the accelerometers attached to a tooth impression was 'suitable for the measurement of the head vibration' because of the high repeatability in the measurements.

The variety of measurement locations and transducer mounting methods makes it difficult to compare the results from different experiments. Paddan and Griffin (1992) estimated the head motion at different locations in the head during the vertical seat vibration by the motions measured at the mouth with the bite-bar in three translational and three rotational axes (Figure 2.28). It is shown in Figure 2.28 that remarkable variations in the vertical head motion due to the different measurement location along the fore-and-aft direction, and in the fore-and-aft head motion due to the different

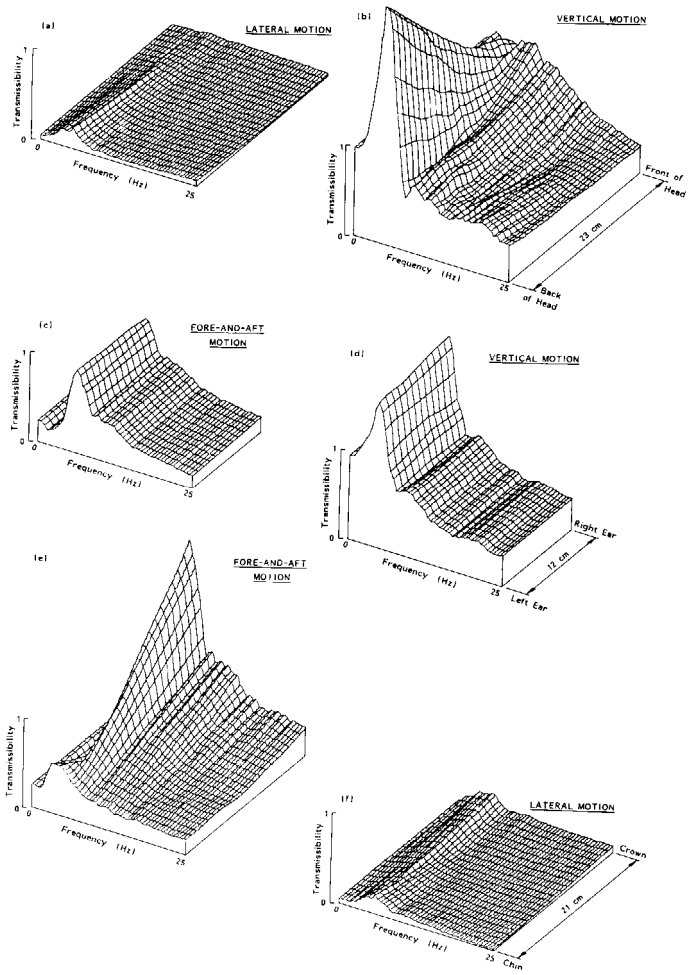

Figure 2.28 Variation in median transmissibilities with position on the head for twelve subjects during vertical seat motion from Paddan and Griffin (1992).

measurement location along the vertical direction. The effect of the pitch head motion on the vertical and fore-and-aft head motion during the exposure to vertical whole-body vibration has been clearly observed. The interpretation of the direct comparison between separate experimental results previously reported is, therefore, required care, although the results from different studies are presented in the following sections. More comprehensive review on the method of head motion measurement method can be found in Paddan (1991).

2.4.2.2 Transmissibility to the head in a normal standing posture

Table 2.7 summarises some principal previous experimental studies of the transmission of vertical whole-body vibration to the head. The experimental conditions used in the studies are summarised. Investigations of the dynamic response of the head of the standing body by Coermann (1962), Rao *et al*. (1975), Kobayashi *et al*. (1981), Rao (1982), Hagena *et al*. (1985, 1986), Herterich and Schnaubar (1992), and Paddan and Griffin (1993) are presented in this section.

Coermann (1962) measured the head motion of the standing body during exposure to vertical floor vibration with eight male subjects, along with the measurement of the mechanical impedance. Sinusoidal vibrations in the frequency range between 1 to 20 Hz were used with magnitudes up to 0.5 g. The measurement of the head motion in the vertical direction was made with an accelerometer mounted to the top of the head with an 'elastic bandage'. The transmissibility to the head of one subject in a 'standing erect' posture was presented, a principal peak at 5 Hz and a broad peak at frequencies around 12 Hz were observed. The transmissibility in the 'standing erect' posture was compared with that in the 'sitting erect' posture for that subject. The principal peak at about 5 Hz with a magnitude of about 1.6 was found in the transmissibilities in both the 'standing erect' and 'sitting erect' postures. It was stated that 'the transmission factor in the standing erect posture is very similar to the sitting erect posture'. However, the transmissibility in the 'sitting erect' posture showed a 'first small peak' at about 3 Hz and two additional peaks at 11 and 15 Hz.

Table 2.7 Summary of experimental conditions used in some principal previous studies of the transmissibility to the head.

Authors (year)	Subjects	Postures, Controls	Measurements	Stimuli (vertical)
Coermann (1962)	8 male subjects Age: 29 to 47 yrs Height: 1.70 to 1.93 m (median: 1.82 m) Weight: 70 to 99 kg (median: 86.9 kg)	'Standing erect' 'Sitting erect' 'Sitting relaxed'	Location: top of the head Mounting: elastic bandage Direction: vertical	Sinusoidal Frequency: 1 to 20 Hz Interval: 0.5 Hz (1 to 14 Hz), 1.0 Hz (14 to 20 Hz) Magnitude: up to 0.5 g Duration: 1 min
Garg and Ross (1976)	8 male and 4 female subjects Age: 23.42 yrs (mean) Height: 1.76 m (mean) Weight: 66.5 kg (mean)	'Standing with normal stance'	Location: top of the head Mounting: bolted to plesiglass frame strapped to head Direction: vertical	Sinusoidal Frequency: 1 to 50 Hz Magnitude: 0.003 to 0.2 in (amplitude)
Griffin (1975)	12 male subjects Age: 21 to 35 yrs Height: 1.71 to 1.89 m Weight: 53 to 88 kg	Sitting 'Most severe' (maximum head vibration) 'Least severe' (minimum head vibration)	Location: mouth Mounting: bite-bar Direction: vertical (all subjects), fore-and-aft, lateral, pitch (4 subjects)	Sinusoidal Frequency: 7, 10, 15, 20, 25, 30, 35, 40, 45, 50, 60, 75 Hz Magnitude: 6 levels, 0.2 to 4.0 ms^{-2} rms
Griffin *et al*. (1978)	11 experiments Various sets: 1 to 56 subjects, male, female, boy	Sitting Various sets including: slouched to erect, relaxed and stiff, different head angle etc.	Location: mouth Mounting: bite-bar Direction: vertical	Sinusoidal, Frequency sweep Frequency: 1 to 100 Hz Magnitude: 0.4 to 2.8 ms^{-2} rms Duration: 1 to 100 sec Random Magnitude: 1 ms^{-2} rms Duration: 100 sec
Hagena *et al*. (1985, 1986)	9 male and 2 female subjects Age: 26 yrs (mean) Height: 1.75 m (mean) Weight: 69 kg (mean)	Standing Sitting	Location: top of the head Mounting: 3 waistbands Direction: vertical	Frequency sweep Frequency: 3 to 40 Hz Magnitude: 0.2 g
Herterich and Schnauber (1992)	14 subjects	Standing	Location: forehead Mounting: attached to Pertinax-board fixed with adhesive tape to the skin Direction: vertical	Sinusoidal Frequency: 0.5 to 200 Hz Magnitude: 0.4 to 2.0 ms^{-2} rms

Table 2.7 (continued) Summary of experimental conditions used in some principal previous studies of the transmissibility to the head.

Authors (year)	Subjects	Postures, Controls	Measurements	Stimuli (vertical)
Kitazaki (1994) Kitazaki and Griffin (1998)	8 male subjects	Sitting 'Normal' 'Erect' 'Slouched'	Location: near cervical spine Mounting: bite-bar Direction: vertical and fore-and-aft	Random Frequency: 0.5 to 35 Hz Magnitude: 1.7 ms^{-2} rms Duration: 1 min
Kobayashi *et al*. (1981)	3 male subjects	Standing ('stood straight') Sitting ('sat straight' and 'without a footrest')	Location: mouth Mounting: tooth impression Direction: vertical, fore-and-aft	Sinusoidal Frequency: 3.15 to 100 Hz (1/3 octave) Magnitude: 0.1 g rms
Mertens (1978)	6 male and 3 female subjects Age: 24 to 44 yrs Weight: 57 to 90 kg	'Upright sitting'	Direction: vertical Location and mounting method were not stated	Vibration type was not stated Frequency: 2 to 20 Hz Magnitude: 0.4 g rms Static acceleration: 1, 2, 3, 4 g
Messenger (1987)	8 male subjects Age: 19 to 37 yrs Weight: 60.3 to 90.7 kg	Sitting 'Normal upright' Different pelvic angles: 105, 95, 85 degrees	Location: mouth Mounting: bite-bar Direction: vertical, fore-and-aft, lateral, pitch	Random Frequency: 0.5 to 40 Hz Magnitude: 1.0 ms^{-2} rms Duration: 60 sec
Messenger (1989)	12 male subjects Age: 20 to 30 yrs	Sitting 'Normal erect'	Location: mouth Mounting: bite-bar Direction: vertical, fore-and-aft, pitch	Random Frequency: 0.5 to 35 Hz Magnitude: 1.0 ms^{-2} rms Duration: 60 sec
Paddan and Griffin (1988)	12 male subjects Age: 18 to 34 yrs (mean 26.1 yrs) Height: 1.65 to 1.91 m (mean 1.80 m) Weight: 58 to 81 kg (mean 70.8 kg)	Sitting 'Back-on' 'Back-off'	Location: mouth Mounting: bite-bar Direction: 6 axes (fore-and-aft, lateral, vertical, roll, pitch, yaw)	Random Frequency: 0.2 to 31.5 Hz Magnitude: 1.75 ms^{-2} rms Duration: 60 sec

Table 2.7 (continued) Summary of experimental conditions used in some principal previous studies of the transmissibility to the head.

Authors (year)	Subjects	Postures, Controls	Measurements	Stimuli (vertical)
Paddan (1987) Paddan and Griffin (1993)	12 male subjects Age: 20 to 41 yrs (mean 28.42 yrs) Height: 1.73 to 1.92 m (mean: 1.81 m) Weight: 60 to 87 kg (mean: 74.33 kg)	Standing 'Legs locked' 'Legs unlocked' 'Legs bent'	Location: mouth Mounting: bite-bar Direction: 6 axes (fore-and-aft, lateral, vertical, roll, pitch, yaw)	Random Frequency: 0.25 to 25 Hz Magnitude: 1.75 ms^{-2} rms Duration: 1 min
Pope *et al*. (1987)	5 male and 5 female subjects Age: 15 to 45 yrs Weight: 65 to 80 kg	Sitting 'Erect' 'Relaxed'	Location: mouth Mounting: wooden bite-block Direction: vertical	Sinusoidal Frequency: 2 to 14 Hz Magnitude: 1.0 ms^{-2} rms Duration: 15 sec Impact Frequency: flat spectrum between 2 to 30 Hz Duration: over 20 to 30 ms 10 repeat impacts
Rao *et al*. (1975) Rao (1982)	8 male subjects Age: 21 to 39 yrs Height: 1.70 to 1.85 m Weight: 55 to 83 kg	'Standing straight' 'Standing with knees bent' 'Sitting straight'...etc.	Location: mouth Mounting: clenched accelerometer between front teeth Direction: vertical	Sinusoidal Frequency: 2.5, 4, 6, 8, 10, 13.5, 15, 17.5, 20, 25, 30 Hz Magnitude: 0.64, 1.32, 2.0 ms^{-2} rms Duration: 1 min Random Frequency: to 30 Hz Magnitude: 0.3, 0.64, 1.32, 2.4 ms^{-2} rms Duration: 90 sec
Wilder *et al*. (1982) Wilder *et al*. (1985)	53 subjects (38 males)	Sitting 'Relaxed' '5º forward flexion' '5º extension' '5º left and right lateral bend' 'Maximum left and right axial rotation' 'Valsalva'	Location: top of head Mounting: rigidly mounted to a hockey helmet Direction: vertical	Frequency sweep Frequency: 1 to 20 Hz Duration: 30 sec

Rao *et al*. (1975) investigated the transmissibility to the head of the standing body at frequencies below 50 Hz with random vibrations having 'constant velocity spectrum' in the frequency range between 0 and 22 Hz. Four levels of vibration magnitudes between 0.03 and 0.24 g r.m.s. were used. The vertical head motion was measured with an accelerometer 'clenched' between subject's front teeth. The transmissibilities to the head obtained from eight male subjects in a 'standing straight' posture showed two peaks: one in the frequency range from 3.5 to 5.5 Hz and another in the frequency range from 12 to 15 Hz. In their subsequent study, Rao (1982), the measurements of the transmissibility to the head were made by using sinusoidal vibrations at 2.5, 4, 6, 8, 10, 13.5, 15, 17.5, 20, 25, and 30 Hz at three different magnitudes, 0.64, 1.32 and 2.0 ms^{-2} r.m.s. The mean transmissibilities to the head of subjects in a 'standing straight' posture at three different magnitudes exhibited a 'first peak' at 4 or 6 Hz with a magnitude of about 1.3 to 1.4, a 'dip' at 8 Hz with a magnitude of about 0.4 to 0.7, and a 'second peak' at 15 Hz with a magnitude of 0.7 to 1.0.

The head motions of standing subjects exposed to vertical whole-body vibration were measured in two axes, the vertical and fore-and-aft directions, with two accelerometers mounted to a 'rigid tooth impression' by Kobayashi (1981). The input stimuli were sinusoidal vibrations at the third-octave centre frequencies between 3.15 and 100 Hz at a magnitude of 0.1 g r.m.s. The mean vertical transmissibility to the head of three subjects when stood straight showed no clear peak in the frequency range between 3.15 and 16 Hz, although that when subjects sat had a marked peak at 5 Hz. The mean transmissibility in the standing posture was maximum at 3.15 Hz and decreased sharply at high frequencies above 25 Hz. A clear peak was found at 5 Hz in the mean transmissibility in the fore-and-aft direction.

The dynamic response of standing subjects to vertical floor vibration was measured at the head and six locations along the spine in the vertical direction by Hagena *et al*. (1985, 1986). Nine male and two female subjects were exposed to swept sinusoidal vibration from 3 to 40 Hz at the constant magnitude of 0.2 g. The measurement of the head motion was made at the top of the head with an accelerometer mounted by three 'waistbands'. Four peak regions were observed in the transmissibility to the head of one subject: at 4 Hz, at 8 Hz, between 11 and 13 Hz, and at 18 Hz. The transmissibility to the head was maximum at 18 Hz for this subject.

Herterich and Schnauber (1992) measured the head motions of fourteen standing subjects in the vertical and fore-and-aft directions, together with the vertical motions at the cervical and lumbar spines. Sinusoidal vibrations in the frequency range between 0.5 and 200 Hz with magnitudes between 0.4 and 2.0 ms^{-2} r.m.s. were used. The head motions were measured with accelerometers mounted to 'Pertinax-board' attached to the forehead with adhesive tape. The mean vertical response showed a peak in the frequency range of 16 to 20 Hz while the mean fore-and-aft response showed a peak at 5 Hz.

The head motions of standing subjects exposed to vertical floor vibration in six, three translational and three rotational, axes have been reported only by Paddan and Griffin (1993). The bite-bar, described in the previous section, was used in the measurements in six axes (see Figure 2.27). The input stimulus was 'Gaussian random' vibration 'with a nominally constant bandwidth acceleration spectrum' between 0.25 and 25 Hz at a magnitude of 1.75 ms^{-2} r.m.s. It was found that head motion occurred principally in the mid-sagittal plane, i.e., in the vertical, fore-and-aft and pitch axes. Variations in the transmissibility between twelve subjects were observed, particularly in the transmissibility in the vertical direction: 20:1 at 5.5 Hz. A 'distinct peak' at about 5 Hz was found in the transmissibilities in all axes, apart from those in the vertical axis which 'often showed two peaks close together'. In the median vertical transmissibility, the peaks at around 5 Hz which were present in the individual data were hardly observed due to the variability between subjects.

The transmissibilities to the head of standing subjects obtained in the previous studies presented above were compared in Figure 2.29. The measurements of the head motion were made at the top of the head by Coermann (1962) and Hagena *et al*. (1985), at the mouth by Rao *et al*. (1975), Kobayashi *et al*. (1981), Rao (1982) and Paddan and Griffin (1993), and at the forehead by Herterich and Schnaubar (1992).

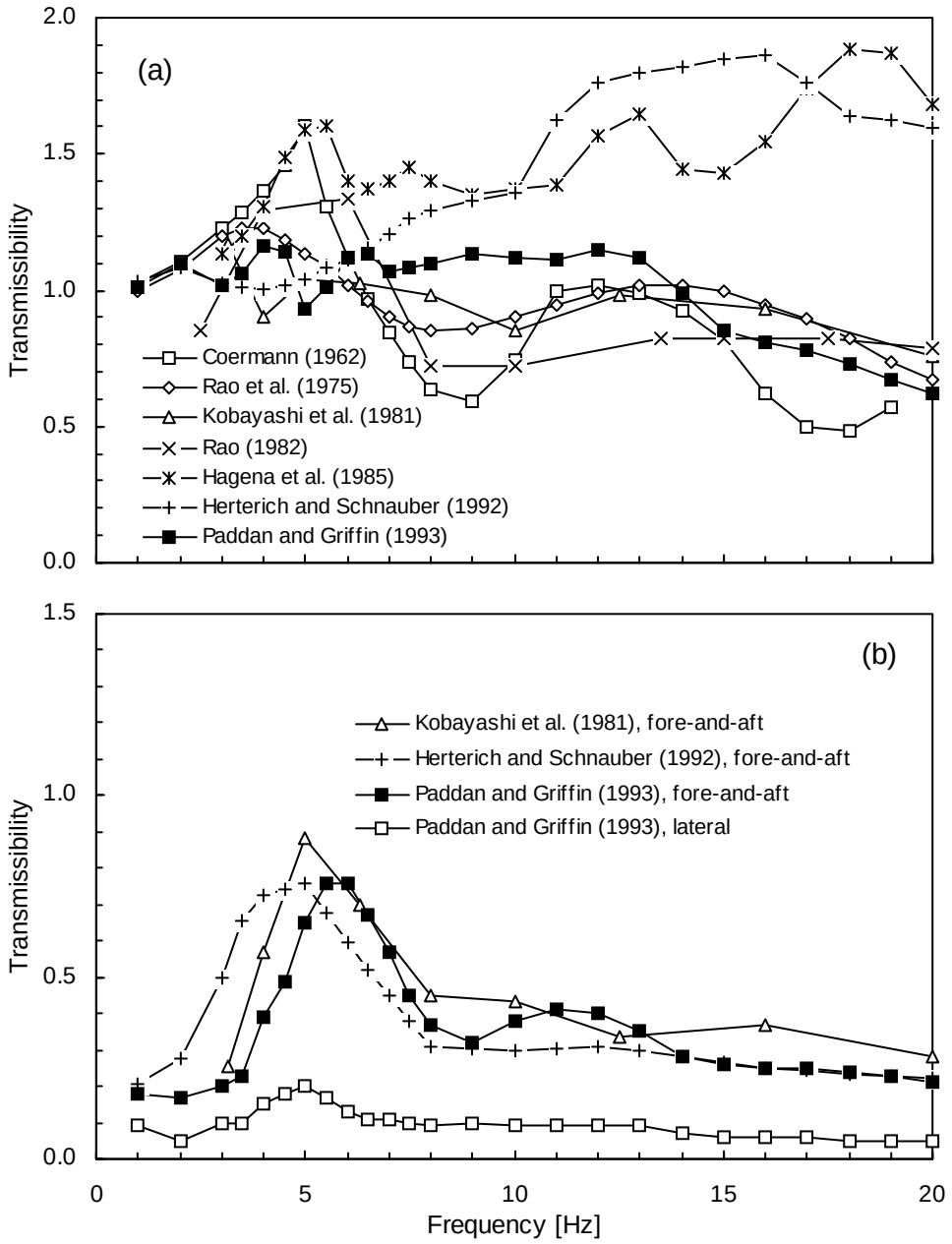

Figure 2.29 Transmissibilities to the head of standing subjects measured in previous studies: (a) vertical, (b) horizontal, (c) rotational axes. Data from one subject from Coermann (1962, 'standing erect' with sinusoidal vibrations at up to 0.5 g). Mean of eight subjects from Rao *et al*. (1975, 'standing straight' with random vibration at 0.132 g r.m.s.). Mean of three subjects from Kobayashi (1981, standing 'straight' with sinusoidal vibrations at 0.1 g r.m.s.). Mean of eight subjects from Rao (1982, 'standing straight' with sinusoidal vibrations at 1.32 ms^{-2} r.m.s.). Data from one subject from Hagena *et al*. (1985, 'standing' with frequency swept vibration at 0.2 g). Mean from 14 subjects by Herterich and Schnauber (1992, 'standing' with sinusoidal vibrations at between 0.2 and 2.2 ms^{-2} r.m.s.). Median from twelve subjects from Paddan and Griffin (1993, 'legs locked' with random vibration from 0.25 to 25 Hz at 1.75 ms^{-2} r.m.s.). -cont.

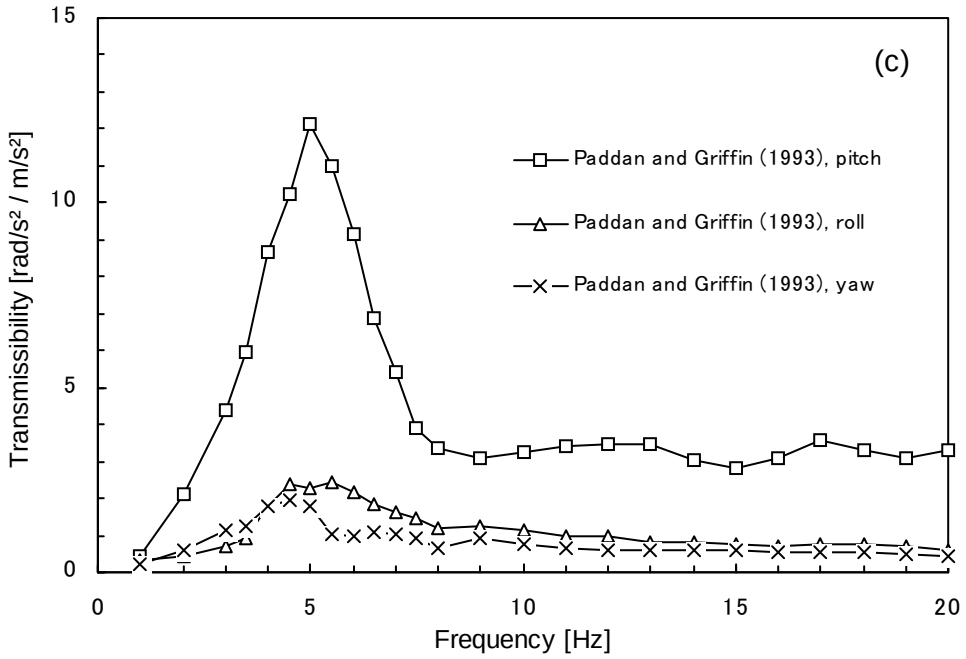

Figure 2.29 (continued) Transmissibilities to the head of standing subjects measured in previous studies: (a) vertical, (b) horizontal, (c) rotational axes.

2.4.2.3 Transmissibility to the head in a normal sitting posture

There have been more studies of the transmission of vertical whole-body vibration to the heads of seated subjects than of standing subjects. Some principal studies of the transmissibility to the head of the seated body are summarised in Table 2.7, shown above. The previous studies using a rigid seat with no backrest are presented here because the effects of the compliance of the seat and the effects of backrests on the dynamic response of the seated body are beyond the scope of this study.

The transmission of vertical whole-body vibration to the head of the seated body was measured by Coermann (1962) who also measured the dynamic response of the heads of subjects in a standing position, as described in Section 2.4.2.2. The transmissibility to the head, measured at the top of the head when one subject was in 'sitting erect' posture on a hard flat seat, had four peaks: a principal peak at about 5 Hz, which was also observed in the transmissibility when the subject was 'standing erect', and three other small peaks at 3, 11 and 15 Hz, which were not present in the transmissibility to the head in the 'standing erect' posture.

Table 2.8 Sources of variability in the seat-to-head transmissibility of the human body from Griffin *et al*. (1978).

INTRINSIC VARIABLES	
INTER-SUBJECT VARIABILITY	effects are large and frequency dependent. (e.g. at 4 Hz about 20% of transmissibility measurements fall outside 0.9 - 1.8 range). Subjects differ in the dominance and frequency of their principal resonances.
Weight	tendency towards lower seat-to-head transmissibilities in heavier subjects.
Sex	men tend to have higher transmissibilities than women from 1.25 - 5 Hz and lower transmissibilities than women from 5 - 100 Hz.
Age	from 10 - 100 Hz the transmissibility of boys tends to be lower than of men.
INTRA-SUBJECT VARIABILITY	large effects of small changes in position and posture. Repeatability in one posture may be 80% of measurements within ±20% of median.
EXTRINSIC VARIABLES	
Vibration frequency	subjects exhibit 1, 2, 3 or more resonance peaks. Without back support transmissibility is often in excess of 1 below about 10 Hz and decreases above 20 Hz.
Vibration axis	vertical seat vibration causes motion in other axes at the head.
Analysis method	transmissibility may be determined by several alterna-methods... The method depends on the type and quality of the input motion. The differences that exist between the results of the alternative methods may often be relatively small but sometimes useful and important.

Griffin *et al*. (1978) investigated various factors that affected the transmission of vertical seat vibration to the head: variables related to the nature of subjects (e.g. gender, body size, age), posture and muscle tension of subjects, type of input vibration, and analysis method. The motions of the head in the vertical direction were measured with an accelerometer secured to a ‘stainless steel bar covered with a nylon sleeve’. The accelerometer was 75 mm from the mid-sagittal plane. Subjects sat on a ‘flat horizontal wooden seat’ in a ‘comfortable upright posture’. Some of the findings summarised by the authors are presented in Table 2.8.

Kobayashi *et al*. (1981) measured the head motions of seated and standing subjects exposed to vertical whole-body vibration in two axes, the vertical and fore-and-aft directions, as described in Section 2.4.2.2. The subjects sat straight on the centre of the vibration table with no footrest. The mean vertical transmissibility to the head in the vertical direction obtained from three male subjects had a clear peak at 5 Hz with a small peak at 12.5 Hz. The mean transmissibility declined sharply at frequencies above 40 Hz. The mean fore-and-aft transmissibility showed a peak at 5 Hz, which

was observed in the fore-and-aft transmissibility of standing subjects. The fore-and-aft transmissibility was smaller than the vertical transmissibility at all frequencies investigated.

The vertical vibration transmission to the head of seated and standing subjects was measured by Rao (1982) with sinusoidal vibrations and with random vibrations having a 'constant velocity spectrum'. The transmissibility to the head was obtained from eight male subjects in a 'sitting straight' posture with an accelerometer held between the subjects' front teeth. Figure 2.30 compares the mean transmissibilities obtained with sinusoidal vibrations at three magnitudes to those obtained with random vibrations at four magnitudes. A principal peak at about 4 Hz, a notch at about 8 Hz and a second broad peak at around 13 Hz was observed in all transmissibilities, irrespective of the type and magnitude of the input stimulus. It seems that the transmissibilities obtained with sinusoidal vibrations tended to be greater than those obtained with random vibrations at around 6 Hz and smaller than those obtained with random vibrations in the frequency range of the second broad peak.

Pope *et al*. (1987) compared the transmissibility to the head in the vertical direction

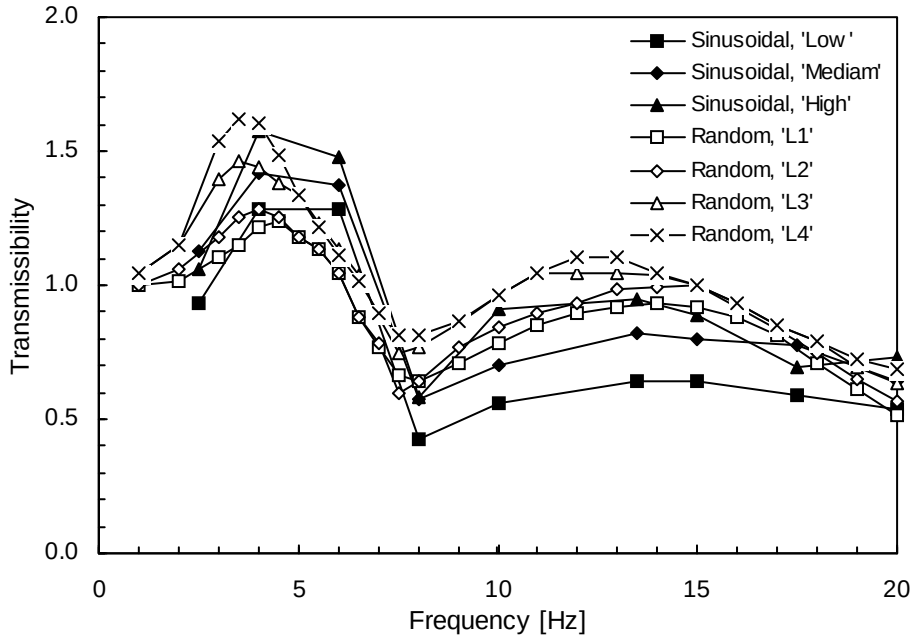

Figure 2.30 Mean transmissibilities of eight male subjects in 'sitting straight' posture obtained with sinusoidal and random vibrations from Rao (1982). Vibration magnitudes for sinusoidal vibrations: Low: 0.64 ms^{-2} r.m.s., Median: 1.32 ms^{-2} r.m.s., High: 2.0 ms^{-2} r.m.s. For random vibrations: L1: 0.3 ms^{-2} r.m.s., L2: 0.64 ms^{-2} r.m.s., L3: 1.32 ms^{-2} r.m.s., L4: 2.4 ms^{-2} r.m.s.

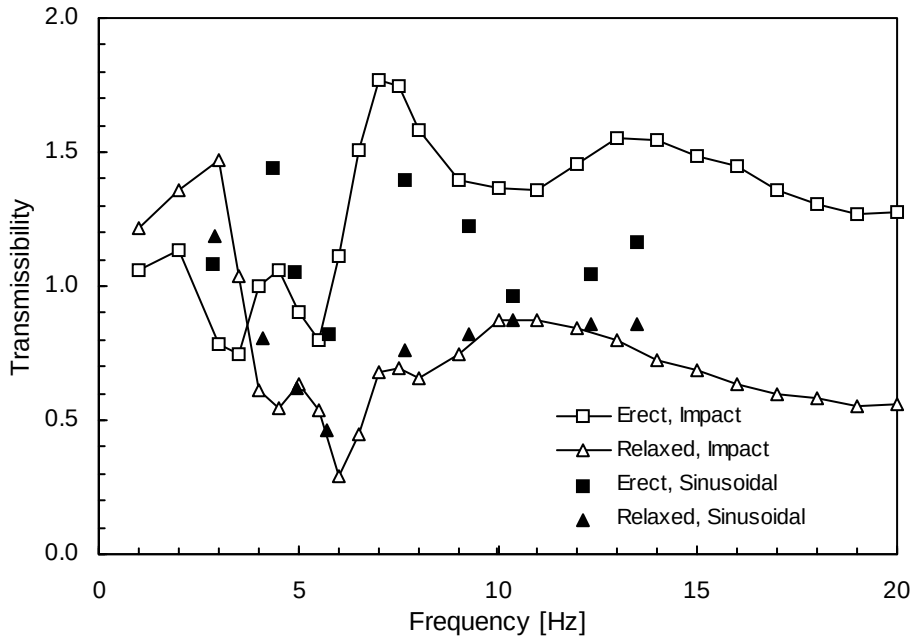

Figure 2.31 Transmissibilities of one seated subject in 'erect' and 'relaxed' postures obtained with impacts and sinusoidal vibrations from Pope *et al*. (1987).

obtained with sinusoidal vibrations and impact inputs. The head responses were measured with five male and five female subjects sitting on a hard flat seat by using an accelerometer mounted to a 'wooden block' which was 'held firmly between the subject's teeth'. Typical transmissibilities to the head of one subject sitting in an 'erect' posture and in a 'relaxed' posture measured with impacts and sinusoidal vibrations shown by the authors are presented in Figure 2.31. Two distinct peaks were observed in the transmissibilities of the subject in the 'erect' posture with sinusoidal vibrations at about 4 and 8 Hz, while the peak at 4 Hz in the transmissibility in the same posture with impact inputs were much smaller than the transmissibility peak at 4 Hz with sinusoidal inputs. It was reported that the transmissibility to the head in the 'erect' posture obtained with sinusoidal vibrations were greater than that obtained with impacts in the frequency range from 2 to 8 Hz. This difference was statistically significant 'at the $p < 0.01$ level' in the frequency range from 2 to 4 Hz and 'at the $p < 0.05$ level' in the frequency range from 4 to 8 Hz.

Messenger (1987) investigated the transmission of vertical seat vibration to the head with eight male subjects in different postures defined in terms of the pelvis angle. The transmissibility to the head was measured in four axes, vertical, fore-and-aft, lateral and pitch, with a random vibration in the frequency range of 0.5 to 40 Hz at a

magnitude of 1.0 ms^{-2} r.m.s. A 'normal upright' posture was defined by the individual's own interpretation, which 'occurred between the 105° and 95° hip angle conditions'. The mean transmissibilities of the subjects in the 'normal upright' posture showed a principal peak at frequencies between 5 and 7 Hz in the fore-and-aft, lateral and pitch axes. In the vertical axis, however, the peak in this frequency was less distinct than a peak at about 2 Hz. A broad peak at about 12 Hz was observed in the mean transmissibilities in the vertical, fore-and-aft and pitch directions, which is most distinct in the vertical direction. The head transmissibilities measured with twelve subjects in a 'normal erect' posture in her successive study (Messenger, 1989) showed larger variability between subjects in the location of peaks in the vertical direction than in the fore-and-aft and pitch directions, particularly in the frequency range between 3 and 10 Hz.

Repeatability in measurements with one subject (i.e., intra-subject variability) and variability between subjects (i.e., inter-subject variability) in the transmissibility to the head were investigated by Paddan and Griffin (1988). Subjects in a 'comfortable upright' posture were exposed to vertical random vibration in the frequency range 0.2 to 31.5 Hz at a magnitude of 1.75 ms^{-2} r.m.s. The head motions were measured in six axes with a bite-bar (see Figure 2.27). For the investigation of intra-subject variability, one male subject was exposed to the input vibration twelve times. Variability was found at high frequencies in the vertical transmissibility to the head: 'near 15 Hz the maximum response was 48 % higher than the minimum response' (Figure 2.32(a)). It seems that the transmissibilities in the vertical direction in the other frequency range and those in the other axes were reasonably repeatable. The inter-subject variability was investigated with twelve male subjects (Figure 2.32(b)). 'Most of the motion at the head' was found to occur in the fore-and-aft, vertical and pitch axes (i.e., in the mid-sagittal plane) with a 'relatively small amount of motion' occurring in the lateral, roll and yaw axes. The variability in the vertical axis was large at frequencies above 2 Hz with a distinct peak in the frequency range between 2 and 8 Hz.

Kitazaki (1994) measured the vertical and fore-and-aft head motions of seated subjects exposed to random vibration in the frequency range from 0.5 to 35 Hz at 1.7 ms^{-2} r.m.s., together with the measurement of the motions at locations over the spine. The head motion measurement was made at '90 mm left and 100 mm behind the mouth', near the cervical spine, using a bite-bar so as to reduce the effect of pitch motion of the head on the translational motions. The mean transmissibility of eight

male subjects in a 'normal' posture, 'with the pelvis rotated most backward with the straightened lumbar spine' and 'upright thoracic and cervical spine', showed a principal peak at about 5 Hz and a second peak at around 12.5 Hz.

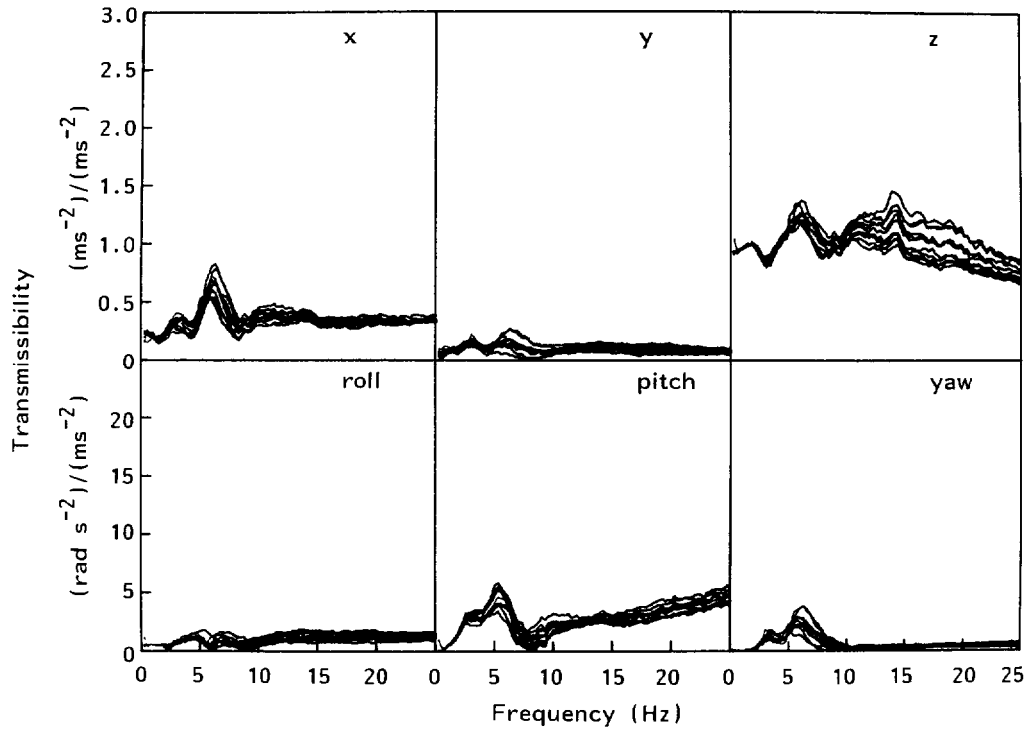

(a)

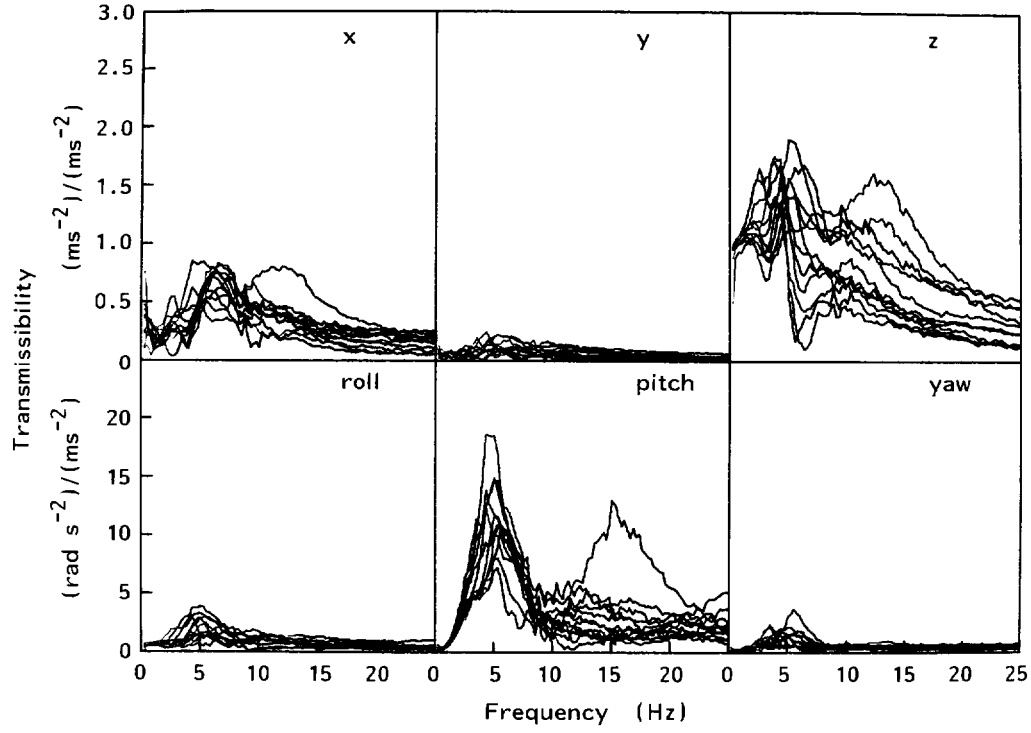

(b)

Figure 2.32 Transmissibilities to the head (a) for one subject during twelve repetitions and (b) for twelve subjects. After Paddan and Griffin (1988).

The transmissibilities to the heads of seated subjects obtained in the previous studies presented above are compared in Figure 2.33. The measurements of the head motion were made at the top of the head by Coermann (1962), at the mouth by Griffin *et al*. (1978), Kobayashi *et al*. (1981), Rao (1982), Pope *et al*. (1987), Messenger (1987) and Paddan and Griffin (1988), and near the cervical spine by Kitazaki (1994).

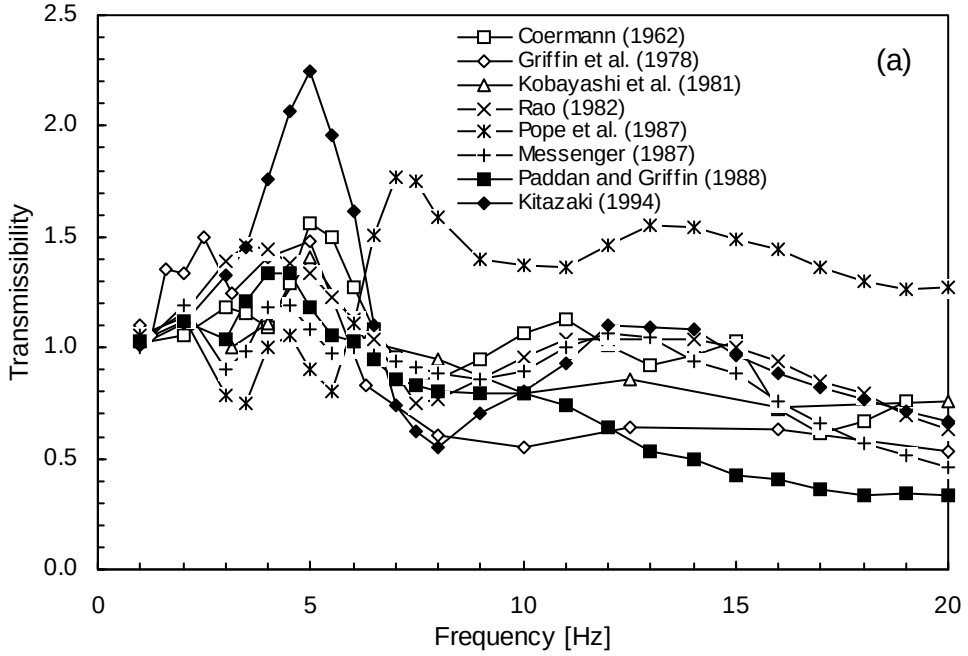

Figure 2.33 Transmissibilities to the head of seated subjects measured in previous studies: (a) vertical, (b) horizontal, (c) rotational axes. Data from one subject from Coermann (1962, 'sitting erect' with sinusoidal vibrations at up to 0.5 g). Mean of 18 subjects from Griffin *et al*. (1978, 'normal upright' with sinusoidal vibrations at 1.0 ms^{-2} r.m.s.). Mean of three subjects from Kobayashi (1981, sitting 'straight' with sinusoidal vibrations at 0.1 g r.m.s.). Mean of eight subjects from Rao (1982, 'sitting straight' with random vibration at 1.32 ms^{-2} r.m.s.). Data from one subject from Pope *et al*. (1987, 'sitting erect' with impact inputs). Mean from eight subjects by Messenger (1987, 'normal upright' with random vibration from 0.5 to 40 Hz at 1.0 ms^{-2} r.m.s.). Median from twelve subjects from Paddan and Griffin (1988, 'back-off' with random vibration from 0.2 to 31.5 Hz at 1.75 ms^{-2} r.m.s.). Mean from eight subjects from Kitazaki (1994, 'normal' with random vibration from 0.5 to 35 Hz at 1.7 ms^{-2} r.m.s.). -cont.

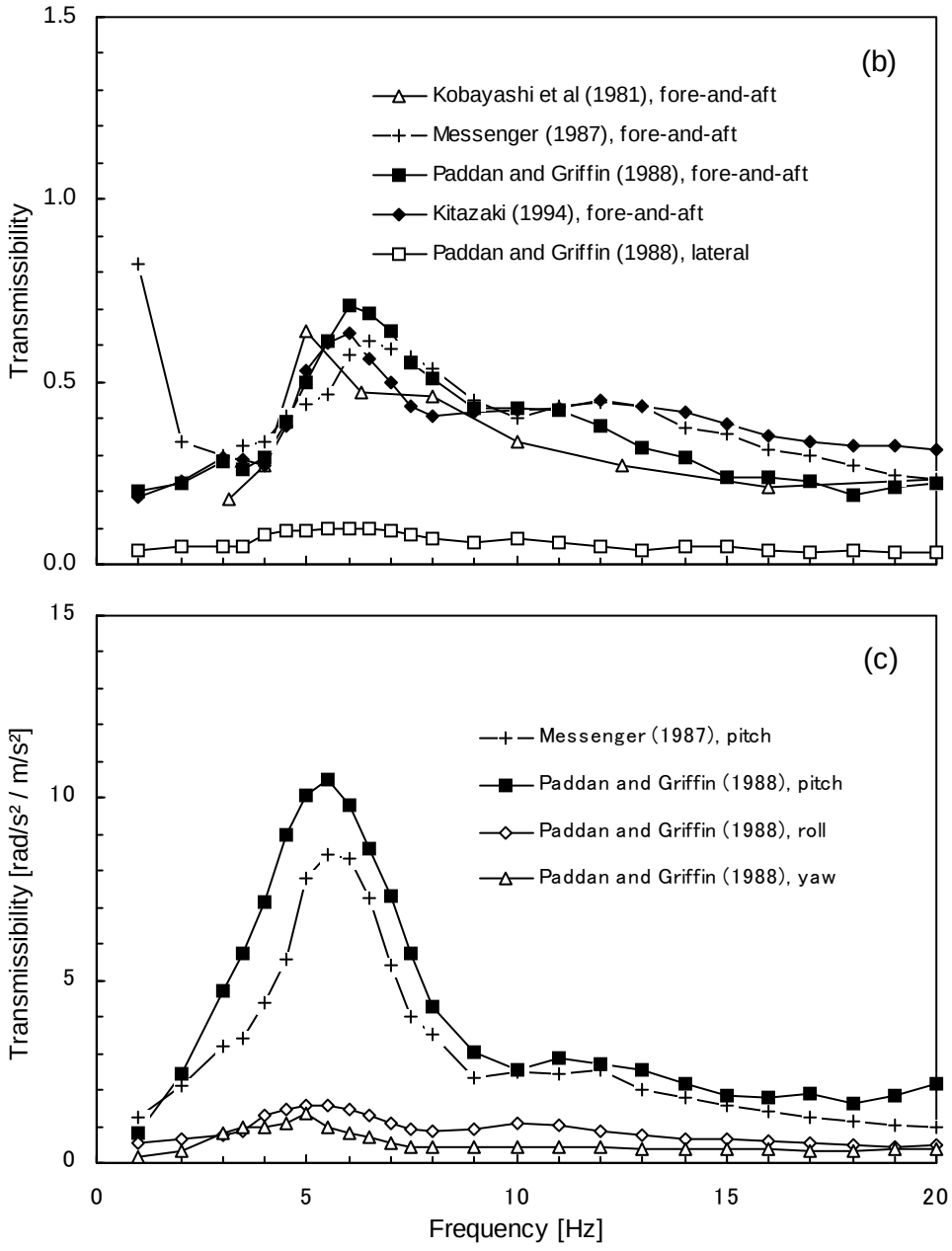

Figure 2.33 (continued) Transmissibilities to the head of seated subjects measured in previous studies: (a) vertical, (b) horizontal, (c) rotational axes.

2.4.2.4 Effects of posture and muscle tension on transmissibility to the head

The transmission of vertical whole-body vibration to the head have been measured with subjects when standing and sitting by Coermann (1962), Kobayashi *et al*. (1981) and Rao (1982). In these studies, the same experimental conditions for standing and seated subjects enables to compare between the head transmissibilities in standing and sitting positions. The transmissibilities from those studies are compared in Figure 2.34. It seemed that the trends of the transmissibilities to the head of standing subjects generally agreed with those of seated subjects. A peak at about 5 Hz was observed in all vertical and fore-and-aft transmissibility curves, apart from the mean vertical transmissibility of three standing subjects reported by Kobayashi *et al*. (1981). The data from Kobayashi *et al*. (1981) showed smaller vertical transmissibility and greater fore-and-aft transmissibility for standing subjects at frequencies around 5 Hz, compared to those for seated subjects. The vertical transmissibility to the head measured by Coermann (1962) with one seated subject showed more local peaks than the vertical transmissibility to the head with same subject when standing.

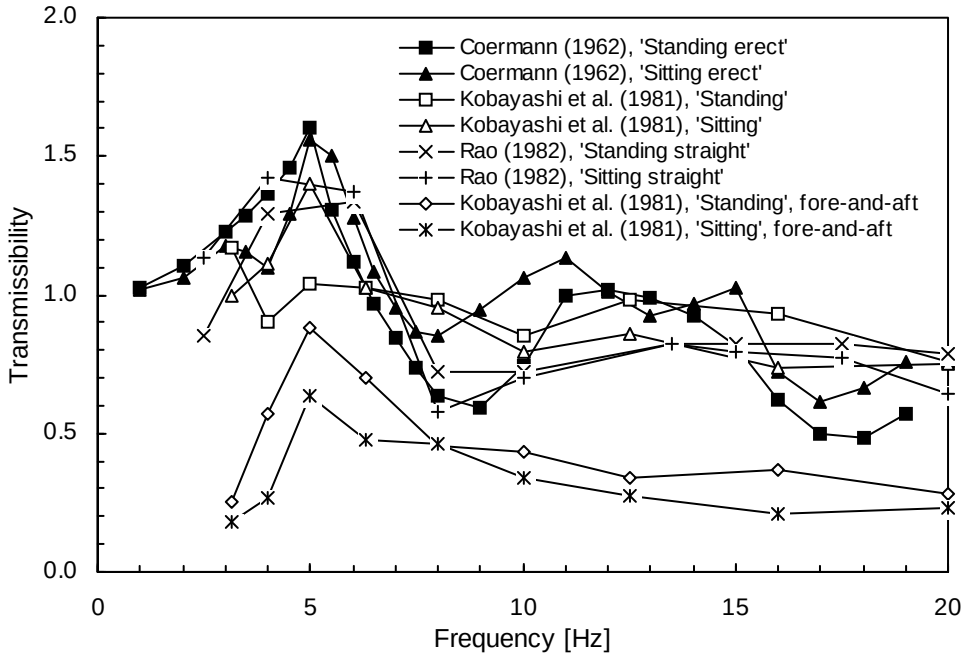

Figure 2.34 Comparison between the transmissibilities to the head of standing subjects and the transmissibilities of seated subjects in the vertical and fore-and-aft axes measured in previous studies. Data from one subject from Coermann (1962, with sinusoidal vibrations at up to 0.5 g). Mean of three subjects from Kobayashi (1981, with sinusoidal vibrations at 0.1 g r.m.s.). Mean of eight subjects from Rao (1982, with sinusoidal vibrations at 1.32 ms^{-2} r.m.s.). Measurements were made at the mouth in all studies, apart from Coermann (1962, at the top of the head).

The effects of posture in the legs of standing subjects on the vibration transmission to the head were investigated by Rao *et al*. (1975) and Paddan and Griffin (1993). A 'legs bent' posture was defined as 'the knees were vertically above the subject's toes' by Paddan and Griffin (1993), whereas the definition of a 'standing with knees bent' posture used by Rao *et al*. (1975) was not clear. Paddan and Griffin (1993) also investigated the difference in the transmissibility to the head between a 'legs locked' posture, in which 'the subject stood in a normal upright stance', and a 'legs unlocked' posture, in which 'the knees were very slightly forward'. The transmissibilities to the head in the vertical axis reported in those two studies are compared in Figure 2.35. The trend that the transmissibility measured with subject's legs bent had a distinct peak at low frequencies, 2 to 3 Hz, and low values at frequencies above the main peak frequency region was consistent in those two studies. This effect is similar to that found in the change in the apparent mass, described in Section 2.4.1.2. The transmissibility in the 'legs unlocked' posture showed lower values than that in the 'legs locked' posture at frequencies above 3 Hz. Paddan and Griffin (1993) also investigated the effect of leg posture on the transmissibilities in the other five axes, fore-and-aft, lateral, pitch, roll and yaw. It was stated that 'the principal differences'

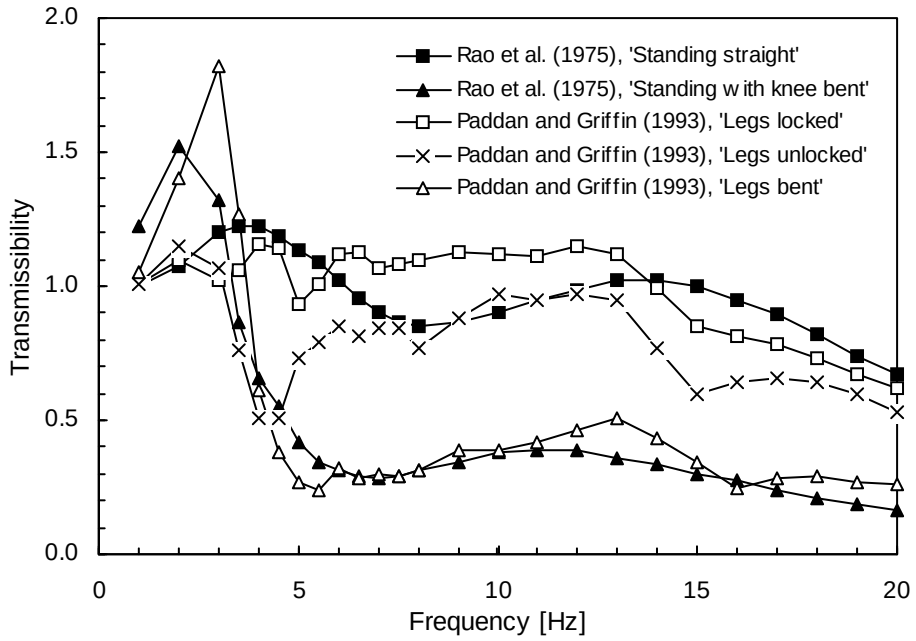

Figure 2.35 Effect of leg posture in the vertical transmissibilities to the head of standing subjects measured in previous studies. Mean of eight subjects from Rao *et al*. (1975, with random vibration at 0.132 g r.m.s.). Median from twelve subjects from Paddan and Griffin (1993, with random vibration from 0.25 to 25 Hz at 1.75 ms^{-2} r.m.s.). Measurements were made at the mouth.

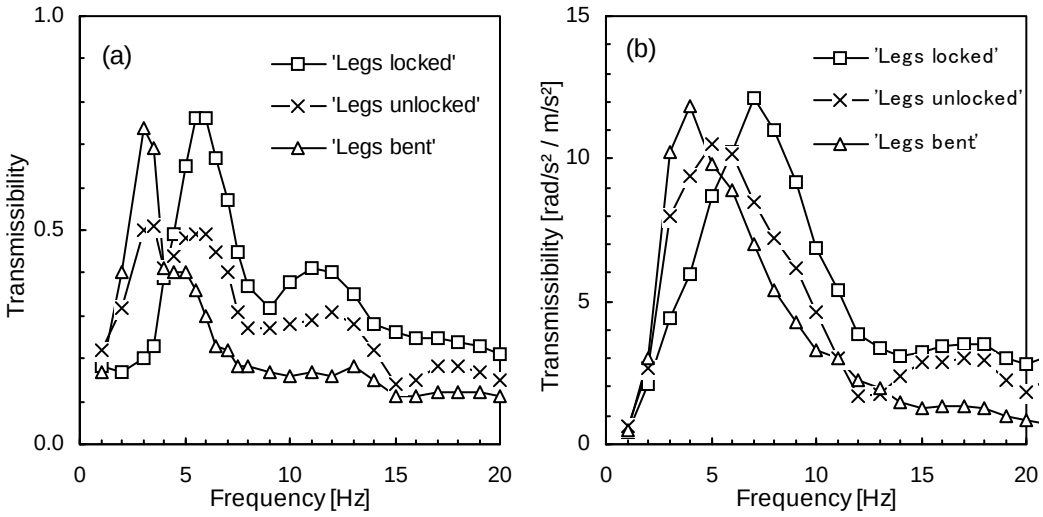

Figure 2.36 Effect of leg posture in the median fore-and-aft and pitch transmissibilities to the head of twelve standing subjects from Paddan and Griffin (1993).

occurred in the fore-and-aft, vertical and pitch axes. The median transmissibilities in the fore-and-aft and pitch axes measured in three postures by Paddan and Griffin (1993) were shown in Figure 2.36. Decreases in the main peak frequency and in the transmissibilities at high frequencies with the postural change from the ‘legs locked’ to the ‘legs bent’ were observed in the transmissibilities in both fore-and-aft and pitch axes.

The effects of posture and muscle tension in the upper-bodies of seated subjects on the transmissibility to the head were investigated in several previous studies. Typical postures used in the studies were ‘normal’, ‘erect’, ‘relaxed’, ‘stiff’, and ‘slouched’. The comparison between the vertical transmissibility obtained with subjects in a ‘relaxed’ posture and the vertical transmissibility obtained with subjects in an ‘erect’ posture were made by Coermann (1962) and Pope *et al*. (1987). The transmissibility in a ‘relaxed’ posture tended to have higher values at low frequencies and lower values at high frequencies than that in an ‘erect’ posture (Figure 2.37). This trend was observed in the results from both studies, although frequency range in which the transmissibility curves in two postures intersected each other was different. Griffin *et al*. (1978) investigated the differences in the vertical transmissibility to the head between a ‘relaxed’, ‘normal’ and ‘stiff’ postures. The transmissibilities in their ‘relaxed’ and ‘normal’ posture showed similar trend, although there were some differences at frequencies around 5 Hz and at higher frequencies above 10 Hz (Figure 2.38). The

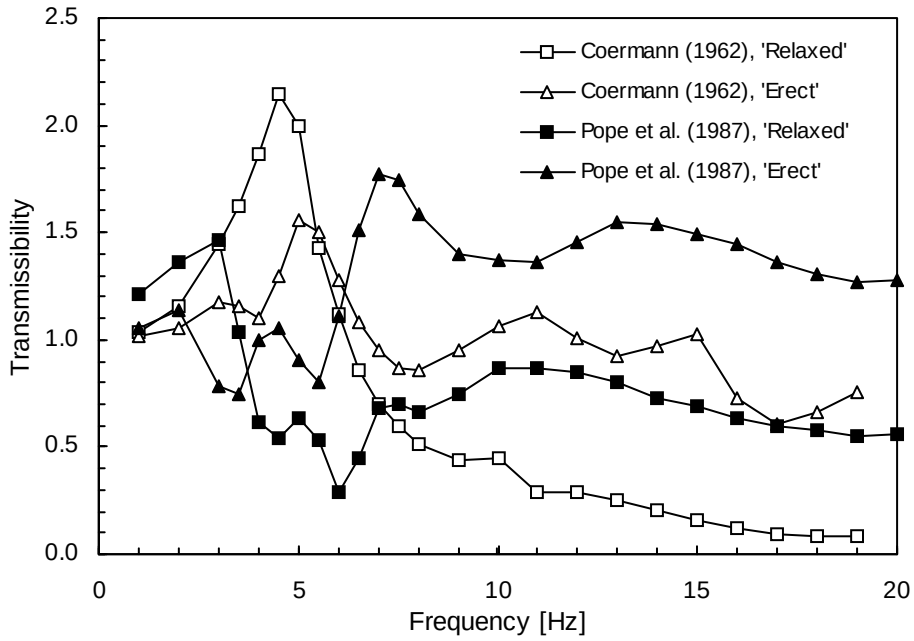

Figure 2.37 Vertical transmissibilities to the head of seated subjects in 'relaxed' and 'erect' postures measured in previous studies. Data from one subject from Coermann (1962, with sinusoidal vibrations at up to 0.5 g). Data from one subject from Pope *et al*. (1987, with impact inputs). Measurements were made at the top of the head by Coermann (1962) and at the mouth by Pope *et al*. (1987).

'stiff' posture flattened the transmissibility curve compared to those in the other two postures. Kitazaki (1994) presented the head transmissibilities measured in a 'slouched', a 'normal' and an 'erect' sitting postures. The differences in the transmissibilities were remarkable at high frequencies above 10 Hz in the vertical and fore-and-aft axes (Figure 2.39): the transmissibilities decreased with the postural change from 'erect' to 'slouched'. The fore-and-aft transmissibility in the 'slouched' posture had greater values at low frequencies below 5 Hz than those in the 'normal' and 'erect' postures.

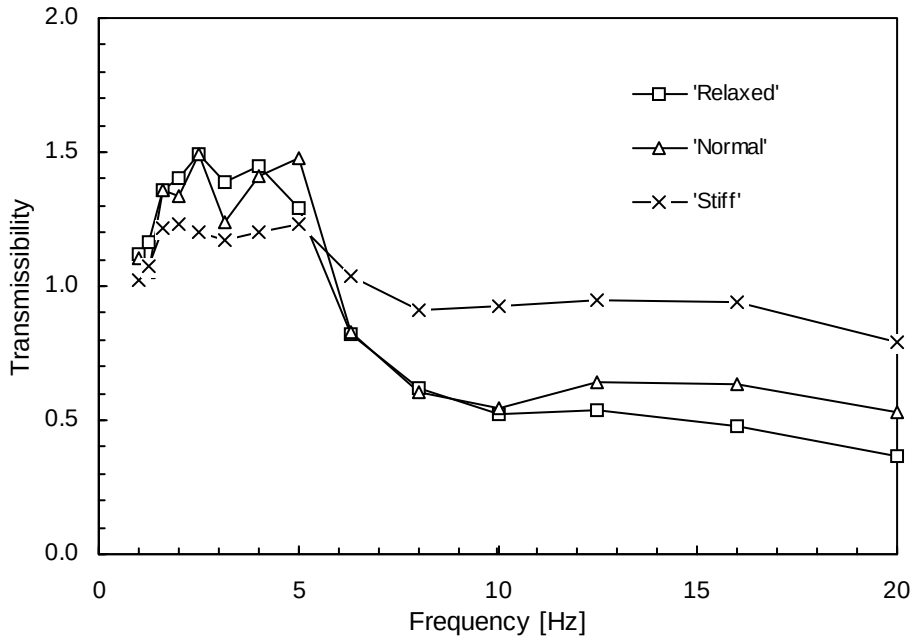

Figure 2.38 Mean vertical transmissibilities to the head of 18 seated subjects in 'relaxed', 'normal' and 'stiff' postures from Griffin *et al*. (1978).

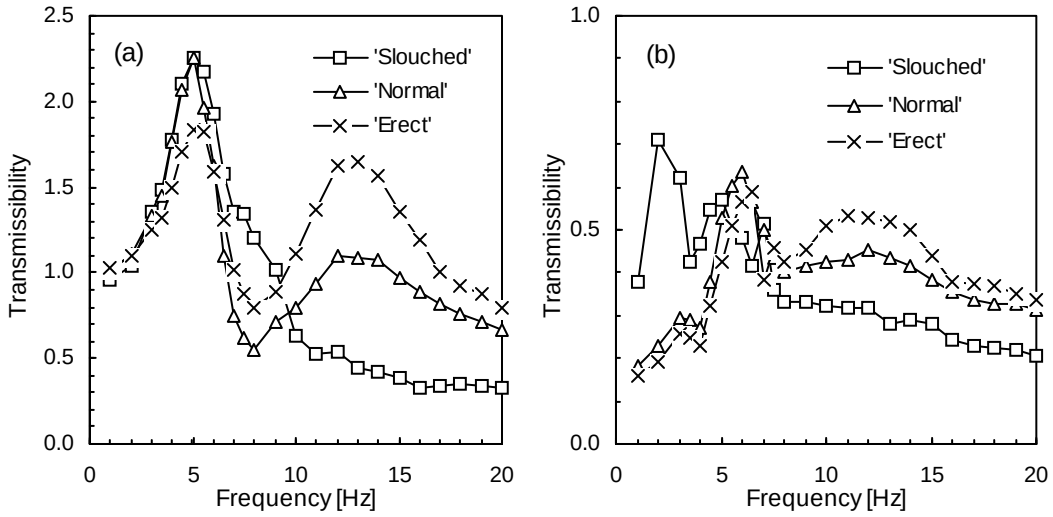

Figure 2.39 Median transmissibilities to the head of eight seated subjects in 'slouched', 'normal' and 'erect' postures from Kitazaki (1994): (a) vertical and (b) fore-and-aft directions. Measurement was made near the cervical spine.

Messenger (1987) defined the change in the posture of sitting subjects in terms of the pelvic angle measured with a 'standard goniometer'. The transmissibilities to the head for sitting postures with the pelvic angles of 85°, 95° and 105° and for a 'normal upright' posture, in which the pelvic angles of eight male subjects varied between 95° and 105°, were investigated. The mean transmissibilities in the vertical, fore-and-aft

and pitch axes are presented in Figure 2.40. It was stated that ‘as the pelvis was rotated forward the magnitude at 4 Hz decreased but the magnitudes at frequencies above 6 Hz increased’ in the vertical axis. ‘Decreased pelvis angles produced increased mean magnitude of the fore-and-aft axis head motion above 3 Hz’. ‘Magnitudes of pitch axis head motion decreased around 5 Hz’ and ‘increased at frequencies above 10 Hz’ with decreases in the pelvic angle. In her subsequent study, the transmissibilities to the head of twelve male subjects in their ‘normal erect’ posture were measured and the correlation between the transmission of vertical vibration from seat to the head and the sitting posture was investigated (Messenger, 1989). Posture was measured in terms of six body angles at the head and five locations on the spine, the six cervical vertebra (C6), the fifth and tenth thoracic vertebrae (T5 and T10) and the second and fourth lumbar vertebrae (L2 and L4). The following correlations were reported: (1) between ‘increased anterior tilting of the pelvis’ and ‘increased straightening of the lumbar region of the back’ and ‘reduced transmissibility’ ‘at approximately 4 Hz’, (2) between ‘increased forward inclination of the upper back’ and ‘increased transmissibility’ ‘at approximately 4 Hz’, (3) between ‘increased anterior tilting of the pelvis’ and ‘increased transmissibility’ ‘at the higher frequencies’, and (4) between ‘increased forward inclination the upper back’ and ‘decreased transmissibility’ ‘at the higher frequencies’.

Griffin (1975) used postures defined by ‘the body positions that maximised and minimised the sensation of vibration at the subjects’ heads’, a ‘most severe’ and ‘least severe’ postures. The subjects determined their posture at each of twelve sinusoidal vibration frequencies between 7 and 75 Hz. The mean vertical transmissibility to the head of twelve subjects in the ‘most severe’ posture had significantly larger values than that in the ‘least severe’ posture at all frequencies investigated: a maximum of an approximate 6:1 difference. The difference in the mean transmissibilities measured in the two posture was relatively small in the other axes measured, fore-and-aft, lateral and pitch.

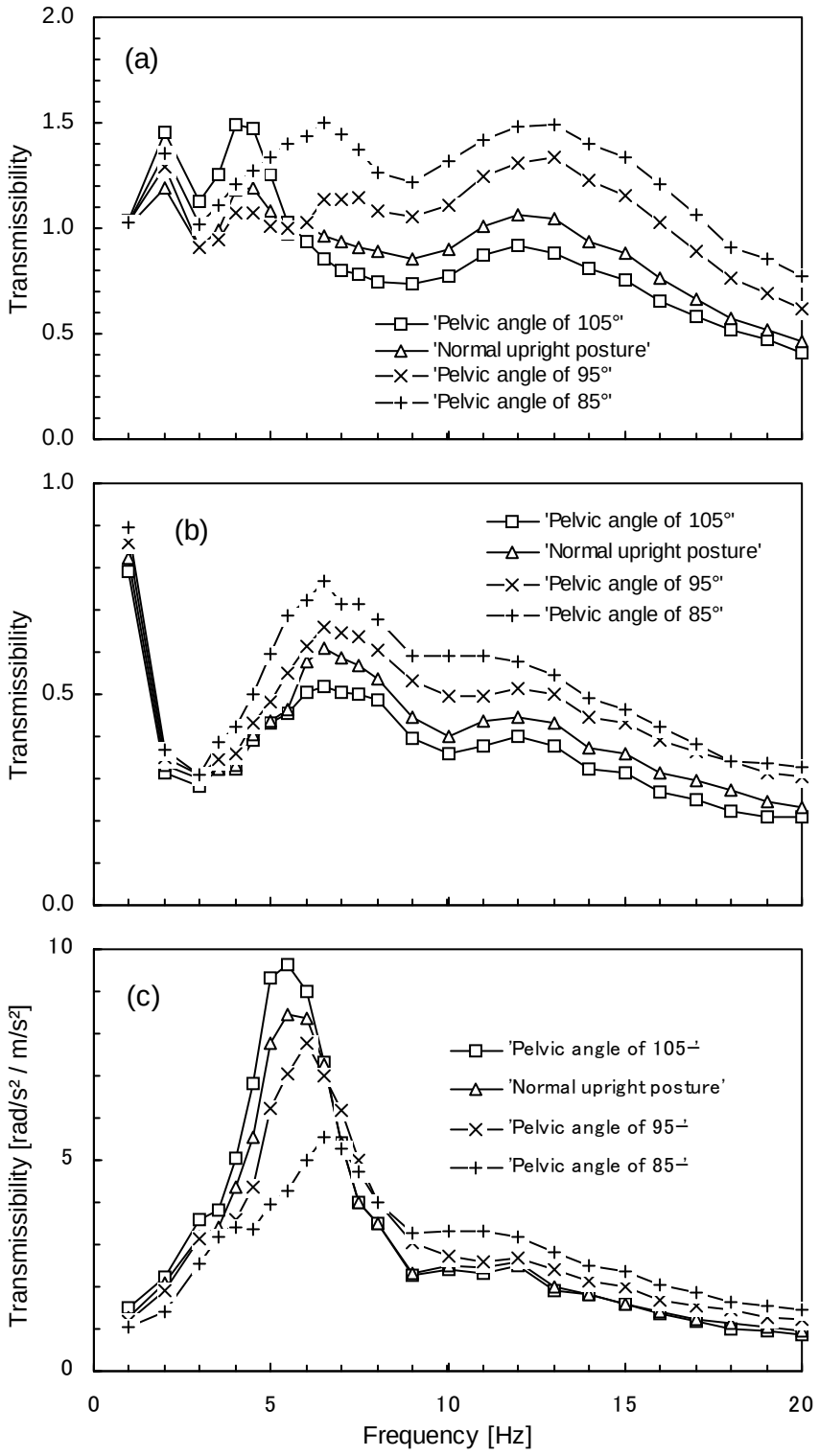

Figure 2.40 Mean transmissibilities to the head of eight seated subjects in four different postures from Messenger (1987): (a) vertical, (b) fore-and-aft, and (c) pitch directions.

2.4.2.5 Effect of excitation magnitude on transmissibility to the head

The effects of excitation magnitude on the transmissibility to the head have been investigated by Rao *et al*. (1975) and Rao (1982). The transmission of vertical vibration to the head were measured with standing and seated subjects with random vibrations at four different magnitudes and with sinusoidal vibrations at three different magnitudes. The mean vertical transmissibilities for standing subjects are shown in Figure 2.41. The data for seated subjects are shown in Figure 2.30. There was a general trend that the transmissibility increased with increasing excitation magnitude. This trend was found in all conditions apart from standing subjects with random vibrations, which showed an opposite effect. There seemed to be an effect of the excitation magnitude on the main resonance frequency, which can be observed in the data obtained with random vibration. As the excitation magnitude increased, the resonance frequency decreased for seated subjects but increased for standing subjects. Griffin (1975) found statistically significant reductions in the transmissibility with increasing levels of vibration in the frequency range from 7 to 75 Hz, which was inconsistent with the trend observed in the data by Rao *et al*. (1975) and Rao (1982).

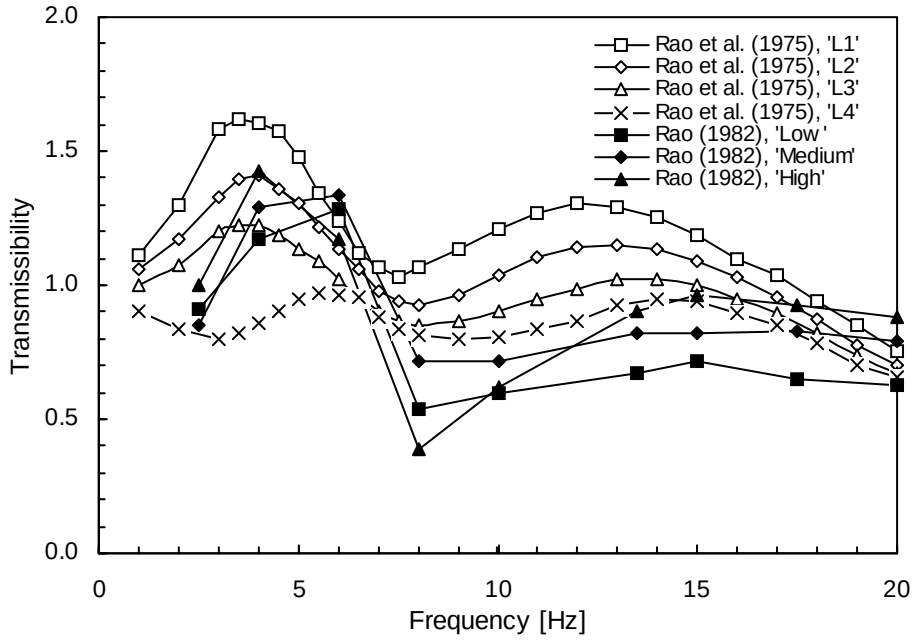

Figure 2.41 Mean transmissibilities of eight male subjects in 'standing straight' posture obtained with sinusoidal and random vibrations from Rao *et al*. (1975) and Rao (1982). Vibration magnitudes for sinusoidal vibrations: Low: 0.64 ms^{-2} r.m.s., Median: 1.32 ms^{-2} r.m.s., High: 2.0 ms^{-2} r.m.s. For random vibrations: L1: 0.3 ms^{-2} r.m.s., L2: 0.64 ms^{-2} r.m.s., L3: 1.32 ms^{-2} r.m.s., L4: 2.4 ms^{-2} r.m.s. See Figure 2.30 for seated subjects.

2.4.3 Dynamic response of the pelvis

2.4.3.1 Basic musculoskeletal anatomy of the pelvis (extracted from Dean and Pegington, 1996b)

The pelvis provides support for the abdominal and pelvis viscera and also transmits the weight of the trunk from the vertebral column to the femoral heads. The two hip bones, or innominate bones, articulate with the sacrum at the sacroiliac joints (Figure 2.42). These are synovial joints. The body of the first sacral segments bears the weight of the trunk which is then passed bilaterally to the sacroiliac joints. In the midline anteriorly, the innominate bones articulate with each other at the pubic symphysis.

Each innominate bone is made up of three separate bones which fuse together. The most superior of the three bones is called the ilium (Figure 2.43). The ilium is surmounted by the iliac crest which runs from the posterior superior iliac spine to the anterior superior iliac spine. The superior part of the acetabulum of the hip joint is part of the ilium and this is the weight-bearing portion of the joint socket. The pubic bone, the second bone of the innominate, has superior and inferior pubic rami which meet each other at the body of the pubic bone anteriorly (Figure 2.43). The bodies of the right and left pubic bones join together at the pubic symphysis. The third bone of the innominate is called the ischium (Figure 2.43). The ischium forms the posterior third of

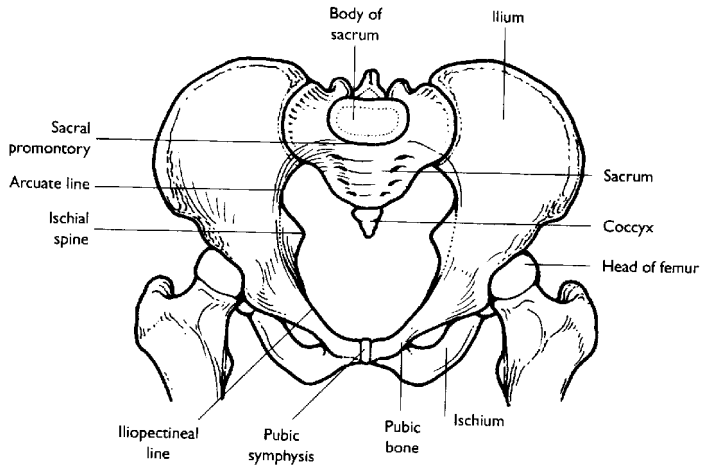

Figure 2.42 The bones and major bony landmarks of the pelvis. After Dean and Pegington (1996b).

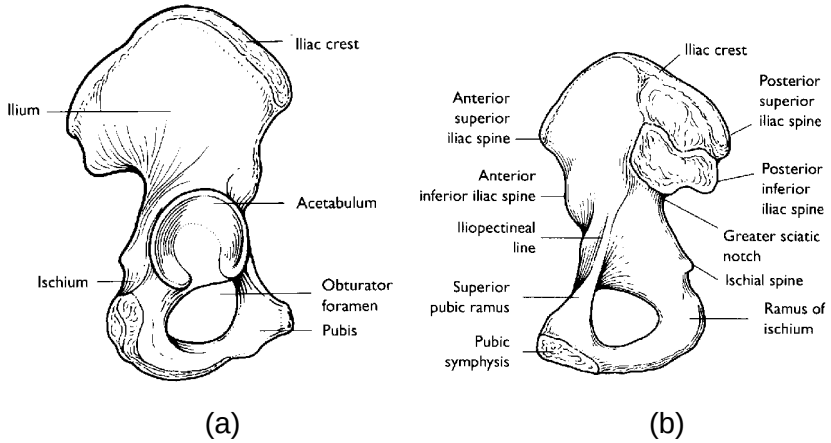

Figure 2.43 The innominate bone with important bony landmarks: (a) seen from the lateral aspect and (b) seen from the medial aspect of the bone when disarticulated. After Dean and Pegington (1996b).

the acetabulum. The part adjoining the ilium is the body of the ischium. The ischial tuberosity is the part of the pelvis people sit on. The tuberosity is roughened and curves round to become the posterior border of the ischium. When people stand upright, the posterior aspect of the body of the pubic bone, the pubic rami and the blocked off obturator foramen provide some support for the pelvic and abdominal viscera above. A muscular diaphragm that fills in the gap between the pubic bone anteriorly and the coccyx and sacrum behind also supports the pelvic and abdominal viscera.

2.4.3.2 Results from previous studies

The motions of the pelvis of the seated body during the exposure to vertical whole-body vibration have been measured in some studies. Kitazaki (1994) measured the dynamic response of the pelvis of seated subjects at the right iliac crest by using the surface measurement method. The mean transmissibilities to the vertical motion at the iliac crest measured in three postures (i.e., ‘slouched’, ‘normal’ and ‘erect’ sitting postures) are presented in Figure 2.44. Two distinct peaks with similar magnitudes were observed in the transmissibilities: the first peak at 5 to 6 Hz and the second peak at 8 Hz. The second distinct peak was not clearly observed in the transmissibilities to the vertical motions over the spine obtained by the author, apart from that to the vertical motion at the sacrum. In the ‘slouched’ and ‘normal’ postures the magnitude of the second peak was greater than that of the first peak, while the first peak was more dominant than the second in the ‘erect’ posture.

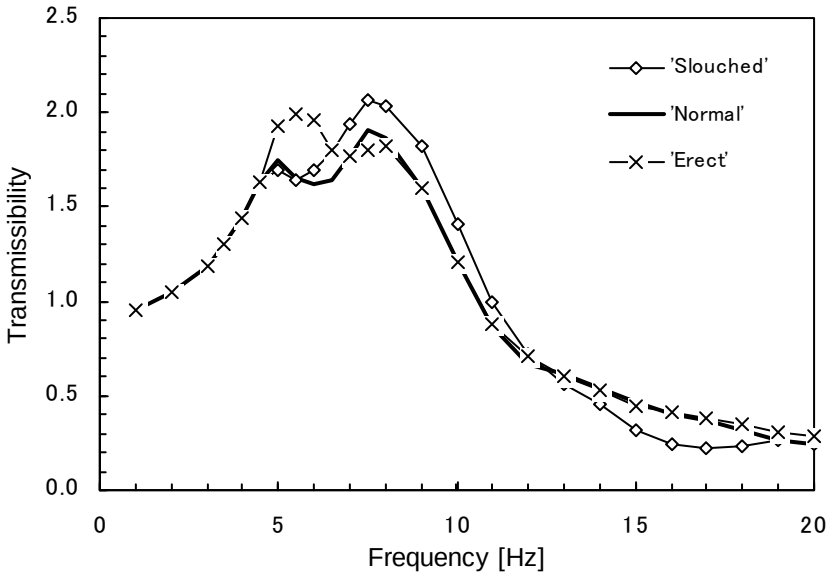

Figure 2.44 Mean vertical transmissibility to the pelvis, the iliac crest, of eight seated subjects in 'slouched', 'normal' and 'erect' postures from Kitazaki (1994).

Mansfield (1998) and Mansfield and Griffin (1999) also measured the pelvis motion of seated subjects exposed to vertical seat vibration by using the surface measurement. The dynamic responses of the pelvis in the vertical direction to vertical seat vibration were measured at the iliac crest (the anterior part of the pelvis) and the posterior superior iliac spine (the posterior part of the pelvis). The transmissibilities measured at the both locations showed the first peak at about 4 Hz and a more dominant second peak at 8 to 10 Hz (see Figures 2.19 and 2.26). It was stated that both of these peaks 'showed a reduction in frequency (from 6 to 4 Hz and from 10 to 7 Hz) with increases in vibration magnitude from 0.25 to 2.5 ms^{-2} r.m.s.' The transmissibility of seat vertical vibration to pitch motion of the pelvis was also calculated from those two measurements. It was stated that 'most subjects showed a peak in the transmissibility' 'at around 10 Hz' with a vibration magnitude of 1.0 ms^{-2} r.m.s., although a large inter-subject variability was observed (Figure 2.45(a)). Median transmissibilities to the pelvis motion in the pitch direction showed a 'broad resonance' at around 11 Hz and a 'smaller peak' at 7 Hz with a vibration magnitude of 0.25 ms^{-2} r.m.s. (Figure 2.45(b)). These peak frequencies decreased to 9 and 5 Hz, respectively, with increases in the vibration magnitude to 2.5 ms^{-2} r.m.s.

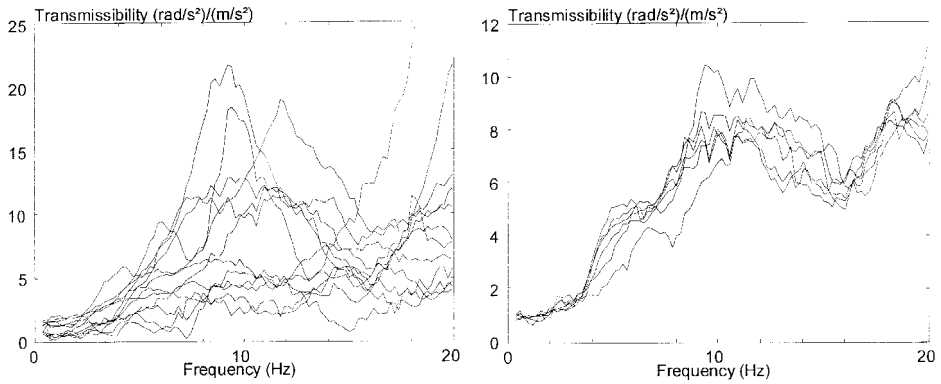

(a) (b)

Figure 2.45 Seat vertical to pitch of the pelvis transmissibility. After Mansfield (1998). (a) variability for twelve subjects measured at 1.0 ms^{-2} r.m.s., (b) median data for twelve subjects at 0.25, 0.5, 1.0 1.5, 2.0, 2.5 ms^{-2} r.m.s.

Mansfield and Griffin (1997) and Mansfield (1998) also obtained the transmissibility to the pelvis pitch motion of seated subjects in several different body postures in a separate study. Individual transmissibilities showed a peak in the frequency range between 10 and 18 Hz, although differences between subjects were observed. It was concluded that 'in comparison with the 'upright posture', no condition showed a significant difference in the 4 to 6 Hz frequency range, implying that changes in pelvis rotation do not contribute greatly to the variation in the apparent mass at resonance caused by postural changes'. Significant differences in the transmissibility to the pelvis pitch motion between different postures were found in higher frequency range, such as between 'upright' and 'posterior lean' postures in the frequency range of 14 to 17 Hz.

2.4.4 Dynamic response of the viscera

2.4.4.1 Basic anatomy of the viscera and trunk cavities (extracted from Dean and Pegington, 1996b)

'Viscera' is a general term for the internal organs, such as the heart, lungs, stomach, and liver, which are contained in the thoracic, abdominal and pelvic cavities of the human body. The bones of the thoracic walls consist of the vertebral column behind and of twelve pairs of ribs both posteriorly and at the sides and the sternum in front. The intercostal muscles fill the spaces between ribs. The thoracic cavity is closed off below by a domed muscle called the diaphragm and is closed over by a thin

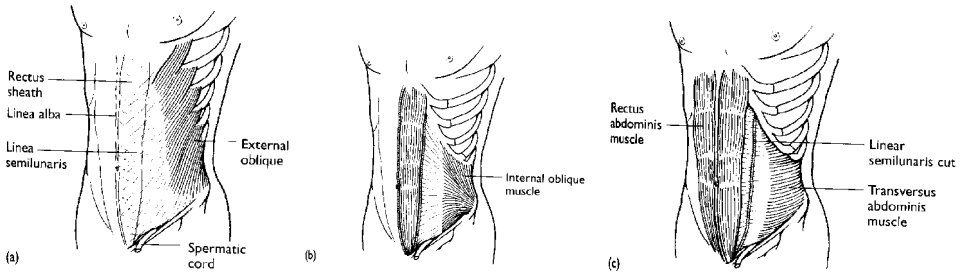

Figure 2.46 Muscles of the anterior and lateral abdominal wall. The rectus abdominis muscle is a strap-like muscle that lies on each side of the midline. After Dean and Pegington (1996b).

membrane called the suprapleural membrane. The main contents in the thoracic cavity are the heart and lungs. The lungs occupy large volume in the thoracic cavity but has relatively light mass.

The abdominal cavity is separated from the thoracic cavity by the diaphragm above, but it is in continuity with the pelvic cavity below. The pelvic cavity is in turn limited by the pelvic diaphragm. The abdominal cavity is bounded by muscular walls at the front, sides and back. The muscles of the anterior and lateral abdominal wall fill the space between the costal margin of the rib cage above and the iliac crest of the pelvis below (Figure 2.46). The rectus abdominis muscle runs from the pubic symphysis and pubic crest below to the margins of the costal cartilages. The rectus abdominis flexes the trunk. The erector spinae muscles are the principal agonists of the rectus abdominis muscles. The internal organs such as the liver and gastrointestinal tract are contained in the abdominal cavity.

2.4.4.2 Results from previous studies

The dynamic response of the visceral part of the upper-body exposed to whole-body vibration has been investigated in some previous studies. There has been difficulties in measuring the motions of the viscera that is a ‘soft’ structure. The definition of the viscera even may vary between investigators. Previous studies presented in this section are, therefore, restricted to those in which the motion of the visceral part of the body exposed to whole-body vibration was measured by transducers mounted on the abdominal wall.

Coermann *et al*. (1960) measured accelerations in the vertical direction at some locations on the abdominal wall of supine subjects exposed to longitudinal sinusoidal vibrations (i.e., horizontal vibrations). The axis of input vibration relative to the human body was the same as that of the vertical motion for standing and seated subjects. Accelerometers were mounted by adhesive tape on the abdominal wall of the subjects who 'rigidly' secured to the shaker table in the frequency range of interest. The transmissibility from the longitudinal input motion to the abdominal displacement response showed a distinct peak at about 3 Hz.

Kitazaki (1994) measured the vertical motion at the abdominal wall at the level of the second lumbar vertebra of seated subjects. An accelerometer attached to a 'stiff card' was attached to the skin by double-sided adhesive tape. The data correction method for the surface measurement developed for the measurement for the motion of the skeleton was applied. The mean transmissibilities to the vertical visceral motion obtained from eight subjects in three postures were presented in Figure 2.47. A principal peak was observed at 5 to 6 Hz in the mean transmissibilities for all three postures. The peak magnitude was greater than those found in the transmissibilities obtained over the spine (see Figure 2.25).

Similar measurement method was used by Mansfield (1998) and Mansfield and Griffin (1999) to measure the motions on the abdominal wall in the vertical and fore-and-aft

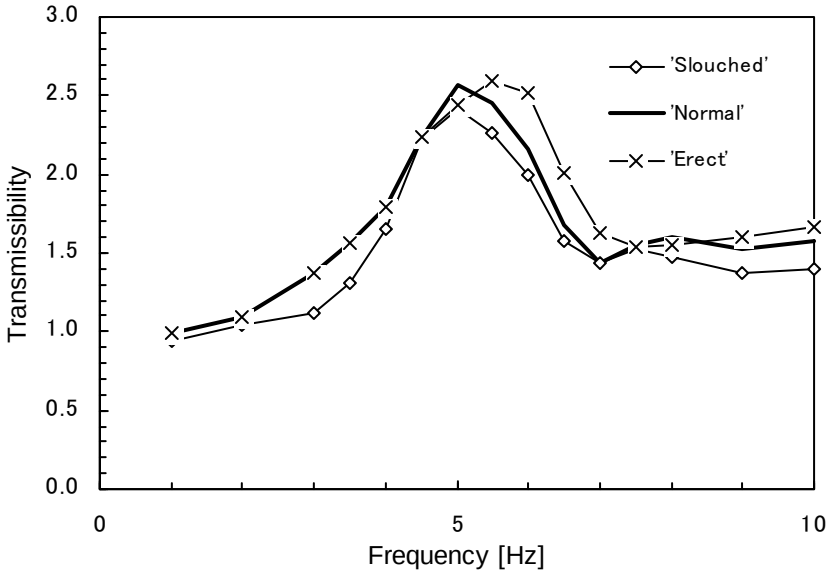

Figure 2.47 Mean vertical transmissibility to the abdominal wall (viscera) of eight seated subjects in 'slouched', 'normal' and 'erect' postures from Kitazaki (1994).

directions of seated subjects exposed to vertical seat vibration. The measurements were made at 20 mm above and below the navel in the two axes. It was stated that for the transmissibilities to the lower location on the abdominal wall, ‘there was evidence of a resonance for both fore-and-aft and vertical directions at approximately 6 Hz’ (see Figures 2.19 and 2.26). For the upper location, a primary resonance was also found at about 6 to 8 Hz in both vertical and fore-and-aft directions with greater transmissibilities than those at the lower location. The transmissibilities to the abdominal wall at about 6 Hz, about 1.7 for the fore-and-aft motion at the lower location to about 4.0 for the vertical motion at the upper location in the median data, were found to be much greater than the transmissibilities simultaneously measured at L3 and the pelvis (see Figures 2.19 and 2.26).

2.4.5 Dynamic response of the whole upper body - modal analysis

The modal analysis technique is a common method to investigate and represent the dynamic characteristics of a mechanical structure. The dynamic properties of the structure are described by natural frequencies, modal damping ratios and mode shapes. The experimental modal analysis is a method to extract those dynamic properties from the measurements of transfer functions of the structure at various locations. The modal analysis technique is well documented in various literature, such as Ewins (1984).

The experimental modal analysis was applied to the apparent mass and transmissibility data of the seated human body by Kitazaki (1994) and Kitazaki and Griffin (1998). The measurements were made at the head, five locations over the spine, the pelvis and on the abdominal wall with eight male subjects. Eight vibration modes were extracted below 10 Hz, as shown in Figure 2.48. It was concluded that ‘a principal resonance of the human body at about 5 Hz consisted of an entire body mode, in which the skeleton moved vertically due to axial and shear deformations of buttocks tissue, in phase with a vertical visceral mode, and a bending mode of the upper thoracic and cervical spine’. The next higher mode located close to the principal mode, at 5.6 Hz as opposed to 4.9 Hz for the principal mode, consisted ‘a bending mode of the lumbar and lower thoracic spine’ ‘with a pitching mode of the head’. Three higher modes including ‘pitching modes of the pelvis and a second visceral mode’ were stated to contribute to the second resonance of the apparent mass at about 8 Hz.

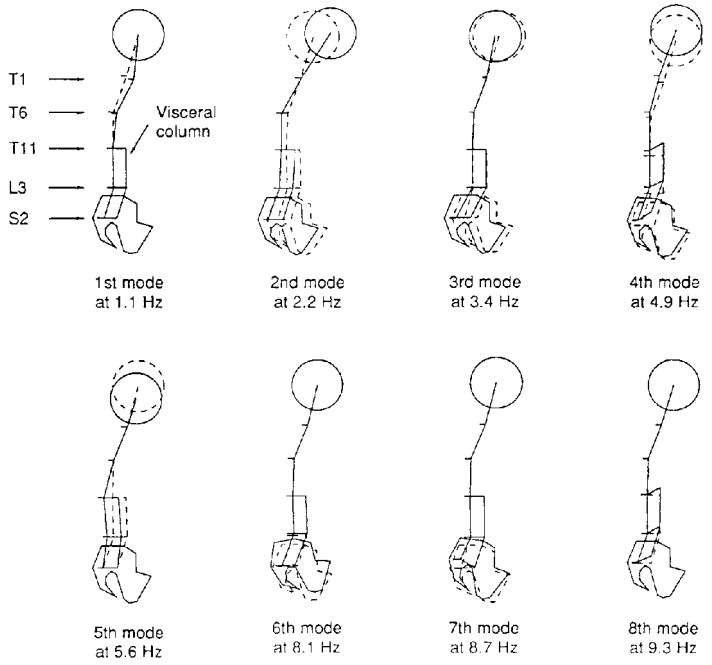

Figure 2.48 Vibration modes in a 'normal' posture extracted from mean transfer functions of eight subjects below 10 Hz (———) and initial posture (- - - -) from Kitazaki (1994) and Kitazaki and Griffin (1998).

With respect to the effect of posture, it was found that shear deformation of buttocks tissue increased in the entire body mode due to postural change from erect to slouched.

2.5 MATHEMATICAL MODELS OF THE BIODYNAMIC RESPONSE TO VERTICAL WHOLE-BODY VIBRATION

In parallel with experimental studies mentioned in the previous sections, mathematical modelling has been another major approach to investigating the dynamic responses of the human body to whole-body vibration. The modelling work, in general, has two main objectives: (1) to obtain a theoretical insight into phenomena observed either in real situations or in laboratory experiments, and (2) to predict what is going to happen to the object modelled in various situations, for example, in a hazardous condition which is not feasible to be produced in a laboratory for safety, financial, ethical, or some other reasons. The most successful biodynamic model should be one that responds to external disturbances of any type, of any direction, and of any level of magnitude in the same way that the human body behaves. That might, however, be too ambitious because the structure of the human body is far too complicated to model precisely. The properties of each body segment are difficult to obtain for use in determining model parameters, particularly for living bodies. Simplification in modelling, based on reasonable assumptions, is therefore required.

The models suggested in early studies tended to be the simplest so that just a single aspect of the dynamic response, such as the driving-point impedance or the transmissibility to the head, was modelled. This may be partly because there had been rather simple measurements of the biodynamic responses for comparison with models and partly because no powerful tools for complicated computation were available. Lumped parameter models with a couple of degrees of freedom, or simple continuum models, for example, a uniform straight rod with a mass at one end, were mainly used in the studies in this period. Analytical solutions of a set of equations of motion, rather than numerical solutions, tended to, or had to, be sought. Although the simplest models could represent a particular aspect of the dynamic response which they were intended to model, they could be used neither to explain nor to predict the other aspects. The representation of the anatomy was poor in the simplest models.

Owing to the development of hardware for improved computation and a wide range of experimental results in recent years, more sophisticated models were developed by some researchers. Lumped parameter models have been extended to those with more degrees of freedom than in the early studies so that the masses of the models could be thought to correspond to particular body parts, such as the head, the torso and the

abdomen. Finite element models which can more faithfully reflect the anatomy have also been developed, although some simplification is still required. The elements of the finite element models have usually represented smaller segments of the body, such as the vertebrae and the connective tissues. Both types of model are similar in that the discretization of the body is required in constructing the model. The lumped parameter model, therefore, could be thought to be a simplified finite element model. Finite element models have usually been constructed either in two or three dimensions, while most of the lumped parameter models have been one dimensional.

The extent of simplification in modelling the dynamic response of the body depends on what aspects are to be investigated, or to be predicted, by a model. If the purpose of modelling was just to have something that provided a similar driving-point response to that of the human body, lumped parameter models with single or two degrees of freedom could be sufficient, according to the experimental results presented in the previous section. There have been several models of this type suggested in previous studies. However, if the mechanisms of the dynamic responses of the body are of interest, more complicated models which represent the anatomy are required.

Some principal models for the biodynamic responses to vertical whole-body vibration suggested in previous studies are tabulated in Table 2.9, most of which have been reviewed elsewhere (Yoganandan *et al*., 1987; Kitazaki, 1994). Among the models in Table 2.9, those which have been compared and validated with experimental data on the dynamic response of the body are reviewed in this section. Most of the continuum models in Table 2.9 (e.g. Krause and Shirazi, 1971; Li and von Rosenberg 1974) are not covered in this section because of the lack of validation, although the assumptions used to construct the models might be reasonable to represent some aspects of the dynamic response of the body. The models reviewed in this section are classified into three groups by the type of experimental data with which they have been correlated: (1) models correlated with the driving-point response, (2) models correlated with the vibration transmission to the head or other location, and (3) comprehensive models.

Table 2.9 Summary of some principal mathematical models of the dynamic response of the body in previous studies.

Authors (year)	Type	Descriptions	Validation with dynamic response
Latham (1957)	Lumped parameter SDOF Vertical Seated body	'Double-mass spring-coupled system' Masses = person, seat Spring = stiffness of person and seat	Acceleration at seat and hip (centre of gravity of body)
Hess and Lombard (1958)	Continuum Vertical Spine	Homogeneous elastic rod Free top end	Comparison between acceleration at free end and acceleration at head
Payne (1965, 1969)	Lumped parameter SDOF Vertical	Mass = head and upper torso Spring = spine Damper = distributed damping in spine and tissue Dynamic Response Index (DRI)	Mechanical impedance
Liu and Murray (1966)	Lumped parameter SDOF Continuum Vertical Spine	Lumped parameter model • Linear and nonlinear spring Continuum model • 'Uniform homogeneous elastic rod' = spine • Mass at top end = head	None
Toth (1966)	Lumped parameter 8 DOF Vertical Lower spine	T11 through L5 Nonlinear stiffnesses and dampings	None
Terry and Roberts (1968)	Continuum Vertical Spine	Uniform viscoelastic rod	Comparison between acceleration at top end and head acceleration
Suggs *et al*. (1969)	Lumped parameter 2 DOF Vertical Seated body	2 uncoupled masses suspended from a frame Lower mass = pelvis and abdomen Upper mass = head and chest	Mechanical impedance
Vulcan and King (1970)	Lumped parameter 4 DOF 2 dimension Seated body	Head rotation Torso rotation Compression of spring supporting head Compression of spring supporting torso	Forces and bending moments at lower vertebral column (Comparison with experimental data from cadavers)

Table 2.9 (continued) Summary of some principal mathematical models of the dynamic response of the body in previous studies.

Authors (year)	Type	Descriptions	Validation with dynamic response
Hopkins (1971)	Lumped parameter 2 DOF Vertical Nonlinear Seated body	2 models with 3 coupled masses • Linear spring and damper with nonlinear geometry of visceral mass motion • Nonlinear effect of lung = piston in cylinder with orifice	Mechanical impedance for nonlinear geometry model Mechanical impedance of pig for nonlinear dynamic model
Kaleps *et al*. (1971)	Lumped parameter 5 DOF Vertical Seated body	Pelvis, abdomen, torso, chest wall, respiratory gas Scaling: to relate 'to geometrically similar primate differing only in total mass'	Mechanical impedance
Krause and Shirazi (1971)	Continuum 2 dimension Lumbar spine	Curved beam = lumbar spine Mass at top end = thorax	None
Li *et al*. (1971)	Continuum 2 dimension Spine	Sinusoidally curved elastic column with end mass Constant cross section cf. Moffatt *et al*. (1971)	None
Moffatt *et al*. (1971)	Continuum 2 dimension Spine	Sinusoidally curved elastic beam with end mass cf. Li *et al*. (1971)	None
Orne and Liu (1971)	Discrete 2 dimension Axial, shear, bending Spine	Vertebrae = rigid bodies (3 DOF), 25 masses Viscoelastic solid for axial axis Elastic solid for shear and bending axes Curved shape of spine Eccentric inertial loading by head and trunk	None
Payne and Band (1971)	Lumped parameter 4 DOF Vertical Linear and nonlinear	Pelvis mass and buttocks spring Upper torso mass and spine spring Viscera mass supported from upper torso mass Head and neck Nonlinearity for spine and buttocks stiffnesses	Mechanical impedance

Table 2.9 (continued) Summary of some principal mathematical models of the dynamic response of the body in previous studies.

Authors (year)	Type	Descriptions	Validation with dynamic response
Rybicki and Hopper (1971)	Continuum Vertical Spine, head	Two-phase solid-fluid continuum model Effect of porosity and fluid of spine Uniform straight porous elastic column Head mass	None
Shirazi (1971)	Continuum Vertical Spine, head	Nonlinear elastic rod More rigid toward base Uniform density Mass at top end	None
Liu and von Rosenberg (1974)	Continuum 2 dimension Spine	Curved beam-column model cf. Li *et al*. (1971), Moffatt *et al*. (1971)	None
Muksian and Nash (1974)	Lumped parameter 6 DOF Vertical Nonlinear Seated body	7 masses = head and atlas, vertebral column, thoracic cage, heart and lungs, diaphragm, abdominal viscera, pelvis and legs Nonlinear stiffness and damping in torso Coulomb friction forces	Transmissibility to head
Prasad and King (1974)	Discrete 2 dimension Seated body	Vertebral bodies, head, pelvis = rigid bodies (3 DOF) Intervertebral discs = springs and dampers in 3 axes Facets and laminae = springs Eccentricity of torso weight Spinal curvature	Force between adjacent vertebral bodies (Comparison with experimental data from cadavers)
Muksian and Nash (1976)	Lumped parameter 2 DOF Vertical Nonlinear Seated body	3 masses = head, body, pelvis and legs Nonlinear damping forces Linear stiffness	Transmissibility to head Transmissibility to shoulder

Table 2.9 (continued) Summary of some principal mathematical models of the dynamic response of the body in previous studies.

Authors (year)	Type	Descriptions	Validation with dynamic response
Belytschko *et al*. (1976, 1978, 1985) Belytschko and Privitzer (1978a, b) Privitzer and Belytschko (1980) Privitzer *et al*. (1982) Williams and Belytschko (1981, 1983)	Finite element 3 dimension Seated body Spine, torso, head	Several models with different levels of sophistication Vertebrae, pelvis, head, ribs = rigid bodies Ligaments, cartilageneous joints, connective tissues = deformable elements (spring, beam) Viscera = hydrodynamic element Linear and nonlinear material properties	Mechanical impedance Comparison between simulation of dynamic deformation of spine exposed to vertical impact acceleration and experiment on primates
Cramer *et al*. (1976)	Continuum 2 dimension Spine	Curved homogeneous beam-column Rigid mass at top end Eccentric inertial loading of torso	Comparison between moment distribution and spinal injury statistics
Mertens and Vogt (1978)	Lumped parameter 5 DOF Vertical Seated body	5 masses = legs resting on seat, buttocks, abdominal system, chest system, head Spine = 3 linear springs and dampers (C1-C7, T1-T12, L1-S1)	Mechanical impedance Transmissibility to head (Under different levels of static accelerations)
Radons *et al*. (1979)	Finite element 2 dimension Spine, torso, head	Vertebrae, head = rigid bodies Intervertebral discs = finite beam elements Internal organs and flesh = elastic substrate Muscles and ligaments = springs Ribs = curved beam elements	Frequency response function between input excitation at L1 and response at T1
International Standard 5982 (1981)	Lumped parameter 2 DOF Vertical Standing and seated	Two masses supported by a common rigid structure Two sets of parameters for standing and seated bodies	Mechanical impedance
International Standard 7962 (1987)	Lumped parameter 4 DOF Vertical Standing and seated	4 masses interconnected by linear springs and dampers Top mass = head	Transmissibility to head

Table 2.9 (continued) Summary of some principal mathematical models of the dynamic response of the body in previous studies.

Authors (year)	Type	Descriptions	Validation with dynamic response
Nigam and Malik (1987)	Lumped parameter 15 DOF Vertical Standing body	Ellipsoid segments truncated at ends Damping properties were ignored	None
Amirouche and Ider (1988)	Lumped parameter 3 dimension Seated body	13 rigid bodies interconnected by spherical, revolvable and free joints Linear and nonlinear stiffnesses and dampings	Transmissibility to middle torso Transmissibility to head
Amirouche *et al*. (1994)	Lumped parameter 12 DOF Vertical Standing and seated	12 masses interconnected by linear springs and dampers Symmetric Optimisation of damping and stiffness of shoes or seat	None
Kitazaki (1994) Kitazaki and Griffin (1997)	Finite element 2 dimension Seated body	Spinal column (C1 to S1) = spinal masses interconnected by beam elements Head, torso, visceral, pelvis masses Buttocks tissue = 2 beam elements 87 master degrees of freedom	Apparent mass Transmissibilities to several parts of body Modal properties
Pankoke *et al*. (1998)	Finite element 2 dimension Seated body	Lower lumbar spine = 3 masses for L3, L4, L5 Head, neck, upper torso, upper arms, forearms, pelvis, thighs, lower legs, feet = rigid masses Linear stiffness, modal damping	Mechanical impedance Transmissibility to head Time history of force between seat and pelvis
Wei and Griffin (1998)	Lumped parameter SDOF and 2 DOF Vertical Seated body	4 models • Single DOF with and without rigid support structures • 2 DOF with and without rigid support structures	Apparent mass

2.5.1 Mathematical models correlated with the driving-point response

The first model which correlated with measured driving-point response might be the one suggested by Payne (1965 and 1969). A lumped parameter model with two degree-of-freedom, one for the human body and another for a seat cushion, was derived so as to predict the potential of spinal injuries during a pilot ejection from aircraft (Figure 2.49). A mass of the human body model was stated to represent the head and upper torso, which was supported by a spring representing the spine and a damper representing 'distributed damping in the spine and associated tissues'. A cushion of an ejection seat was modelled by massless spring and damper. It was suggested that the damping parameters of the human body model could be determined by comparing calculated mechanical impedance with measured mechanical impedance because the measurement of the mechanical impedance was 'probably the simplest and the most accurate'. A dynamic response index (DRI) which provided a single number related with the peak stress in the spine was suggested using the model so as to predict the potential of spinal injuries.

$$DRI = k\delta_{\max} / m = \omega^2 \delta_{\max} \tag{2.7}$$

where k and m are the spring constant and the weight of the mass of the human body model, respectively. $\omega = \sqrt{k/m}$ is the natural angular frequency of the human body model. $\delta_{\max}$ is the maximum deflection of the spinal spring. Therefore, $k\delta_{\max}$ corresponds to the peak force in the spine induced by an excessive acceleration during an ejection. Upon assuming that the cross sectional area of the spine was proportional to the effective mass of the person, Equation (2.7) could be considered to be proportional to the peak stress in the spine. The natural angular frequency of $\omega = 52.9$ rad/s (8.42 Hz)

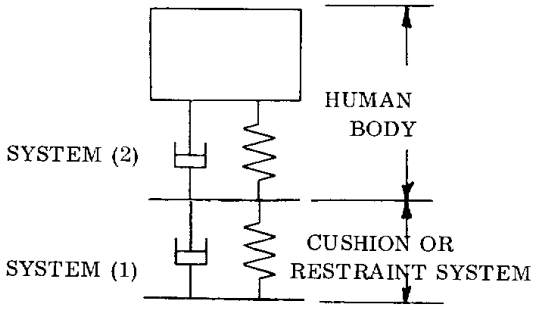

Figure 2.49 A two degree-of-freedom model of the seated human body and the seat by Payne (1965, 1969).

and the damping ratio of $\varsigma = 0.2245$ were used in calculation of the maximum deflection $\delta_{\max}$ to given seat accelerations. It was reported that the DRI was found to give a reliable prediction of the spinal-injury potential of various rocket/catapult accelerators used in aircraft and was used as a standard tool in the design of ejection seats in the U.S. Air Force in that period.

Suggs *et al*. (1969) proposed a two degree-of-freedom lumped parameter model with the aim of building a standardised vehicle seat testing procedure. As shown in Figure 2.50, the model consisted of two uncoupled masses which were suspended from a rigid frame. It was stated that the larger lower mass represented the pelvis and the abdomen while the upper mass represented the head and chest, although these two masses were parallel so that the position of the masses did not affect the response of the model. The frame was considered to be analogous to the spinal column. The parameters of the model was derived from the comparison between the mechanical impedance calculated by the model and the mechanical impedance of eleven males sitting in a 'natural upright position' measured by the authors. The mean measured mechanical impedance showed a primary resonance at about 4.5 Hz and a lower secondary resonance at about 8 Hz. The model parameters that might have been derived from the mean mechanical impedance were presented, which corresponded to two damped natural frequencies of 4.9 Hz and 6.1 Hz. A mechanical model with two degrees of freedom was also constructed, which gave a similar mechanical impedance curve to that of the mean of eleven subjects measured.

Two nonlinear lumped parameter models having three masses with two degrees of freedom were proposed by Hopkins (1971) for the seated body. Three masses were thought to be the representations of the 'upper torso', 'lower torso' and 'viscera'. In his

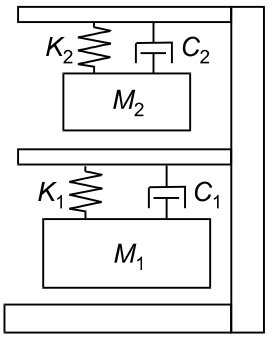

Figure 2.50 A two degree-of-freedom model of the seated human body by Suggs *et al*. (1969).

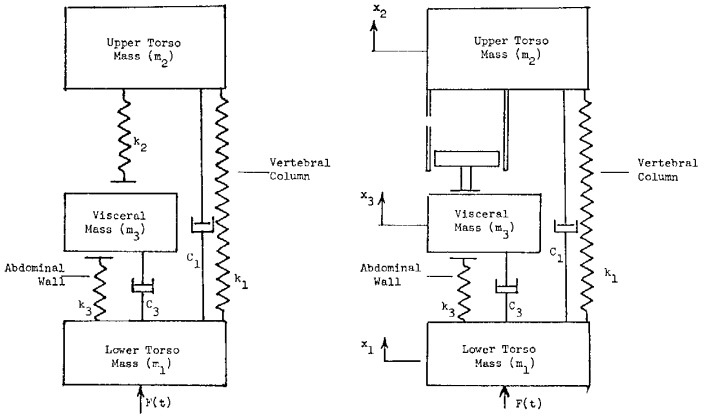

(a) (b)

Figure 2.51 Two degree-of-freedom nonlinear models by Hopkins (1971): (a) nonlinear geometry model, and (b) nonlinear model.

first model, a ‘nonlinear geometry’ of the visceral organs during vibration was taken into account: ‘the visceral organs were not tethered but were supported in the abdominal cavity by the abdominal muscle wall, the pelvis, and the diaphragm’ so that they would not put any tension on the organs located behind the visceral organs when moving in a certain direction. This nonlinearity was modelled by linear springs which were not rigidly attached to the visceral mass (Figure 2.51(a)). The ‘nonlinear geometry model’ was found to be able to reproduce the mechanical impedance and the phase of the human body measured by Coermann (1962) adequately. It was stated that the nonlinear geometry model showed an independence of the magnitude of input vibration, although nonlinearity with respect to the magnitude of input vibration in the mechanical impedance of pigs was observed by Krause and Lange (1967). The second nonlinear model was, therefore, constructed so as to investigate the dynamic response of pigs at greater magnitude of vibration. The nonlinear effects of the lungs was included in the nonlinear geometry model ‘by modelling them as a piston in a cylinder with an orifice’ (Figure 2.51(b)). It was shown that the mechanical impedance curve became flatter with an increase in the magnitude of input vibration.

Kaleps *et al*. (1971) constructed a linear five degree-of-freedom lumped parameter model so as to simulate thoracic, abdominal and spinal response to various dynamic environments: impact, vibration, blast, acoustic fields. Five masses in the model were stated to correspond to the ‘pelvis’, ‘abdomen’, ‘torso’, ‘chest wall’ and ‘respiratory gas’ (Figure 2.52). The thorax was ‘simulated by an air-filled cavity with the abdomen, chest wall, and airway to the mouth acting as pistons’ so that these masses were coupled by the ‘gas pressure’. It was stated that model parameters were ‘selected as a compromise from segmental and whole body dynamic and static measurements, other lumped

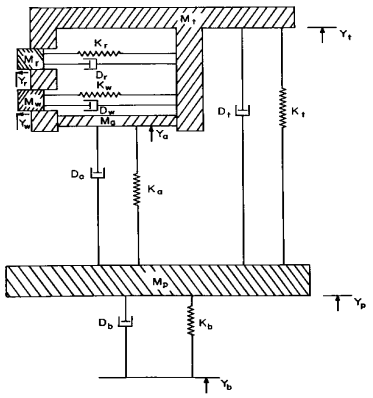

Figure 2.52 A five degree-of-freedom model by Kaleps *et al*. (1971).

parameter models, and the requirements for stability and proper behaviour of the present model'. The authors proposed scaling relations for different total weights, which made the dynamic characteristics of the model, such as resonance frequency, dependent on its total weight. The mechanical impedance calculated from the model was compared with unpublished data, which showed a good agreement in the shape of the impedance curve, although the total weight of the model was about a third of that of a subject used in the experiment.

Payne and Band (1971) proposed a four degree-of-freedom lumped parameter model so as to expand the single degree-of-freedom model developed by Payne (1965 and 1969) mentioned above. The model consisted of four parts: the 'pelvic mass' and the 'buttocks spring', the 'upper torso mass' and the 'spine spring', the 'viscera mass' sprung from the upper torso mass, and the 'head mass' and the 'neck spring' (Figure 2.53). Dampings were incorporated with each spring element. The model parameters for each of four parts of the model, i.e. 'the buttock, spinal, visceral and neck modes', were derived from various previous experiments. For some parameters, only a range of reasonable variation determined from the experimental data was assigned because of the difficulty in transferring experimental data with variation or nonlinearity to a single value. A parametric study was, therefore, conducted by varying those parameters and comparing the driving point impedance of the model with those measured in the previous experiments, such as Vogt *et al*. (1968). The weights of each mass, the stiffness for the viscera, and the stiffness and damping for the neck were fixed. The driving point impedance of the linear model with a set of parameters showed a good agreement with the measured data at frequencies below 8 Hz. It was stated that the frequency and magnitude of the first peak of the impedance were largely dependent on the spring and damping parameters of the closest part of the model to the driving point. The model was

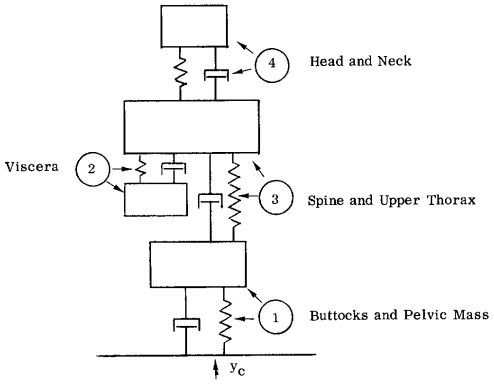

Figure 2.53 A four degree-of-freedom model by Payne and Band (1971).

further expanded by assigning nonlinear properties to the stiffness and damping of the spinal and buttock modes, although sufficient results to validate the model had not been obtained by the authors.

Mertens and Vogt (1978) developed a five degree-of-freedom lumped parameter model of the seated body (Figure 2.54). The five masses represented the ‘head’, ‘chest’, ‘abdomen’, ‘buttocks’ and ‘legs resting on the seat’ whose weights were determined from the anthropometric measurements. Some stiffness parameters, such as one hanging the abdominal mass, were derived from the experimental data in the literature. The other stiffness and all damping parameters were determined by comparing the driving point mechanical impedance and the transmissibility from the seat to the head of the model with those measured in experiments at a small vibration magnitude (0.3 g). Another three sets of parameters were obtained for increased static accelerations, 2, 3 and 4 g, by varying the stiffnesses and dampings so as to provide the nonlinearity in the mechanical impedance and in the transmissibility to the head found in the experiment with different static vertical accelerations (Mertens, 1978). The model was intended to be used to simulate situations where the human body was subjected to a great magnitude of vertical

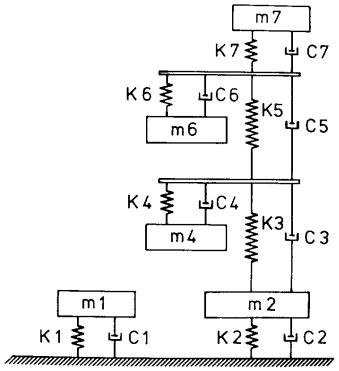

Figure 2.54 A five degree-of-freedom model by Mertens and Vogt (1978).

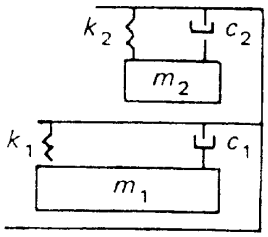

Figure 2.55 A two degree-of-freedom model correlated with the driving point mechanical impedance of the human body in standing and sitting positions proposed in International Standard 5982 (1981).

impact or pulse, although the model parameters were based on the experimental data obtained in steady state environments. The stiffnesses and dampings were doubled compared with those with the static acceleration of 4 g in the simulations.

Three lumped parameter models for calculating the driving point impedances of the human body in standing, sitting, and supine positions have been presented in the International Standard 5982 (1981). A two degree-of-freedom model whose two masses are supported by a common rigid structure is used for the standing and sitting bodies (Figure 2.55). Two sets of model parameters are assigned to standing and sitting bodies, respectively, by comparing with experimental values obtained from available literature. Results from five subjects were used in deriving the parameters for the standing body whereas those from 39 subjects were used for the sitting body.

Lin and Griffin (1998) developed alternative models of the vertical apparent mass of the seated body for predicting seat transmissibility. Four lumped parameter models, 2 single degree-of-freedom models and 2 two degree-of-freedom models (Figure 2.56), were used to seek optimum parameters for the mean apparent masses of 60 people measured by Fairley and Griffin (1989). Single degree-of-freedom and two degree-of-freedom models with rigid support structures provided the ‘best fits’ to the mean measured apparent mass and phase. These two models were, therefore, used to obtain optimum parameters for each subject, including adult males, adult females and children. The model parameters showed large variability between different individuals, although the mean parameters of the two adult groups of subjects were found to be similar. The two degree-of-freedom model was found to provide ‘a better fit to the phase’ ‘at frequencies greater than about 8 Hz’ and ‘an improved fit to the modulus’ ‘at frequencies around 5 Hz’. It was concluded that ‘the two degree-of-freedom model provided an apparent mass similar to that of the human body, but this does not imply that the body

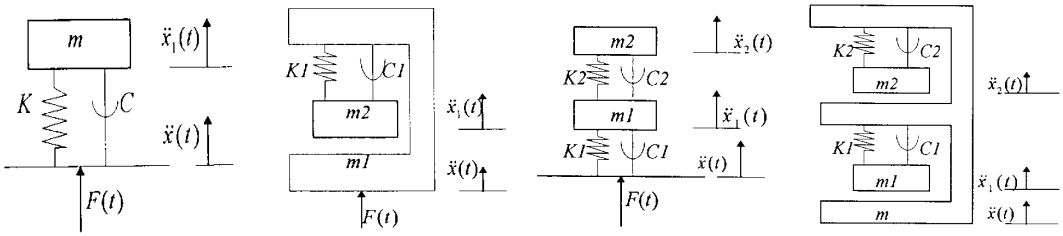

(a) (b) (c) (d)

Figure 2.56 Lumped parameter models of the driving point apparent mass by Lin and Griffin (1998). (a) Single degree-of-freedom model, (b) single degree-of-freedom model with support structure, (c) two degree-of-freedom model, and (d) two degree-of-freedom model with support structure.

moved in the same manner as the masses in the optimised two degree-of-freedom model'.

2.5.2 Mathematical models correlated with the vibration transmission to the head or other location

Earlier than Payne (1965) mentioned in the previous section, the first mathematical model that correlated with the vibration transmission through the human body was developed by Latham (1957). Pilot ejection situations with different cushions were investigated using a 'double-mass spring-coupled' lumped parameter model which represented the human body and the ejection seat (Figure 2.57). Acceleration responses of the mass representing the human body to a step function disturbance in the time domain were compared with accelerations measured at the hip, which was considered as the centre of gravity of the body, in 'seat-drop experiments' conducted by the authors. The calculated acceleration time histories showed good agreements with the experimental results, although large overshoots observed in measured accelerations were not reproduced by the model.

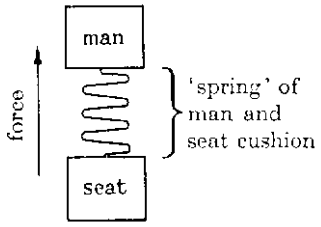

Figure 2.57 A single degree-of-freedom model by Latham (1957).

Hess and Lombard (1958) also proposed a model for the investigation of a pilot ejection from military jet aircraft. As ‘the simplest possible model’, a homogeneous elastic straight rod (i.e. continuum model) was used so as to model the human upper-body. One end of the model, which was considered as the head, was free while the other was subjected to a ‘prescribed acceleration in the direction of its length’. No damping properties were included in the model. The calculated acceleration at the free end of the model was fitted to experimental data recorded at the head of subjects in ‘ejection seat tests’ conducted by the authors. ‘The acceleration at points of the rod’ depended on only ‘the time required for a stress or acceleration wave to travel the length of the rod’ which was optimised. It was shown that ‘the best fits were obtained for approximately the same value of time of wave travel, about 0.025 seconds’. It was suggested that ‘the degree of approximation of the model could be improved’ ‘by the addition of damping’.

Terry and Roberts (1968) used a uniform rod of a ‘viscoelastic medium’ to model the dynamic response of the spine so that the model proposed by Hess and Lombard (1958) was improved by adding damping properties, as they recommended. The model was subjected to a ‘ramp input acceleration pulse’ at one end. ‘The resulting acceleration at the far end of the rod’ was compared with the acceleration at the head obtained in experiments. The elasticity and viscosity of the model were adjusted so as to minimise the error between the theoretical and experimental head acceleration curves. ‘The values of the theoretical curves closely matched the experimental ones for low acceleration level’ while ‘the difference between the theoretical and experimental curves’ increased ‘as the acceleration level increased’. The use of nonlinear properties for both the elasticity and the viscosity of the model was recommended for further modifications of the model.

Muksian and Nash (1974) developed a six degree-of-freedom lumped parameter model which was correlated with the transmissibility to the head of seated subjects measured by Goldman and von Gierke (1961) and Pradko *et al*. (1965, 1967). Seven masses represented the ‘head’, ‘vertebral column’, ‘thoracic cage’, ‘heart and lungs’, ‘diaphragm’, ‘viscera’, and ‘pelvis and legs’, respectively (Figure 2.58). The weight of each mass was determined by some literature on the anthropometry and anatomy of the body. Linear springs and viscous dampers were used to represent the stiffness and damping in the vertebral column while those in the other part of the body were modelled by nonlinear cubic springs and dampers. In addition, the longitudinal forces and the muscle contraction at the ‘gliding joints between the ribs and vertebrae’ were represented by a Coulomb friction force. The forces acting on the thorax due to the ‘heartbeat’ and those

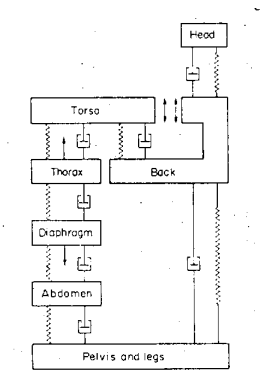

Figure 2.58 A six degree-of-freedom nonlinear model by Muksian and Nash (1974).

acting on the diaphragm due to the 'respiration' were also included in the model. The calculated transmissibility to the head by the model showed a good agreement with the experimental results at frequencies below 8 Hz with a set of damping coefficients originally estimated by the authors. The agreement between the calculated and measured transmissibilities were improved with greater damping coefficients. It was stated that the damping properties of the human body might be frequency dependent, which was also supported by their preliminary study using a two degree-of-freedom nonlinear model (Muksian and Nash, 1976).

International Standard 7962 (1987) presents a four degree-of-freedom lumped parameter model which are correlated with the transmissibilities to the head obtained from available literature. The experimental data are related to approximately 50 subjects, in general, in an upright standing or sitting position. It is stated that 'the experimental data indicated that the transmissibility curves for sitting and standing positions (standing erect) were essentially the same'. A common model is, therefore, presented for calculating the transmissibilities to the head in both standing and sitting positions (Figure 2.59). The top mass is considered to correspond to the head and the transmissibility to that mass is correlated with the transmissibilities to the head measured in experiments.

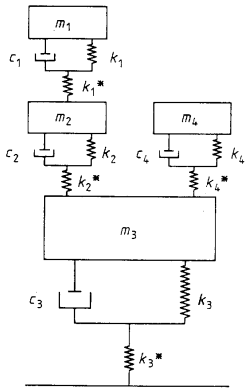

Figure 2.59 A four degree-of-freedom model correlated with the transmissibility to the head proposed in International Standard 7962 (1987).

2.5.3 Comprehensive mathematical models

Three dimensional discrete element models of the seated human body with several extents of complexity were developed by Belytschko and his colleagues (Belytschko *et al*. 1976, 1978, 1985; Belytschko and Privitzer, 1978a, 1978b; Privitzer and Belytschko, 1980; Williams and Belytschko, 1981, 1983; and Privitzer *et al*. 1982). For their most complicated model, the human body was modelled as faithfully as possible by considering each element of the body with the use of the finite element method. In general, the skeletal segments were modelled by rigid bodies while the intervertebral discs were modelled by beam elements with axial, torsional and bending stiffnesses. The stiffnesses could be nonlinear, if required. Spring elements, which could have resistance in tension only, were used to represent the ligaments and articular facets. Hydrodynamic elements, which had a 'linear pressure-dilatation relationship' and a 'linear viscosity' and deform only in the axial direction, were used to model the viscera and the articular facets in the cervical spine. The other connective tissues and cartilaginous joints were also modelled by 'deformable elements'. Inertial, stiffness, and damping properties and geometry of the model elements were derived from various literature.

Three finite element models with different complexity were presented by Belytschko *et al*. (1976), which were named 'isolated ligamentous spine model (ILS)', 'complete spine model', and 'cervical spine model', respectively. The isolated ligamentous spine model, ILS, was consisted of a model of the 'thoracolumbar spine', 'a single beam element' representing the 'cervical spine', the 'pelvis', and the 'head' (Figure 2.60(a)). The vertebral rigid bodies were interconnected by seven spring elements, which represented the ligaments and the connective tissues, and a beam element representing the

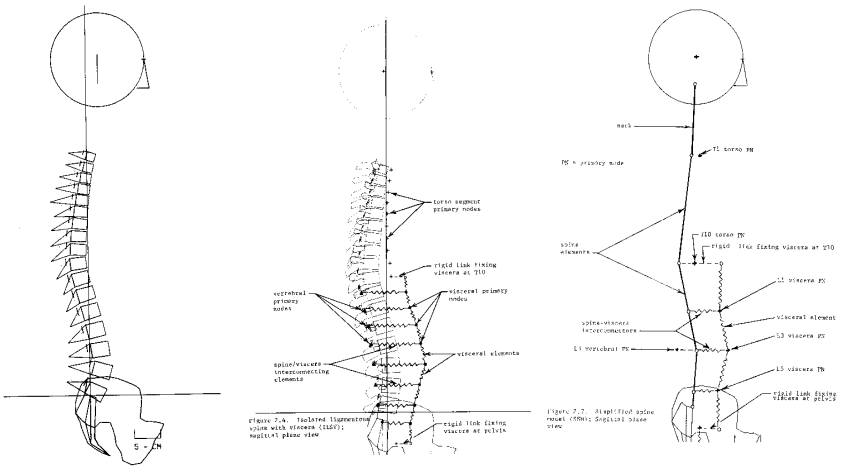

(a) (b) (c)

Figure 2.60 Three discrete models of the spine by Belytschko *et al*. (1976), Belytschko *et al*. (1978), Belytschko and Privitzer (1978a, b): (a) ‘isolated ligamentous spine model’, (b) ‘isolated ligamentous spine with viscera’, and (c) ‘simplified spine model’.

intervertebral disc in the model of the thoracolumbar spine. An additional beam element was used to model the ‘stiffness of the torso and ‘rib cage’ for the ILS. Models of the viscera and rib cage were included in the ILS so that the ‘complete spine model’ was constructed. Each rib was modelled by a rigid body which was connected to two vertebral bodies by three deformable elements at one end and to the sternum by a deformable element at another end. The viscera was represented by a ‘stack of hydrodynamic elements’ which was connected to the pelvis at its bottom and to the ribs at the level of T10 at its top. For the cervical spine model, the single beam representing the cervical spine in the ILS was replaced by a complicated model of the cervical spine. The cervical vertebrae modelled by rigid bodies were interconnected by a beam, a spring, and a hydrodynamic element which represented the ‘intervertebral disc’, ‘interspinous ligament’, and ‘articular facet’, respectively. Several simulations and the modal analysis were conducted using the models to investigate the behaviour of the spine under situations with excessive accelerations, although they were not validated with any experimental data on the dynamic response of the body at that stage.

Belytschko *et al*. (1978) and Belytschko and Privitzer (1978a) modified the isolated ligamentous spine model, ILS, by including the representations of the viscera and rib cage which were simpler than those proposed in their previous study (Figure 2.60(b)). The modified model was called ‘isolated ligamentous spine with viscera (ILSV)’. The viscera, which might be a secondary force transmission path through the body, was modelled by a series of masses and springs interconnected to the vertebral bodies. The

weights of each level of the vertebral body below the tenth thoracic vertebra were ‘apportioned between the vertebral body and viscera according to the ratio of the area’ measured in the graphical data of the torso cross-sections. The rib cage was modelled by a series of beams which represented the ‘flexural resistance of the rib cage’. The driving point mechanical impedance of the ILSV was compared with the experimental data by Vogt *et al*. (1968). The mechanical impedance calculated by the ILSV showed two peaks at 6 Hz and 13.5 Hz, compared to at 4.9 Hz and 13.5 Hz in the measured impedance. However, the magnitude of the peaks and the shapes of the calculated impedance curve were substantially different from those obtained in the experiment. The validation of the models with the mechanical impedance measured in the experiment was also reported by Privitzer and Belytschko (1980).

A simplified model was proposed in this series of studies by Belytschko and Privitzer (1978b) (Figure 2.60(c)). The thoracolumbar spine, from the first thoracic vertebra to the sacrum, was divided into three parts at the tenth thoracic vertebra and at the third lumbar vertebra so that each spinal part was modelled by a beam element. The viscera was represented by a series of three masses and four springs placed between the pelvis and the level of the tenth thoracic spine. The stiffnesses of the element in this ‘simplified spine model (SSM)’ were calculated by ‘series combinations’ of the corresponding elements of the ILSV. The comparison between the mechanical impedance of the model and the experimental data implied that an additional spring for the buttocks tissue was required. A vertical spring beneath the pelvic mass was, therefore, included in the models so that the mechanical impedance of both the SSM and ILSV showed good agreement with the experimental data. It was concluded that the first peak in the mechanical impedance in the range between 5 and 7 Hz ‘resulted from a combination of the buttock-seat resonance, the flexural response of the spine and the visceral resonance’.

The improvement and validation of the models mentioned above were sought in their subsequent studies. Privitzer *et al*. (1982) constructed a three dimensional finite element model of the baboon body in the same manner as the development of the models mentioned above. The model was validated by comparing the configuration of the spine of the baboon measured in their drop test and the results of model simulations. The purpose of the study was to validate the models of the human body developed by the authors’ group (Belytschko *et al*. 1976, 1978; Belytschko and Privitzer, 1978a, 1978b; and Privitzer and Belytschko, 1980) on the assumption that the mechanisms of the dynamic response of the primate were similar to those of the human body. The model of

the head and cervical spine was refined by Williams and Belytschko (1981, 1983) by revising the geometric and stiffness data and including a muscle model. A model of the diaphragm was developed by Belytschko *et al*. (1985), which was stated to be able to 'replicate the effects of the secondary $+G_z$ loading path through the viscera-abdominal wall/diaphragm/rib cage system'.

A three dimensional multi-degree-of-freedom model was developed by Amirouche and Ider (1988) by using rotational connections between model masses. Thirteen masses represented the 'head', 'neck', 'upper-torso', 'centre-torso', 'lower-torso', 'upper-arms', 'lower-arms', 'upper-legs' and 'lower-legs' (Figure 2.61). These masses were interconnected by vertical and rotational linear springs and dampers. Each rotational connection was assigned a three dimensional degree of freedom. The model was symmetrical about the mid-sagittal plane so that two dimensional responses would be obtained with pure vertical input stimuli. Stiffness and damping parameters were determined by comparing the calculated vertical and pitch transmissibilities to the middle torso mass and the vertical transmissibility to the head mass using experimental data obtained elsewhere (Coermann, 1962; Pradko *et al*., 1965; Sandover, 1978; Griffin *et al*., 1978; Panjabi *et al*., 1986). Four natural frequencies in the frequency range below 20 Hz were obtained by modal analysis of the model.

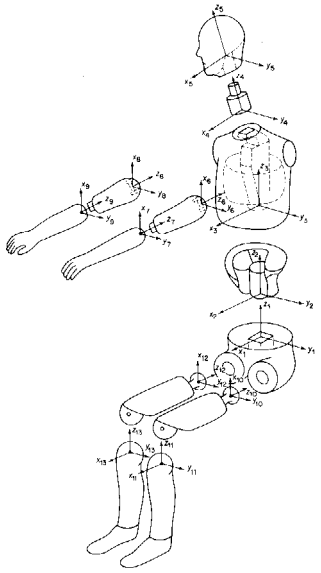

Figure 2.61 Three dimensional 'multi-body' model by Amirouche and Ider (1988).

Kitazaki (1994) and Kitazaki and Griffin (1997) developed a two dimensional finite element model of the seated body in the mid-sagittal plane which was based on the three dimensional models presented by Belytschko and Privitzer (1978) (Figure 2.62(a)). The spinal column from the first cervical vertebra to the sacrum was modelled by 24 beam elements 'representing all the intervertebral discs'. 'Mass elements for the torso' were assigned for each vertebral level. They were located 'anterior to the spine' in the region between the first and tenth thoracic vertebrae, while they were separated into the 'spinal masses' and the 'visceral masses' at the levels below the tenth thoracic vertebra. The mass eccentricity was not considered in the cervical region. The 'visceral masses' which were 'interconnected by spring elements' were connected to the 'spinal beam' at the level of the tenth thoracic vertebra at the top and to the 'pelvic mass' at the bottom by 'massless rigid links'. 'The interaction between the viscera and the spine was modelled by horizontal spring elements interconnecting the visceral masses and the spinal beams'. Two beam elements were used to model the buttocks tissue which allowed 'rotational and fore-and-aft motion of the pelvis'. The head was modelled by a rigid mass which connected to the top of the spinal beam by a beam element 'representing the atlanto-

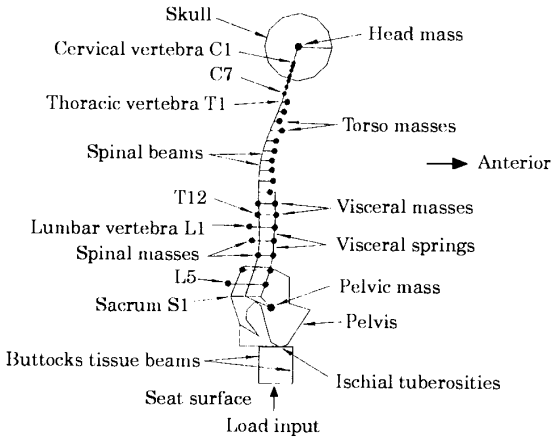

(a)

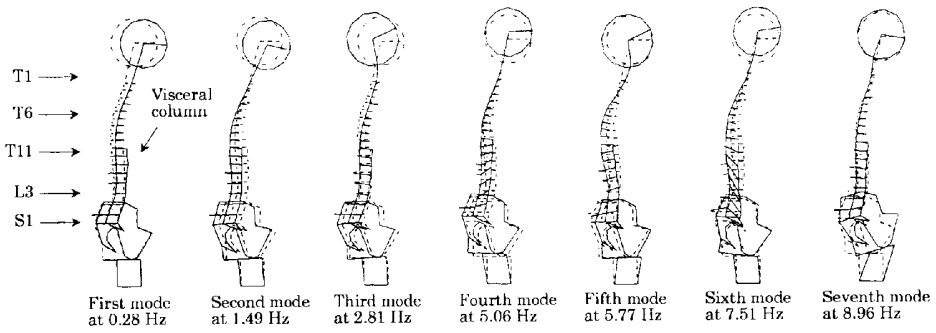

(b)

Figure 2.62 (a) Finite element model of the seated body and (b) calculated mode shapes below 10 Hz by Kitazaki (1994) and Kitazaki and Griffin (1997).

occipital joint'. The spinal curves of the model in three different postures were determined by their measurements with living subjects. The relative horizontal locations of the mass elements to the corresponding vertebrae, the mass eccentricity, were common in three postures. The other geometry and inertial data of the model were derived from several literature. Linear stiffnesses were assigned to each beam and spring element initially by using those obtained from the literature. The axial and bending stiffnesses of the 'buttocks tissue beams', axial stiffnesses of the 'visceral springs' and bending stiffnesses of the 'spinal beams', for which no reliable data were available, were then adjusted 'by comparing the natural frequencies and the vibration mode shapes of the model with the measurements' by the authors. The damping properties were incorporated by using modal damping ratios determined by comparing the driving point apparent mass of the model with their measurements. 'A total of seven vibration modes' was calculated for a normal body posture at the frequencies below 10 Hz (Figure 2.62(b)). It was concluded that 'the fourth mode at 5.06 Hz (in the normal posture) corresponded to the principal resonance seen in the driving point response of the seated body'. The mode consisted of 'an entire body mode with vertical and fore-and-aft pelvic motion due to deformation of tissue beneath the pelvis occurring in phase with a vertical visceral mode'. It was found that 'a bending mode of the lumbar spine was included in the next higher mode at 5.77 Hz'. 'A shift of the principal resonance' of the driving point apparent mass due to postural changes, observed in their experiment, was 'achieved only by changing the axial stiffness of the buttocks tissue'.

A simpler two dimensional model of the seated body than those mentioned above was developed by Pankoke *et al*. (1998) so as to estimate the compressive and shear forces in the intervertebral discs in the lumbar spine caused by whole-body vibration (Figure 2.63). The vertebrae in the region between the third lumbar vertebra and the fifth lumbar vertebra were modelled by rigid bodies which were interconnected by linear springs representing the intervertebral discs, ligaments, and the articular facets. The viscera in this region was modelled by three rigid masses interconnected to each other by spring elements which were also connected to the vertebrae by springs at each vertebral levels. The other parts of the body were represented in a more collective manner: eight rigid bodies represented the 'head', 'neck', 'upper torso', 'upper arm', 'forearm', 'pelvis', 'thigh', 'lower leg and foot' were used. These masses were interconnected by linear springs. The 'back muscles' in the lower lumbar region were modelled by a linear spring connected to the upper torso mass at the top and to the pelvic mass at the bottom. Some model parameters were derived directly from various literature and some were determined by 'parameter identification' using the experimental results of the dynamic response of the

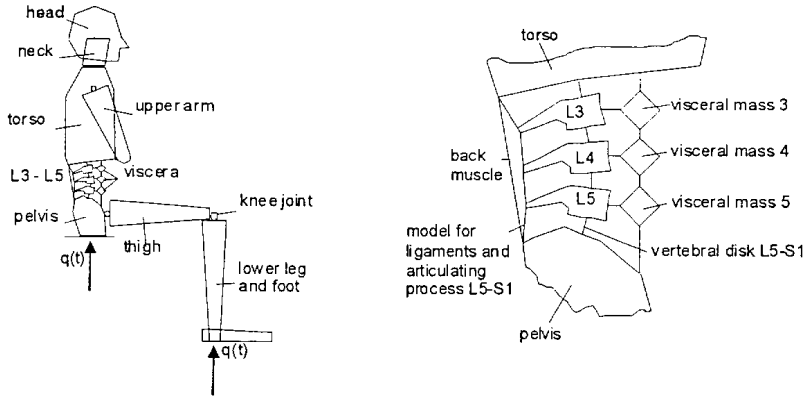

Figure 2.63 A discrete model of the lower lumbar spine and the seated body by Pankoke *et al*. (1998).

human body obtained from literature. The geometry and inertial parameters of the model were adjustable to a specific body height and weight while the stiffnesses and dampings were unchanged. The mechanical impedance calculated by the model showed a good agreement with the measured impedance obtained from the literature at frequencies below about 7 Hz. The vibration transmissibility of the vertical seat vibration to the fore-and-aft head motion of the model were similar to the measurement obtained from the same literature in the frequency range below 5 Hz. It was stated that the discrepancy between the model and the measurement at high frequencies resulted from the way damping properties were modelled (by modal damping), and in modelling the muscles, which were represented by a linear passive spring.

2.6 DISCUSSION AND CONCLUSIONS

The driving-point response of the human body exposed to vertical whole-body vibration can be considered as a representation of the overall response of the body. A consistent finding through the literature on experimental studies of the driving-point response of the seated body is that a principal resonance in the frequency response function (i.e., mechanical impedance or apparent mass) is observed in the frequency range of 4 to 6 Hz. This consistency in the previous data is based on various experiments conducted in different places and at different times with more than 150 subjects, as introduced in this chapter. The principal resonance at about 5 Hz can, therefore, be accepted as a true phenomenon occurring in the seated human body exposed to vertical seat vibration. With respect to the driving-point response of the standing body, a similar conclusion may be drawn. However, the resonance frequency reported in the previous studies varies between 4 and 7 Hz, a wider variation than in seated subjects. The total number of subjects involved in the previous studies with the standing body appears to be about 50. A resonance at 7 Hz, a rather high frequency, was derived from the study by Miwa (1975) in which 20 subjects, 40% of the total of 50 subjects in the previous studies presented in this chapter, participated. Therefore, further experimental studies of the driving-point response of the standing body are required so as to determine the principal resonance frequency of the standing body and to understand the difference in the dynamic response between the standing body and seated body.

The transmissibilities measured at various body parts provide understanding of motions occurring in particular body parts of interest during exposure to whole-body motion. The motion of the spine is important so as to understand the mechanisms of the dynamic response of the body, as well as to estimate the risk of spinal disorders, because the spine should be a major transmission path for longitudinal vibration. For the measurement of spinal motion, there have been mainly two methods used in the previous studies. The ‘direct measurement’ method may have the advantage of a rigid fixation on the vertebra. However, ethical conditions limit the number of subjects and measurement locations to a few. Further, local anaesthesia may alter the muscle activity in the region interest, which may alter the body response to the input stimulus. The results from ‘surface measurement’ shows an agreement with those using direct measurements within the expected variability between subjects, although some

assumptions are involved in surface measurement method. The number of subjects is not limited by using surface measurement. It is, therefore, reasonable to measure the spinal motion with transducers attached to the skin as long as local dynamics of the transducer-skin-tissue system is taken into account.

Transmissibilities to the vertebrae generally show a peak at about 5 Hz, close to the principal resonance frequency of the driving-point responses, for both standing and seated subjects. Reliable data on the transmissibilities to the spine for the standing body available in the literature have been obtained from only a few subjects. Measurements in the previous studies were usually made only at a couple of points over the lumbar spine so that it is difficult to understand the dynamic response of the whole vertebral column from the results. The causes of the peak observed in the transmissibilities at about 5 Hz were hypothesised in some previous studies. However, there is clearly a limitation in the discussion of the complex human body mechanisms based on only a couple of measurements. There have been two studies, Hagena *et al*. (1985) and Kitazaki (1994), in which the transmissibility measurement covers the whole spine over a wide frequency range. Similar measurements have been made on cadavers by El-Khatib *et al*. (1998). However, the absence of the muscle activity in the cadavers and the presence of some support to maintain the posture of subjects may alter the dynamic response of the body. It is not, therefore, reasonable to compare the results with those presented in this chapter.

The head motions during exposure to vertical whole-body vibration and shock measured in the previous studies tend to show larger variability than the motions of the vertebrae for both standing and seated bodies. This may be partly caused by the difference in the measurement location, as Paddan and Griffin (1992) showed. It has been found that inter-subject variability is large even in a single study. Peaks observed in individual transmissibilities are smoothed out by some sort of averaging between subjects due to the inter-subject variability. However, it is interesting to see that the mean vertical transmissibility from Kitazaki (1994) shows a clear peak at about 5 Hz while the median data from Paddan and Griffin (1988) shows a much less obvious peak at the same frequency. The same measurement device was used in both studies but the definition of vertical motion at the head was different: the motion near the cervical spine for Kitazaki (1994) and the motion at the mouth for Paddan and Griffin (1988). Therefore, there may be individual differences in the phase between vertical motion transmitted through the spine to the head and the pitch motion of the head.

There has been only one study, Kitazaki (1994) and Kitazaki and Griffin (1997, 1998), which investigated the dynamic mechanisms of resonances of the seated body based on a comprehensive set of measurement locations in the body. By using the experimental modal analysis technique, it was concluded that the principal resonance at about 5 Hz could be attributed to an entire body motion due to axial and shear deformations of the buttocks tissue, in phase with a vertical visceral motion, and a bending motion of the upper thoracic and cervical spine. In a related mathematical modelling study, Kitazaki (1994) and Kitazaki and Griffin (1997), a similar conclusion about the causes of the principal resonance was derived, but the contribution of bending motion of the spine was excluded. There have been no such studies for the standing body.

The effect of changes in posture and muscle tension may contribute to intra- and inter-subject variability found in the experimental data, as pointed out by Griffin (1990). The understanding of postural effects will be useful to determine the ability to change the dynamic response voluntarily and define a ‘good posture’ in various circumstances. It may also provide some insight into the mechanisms of the resonance of the body. A difficulty in investigations of the postural effect is the definition of posture. In the majority of the previous studies, the posture definition was, for example, ‘relaxed’ which is dependent on the interpretation of subjects, so that the ‘relaxed’ posture might vary between subjects and between experiments. However, the trend in the postural change in individuals may be consistent: a change from ‘erect’ to ‘relaxed’, for example, would induce loosening in the muscles. It is, therefore, reasonable to investigate trends in changes in the dynamic response with postural changes. In this context, decreases in the main resonance frequency of the driving-point response and transmissibilities to various body parts with postural change from ‘erect’ to ‘relaxed’ for the seated subjects found in some studies may be useful. It has also been found in some studies that bending the legs reduces the main resonance frequency compared to standing with straight legs. It will be useful for understanding of standing body responses to investigate the effects of postural change in the upper-body on the driving-point response of standing subjects and to see if there is a difference in the effect of postural change between standing and seated bodies.

Decreases in the resonance frequency of the driving-point response of the seated body have been found with increases in input vibration magnitude in some previous

studies. The same nonlinear effect for the standing body was observed by Edwards and Lange (1964) with one subject but not observed with their other subject. No other studies have investigated the effect of excitation magnitude on the driving-point response of the standing body. The ‘softening’ nonlinearity has also been shown in the transmissibilities to the abdomen of the seated body by Mansfield (1998). This nonlinear effect may be caused either by nonlinear properties of the soft tissues in the body, by the muscle activity which differs depending on the magnitude of the motion, or by some geometrical effect when the body exposed to vertical translational motion moves in some rotational directions, or a combination of these features. An understanding of the nonlinearity of the body will be important information helping to identify the causes of the resonance. It is also required with a view to extrapolating to the behaviour of the body at hazardous magnitudes of input stimuli from the findings obtained with low magnitude of input motions.

There have been various types of mathematical model developed in the previous studies, mainly for the seated body. Simple models, such as lumped parameter models with one or a few degree-of-freedom, have been used to represent basically one aspect of the dynamic response of the human body. For example, lumped parameter models with two degree-of-freedom have been preferred to represent the driving-point response and adopted in an International Standard. More complicated models have also been developed for the same purpose. However, having more degrees of freedom is not necessarily required to represent one aspect of the response reasonably and practically. The cost in computation due to the more complicated structure of the model may become disadvantage.

Sophisticated models, such as finite element models, may be required so as to represent the mechanisms of the dynamic response of the human body that has a highly complex structure. Validation of such models tends to be difficult because of the absence of information on many mechanical properties of the living human body and the lack of the experimental data on the dynamic responses measured at a sufficient number of locations in the body. Some finite element models have been developed and some seem to represent the human body response reasonably, as described in this chapter. However, there is still a potential disadvantage with complicated models in that uncertain data on model properties with a complicated model structure may lead to a wrong result. It is, therefore, worth investigating some ‘compromised’ model which has a simplified structure representing some parts of the body reasonably and

validating the simplified model with a sufficient set of experimental results. This model would be used to investigate the causes of the body resonance observed in experimental studies.

The main objective of the following research was to understand the dynamic mechanisms of the principal resonance observed in the driving-point frequency response function for standing and seated bodies exposed to vertical whole-body vibration. The following information is thought to be required to achieve the main objective, based on the literature review described in this chapter:

1) To identify the principal resonance in the driving-point frequency response function (i.e., the apparent mass in this research) of the standing body. To investigate the effect of posture and excitation magnitude on the resonance.
2) To identify characteristics of the transmissibilities to the various parts of the standing body. To investigate the effect of posture and excitation magnitude on the transmissibilities. To understand the relation between the principal resonance in the apparent mass and peaks in the transmissibilities.
3) To obtain sufficient experimental data to represent possible dynamic mechanisms of the principal resonance of standing and seated bodies.
4) To develop a reasonably simple mathematical model to represent the human body structure and validate the model with a sufficient set of experimental data on the dynamic response of the standing and seated body. To interpret the experimental data with the aid of the model.

CHAPTER 3

EXPERIMENTAL APPARATUS AND DESIGN, AND DATA ANALYSIS

3.1 INTRODUCTION

Three major experiments was conducted in the laboratory of the Human Factors Research Unit, the Institute of Sound and Vibration Research, the University of Southampton, so as to investigate the dynamic mechanisms of the human body in standing and sitting positions when exposed to vertical whole-body vibration. This chapter describes the apparatus used in the experiments and the experimental designs of three experiments (referred to in this thesis as Experiments 1, 2, and 3, respectively). The analysis methods applied to the experimental data, including frequency domain analysis and statistical analysis, are also described in this chapter.

3.2 APPARATUS

3.2.1 Vibrators

3.2.1.1 Electro-magnetic vibrator

The first experiment, Experiment 1, was conducted using an electro-dynamic vibrator. Derritron VP85 electro-magnetic vibrator driven by an amplifier with the power of 1.0 kW had a capability of producing an acceleration of up to 55 g with no load, a peak-to-peak displacement of up to 2.54 cm (1 inch), and a force of 3.3 kN. A lowest operating frequency of 1.5 Hz and a first major resonance of 3700 Hz were reported by the manufacturer.

3.2.1.2 Electro-hydraulic vibrator

An electro-hydraulic vibrator, which was designed to be used in a variety of studies of human response to vertical motion, was used in Experiments 2 and 3. The vibrator consisted of a servo-hydraulic actuator, a vibration table, electronic control equipment and hydraulic power supply. The vibrator was capable of producing a 10 kN dynamic force with an 8.8 kN preload and a peak-to-peak displacement of 1 m. The maximum payload was 400 kg. In the frequency range between 0.05 to 50 Hz, the vibrator could be operated at low acceleration magnitudes below about 10 ms^{-2} r.m.s. with a waveform distortions specified as below 5%. The support for test subjects and equipment consisted of a removable aluminium alloy plate with dimensions of 1.5 by 0.9 m attached to the upper surface of the vibrator table, which in turn was fixed to the end of the piston rod driven by the servo-hydraulic actuator and fitted with an anti-rotation assembly. The performance of the vibrator was in accordance with BS 7085 (1989): Guide to safety aspects of experiments in which people are exposed to mechanical vibration and shock. Specific safety measures were incorporated into the mechanical, hydraulic, and electrical parts of the system.

3.2.2 Transducers

3.2.2.1 Accelerometers

The input motion to test subjects was measured using a piezo-resistive accelerometer, either Entran EGCSY-240D*-10 or Entran EGCS-DO-10. Entran EGCSY-240D*-10 had a sensitivity of approximately 13 mV/g with an operating range of ±10 g. The sensitivity of Entran EGCS-DO-10 was approximately 10 mV/g with an operating range of ±10 g.

Miniature piezo-resistive accelerometers were used to measure the motion of various locations of the body. Entran EGA-125(F)*-10D had a sensitivity of approximately 7 mV/g with an operating range of ±10 g. The mass of Entran EGA-125(F)*-10D was approximately 1 gram. Additionally, EGAX-F-5 which had a sensitivity of approximately 8 mV/g with an operating range of ±5 g was also used.

Signals from the accelerometers were used to calculate ratios between accelerations measured at two distant points (i.e., the transmissibilities). Figure 3.1 shows the range in the ratios of accelerations measured with 26 accelerometers to acceleration measured

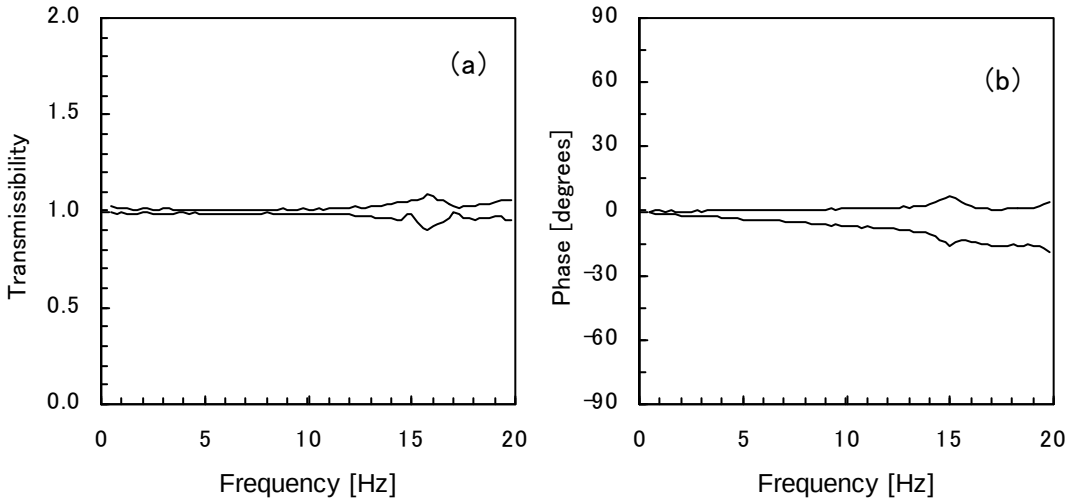

Figure 3.1 Maximum and minimum transmissibilities and phases between accelerations measured with 27 calibrated accelerometers shaken simultaneously. Measured before an experiment. Data at frequencies below 10 Hz were investigated.

with another accelerometer when these accelerometers were attached to the vibrator platform and shaken simultaneously. These accelerometers were calibrated for an experiment. Ideally, the transmissibility was unity and the phase was zero degree at all frequencies, assuming a pure uni-axis vibration was produced by the vibrator and the vibrator platform was rigid. Errors observed in the data were: for the transmissibility, ±2% below 10 Hz and ±10% below 20 Hz; for the phase, between -7 and 1 degrees below 10 Hz and -19 to 7 degrees below 20 Hz.

3.2.2.2 Force transducers

The force at the interface between test subjects and the vibrating platform was measured with a force platform, Kistler 9281 B. It incorporated four quartz piezo-electric force transducers mounted at the corners of a rectangular welded steel frame. An aluminium alloy plate, 0.6 by 0.4 m with 0.02 m thick, was bolted on to the pre-loaded force transducers. The force transducers had closely matched sensitivities so that the total force was obtained by summing the charges from each of the four outputs. The force acting on the mass of the top plate and the force transducers above the measuring equipment, approximately 15 kg, was included in the total force obtained. This force was subtracted so as to obtain the force acting on the subjects. The theoretical lowest resonance frequencies of the force platform with a 100 kg mass were 320 Hz and 480 Hz in the vertical and horizontal directions, respectively. This ensured that

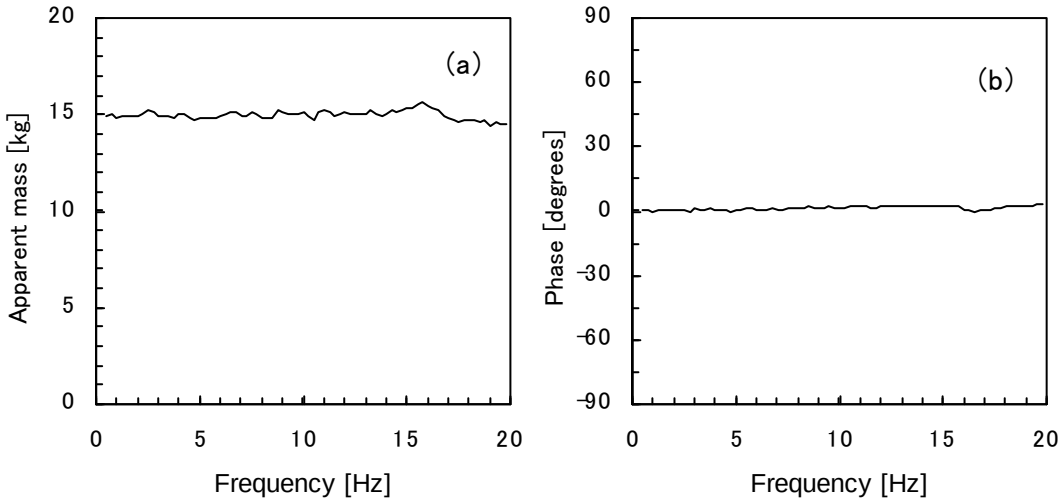

Figure 3.2 Apparent mass obtained with no additional mass on the force platform.

measurements were not likely to be affected by a resonance of the force platform. Figure 3.2 shows the ratio between a force signal obtained from the force platform and an acceleration signal obtained from an accelerometer which was mounted on the top plate of the force platform. This ratio was interpreted as the apparent mass of the top plate of the force platform which ideally coincided with the mass of the top plate, 15 kg. The phase would be zero on the assumption that the top plate was rigid and the force platform was rigidly connected to the vibrator platform. The errors observed in Figure 3.2 were: for the apparent mass, ±2% below 10 Hz and ±4% below 20 Hz; for the phase, between -0.1 and 2.2 degrees below 10 Hz and between -0.1 and 3.2 degrees below 20 Hz.

3.2.3 Data acquisition

A 16-channel *HVLab* data acquisition and analysis system, which was developed at the Human Factors Research Unit, the Institute of Sound and Vibration Research, the University of Southampton, was used to control the vibrator and to acquire the output signals from the accelerometers and force transducers. The system used an Advantech PCL-818 data acquisition card and Techfilter TF-16 anti-aliasing card. The signals from the force transducers were amplified through a charge amplifier, Kistler 5001 SN, before acquired.

3.3 SUMMARY OF EXPERIMENTAL DESIGNS

Three major experiments were designed so as to understand the dynamic mechanisms of the human body in standing and seated positions. The objectives and measurements performed in the experiments are summarised in Table 3.1.

All experimental procedures presented in this thesis received the prior approval of the Human Experimentation Safety and Ethics Committee of the Institute of Sound and Vibration Research before the experiments commenced.

The conditions used in the three experiment in which the apparent mass and transmissibility of subjects were measured are summarised in Table 3.2. The details of the experimental designs are described in the corresponding chapters.

Table 3.1 Objectives and measurements of three experiments described in this thesis.

Experiment	Objectives	Measurements	Positions
1	To compare the apparent mass of the standing body to that of the seated body. To investigate the effects of postural changes of standing subjects on the apparent mass.	Apparent mass	Standing Sitting
2	To investigate the relation between driving-point response and body motions for subjects standing with different postures of their legs. To investigate the effect of vibration magnitude on the dynamic response of the standing body.	Apparent mass Transmissibility (vertical, fore-and-aft)	Standing
3	To measure the dynamic responses of various body locations of standing and seated subjects in vertical, fore-and-aft and pitch axes so as to define the form of body movements during exposure to vertical whole-body vibration. To identify the mechanism contributing to the principal resonance observed in the apparent mass.	Apparent mass Transmissibility (vertical, fore-and-aft, pitch)	Standing Sitting

Table 3.2 Summary of the conditions of three experiment measuring the apparent mass and transmissibility of human body.

Experiment	Postures	Input stimuli
1	Standing normally Standing with erect upper-body Standing with slouched upper-body Standing with upper-body tensed Standing with legs bent Standing on one leg Sitting normally	Gaussian random 1.0 to 50 Hz 1.0 ms^{-2} r.m.s.
2	Standing normally (Normal) Standing with legs bent (Legs bent) Standing on one leg (One leg)	Gaussian random 0.5 to 30 Hz 0.125, 0.25, 0.5, 1.0, 2.0 ms^{-2} r.m.s. for normal and legs bent 0.25, 1.0 ms^{-2} r.m.s. for one leg
3	Standing normally Sitting normally	Gaussian random 0.5 to 20 Hz 0.125, 0.25, 0.5, 1.0, 2.0 ms^{-2} r.m.s.

3.4 DATA ANALYSIS

3.4.1 Frequency response functions

3.4.1.1 Apparent mass

The apparent mass, *M(f)*, was calculated using the 'cross spectral density method', that is, by dividing the cross spectral density function between the input acceleration and the resulting force at the driving point, $S_{af}(f)$, by the power spectral density function of the input acceleration, $S_a(f)$:

$$M(f) = \frac{S_{af}(f)}{S_a(f)} \tag{3.1}$$

The apparent mass, *M(f)*, is a frequency response function in complex numbers. The modulus, $M_m(f)$, and phase, $M_p(f)$, of the apparent mass, *M(f)*, were calculated by:

$$M_m(f) = |M(f)| = \sqrt{(\mathrm{Re}\{M(f)\})^2 + (\mathrm{Im}\{M(f)\})^2} \tag{3.2}$$

$$M_p(f) = \tan^{-1}\frac{\mathrm{Im}\{M(f)\}}{\mathrm{Re}\{M(f)\}} \tag{3.3}$$

The ordinary coherence function for the apparent mass, $\gamma^2_m(f)$, was obtained by:

$$\gamma^2_m(f) = \frac{|S_{af}(f)|^2}{S_a(f)S_f(f)} \tag{3.4}$$

where $S_f(f)$ is the power spectral density function of the force measured at the driving point. The ordinary coherence function indicates the linearity of the system and the effect of noise in the measurements by giving a value between zero and unity. A coherence of unity means that the input is linearly related to the output and the input and output signals contain no noise. If the coherence function has a value between zero and unity, the input and output are partly linearly related but at least one of the following holds: (1) the signals contain measurement noise, (2) the input and output are not only linearly related, (3) some inputs, other than the input of interest, also contributes to the output.

The measured force was caused not only by the body of the subject but also the mass of the top plate of the force platform as mentioned in Section 3.2.2.2. In order to eliminate this effect, mass cancellation was taken into account as follows (Figure 3.3):

$$\begin{aligned} &\textit{Apparent mass of subject}, M(f) \\ &= \frac{\textit{Measured force}, F(f) - \textit{Force acting on equipment}, F_e(f)}{\textit{Measured acceleration}, A(f)} \\ &= \textit{Measured Apparent mass}, M_m(f) - \textit{Apparent mass of equipment}, m_e \end{aligned} \tag{3.5}$$

The apparent mass of the top plate was identical to its static mass on the assumption that the plate behaved as a rigid body when its apparent mass was measured without a subject (see Figure 3.2). In practice, the apparent mass measured without a subject, rather than the static mass of the top plate, was subtracted from the apparent masses measured with subjects in the procedure for mass cancellation.

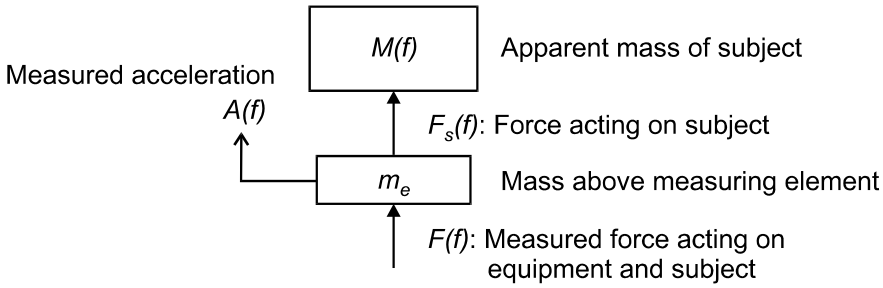

Figure 3.3 Model of mass cancellation.

A large variability in the apparent masses of subjects was partly attributed to their different static masses, as in previous studies with seated subjects (e.g. Fairley and Griffin, 1989). Hence, each apparent mass was 'normalised' by dividing it by the measured value of the apparent mass at the lowest frequency, either 0.5 or 1.0 Hz, which was almost equal to the static mass of the subject.

$$M_n(f) = \frac{M(f)}{M(f_{lowest})} \tag{3.6}$$

where f_{lowest} is the lowest frequency of the measurements. The normalised apparent mass assisted the comparison of apparent masses across subjects.

3.4.1.2 Transmissibility

The transmissibility, $T(f)$, the ratio between motions at two distant points, was calculated by the 'cross spectral density method', as in the case of the apparent mass. From the cross spectral density between the accelerations at 'input' and 'output' points, $S_{io}(f)$, and the power spectral density of the acceleration at the input point, $S_i(f)$, the transmissibility in complex numbers, $T(f)$, was obtained by:

$$T(f) = \frac{S_{io}(f)}{S_i(f)} \tag{3.7}$$

The driving point was usually selected as the input point in the calculation. The modulus and phase of the transmissibility were obtained in the same way as the apparent mass shown in Equations (3.2) and (3.3). The linear correlation between the input and output signals was examined by calculating the ordinary coherence function as Equation (3.4):

$$\gamma_t^2(f) = \frac{|S_{io}(f)|^2}{S_i(f)S_o(f)} \qquad (3.8)$$

Here $\gamma^2_t(f)$ is the ordinary coherence function for the transmissibility, $S_o(f)$ is the power spectral density function of the output acceleration.

A consideration of the relation between apparent mass, normalised apparent mass and transmissibility in lumped parameter models is given in Appendix A.

3.4.2 Statistical analysis (mainly extracted from Siegel and Castellan, 1988)

Statistical inference can be generally used to draw conclusions about large groups of samples on the basis of observation of a few samples. Nonparameteric statistical techniques were adopted in the course of the studies presented in this thesis. The main reason for the choice of nonparametric techniques was that the nature of the population from which the samples were drawn was not clearly known: various values obtained from experiments with human subjects were not necessarily distributed in a particular form, such as, a normal distribution. Statistical tests were used in the present study so as to: (i) determine whether differences between two or more variables, or conditions, observed in experiments with several subjects signify that those were really different in the population from which the sample was drawn, and (ii) determine whether or not some observed association in variables used in experiments indicated that the variables under study were associated in the population (for details, see Siegel and Castellan, 1988).

3.4.2.1 Wilcoxon matched-pairs signed ranks test

The Wilcoxon matched-pairs signed ranks test can be used to test the differences between samples of paired or related data which are on an ordinal scale both within and between paired data (i.e., the direction as well as the relative magnitude of the differences within pairs can be considered). For example, the Wilcoxon matched-pairs signed ranks test may be used to test the difference between the moduli of the apparent mass at a frequency of interest measured in two experimental conditions for each subject, so that it indicates whether the two experimental conditions cause a significant difference in the magnitude of the apparent mass at that frequency.

Table 3.3 shows an example of the data: the magnitudes of the apparent mass at a frequency for eight subjects in two conditions. The values in the fourth column in Table 3.3, *d*, were the differences between the apparent masses at the frequency in two conditions for each subject (i.e., the difference scores for each matched pair). The difference scores, *d*, are ranked by its absolute value and then affixed the sign of the difference to each rank, as shown in the fifth column in Table 3.3.

The null hypothesis is that the change between conditions A and B has no effect on the magnitude of the apparent mass at that particular frequency. If this was true, it would be expected that the sum of those ranks having positive values is about equal to the sum of those ranks having negative values. However, if those sums were very much different, it could be inferred that the apparent mass at the frequency in condition A differs from that in condition B. In Table 3.3, the sum of those ranks having plus signs, T^+, is 34, while the sum of those ranks having negative signs, T^-, is 2.

For small samples (i.e., $N < 15$, $N = 8$ for the example shown in Table 3.3), various values of the sum of the positive ranks, T^+, and their associated probabilities of occurrence under the assumption of no difference between two groupings, conditions A and B in this example, are previously obtained and tabulated (see e.g. Siegel and Castellan, 1988). An upper-tail probability of 0.0117 can be obtained from the table for $T^+ = 34$ when $N = 8$, which corresponds to 0.0234 for a two-tailed test since the direction of the difference is not predicted in this example. It can be, therefore, concluded that the null hypothesis that the change between conditions A and B has no effect on the

Table 3.3 Example of Wilcoxon matched-pairs signed ranks test. Moduli of the apparent mass at a frequency measured in two experimental conditions.

Subject	Condition A [kg]	Condition B [kg]	*d* [kg]	Rank of *d*
1	92.2	109.5	17.3	5
2	84.3	97.7	13.4	4
3	92.5	123.8	31.3	6
4	136.1	125.9	-10.2	-2
5	88.4	123.6	35.2	8
6	123.8	132.5	8.7	1
7	95.3	130.4	35.1	7
8	101.1	111.4	10.3	3

magnitude of the apparent mass at that particular frequency may be rejected at a significance level of α = 0.05, which is a widely used significance level: the difference in the apparent mass at that frequency between condition A and B is statistically significant.

3.4.2.2 Friedman two-way analysis of variance

The Friedman two-way analysis of variance can be used to test the null hypothesis that the *k* (greater than two) repeated measures or matched samples come from the same population or populations with the same median. The samples are required to be on at least an ordinal scale. For example, whether or not the resonance frequency of the apparent mass differs in several experimental conditions can be tested by the Friedman two-way analysis of variance.

Table 3.4 presents the resonance frequencies of the apparent mass for eight subjects (*N* = 8) measured in four experimental conditions (*k* = 4) in a two-way table having eight rows and four columns. The scores in each row are then ranked separately in a range from 1 to 4, i.e., the number of conditions, as shown in Table 3.5.

If the null hypothesis that any changes in experimental condition, as far as four conditions used are concerned, have no effect on the resonance frequencies of the apparent mass was true, the distribution of ranks in each column would be a matter of

Table 3.4 Example of Friedman two-way analysis of variance. Resonance frequencies of the apparent mass measured in four experimental conditions.

Subject	Condition			
	A [Hz]	B [Hz]	C [Hz]	D [Hz]
1	5.2	5.0	6.5	6.0
2	5.5	5.3	7.0	5.8
3	5.5	4.8	5.0	6.0
4	5.2	5.0	5.3	6.0
5	6.5	5.2	6.2	5.3
6	5.5	5.7	6.5	7.0
7	5.3	5.0	5.5	5.8
8	5.3	5.2	5.0	6.0

Table 3.5 Ranks of the resonance frequencies of eight subjects under four conditions.

Subject	Condition			
	A	B	C	D
1	2	1	4	3
2	2	1	4	3
3	3	1	2	4
4	2	1	3	4
5	4	1	3	2
6	1	2	3	4
7	2	1	3	4
8	3	2	1	4
R_j	19	10	23	28

chance. It would be then expected that the sum of ranks in each column, R_j, to be $N(k+1)/2$ (20 for the example), i.e., the sum of all ranks in the table divided by the number of column. However, if the resonance frequencies were dependent on conditions, the rank totals would vary from one column to another.

The Friedman test determines whether the rank totals, R_j, for each condition or variable differ significantly from the values which would be expected by chance. The statistics, F_r, is calculated so as to do this test:

$$F_r = \left[\frac{12}{Nk(k+1)} \sum_{j=1}^{k} R_j^2 \right] - 3N(k+1) \tag{3.9}$$

Probabilities associated with various values of F_r when the null hypothesis is true have been tabulated for various sample sizes and various numbers of variables (e.g. see Siegel and Castellan, 1988). If the observed value of F_r is larger than the value in the table of F_r at the chosen significance level, the null hypothesis may be rejected in favour of the alternative hypothesis that the resonance frequency differs for at least two conditions. For $N = 8$ and $k = 4$, $F_r = 7.50$ for a significance level of $\alpha = 0.05$, while $F_r = 13.05$ is obtained from Table 3.5 and Equation (3.9). Therefore, for the example data, the null hypothesis that any changes in experimental condition have no effect on the resonance frequencies of the apparent mass may be rejected at the significance level of

α = 0.05: there is a statistically significant difference in the resonance frequency between at least two conditions.

3.4.2.3 Kendall rank-order correlation coefficient

The Kendall rank-order correlation coefficient, *T*, (referred to as Kendall's tau, τ, by some authors) is suitable as a measure of association between two variables which requires that both variables be measured on at least an ordinal scale so that the objects or individuals under study may be ranked in two ordered series. The sampling distribution of *T* under the null hypothesis of independence is known and *T* may be used in tests of significance.

An example of data is shown in Table 3.6: the apparent masses measured at a frequency, 5 Hz for example, and static weights for eight subjects (*N* = 8). The null hypothesis for this example is that the apparent mass measured at 5 Hz is independent of the static weight of subjects. Table 3.7 shows the ranks of two sets of example data. The order of the subjects is then rearranged so that the ranks for the apparent mass appear in ascending order, as shown in Table 3.8.

Table 3.6 Example of Kendall rank-order correlation coefficient. Apparent masses at 5 Hz and static weights of eight subjects.

Subject	1	2	3	4	5	6	7	8
Apparent mass [kg]	122.3	134.9	100.1	120.9	111.1	140.7	102.2	141.4
Static weight [kg]	77	84	65	74	68	82	71	85

Table 3.7 Ranks of the apparent masses and static weights of eight subjects.

Subject	1	2	3	4	5	6	7	8
Apparent mass	5	6	1	4	3	7	2	8
Static weight	5	7	1	4	2	6	3	8

Table 3.8 Ranks of the apparent masses and static weights of eight subjects. Rearranged according to the ranks of the apparent masses.

Subject	3	7	5	4	1	2	6	8
Apparent mass	1	2	3	4	5	6	7	8
Static weight	1	3	2	4	5	7	6	8

The number of agreements in ordering and the number of disagreements in the observed ordering of ranks are counted for all possible pairs of ranks in Table 3.8. Consider first all possible pairs of ranks in which the rank of static weight is 1 (the first rank for the static weight in Table 3.8) is a member and the other member is a later rank (to the right). If a pair is in the correct order, that pair is assigned a score of +1. If not in the correct order, a score of -1 is assigned to the pair. In this example, the all possible pairs of ranks including rank 1 for the static weight are in the correct order so that +1 is assigned to seven pairs. For all possible pairs including rank 3 (the rank second from the left in the static weight), five pairs are in the correct order but a pair (3 - 2) is in the wrong order. The total of these score is 5 - 1 = 4. The same procedure is repeated for succeeding ranks so that the total of all of the scores assigned is 7 + 4 + 5 + 4 + 3 + 0 + 1 = 24

The maximum possible total, the one which would occur in the case of perfect agreement between the ranks of two sets of data, would be the combination of N objects taken two at a time, $N(N\text{-}1)/2$ (28 for N = 8). The Kendall rank-order correlation coefficient, T, is defined by the ratio of the actual total of +1s and -1s to the maximum possible total, the number of possible pairs:

$$T = \frac{Number\ of\ agreements - Number\ of\ disagreements}{Total\ number\ of\ pairs} = \frac{24}{28} = 0.857 \qquad (3.10)$$

The significance of T can be tested based on probability of occurrence of T under the null hypothesis of independence. For large sample sizes, $N > 10$, the sampling distribution of T may be approximated by the normal distribution. When $N \leq 10$, previously calculated data which may be used to determine the exact probability associated with the occurrence under the null hypothesis are available (see e.g. Siegel and Castellan, 1988). For N = 8 and T = 0.857, a probability of p = 0.001, that is the probability of obtaining a Kendall rank-order correlation coefficient of T = 0.857 when the apparent mass at 5 Hz is independent of the static weight is less than 0.005. The null hypothesis that the apparent mass at 5 Hz and static weight are independent may be rejected and it can be concluded that there is a statistically significant correlation between two values.

The advantage of the Kendall rank-order correlation coefficient is that *T* can be generalised to a partial correlation coefficient, although it is not presented in this thesis. The Kendall coefficient of concordance, *W*, can be used to determine the association among *k* (more than two) sets of rankings.

CHAPTER 4

APPARENT MASS OF THE HUMAN BODY IN STANDING POSITION EXPOSED TO VERTICAL WHOLE-BODY VIBRATION: INFLUENCE OF POSTURE

4.1 INTRODUCTION

The driving-point dynamic response, such as mechanical impedance or apparent mass, of the human body has been investigated as one of the objective methods to measure the biodynamic response to whole-body vibration, as reviewed in Section 2.3. There have been many studies of the seated body in which, for example, the effects of changes in posture as well as the effects of magnitude of stimuli on the driving-point response have been investigated. However, the driving-point response of the human body in a standing position has been reported in few studies.

Previous studies in which the mechanical impedance, or the apparent mass, of subjects has been measured while standing in a normal posture during exposure to vertical whole-body vibration have found a main resonance at around 5 Hz (Coermann, 1962; Edwards and Lange, 1964; Fairley, 1981 and 1986). In some subjects, a second broad peak at 10 to 15 Hz was also observed. An exception is a study by Miwa (1975) who found resonances at 7 Hz and 20 Hz. A body resonance at about 5 Hz in a standing position is consistent with a resonance at this frequency in a sitting position (e.g. Fairley and Griffin, 1989).

An influence of posture on the driving-point response of standing subjects has been investigated in few studies. Coermann (1962) mentioned that the natural frequency of the mechanical impedance decreased to about 2 Hz with the legs bent, compared to 5.9 Hz when ‘standing erect with stiff knees posture’, although no data were presented. Miwa (1975) investigated mechanical impedance in various standing postures. In a ‘knee-bending’ posture, three peaks with similar magnitude were found at 3 Hz (the lowest frequency investigated), at 20 Hz and at 60 Hz. He stated that there was no obvious difference between two upper-body postures, ‘erect’ and ‘relaxed’, when the legs were in an ‘erect state’, although no data were shown. When subjects stood on one

leg, a single peak frequency of 5 Hz was lower than the lowest peak frequency in the 'erect' posture (i.e. 7 Hz). Miwa also investigated mechanical impedance in other standing postures, such as 'standing on heels'. Fairley (1981) showed that a 'legs slightly bent' posture caused a decrease in the first resonance frequency to 3 Hz while a 'knee bent' posture caused a main resonance at 2.5 Hz.

This chapter presents an experiment (referred to in this thesis as Experiment 1) that has been conducted so as to investigate the driving-point response (i.e., apparent mass) of the standing body to vertical whole-body vibration. The apparent mass of the seated body has also been measured in the experiment so as to compare the apparent mass of the standing body with that of the seated body. It was hypothesised that the apparent masses of both standing and seated bodies had a main resonance at about 5 Hz. The effects of changes in subject posture and muscle tone on the apparent mass of the standing body have been investigated.

Additionally, an investigation of simple mathematical modelling of the apparent mass obtained in the experiment is also presented in this chapter. A single degree-of-freedom and two types of two degree-of-freedom linear lumped parameter models were used to model the measured apparent mass for some body postures. The purpose of the modelling was to identify the validity of the models provided in the International Standard 5982 (1981) and also to understand the mechanisms causing differences in the apparent masses among different body postures.

4.2 EXPERIMENTAL METHOD

4.2.1 Apparatus and procedure

The experiment was conducted using an electro-dynamic vibrator. A force platform, Kistler 9281B, was rigidly secured to the vibrator. An accelerometer, Entran EGCSY-240D*-10, was mounted on the centre of the top plate of the force platform using double-sided adhesive tape. Gaussian random vertical vibration with bandpass filtered constant acceleration power spectral density at frequencies between 1.0 and 50 Hz was used as the input stimulus. An analogue filter was used to amplify signals in the low frequency range. A limitation of accuracy due to the apparatus, especially the vibrator, allowed the lower limit of the frequency range to be at 1 Hz while maintaining a flat

constant bandwidth acceleration power spectrum over the frequency range. A vibration magnitude of 1.0 ms^{-2} r.m.s. was used and the duration of each run was 60 seconds. The output signals from the accelerometer and the force platform were acquired at 256 samples/second after low-pass filtering at 50 Hz to avoid aliasing. The details of the apparatus used in the experiment are described in Section 3.2.

Twelve male subjects, median age 24.5 yr, height 1.80 m and weight 75.5 kg, took part in the experiment. The details of the subjects were presented in Appendix B. Repeatability of the measurements, intra-subject variability, was also examined through twelve runs with one of the subjects with arbitrary intervals over several days. The effect of postural changes on the dynamic response were investigated in seven different conditions:

1) 'Standing normally': comfortable and upright posture with normal muscle tension.
2) 'Standing with erect upper-body': straight back and shoulders held back with normal muscle tension.
3) 'Standing with slouched upper-body': with a slight stoop and shoulders held forward with normal muscle tension.
4) 'Standing with upper-body tensed': with all the muscles of the upper-body tensed as much as possible.
5) 'Standing with legs bent': knees held vertically above the toes with comfortable and upright upper-body with normal muscle tension.
6) 'Standing on one leg': on left leg with comfortable and upright upper-body with normal muscle tension.
7) 'Sitting normally': comfortable and upright posture with normal muscle tension.

Legs were straight with normal muscle tension (unlocked) for all the standing postures, except for the legs bent posture. In all the standing postures, the stance between the subjects' feet was set to be 0.3 m and the mid-sagittal plane of subjects coincided with the central plane of the force platform in the direction of its shorter side. Measurements were obtained with subjects barefoot so as to eliminate any effects of footwear. When subjects stood on one leg, they touched slightly with their finger tips on a wall by the shaker so as not to lose their balance. In order to have the same contact area between the subject and the platform in the sitting position, subjects were ordered to sit on the platform with their ischial tuberosities over the centre line of the platform, which was 0.3 m away from the edge. A footrest was not used in the sitting position. The feet of the

subjects were hanging freely. An instruction sheet shown to the subjects before the exposures are presented in Appendix B.

4.2.2 Analysis

The apparent mass, *M(f)*, was calculated using the cross spectral density method with a resolution of 0.25 Hz:

$$M(f) = \frac{S_{af}(f)}{S_a(f)} \tag{4.1}$$

where $S_{af}(f)$ is the cross spectral density function between the input acceleration and the force at the driving point and $S_a(f)$ is the power spectral density function of the input acceleration. The effect of the mass of the top plate of the force platform was eliminated by mass cancellation as described in Section 3.4.1.1: the apparent mass measured without a subject was subtracted from the apparent mass measured with a subject.

The ordinary coherence function of the apparent mass, $\gamma_m^2(f)$, was obtained by:

$$\gamma_m^2(f) = \frac{\left|S_{af}(f)\right|^2}{S_a(f)S_f(f)} \tag{4.2}$$

where $S_f(f)$ was the power spectral density function of the force measured at the driving-point.

The normalised apparent mass, $M_n(f)$, defined by Fairley and Griffin (1989), was obtained by:

$$M_n(f) = \frac{M(f)}{M(f_{lowest})} \tag{4.3}$$

where $M(f_{lowest})$ is the apparent mass at the lowest frequency of the measurement, 1.0 Hz, which was almost equal to the total mass of the subject.

4.3 EXPERIMENTAL RESULTS

The apparent masses of the human body obtained from the experiment are presented in this section. The apparent masses in the standing and sitting positions are compared and the effect of changes in the postures of subjects are shown. The ‘main’, ‘primary’, or ‘principal resonance of the apparent mass’ used in this thesis is defined as the maximum apparent mass in the frequency range investigated.

4.3.1 Standing and sitting

4.3.1.1 Repeatability - intra-subject variability

The apparent masses, phases and coherences of a subject measured on twelve separate occasions in the normal upright standing posture and normal upright sitting posture are shown in Figure 4.1. The apparent masses of the subject measured in both the normal upright standing posture and the normal upright sitting posture through twelve runs showed high repeatability. Variability in twelve runs was represented by dividing the inter-quartile range by the median at each frequency:

$$Normalised\ variability = \frac{Inter\text{-}quartile\ range}{Median} \tag{4.4}$$

The normalised variability was greater for the standing posture than for the sitting postures at frequencies between 15 and 27 Hz and above 35 Hz. Similar normalised variability was observed for the two postures at the other frequencies.

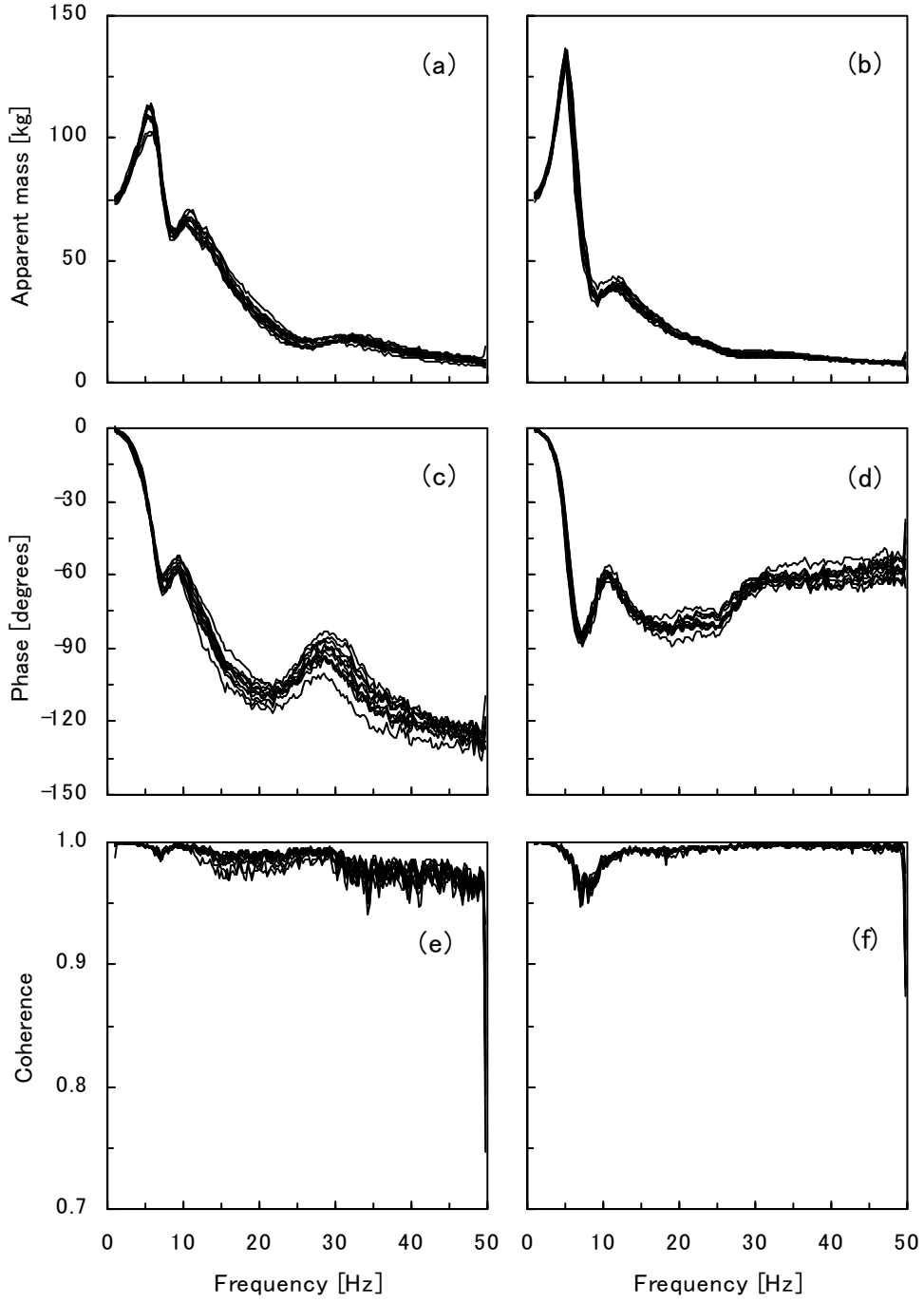

Figure 4.1 Apparent masses, phases, and coherences of a subject through twelve runs: (a) apparent masses in the normal standing posture, (b) apparent masses in the normal sitting posture, (c) phases in the normal standing posture, (d) phases in the normal sitting posture, (e) coherences in the normal standing posture, and (f) coherences in the normal sitting posture.

4.3.1.2 Variability across subjects - inter-subject variability

Figure 4.2 shows the apparent masses, phases and coherences of the twelve subjects in the normal standing and normal sitting postures. The measured apparent mass of the seated body, which had a main peak at about 5 Hz for all subjects, was found to have a similar trend to previous results (e.g. Fairley and Griffin, 1989). The apparent mass when subjects were in the normal standing posture also had a primary resonance at about 5 Hz. The normalised variability calculated by Equation (4.4) had greater values for the standing posture than for the sitting posture at frequencies between 3.5 and 7 Hz, between 14 and 28.5 Hz and above 36 Hz, while the opposite trends were found in the frequency range between 7.5 and 10.5 Hz.

Figures 4.3(a) and (b) shows the apparent masses normalised by the values of the apparent mass at 1 Hz. The apparent masses at 1 Hz was close to the total mass of a subject measured with a weighing machine. Figures 4.3(c) and (d) showed the normalised variability for the apparent masses and normalised apparent masses in the two postures. As shown in the figures, the variability across the subjects tended to reduce for both postures by normalising the apparent mass. The normalised apparent mass in the normal sitting posture was more consistent across the subjects than that in the normal standing posture, except at frequencies between 7.25 and 14 Hz.

The apparent masses for both the standing and sitting postures of each of the twelve subjects are presented in Figure 4.4. The median value of the principal resonance frequencies, the frequencies at which the apparent masses were the greatest, for all subjects in the standing posture was 5.25 Hz, with an inter-quartile range from 4.69 to 5.5 Hz. The median principal resonance frequency for seated subjects was 5.13 Hz, with an inter-quartile range from 5.0 to 5.25 Hz. The difference between the principal resonance frequency in the standing posture and that in the sitting posture was not statistically significant (Wilcoxon matched-pairs signed ranks test). The principal resonance magnitude of the apparent mass of standing subjects, median of 1.45 obtained from the normalised values, was lower than that of seated subjects, 1.69 ($p < 0.01$).

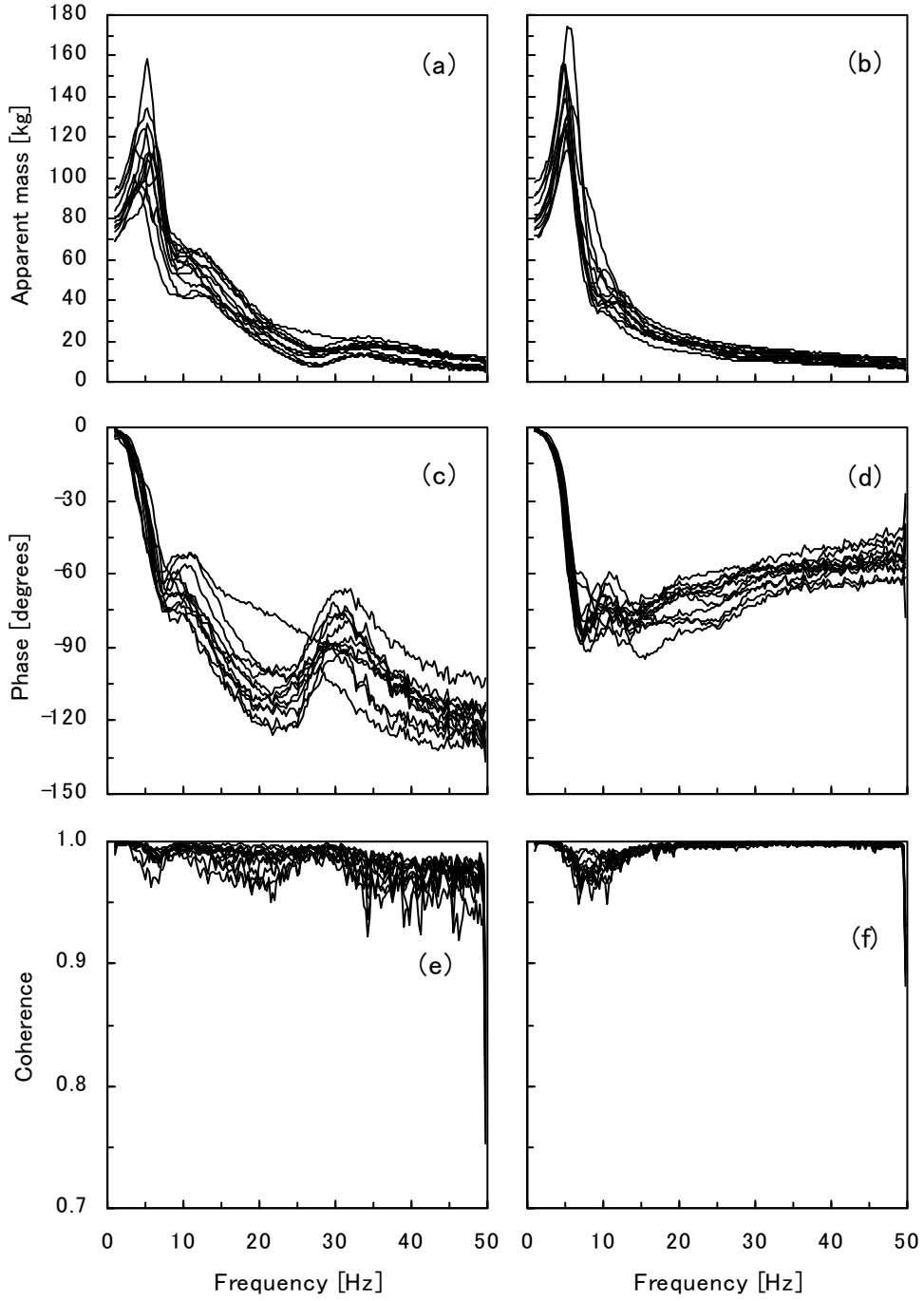

Figure 4.2 Apparent masses, phases, and coherences of twelve subjects: (a) apparent masses in the normal standing posture, (b) apparent masses in the normal sitting posture, (c) phases in the normal standing posture, (d) phases in the normal sitting posture, (e) coherences in the normal standing posture, and (f) coherences in the normal sitting posture.

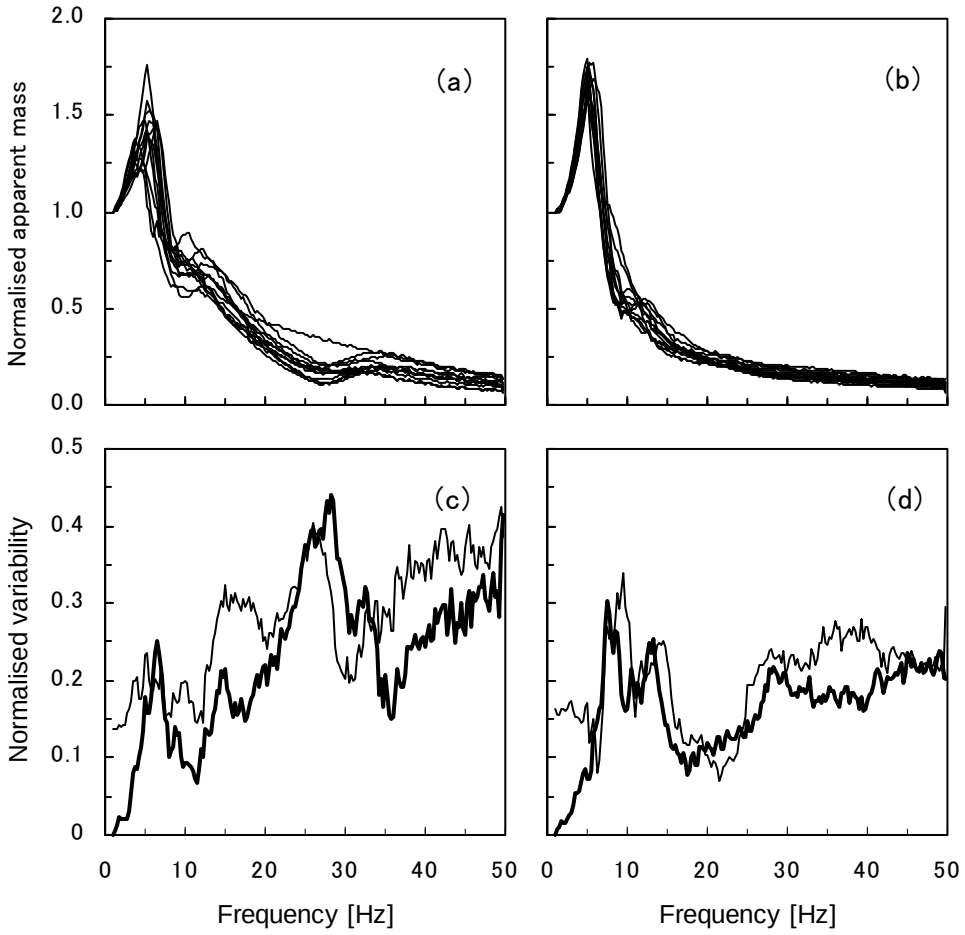

Figure 4.3 Normalised apparent masses and normalised variabilities for the apparent mass and normalised apparent mass of twelve subjects: (a) normalised apparent masses in the normal standing posture, (b) normalised apparent masses in the normal sitting posture, (c) normalised variabilities in the normal standing posture, and (d) normalised variabilities in the normal sitting posture. Keys for (c) and (d): apparent mass ——— ; normalised apparent mass ━━━ .

Two other local broad peaks in the apparent mass were found in the standing posture: one in the frequency range from 10 to 15 Hz, which was a clear peak in some subjects and might be found in the apparent masses of the sitting subjects, and another at around 35 Hz which was not seen in the sitting posture. The apparent mass of the standing body was significantly greater than that of the sitting body in the frequency range 8 to 22 Hz and 31 to 41 Hz, while the apparent mass of the sitting body was greater than that of the standing body at frequencies between 3.75 and 5.75 Hz (p < 0.05). The median normalised apparent masses and phases in the standing and sitting positions are shown in Figure 4.5.

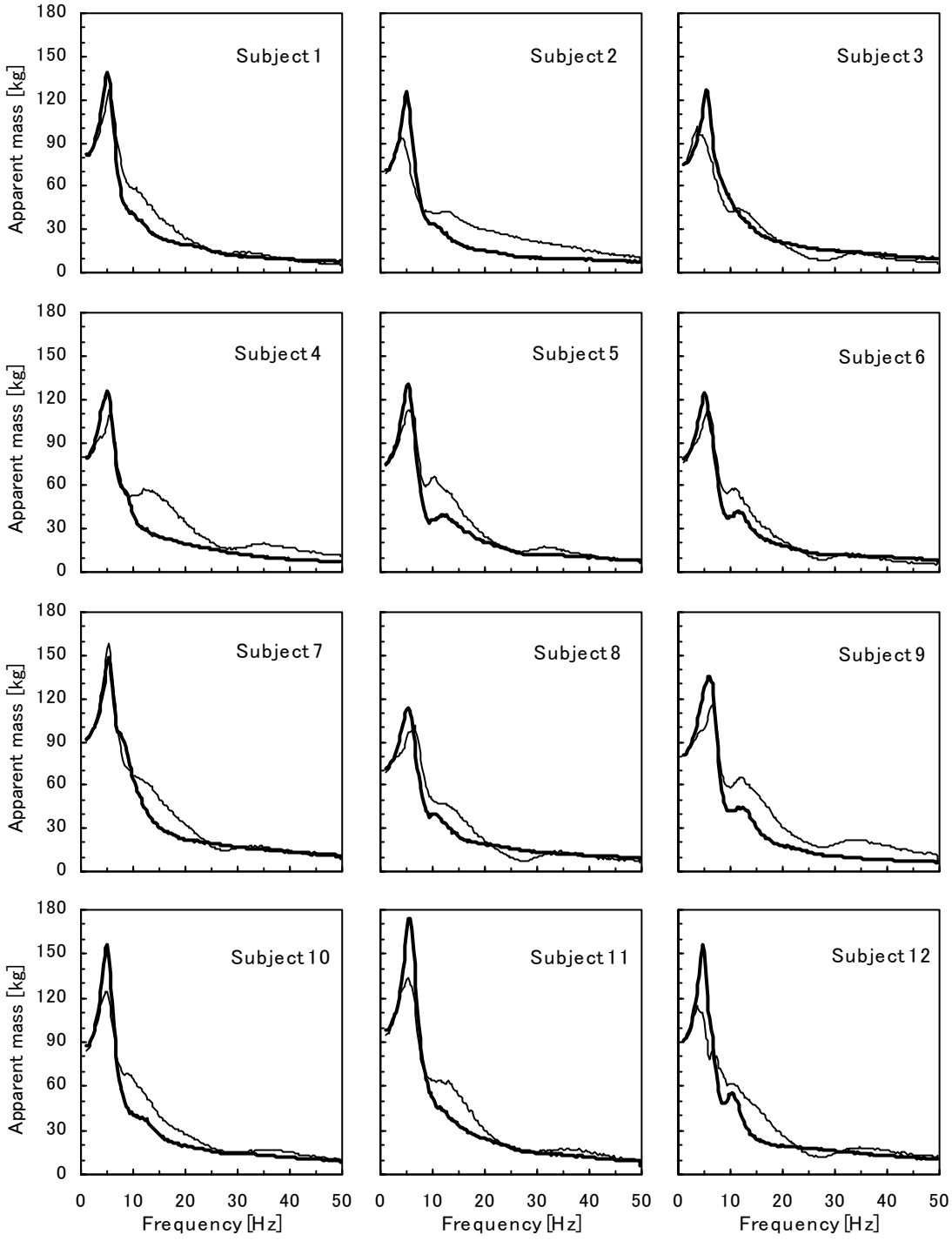

Figure 4.4 Apparent masses of the twelve subjects in the normal standing and sitting positions: standing posture ——— , sitting posture ━━━ .

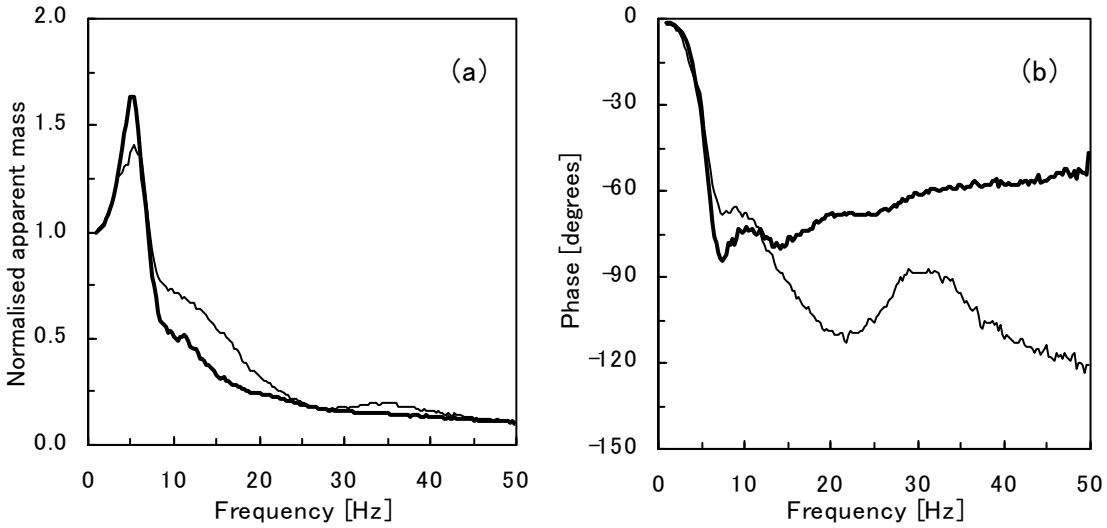

Figure 4.5 Median normalised apparent masses and phases of the twelve subjects in the normal standing and sitting positions: standing posture ——— ; sitting posture ━━━ .

4.3.2 Effect of posture and muscle tension in standing position

4.3.2.1 Effect of upper-body posture in standing position

The apparent masses of the twelve subjects in three different upper-body postures, upright (normal), erect and slouched in a standing position, measured in Experiment 1, are shown in Figure 4.6. The effect of postural changes in the upper-body were more evident at frequencies around the principal resonance frequency of the apparent mass. Variability between subjects was found to be large in the apparent masses in the slouched posture.

Figure 4.7 shows the median normalised apparent masses in three upper-body postures. The change in the upper-body posture, from normal upright to slouched, tended to decrease the frequency and magnitude of the main peak of the apparent mass from 5.25 Hz, with a magnitude of 1.41, to 4.25 Hz with a magnitude of 1.26, obtained from the median curves in Figure 4.7 ($p < 0.05$, Wilcoxon matched-pairs signed ranks test). Although the change to an erect posture showed some effects on the apparent mass of each subject shown in Figure 4.6, these were not consistent over the subjects so that no statistically significant differences were found.

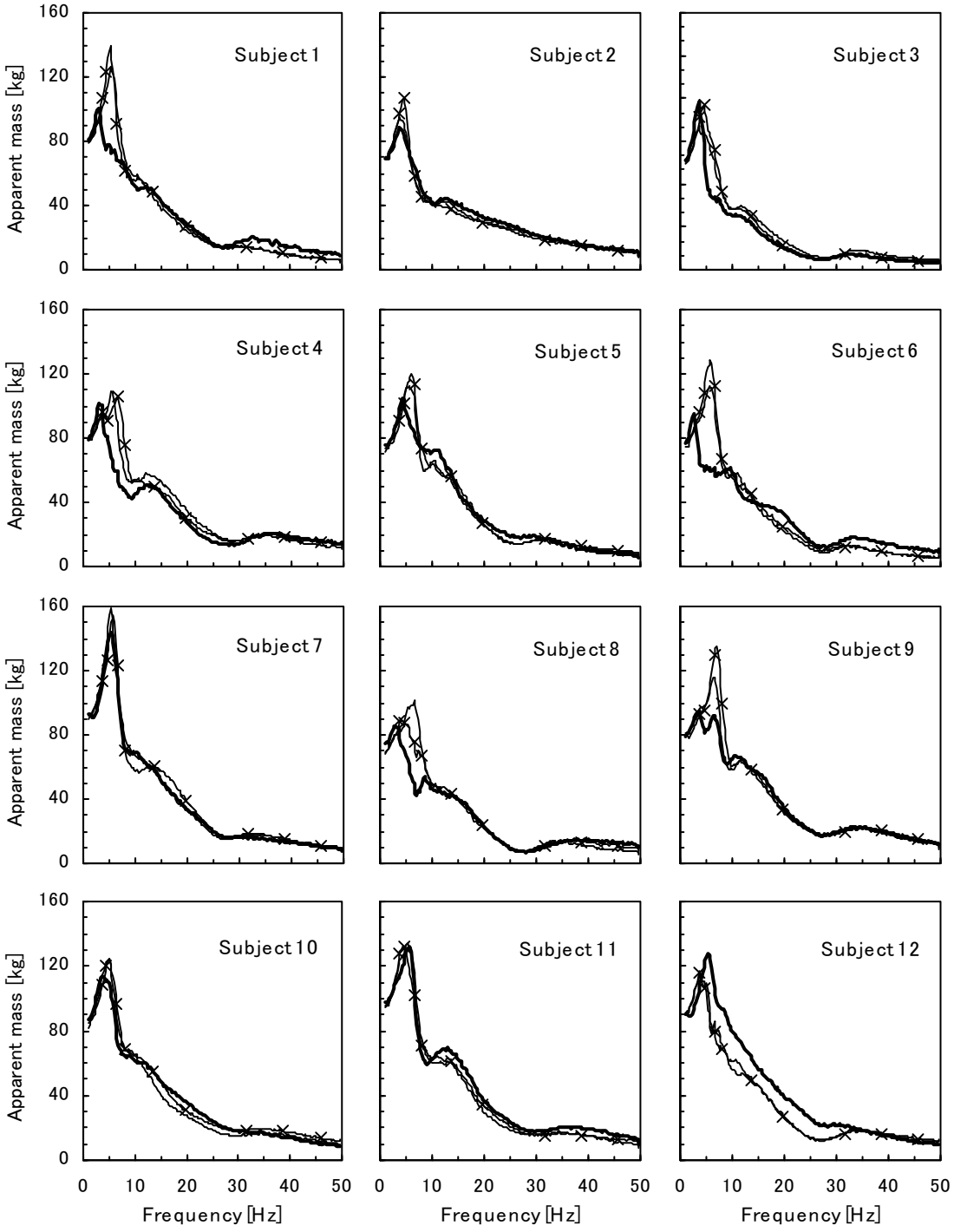

Figure 4.6 Apparent masses of the twelve subjects in the normal standing, erect standing and slouched standing postures: normal standing posture ——— ; erect standing posture —x— ; slouched standing posture ━━━ .

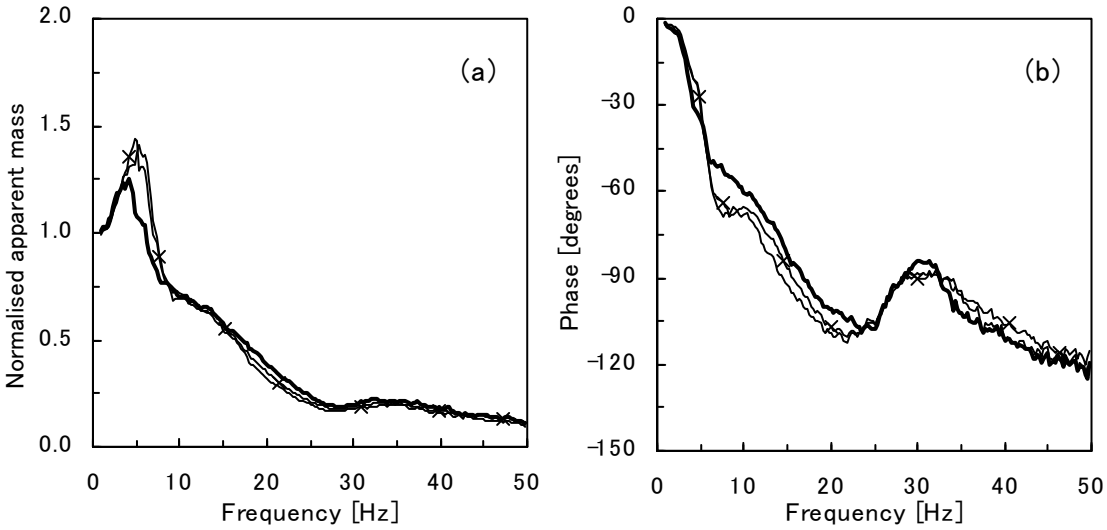

Figure 4.7 Median normalised apparent masses and phases of the twelve subjects in the normal standing, erect standing and slouched standing postures: normal standing posture ——— ; erect standing posture —x— ; slouched standing posture ▬▬ .

4.3.2.2 Effect of muscle tension

The apparent masses of the twelve subjects in the tensed standing posture, standing with all the muscles of the body tensed as much as possible, are compared with those in the normal standing posture in Figure 4.8. The effect of muscle tension was found to be inconsistent through the subjects, although the principal resonance frequency was higher in the tensed posture than in the normal posture for seven subjects.

The median normalised apparent mass in the tensed posture is compared with that in the normal posture in Figure 4.9. The principal resonance frequency was 6.0 Hz, with a magnitude of 1.57, in the tensed posture, although the changes in the principal resonance frequency and magnitude from those in the normal posture were not statistically significant.

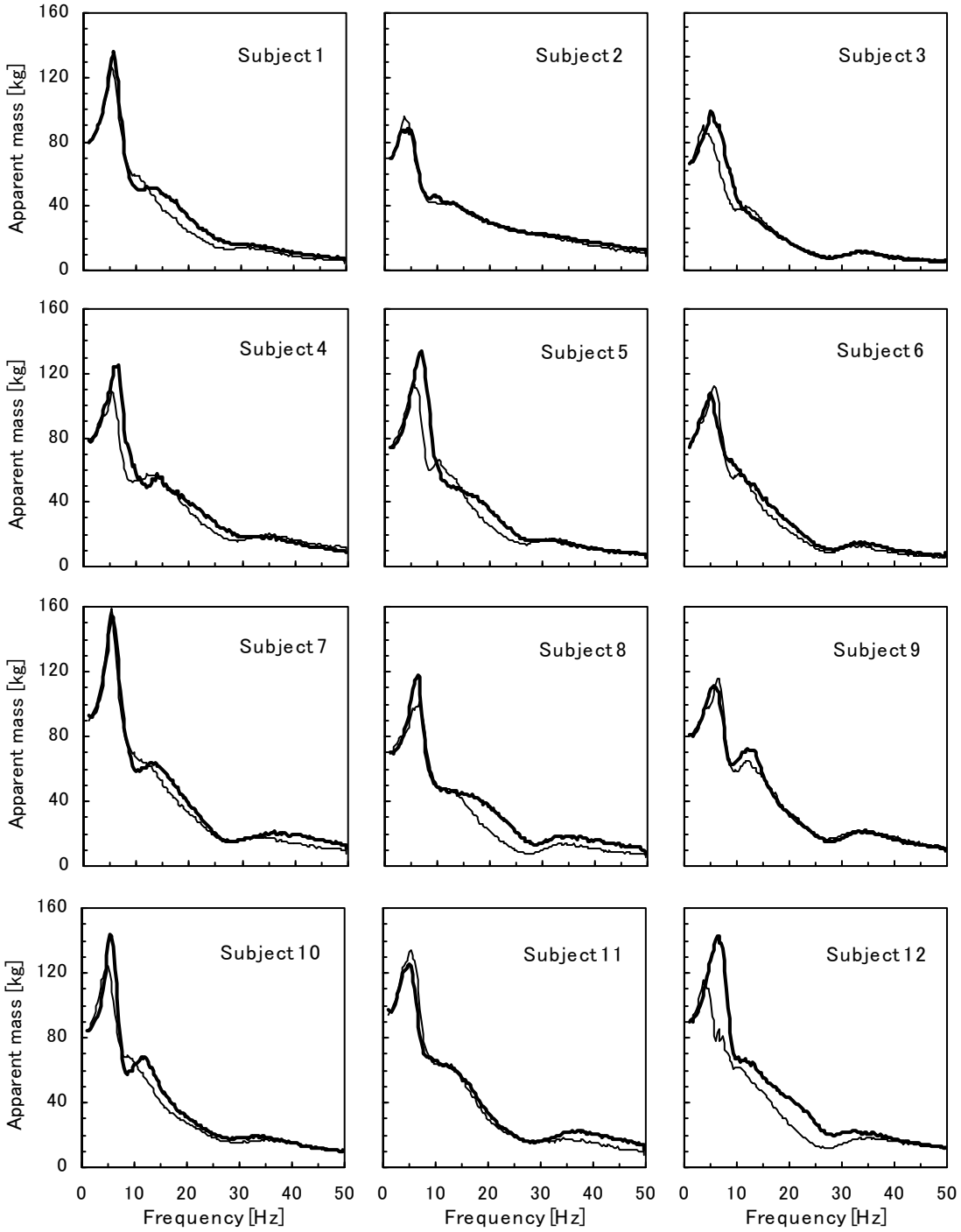

Figure 4.8 Apparent masses of the twelve subjects in the normal standing and tensed standing postures: normal standing posture ——— ; tensed standing posture ▬▬ .

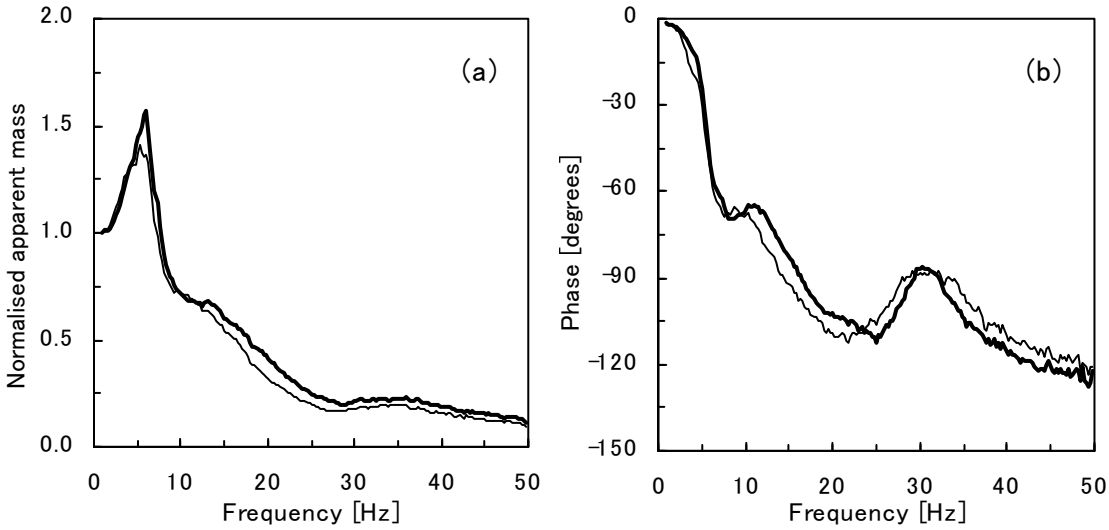

Figure 4.9 Median normalised apparent masses and phases of the twelve subjects in the normal standing and tensed standing postures: normal standing posture ——— ; tensed standing posture ━━━ .

4.3.2.3 Effect of leg posture

Figure 4.10 shows the effect of postural changes in the legs on the apparent mass for each subject. The apparent masses for the normal standing posture, legs bent posture, and one leg posture are compared in the figure. The median normalised apparent masses and phases for the three different leg postures are shown in Figure 4.11.

The apparent mass while subjects held their legs bent showed a clear difference in the main peak from that in the normal standing posture. With the legs bent, a principal resonance appeared at 2.75 Hz in the median normalised apparent mass, compared to 5.25 Hz in the normal posture (Figure 4.11). An increase in the resonance magnitude of the normalised apparent mass, from 1.41 for the normal posture to 1.81 for the legs bent posture, is also clear. These differences in the frequency and the magnitude were statistically significant ($p < 0.005$ according to the Wilcoxon matched-pairs signed ranks test).

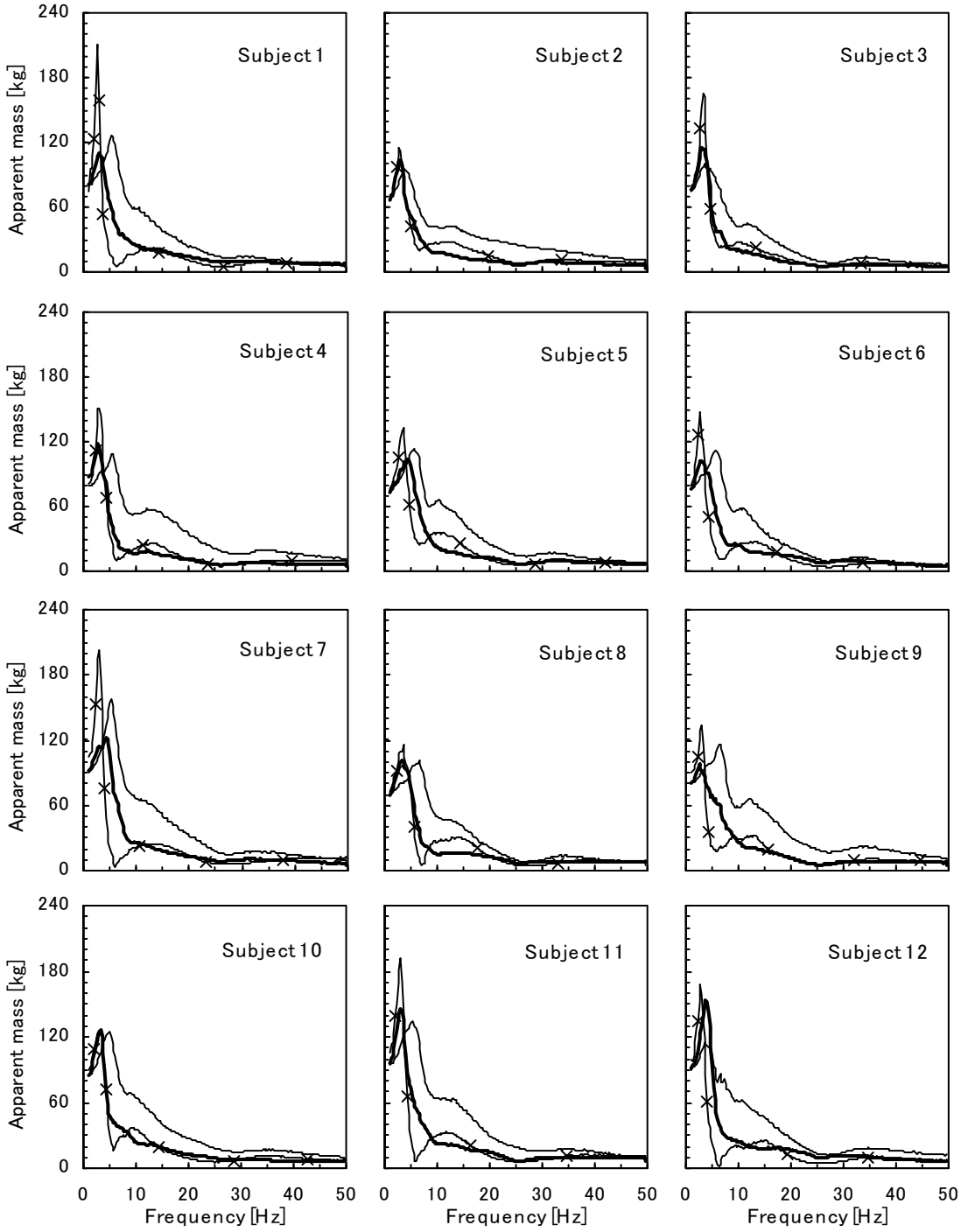

Figure 4.10 Apparent masses of the twelve subjects in the normal standing, legs bent and one leg postures: normal standing posture ——— ; legs bent posture —×— ; one leg posture ━━━ .

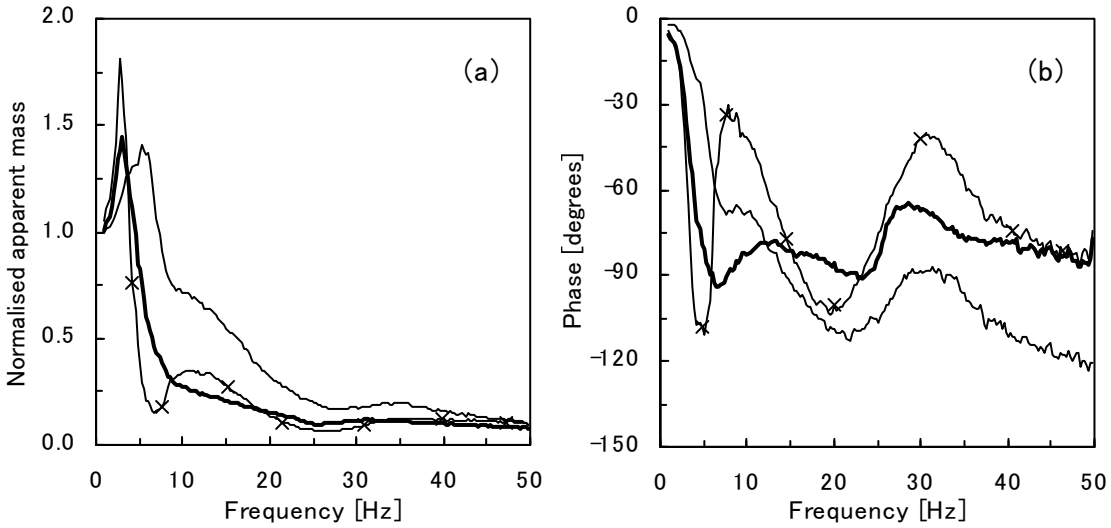

Figure 4.11 Median normalised apparent masses and phases of the twelve subjects in the normal standing, legs bent and one leg postures: normal standing posture ——— ; legs bent posture —×— ; one leg posture ━━━ .

The magnitude of the apparent mass in the legs bent posture dramatically decreased over the frequency range just above the frequency of the main resonance and showed much lower values than those during normal standing ($p < 0.05$ above 4 Hz). Two local peaks seen with the normal posture at about 12 and 35 Hz were found to exist at the same frequencies with the legs bent. There is a frequency region around 6 Hz where the apparent mass is small with the legs bent, while the apparent mass in the normal standing posture has a main peak in this frequency range. These changes were consistent with all subjects.

The apparent mass in the one leg posture showed a lower principal resonance frequency than in the normal posture, as seen in Figure 4.10 ($p < 0.005$, Wilcoxon matched-pairs signed ranks test). The median normalised apparent mass in the one leg posture had a principal resonance at 3.0 Hz, with a magnitude of 1.45 (Figure 4.11). The apparent mass in the one leg posture was smaller at frequencies above the principal resonance, compared to that in the normal posture ($p < 0.05$ above 4.25 Hz). The local peak seen with the normal posture and legs bent posture at about 12 Hz were not clear in the one leg posture.

Table 4.1 Medians and inter-quartile ranges of the frequency and magnitude of the principal resonance of the normalised apparent mass in different standing postures.

	Normal	Erect	Slouched	Tensed	Bent	One leg
Frequency [Hz]						
25th percentile	4.69	4.51	3.00	5.00	2.75	2.94
Median	5.25	5.13	3.63	5.38	2.88	3.00
75th percentile	5.50	5.82	4.50	6.31	3.07	3.38
Magnitude						
25th percentile	1.38	1.38	1.25	1.41	1.67	1.37
Median	1.45	1.53	1.32	1.59	1.89	1.48
75th percentile	1.49	1.67	1.42	1.70	2.07	1.51

Table 4.1 shows medians and inter-quartile ranges of the frequency and magnitude of the principal resonance of the normalised apparent masses in the different standing postures.

4.4 MATHEMATICAL MODELS OF APPARENT MASS

A simple modelling of the apparent mass of the standing and seated body measured in the experiment was carried out by using linear lumped parameter models. A single degree-of-freedom model was used first to obtain a general understanding of the characteristics of the apparent masses for subjects in the normal standing and sitting postures. Two types of two degree-of-freedom models were then used to obtain reasonable representations of the apparent masses for some different postures measured in the experiment.

4.4.1 Single degree-of-freedom models

It seems that the apparent masses measured with the subjects in the normal standing and normal sitting postures presented in the preceding sections showed characteristics of a two degree-of-freedom system in the frequency range below 20 Hz. The apparent mass for seated subjects obtained in this study showed similar trends to those measured in previous studies (e.g. Fairley and Griffin, 1989). The contribution of the

second mode of the system found at frequencies between 10 and 15 Hz, however, was smaller, compared to that of the first mode. The use of a single degree-of-freedom model was, therefore, reasonable to represent the apparent mass roughly and to obtain general ideas about the characteristics of the apparent masses for those two positions.

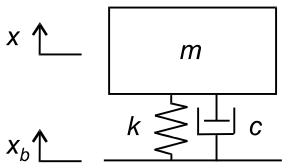

Figure 4.12 Single degree-of-freedom model.

The normalised apparent mass, normalised by the value at 1 Hz, calculated from a single degree-of-freedom linear lumped parameter model shown in Figure 4.12 was compared with the median normalised apparent masses for the normal standing and sitting postures measured in the experiment. The equation of motion of the model shown in Figure 4.12 was:

$$m\ddot{x} + c(\dot{x} - \dot{x}_b) + k(x - x_b) = 0 \tag{4.5}$$

where x was the displacement of the mass element and x_b was the displacement of the base. Using the Laplace Transform on the assumption that $x(0)=0$, $\dot{x}(0) = 0$, $x_b(0)=0$, and $\dot{x}_b(0) = 0$, and replacing the Laplace Transform variable s with the angular frequency ω based on the relation of $s = i\omega$, the apparent mass of the model was able to be obtained by:

$$M(i\omega) = \frac{m(ic\omega + k)}{-m\omega^2 + ic\omega + k} \tag{4.6}$$

The experimental results showed that the principal resonance frequencies of the apparent mass for those two postures were similar to each other, as mentioned in Section 4.3.1.2. Therefore, the undamped natural frequencies of the models for the two postures were set at an identical frequency, 5.5 Hz. The model mass was determined arbitrarily because the normalised apparent mass was compared with the experimental data. The model mass did not affect the frequency profile of the normalised apparent mass of the model. The damping ratio of the model was altered by trial and error so as to obtain reasonable representations of the measured apparent masses.

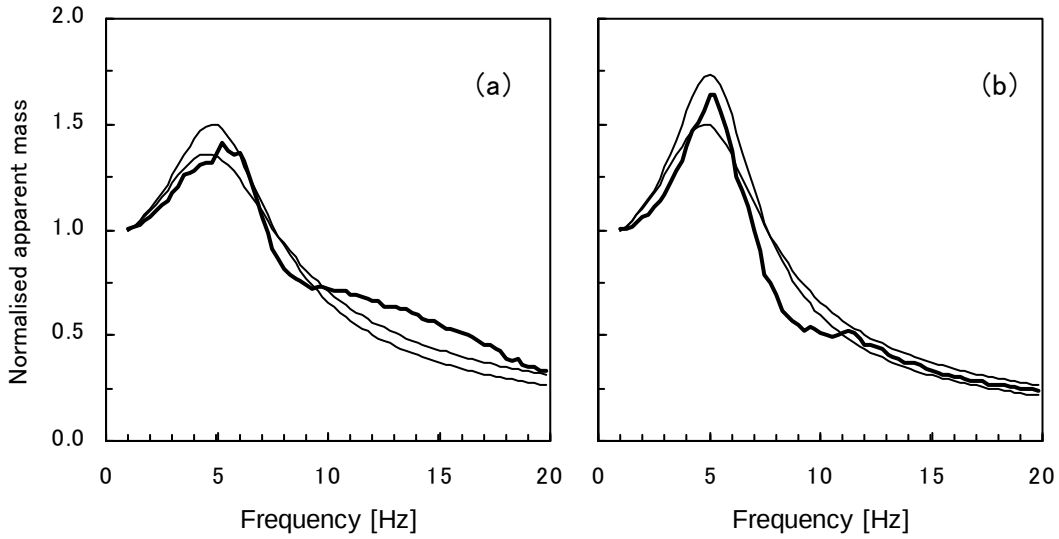

Figure 4.13 Normalised apparent mass measured in the experiment and calculated from the models. (a) Normal standing posture: experiment ━━━, models with two damping ratios, 0.45 and 0.55 ——; (b) normal sitting posture: experiment ━━━, models with two damping ratios, 0.35 and 0.45 ——.

Figure 4.13 compares the median normalised apparent masses for the normal standing and sitting postures obtained in the experiment with the normalised apparent masses calculated from the models. Two different damping ratios were used for each posture so as to show the range of damping ratios which provide reasonable representations of the apparent mass: 0.45 to 0.55 for the standing posture and 0.35 to 0.45 for the sitting posture. These damping ratios are much greater than those obtained for ordinary mechanical structures.

4.4.2 Two degree-of-freedom models

It was found that the apparent masses for the three standing postures (i.e. normal posture, legs bent posture and one leg posture) and for the sitting posture were distinguishable from each other in the experimental data, as presented in Section 4.3. These four postures were, therefore, selected for a further investigation using mathematical models so as to understand possible mechanisms causing the differences in the apparent masses among these different body postures.

4.4.2.1 Standing and sitting

The International Standard 5982 (1981) provides two degree-of-freedom linear lumped parameter models for the apparent masses of standing and seated subjects, as mentioned in Section 2.5.1. The model provided in ISO 5982 has two mass-spring-damper systems in parallel which do not dynamically couple with each other. It is unlikely, however, that some part of the body, or vibration mode of the body, is dynamically independent of the others in the human body at low frequencies of interest. Figure 4.14 shows two types of lumped parameter models with two degree-of-freedom, one of which was the same type as that suggested in ISO 5982. The equations of motion, and the apparent mass, were derived from the equations in the same way as described in the preceding section:

(a) Model 1

Equations of motion

$$\begin{aligned} m_1\ddot{x}_1 + c_1(\dot{x}_1 - \dot{x}_b) + k_1(x_1 - x_b) &= 0 \\ m_2\ddot{x}_2 + c_2(\dot{x}_2 - \dot{x}_b) + k_2(x_2 - x_b) &= 0 \end{aligned} \qquad (4.7\text{ a, b})$$

Apparent mass

$$M(i\omega) = \frac{m_1(ic_1\omega + k_1)}{-m_1\omega^2 + ic_1\omega + k_1} + \frac{m_2(ic_2\omega + k_2)}{-m_2\omega^2 + ic_2\omega + k_2} \qquad (4.8)$$

(b) Model 2

Equations of motion

$$\begin{aligned} m_1\ddot{x}_1 + c_1(\dot{x}_1 - \dot{x}_b) + c_2(\dot{x}_1 - \dot{x}_2) + k_1(x_1 - x_b) + k_2(x_1 - x_2) &= 0 \\ m_2\ddot{x}_2 + c_2(\dot{x}_2 - \dot{x}_1) + k_2(x_2 - x_1) &= 0 \end{aligned} \qquad (4.9\text{ a, b})$$

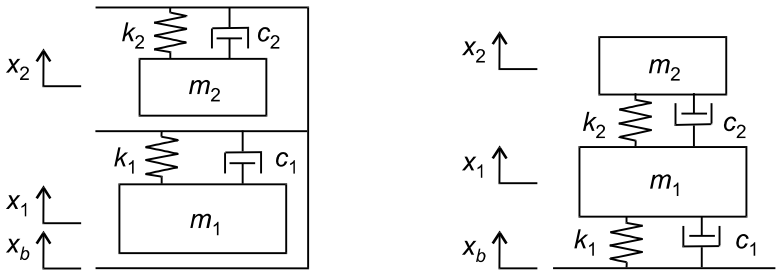

(a) Model 1 (b) Model 2

Figure 4.14 Two degree-of-freedom models. Model 1 is the same type as that provided in ISO 5982 (1981).

Apparent mass

$$M(i\omega) = \frac{(ic_1\omega + k_1)\left\{m_1(-m_2\omega^2 + ic_2\omega + k_2) + m_2(ic_2\omega + k_2)\right\}}{(-m_1\omega^2 + ic_1\omega + k_1)(-m_2\omega^2 + ic_2\omega + k_2) - m_2(ic_2\omega + k_2)\omega^2} \qquad (4.10)$$

The two degree-of-freedom model of standing subjects provided in ISO 5982 is based on data from only five subjects while that of seated subjects is based on 39 subjects. The validity of the ISO models for standing and seated subjects was examined by comparing the normalised apparent masses calculated from the ISO models with those measured in the experiment.

The model parameters for Models 1 and 2 were then optimised by a curve fitting method using the median normalised apparent masses obtained at frequencies below 20 Hz. The mass distribution for both models was the same as that given in ISO 5982 for each position: [m_1, m_2] = [62 kg, 13 kg] for a standing position and [m_1, m_2] = [69 kg, 6 kg] for a sitting position. The stiffness and damping parameters were obtained from parameter identification. A non-linear optimisation method, the Nelder-Meade simplex search available in MATLAB (MathWorks Inc.), was used to find an optimum set of parameters for the model.

Figure 4.15 compares the median normalised apparent mass and phase for the normal standing posture measured in the experiment, the normalised apparent mass and phase

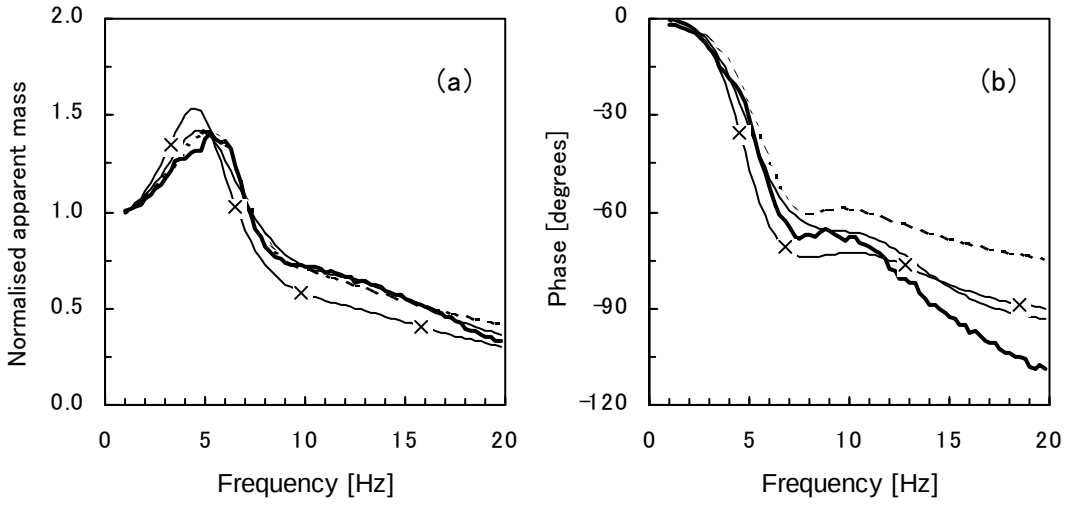

Figure 4.15 Median normalised apparent mass and phase for the normal standing posture measured in Experiment 1 and normalised apparent masses and phases calculated from models: experiment ——— ; ISO model —×— ; Model 1 ——— ; Model 2 - - - - . (Mass distribution was fixed.)

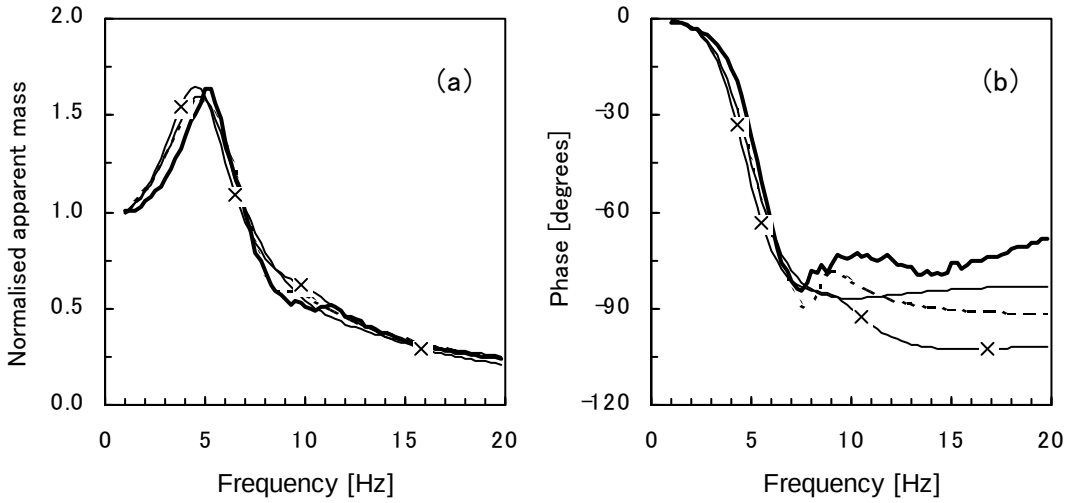

Figure 4.16 Median normalised apparent mass and phase for the normal sitting posture measured in Experiment 1 and normalised apparent masses and phases calculated from models: experiment ——; ISO model —×—; Model 1 ——; Model 2 - - - -. (Mass distribution was fixed.)

calculated from the ISO models, and those calculated from Models 1 and 2 with optimised stiffness and damping parameters. Those for the normal sitting posture are shown in Figure 4.16. The model parameters obtained from the parameter identification are tabulated in Table 4.2.

For a standing position, the normalised apparent mass and phase calculated from the ISO model was fairly close to the experimental data of the normal standing posture (Figure 4.15). However, a better result could be obtained if the parameters for the stiffness and damping of the model were adjusted while the mass distribution of the two masses were fixed (see the curve for Model 1 in Figure 4.15). The apparent masses

Table 4.2 Optimised model parameters for the standing and sitting postures. (Mass distribution was fixed.)

	Standing			Sitting		
	ISO 5982	Model 1	Model 2	ISO 5982	Model 1	Model 2
m_1 [kg]	62	62	62	69	69	69
k_1 [N/m]	6.2×10^4	7.4×10^4	1.4×10^5	6.8×10^4	7.5×10^4	8.5×10^4
c_1 [Ns/m]	1.46×10^3	1.9×10^3	4.0×10^3	1.54×10^3	1.7×10^3	2.2×10^3
m_2 [kg]	13	13	13	6.0	6.0	6.0
k_2 [N/m]	8.0×10^4	8.8×10^4	2.7×10^4	2.4×10^4	4.9×10^4	1.5×10^4
c_2 [Ns/m]	9.3×10^2	7.4×10^2	3.2×10^2	1.9×10^2	8.9×10^2	5.9×10^1

calculated from Models 1 and 2 were very similar, although the phase calculated from Model 1 was closer to the experimental data than that from Model 2.

It can be seen in Figure 4.16 that the normalised apparent mass calculated from the ISO model of seated subjects showed a good agreement with the measured normalised apparent mass, except in the frequency range between 8 and 11 Hz. The phase calculated from the ISO model did not fit the experimental data at frequencies above 8 Hz. That discrepancy was also observed in the figure provided in ISO 5982 (1981). The results obtained from Models 1 and 2 showed a better agreement with the measured phase, compared to that from the ISO model, although differences between the measured and calculated values were still observed at high frequencies.

In the results mentioned above, parameters for the stiffness and damping of the models were optimised while the mass distribution of the two masses were retained. The parameters for the two masses were then involved in the optimisation procedure so as to obtain a better fit to the experimental data. The total mass of the two masses in the models was fixed at 75.0 kg, as in the case of ISO 5982, although this did not affect the normalised apparent mass. The ratio between the two masses and the parameters for stiffness and damping were optimised simultaneously.

Figures 4.17 and 4.18 compare the measured median normalised apparent mass and phase with those calculated from Models 1 and 2 for the normal standing and normal

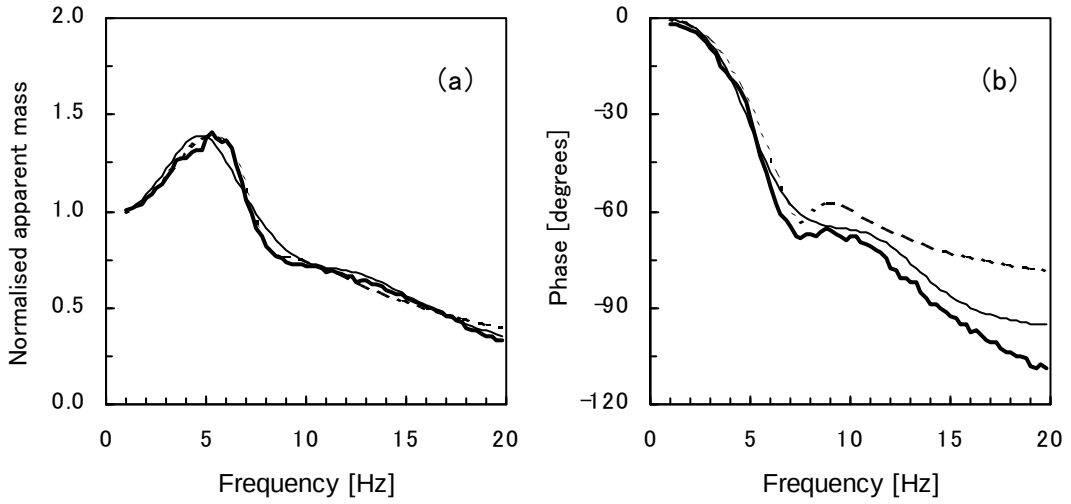

Figure 4.17 Median normalised apparent mass and phase for the normal standing posture measured in Experiment 1 and normalised apparent masses and phases calculated from models: experiment ━━━; Model 1 ——; Model 2 - - - - -. (Mass distribution was optimised.)

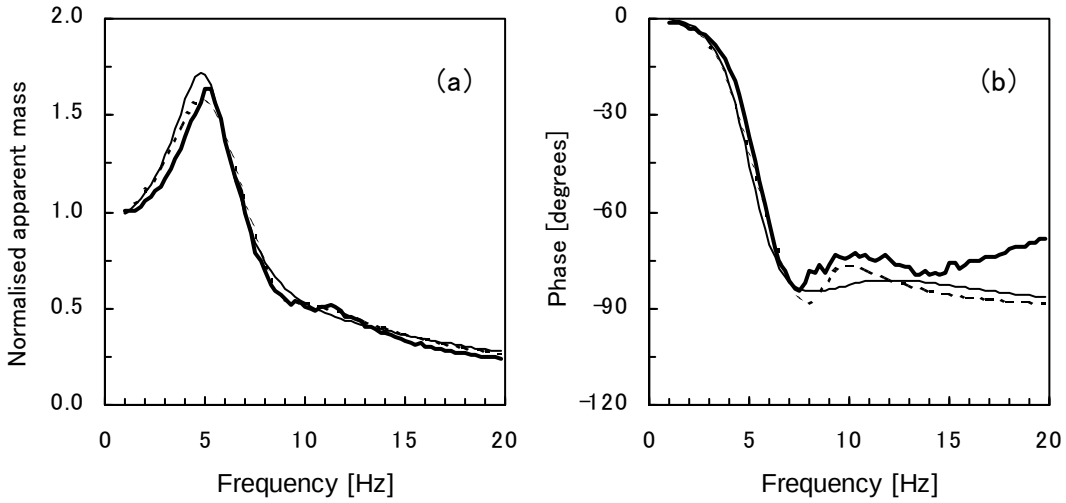

Figure 4.18 Median normalised apparent mass and phase for the normal sitting posture measured in Experiment 1 and normalised apparent masses and phases calculated from models: experiment ——— ; Model 1 ——— ; Model 2 - - - - - . (Mass distribution was optimised.)

sitting postures, respectively. Table 4.3 shows the model parameters obtained from curve fitting.

The mass distribution of Model 1 obtained for the standing posture coincided with that for the sitting posture (Table 4.3). That mass distribution for Model 1 was close to that of the ISO model of standing subjects. The masses of the ISO model of standing subjects may be reasonable to represent the apparent mass. The mass distribution of Model 2 obtained was different from that of the ISO model for both standing and seated subjects. That could be expected because the structure of Model 2, a series of two mass-spring-damper systems, was different from Model 1, parallel two mass-spring-damper systems.

Table 4.3 Optimised model parameters for the standing and sitting postures. (Mass distribution was optimised.)

	Standing		Sitting	
	Model 1	Model 2	Model 1	Model 2
m_1 [kg]	64	68.2	64	65
k_1 [N/m]	7.7×10^4	1.2×10^5	6.9×10^4	9.0×10^4
c_1 [Ns/m]	2.1×10^3	3.7×10^3	1.3×10^3	2.4×10^3
m_2 [kg]	11	6.8	11	10
k_2 [N/m]	7.4×10^4	1.5×10^4	7.0×10^4	2.6×10^4
c_2 [Ns/m]	5.2×10^2	9.4×10^1	1.1×10^3	1.4×10^2

It was observed that the models, Models 1 and 2, with masses optimised improved the representation of the phase at frequencies above 8 Hz for the sitting posture, compared to those with the same mass distribution as the ISO model (Figures 4.16(b) and Figure 4.18(b)). For the standing posture, the results from the models with optimised masses were very similar to those from the models with the mass distribution given in ISO 5982.

4.4.2.2 Standing with different leg postures

Two types of two degree-of-freedom models shown in Figure 4.14 were used to model the apparent mass for the legs bent posture and the one leg posture. First, as in the previous section, the stiffness and damping parameters were obtained by the curve fitting, while the two masses were fixed at 62 and 13 kg as provided in ISO 5982 for standing subjects. The median normalised apparent masses measured at frequencies below 20 Hz were used for determining the model parameters.

The difference in the three standing postures used in the experiment was only in the attitude of the legs. It might, therefore, be hypothesised that the differences of the apparent mass in the three postures were caused by changes in the dynamic mechanism of the body which mainly contributed to the first resonance of the apparent mass. Therefore, the stiffness and damping of the lower system with a heavier mass (i.e., k_1 and c_1) in Figure 4.14, were optimised to obtain the apparent mass in the legs

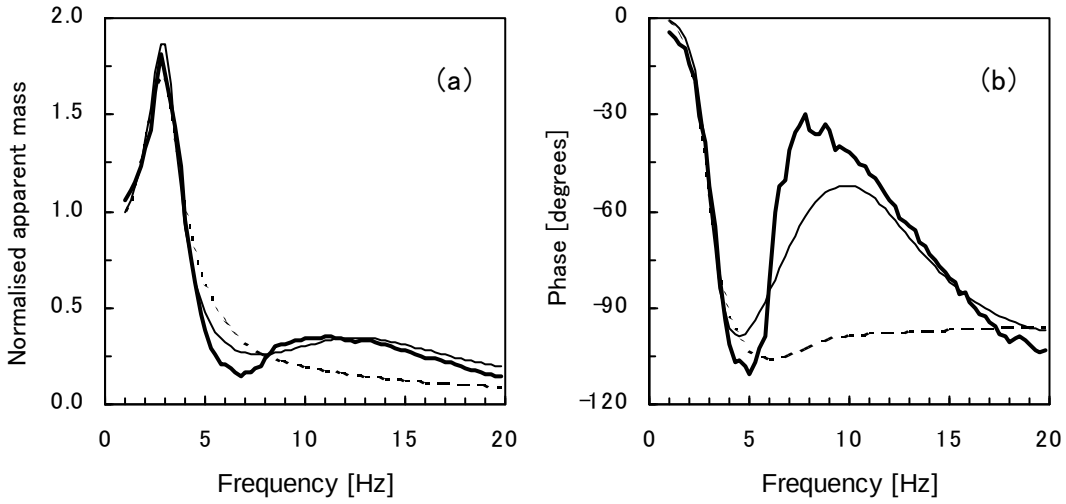

Figure 4.19 Median normalised apparent mass and phase for the legs bent posture measured in Experiment 1 and normalised apparent masses and phases calculated from models: experiment ━━━ ; Model 1 ——— ; Model 2 - - - - - . (Stiffness and damping for Mass 1 were optimised.)

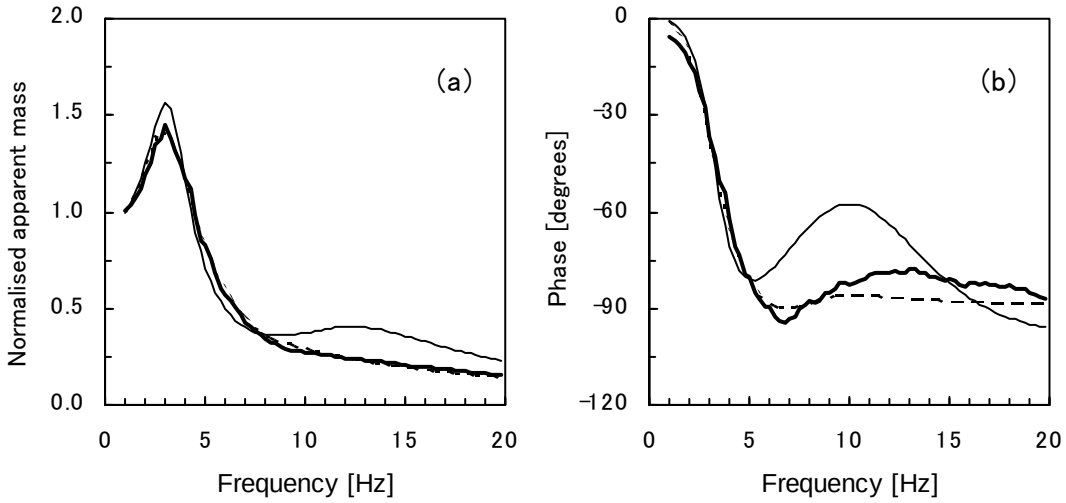

Figure 4.20 Median normalised apparent mass and phase for the one leg posture measured in Experiment 1 and normalised apparent masses and phases calculated from models: experiment ━━━; Model 1 ——; Model 2 - - - - -. (Stiffness and damping for Mass 1 were optimised.)

bent and one leg postures. The other parameters were the same as those obtained above for the normal standing posture (see Table 4.2).

The median normalised apparent mass and phase measured in the experiment and those calculated from Models 1 and 2 are shown in Figure 4.19 for the legs bent posture and in Figure 4.20 for the one leg posture. The parameters used to calculate the apparent masses and phases of the models are presented in Table 4.4.

The results presented in Figures 4.19 and 4.20 showed that the differences in the apparent masses among the three standing postures could be represented by the

Table 4.4 Optimised model parameters for the legs bent and one leg postures. (k_1 and c_1 were optimised.)

	Legs bent		One leg	
	Model 1	Model 2	Model 1	Model 2
m_1 [kg]	62	62	62	62
k_1 [N/m]	2.3×10^4	2.7×10^4	2.8×10^4	3.3×10^4
c_1 [Ns/m]	5.5×10^2	9.5×10^2	8.7×10^2	1.5×10^3
m_2 [kg]	13	13	13	13
k_2 [N/m]	8.8×10^4	2.7×10^4	8.8×10^4	2.7×10^4
c_2 [Ns/m]	7.4×10^2	3.2×10^2	7.4×10^2	3.2×10^2

changes only in the stiffness and damping of the lower system with a heavier mass. For the legs bent posture, the normalised apparent mass and phase calculated from Model 1 showed a better agreement with the experimental data than those calculated from Model 2 (Figure 4.19). The change in the apparent masses between the normal and legs bent posture may be explained by Model 1. For the one leg posture, however, the measured normalised apparent mass and phase were more closely fitted by those obtained from Model 2 than those calculated from Model 1. It might, therefore, be concluded that different leg postures alter the characteristic of only the dynamic mechanism which mainly contributes to the principal resonance of the apparent mass while the other dynamic properties are not influenced. However, neither Model 1 nor 2 could provide reasonable representations for both the legs bent posture and the one leg posture.

The parameters that were fixed in the parameter identification method mentioned above were then optimised so as to investigate if the changes in all parameters could improve the representation of the apparent masses for the legs bent and one leg postures. As in the case of Section 4.4.2.1, the total mass of the model was fixed at 75.0 kg. The results of curve fitting are presented in Figure 4.21 for the legs bent posture and in Figure 4.22 for the one leg posture. The optimised model parameters are tabulated in Table 4.5.

The masses of Model 1 were not very different from those provided by ISO 5982, even if

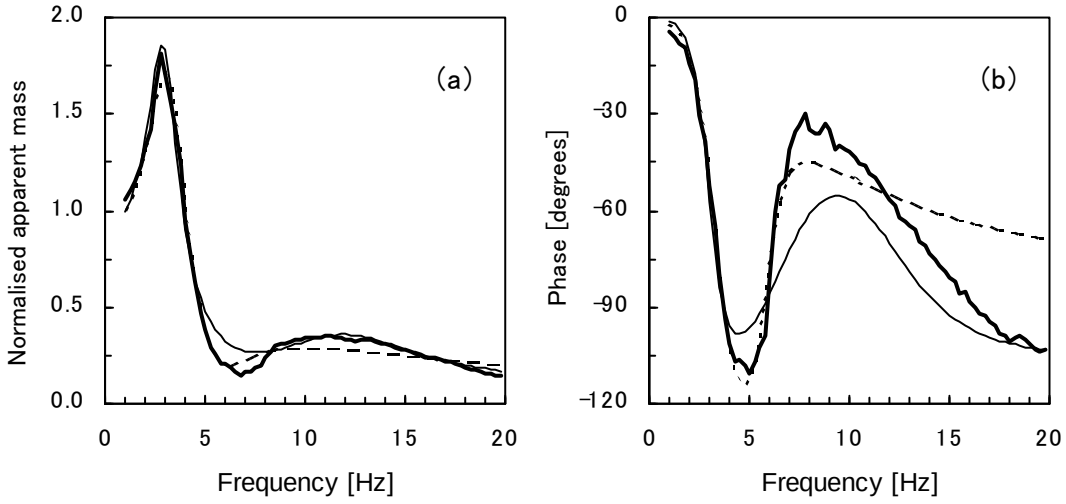

Figure 4.21 Median normalised apparent mass and phase for the legs bent posture measured in Experiment 1 and normalised apparent masses and phases calculated from models: experiment ━━━; Model 1 ——; Model 2 - - - - -. (All parameters were optimised.)

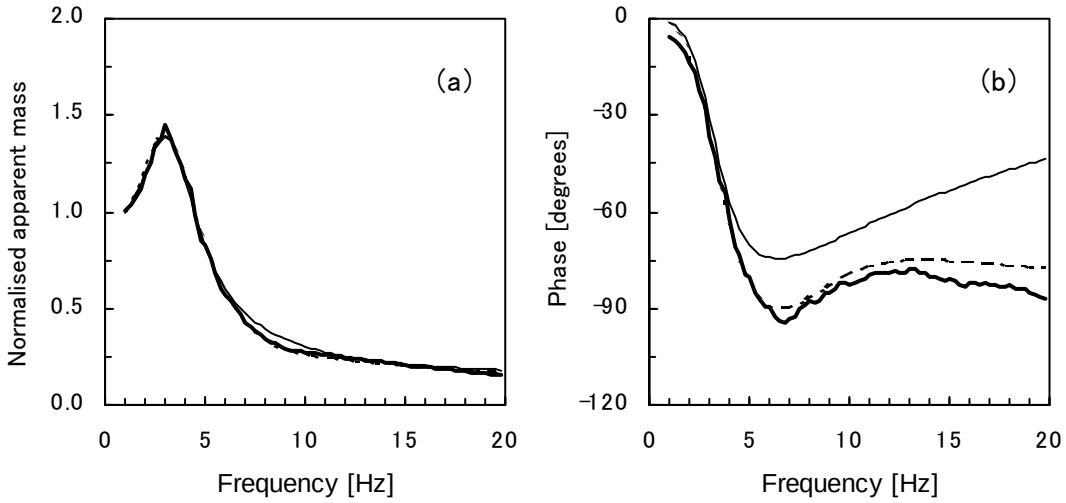

Figure 4.22 Median normalised apparent mass and phase for the one leg posture measured in Experiment 1 and normalised apparent masses and phases calculated from models: experiment ━━━; Model 1 ——; Model 2 - - - - -. (All parameters were optimised.)

those parameters were involved in the optimisation procedure. However, the stiffness and damping parameters for the smaller mass system (i.e., k_2 and c_2) of Model 1 obtained for the one leg posture were too large, so that the performance of that mass-spring-damper system hardly influenced the response of the whole model up to 20 Hz. Model 1 did not seem to be suitable to represent the apparent mass for the one leg posture.

The normalised apparent mass and phase calculated from Model 2 showed a good agreement with the experimental data for the one leg posture (Figure 4.22). The parameters of Model 2 for the one leg posture were not similar to those for the normal

Table 4.5 Optimised model parameters for the legs bent and one leg postures. (All parameters were optimised.)

	Legs bent		One leg	
	Model 1	Model 2	Model 1	Model 2
m_1 [kg]	63	36	64	39
k_1 [N/m]	2.3×10^4	4.0×10^4	3.1×10^4	3.7×10^4
c_1 [Ns/m]	5.9×10^2	2.3×10^3	1.2×10^3	1.9×10^3
m_2 [kg]	12	39	11	36
k_2 [N/m]	7.1×10^4	2.5×10^4	1.3×10^{19}	5.6×10^4
c_2 [Ns/m]	5.7×10^2	2.1×10^2	1.6×10^{17}	9.0×10^2

standing posture (Tables 4.3 and 4.5). For the legs bent posture, the results obtained from both models showed a good agreement with the measured values, except for the discrepancy in the phase calculated from Model 2 at frequencies above 10 Hz (Figure 4.21). The parameters of Model 2 for the legs bent posture were significantly different from those for the normal standing posture, as in the case of the one leg posture (Tables 4.3 and 4.5).

4.5 DISCUSSION

4.5.1 Discussion of experimental results

The apparent mass was obtained when subjects were standing in several different postures and sitting on a rigid seat in the experiment. Twelve repeat measurements of the apparent mass with a subject showed high repeatability of the measurement for the normal standing and sitting postures, which were chosen as typical postures (Section 4.3.1.1). This high repeatability assured that reliable apparent mass data could be obtained from a measurement for each individual. It seemed that variability among twelve runs with a subject, intra-subject variability, was larger for the standing position than for the sitting position (Figure 4.1). It is more difficult to reproduce exactly the same posture for each exposure in a standing position than in a sitting position because more degrees of freedom (i.e., the legs) were involved when standing, even when a subject is well trained to maintain the same posture on every occasion. This might cause the slightly larger variability in the standing posture than in the sitting posture.

The median apparent mass for the normal standing posture obtained in the experiment is compared with the apparent masses measured in previous studies presented in Section 2.3.1.1 in Figure 4.23. The trends in the apparent mass seemed to agree with the previous data: the principal resonance at around 5 Hz and the second broad peak at frequencies between 9 and 15 Hz can be observed in Figure 4.23. The principal resonance magnitude of the measured apparent mass was smaller than the previous results by Coermann (1962) and Edwards and Lange (1964) but similar to the result by Fairley (1981). This might be mainly caused by the difference in the static weight of subjects used in the studies: 83.9 kg for the subject used by Coermann (1962), 84 and 78 kg for the two subject in Edwards and Lange (1964), a median of 75 kg for the eight

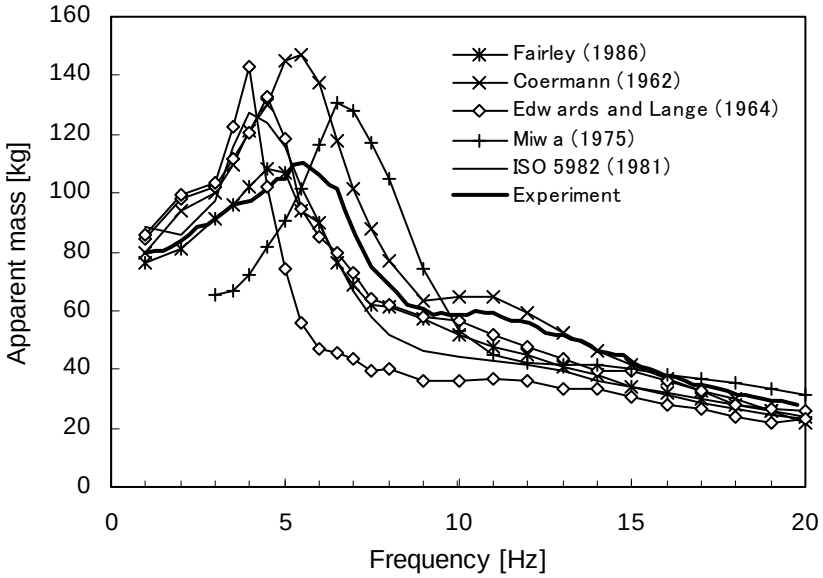

Figure 4.23 Median apparent mass for the normal standing posture measured in Experiment 1 and the apparent mass for a normal standing position in previous studies and ISO 5982. (See Section 2.3.1.1 for details of the previous studies.)

subjects used by Fairley (1981), a median of 75.5 kg for the twelve subjects in this study.

The apparent masses of subjects when standing normally showed two similar peaks to those found in the apparent masses of normally sitting subjects in the frequency range from 1 to 50 Hz: a principal resonance at about 5 Hz and a local broad peak in the frequency range of 10 to 15 Hz (Figures 4.2 to 4.5). This may imply that it is possible to consider these two resonances in the dynamic response of the standing body to be attributed to the same dynamic mechanisms, vibration modes, as when sitting (Kitazaki and Griffin, 1997 and 1998). A broad peak at around 35 Hz, which was relatively small, was found only in the apparent mass of the standing body. This might be caused by the contribution of some local dynamic response of the lower limbs.

Postural changes of the upper-body had some effects on the dynamic response of the standing subjects, in particular in the frequency region around the principal resonance (Figure 4.7). In the present study, the frequency of the principal resonance decreased by about 1 Hz with a change of the upper-body posture from normal to slouched. The magnitude of the principal resonance also decreased with the same postural change. However, different influences were observed in a few subjects, which may be caused by the difficulty in maintaining required postures, particularly when standing (Figure 4.6).

There was also some difference between the apparent masses in normal and erect postures at about 5 Hz. These effects might be mainly caused by a change in the angle between the upper-body, or the pelvis, and the legs. The change from normal posture to slouched, in which subjects leant their upper-body forward slightly, caused a larger change in the apparent mass than the change from normal to erect in which the upper-body was held upright without a significant change in the angle of the pelvis.

It was thought that the 'standing with the upper-body tensed' posture used in the study might change the constant muscle force in the upper-body. The muscle force in subjects might fluctuate either voluntarily or involuntarily about its constant level during exposure to vibration. The tensed posture might increase that constant muscle force and make the body stiffer. It was found that the change in the muscle tone used here did not have any significant effects on the apparent mass, although the principal resonance frequency increased with the change from normal muscle tone to tensed for several subjects (Figure 4.8).

With the legs bent in a standing position, the principal resonance in the apparent mass of all subjects appeared at about 3 Hz, while in the normal standing posture the resonance was at about 5 Hz (Figure 4.10). The trends of the apparent mass for the legs bent posture agreed with those obtained by Fairley (1981), although a difference in the principal resonance magnitude was able to be seen (Figure 4.24). There was an

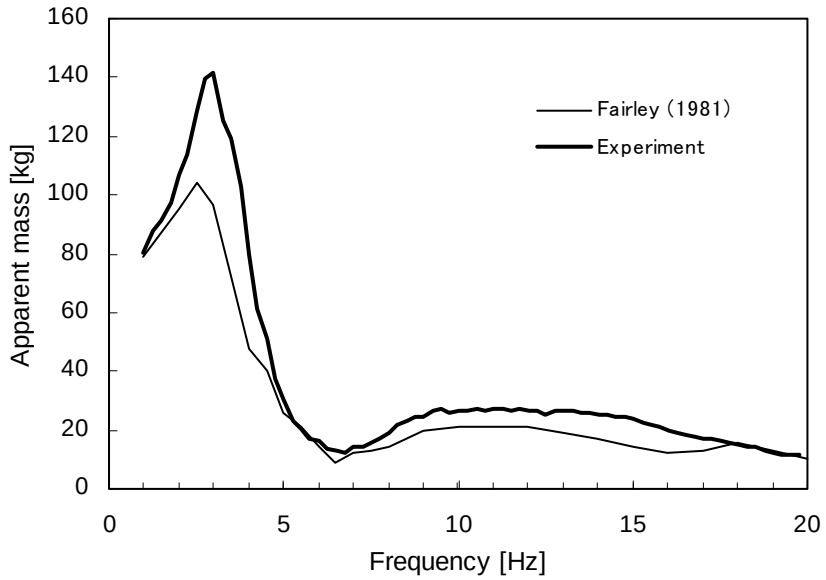

Figure 4.24 Median apparent mass for the legs bent posture measured in Experiment 1 and that for the 'knee bent' posture by Fairley (1981). (See Section 2.4.1.2 for the details of the study by Fairley.)

increase in the principal resonance magnitude by about 30% while the magnitude of the apparent mass showed remarkably low values in the frequency region just above the main resonance frequency (Figures 4.10 and 4.11). This may imply that, when bent, the legs worked as springs with low stiffness giving amplification at low frequencies and isolation at higher frequencies. At about 6 Hz, where the apparent mass dramatically decreased to a minimum, the absolute movement of the upper-body was probably small, owing to the isolation provided by the legs.

The postural change from normal standing to standing on one leg also decreased the principal resonance frequency from 5.25 to 3.0 Hz in the median apparent mass of the twelve subjects (Figure 4.11). At frequencies above the principal resonance, the apparent mass for the one leg posture was smaller than that for the normal posture (Figures 4.10 and 4.11). It is likely that some vibration isolation was provided when subjects stood on one leg, as in the case of the legs bent posture. However, the local peak in the frequency range between 10 and 15 Hz disappeared in the one leg posture, although that could be seen in the apparent mass for the legs bent posture in which the effect of vibration isolation was observed. The cause of the vibration isolation in the one leg posture, therefore, might be different from that in the legs bent posture.

4.5.2 Discussion of mathematical modelling

The investigation of mathematical models using linear lumped parameter models provided some insights into the mechanisms of the resonances observed in the apparent mass. Single degree-of-freedom models with a constant stiffness but with different damping could roughly represent the measured apparent masses for both standing and sitting postures at frequencies below 20 Hz. A damping ratio about 0.5 was used for the standing posture while about 0.4 for the sitting posture (Figure 4.13). In the single degree-of-freedom model shown in Figure 4.12, heavier damping provided smaller apparent masses at around resonance frequency and greater apparent masses at frequencies above $\sqrt{2}f_n$ Hz (f_n: undamped natural frequency; the apparent mass at $\sqrt{2}f_n$ Hz corresponds to the static mass for any damping ratio). This trend can be observed in the apparent mass for the standing posture, compared to that for the sitting posture. This may imply that, when standing, the legs provided additional damping on some dynamic mechanisms in the upper-body which caused the principal resonance of the apparent mass for both standing and sitting postures.

The two degree-of-freedom models of the mechanical impedance for standing and seated subjects defined in ISO 5982 were compared with the measured apparent masses. The ISO model of seated subjects showed a good agreement with the median normalised apparent mass measured with the twelve subjects, although the ISO model was based on seated subjects with the feet supported by a footrest while the feet of the subjects hung freely in Experiment 1 (Figure 4.16). It was stated in ISO 5982 that 'the subject posture was usually poorly defined. In general, the values relate to an upright posture and for at least ten subjects, the feet were supported by a footrest moving with the seat'. The agreement of the ISO model of standing subjects with the experimental data was not as good as that for seated subjects (Figure 4.15). As mentioned above, the model of standing subjects was based on available experimental data from five subjects. The model for standing subjects, therefore, might be open to be revised if more experimental data are available. The representation of the apparent mass and phase for standing subjects was improved by optimising the model parameters (Model 1 in Figures 4.15 and 4.17). The mass distribution of the ISO models seemed to be reasonable because the optimised mass distribution was not significantly different from the original value provided in ISO 5982 (Model 1 in Tables 4.2 and 4.3).

Although the ISO model for seated subjects represented the apparent mass well, there were discrepancies in the phase of the driving-point response between the model and experimental data, as seen in Figure 4.16. This may not be attributed to the difference in

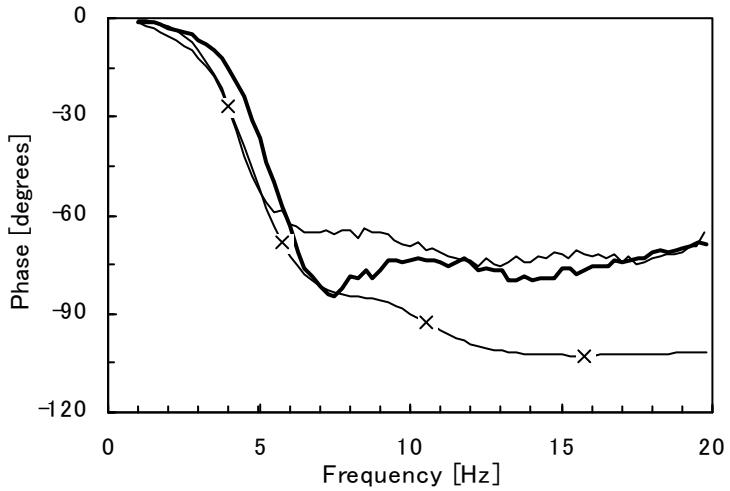

Figure 4.25 Phases of seated subjects: median in Experiment 1 (without footrest) ——; ISO model —x—; median by Fairley and Griffin (1989) (with footrest) — — .

the experimental condition of subjects' feet between this experiment and the standard because similar discrepancies can be seen in the comparison between the model and the experimental data in ISO 5982. Figure 4.25 compares the median phase measured in Experiment 1, the phase calculated from the ISO model and the median phase measured with 60 seated subjects with their feet supported by Fairley and Griffin (1989). It can be seen that the discrepancy between the phase calculated from the ISO model and the phase measured in this experiment is not attributed to the effect of a footrest. The representation of the phase was able to be improved by changing the model parameters (Model 1 in Figures 4.16 and 4.18). However, it might be difficult to obtain a very good representation at higher frequencies by two degree-of-freedom models because the dynamic response at those frequencies might be affected by the third or higher vibration modes. The development of alternative two degree-of-freedom models of the apparent mass of seated subjects has been underway elsewhere (e.g. Wei and Griffin 1998).

Model 2 shown in Figure 4.14 had a series of two mass-spring-damper systems which coupled with each other, as opposed to Model 1 with two parallel independent systems. The apparent mass was able to be represented well generally by both types of model. The difference between Model 1 and Model 2 was clear in the calculated phase at frequencies above about 7 Hz (Figures 4.15 to 4.18). It seemed that Model 1 was better for the standing posture while Model 2 was better for the sitting posture in the figures. However, the effects of higher vibration modes which might alter the calculated phase at higher frequencies were neglected in this study. It was, therefore, difficult to conclude which type of model was better able to represent the apparent mass for standing and seated subjects.

The apparent masses for the legs bent posture and the one leg posture were reasonably represented by the models with the same mass distribution and the same stiffness and damping parameters for the smaller mass system as those for the normal standing posture (Figures 4.19 and 4.20). This might imply that the postural changes in the legs used in the study caused some change in the dynamic mechanisms which contributed to the principal resonance but left higher vibration modes unchanged. However, neither Model 1 nor 2 could provide reasonable representations for both the legs bent posture and the one leg posture.

The results from the models with all parameters optimised showed that the apparent mass and phase for the legs bent posture could be represented by both Models 1 and 2 while those, particularly the phase, for the one leg posture could be represented only by Model 2 (Figures 4.21 and 4.22). The mass distribution of Model 2 obtained for both the legs bent posture and the one leg posture were found to be very different from that obtained for the normal standing posture while the mass distribution of Model 1 for the legs bent posture were similar to that for the normal posture (Tables 4.3 and 4.5). As mentioned above, when the mass distribution of the model was optimised, the apparent mass and phase for the one leg posture were represented only by Model 2. This may imply that the mechanism of the dynamic response in one leg posture is different from that with standing on both legs. For the legs bent posture, it was difficult to conclude in the same way as the one leg posture because both models showed reasonable agreement with the experimental data.

4.6 CONCLUSIONS

The apparent masses measured with both standing and sitting subjects showed a principal peak at about 5 Hz. A local broad peak in the frequency range of 10 to 15 Hz was also found in both positions. The dynamic mechanisms which contributed to the principal resonance and the second broad peak might be common in standing and sitting positions. It is likely that vibration transmission through the legs provided additional damping to the principal resonance of the apparent mass of standing subjects. There was another small broad peak at frequencies around 35 Hz only in the apparent mass of the standing body. The dynamic response of the legs might cause this broad peak in the standing posture.

Changing the upper-body posture from normal upright to slouched in a standing position decreased the principal resonance frequency by about 1 Hz. The magnitude of the principal resonance also decreased with the same postural change. The angle of the upper-body relative to the legs might be the main cause of the change in the apparent mass.

With the legs bent posture, the principal resonances for all subjects appeared at a frequency below 3 Hz and the resonance magnitude was greater than that in the normal standing posture by about 30%. The magnitude of the apparent mass decreased sharply at frequencies above the principal resonance frequency and was very low at about 6 Hz.

It is likely that the legs, which had low stiffness in the vertical direction when bent, isolated the upper-body at frequencies above 3 Hz.

The apparent mass for the one leg posture also showed a lower principal resonance frequency, about 3 Hz, and low apparent mass at frequencies above the principal resonance. The upper-body might be isolated by standing on one leg, as observed in the legs bent posture. The local peak in the frequency range between 10 and 15 Hz found in the apparent masses for the normal standing posture and the legs bent posture was not observed in the apparent mass for the one leg posture. The dynamic response in the one leg posture, including the vibration isolation mechanism, might be different from that when standing on both legs.

CHAPTER 5

INFLUENCE OF LEG POSTURE AND VIBRATION MAGNITUDE ON DYNAMIC RESPONSE OF THE STANDING HUMAN BODY EXPOSED TO VERTICAL WHOLE-BODY VIBRATION

5.1 INTRODUCTION

In the previous chapter, the driving-point apparent mass was measured with subjects in several different postures, including standing and sitting positions, so as to investigate the overall characteristics of the dynamic response of the human body. The transmissibility, the ratio between two motions measured at distant points, is another useful frequency response function to represent the dynamic response of the body objectively, as mentioned in Section 2.2. The transmissibility can be used to measure the dynamic response of some particular parts of the body of interest to input motion and related to the apparent mass data so as to identify the dynamic mechanisms of the body contributing to the resonances observed in the apparent mass. There have been a few studies which measured the transmissibility of the human body, for example, over the spine and at the head, when standing. This chapter documents an experiment (referred to in this thesis as Experiment 2) in which the transmissibility as well as the apparent mass of subjects when standing were measured. Influences of the posture of the legs and the input vibration magnitude were investigated.

Hagena *et al.* (1985) measured the vertical transmissibilities of the standing body from the sacral bone to the head and to five points over the spine: the first, fourth and fifth lumbar vertebrae (L1, L4 and L5), the sixth thoracic vertebra (T6) and the seventh cervical vertebra (C7). Using Kirschner-wires (*K*-wires) inserted into the spinous processes with local anaesthesia, direct measurements of the movements of vertebral bodies were obtained. They found three peaks: at 4 Hz (at all the measurement points, particularly marked at L5, L1 and C7), at 8 Hz (with equally large magnitudes at all points), and at 18 Hz. It was said that the peak at 4 Hz corresponded with the entire body mode and that ‘the independent resonance of the spine’ was represented by the peak at 8 Hz. The transmissibilities of seated subjects were also measured and showed there were small differences between standing and seated bodies.

The transmissibility to the spine of a standing subject exposed to impacts has been measured by Pope *et al*. (1989) by using the direct measurement method with *K*-wires. A single peak at about 5.5 Hz in the transmissibility to the third lumbar vertebra (L3) in the vertical direction was found when standing in a 'rigid erect (at attention)' posture. The effect of posture was investigated and an attenuation of the response, with small peaks at about 2, 6 and 15 Hz, was found in a 'knees slightly flexed (at 30º)' posture. It was found that the angle of the pelvis and muscle tone had some effect on the response of L3. There were only minor differences due to different energies of the impact. Herterich and Schnauber (1992) also measured the transmissibility to the spines and heads of standing subjects. Using transducers attached to the skin, the maximum transmissibility in the vertical direction was located at about 8 Hz for the lumbar spine and at 16 to 20 Hz for the head and cervical spine.

Paddan and Griffin (1993), using a bite-bar to measure motion of the head in six axes in standing subjects exposed to vertical floor vibration, reported a distinctive peak at about 5 Hz, particularly in the mid-sagittal plane (i.e. in the vertical, fore-and-aft and pitch axes) in a 'legs locked' posture. A 'legs unlocked' posture did not change the transmissibilities, but in a 'legs bent' posture, a resonance at about 3 Hz appeared in all axes, especially in the mid-sagittal plane. Other studies have shown similar results, but have not considered the potentially large effects of rotational motions on the translational motions of the head (e.g. Kobayashi *et al*., 1981; Rao, 1982).

With respect to the effect of input vibration magnitude on the dynamic response, Edwards and Lange (1964) measured the mechanical impedance of the standing body at three different vibration magnitudes: 0.2, 0.35 and 0.5 g. One subject showed a decrease in the first resonance frequency (from 5 to 4 Hz) and a decrease in resonance magnitude as the vibration magnitude increased when in a 'standing relaxed' posture, although the effect on another subject was within the limits of the accuracy of measurement. A decrease in the main resonance frequency with an increase of the vibration magnitude has been found in studies with the seated body (e.g. Fairley and Griffin, 1989; Hinz and Seidel, 1987; Mansfield, 1998; Mansfield and Griffin, 1999).

In the study presented in this chapter, the apparent masses and transmissibilities to various body locations of standing subjects were measured with three different standing postures (normal, legs bent and one leg) at five different vibration magnitudes (0.125 to 2.0 ms^{-2} r.m.s.). The objectives were to: (i) investigate the relation between the driving-

point response and body motions for subjects standing with different postures of their legs, and (ii) investigate the effect of vibration magnitude on the dynamic response of the standing body.

5.2 METHOD

Vibration was measured at six locations on the surface of the body: at the first and eighth thoracic vertebrae (T1 and T8), the fourth lumbar vertebra (L4), the left and right iliac crests, and the knee of the left leg. Two types of piezoresistive accelerometer (Entran EGCSY-240D*-10 and EGA-125F-10D) were used for the measurements. One accelerometer of each type was orientated orthogonally and attached to a stiff paper card, 30 mm (horizontal) by 35 mm (vertical). The combined mass of the card and accelerometers was 12 g. The card was mounted to the skin, by double-sided adhesive tape and surgical tape, over the spinous processes of T1, T8 and L4 to measure the motions in both the vertical (z-axis) and the fore-and-aft (x-axis) directions, and over the left iliac crest to measure the vertical and the lateral (y-axis) motions. For the measurement of the vertical and fore-and-aft motion at the knee, a pair of small accelerometers (Entran EGA-125F-10D) were attached to a smaller card, 20 mm (horizontal) by 30 mm (vertical), weighing 2 g all together, and fixed to the patella of the left leg. A small accelerometer was attached to a 30 mm by 35 mm card and fixed to the skin over the right iliac crest so as to measure the vertical motion. The combined mass of the card and accelerometer was 2 g.

As shown by Pope *et al*. (1986), a motion measured on the body surface over a bone may be modified by the tissue and skin between the bone and the transducer. Accordingly, data correction methods for surface measurements have been developed (Hinz *et al*., 1988a; Smeathers, 1989; Kitazaki and Griffin, 1995). For these methods it is assumed that the local dynamic system consisting of the tissue and the accelerometer can be analogised with a single degree of freedom linear system. In this study, the method developed by Kitazaki and Griffin (1995) was applied. To use their correction method, the natural frequency and damping ratio of the local tissue-accelerometer system at each measurement point and in each direction was derived from the response to free damped oscillations. The method used in this study was identical to that of the former study (Kitazaki and Griffin, 1995) and was performed before vibration exposures. It was assumed that the behaviour of the local system was not affected by changes in subject posture.

A 1 metre stroke electro-hydraulic vibrator described in Section 3.2.1.2 was used in the experiment. A force platform, Kistler 9281B, was secured to the vibrator platform to measure the force at the interface between vibrator and subjects. The input motion of the top plate of the force platform, just under the feet of subject, was measured with an accelerometer, Entran EGCSY-240D*-10. A computer-generated Gaussian random signal having a flat constant bandwidth acceleration spectrum over the frequency range from 0.5 to 30 Hz was fed to the vibrator. Subjects were exposed to this vibration at five different magnitudes, 0.125, 0.25, 0.5, 1.0 and 2.0 ms^{-2} r.m.s., for 60 seconds. The output signals from the twelve accelerometers and the force platform were acquired at 128 samples/second after low-pass filtering at 31.5 Hz.

Twelve healthy male volunteers, median age 28 yr, height 1.79 m and weight 73.5 kg, took part in the experiment. The details of the subjects are presented in Appendix C. The effects of posture on the dynamic response of the standing body were investigated for three postures:

1) 'Normal': keep the legs straight and locked with 0.3 m separation between the feet.
2) 'Legs bent': hold the legs bent so that the knees were vertically above the toes with 0.3 m separation between the feet.
3) 'One leg': stood on the left leg and kept it locked as in the 'normal' posture.

In all postures, subjects were ordered to keep their upper-body in a comfortable and upright position and look forward. For safety purposes, subjects held lightly with both hands to a frame in front of them which was rigidly fixed to the vibrator platform; no subject needed to change upper-body position to hold the frame. Measurements were obtained with subjects barefoot so as to eliminate any effects of footwear. Only two different magnitudes of vibration, 0.25 and 1.0 ms^{-2} r.m.s., were used for the one leg posture, so a total of twelve conditions completed the experiment. The written instructions given to the subjects are shown in Appendix C.

5.3 ANALYSIS

The apparent mass, *M(f)*, was calculated by the 'cross spectral density method', as in the previous chapter:

$$M(f) = \frac{S_{af}(f)}{S_a(f)} \tag{5.1}$$

using the cross spectral density function between the input acceleration and the resulting force at the driving point, $S_{af}(f)$, and the power spectral density function of the input acceleration, $S_a(f)$. The effect of the top plate mass of the force platform was eliminated by the mass cancellation described in Section 3.4.1.1. A resolution of 0.25 Hz was used for the calculation of spectra. A large variability in the apparent masses of subjects was partly attributed to their different static masses, as in previous studies with seated subjects (e.g. Fairley and Griffin, 1989). Hence, each apparent mass was normalised by dividing it by the measured value of the apparent mass at 0.5 Hz, which was almost equal to the static weight of the subject. This assisted the comparison of apparent masses across subjects.

Frequency response functions between the acceleration measured at the driving point and those at each measurement point of the body, the transmissibilities, $T(f)$, were also calculated using the cross spectral density method with a 0.25 Hz resolution:

$$T(f) = \frac{S_{io}(f)}{S_i(f)} \tag{5.2}$$

Here $S_{io}(f)$ is the cross spectral density between the accelerations at two points and $S_i(f)$ is the power spectral density of the acceleration at the driving point. Each transmissibility was corrected using the method developed by Kitazaki and Griffin (1995), as mentioned above, to reduce the discrepancy between the motion of the skeleton and that measured at the body surface:

$$T_b(f) = C(f)T_s(f) \tag{5.3}$$

where $T_b(f)$ and $T_s(f)$ are the transmissibilities to the bone and to the surface over the bone, respectively, and $C(f)$ is a correction frequency function defined by the natural frequency and damping ratio of the local tissue-accelerometer system obtained by a free oscillation test:

$$C(f) = \frac{1 - \left(f/f_0\right)^2 + 2i\zeta\left(f/f_0\right)}{1 + 2i\zeta\left(f/f_0\right)} \tag{5.4}$$

where f_0 and ζ are the natural frequency and damping ratio of the local system, respectively, and $i^2 = -1$.

The effect of the inclination of the body surface on the measurements seemed to be large at some measurement locations, particularly at the first thoracic vertebrae (T1). The angles of the body surface to the vertical axis were measured and found to range from 28 to 38 degrees at T1 for the twelve subjects. The measured transmissibilities over the spine were therefore compensated linearly by the angles between the body surface and the vertical axis, θ, in the frequency domain:

$$T_x(f) = T_{x1}(f)\cos\theta + T_{z1}(f)\sin\theta \quad (5.5)$$

$$T_z(f) = -T_{x1}(f)\sin\theta + T_{z1}(f)\cos\theta \quad (5.6)$$

where $T_{x1}(f)$ and $T_{z1}(f)$ are measured transmissibilities in the fore-and-aft and vertical directions, respectively. It was assumed that the displacement responses were small at each measurement point and the inclination angles were able to consider to be constant. After the correction, all the vertical transmissibilities over the spine at the lowest frequency were almost unity, which agreed with the expectation that the body would respond rigidly at low frequencies. The correction could reduce the fore-and-aft transmissibility to T1 of a subject from about 0.5 to about 0.1 at the lowest frequencies.

Rotational motions of the pelvis might contribute to the dynamic response of the body. On the assumption that the pelvis is rigid at frequencies investigated in this study, the transmissibilities between vertical floor vibration and the roll of the pelvis were obtained. Roll of the pelvis was calculated by dividing the difference between the vertical transmissibilities to the iliac crests on both sides by the distance between the two measurement points on the assumption that the roll displacement was small.

Pitch motion of the pelvis, which has an effect on the lordosis of the lumbar spine, might be one of the more important factors affecting the dynamic response of the spine and, consequently, the whole body. Upon assuming the relative motion between the pelvis and the lower lumbar spine was small enough to be neglected, the transmissibilities for vertical floor vibration to pitch motion of the pelvis were calculated. Pitch motion was obtained by dividing the difference between the mean values of the two vertical motions measured at the iliac crests and the vertical motion at L4 by the distance between the

iliac crests and L4 measured in the sagittal plane. The calculation of rotational motion was conducted in the frequency domain.

5.4 RESULTS

5.4.1 Influence of leg posture on apparent mass

The apparent masses, normalised apparent masses, phases and coherences of the twelve subjects in the three different standing postures at a vibration magnitude of 1.0 ms^{-2} r.m.s. are shown in Figure 5.1. Variability between subjects (i.e. inter-subject variability) in the magnitude of the apparent mass was reduced by the normalisation so that each curve shows a similar trend. The apparent masses in three postures at 1.0 ms^{-2} r.m.s. are compared for each subject in Figure 5.2. Median normalised apparent masses and phases from the twelve subjects in the three postures at 1.0 ms^{-2} r.m.s. are shown in Figure 5.3.

For the normal standing posture, a main resonance at around 5.5 Hz is observed in the apparent mass of most subjects (Figures 5.1(a), (d), and 5.2). The frequency and magnitude of the main resonance ranged from 4.0 to 6.0 Hz and from 1.23 to 1.72 in the normalised apparent mass, respectively, at this vibration magnitude. A local broad peak can also be seen in the frequency range from 9 to 15 Hz, although it is ambiguous for some subjects (Figure 5.2). Inter-subject variability in the phase at frequencies above 10 Hz was relatively large (Figure 5.1(g)).

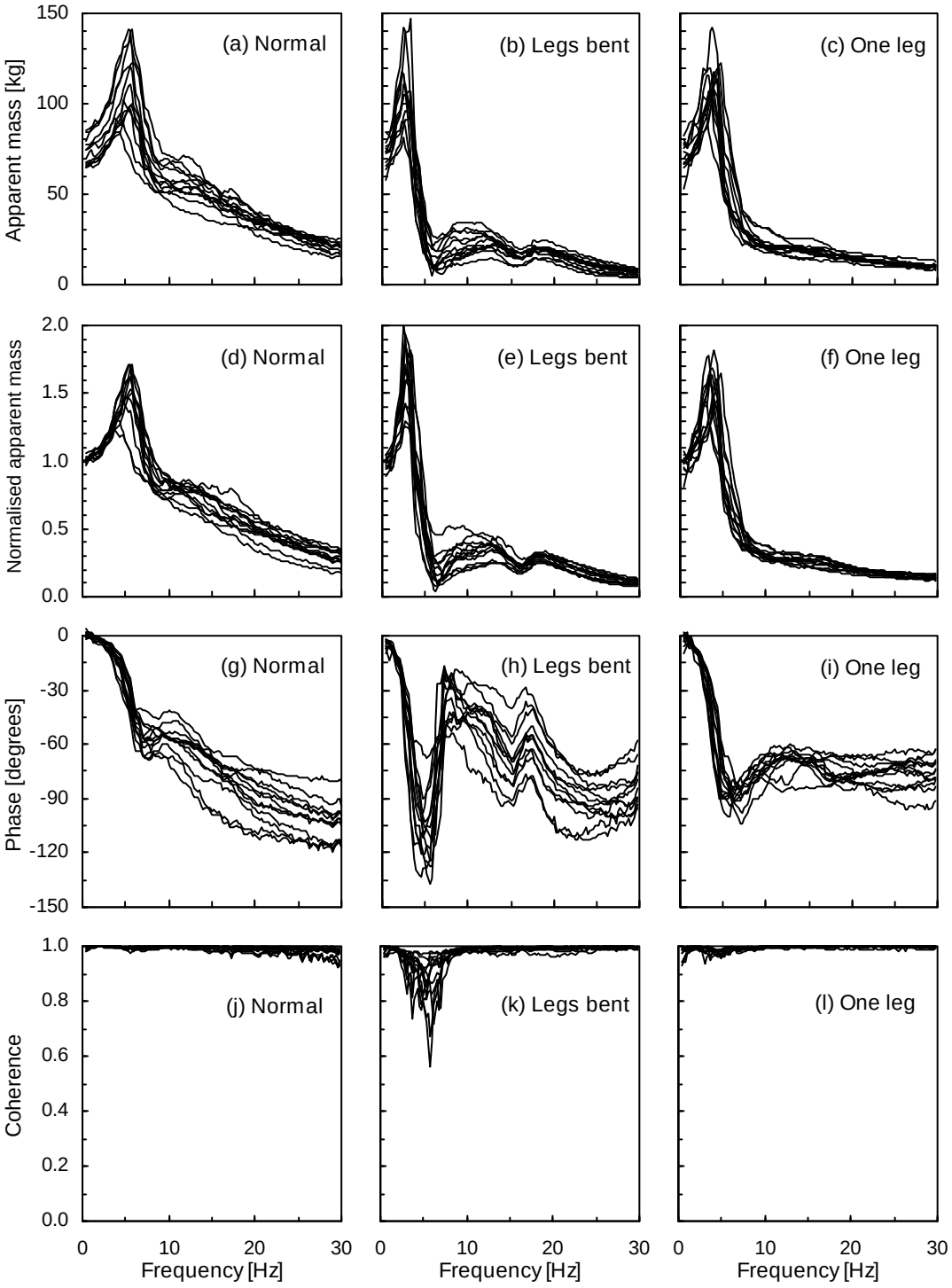

Figure 5.1 Apparent masses, normalised apparent masses, phases, and coherences of the twelve subjects in the normal standing posture, legs bent posture, and one leg posture measured at a vibration magnitude of 1.0 ms^{-2} r.m.s.

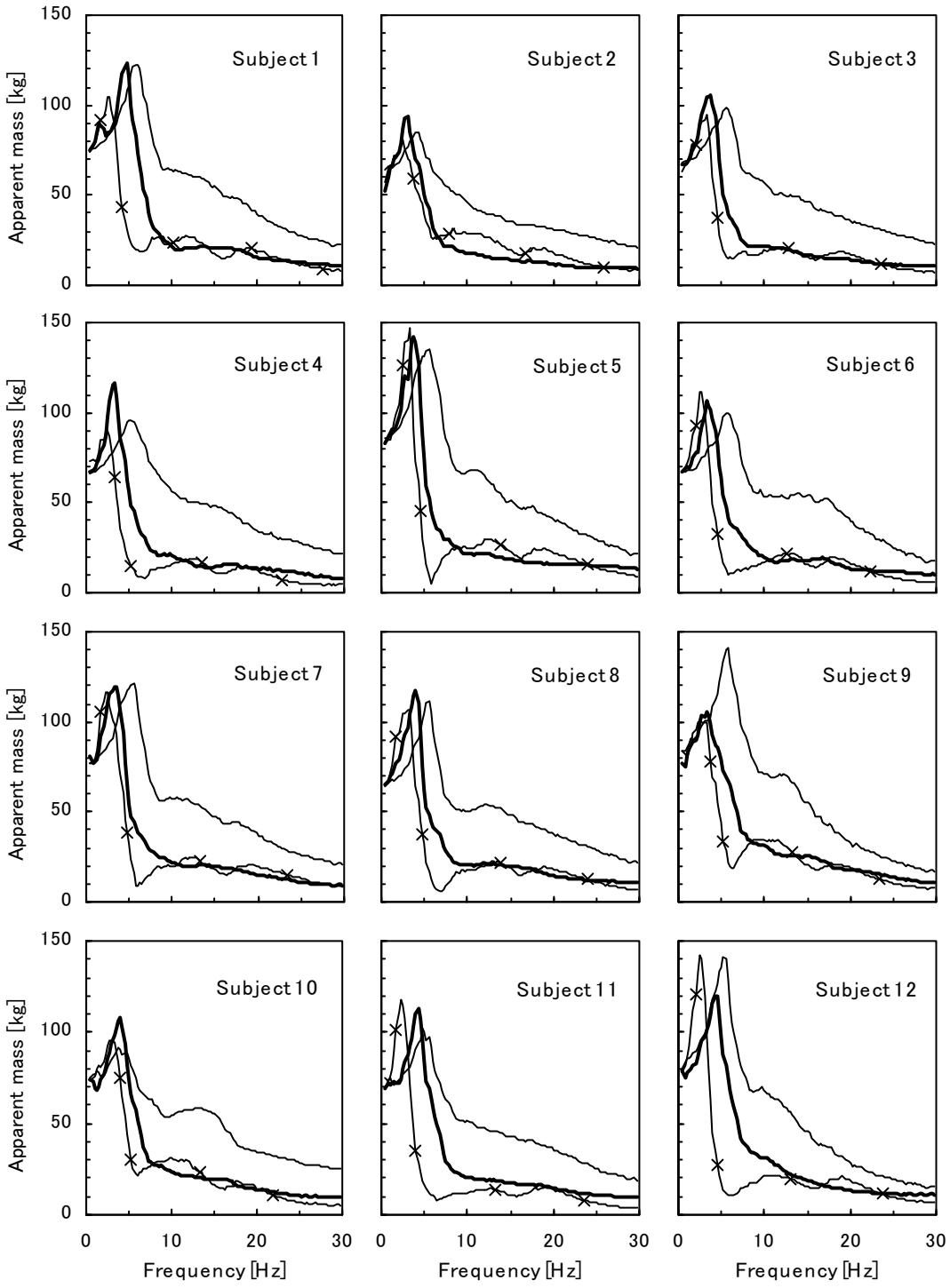

Figure 5.2 Apparent masses of the twelve subjects in the normal standing, legs bent and one leg postures measured at a vibration magnitude of 1.0 ms^{-2} r.m.s.: normal standing posture ——— ; legs bent posture —×— ; one leg posture ━━━ .

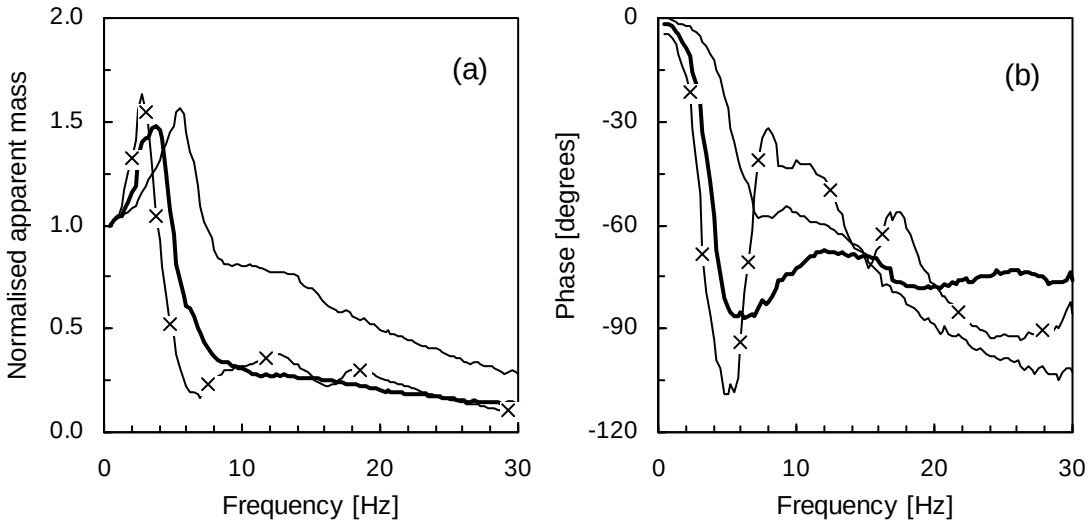

Figure 5.3 Median normalised apparent masses and phases of the twelve subjects in the normal standing, legs bent and one leg postures measured at a vibration magnitude of 1.0 ms^{-2} r.m.s.: normal standing posture ——— ; legs bent posture —x— ; one leg posture ━━━ .

There was an appreciable effect of leg posture on the apparent mass. A main resonance in the apparent mass for the legs bent posture was observed at a frequency between 2.5 and 3.25 Hz for the twelve subjects, at 2.75 Hz in the median normalised apparent mass (Figures 5.1(b), (e), 5.2, and 5.3). The difference in the main resonance frequency between the legs bent and normal postures was found to be statistically significant (p < 0.005, Wilcoxon matched-pairs signed ranks test). The normalised apparent mass at the main resonance ranged from 1.25 to 2.0 for the legs bent posture. The resonance magnitude in the normalised apparent mass tended to be greater for the legs bent posture than for the normal posture (p < 0.1). Two small broad peaks at about 13 and 18 Hz and troughs at around 7 and 16 Hz were seen in the individual and median apparent mass data in the legs bent posture. A significant phase shift was observed in the frequency region around 7 Hz at which the apparent mass showed a trough (Figure 5.1(h)). The coherence had relatively low values, about 0.6 at the lowest, at about 7 Hz, as seen in Figure 5.1(k).

The postural change to the one leg posture also decreased a main resonance frequency of the apparent mass compared to that in the normal posture. The main resonance frequencies and magnitudes of the normalised apparent mass were found between 3.0 and 4.75 Hz and between 1.28 and 1.82, respectively, for twelve subjects (Figures 5.1(c), (f) and 5.2). The main resonance frequency in the median normalised apparent mass was found at 3.75 Hz (Figure 5.3). The difference in the resonance frequency between

the one leg posture and the normal posture was found to be statistically significant ($p < 0.005$), while the difference in the resonance magnitude was not significant. No obvious peaks, except for the main one, were found for the one leg posture. The phase shift at frequencies below 6 Hz was greater for the one leg posture than for the normal posture (Figure 5.1(g) and (l)).

The main resonance frequencies, resonance magnitudes and corresponding phases of the apparent masses are tabulated in Table 5.1 for each subject in the three posture. The corresponding median values obtained for each posture are also presented in Table 5.1. The median resonance frequencies obtained from the resonance frequencies for each subject shown in Table 5.1 coincided with those obtained from the maximum point of the median normalised apparent mass curves shown in Figure 5.3 for all three postures. The phase at the main resonance frequency was about -30 degrees for the normal standing posture (median: -32.77 degrees, inter-quartile range: -37.35 to -27.91 degrees), while it was about -45 degrees for the legs bent posture (median: -43.43 degrees, inter-quartile range: -44.66 to -39.78 degrees) and for the one leg posture (median: -48.10 degrees, inter-quartile range: -50.55 to -41.96 degrees).

Table 5.1 Main resonance frequencies, magnitudes and phases of the apparent mass of the twelve subjects in the three postures measured at 1.0 ms^{-2} r.m.s.

	Frequency [Hz]			Apparent mass [kg]			Phase [degrees]		
Subject	Normal	Bent	One	Normal	Bent	One	Normal	Bent	One
1	6.0	2.75	4.75	122.4	119.5	123.0	-36.1	-40.5	-59.7
2	4.0	2.75	3.0	84.79	84.23	93.86	-23.3	-34.3	-37.7
3	5.5	3.25	3.75	98.58	96.60	105.2	-29.4	-43.6	-49.5
4	5.25	2.75	3.25	96.17	112.1	116.1	-28.2	-43.3	-45.0
5	5.5	2.75	3.75	134.9	139.7	141.7	-37.5	-44.0	-53.6
6	5.75	2.5	3.25	100.1	132.3	106.6	-30.7	-51.6	-33.2
7	5.5	2.75	3.5	120.9	139.3	119.5	-41.4	-43.1	-49.4
8	5.5	3.25	4.0	111.1	116.5	117.4	-34.8	-44.3	-55.7
9	5.75	2.75	3.25	140.7	117.1	106.0	-37.3	-35.6	-35.2
10	3.75	2.75	4.0	91.91	93.60	108.1	-16.9	-37.6	-47.0
11	4.75	2.75	4.25	102.2	136.9	113.3	-27.1	-45.8	-49.3
12	5.25	2.75	4.25	141.4	153.7	120.1	-41.0	-61.3	-43.4
Median	5.5	2.75	3.75	106.7	118.3	114.7	-32.8	-43.4	-48.1

5.4.2 Transmissibility in normal standing posture

The transmissibilities from the floor to each measurement point on the bodies of the twelve subjects in the normal posture at 1.0 ms^{-2} r.m.s. are shown in Figure 5.4. The corresponding phases and coherences of the transmissibilities in the vertical and fore-and-aft directions are presented in Figures 5.5 and 5.6, respectively. The coherences were obtained for the transmissibilities before correction for the local motion and the inclination effects by using Equations (5.3) to (5.6). The phase data for the fore-and-aft direction are shown in the range between -180 and 180 degrees because the range of inter-subject variability in the phase exceeded 360 degrees (i.e., one cycle). This was partly because low coherence for the fore-and-aft transmissibilities (Figure 5.6). Because of the limitation of the data correction method, which is not effective at frequencies above the natural frequency of the local tissue-accelerometer system (Kitazaki and Griffin, 1995), transmissibility data are only presented at frequencies below 20 Hz. The natural frequencies and damping ratios of local tissue-accelerometer systems obtained in the experiment are tabulated in Appendix C.

Relatively large inter-subject variability can be seen in the transmissibilities to some measurement points, compared to the variability in the apparent masses. The principal peak frequency of the transmissibility to the fourth lumbar vertebra in the vertical direction, for example, varied in the range between 5.5 and 9.75 Hz across subjects, although in ten subjects it was found below 7 Hz (Figure 5.4(e)). The transmissibility to the knee in the vertical direction showed a large variability at high frequencies (Figure 5.4(i)).

When subjects stood in the normal posture, transmissibilities to the pelvis and the lower lumbar spine in the vertical direction had a similar trend to the apparent masses (Figures 5.1(a), (d) and 5.4(e), (g), (h)). Most transmissibilities to the spine (T1, T8 and L4) in both the vertical and fore-and-aft directions show a peak at around 6 Hz, close to the principal resonance frequencies of the apparent masses for most subjects in this posture (Figures 5.4(a) to (f)). The transmissibilities to the thoracic vertebrae, T1 and T8, in the vertical direction were similar and remained at about unity at high frequencies, even though those to the lumbar vertebra (L4) were greater at low frequencies and decreased below unity at high frequencies. The phase lags at T1 and T8 were also similar while those at L4 were much larger above 6 Hz (Figure 5.5).

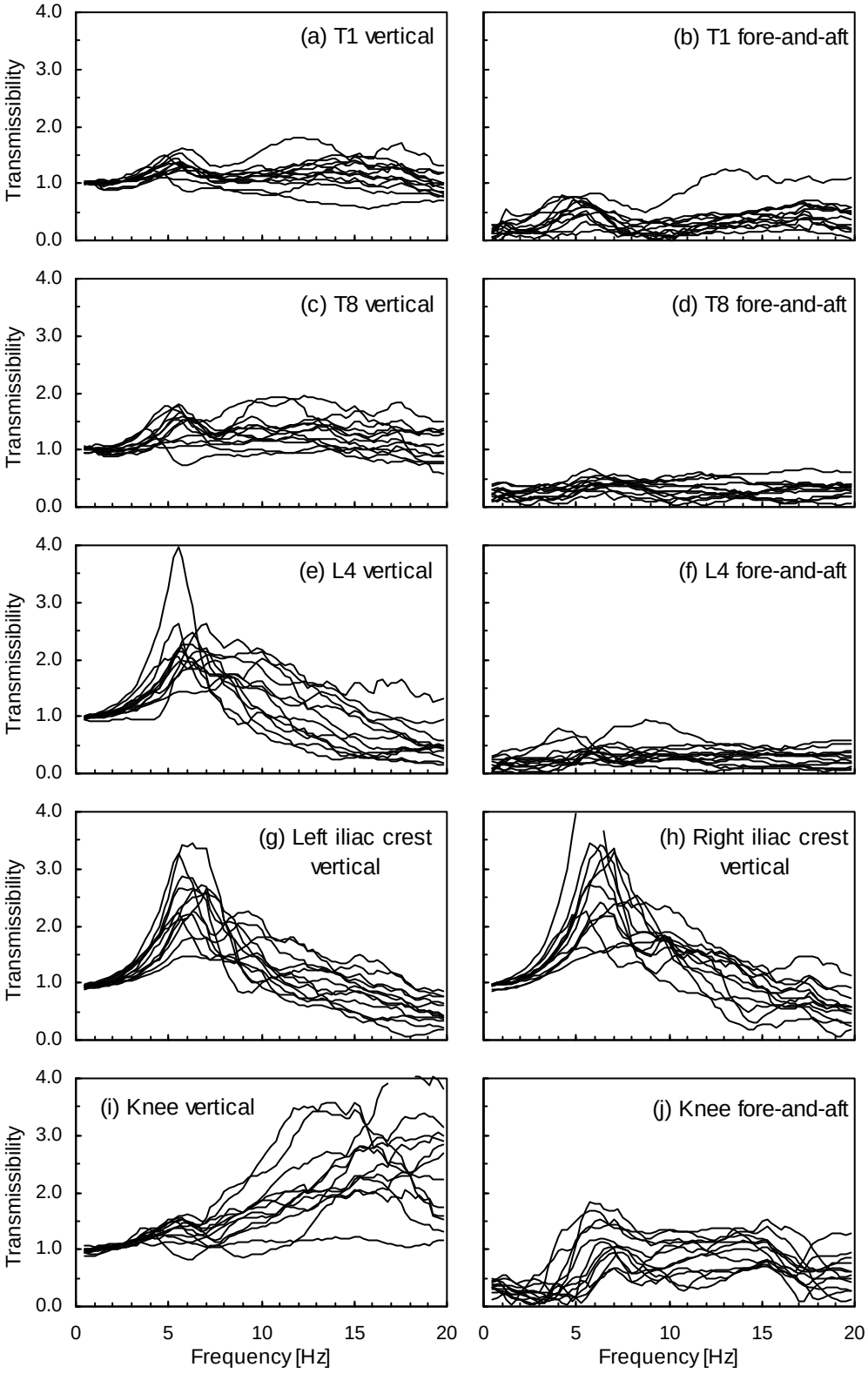

Figure 5.4 Transmissibilities to each measurement point of twelve subjects in the normal standing posture at 1.0 ms^{-2} r.m.s.

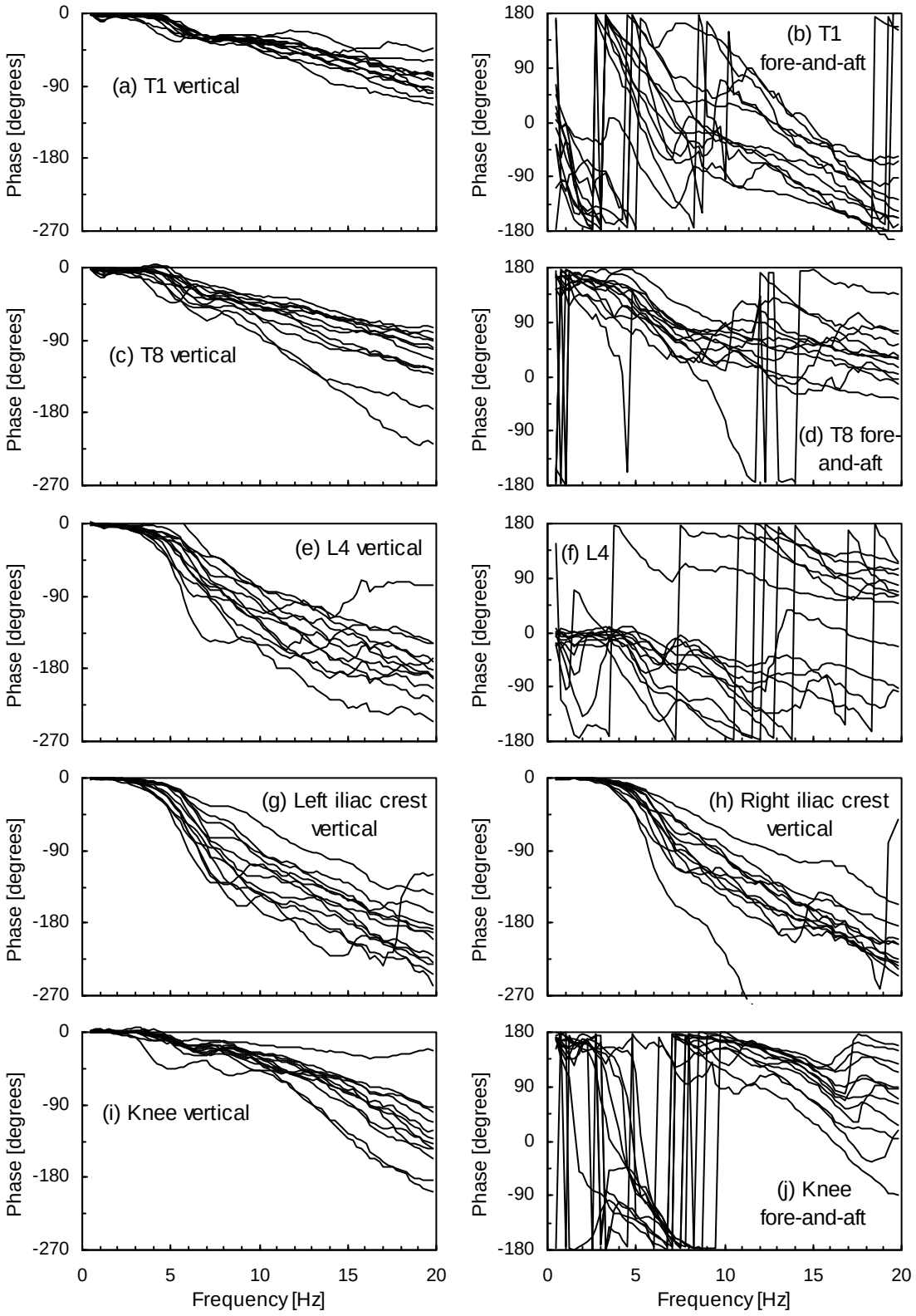

Figure 5.5 Phases of transmissibilities of twelve subjects in the normal standing posture at 1.0 ms^{-2} r.m.s.

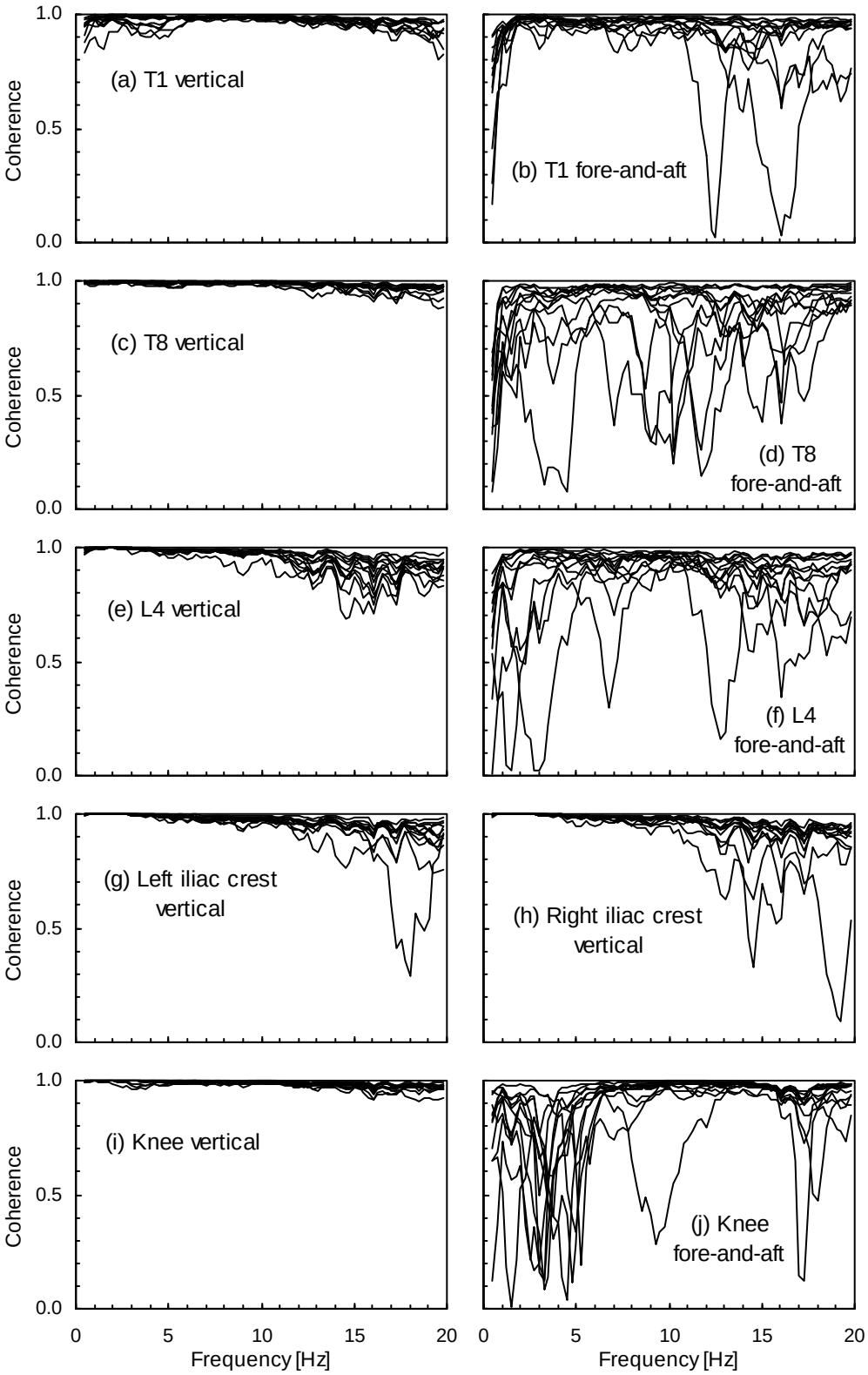

Figure 5.6 Coherences of transmissibilities of twelve subjects in the normal standing posture at 1.0 ms^{-2} r.m.s.

5.4.3 Influence of leg posture on transmissibility

5.4.3.1 Transmissibility to the pelvis region

When subjects stood on one leg, the dynamic response of the pelvis region was different from when they stood on both legs. The median transmissibilities to the pelvis region (i.e., L4, right and left iliac crests) in the vertical direction in the three postures at 1.0 ms^{-2} r.m.s. are shown in Figure 5.7. In the vertical direction, the transmissibilities to both sides of the iliac crests were similar to that to the fourth lumbar vertebra (L4) in both the normal posture and in the legs bent posture (Figures 5.7 (a), (b)). However, when subjects stood on their left leg, the transmissibility to the right iliac crest was much larger at the resonance frequency, 2.63 at 4.25 Hz (median), than that to the left iliac crest and L4, 1.32 and 1.57, respectively, at the same frequency (Figure 5.7(c)).

Figure 5.8 shows the transmissibilities from vertical floor vibration to roll motion of the pelvis for twelve subjects in the three postures at 1.0 ms^{-2} r.m.s., calculated by the method mentioned above. It is clear that there were significant roll motions of the pelvis when standing in the one leg posture compared to the normal and legs bent postures: an increase in roll at the lowest frequencies and a peak region between 4 and 10 Hz.

The transmissibilities to pitch motion of the pelvis in the three postures at 1.0 ms^{-2} r.m.s. are presented in Figure 5.9. The transmissibilities to pitch motion of the pelvis, particularly in the normal and the one leg postures, show a large variability between subjects. In the normal posture, the transmissibilities for nine of the subjects show a peak

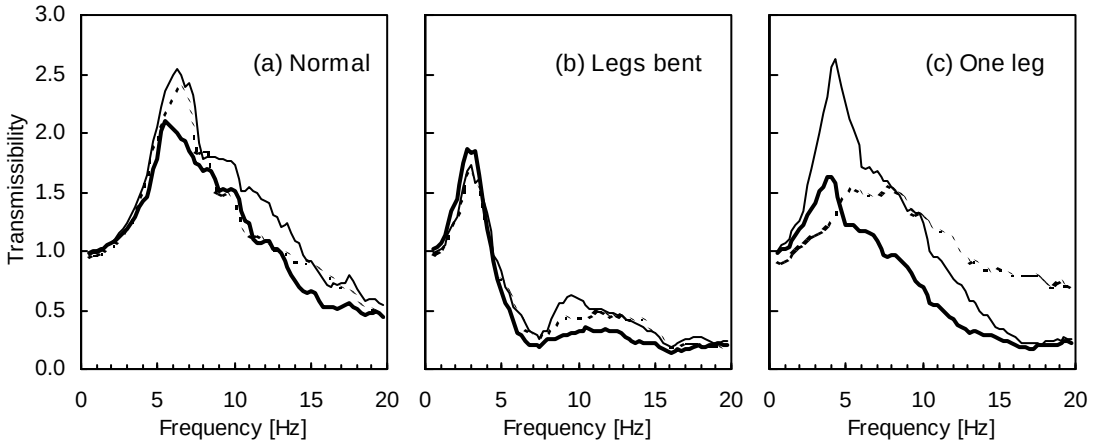

Figure 5.7 Median vertical transmissibilities to the pelvis region in three postures at 1.0 ms^{-2} r.m.s.: L4 ━━━ ; right iliac crest ——— ; left iliac crest - - - - .

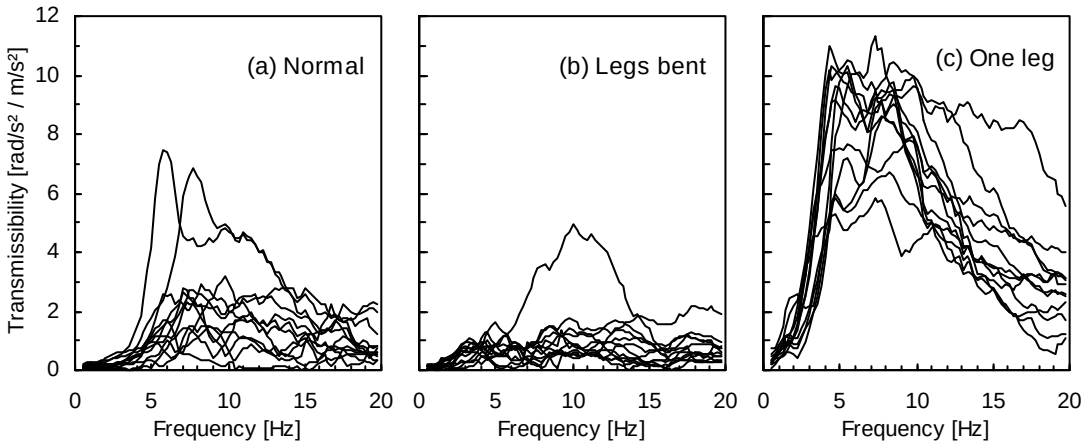

Figure 5.8 Transmissibilities to roll motion of the pelvis of twelve subjects in three postures at 1.0 ms^{-2} r.m.s.

at frequencies below 10 Hz, although some had a greater peak at high frequencies (Figure 5.9(a)). It can be seen that pitch motion occurred at frequencies above about 5 Hz. However, because of the large inter-subject variability, it is difficult to identify general characteristics of the calculated pitch motion of the pelvis.

The variability between subjects in the legs bent posture was smaller (Figure 5.9(b)). A peak at 3 to 4 Hz where the resonance of the apparent mass was located was clear in the transmissibilities for most subjects. In addition, two troughs at about 7 and 16 Hz were consistent, and could be found in the apparent mass (Figures 5.1(b), (e) and 5.9(b)). Some transmissibilities had relatively large magnitudes at high frequencies.

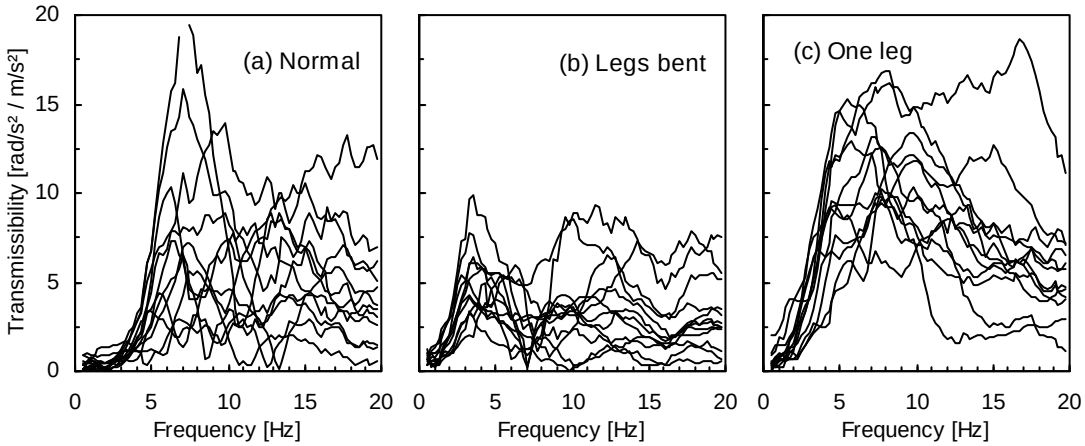

Figure 5.9 Transmissibilities to pitch motion of the pelvis of twelve subjects in three postures at 1.0 ms^{-2} r.m.s.

The transmissibilities to pitch motion of the pelvis in the one leg posture tended to have greater magnitudes than those in the other postures for all subjects (Figure 5.9(c)). Relative movements between the pelvis and L4, resulting from lateral bending or roll motion of the lumbar spine due to roll motion of the pelvis, may have affected the calculated pitch motion.

5.4.3.2 Transmissibility to the spine

Figure 5.10 compares the median transmissibilities to the vertical and fore-and-aft motions measured at three locations over the spine in the three postures at 1.0 ms^{-2}

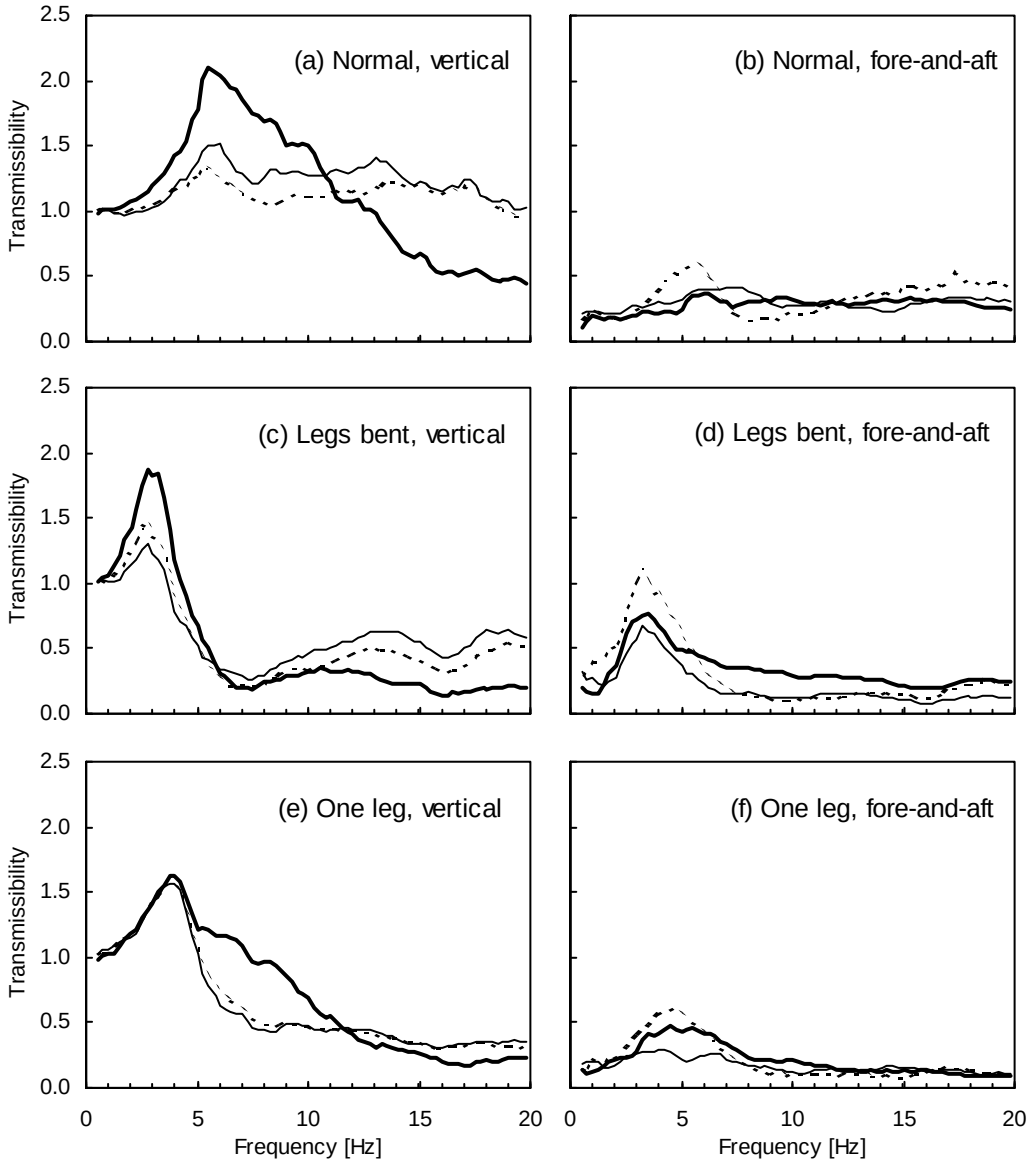

Figure 5.10 Median transmissibilities to the spine in the vertical and fore-and-aft directions in three postures at 1.0 ms^{-2} r.m.s.: L4 ——— ; T8 ——— ; T1 - - - - - .

r.m.s. The transmissibilities measured over the spine showed a peak at about the resonance frequency of the apparent mass in both the legs bent and the one leg postures, as for the normal posture.

In the legs bent posture, there was substantial fore-and-aft motion over the spine at about 3 Hz, the resonance frequency of the apparent mass, which was greatest at T1 (Figure 5.10(d)). This implies a rocking or bending motion of the upper-body about the hip joint. In the legs bent posture, the vertical transmissibilities to the vertebrae at frequencies above about 7 Hz, where a trough was found for each measurement point, were much less than those in the normal posture. In the high frequency range, the transmissibilities in the vertical direction to the thoracic vertebrae, T1 and T8, were greater than to the lumbar spine, which showed greater transmissibility at around 3 Hz, the same trend as found in the normal posture.

The vertical transmissibilities to the three measurement points over the spine in the one leg posture were almost identical at frequencies below 5 Hz (Figure 5.10(e)). This was also found in most individual data, although the data are not presented. In the one leg posture, the vertical transmissibilities to the thoracic vertebrae at high frequencies were much less than those in the normal posture.

5.4.3.3 Transmissibility to the knee

Figure 5.11 shows the median transmissibilities to the knee in the vertical and fore-and-aft directions at 1.0 ms^{-2} r.m.s. in the three postures. There was a principal peak at about

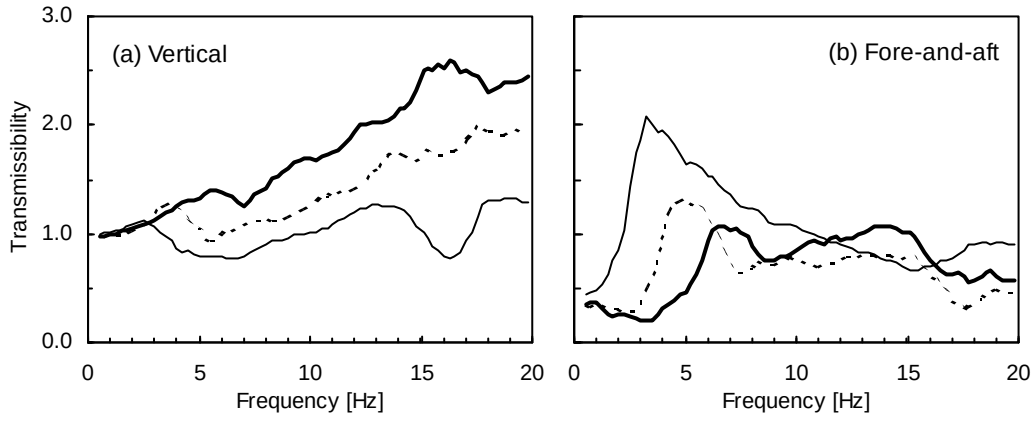

Figure 5.11 Median transmissibilities to the knee in the vertical (a) and fore-and-aft (b) directions in three postures at 1.0 ms^{-2} r.m.s.: normal posture ——— ; legs bent posture ——— ; one leg posture - - - - - .

3 Hz in the transmissibilities to the knee in the fore-and-aft direction in the legs bent posture (Figure 5.11(b)). A significant bending motion of the legs at the knee may have occurred at this frequency. In both the normal and the one leg postures, there was a peak in the vertical transmissibilities to the knee at around the resonance frequency of the apparent mass, although the peak magnitude was small compared to that of the transmissibilities to L4 and the pelvis (Figures 5.7(a), (c) and 5.11(a)). These vertical transmissibilities to the knee tended to increase with increasing frequency. The fore-and-aft transmissibilities in these postures increased above unity at the resonance frequency of the apparent mass (Figure 5.11(b)).

5.4.4 Influence of vibration magnitude

5.4.4.1 Apparent mass in normal standing posture

Figure 5.12 shows the median and the 10th and 90th percentiles for the apparent masses of the twelve subjects in the normal standing posture measured at each vibration magnitude. The corresponding phases and coherences are presented in Figures 5.13 and 5.14, respectively. The coherence was relatively low over the frequency range used for 0.125 ms^{-2} r.m.s. and for 2.0 ms^{-2} r.m.s. at high frequencies (Figure 5.14). The apparent mass and phase curves appeared not to be smooth when the coherence had a relatively low value, which can be seen in the percentile curves in Figures 5.12 and 5.13. It was difficult to determine resonance frequencies in the apparent mass measured at 0.125 ms^{-2} r.m.s. for some subjects due to the existence of a number of small notches. Variability between subjects, inter-subject variability, in the apparent mass and phase seemed to be similar for all vibration magnitudes used in this investigation.

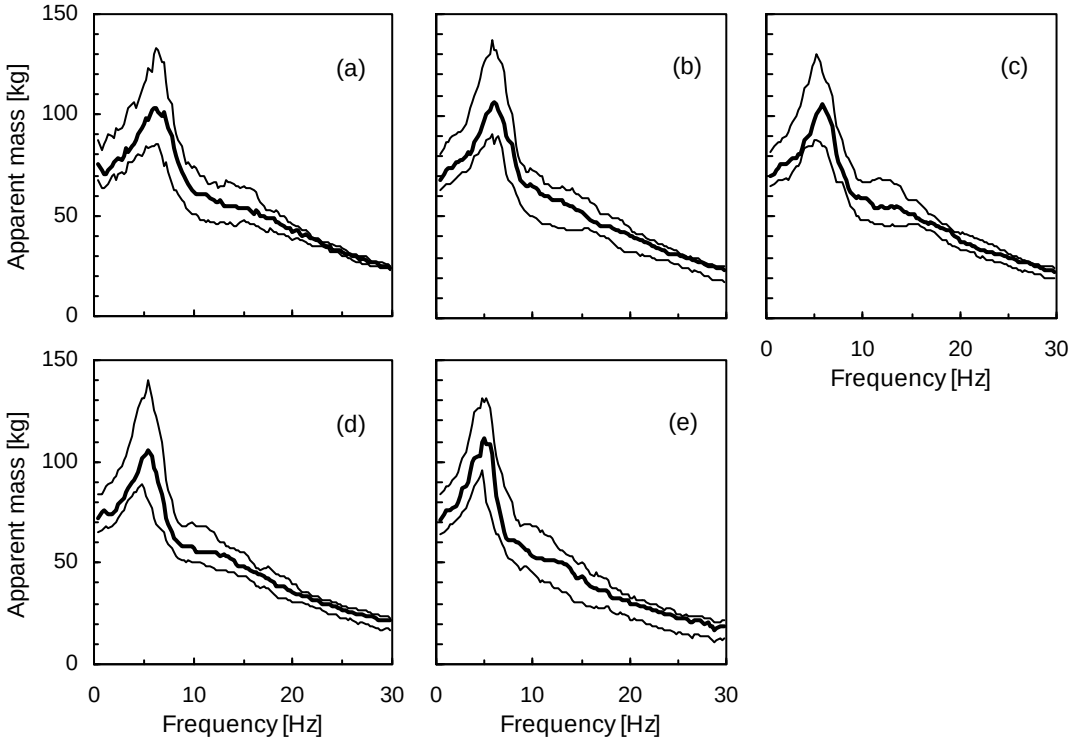

Figure 5.12 Median and 10th and 90th percentiles for the apparent masses of the twelve subjects in the normal standing posture measured at five different magnitudes: (a) 0.125, (b) 0.25, (c) 0.5, (d) 1.0, and (e) 2.0 ms^{-2} r.m.s.

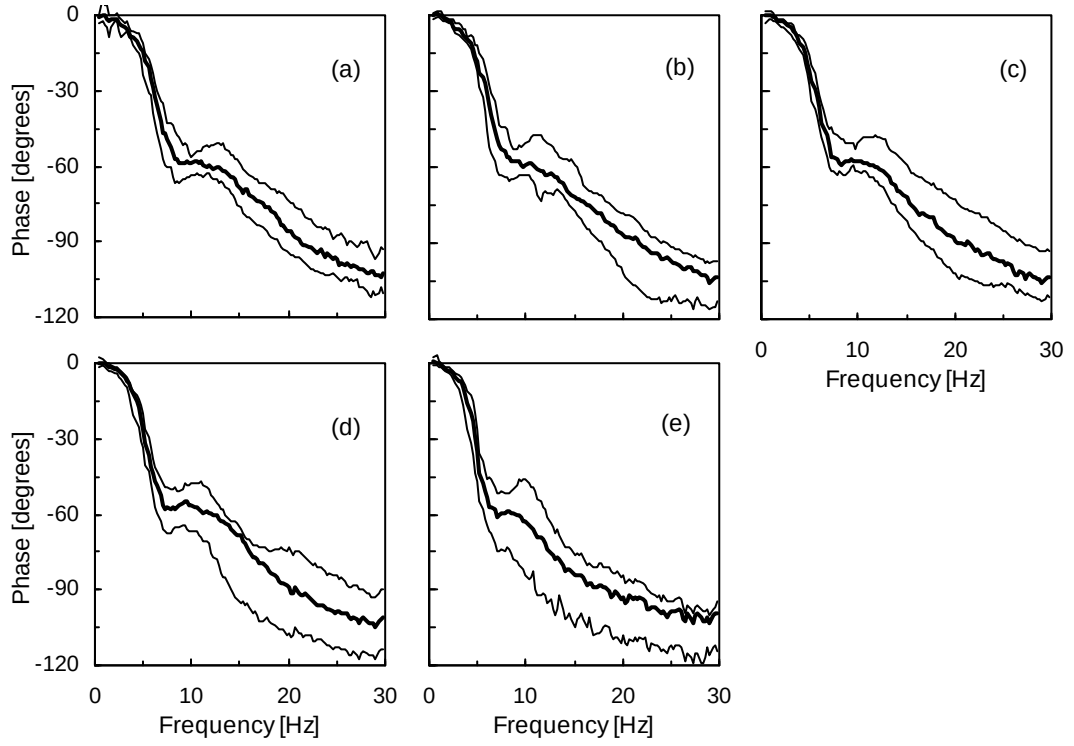

Figure 5.13 Median and 10th and 90th percentiles for the phases of the twelve subjects in the normal standing posture measured at five different magnitudes: (a) 0.125, (b) 0.25, (c) 0.5, (d) 1.0, and (e) 2.0 ms^{-2} r.m.s.

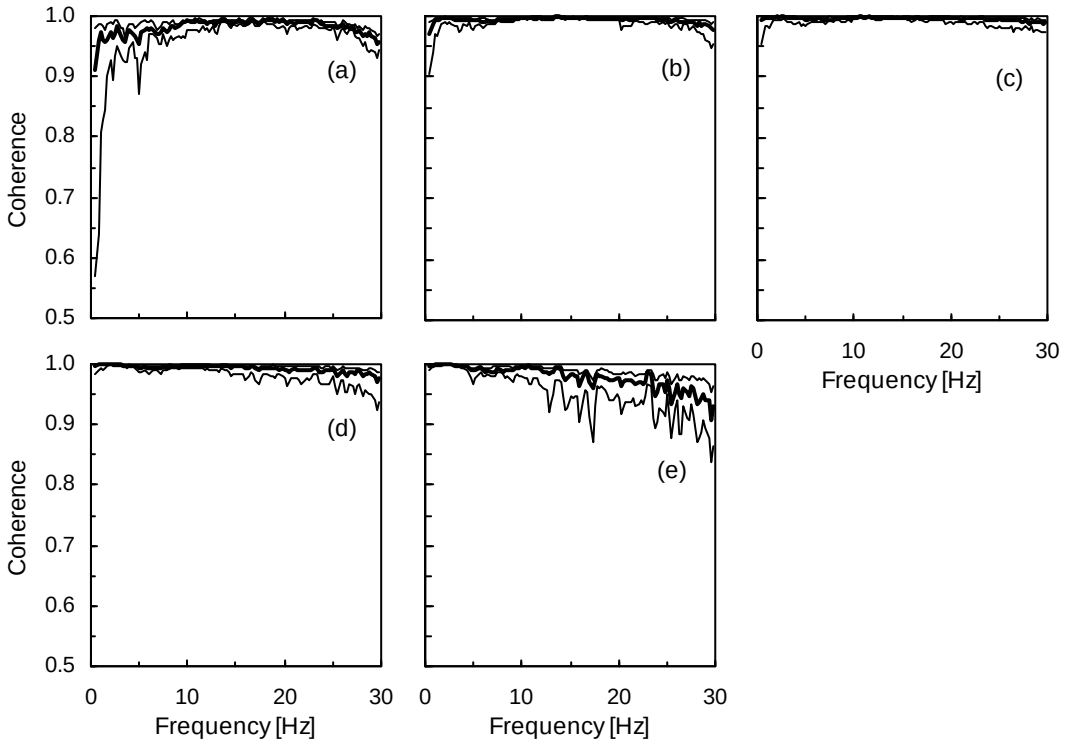

Figure 5.14 Median and 10th and 90th percentiles for the coherences of the twelve subjects in the normal standing posture measured at five different magnitudes: (a) 0.125, (b) 0.25, (c) 0.5, (d) 1.0, and (e) 2.0 ms^{-2} r.m.s.

The apparent masses measured at five different vibration magnitudes are presented for each individual in the normal standing posture in Figure 5.15. The principal resonance frequency was found to decrease with increases in the input vibration magnitude. Medians and inter-quartile ranges of the principal resonance frequency and magnitude of the normalised apparent mass of the twelve subjects in the normal standing posture at five different magnitude are shown in Figure 5.16. The median resonance frequency obtained from the resonance frequency for each subject decreased from 6.25 to 4.75 Hz (Figure 5.16). The decrease in the principal resonance frequency with each increase in the vibration magnitude was statistically significant ($p < 0.05$, Wilcoxon matched-pairs signed ranks test), except for the increase from 0.125 to 0.25 ms^{-2} r.m.s. An influence of the vibration magnitude on the resonance magnitude was not clear, although the resonance magnitude at 2.0 ms^{-2} r.m.s. was greater than that at 1.0 ms^{-2} r.m.s., which was statistically significant ($p < 0.05$). The broad peak observed in the frequency range from 9 to 15 Hz also seemed to shift to a lower frequency by increasing vibration magnitude.

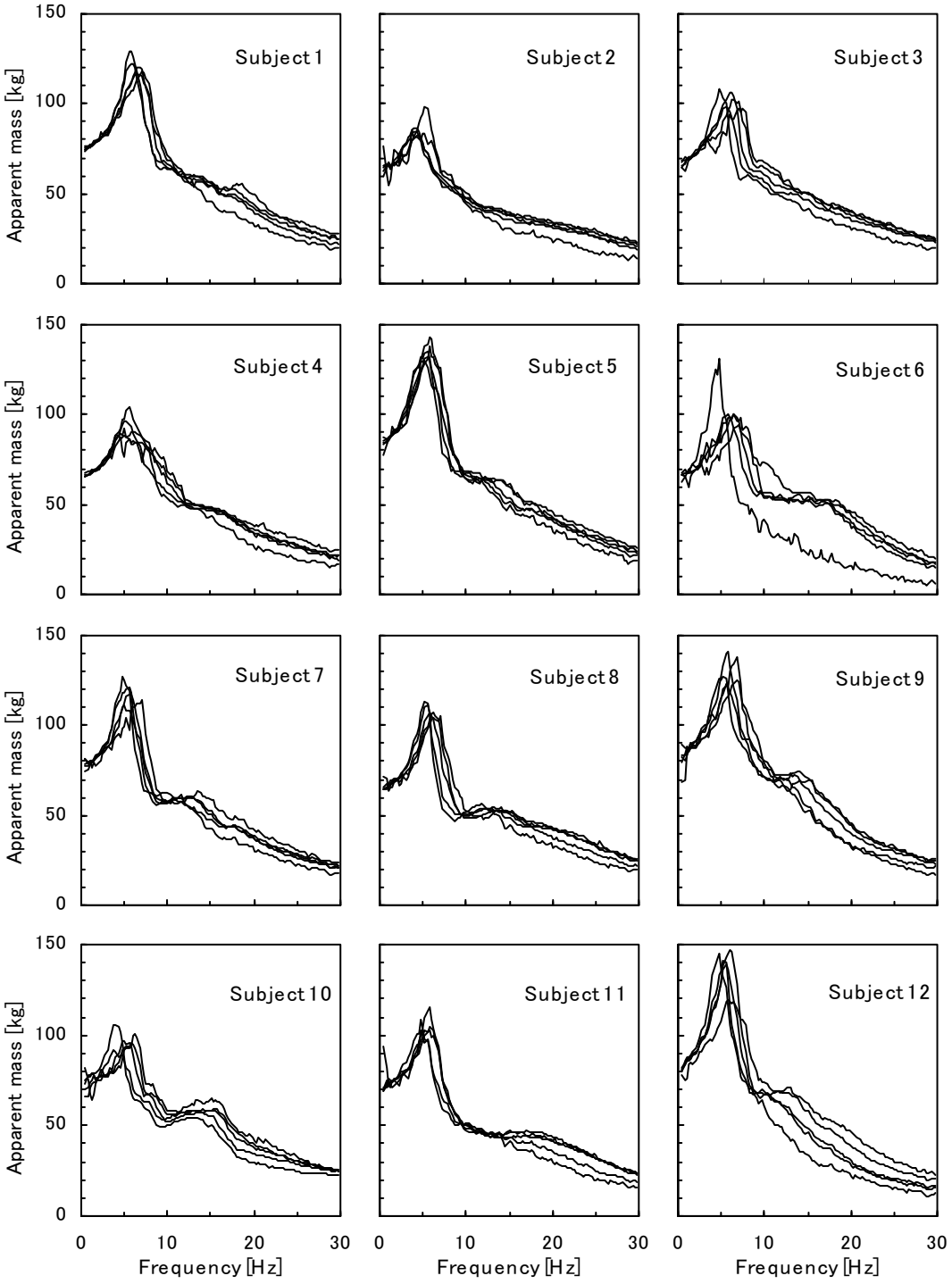

Figure 5.15 Apparent masses measured at five different magnitudes for each subject in the normal standing posture.

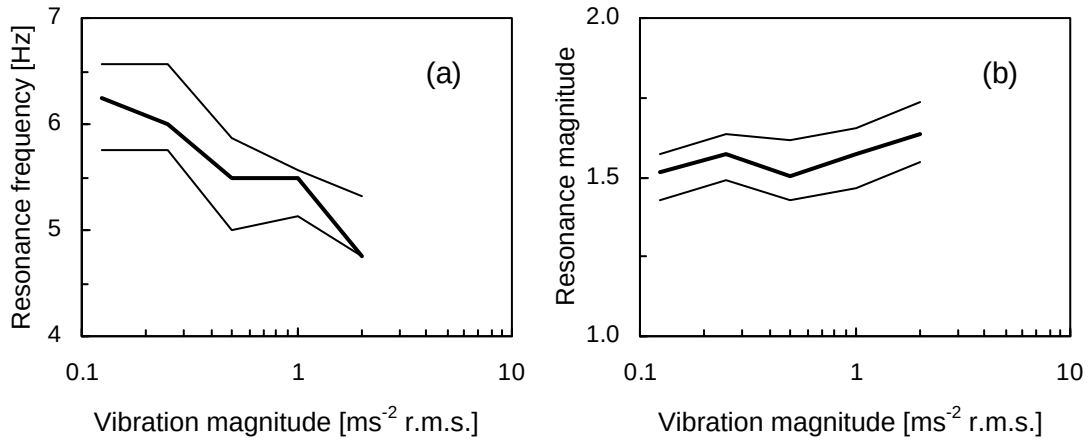

Figure 5.16 Medians and inter-quartile ranges of the principal resonance frequency and magnitude of the normalised apparent mass for the normal standing posture measured at five different vibration magnitudes.

Medians for the apparent mass, normalised apparent mass, phase and coherence at five vibration magnitudes are compared in Figure 5.17. A decrease in the principal resonance frequency was observed with an increase in the vibration magnitude in the median apparent mass and median normalised apparent mass for the twelve subjects (Figures 5.17(a), (b)), which was found to be statistically significant as mentioned above. The median phase also indicated the decrease in the resonance frequency as the vibration magnitude increased (Figure 5.17(c)). By increasing the vibration magnitude from 0.125 to 2.0 ms^{-2} r.m.s., the frequency of the principal resonance decreased from 6.25 to 5.0 Hz for the median normalised apparent mass curves (Figure 5.17(a)) and from 6.75 to 5.25 Hz for the median normalised apparent mass curves (Figures 5.17(b)). The median curves showed the decrease in the frequency of the broad peak at around 12 Hz with increasing the vibration magnitude, as seen in the individual data in Figure 5.15.

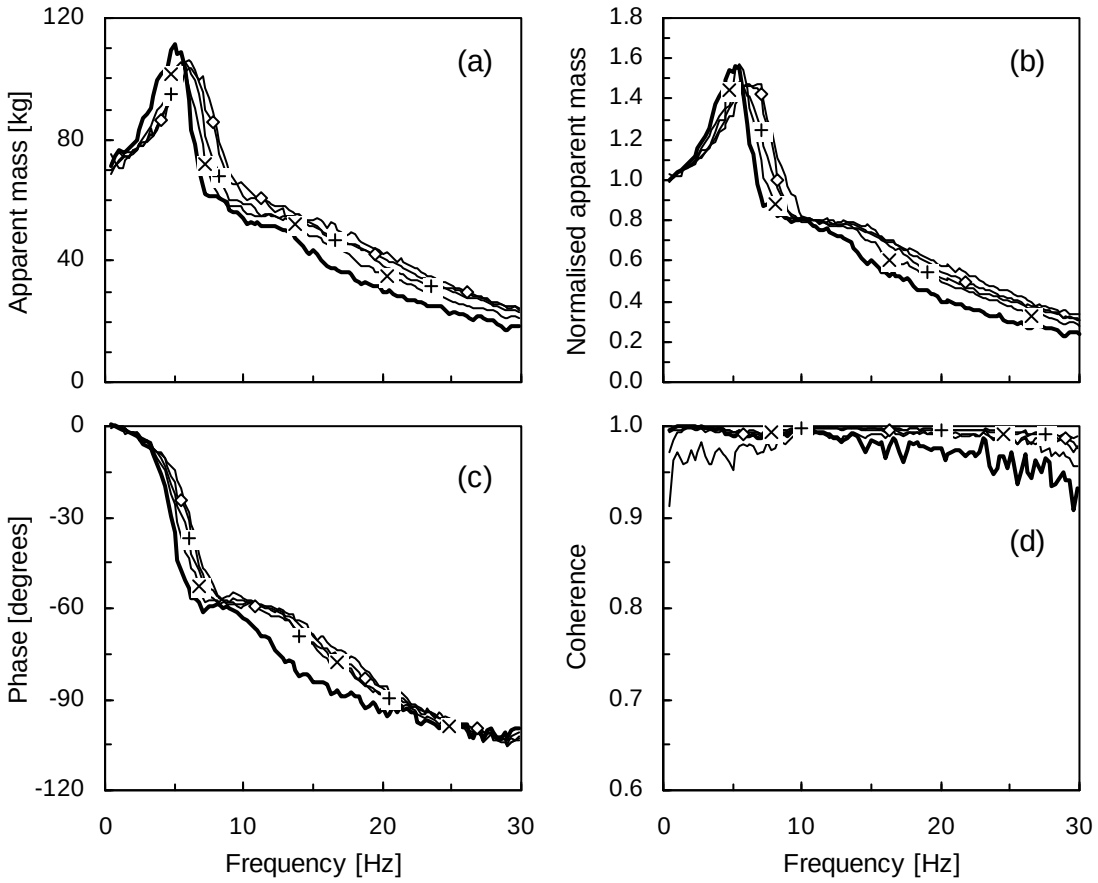

Figure 5.17 Medians for apparent masses, normalised apparent masses, phases and coherences of the twelve subjects in the normal standing posture measured at five different magnitudes: 0.125 ——— ; 0.25 —◇— ; 0.5 —+— ; 1.0 —×— ; 2.0 ms^{-2} r.m.s. ━━━ .

5.4.4.2 Apparent mass in legs bent and one leg postures

The principal resonance frequency of the apparent mass for the legs bent posture tended to decrease with increases in the vibration magnitude, although this was not so clear as in the normal posture. Figure 5.18 shows medians and inter-quartile ranges of the principal resonance frequency and magnitude of the normalised apparent mass of the twelve subjects for the legs bent posture at five vibration magnitudes. Friedman two-way analysis of variance showed a significant difference between the resonance frequencies at the five different magnitudes ($p < 0.005$). By Wilcoxon matched-pairs signed ranks tests, only the difference between 0.25 and 0.5 ms^{-2} r.m.s. was statistically significant ($p < 0.05$). With respect to the resonance magnitude, a significant difference was not found by Friedman two-way analysis of variance, although the resonance magnitude at 1.0 ms^{-2}

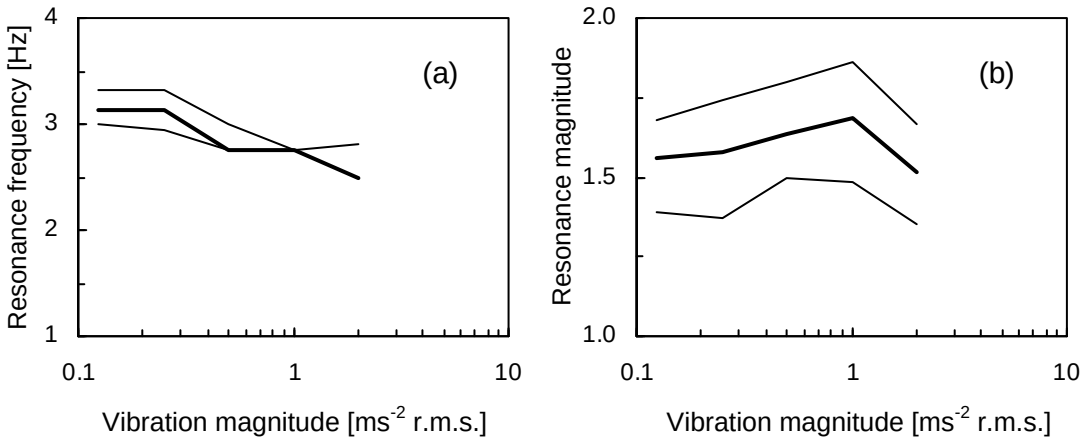

Figure 5.18 Medians and inter-quartile ranges of the principal resonance frequency and magnitude of the normalised apparent mass for the legs bent posture measured at five different vibration magnitudes.

r.m.s. was found to be significantly greater than that at 2.0 ms^{-2} r.m.s. ($p < 0.05$, Wilcoxon matched-pairs signed ranks tests).

Figure 5.19 shows medians for the apparent mass, normalised apparent mass, phase and coherence at five vibration magnitudes for the legs bent posture. In the median apparent mass, the principal resonance frequency was found at 3.0 Hz at 0.125 ms^{-2} r.m.s. and at 2.75 Hz at 2.0 ms^{-2} r.m.s. (Figure 5.19(a)). The change in the principal resonance frequency in the median normalised apparent mass was from 3.0 Hz at 0.125 ms^{-2} r.m.s. to 2.5 Hz at 2.0 ms^{-2} r.m.s. (Figure 5.19(b)). The principal resonance frequency tended to decrease with an increase in the vibration magnitude in the legs bent posture, although this is not so clear as in the normal posture. The apparent mass and normalised apparent mass had smaller magnitudes at frequencies above the principal resonance frequency as the vibration magnitude increased (Figure 5.19(a), (b)). The phase shift at low frequencies seemed to be greater with increasing the vibration magnitude (Figure 5.19(c)). As in the case for the normal standing posture, the coherence was lower for the measurement at 0.125 ms^{-2} r.m.s., particularly at frequencies around 7 Hz, compared to those at the other vibration magnitude (Figure 5.19(d)).

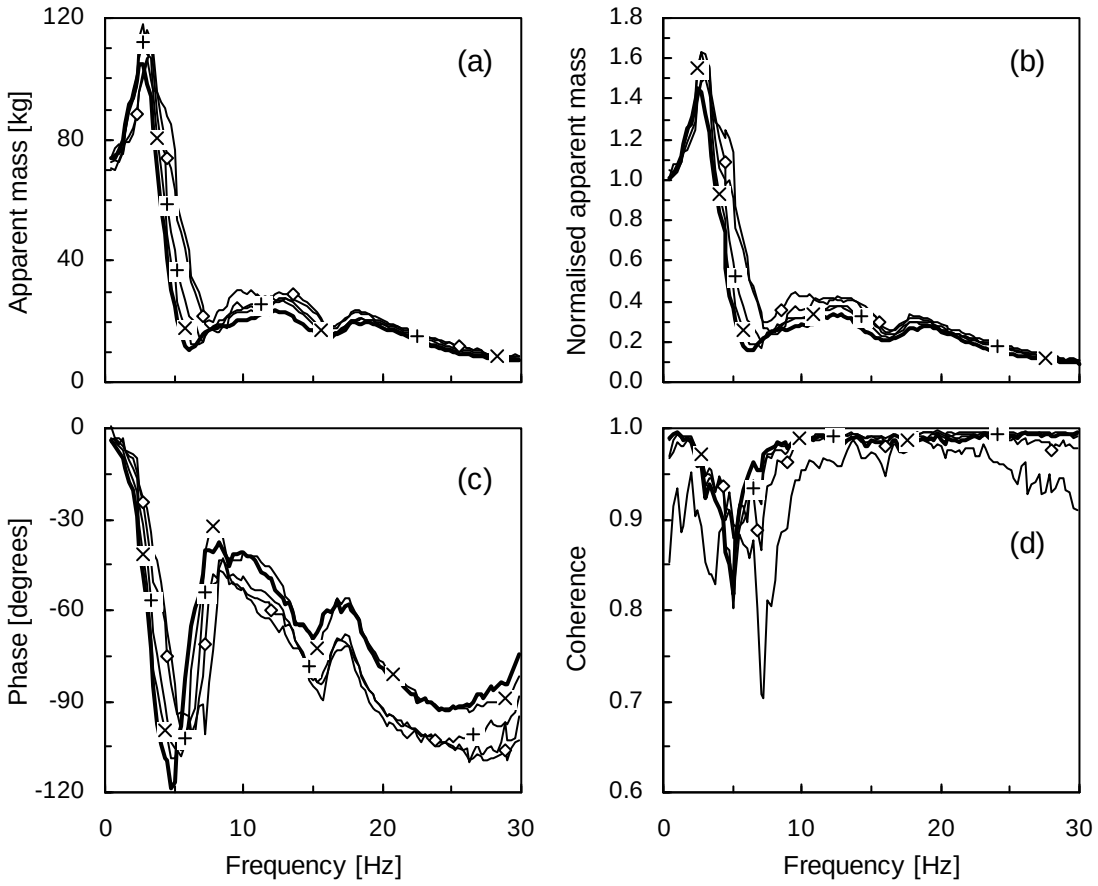

Figure 5.19 Medians for apparent masses, normalised apparent masses, phases and coherences of the twelve subjects in the legs bent posture measured at five different magnitudes: 0.125 ——— ; 0.25 —◇— ; 0.5 —+— ; 1.0 —×— ; 2.0 ms^{-2} r.m.s. ▬▬ .

For the one leg posture, there does not seem to be any consistent effects of the vibration magnitude on the apparent mass. Medians for the apparent mass, normalised apparent mass, phase and coherence at five vibration magnitudes are presented in Figure 5.20. It was difficult to detect a consistent influence of the vibration magnitude on the apparent mass of the subjects in the one leg posture. The differences in the principal resonance frequency and magnitude between two vibration magnitudes were not found to be statistically significant by Wilcoxon matched-pairs signed ranks test. The principal resonance in the apparent mass was observed at 3.5 Hz at 0.25 ms^{-2} r.m.s. and 4.0 Hz at 1.0 ms^{-2} r.m.s. In the normalised apparent mass, the principal resonance frequency was 3.5 Hz for 0.25 ms^{-2} r.m.s. and 3.75 Hz for 1.0 ms^{-2} r.m.s. It was found that two apparent mass curves for each subject were similar to one another at most frequencies used, although the data are not presented here.

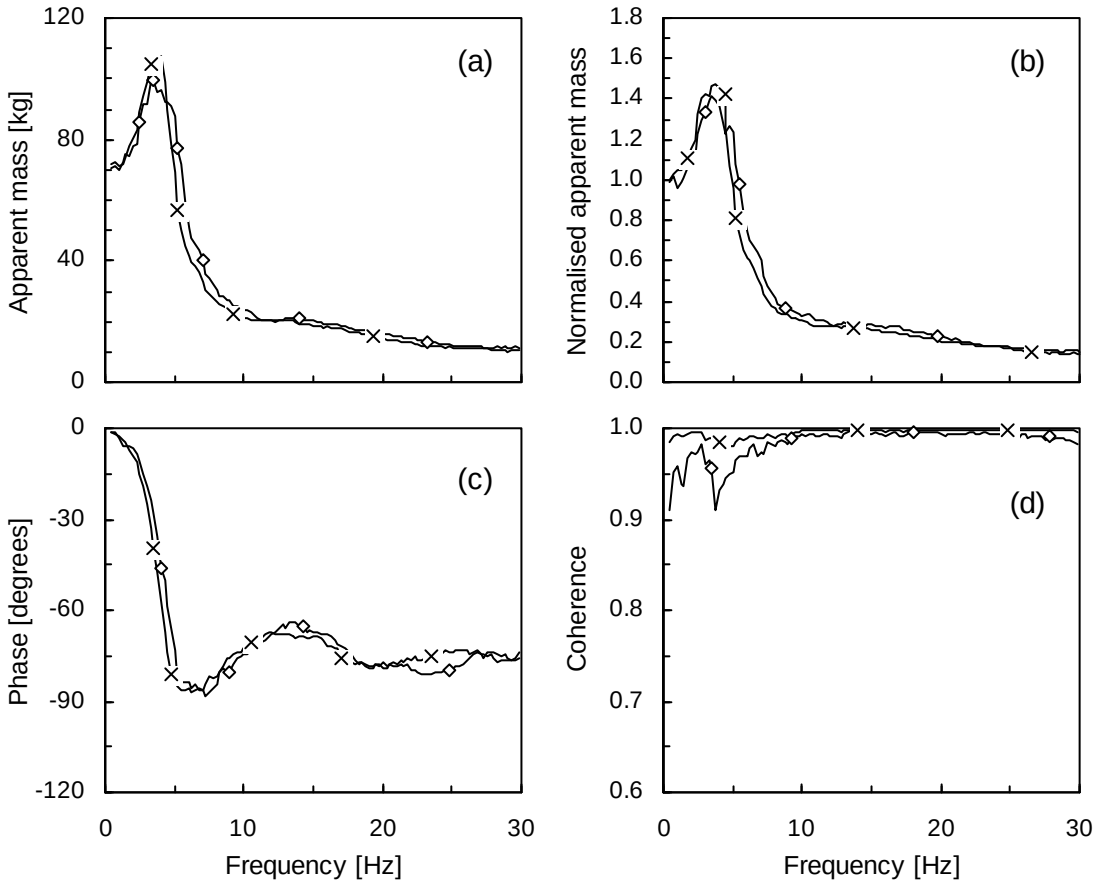

Figure 5.20 Medians for apparent masses, normalised apparent masses, phases and coherences of the twelve subjects in the one leg posture measured at two different magnitudes: 0.25 —◇— ; 1.0 ms^{-2} r.m.s. —×— .

5.4.4.3 Influence of vibration magnitude on transmissibility

An effect of vibration magnitude was found in the transmissibilities to the lower upper-body in all postures. As found in the apparent mass, the peak frequency of the vertical transmissibility to L4 in the normal posture decreased with increasing vibration magnitude (Figure 5.21(a)). The differences in the peak frequencies were statistically significant ($p < 0.05$, Wilcoxon matched-pairs signed ranks tests), except for that between 0.125 and 0.25 ms^{-2} r.m.s. The peak frequency of the vertical transmissibility to L4 in the legs bent posture was affected by changes in vibration magnitude in the same manner as in the case of the normal posture (Figure 5.21(b)). However, statistically significant differences were found only between 0.125 and 0.25 ms^{-2} r.m.s. and between 0.25 and 0.5 ms^{-2} r.m.s. ($p < 0.05$). The peak frequency of the transmissibility to the right iliac crest in the one leg posture also decreased with increasing vibration magnitude from

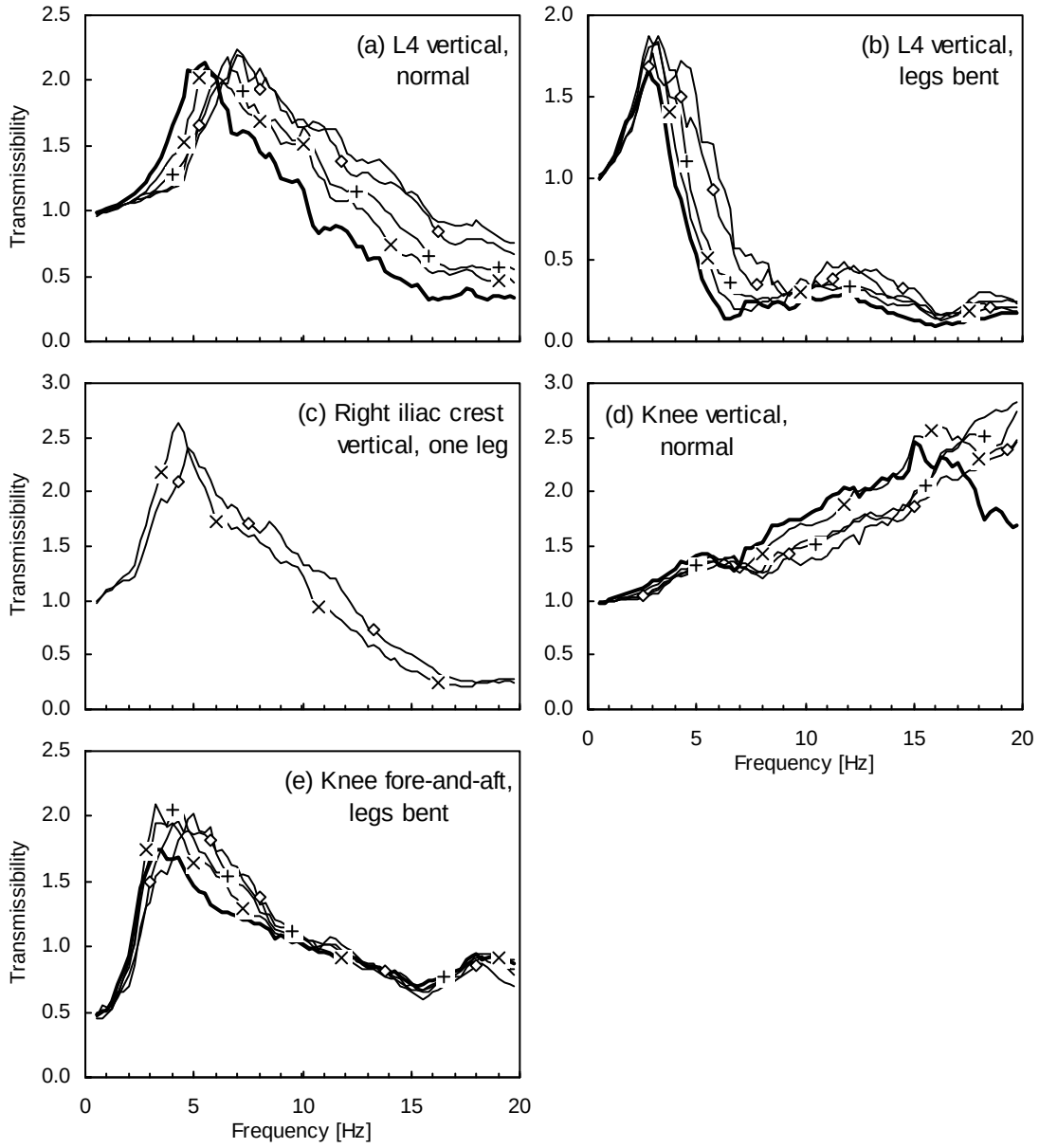

Figure 5.21 Median transmissibilities at different vibration magnitudes. 0.125 ——— ; 0.25 —◇— ; 0.5 —+— ; 1.0 —×— ; 2.0 ms^{-2} r.m.s. ━━━ .

0.25 to 1.0 ms^{-2} r.m.s. ($p < 0.01$), although no clear effect of the vibration magnitude on the apparent mass was found in this posture (Figure 5.21(c)).

The transmissibilities to the knee were also affected by changes in vibration magnitude. In the normal posture, the vertical transmissibilities to the knee at 10 Hz increased with increasing vibration magnitude ($p < 0.05$ for the differences between 0.125 and 0.25 ms^{-2} r.m.s. and between 0.5 and 1.0 ms^{-2} r.m.s., Figure 5.21(d)). This implies either a decrease in the main peak frequency or an increase in the main peak transmissibility, because the main peaks of the transmissibilities were located above 10 Hz (see Figures

5.4(i) and 5.11(a)). The effect of the vibration magnitude on the transmissibility to the knee in the fore-and-aft direction in the legs bent posture was similar to that on the apparent mass (Figure 5.21(e)). The peak frequency tended to decrease as the vibration magnitude increased, although statistical significance was found only between 0.25 and 0.5 ms^{-2} r.m.s. ($p < 0.05$), as in the case of the apparent mass.

5.5 DISCUSSION

The apparent mass of each subject when standing normally showed a main peak at around 5 Hz. This is consistent with previously reported resonance frequencies for both the mechanical impedance and the apparent mass of subjects in similar standing postures (e.g. Coermann, 1962; Fairley, 1986). The resonance frequency in the normal standing posture found in this study was also close to that of the seated body measured in many studies (see Fairley and Griffin, 1989). This implies that the same dynamic mechanism of the upper-body may contribute to the main resonance of the driving point responses of both standing and seated people, as hypothesised in the preceding chapter. In addition, the frequency range of a second broad peak in the apparent mass is similar when standing and when seated. It is, therefore, likely that there is no resonance in the legs held straight that affects the driving point response to vertical vibration at frequencies below about 15 Hz. A small peak in the vertical transmissibility to the knee at around the resonance frequency of the apparent mass may be caused by the motion transmitted from the lower upper-body (Figures 5.4(i) and 5.11(a)). An increase in vibration transmission to the knee was found with increases in frequency above 5 Hz (Figures 5.4(i), (j)).

Figure 5.22 compares the median transmissibilities measured at the three locations over the spine, T1, T8 and L4, in the normal standing posture with the transmissibilities to the spine obtained in previous studies. The median transmissibility to L4 showed a greater peak at frequencies around 5 Hz than those observed in the previous studies. Although some discrepancies can be found between the measured transmissibility to L4 and the transmissibilities reported in the previous experiment, the previously reported transmissibilities also showed differences among the three studies shown in Figure 5.22(a). It is, therefore, difficult to conclude whether the discrepancies found between the measured transmissibility to L4 and the transmissibilities to the lumbar spine previously presented were due to either measurement error, inter-subject variability, or the difference in measurement location. The median transmissibilities to T1 and T8

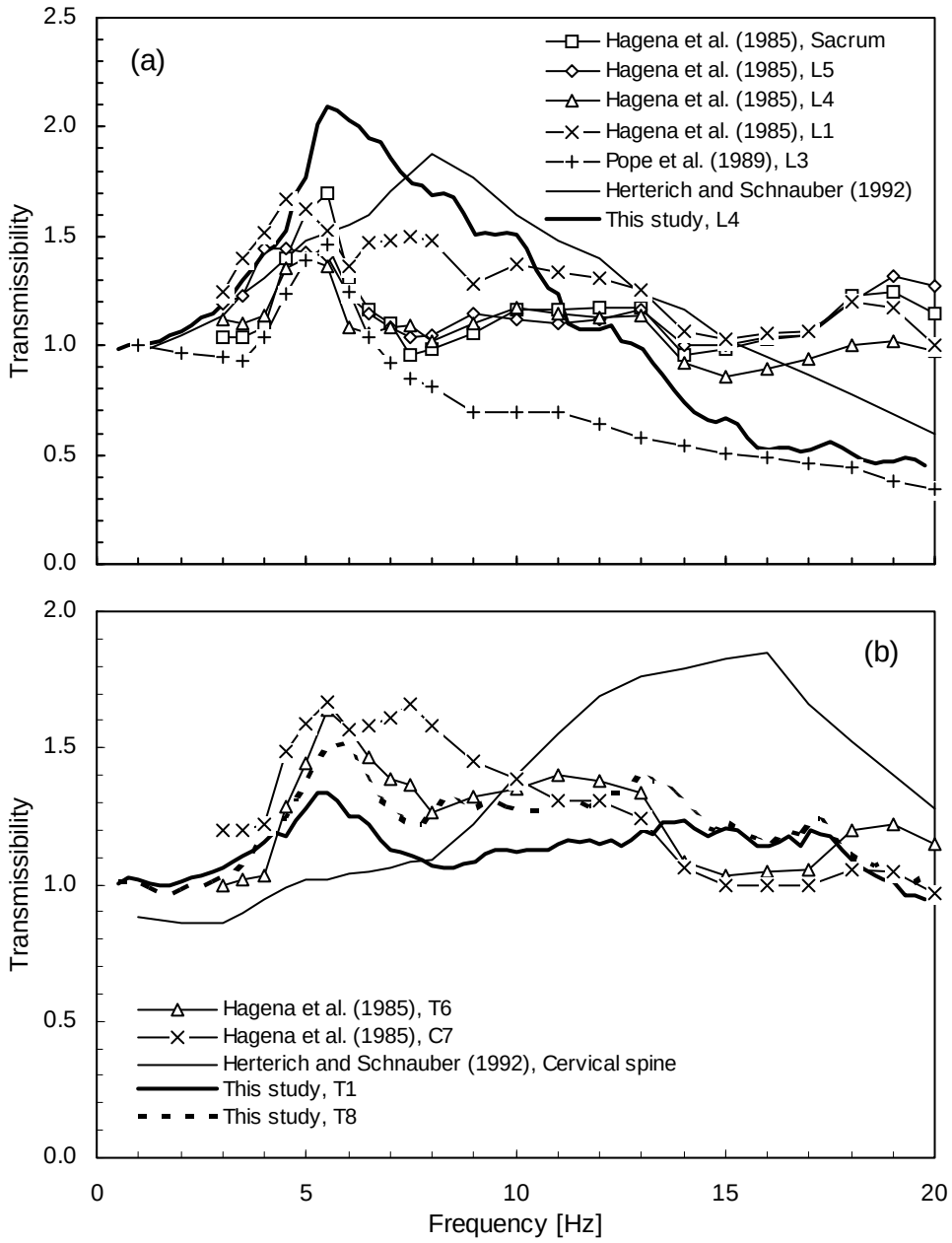

Figure 5.22 Median transmissibilities to the spine in the normal standing posture measured in Experiment 2 and the transmissibilities to the spine in previous studies. (a) To the sacrum and the lumbar spine, (b) to the thoracic and cervical spine. (See Section 2.4.1.3 for details of the previous studies.)

measured in this study showed similar trends to the transmissibilities to C7 and T6 measured by Hagena *et al*. (1985) with one subject (Figure 5.22(b)).

Several studies of the dynamic response of the lumbar spines of seated subjects to either vibration or impact have reported a peak response at around 5 Hz (e.g. Panjabi *et al*., 1986; Magnusson *et al*., 1993), which is close to previously reported resonance frequencies for the mechanical impedance and the apparent mass (e.g. Coermann, 1962; Fairley and Griffin, 1989). For many subjects used in the present study, vertical transmissibility to the fourth lumbar vertebra (L4) showed a prominent peak at a frequency close to the resonance frequency of the apparent mass in all three postures (Table 5.2). Kendall correlation coefficients between the peak frequencies of the transmissibility to L4 and the resonance frequencies of the apparent mass were found to be quite high: 0.462 (p = 0.053) in the normal posture, 0.720 (p = 0.010) in the legs bent posture, and 0.600 (p = 0.011) in the one leg posture. In the legs bent posture, the transmissibilities to the iliac crests also had a peak at the same frequency as that of the apparent mass. This implies that the dynamic mechanisms producing increased motion

Table 5.2 Medians and quartiles of the peak frequencies of the apparent masses and the transmissibilities to the pelvis region at 1.0 ms^{-2} r.m.s. and Kendall correlation coefficients between the peak frequency of the apparent mass and that of the transmissibilities (*: $p < 0.05$, **: $p < 0.01$).

	Apparent mass	**L4**	**Right iliac crest**	**Left iliac crest**
Normal				
25 % [Hz]	5.14	5.70	5.76	5.95
Median [Hz]	5.51	5.89	6.51	6.51
75 % [Hz]	5.57	7.01	7.14	7.01
Correlation (Significance)	---	0.462 (p = 0.053)	0.050 (p = 0.831)	-0.017 (p = 0.943)
Legs bent				
25 % [Hz]	2.75	2.75	2.75	2.75
Median [Hz]	2.75	2.75	2.75	2.75
75 % [Hz]	2.75	3.26	3.26	3.26
Correlation (Significance)	---	0.720 * (p = 0.010)	0.777 ** (p = 0.004)	0.786 ** (p = 0.004)
One leg				
25 % [Hz]	3.26	3.20	4.01	5.51
Median [Hz]	3.76	3.76	4.26	6.51
75 % [Hz]	4.07	4.57	4.39	7.89
Correlation (Significance)	---	0.600 * (p = 0.011)	0.547 (p = 0.024)	-0.464 * (p = 0.043)

at the lower spine may make a significant contribution to the resonance of the whole body. It is likely that the motion of the lower spine is closely related to that of the pelvis: the trends in the transmissibilities to the iliac crests were almost the same as those to L4 up to the peak frequency, when standing on both legs (Figures 5.7(a), (b)).

Peaks in transmissibilities to the thoracic vertebrae at around 5 Hz were not so remarkable as those in the transmissibilities to the lumbar vertebra at this frequency. The transmissibilities to two measurement points over the thoracic spine (at T1 and T8) were found to be similar to each other but different from that to the lumbar spine, in both the normal posture and in the legs bent posture (Figure 5.10). The transmissibilities between adjacent measurement points over the spine in the vertical axis were calculated to investigate motions within the spine (Figure 5.23). It is clear that there was little amplification or attenuation of vertical motion between the first and eighth thoracic vertebrae (T1 and T8) for most subjects in all the postures: the transmissibility was almost unity over the frequency range used.

The transmissibility from the fourth lumbar vertebra to the eighth thoracic vertebra suggested that larger relative motions occurred in the lower spine than in the upper spine (Figure 5.23(a), (c), (e)). The difference in the transmissibilities between subjects were small at low frequencies in all the postures. The magnitudes of the transmissibilities in the normal posture and in the legs bent posture decreased from unity as the frequency increased up to about the resonance frequency of the apparent mass: the vertical motion measured at L4 was greater than that at T8. However, as Sandover and Dupuis (1987) and Hinz *et al*. (1988b) stated, axial motion of lumbar vertebrae may be accompanied by rotational motion that affects measurements over the spinous process of L4: a pitch motion of the vertebral body could have been measured as a vertical motion. The pitch motion could result from bending of the lumbar spine. If the lumbar spine flexed during upward movement of the floor, the tip of the spinous process of L4 would move upward more than the centre of the vertebral body of L4. There may be smaller rotational motions of the vertebral bodies in the thoracic region if the rib cage connected to thoracic vertebral bodies restricts relative rotational motion between adjacent vertebrae. Therefore, the relative motion found between L4 and T8 at low frequencies possibly arose from either a greater axial motion at L4 than that at T8, or a rotational motion of L4 while vertical motions of the vertebral bodies at L4 and T8 may have been similar, or both. It was not possible to separate vertical and rotational motions of the vertebral body by the measurement method used. In the one leg posture, the transmissibility between

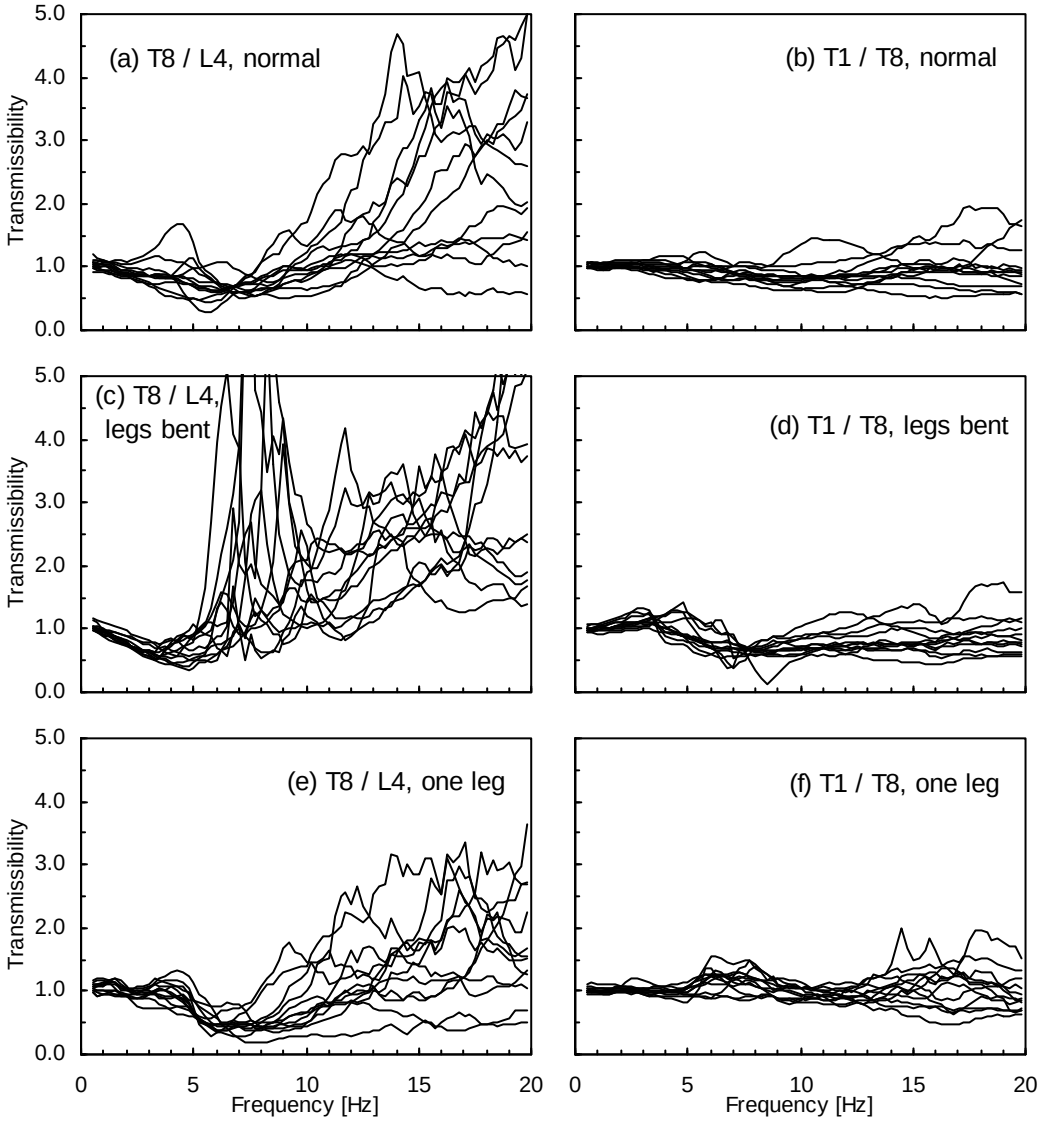

Figure 5.23 Transmissibilities between two points over the spines of twelve subjects at 1.0 ms^{-2} r.m.s. (a) T8/L4, normal; (b) T1/T8, normal; (c) T8/L4, legs bent; (d) T1/T8, legs bent; (e) T8/L4, one leg; (f) T1/T8, one leg.

L4 and T8 remained unity up to the resonance frequency of the apparent mass, as did the transmissibility between T8 and T1.

A large inter-subject variability in the vertical transmissibilities between L4 and T8 was found at high frequencies for all postures (Figures 5.23(a), (c), (e)). This large variability might be caused not only by the difference in the response itself but by small 'input' motions at L4 not being accurately resolved. The very high variability in the transmissibility between L4 and T8 in the legs bent posture at around 7 Hz was also caused by little motion at L4 (Figure 5.23(c)). At high frequencies, the vertical motion measured at L4, in the lower part of the spine, was consistently smaller than that at T1

and T8, in the higher parts of the spine, for most subjects, although the variability was large. In addition, the phase lags in the transmissibilities from the floor to L4 were much larger than the phase lags to T1 and T8 in this frequency range (Figure 5.5, for the normal posture). It seems unlikely that the axial motion of the vertebrae were different enough to produce such a large relative motion and phase lag between the thoracic and lumbar spine. It may be hypothesised that vertical motion of the vertebral body is partially cancelled by a rotational motion which is out of phase with the vertical motion in this frequency range.

5.6 CONCLUSIONS

In a normal standing posture, with a vibration magnitude of 1.0 ms^{-2} r.m.s., there was a main resonance of the apparent mass of the human body at about 5.5 Hz, with a second broad resonance in the range 9 to 15 Hz. Almost all transmissibilities to the spine measured in both the vertical and fore-and-aft directions showed a peak at almost the same frequency as that of the apparent mass, while some peaks, particularly in the fore-and-aft direction, were small. Transmissibilities to the fourth lumbar vertebra (L4) in the vertical direction, in particular, had a clear peak at this frequency. The relative vertical motions between two points within the thoracic spine (at T1 and T8) were smaller than the relative vertical motions between the thoracic and the lumbar spine (at T8 and L4) over the frequency range up to 20 Hz. Vertical transmissibilities to the iliac crests had similar trends to the transmissibilities to L4, although the peak frequencies for the iliac crests were slightly higher. Pitch motion of the pelvis, which might alter the lordosis of the lumbar spine and cause motion of the lumbar vertebrae, occurred at frequencies somewhat above 5 Hz. No resonance in the legs held straight that affected the apparent mass was found at frequencies below 15 Hz.

When the legs were bent, with a vibration magnitude of 1.0 ms^{-2} r.m.s., the resonance frequency of the apparent mass decreased to about 2.75 Hz. There was a trough in the apparent mass at around 7 Hz and low magnitudes above 7 Hz, compared to those in the normal posture. The peak frequencies of the transmissibilities to L4 and the iliac crests were strongly correlated with the resonance frequency of the apparent mass. At the resonance frequency of the apparent mass in this posture, the fore-and-aft motions at the knee and at T1 were much greater than those in the other postures. A bending motion of the legs at the knee, which is probably coupled with a pitching or bending motion of the whole upper-body about the hip joint, may be the cause of the resonance of

the whole body. A bending motion of the legs also attenuated the vibration transmission to the upper-body at frequencies well above the natural frequency of the bending mode, at about 3 Hz.

When subjects stood on one leg, with a vibration magnitude of 1.0 ms^{-2} r.m.s., a main resonance of the apparent mass appeared at about 3.75 Hz, with no other distinguishable peaks at frequencies below 30 Hz. The vertical transmissibilities to three measurement points over the spine were almost identical up to 5 Hz, which implied that the upper-body tended to move as a whole. Both roll and pitch motions of the pelvis in the one leg posture were relatively large, particularly at frequencies below 10 Hz, compared to those in the other postures when standing on both legs. Coupled rotational motions about the hip joint may cause a whole upper-body movement at low frequencies, rather than a resonance of local body parts, and attenuate vertical vibration transmission at high frequencies.

The main resonance frequency of the apparent mass in the normal posture decreased from 6.75 Hz to 5.25 Hz as the vibration magnitude increased from 0.125 ms^{-2} r.m.s. to 2.0 ms^{-2} r.m.s. This ‘softening’ effect was also found for the second broad peak in the apparent mass for most subjects, as well as in the transmissibilities to most parts of the body where a clear peak was evident. The resonance frequency of the apparent mass in the legs bent posture also tended to decrease with an increase in vibration magnitude, although the change was small: 3.0 Hz at 0.125 ms^{-2} r.m.s. to 2.5 Hz at 2.0 ms^{-2} r.m.s. A similar effect was found in the transmissibility to the knee in the fore-and-aft direction which might be responsible for the resonance seen in the apparent mass. In the one leg posture, the ‘softening’ effect was found to be significant in the transmissibility to the pelvis, although the influence of vibration magnitude on the apparent mass was not statistically significant.

CHAPTER 6

DIFFERENCES IN DYNAMIC RESPONSES BETWEEN STANDING AND SEATED BODIES AND THE NONLINEARITY IN BIODYNAMIC RESPONSES

6.1 INTRODUCTION

The two experiments described in the previous chapters showed that the principal and second resonances in the apparent mass of standing subjects were observed at similar frequencies to those of seated subjects. The measurements of the motions at the knee when subjects stood with their legs locked showed that the dynamic response of the legs when straight might not make a main contribution to the principal resonance of the apparent mass at about 5 Hz. It is, therefore, hypothesised that the principal resonance in the apparent mass for both the standing and seated body is caused by the same dynamic mechanisms in the upper-body above the pelvis.

In Experiment 2 described in Chapter 5, the dynamic response of the upper-body to vertical whole-body vibration was measured at several locations along the spine and over the pelvis when subjects were standing. It seemed from the measurements of the motions at three locations along the spine that the motion of the spine might make some contribution to the principal resonance of the apparent mass. More relative motion within the spine was found to occur in the lower spine than in the higher spine. It was thought likely that the translational motions of the vertebrae were coupled with the rotational motions.

This chapter presents an experiment (referred to in this thesis as Experiment 3) in which the dynamic responses of the body in both standing and seated subjects to vertical vibration were measured. The measurements were made at more locations than those in Experiment 2, including more locations along the spine, particularly in the lower spine, and the head, at five different vibration magnitudes. Rotational motions in the sagittal plane (i.e., pitch) were measured at all locations together with translational (i.e., vertical and fore-and-aft) motions.

The driving-point impedances have been obtained with subjects when standing and sitting by Coermann (1962) and Miwa (1975). Coermann (1962) presented the mechanical impedance of one subject in three postures, ‘standing erect’, ‘sitting erect’ and ‘sitting relaxed’. A main resonance was observed at 5.9, 6.3 and 5.2 Hz, respectively. The impedance at the resonance was greater in a ‘sitting erect’ posture than in the other two postures. Miwa (1975) found a main peak at 7 Hz, together with a minor peak at 20 Hz, in the mean mechanical impedance of 20 standing subjects. For seated subjects, a main peak at a frequency 6 to 8 Hz with a minor peak in the 16 to 20 Hz frequency range was found.

Coermann (1962) compared the vertical vibration transmissibilities to the head between standing and sitting subjects. It was observed in the data from one subject that the transmissibility to the head had a similar main peak at about 5 Hz with ‘standing erect’ and ‘sitting erect’ postures, while differences at higher frequencies were observed. Kobayashi *et al*. (1981) and Rao (1982) also measured the vibration transmission to the head with standing and sitting subjects exposed to vertical vibration. Kobayashi *et al*. (1981) showed smaller vertical transmissibilities and greater fore-and-aft transmissibilities at around 5 Hz for standing subjects than for seated subjects. The data from Rao (1982) showed the trend in the transmissibility curve was consistent in standing and sitting positions.

In a study by Hagena *et al*. (1986), the vertical vibration transmission from the sacrum to six upper locations along the spine, including the head, was presented for standing and sitting positions at seven discrete frequencies up to 40 Hz. The variation in the transmission between measurement locations was within ± about 15% at frequencies below 14.3 Hz for a standing position and below 8.1 Hz for a sitting position. The transmission through the spine was less for a sitting posture than for a standing posture at 4 Hz.

Nonlinear characteristics observed in the dynamic response of the human body due to changes in input vibration magnitude have been reported in some previous studies of the seated body (e.g., Hinz and Seidel, 1987; Mansfield, 1998; Mansfield and Griffin, 1999). Mansfield (1998) and Mansfield and Griffin (1999) showed decreases in resonance frequencies observed in the apparent mass and transmissibilities to the abdominal region with increasing vibration magnitude: for example, 5.4 Hz at 0.25 ms^{-2} r.m.s. to 4.2 Hz at 2.5 ms^{-2} r.m.s. in the median apparent mass. However, some have not observed

any nonlinear effects in the dynamic response measurements with different input magnitudes. (e.g., Panjabi *et al*. 1986; Pope *et al*. 1989).

The objectives of the study presented in this chapter were: (i) to identify the differences in the apparent mass and transmissibilities between standing and seated people by measuring the motions at several locations on the body in three axes in the mid-sagittal plane (i.e., vertical, fore-and-aft and pitch), and (ii) to confirm the presence of nonlinear effects in the apparent mass and transmissibilities of standing and seated subjects, which have been inconsistent in previous studies of the seated body.

6.2 METHOD

The 1 metre stroke electro-hydraulic vibrator described in Section 3.2.1.2 was used in Experiment 3. The force platform, Kistler 9281B, was secured to a flat rigid seat which was mounted on the vibrator platform to measure the force at the interface between the seat and seated subjects. The force platform was rigidly mounted on the vibrator platform for standing subjects, as opposed to on the seat for seated subjects. A computer generated Gaussian random signal, which was common for all subjects, was fed into the vibrator which produced a random vertical vibration having a flat constant bandwidth acceleration spectrum over the frequency range between 0.5 and 20 Hz. Five different magnitudes of vibration, 0.125, 0.25, 0.5, 1.0, 2.0 ms^{-2} r.m.s., for 60 seconds were used as input stimuli. The acceleration at the vibrating surface, either the seat or the floor, was measured at the centre of the top plate of the force platform with a piezoresistive accelerometer, Entran EGCS-DO-10.

Eight male volunteers, median age 28 yr, height 1.76 m and weight 72 kg, took part in the experiment. The details of the subjects are presented in Appendix D. The sitting posture of the subjects was a ‘normal sitting posture’ defined as sitting looking straight ahead and with the upper-body in a comfortable and upright posture without backrest. No footrest was used: the feet were allowed to hang freely. The standing posture of the subjects was a ‘normal standing posture’ defined as standing looking straight ahead and with the upper-body in a comfortable, upright position and the legs straight and locked. When standing, subjects held lightly with both hands to a rigid frame in front of them which was rigidly secured to the vibrator platform for safety purposes; no subject needed to alter upper-body position to hold the frame. Measurements were made while barefoot so as to eliminate any effects of footwear. Subjects were asked to avoid any voluntary

movements in both postures. Half of the subjects started the experiment with the standing posture and the rest started with the sitting posture. The order of presentation of the five vibration magnitudes was randomised. The written instructions given to the subjects is shown in Appendix D.

The motions of the body in three axes in the mid-sagittal plane (i.e., vertical, fore-and-aft, and pitch) were measured at eight locations in the upper-body: at the head, six points along the spine (the first, fifth and tenth thoracic vertebrae, and the first, third and fifth lumbar vertebrae: T1, T5, T10, L1, L3, L5) and the pelvis (on the posterior-superior iliac spine of the right ilium, 50 mm away from the mid sagittal plane). Additionally, the vibration was measured at the left knee (just below the patella) in the vertical and fore-and-aft direction in the standing posture. The locations of all measurement sites were measured so as to identify the motion of the whole spine at the resonance frequency described in the subsequent chapter. A bite-bar in which three translational accelerometers (Entran EGA-125(F)*-10D and EGAX-F-5) were installed was used for measuring the head motion in the vertical, fore-and-aft and pitch directions (see Paddan and Griffin, 1988). The separation between two accelerometers measuring the vertical motions for calculation of the pitch motion of the head was 115 mm.

The motions of the vertebrae and the pelvis were measured with accelerometers attached to the body surface. As suggested by Sandover and Dupuis (1987) and Hinz *et al*. (1988b), potential pitch motion of the vertebrae has an effect on the measurement of translational motions at the body surface (i.e., those at the centre of the vertebral bodies could be different from those at the spinous processes). Therefore, the vertebral motions in the vertical, fore-and-aft and pitch axes were measured at the body surface such that the motions at the centres of the vertebral bodies could be estimated. Sets of two miniature accelerometers (either Entran EGA-125(F)*-10D or EGAX-F-5) were attached to T-shaped blocks of balsa wood with a separation of 30 mm so as to measure both the vertical and pitch motions at the body surface over the spine and the pelvis (see Figure 6.1). The fore-and-aft motion was also measured with another miniature accelerometer attached to a different face of the block. The weight of the block, including the accelerometers and their cables, was about 4 g. The block was attached to the body surface by double-sided adhesive tape and adhesive plaster with a contact area of 20 mm (horizontal) by 30 mm (vertical). The motions at the knee were measured with two miniature translational accelerometers (Entran EGA-125*-10D) orientated orthogonally and attached to a balsa wood card, 20 mm (horizontal) by 30 mm (vertical) with 3 mm in

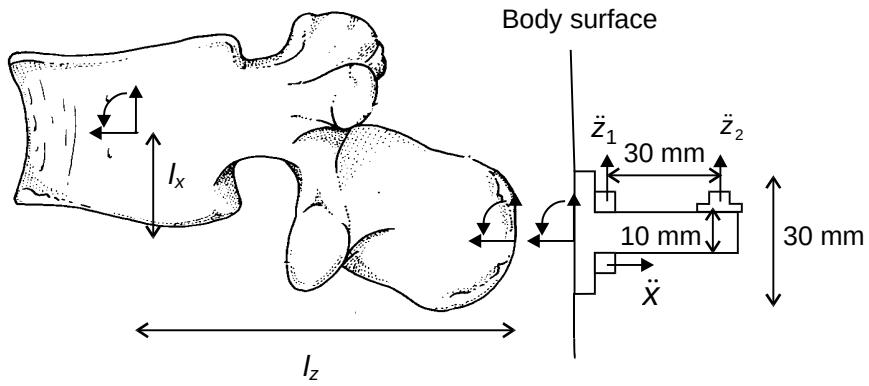

Figure 6.1 Measurements over a vertebra showing the T-shaped balsa block and miniature accelerometers. (Transmissibilities to the centre of the vertebra were estimated from those to the spinous process obtained from surface measurement.)

thickness. Signals from all the accelerometers and the force platform were acquired at 128 samples per second after low-pass filtering at 20 Hz.

As in Experiment 2, a data correction method for surface measurements developed by Kitazaki and Griffin (1995) was applied, assuming that the local dynamic system consisting of the tissue and the accelerometer could be analogised with a single degree-of-freedom linear system. The natural frequency and damping ratio of the local tissue-accelerometer system at each measurement location and in each direction was derived from the response to free damped oscillation tests performed before vibration exposure. The correction method made it possible to obtain the motions at the spinous processes from those measured on the body surface.

6.3 ANALYSIS

In the analysis, upward and forward motions were taken as positive vertical (*z*-axis) and fore-and-aft (*x*-axis) motions, respectively, as defined in ISO 2631-1 (1997). Pitch motions which rotated clockwise when looked at from the right hand side of the body were taken as positive.

The apparent mass, $M(f)$, was calculated by dividing the cross spectral density function between the seat or floor acceleration and the resulting force at the seat or floor surface, $S_{sf}(f)$, by the power spectral density function of the seat or floor acceleration, $S_s(f)$:

$$M(f) = S_{sf}(f)/S_s(f) \qquad (6.1)$$

The effect of the top plate of the force platform on the apparent mass was eliminated by mass cancellation as described in Section 3.4.1.1.

The transmissibilities, $T(f)$, were also obtained using the cross spectral density method, using the seat or floor acceleration as a reference:

$$T(f) = S_{sb}(f)/S_s(f) \tag{6.2}$$

where $S_{sb}(f)$ is the cross spectral density between the acceleration at the seat or the floor and the acceleration measured at a location of the body. A resolution of 0.25 Hz was used for the calculation, which gives 60 degrees-of-freedom corresponding to accuracy and confidence levels of about 80% at ± 1 dB.

Accelerations in the *z*-axis obtained from accelerometers attached to a balsa block near the body surface, $\ddot{z}_1$ in Figure 6.1, were regarded as those along the body surface on the assumption that the distance between the body surface and the accelerometers, 5 mm, could be neglected. Those from the accelerometers on a different face of the block were regarded as being normal to the surface ($\ddot{x}$ in Figure 6.1). Pitch motion was obtained by dividing the difference between the two vertical accelerations ($\ddot{z}_1$ and $\ddot{z}_2$ in Figure 6.1) by the distance between two accelerometers (i.e., 30 mm). It was assumed that both the bite-bar and balsa blocks were rigid in the frequency range used in the experiment.

The transmissibilities to each location and in each axis were corrected to reduce the discrepancy between the motion of the skeleton and that measured at the body surface (Kitazaki and Griffin, 1995), as in the previous chapter:

$$T_b(f) = C(f)T_s(f) \tag{6.3}$$

where $T_b(f)$ and $T_s(f)$ are the transmissibilities to the bone and to the surface over the bone, respectively, expressed in complex numbers. The values of the correction frequency functions, $C(f)$, were determined from the natural frequencies and the damping ratios of the local tissue-accelerometer systems obtained from free oscillation tests:

$$C(f) = \frac{1-(f/f_0)^2 + 2i\varsigma(f/f_0)}{1+2i\varsigma(f/f_0)} \quad (6.4)$$

where f_0 and ζ are the natural frequency and the damping ratio of the local system, respectively, and $i^2 = -1$.

The effect of the inclination of the body surface on the measurement was reduced using the angle of the surface relative to the vertical axis. This effect was particularly significant at T1 where the angle of the surface to the vertical axis varied between 14 and 35 degrees among the eight subjects. The corrected transmissibilities to the spinous processes along the body surface, $T_{z1}(f)$, and normal to the surface, $T_{x1}(f)$, expressed in complex numbers were compensated linearly by the angle between the body surface and the vertical axis, θ, in the frequency domain:

$$T_x(f) = T_{x1}(f)\cos\theta + T_{z1}(f)\sin\theta \quad (6.5)$$

$$T_z(f) = -T_{x1}(f)\sin\theta + T_{z1}(f)\cos\theta \quad (6.6)$$

where $T_x(f)$ and $T_z(f)$ are the required transmissibilities in the *x*-axis (i.e. fore-and-aft) and the *z*-axis (i.e. vertical) in an earth-based co-ordinate system. The pitch displacements at each measurement point were assumed to be small so that the angle of the surface did not change during exposure. This was a reasonable assumption according to the results

Table 6.1 Angles between body surface and vertical axis at each measurement location for the standing posture. In degrees. Based on the same co-ordinate for pitch motion.

	Subject 1	Subject 2	Subject 3	Subject 4	Subject 5	Subject 6	Subject 7	Subject 8
T1	14	30	33	22	22	29	26	21
T5	7	0	10	4	13	19	4	10
T10	-12	-26	-15	-15	-18	-14	-11	-15
L1	-23	5	-11	-15	-8	-8	-16	-8
L3	-8	27	4	-13	-2	0	0	6
L5	9	14	8	-4	2	8	-4	15
Pelvis	9	14	8	-4	14	8	-4	15
Knee	13	15	12	15	12	13	15	17

Table 6.2 Angles between body surface and vertical axis at each measurement location for the sitting posture. In degrees. Based on the same co-ordinate for pitch motion.

	Subject 1	Subject 2	Subject 3	Subject 4	Subject 5	Subject 6	Subject 7	Subject 8
T1	24	34	30	35	28	24	24	30
T5	16	5	11	11	15	4	16	14
T10	4	-5	-6	-3	-10	-16	10	-3
L1	-6	-1	0	0	-2	-2	8	-5
L3	-6	-6	-2	0	0	3	0	-2
L5	-16	-10	-2	0	0	5	-4	-2
Pelvis	-16	-10	-2	0	0	5	-4	15

presented below. The angles between the body surface and the vertical axis, θ, at each measurement point measured with an angle meter are given for all subjects in the standing and sitting postures in Tables 6.1 and 6.2, respectively.

As mentioned above, if there is pitch motion of the vertebrae, transmissibilities to the spinous processes will be different from those to the centres of the vertebral bodies. Therefore, assuming that the vertebrae were rigid and that their velocities in the pitch direction were small, transmissibilities to the centres of the vertebral bodies were estimated using those determined for the spinous processes for the three directions within the sagittal plane:

$$T_{xc}(f) = T_{xs}(f) + l_z T_{ps}(f) \tag{6.7}$$

$$T_{zc}(f) = T_{zs}(f) - l_x T_{ps}(f) \tag{6.8}$$

where $T(f)$ is the complex transmissibility and the subscripts x, z and p represent the fore-and-aft, vertical and pitch directions, respectively. The subscripts c and s represent the centres of the vertebral bodies and the spinous processes, respectively. The assumed horizontal and vertical distances, l_x and l_z, between the centres of the vertebral bodies and the tips of the spinous processes are given in Table 6.3 (see Figure 6.1).

Table 6.3 Horizontal and vertical distances between the centres of the vertebral bodies and the tips of the spinous processes, used in the estimation of the transmissibilities to the centres of the vertebral bodies.

Location	Horizontal, l_x [mm]	Vertical, l_z [mm]
T1	50	10
T5	50	30
T10	55	15
L1	60	10
L3	65	10
L5	60	15

6.4 RESULTS

6.4.1 Effect of data correction method on transmissibility

In a preliminary experiment, a significant variability in measured vertebral pitch motion was found at frequencies above about 10 Hz when using different sizes of balsa blocks (Figure 6.2). It was concluded that the estimated transmissibilities to the centres of the vertebrae were reliable in the frequency range below 10 Hz.

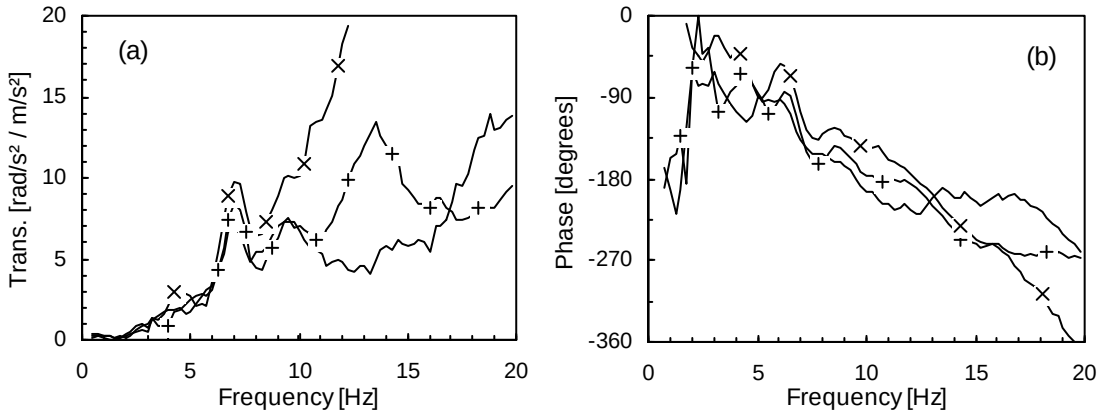

Figure 6.2 Pitch transmissibility to L3 measured with three T-shaped balsa blocks having different sizes: —+—, 25 mm of separation between two accelerometers; ———, 30 mm of separation; —x—, 35 mm of separation. (Results from a preliminary experiment.)

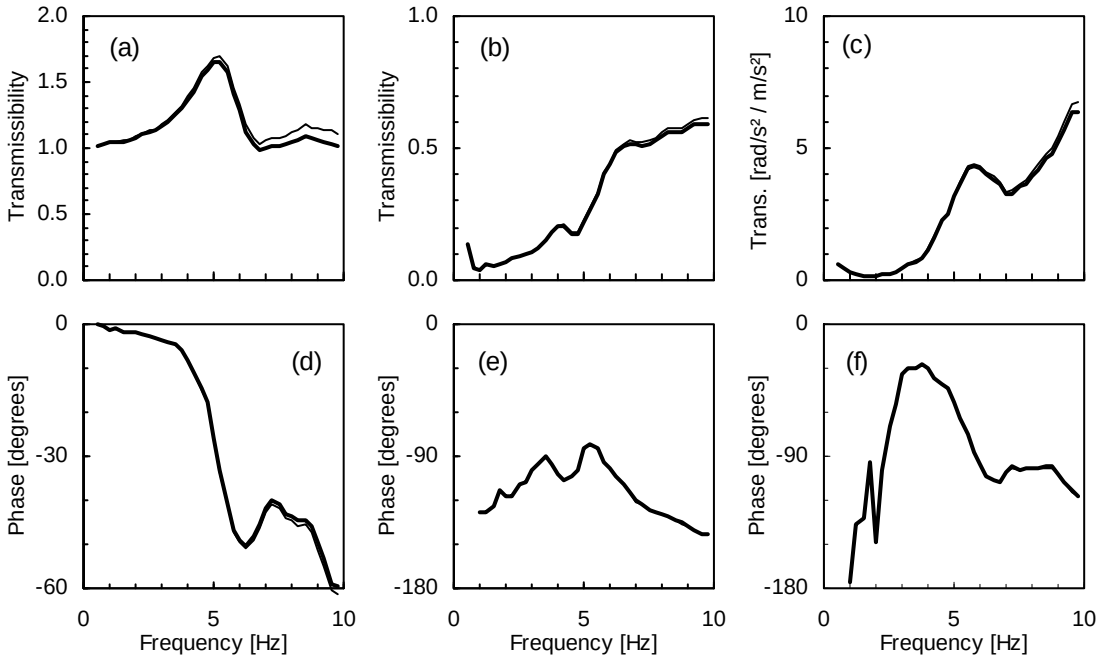

Figure 6.3 Examples of the effects of the local tissue-accelerometer system on the transmissibility. Transmissibilities and phases for the motions at L3 of a subject in the sitting position: (a) and (d), the vertical motion; (b) and (e), the fore-and-aft motion; (c) and (f) the pitch motion. ——— , before correction; ━━━ , after correction.

The first step of the data correction method for the transmissibility was to reduce the discrepancy between the motion of the skeleton and that measured at the body surface by using Equations (6.3) and (6.4). Appendix D presents the natural frequencies and damping ratios of the local tissue-accelerometer systems obtained prior to vibration exposures. Examples of the effect of the local tissue-accelerometer system are shown in Figure 6.3. As seen in the figure, the effects were generally small in the frequency range below 10 Hz, with the local natural frequencies generally above 15 Hz, which was also seen by Kitazaki and Griffin (1995).

The effect of the inclination of the body surface on the transmissibility was reduced by using Equations (6.5) and (6.6). The effect was most significant on the measurements at T1, as mentioned above. Examples of the effect of the inclination are shown in Figure 6.4. For these examples, the correction reduced the fore-and-aft transmissibility to T1 of a subject from about 0.4 to about 0.1 or less at the lowest frequencies (e.g. about 1.0 Hz), agreeing with the expectation that the body would mainly move in the vertical direction at low frequencies.

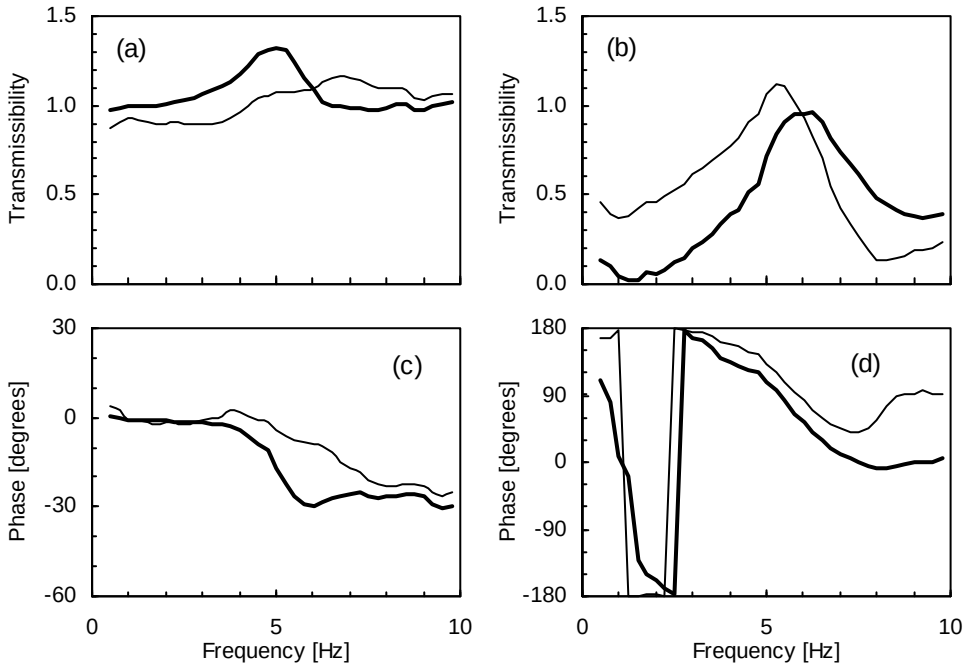

Figure 6.4 Examples of the effects of the inclination of the body surface on the transmissibility. Transmissibilities and phases for the motions at T1 of a subject in the sitting posture: (a) and (c), the vertical motion; (b) and (d), the fore-and-aft motion. ——— , before correction; ━━━ , after correction.

It was found that the pitch motions of the vertebrae resulted in up to about 20% difference in transmissibility to the vertebral bodies compared to the transmissibility to the spinous processes around 5 Hz, which agreed with the observation by Sandover and Dupuis (1987). Figure 6.5 illustrates the transmissibility to the spinous process, after correction by Equations (6.3) to (6.6), and the transmissibility to the centre of the vertebra using Equations (6.7) and (6.8), at L3 of the same subject shown in Figure 6.3. The median estimated transmissibility to the centre of the vertebral body of L3 was compared with the transmissibilities to L3 and the vicinity reported in previous studies of seated subjects using transducers mounted on pins directly threaded into the spinous processes (see Figure 6.6, Panjabi *et al*., 1986; Pope *et al*., 1990; Magnusson *et al*., 1993). The median transmissibility obtained in this study was found to be similar to measurements obtained with transducers rigidly mounted to the spinous processes. The difference between the present study and the previous studies may be partly attributed to the difference in transmissibility between the centre of the vertebral body and the spinous process.

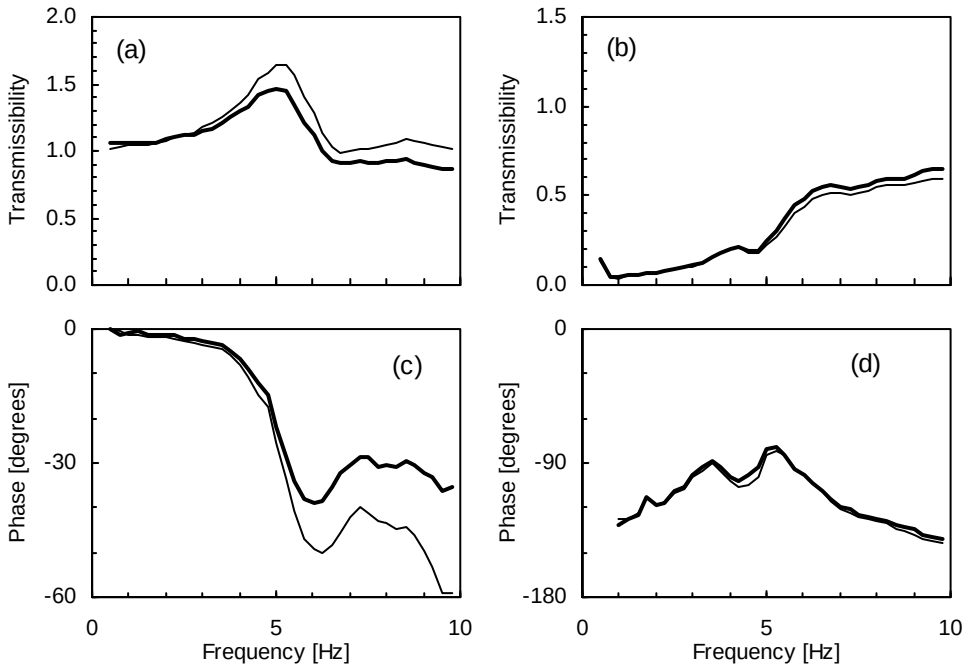

Figure 6.5 Transmissibilities and phases to the spinous process and to the centre of the vertebra at L3 of a subject in the sitting posture: (a) and (c), in the vertical direction; (b) and (d), in the fore-and-aft direction. ——— , spinous process; ━━━ , centre of vertebra.

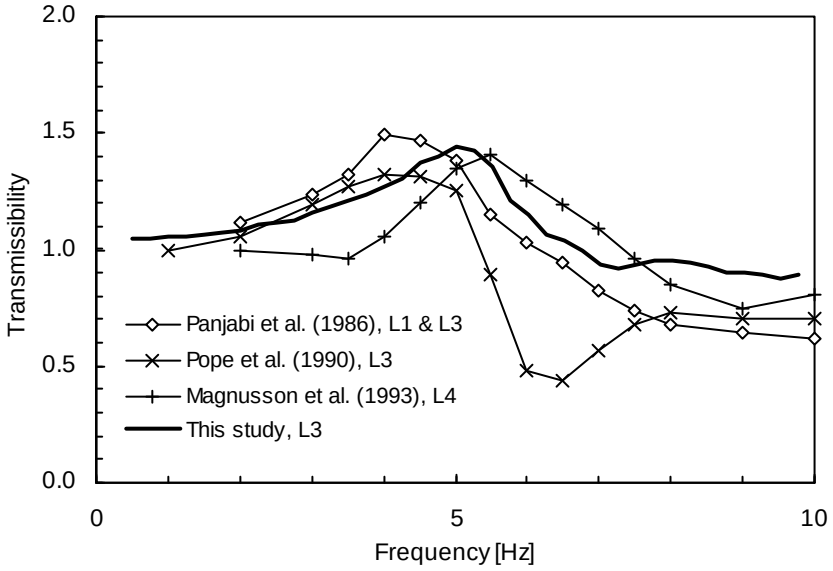

Figure 6.6 Comparison of the median estimated transmissibility to the centre of the vertebral body of L3, to the transmissibilities to L3, and to this vicinity reported in previous studies. (See Section 2.4.1.4 for details of the previous studies.)

6.4.2 Dynamic responses of the body in standing and sitting positions

Figure 6.7 compares the median normalised apparent masses of the eight subjects when sitting and standing measured at a vibration magnitude of 1.0 ms^{-2} r.m.s. The principal resonance frequencies in the standing posture were found to be somewhat greater than those in the sitting posture at 1.0 ms^{-2} r.m.s. ($p < 0.05$, Wilcoxon matched-pairs signed ranks test). The same statistically significant difference was found in the apparent masses measured at 0.5 and 2.0 ms^{-2} r.m.s. ($p < 0.05$). The moduli of the apparent masses at the principal resonance frequency in the standing posture tended to be smaller than those in the sitting posture ($p < 0.05$, at 0.5, 1.0 and 2.0 ms^{-2} r.m.s.). At frequencies above 10 Hz, the apparent masses in the standing posture were found to be greater than those in the sitting posture for all the subjects.

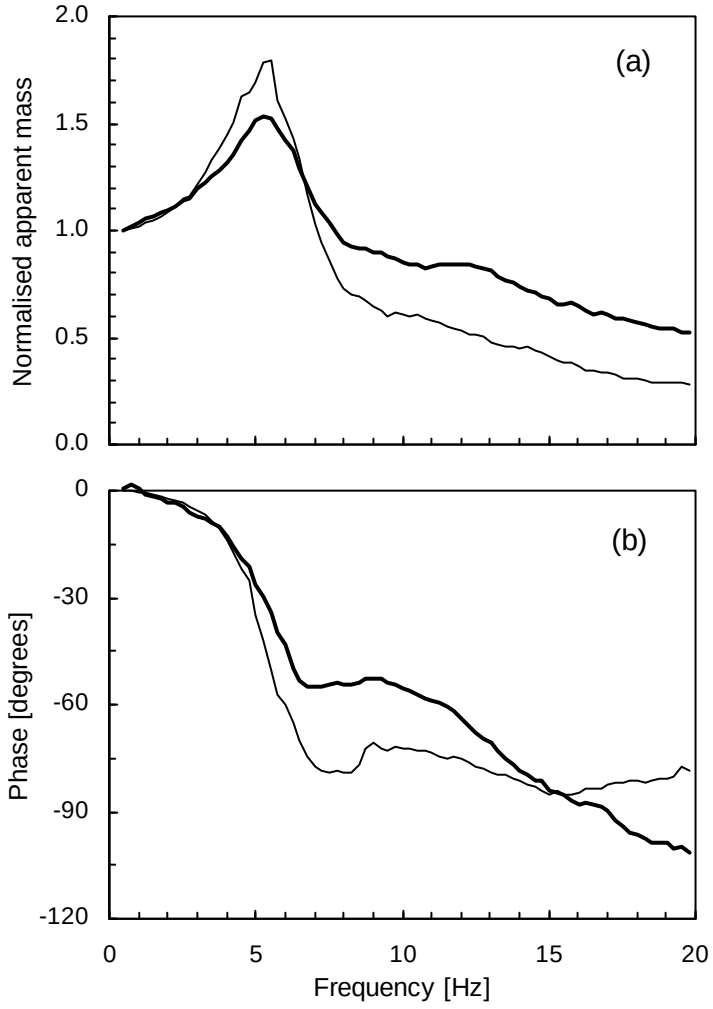

Figure 6.7 Median normalised apparent masses in the standing and sitting postures measured at 1.0 ms^{-2} r.m.s.: standing posture ━━━ ; sitting posture ——— .

The median transmissibilities of vertical (either floor or seat) vibration to each measurement location in the upper-body in the vertical, fore-and-aft and pitch directions measured with the subjects when standing and sitting at 1.0 ms^{-2} r.m.s. are shown in Figures 6.8, 6.9, and 6.10, respectively.

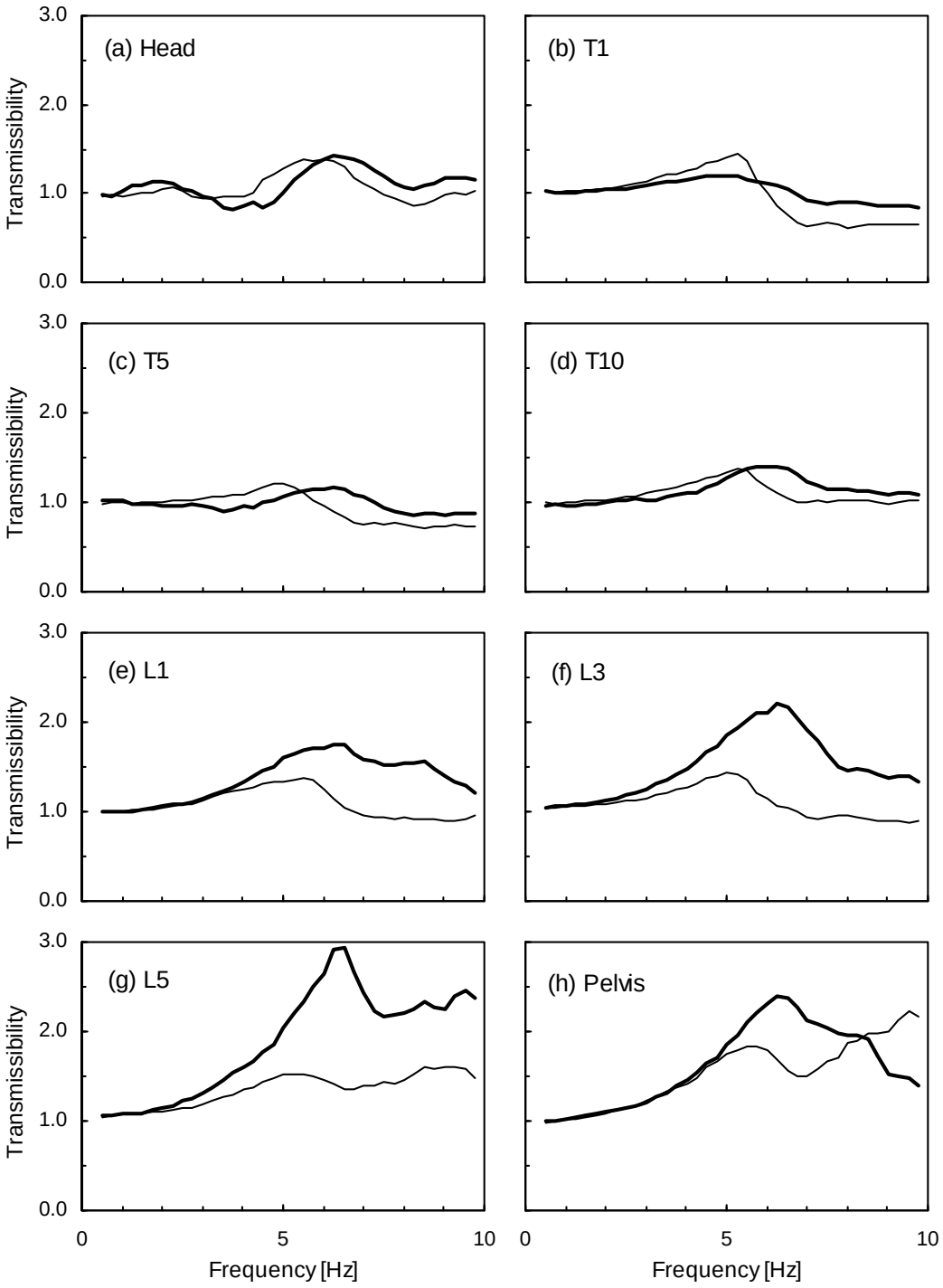

Figure 6.8 Median transmissibilities to vertical vibration at each measurement location measured with the subjects in the standing and sitting postures at 1.0 ms^{-2} r.m.s.: standing posture ━━━ ; sitting posture ——— .

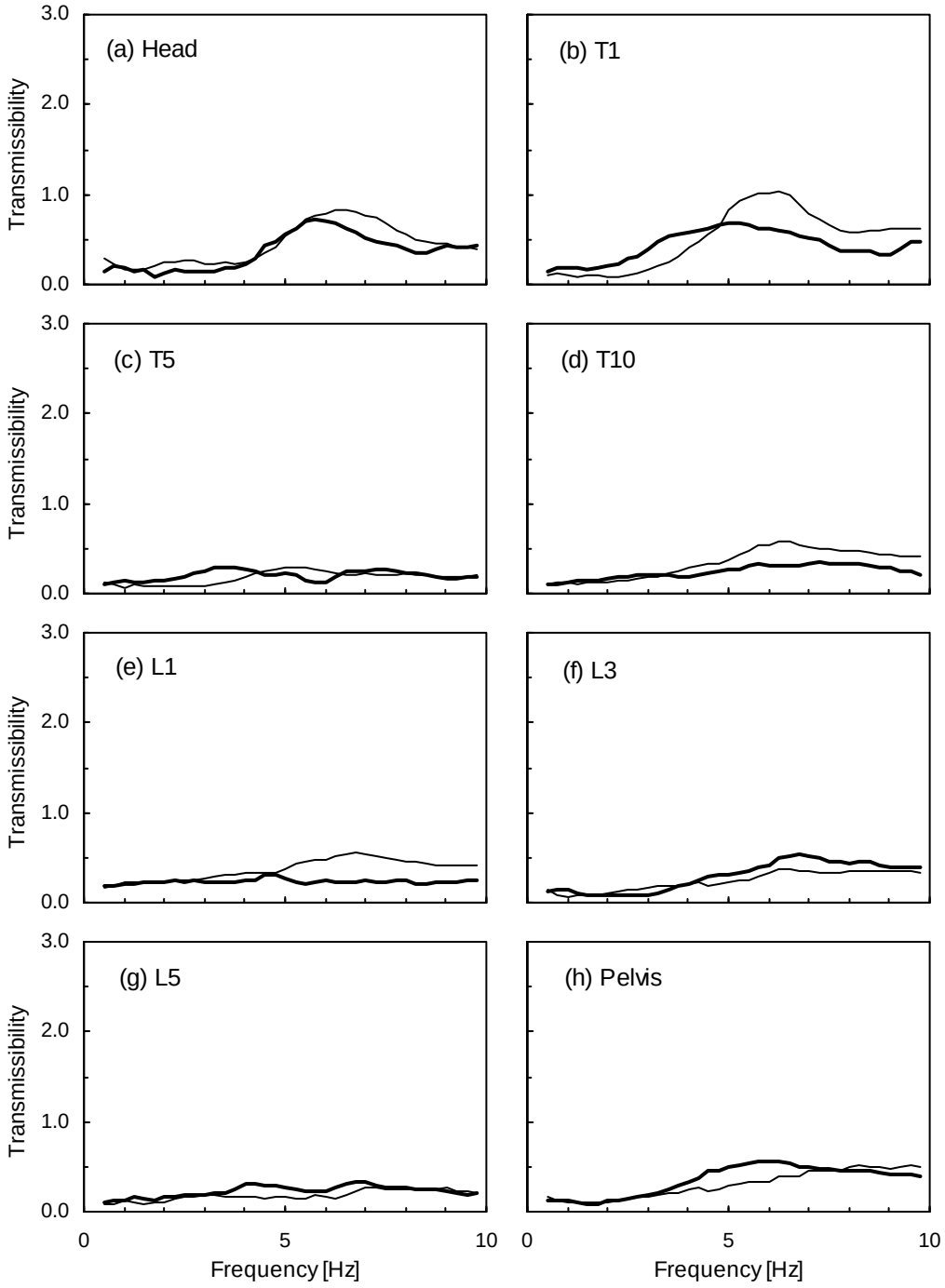

Figure 6.9 Median transmissibilities to fore-and-aft vibration at each measurement location measured with the subjects in the standing and sitting postures at 1.0 ms^{-2} r.m.s.: standing posture ━━━ ; sitting posture ——— .

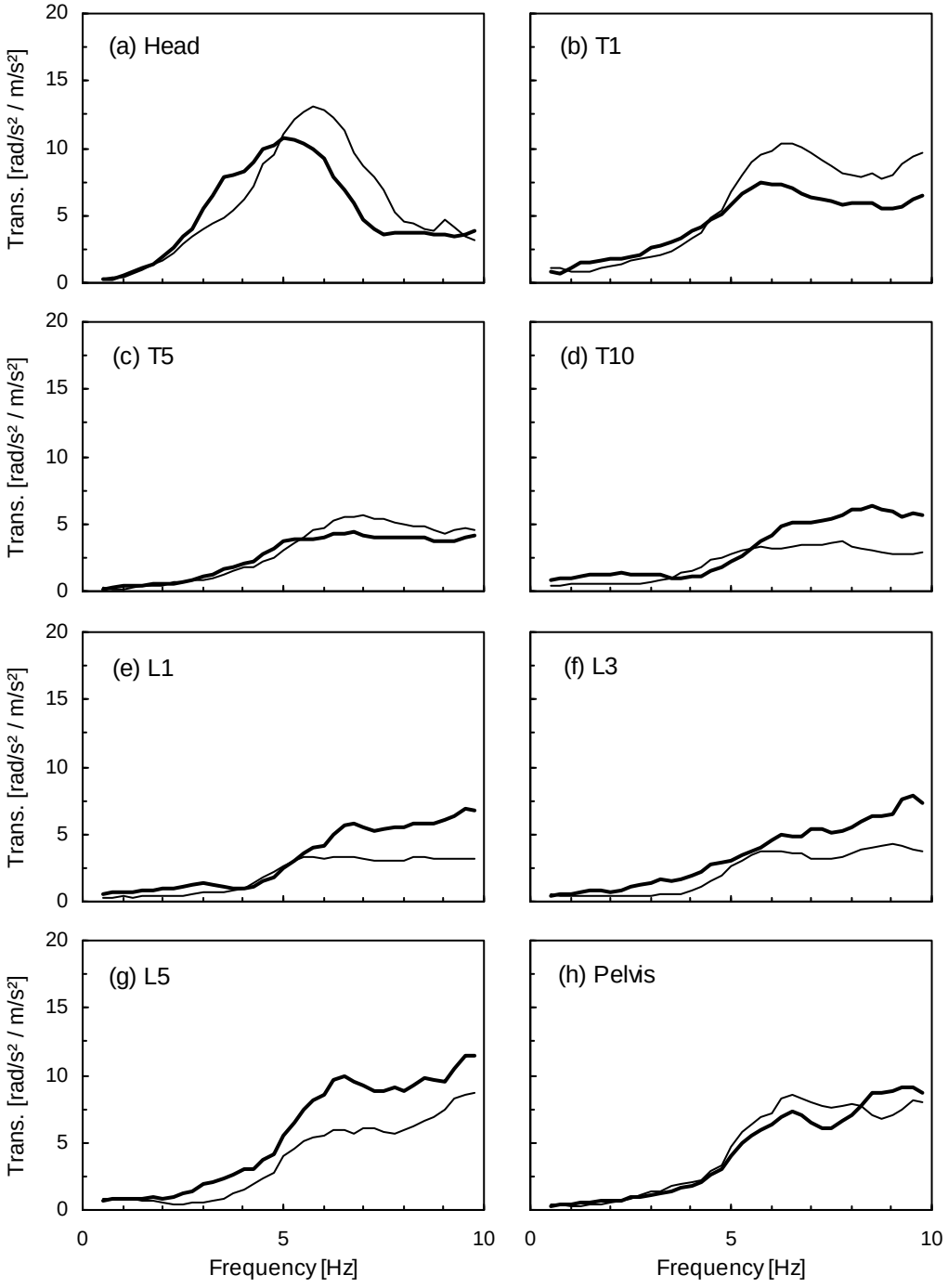

Figure 6.10 Median transmissibilities to pitch vibration at each measurement location measured with the subjects in the standing and sitting postures at 1.0 ms^{-2} r.m.s.: standing posture ━━━ ; sitting posture ——— .

Differences in the transmissibilities to the vertical motions between the standing and sitting postures were more significant at the lower spine (Figure 6.8). The transmissibilities showed similar magnitudes for the standing and sitting postures at the head and in the thoracic region, while the transmissibilities to the vertical motions in the lumbar region and at the pelvis for the standing posture was greater than those for the sitting posture. The differences in the vertical transmissibilities between the standing posture and the sitting posture were statistically significant at frequencies above 6 Hz for L1, above 3 Hz for L3 and L5, and 6 to 7 Hz for the pelvis ($p < 0.05$). A peak was observed in most vertical transmissibilities in the frequency range around 5 to 6 Hz for the standing and sitting postures. The frequency of the peak tended to be higher in the vertical transmissibilities in the standing posture than those in the sitting posture, irrespective of the measurement location. For example, the peak frequency of the vertical transmissibility to L3 in the standing posture was significantly higher than that in the sitting posture at all five vibration magnitudes ($p < 0.05$).

The transmissibilities to the fore-and-aft motions at all measurement locations were similar in the standing and sitting postures, although some differences can be observed in Figure 6.9, for example in the measurement at T1. The transmissibilities to the pitch motions also showed some differences between the standing posture and the sitting posture (Figure 6.10). In the lower spine region, the pitch transmissibilities tended to be greater for the standing posture than for the sitting posture, particularly at frequencies above 6 Hz (Figures 6.10(d), (e), (f), (g)). This trend was also observed in the vertical transmissibilities, as mentioned above. However, at the head and at T1, the pitch transmissibilities in the standing posture tended to be smaller than those in the sitting posture at higher frequencies. In this region, the peak frequency was higher in the sitting posture than in the standing posture ($p < 0.05$ for the head), which was inconsistent with those observed in the apparent mass and vertical transmissibilities.

6.4.3 Nonlinearity in dynamic responses

6.4.3.1 Nonlinearity in apparent mass

The apparent masses measured at five different vibration magnitudes, 0.125, 0.25, 0.5, 1.0 and 2.0 ms^{-2} r.m.s., are shown for each subject in the standing posture in Figure 6.11. Those for the sitting posture are shown in Figure 6.12.

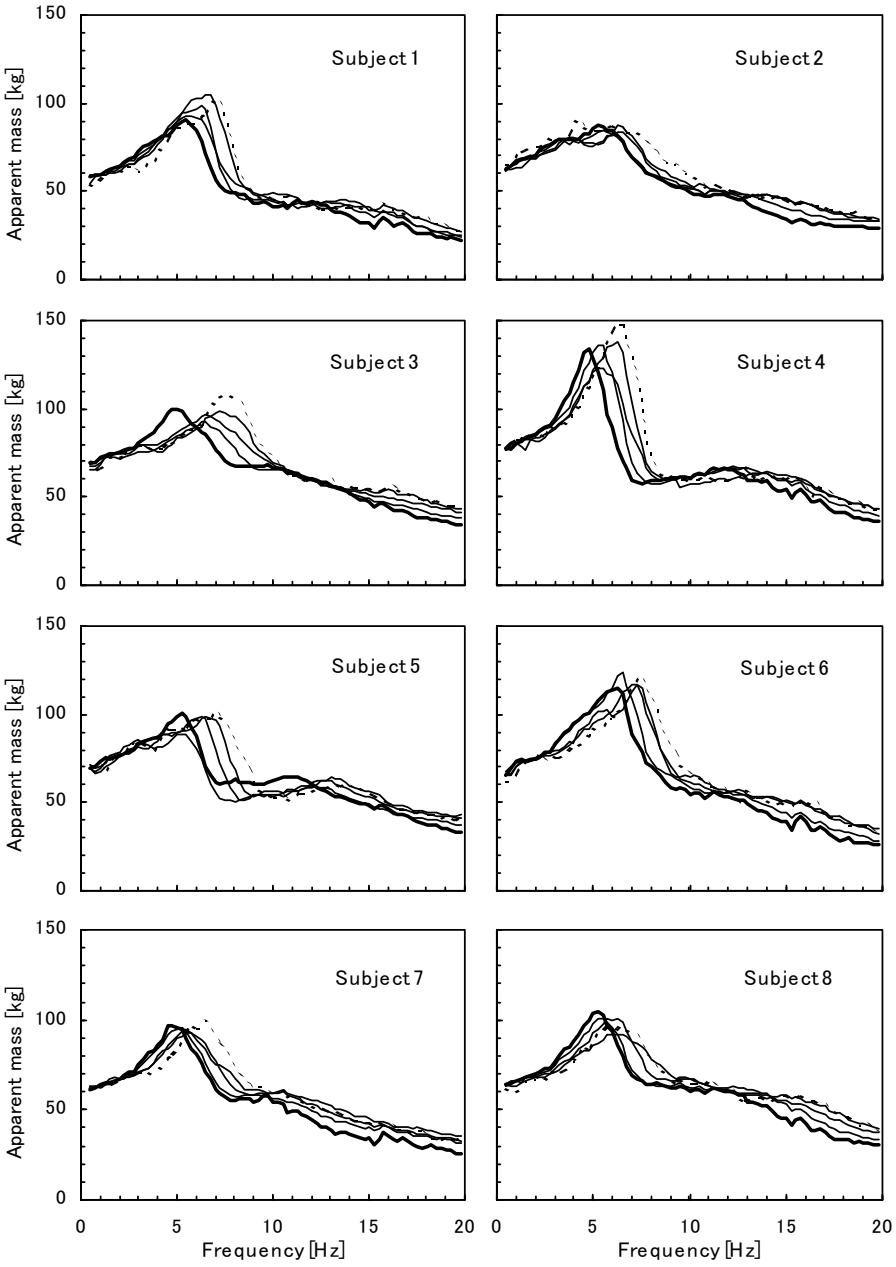

Figure 6.11 Apparent masses measured at five vibration magnitudes for each subject in the standing posture: the lowest magnitude, 0.125 ms^{-2} r.m.s. - - - - - ; the greatest magnitude, 2.0 ms^{-2} r.m.s. ——— .

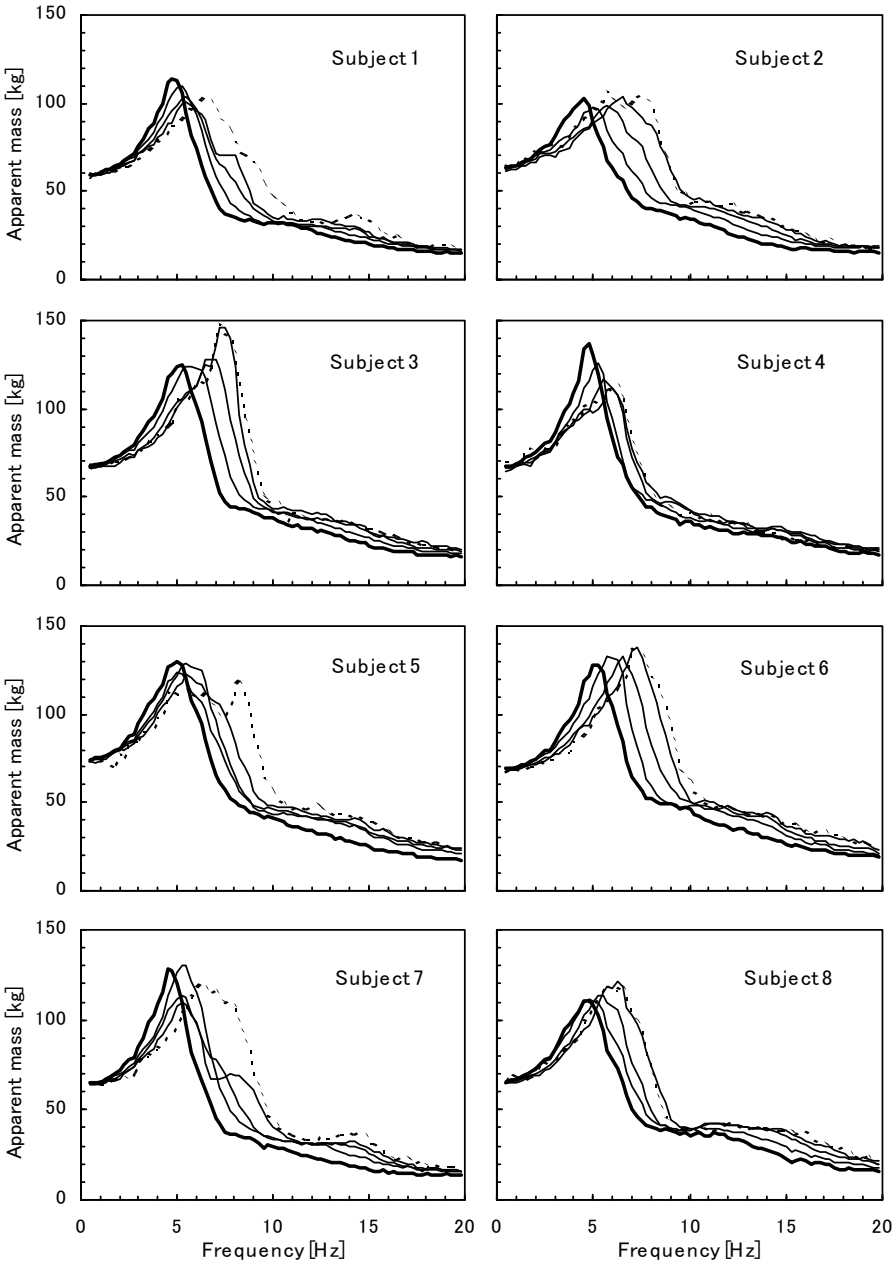

Figure 6.12 Apparent masses measured at five vibration magnitudes for each subject in the sitting posture: the lowest magnitude, 0.125 ms^{-2} r.m.s. - - - - ; the greatest magnitude, 2.0 ms^{-2} r.m.s. ——— .

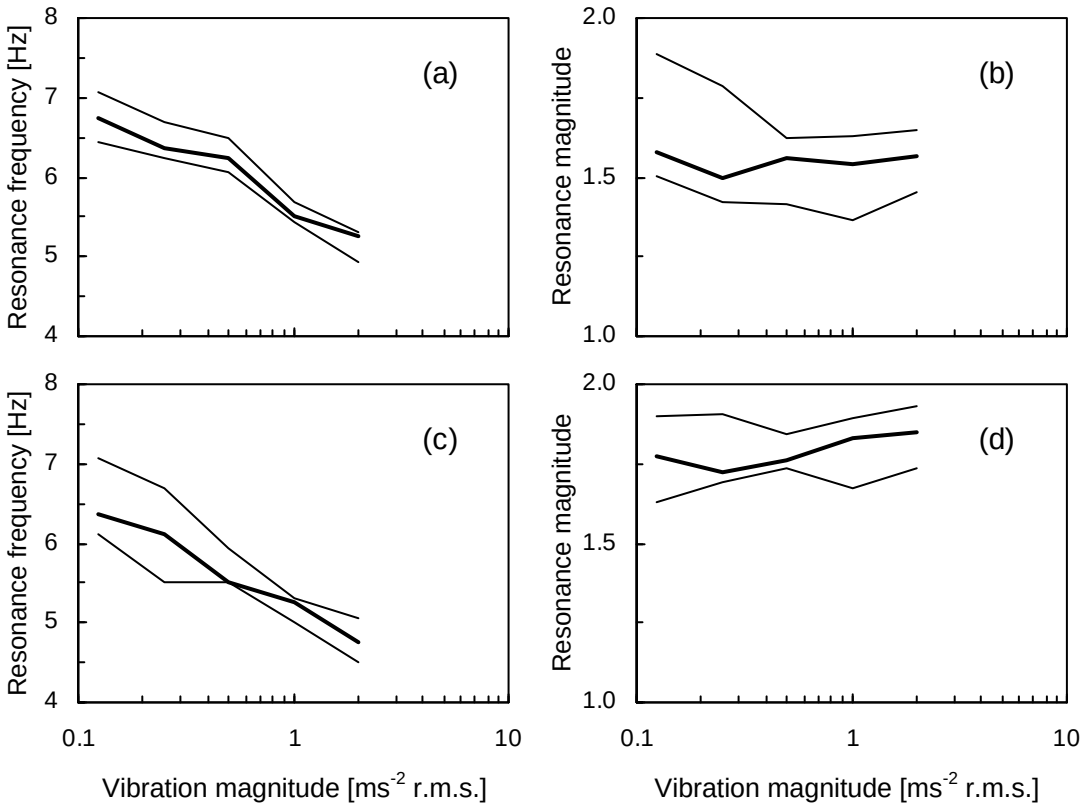

Figure 6.13 Medians and inter-quartile ranges of the principal resonance frequency and the normalised apparent mass at the resonance measured at five vibration magnitudes: (a) and (b), standing posture; (c) and (d), sitting posture.

Decreases in the principal resonance frequency in the apparent mass with increasing the vibration magnitude were observed for both the standing and sitting postures in Figures 6.11 and 6.12, as found in Experiment 2 for standing subjects (see Chapter 5) and in the previous studies for seated subjects (e.g. Mansfield, 1998). Medians and inter-quartile ranges of the principal resonance frequency and the normalised apparent mass at the resonance of the eight subjects in the standing and sitting postures are shown for five input vibration magnitudes in Figure 6.13. It is clearly seen that the principal resonance frequency decreased as the vibration magnitude increased: 6.75 to 5.25 Hz for the standing posture and 6.4 to 4.75 Hz for the sitting posture, when increasing the vibration magnitude from 0.125 to 2.0 ms^{-2} r.m.s. Decreases in the resonance frequency were statistically significant with increases in the vibration magnitude from 0.25 to 0.5 ms^{-2} r.m.s. for the sitting posture and from 0.5 to 1.0 ms^{-2} r.m.s. and from 1.0 to 2.0 ms^{-2} r.m.s. for both postures ($p < 0.05$). The change in the apparent mass at the resonance due to different vibration magnitude was not found to be statistically significant. Figure 6.14

shows the median normalised apparent masses, phases and coherences of the eight subjects in the standing and sitting postures measured at five vibration magnitudes.

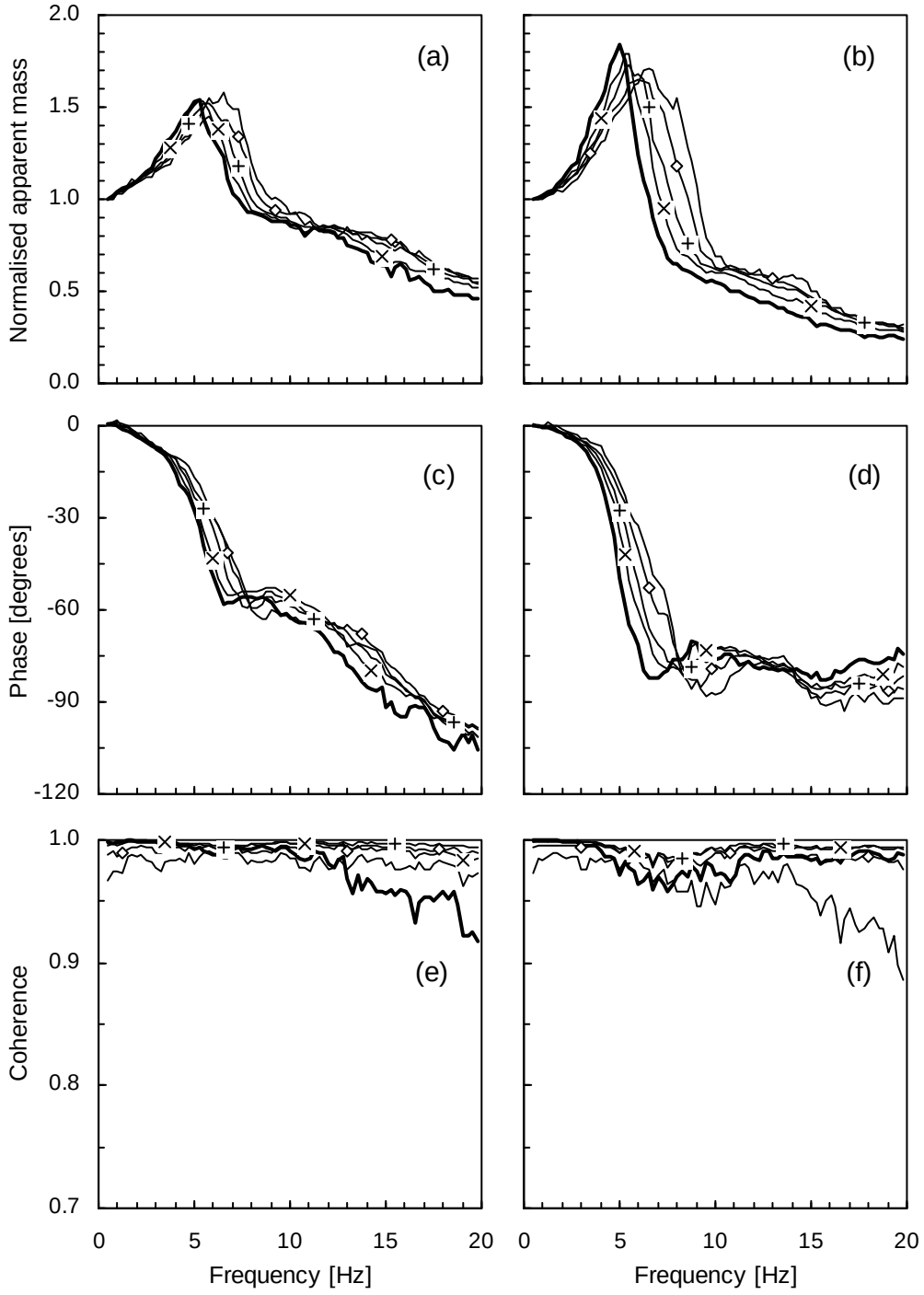

Figure 6.14 Medians for normalised apparent masses, phases, and coherences of the eight subjects in the standing and sitting postures measured at five vibration magnitudes: (a), (c), (e), standing posture; (b), (d), (f), sitting posture. 0.125 ——; 0.25 —◇—; 0.5 —+—; 1.0 —×—; 2.0 ms^{-2} r.m.s. ▬.

6.4.3.2 Nonlinearity in transmissibility

The median transmissibilities to motions at each measurement location in the upper-body in the standing posture obtained at five vibration magnitudes are compared for the vertical, fore-and-aft, and pitch axes in Figures 6.15, 6.16 and 6.17, respectively. The median transmissibilities in the sitting posture measured at five magnitudes are also shown for three axes in Figures 6.18 to 6.20.

Nonlinear characteristics were observed in the transmissibilities of standing and seated bodies due to changes in the vibration magnitude. The effect of vibration magnitude was particularly clear in the transmissibilities which showed a peak in the frequency range below 10 Hz, as shown in Figures 6.15 to 6.20. The peak frequency in the transmissibilities in both standing and sitting postures tended to decrease as the vibration magnitude increased. This trend was also found in the transmissibilities for standing subjects measured at some locations in Experiment 2, as presented in Section 5.4.4.3, and in the apparent masses described in the preceding section.

The transmissibilities to the vertical motion measured at L3 had a clear peak in the frequency range presented for both standing and sitting postures. The peak frequency in the vertical transmissibilities to L3 showed decreases with increasing vibration magnitude, as seen in the median data shown in Figures 6.15(f) and 6.18(f). Figures 6.21(a) and (b) show the medians and inter-quartile ranges of the peak frequency and magnitude of the transmissibilities to the vertical vibrations at L3 of the eight subjects in the standing and sitting postures at five vibration magnitudes. The peak frequency decreased from 7.5 to 5.6 Hz for the standing posture and 6.25 to 4.75 Hz for the sitting posture when increasing vibration magnitude from 0.125 and 2.0 ms^{-2} r.m.s. Statistically significant differences in the peak frequency were found between vibration magnitudes of 0.25 and 0.5 ms^{-2} r.m.s. for the sitting posture and between 0.5 and 1.0 ms^{-2} r.m.s. and 1.0 and 2.0 ms^{-2} r.m.s. for both standing and sitting postures ($p < 0.05$). Similar findings were drawn from the transmissibilities to the vertical motions at locations over the spine, as seen in Figures 6.15 and 6.18.

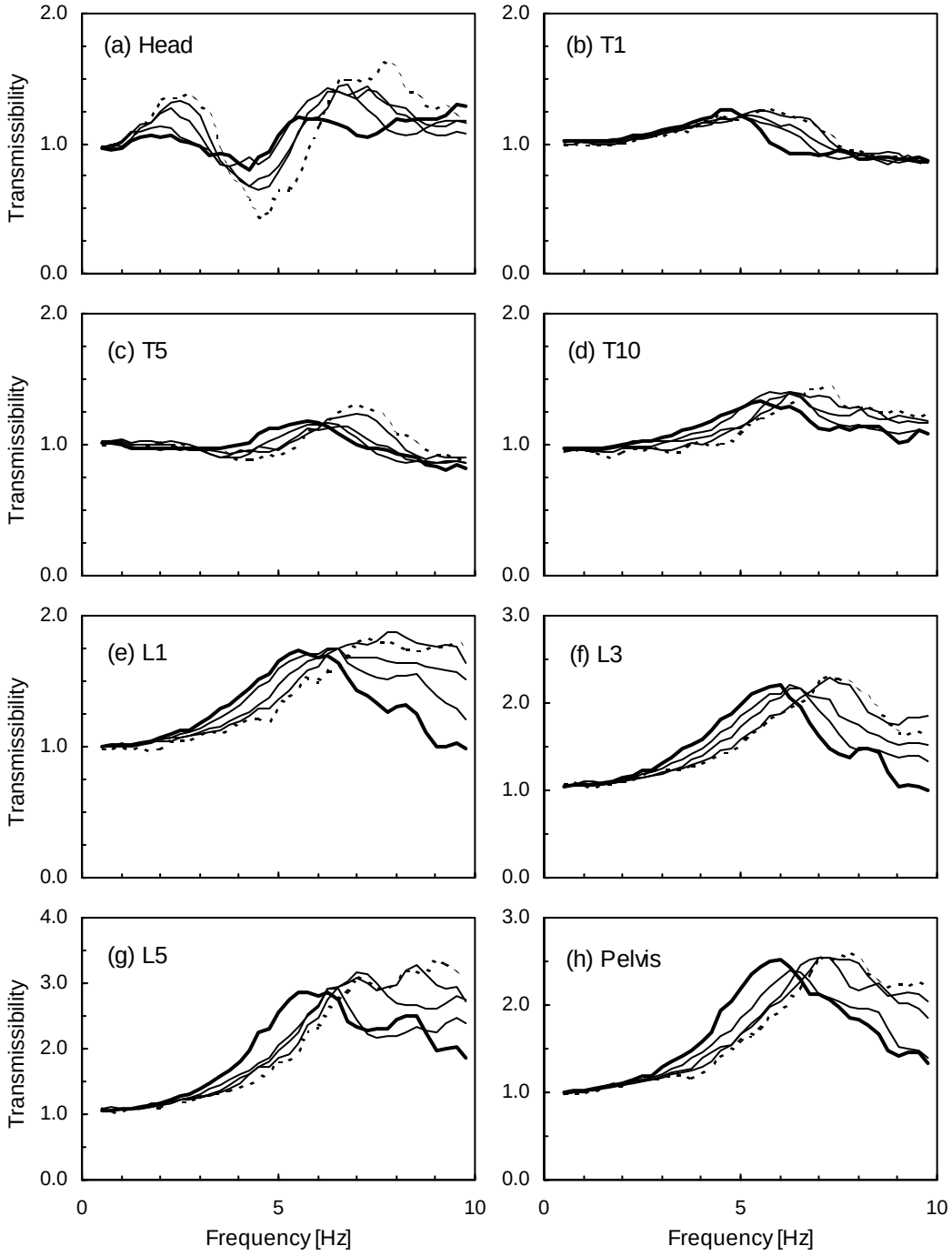

Figure 6.15 Median transmissibilities to vertical motions at each measurement location in the upper-body in the standing posture at five vibration magnitudes: the lowest magnitude, 0.125 ms^{-2} r.m.s. - - - - ; the greatest magnitude, 2.0 ms^{-2} r.m.s. ——— .

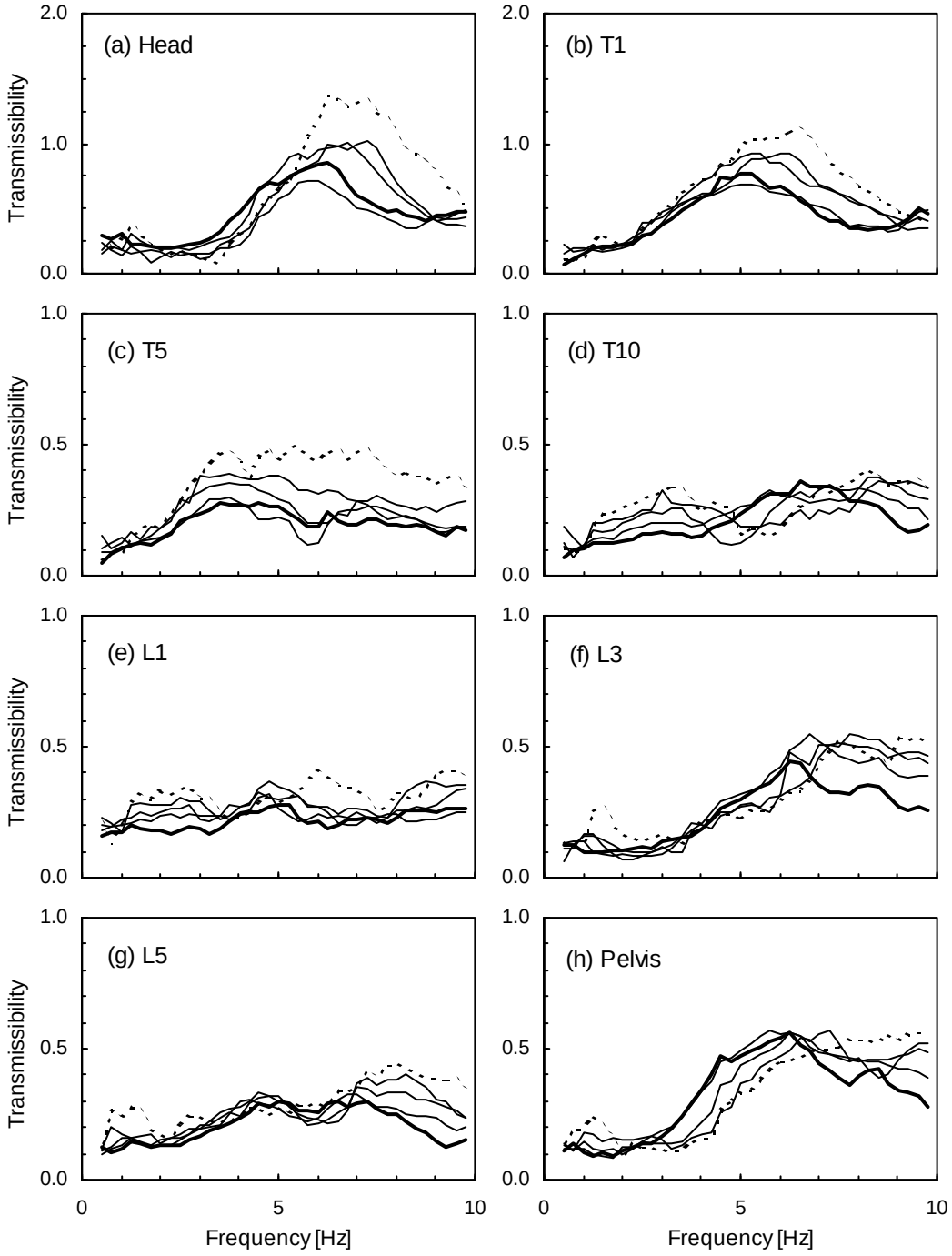

Figure 6.16 Median transmissibilities to fore-and-aft motions at each measurement location in the upper-body in the standing posture at five vibration magnitudes: the lowest magnitude, 0.125 ms^{-2} r.m.s. - - - - ; the greatest magnitude, 2.0 ms^{-2} r.m.s. ——— .

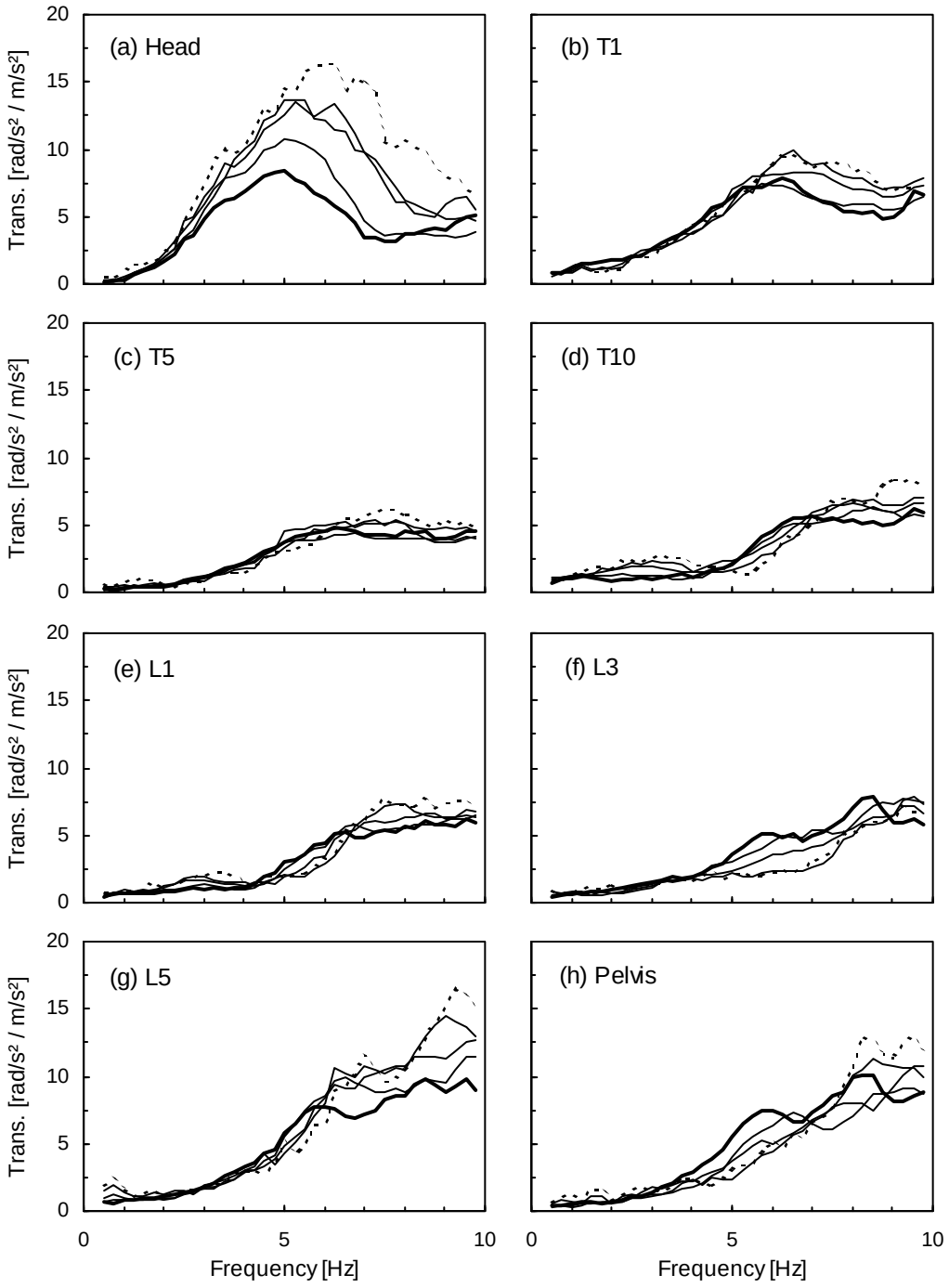

Figure 6.17 Median transmissibilities to pitch motions at each measurement location in the upper-body in the standing posture at five vibration magnitudes: the lowest magnitude, 0.125 ms^{-2} r.m.s. - - - - ; the greatest magnitude, 2.0 ms^{-2} r.m.s. ——— .

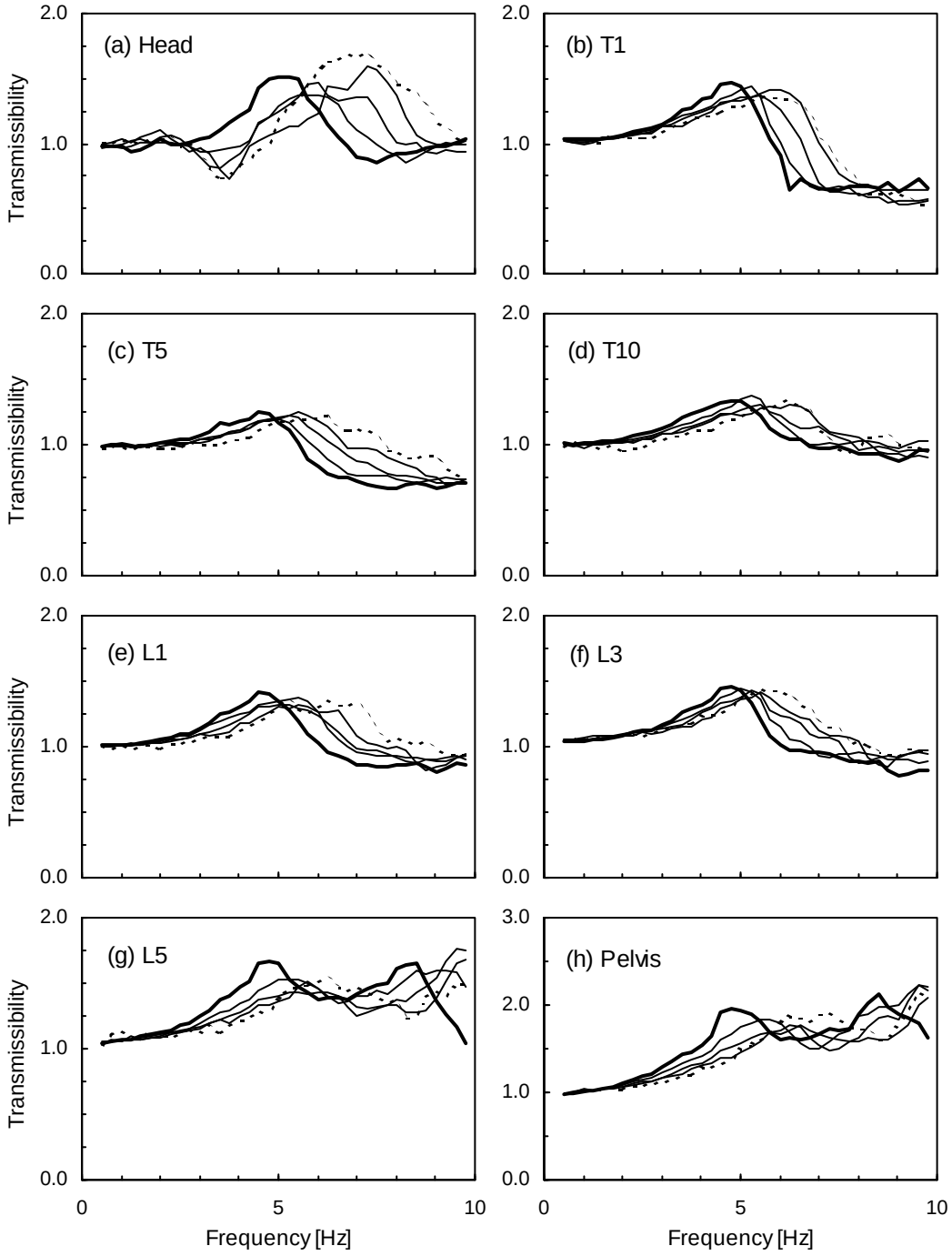

Figure 6.18 Median transmissibilities to vertical motions at each measurement location in the upper-body in the sitting posture at five vibration magnitudes: the lowest magnitude, 0.125 ms^{-2} r.m.s. - - - - - ; the greatest magnitude, 2.0 ms^{-2} r.m.s. ——— .

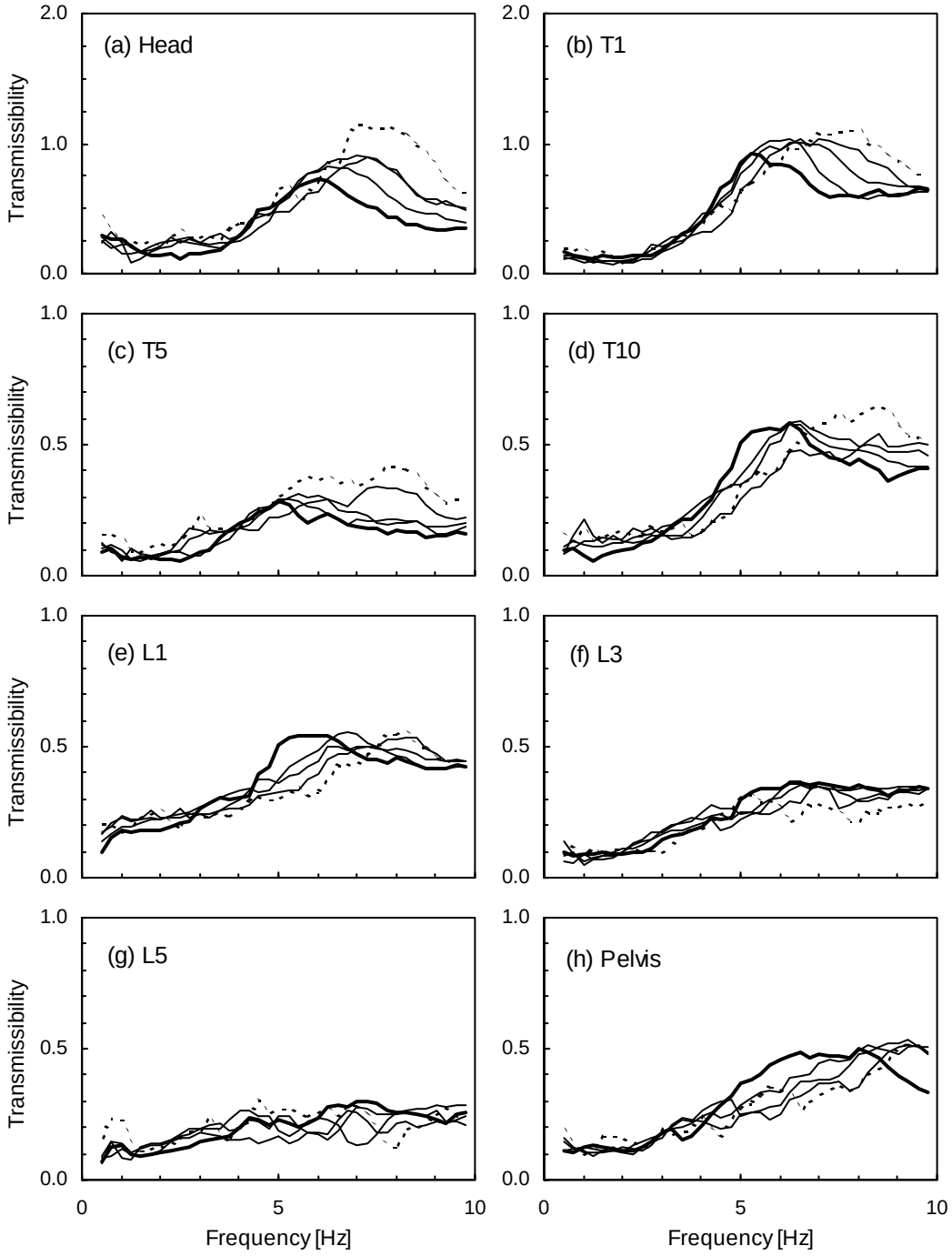

Figure 6.19 Median transmissibilities to fore-and-aft motions at each measurement location in the upper-body in the sitting posture at five vibration magnitudes: the lowest magnitude, 0.125 ms^{-2} r.m.s. - - - - - ; the greatest magnitude, 2.0 ms^{-2} r.m.s. ——— .

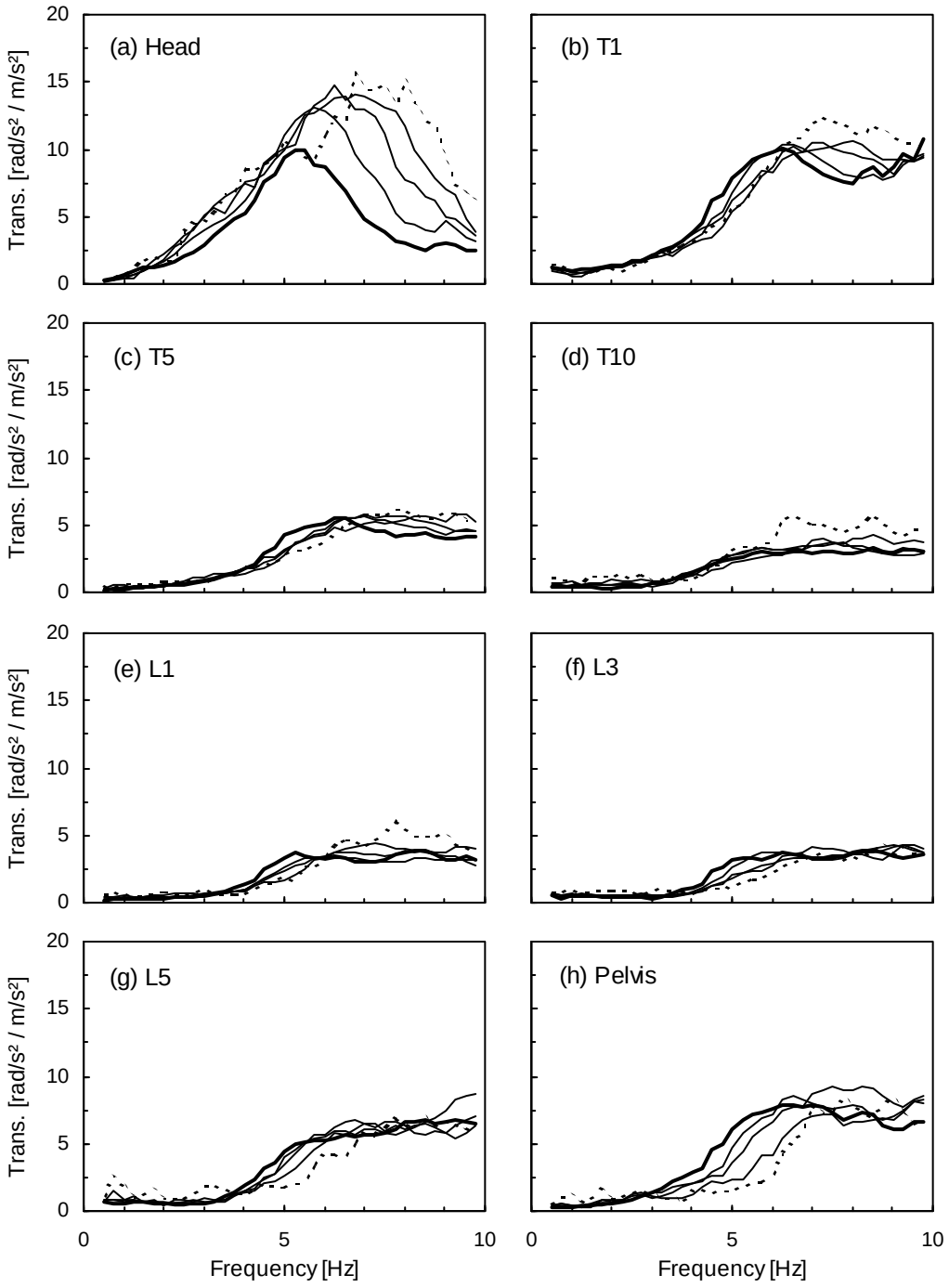

Figure 6.20 Median transmissibilities to pitch motions at each measurement location in the upper-body in the sitting posture at five vibration magnitudes: the lowest magnitude, 0.125 ms^{-2} r.m.s. - - - - ; the greatest magnitude, 2.0 ms^{-2} r.m.s. ——— .

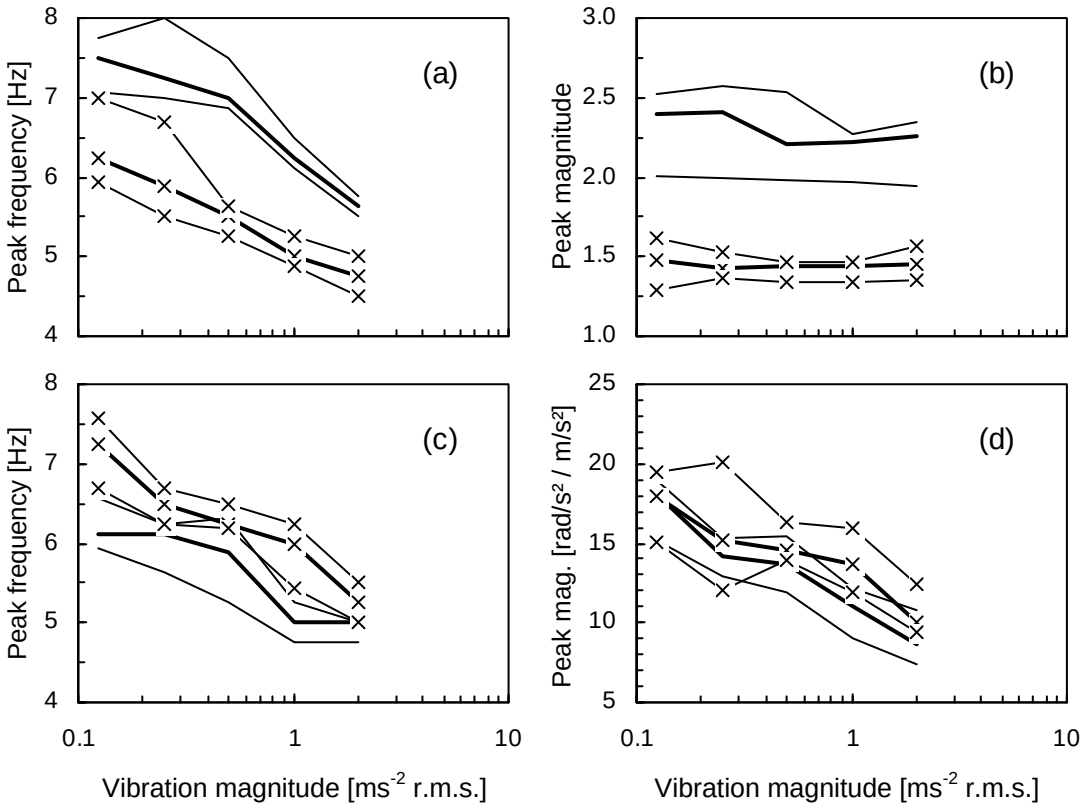

Figure 6.21 Medians and inter-quartile ranges of the peak frequency of the transmissibilities in the standing and sitting postures measured at five vibration magnitude: (a) and (b), the transmissibility to the vertical vibration at L3; (c) and (d), the transmissibility to the pitch vibration at the head. ——— : standing posture; —x— : sitting posture.

The effect of vibration magnitude on the moduli of transmissibilities can be observed in those to the pitch motion at the head for both standing and sitting postures, together with an effect on the peak frequency (Figures 6.17(a) and 6.20(a)). The peak magnitude and frequency of the transmissibilities tended to decrease with increases in the vibration magnitude. The medians and inter-quartile ranges of the peak frequency and magnitude of the transmissibilities to the pitch vibrations at the head for the standing and sitting postures at five vibration magnitudes are shown in Figures 6.21(c) and (d). The differences in the peak magnitude were statistically significant between 0.125 and 0.25 ms^{-2} r.m.s. and between 0.5 and 1.0 ms^{-2} r.m.s. for the standing posture and between 1.0 and 2.0 ms^{-2} r.m.s. for the sitting posture. The differences in the peak frequency were statistically significant between 0.5 and 1.0 ms^{-2} r.m.s. for the standing posture and between 0.5 and 1.0 ms^{-2} r.m.s. and between 1.0 and 2.0 ms^{-2} r.m.s. for the sitting posture ($p < 0.05$). By comparing the pitch transmissibilities to the head with the vertical transmissibilities to the head, it seems that the pitch motion of the head at about 5 Hz

decreases the vertical motion measured at the mouth, particularly for the standing posture (Figures 6.15(a) and 6.17(a) for the standing posture, and Figures 6.18(a) and 6.20(a) for the sitting posture).

6.5 DISCUSSION

The principal resonance of the apparent mass was found at a frequency around 5 Hz for both the standing and sitting postures, as observed in Chapter 4. It was found in this experiment that the principal resonance frequency of the apparent mass in the standing posture was slightly higher than that in the sitting posture. This difference was statistically significant with the three greatest vibration magnitudes but not significant with the two lowest magnitudes. The differences in the resonance frequency between the standing and sitting postures were mostly within 1 Hz for each subject. There might be a slight shift of the principal resonance frequency in the apparent mass between standing and sitting positions, generally less than 1 Hz, although this difference was not found in Experiment 1 presented in Chapter 4. The apparent mass at the principal resonance frequency was found to be significantly greater for the sitting posture than for the standing posture. It can be hypothesised that, for both standing and sitting bodies, common dynamic mechanisms in the upper-body contribute to the principal resonance of the apparent mass, although a slight change was observed in the resonance frequency between the standing and sitting postures.

The median transmissibilities to vertical and fore-and-aft motions measured at all locations in the spine are compared with the transmissibilities to the spine reported in previous studies in Figures 6.22 to 6.24: the vertical transmissibilities in the standing posture in Figure 6.22, the vertical transmissibilities in the sitting posture in Figure 6.23, and the fore-and-aft transmissibilities in the sitting posture in Figure 6.24. The transmissibilities to fore-and-aft motions of the spines of standing subjects were not available in the literature.

For the standing body, the median transmissibility to the vertical vibration at L1 showed similar magnitudes of transmissibility to those reported in Hagena *et al*. (1985) and Pope *et al*. (1989), while the median vertical transmissibilities to L3 and L5 are greater than the previous results at frequencies between 5 and 7 Hz for L3 and above 5 Hz for L5 (Figure 6.22(a)). In the lumbar region, inter-subject variability in the vertical transmissibility was relatively large in the experimental data obtained. The data from the two previous studies were obtained with one subject and were within the variability between the eight subjects

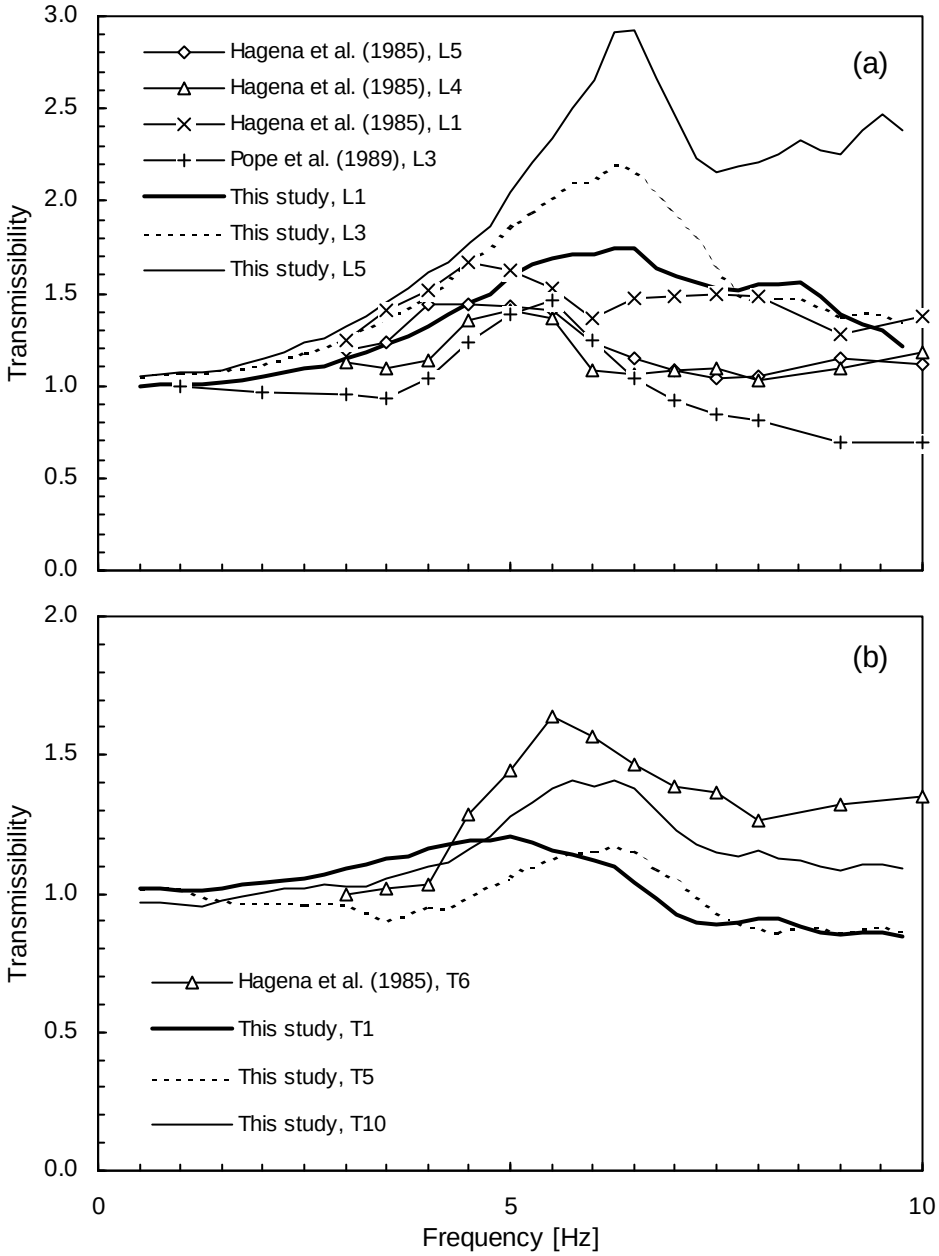

Figure 6.22 Median vertical transmissibilities to the spine in the standing posture measured in Experiment 3 and the vertical transmissibilities to the spine of standing subjects in the previous studies: (a) to the lumbar vertebrae; (b) to the thoracic vertebrae. (See Section 2.4.1.3 for details of the previous studies.)

in this study for L1 and L3. For the thoracic region, only a set of data for one location from one subject was available, therefore, it was difficult to conclude anything from the comparison. However, the median vertical transmissibilities to thoracic spine obtained in this study showed a similar trend to the vertical transmissibility to T6 reported in Hagena *et al*. (1985), as seen in Figure 6.22(b).

For the seated body, the median transmissibilities to vertical motions measured at the

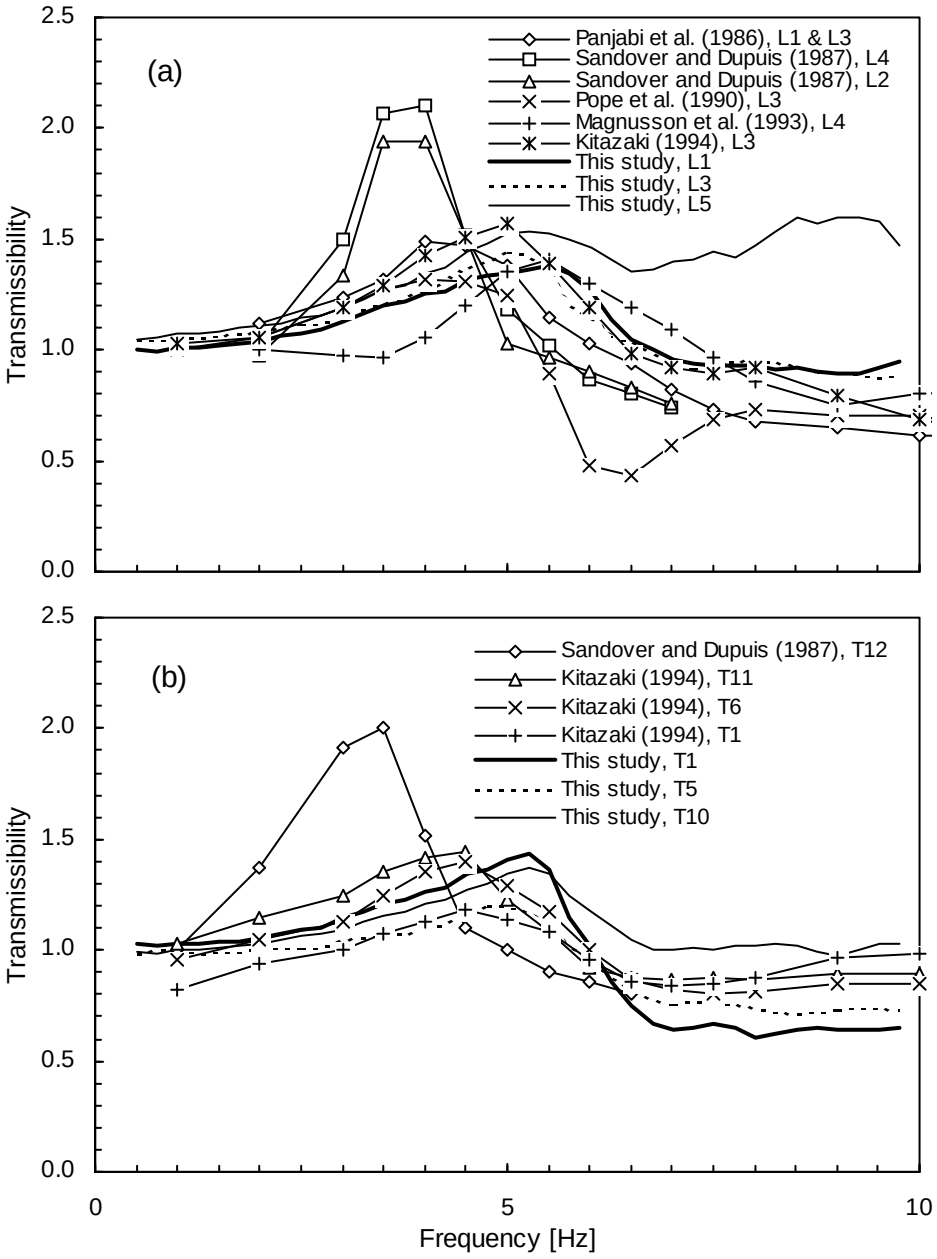

Figure 6.23 Median vertical transmissibilities to the spine in the sitting posture measured in Experiment 3 and the vertical transmissibilities to the spine of seated subjects in the previous studies: (a) to the lumbar vertebrae; (b) to the thoracic vertebrae. (See Section 2.4.1.4 for details of the previous studies.)

locations along the spine in this study, apart from that to L5, showed good agreements with the previous experimental data (Figure 6.23). The median vertical transmissibility to L5 had a second peak at the 8 to 10 Hz frequency region. There have been no data on the transmissibility to L5 in the previous studies. The second peak was not seen in the data for L4 obtained by Magnusson *et al*. (1993, Figure 6.23(a)) but was seen in the data for S2 obtained by Kitazaki (1994, Figure 2.20(a)).

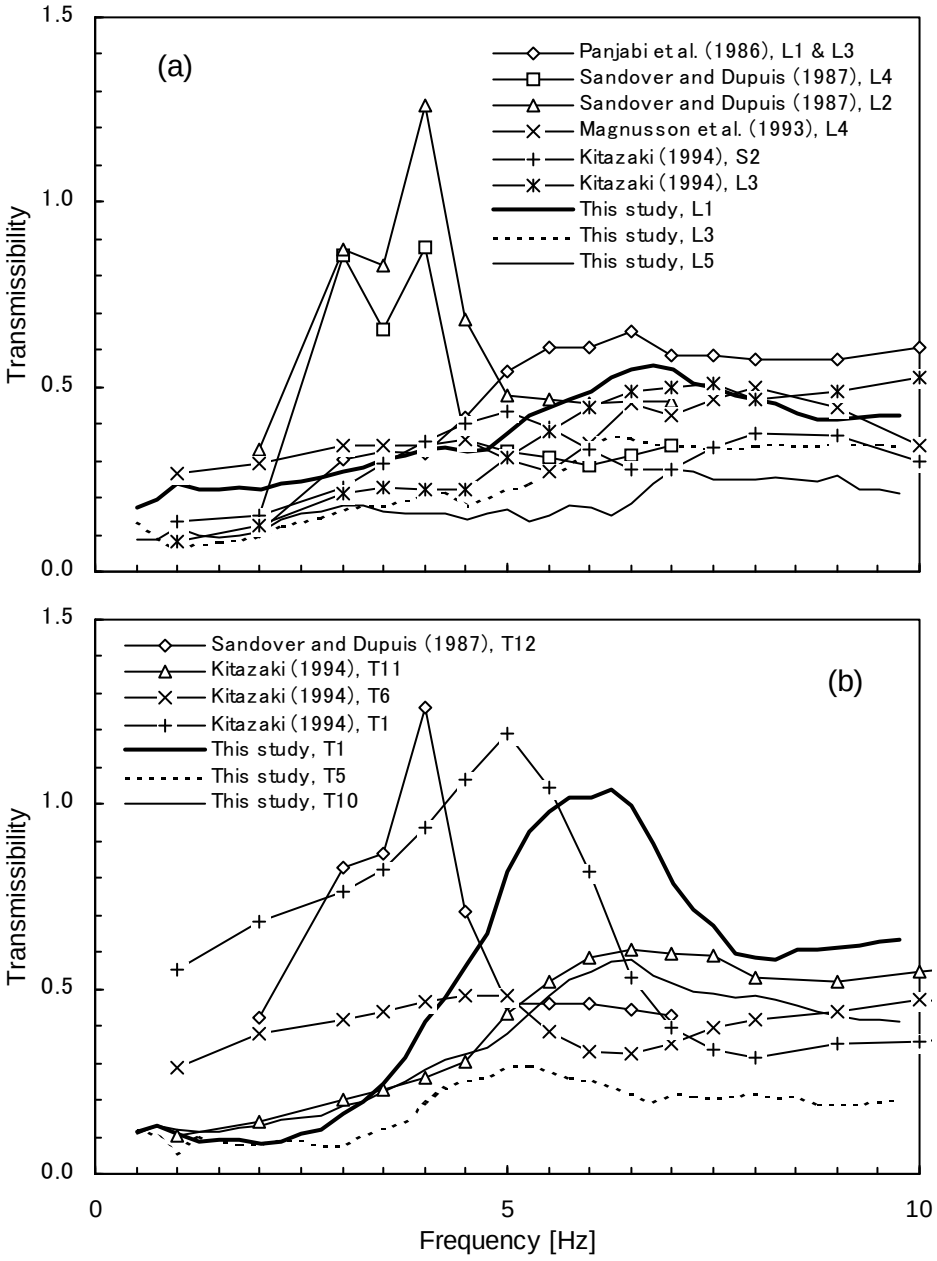

Figure 6.24 Median fore-and-aft transmissibilities to the spine in the sitting posture measured in Experiment 3 and the fore-and-aft transmissibilities to the spine of seated subjects in the previous studies: (a) to the lumbar vertebrae; (b) to the thoracic vertebrae. (See Section 2.4.1.4 for details of the previous studies.)

The median fore-and-aft transmissibilities to the spine obtained in this study were generally similar to those shown in the previous studies (Figure 6.24). Differences in the transmissibilities to the upper thoracic spine between this study and Kitazaki (1994) seen in Figure 6.24 were attributed to the data correction for the inclination of the body surface described in Equations (6.5) and (6.6). The fore-and-aft transmissibilities before the correction were similar to those in Kitazaki (1994), as seen in Figure 6.4.

As seen in Figures 6.23 and 6.24, good agreements were found between the transmissibilities for the seated body obtained by the surface measurement method used in this study and those from the previous studies in which either the direct measurement method or surface measurement method was used (see Section 2.4.1.2). It can be, therefore, concluded that the surface measurement method with the data corrections described in Section 6.3 provide with reliable measurements of motions at locations along the spine.

The vertical transmissibilities for the standing body measured in this experiment showed consistency with those in Experiment 2 (see Figures 5.22 and 6.22). However, there were some differences between the vertical transmissibilities to the lumbar spines of standing subjects measured in this study and those in the previous studies, as seen in Figure 6.22(a). The transmissibility curves available in the previous studies were obtained from only two subjects with some direct measurement methods. It was difficult to compare the data in the present study with the previous studies using only two subjects in a reliable sense. However, it is reasonable to claim that the surface measurement method would work for the standing body as well as for the seated body. Therefore, the differences between the transmissibilities of standing subjects in this study and those in the previous study may not be caused by the difference in the measurement method. Possible reasons for the differences observed might be the variability between subjects, as mentioned above, the effect of the pitch motion of the vertebrae on the translational motions, and the effect of the inclination of the sensitive axis of the transducer to the vertical axis. An example of the effects of the inclination and the pitch motion can be seen in Figures 6.4 and 6.5 respectively.

The median transmissibilities to the vertical, fore-and-aft and pitch motions at the head are compared with the transmissibilities to the head measured in previous studies for standing and sitting subjects in Figures 6.25 and 6.26, respectively.

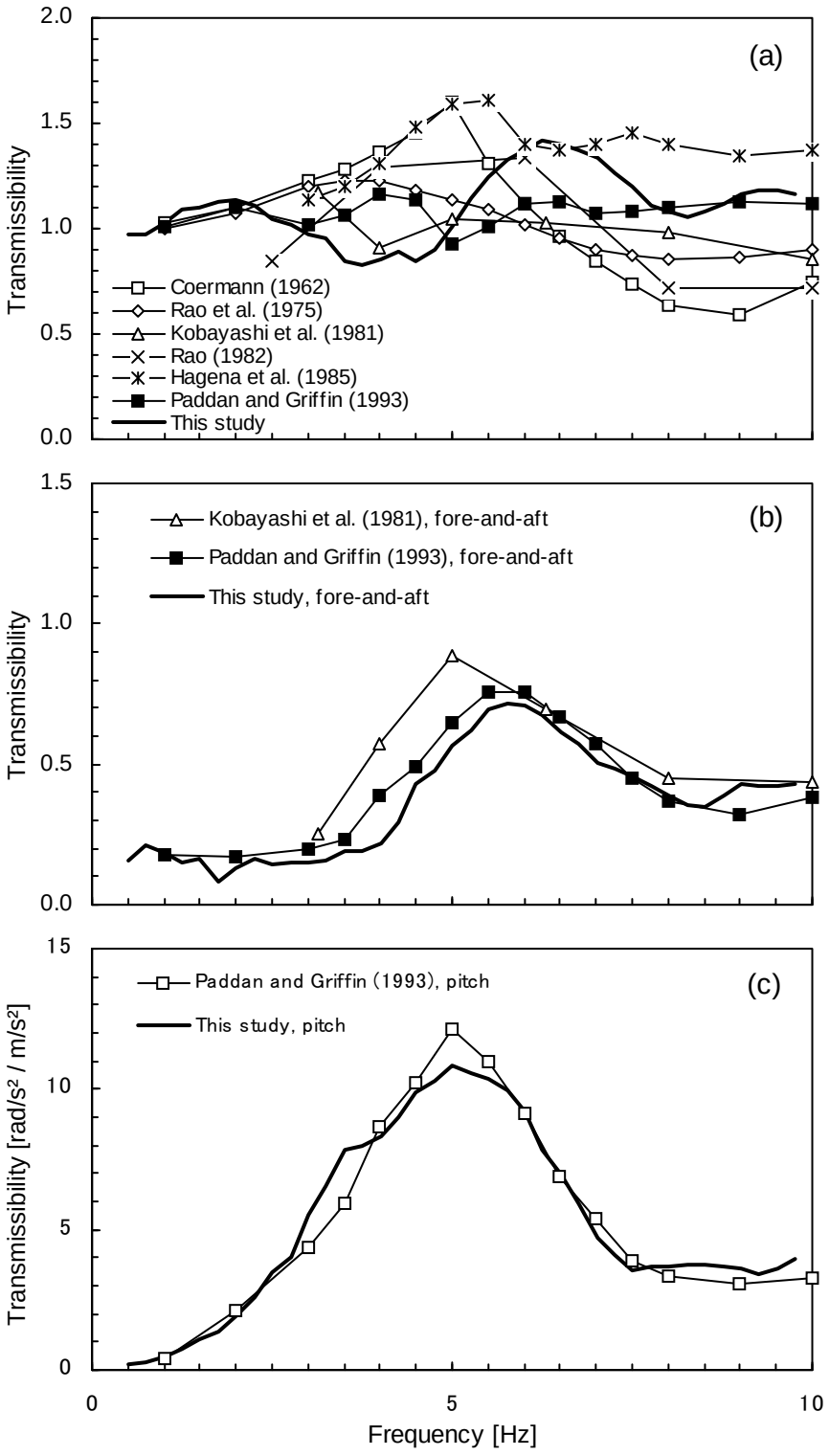

Figure 6.25 Median transmissibilities to the head in the standing posture measured in Experiment 3 and the transmissibilities to the head of standing subjects in the previous studies: (a) in the vertical axis; (b) in the fore-and-aft axis; (c) in the pitch axis. (See Section 2.4.2.2 for details of the previous studies.)

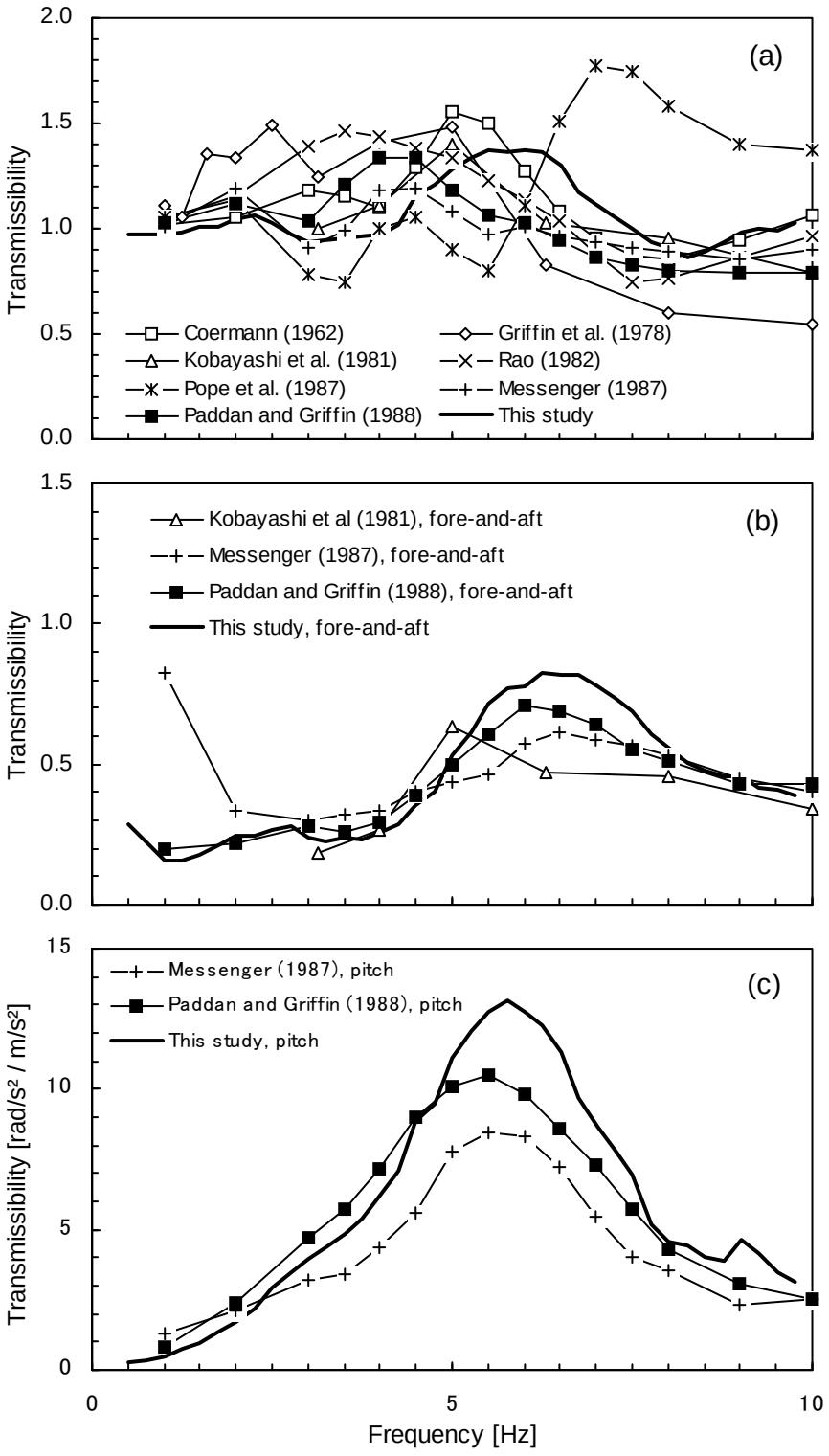

Figure 6.26 Median transmissibilities to the head in the sitting posture measured in Experiment 3 and the transmissibilities to the head of seated subjects in the previous studies: (a) in the vertical axis; (b) in the fore-and-aft axis; (c) in the pitch axis. (See Section 2.4.2.3 for details of the previous studies.)

It is seen in Figures 6.25 and 6.26 that the transmissibilities to the fore-and-aft and pitch motions at the head measured in this experiment show good agreements with those obtained in the previous studies. The median transmissibility to the vertical vibration at the head measured in this study was generally within the variability between the results from the previous studies.

With respect to the difference in the vibration transmissibility to various locations in the body between standing and sitting positions, the peak frequency observed in most transmissibilities at 5 to 7 Hz tended to be higher in the standing posture than in the sitting posture, as found in the apparent mass (Figures 6.7 to 6.10). The transmissibility to the lower part of the upper-body, for example L3, showed a more clear frequency shift between standing and sitting positions than that seen in the apparent mass: statistically significant differences between the standing and sitting postures were found at three vibration magnitudes for the apparent mass but at all five magnitudes for the vertical transmissibility to L3. It is likely that the natural frequency of some vibration mode in the lower trunk which makes major contributions to the resonance of the driving-point response slightly changes between the standing and sitting postures. This change between standing and sitting positions might be attributed to the differences in the posture (e.g., the pelvis angle, spinal curvature or muscle tension) or in the manner of vibration transmission to the upper-body.

According to Pheasant (1996), in an upright standing position, ‘the pelvis is more or less vertical and the first lumbar vertebra and sacrum make angle of about 30º above and below the horizontal plane respectively’ (Figure 6.27(a)). The lumbar spine is concave to the rear (i.e., in a lordosis). In a sitting posture, however, the rotation of the pelvis is opposed by tension in the hamstring muscles and the movement tends to be completed by a backward rotation of 30º or more (Figure 6.27(b)). This backward rotation is ‘compensated by an equivalent degree of flexion in the lumbar spine’ so that the lordosis of the lumbar region tends to be flattened out. In this posture, a relaxed sitting posture, the lumbar spine may ‘well be flexed close to the limit of its range of motion’ with relaxed muscles. ‘The weight of the trunk will be supported by tension in passive structures such as ligaments’. A muscular effort, which ‘probably comes from a muscle deep within the pelvis called iliopsoas’, is required to keep the pelvis vertical and regain the lordosis of the lumbar spine in an upright sitting posture. Back muscle activity may be also required ‘to support the weight of the trunk’. The sitting posture used in this study was thought to be closer to the relaxed posture than to the upright posture. It was reported that the pressure in the L3 intervertebral disc ‘in a person sitting upright’ was ‘40% in excess of

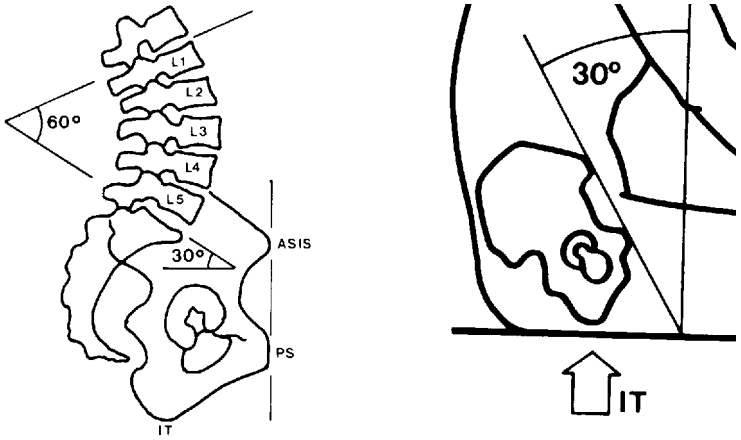

(a) (b)

Figure 6.27 Typical orientation of the pelvis and lumbar spine. (a) In the upright standing posture: the pelvis in the vertical position and the lordosis of the lumbar spine. (b) In the relaxed sitting posture: the pelvis with back rotation and the lumbar spine flexed (the spine is not seen in the figure). From Pheasant (1996).

the value obtained in upright standing', although this upright sitting posture was not necessarily the same as the one defined above (Nachemson and Morris, 1964; Nachemson, 1981). This increase in the lumbar intradiscal pressure due to postural change from the standing position to the sitting position might be caused by the increase in the muscle activity and less lordosis in the lumbar spine.

It could be expected that the lumbar spine is more compressed and less flexible in the sitting posture than in the standing posture due to both anterior and posterior trunk muscle activities and a less lordosis of the lumbar spine mentioned above. This might be one of the causes of the transmissibilities to the three locations in the lumbar spine in the sitting posture, particularly in the vertical and pitch axes, being less than those in the standing posture in this study (Figures 6.8 and 6.10). Less difference between the transmissibilities to the lumbar vertebrae in the sitting posture might also be caused by the lumbar spine being in a more compressed and less flexible state.

The difference in the geometry of the lumbar spine between the standing and sitting positions may make some contribution to the differences between the transmissibilities. The vertical load in the upper-body should mainly transmit through the spine. The vertical transmissibilities in the thoracic region were similar for both the standing and sitting postures, so that the vertical load acting on the lumbar spine would be at similar magnitudes (Figure 6.8). However, more lordosis in the lumbar spine in the standing posture might result in longer lever arms for the vertical load for some spinal motion

segments: a greater moment in the pitch axis acting on a motion segment with more inclination to the vertical axis. This might cause more bending motions in the lumbar region in the standing position than in the sitting position, which could partly result in greater pitch transmissibilities and partly result in greater vertical transmissibilities. A more distinct lordosis in the lumbar spine in the standing posture than in the sitting posture might, therefore, be one of the causes of the differences in the transmissibilities.

Floor vibration is transmitted through the tissue beneath the feet and then the legs to the hip joints in the pelvis in the standing posture, while the seat vibration is transmitted through the tissue beneath the pelvis to the ischial tuberosities in the pelvis in the sitting posture. The transmission of vertical floor vibration to the knee was measured in the vertical and fore-and-aft directions in the present study (Figure 6.28). It was found that the vertical transmissibility to the knee generally showed monotonous increases with increasing frequency without any remarkable peak at frequencies below 10 Hz. The fore-and-aft transmissibility to the knee, however, had a peak in the 6 to 7 frequency range that was close to the frequency range of the principal resonance of the apparent mass but a little bit higher. This implied the existence of some bending motion of the legs at the ankle and knee or some shear deformation of the tissue beneath the feet in this frequency range. There might also be an axial deformation of the foot tissue, although this might not make a main contribution to the resonance of the body in this frequency range. The vibration transmitted through the hip joint to the pelvis might, therefore, be both in the vertical and fore-and-aft axes. In the sitting posture, the deformation of the tissue beneath the pelvis in the shear and axial directions might alter the vertical seat vibration to two dimensional motions which is transmitted to the ischial tuberosities. This transmitted motion to the pelvis in the sitting position would be different from that in the standing posture, although both are two dimensional. Such two dimensional input motions to the pelvis might result in two dimensional pelvis motions, including pitch motion. During pitch motion, the pelvis would rotate about the hip joint in the standing posture but about the ischial tuberosities in the standing

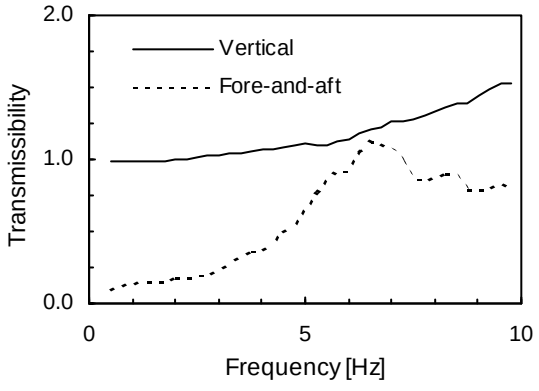

Figure 6.28 Median transmissibilities to the knee in the vertical and fore-and-aft axes measured at 1.0 ms^{-2} r.m.s. in Experiment 3.

posture. The difference in the pitch motion of the pelvis between the standing and sitting postures can be seen in the phases shown in Figure 6.29. There were greater phase lags in the pitch transmissibility in the standing posture than in the sitting posture, although the phases of the vertical transmissibilities and the moduli of the pitch transmissibilities to the pelvis were similar in the two postures (Figures 6.10 (h) and 6.29). The transmissibilities to the upper trunk were similar as observed in Figures 6.8 to 6.10. It was likely, therefore, that the vibration transmitted to the pelvis and upper-body differed between the standing and sitting postures and that the dynamic mechanisms in the lower trunk compensated for the difference somehow so that the difference in the vibration transmitted to the upper trunk was not remarkable. This difference in the dynamic response of the lower upper-body including the pelvis might make contributions to the differences observed in the transmissibilities to that region observed in Figure 6.8.

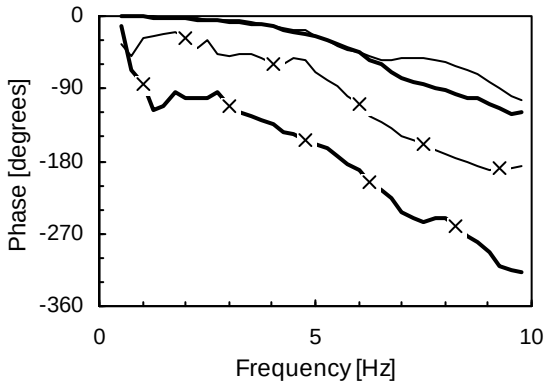

Figure 6.29 Median phases of the transmissibilities to the pelvis in the vertical and pitch axes in the standing and sitting postures. ━━━ , standing posture; ——— , sitting posture. x: pitch.

At the upper locations in the body (i.e., the head and T1), an opposite shift in the peak frequency to that observed in the apparent mass and the transmissibilities to the lower locations was found: the peak frequencies in the pitch transmissibilities at those locations tended to be lower in the standing posture than in the sitting posture. This may imply the existence of some local motion of the head, mainly in the pitch direction, that does not make any clear contribution to the driving-point response. Pitch motion of the head may be induced mainly by an eccentricity of the centre of gravity of the head relative to the location of the input motion transmitted through the neck. The position of the head-neck system, including the muscle tension in the neck, will, therefore, significantly affect the resulting pitch motion of the head. In the present study, the posture of subjects was dependent on their interpretation of a ‘comfortable, upright position’. This could result in a variability in the head-neck position between subjects and, consequently, a variability in pitch motion of the head between subjects. Larger variability observed in the vertical transmissibility to the head reported in the present

study, as well as in the previous studies, might be attributed to this variability in pitch motion of the head.

Decreases in the principal resonance frequency of the apparent mass for seated subjects were found with increases in the vibration magnitude in the present study: decreases from 6.4 to 4.75 Hz with increases from 0.125 to 2.0 ms^{-2} r.m.s. This frequency shift was consistent with that found by Mansfield (1998): 5.9 to 4.5 Hz by increasing from 0.25 to 2.5 ms^{-2} r.m.s. with a similar frequency range, 0.2 to 20 Hz, to that used in this study, 0.5 to 20 Hz. The decreases in the principal resonance frequency of the apparent mass for standing subjects with increases in the vibration magnitude were also observed: 6.75 to 5.25 Hz with increases from 0.125 to 2.0 ms^{-2} r.m.s. The same trend was also found in the transmissibilities measured at various body locations, particularly in those with a clear peak in the frequency range used, as shown in Figures 6.15 to 6.20. This nonlinear characteristic observed in both standing and seated bodies may support the hypothesis made above that the dynamic mechanisms of the principal resonance are common for standing and seated bodies.

6.6 CONCLUSIONS

The apparent masses and transmissibilities of standing and seated subjects measured at five vibration magnitudes have been compared. The principal resonance in the apparent mass was observed in the 5 to 6 Hz frequency range for both standing and seated bodies. The principal resonance frequency for the standing posture tended to be higher than that for the seated posture, although the differences were within 1 Hz for most subjects. The apparent mass at the principal resonance was greater in the sitting posture than in the standing posture, while those at higher frequencies, above about 7 Hz, were less in the sitting posture than in the standing posture. The legs which worked as vibration transmission paths in the standing posture and as additional masses in the sitting posture may have made a contribution to the difference in the apparent masses between the standing and sitting postures.

The transmissibilities measured at locations in the lower upper-body showed differences between standing and sitting subjects. It was found that the vertical transmissibilities to the lumbar vertebrae were greater in the standing posture than in the sitting posture at frequencies around the principal resonance of the apparent mass and above. The median transmissibilities to the vertical vibrations at L3 and L5 in the standing posture

exceeded 2.0 at the peak while those in the sitting posture were less than 1.5 at 1.0 ms^{-2} r.m.s. The first peak frequency was found to be higher in the standing body than in the sitting body, which was consistent with the trend observed in the apparent mass. The differences in the pelvis angle, spinal curvature and muscle tension, and the differences in the vibration transmission path between standing and sitting positions may make some contributions to those differences in the vertical transmissibilities to the lumbar region. The transmissibilities to the thoracic region showed similar magnitudes in the frequency range used in both positions, although the peak frequency was higher in the standing posture, which might be caused by the dynamics of the lower part of the body. Some evidence of local pitch motions of the head were observed, which might not make major contributions to the dynamic characteristics seen in the apparent mass.

Nonlinear characteristics were found in the dynamic responses of both standing and seated subjects. The resonance frequency in the apparent mass decreased with increasing vibration magnitude from 0.125 to 2.0 ms^{-2} r.m.s.: 6.75 to 5.25 Hz and 6.4 to 4.75 Hz for the standing posture and the sitting posture, respectively. Decreases in the frequencies of the first peaks in the transmissibilities were also observed as the vibration magnitude increased from 0.125 to 2.0 ms^{-2} r.m.s.: for the vertical transmissibilities to L3, 7.5 to 5.6 Hz and 6.25 to 4.75 Hz for the standing posture and the sitting posture, respectively. The same nonlinear trend in the principal resonance in both standing and seated bodies indicated that the dynamic mechanisms contributing to the resonance were probably common for the standing and seated body.

CHAPTER 7

MOVEMENT OF THE BODY OF SEATED AND STANDING SUBJECTS EXPOSED TO VERTICAL WHOLE-BODY VIBRATION AT THE PRINCIPAL RESONANCE FREQUENCY

7.1 INTRODUCTION

The previous chapter, Chapter 6, presents the apparent masses and transmissibilities measured in Experiment 3. This chapter is concerned with the identification of the dynamic mechanisms of the principal resonance of the apparent mass. The movements of the body in sitting and standing positions at the principal resonance frequency are presented, based on the measurements of the apparent mass and transmissibility obtained in Experiment 3. The hypothesis was that the principal resonance of the apparent mass in both standing and seated subjects located at about 5 Hz might be caused by the same dynamic mechanisms in the upper-body, as mentioned in the introduction of Chapter 6.

The principal resonance of the seated body at about 5 Hz has been previously suggested to be associated with some dynamic mechanisms of the body. Hagena *et al*. (1985) measured the dynamic response of both standing and seated subjects at the head, the seventh cervical vertebra, the sixth thoracic vertebra, the first, fourth and fifth lumbar vertebrae and the sacrum. Comparing the vertical transmissibilities from the vibrator platform vibration to each measurement location with those from the sacrum to each upper location, they concluded that the resonance observed at around 4 and 5 Hz corresponded to motion of the entire body, while the second resonance between 7 and 10 Hz represented motion of the spinal column. Sandover and Dupuis (1987) reanalysed film of the motion of the lower spine as investigated by Christ and Dupuis (1966) and hypothesised that the resonances at about 4 Hz observed during human response to vertical vibration were related to bending in the lumbar spine and possibly a rocking motion of the pelvis. Bending motion of the lumbar spine was also suggested by Hinz *et al*. (1988b). They stated that the relative vertical accelerations between L3 and L4 found at 4.5 Hz were mainly caused by bending of the spine. It was also stated that the time relations between extreme accelerations at the lumbar vertebrae and those at

the head and the acromion indicated that the vertical motion of the body parts above L3, rather than a pitching of the pelvis which might be a secondary effect, caused a bending of the lumbar spine. Pope *et al*. (1990) suggested that the first natural frequency of the vertical transmissibility to the third lumbar vertebra is 'due primarily to a vertical response of the buttocks-pelvis system': 'due to compression of the buttocks tissue and to the interaction of this vertical response with the rotational subsystem'.

Kitazaki (1994) and Kitazaki and Griffin (1998) investigated vibration modes of the seated body in the mid-sagittal plane at frequencies below 10 Hz using experimental modal analysis. They extracted a total of eight vibration modes in which acceleration responses of the spine (i.e., at the first, sixth and eleventh thoracic vertebrae, the third lumbar vertebra, and the sacrum), of the pelvis, viscera and the head to whole-body vertical vibration were measured. The fourth mode they obtained, at 4.9 Hz, was found to be a combination of 'an entire body mode, in which the head, spinal column and the pelvis moved vertically due to axial and shear deformations of the buttocks tissue, in phase with a vertical visceral mode, and a bending of the upper thoracic and cervical spine'. The fifth mode at 5.6 Hz appeared to contain a bending mode of the lumbar and lower thoracic spine and a motion of the head which might have been pitch motion. A rotational mode of the pelvis was contained in the sixth mode at 8.1 Hz and the seventh mode at 8.7 Hz. The authors also conducted a study of vibration modes of the seated body using the finite element method (1994, 1997). A two-dimensional model was developed by comparison of the vibration mode shapes with those extracted from experimental data (1994, 1998). A total of seven modes was obtained from the mathematical model. It was concluded that 'the principal resonance of the driving point response at about 5 Hz consisted of an entire body mode, in which the head, spinal column and the pelvis move almost rigidly, with axial and shear deformation of tissue beneath the pelvis occurring in phase with a vertical visceral mode', which was the fourth mode at 5.06 Hz. A bending mode of the entire spine was found in the fifth mode at 5.77 Hz which was stated to make a minor contribution to the principal resonance. As in the experimental results, a pelvis rotation was found in both the sixth mode (at 7.51 Hz) and in the seventh mode (at 8.96 Hz).

There have been few studies that investigate the dynamic mechanisms of the standing body based on the measurement of the body motion, not just based on the driving-point responses. Hagena *et al*. (1985, 1986) measured the spinal motion of eleven subjects in both standing and sitting positions exposed to vertical swept sinusoidal vibration from 3 to 40 Hz at a magnitude of 0.2 g. The spinal motion was measured with accelerometers

mounted on the spinous processes by Kirschner-wires (*K*-wires) at six spinal levels: at the seventh cervical vertebra (C7), the sixth thoracic vertebra (T6), the first, fourth and fifth lumbar vertebrae (L1, L4 and L5), and the sacrum. Three resonance phenomena were found in the transmissibilities in the frequency range investigated: between 4 and 5 Hz, between 7 and 10 Hz, and at about 18 Hz. They seemed to assume that the causes of the resonances were consistent in both standing and sitting positions. It was concluded that the resonance between 4 and 5 Hz corresponded with a vibration mode of the entire body, the resonance between 7 and 10 Hz represented an independent resonance of the spinal column, and the resonance at about 18 Hz could be considered to correspond with the head motion. Pope *et al*. (1989) measured the dynamic response of standing subjects to impacts at the level of the third lumbar vertebra (L3) of a female subject with an accelerometer mounted on a *K*-wire. They stated that, for the subject in a rigid erect posture ('at attention'), the transmissibility was similar in form to that of sitting subjects measured in their separate study (Broman *et al*., 1991), however, the response was attenuated. It was concluded that 'the standing subject has an ability to attenuate vibrations through the lower extremities'.

The objectives of the study presented in this chapter were: (i) to define the form of body movements in sitting and standing positions during exposure to vertical whole-body vibration, (ii) to identify the mechanisms contributing to the principal resonance seen in the apparent mass of seated and standing bodies, and (iii) to identify any differences in the dynamic mechanisms contributing to the principal resonance between standing and seated bodies.

7.2 METHOD AND ANALYSIS

The experimental set-up, input stimuli, subjects, posture and analysis method used were described in Section 6.2.

The locations of all measurement sites were measured so as to illustrate the movement of the body by using the transmissibility data to the sites. For the sitting position, the vertical location (in the *z*-axis) was the height of each point above the seat surface. The horizontal location (in the *x*-axis) was the distance between the body surface at the measurement point and a reference vertical surface fixed to the rear of the seat. For the standing position, the vertical location (in the *z*-axis) was the height of each point above the floor. The horizontal location (in the *x*-axis) was the distance between the body

surface at the measurement point and a reference vertical surface which was measured prior to vibration exposures. The positions of vertebrae were then estimated using distances between the centres of the vertebral bodies and the tips of the spinous processes using the values shown in Table 6.3. The thickness of the tissue between the body surface and the spinous processes was neglected. The location of the head (the mouth) and the pelvis (the posterior-superior iliac spine) and the estimated centres of the vertebral bodies as measured for each subject in the seated and standing postures are shown in Tables 7.1 and 7.2, respectively.

Table 7.1 Location of the head (the mouth), estimated centres of the vertebral bodies and the pelvis (the posterior-superior iliac spine) in the sitting posture. (The origin of the co-ordinate system was taken at the seat surface, vertically below the body surface over L5 on the vertical middle line of the back. The *y*-component (in the lateral axis) was zero for all measurement points, apart from the pelvis which was -0.05 for all subjects).

[m]	Subject 1, (*x, z*)	Subject 2, (*x, z*)	Subject 3, (*x, z*)	Subject 4, (*x, z*)
Head	(0.21, 0.72)	(0.27, 0.75)	(0.24, 0.70)	(0.23, 0.78)
T1	(0.080, 0.60)	(0.070, 0.64)	(0.080, 0.62)	(0.080, 0.68)
T5	(0.040, 0.49)	(0.020, 0.51)	(0.040, 0.50)	(0.040, 0.56)
T10	(0.060, 0.34)	(0.035, 0.36)	(0.045, 0.35)	(0.050, 0.42)
L1	(0.075, 0.26)	(0.050, 0.27)	(0.060, 0.28)	(0.065, 0.36)
L3	(0.075, 0.21)	(0.065, 0.21)	(0.065, 0.24)	(0.075, 0.30)
L5	(0.060, 0.15)	(0.060, 0.15)	(0.060, 0.18)	(0.060, 0.23)
Pelvis	(0.0, 0.15)	(0.0, 0.15)	(0.0, 0.18)	(0.0, 0.23)
[m]	Subject 5, (*x, z*)	Subject 6, (*x, z*)	Subject 7, (*x, z*)	Subject 8, (*x, z*)
Head	(0.22, 0.75)	(0.18, 0.76)	(0.22, 0.72)	(0.17, 0.75)
T1	(0.070, 0.67)	(0.070, 0.66)	(0.090, 0.61)	(0.070, 0.65)
T5	(0.040, 0.57)	(0.030, 0.56)	(0.060, 0.49)	(0.050, 0.55)
T10	(0.045, 0.41)	(0.045, 0.38)	(0.050, 0.36)	(0.045, 0.40)
L1	(0.065, 0.33)	(0.060, 0.32)	(0.055, 0.30)	(0.060, 0.32)
L3	(0.075, 0.27)	(0.070, 0.25)	(0.065, 0.24)	(0.070, 0.26)
L5	(0.060, 0.21)	(0.060, 0.20)	(0.060, 0.18)	(0.060, 0.20)
Pelvis	(0.0, 0.21)	(0.0, 0.20)	(0.0, 0.18)	(0.0, 0.20)

Table 7.2 Location of the head (the mouth), estimated centres of the vertebral bodies and the pelvis (the posterior-superior iliac spine) and the knee (just below the patella) in the standing posture. (The origin of the co-ordinate system was taken at the floor, vertically below the body surface over L5 on the vertical middle line of the back.)

[m]	Subject 1, (*x, z*)	Subject 2, (*x, z*)	Subject 3, (*x, z*)	Subject 4, (*x, z*)
Head	(0.17, 1.46)	(0.20, 1.59)	(0.19, 1.58)	(0.19, 1.62)
T1	(0.020, 1.36)	(0.030, 1.50)	(0.060, 1.50)	(0.030, 1.52)
T5	(0.0, 1.25)	(0.0, 1.35)	(0.030, 1.38)	(0.010, 1.40)
T10	(0.015, 1.12)	(0.050, 1.22)	(0.060, 1.23)	(0.035, 1.25)
L1	(0.050, 1.05)	(0.070, 1.15)	(0.070, 1.17)	(0.055, 1.18)
L3	(0.070, 0.99)	(0.080, 1.11)	(0.080, 1.12)	(0.065, 1.13)
L5	(0.060, 0.94)	(0.060, 1.05)	(0.060, 1.07)	(0.060, 1.08)
Pelvis	(0.0, 0.94)	(0.0, 1.05)	(0.0, 1.07)	(0.0, 1.08)
Knee	(0.050, 0.38)	(0.070, 0.46)	(0.070, 0.49)	(0.080, 0.45)
[m]	Subject 5, (*x, z*)	Subject 6, (*x, z*)	Subject 7, (*x, z*)	Subject 8, (*x, z*)
Head	(0.17, 1.58)	(0.21, 1.57)	(0.16, 1.49)	(0.135, 1.59)
T1	(0.050, 1.48)	(0.070, 1.47)	(0.030, 1.38)	(0.035, 1.46)
T5	(0.010, 1.36)	(0.030, 1.36)	(0.0, 1.24)	(-0.050, 1.34)
T10	(0.025, 1.20)	(0.030, 1.21)	(0.035, 1.10)	(0.030, 1.19)
L1	(0.050, 1.12)	(0.060, 1.13)	(0.060, 1.04)	(0.055, 1.11)
L3	(0.070, 1.08)	(0.075, 1.07)	(0.075, 0.99)	(0.070, 1.06)
L5	(0.060, 1.03)	(0.060, 1.02)	(0.060, 0.95)	(0.060, 1.01)
Pelvis	(0.0, 1.03)	(0.0, 1.02)	(0.0, 0.95)	(0.0, 1.01)
Knee	(0.080, 0.43)	(0.080, 0.43)	(0.070, 0.38)	(0.055, 0.42)

The transmissibilities in the vertical and fore-and-aft axes, obtained by the method explained in Section 6.3, were used to determine the movement of the body at the principal resonance frequency determined from the apparent mass for each subject. Using the moduli and the phases of the transmissibilities at the resonance frequency measured at a vibration magnitude of 1.0 ms^{-2} r.m.s., the position of each measurement point in the sagittal plane was calculated:

$$x_j = x_{0j} + T_{xj} A \sin(2\pi f_r t + \phi_x) \quad (7.1)$$

$$z_j = z_{0j} + T_{zj} A \sin(2\pi f_r t + \phi_z) \quad (7.2)$$

where j indicates the position of the measurement point, and x and z are the horizontal and vertical components in the co-ordinate defined in the captions of Tables 7.1 and 7.2, respectively. The values of x_0 and z_0 represent the initial position of the measurement point, j, as given in Tables 7.1 and 7.2; f_r is the principal resonance frequency determined from the apparent mass; T_x and ϕ_x are the modulus and the phase of the fore-and-aft transmissibility at f_r; T_z and ϕ_z are the modulus and the phase of the vertical transmissibility at f_r; A is the amplitude of the vertical displacement of the reference motion (i.e. the seat surface displacement) at the frequency f_r; t is the time.

7.3 RESULTS

7.3.1 Seated position

As reported in the preceding chapters and previous studies, the apparent masses of the eight subjects when seated measured at a vibration magnitude of 1.0 ms^{-2} r.m.s. showed a clear peak in the frequency range between 4.75 and 5.75 Hz (Figure 7.1). The frequencies at which the apparent masses had a principal peak are listed in Table 7.3. The frequencies at which the apparent mass was greatest were assumed to be the principal resonance frequencies of the subjects and are referred to as the principal resonance frequencies of the apparent mass in this study.

The transmissibilities between the vertical seat motion to the vertical motions at the head (i.e., the mouth), the centre of each vertebral body and the pelvis (i.e., the posterior-superior iliac spine) for the eight subjects are shown in Figure 7.2. The variability between subjects, inter-subject variability, was large for the head, and for transmissibilities to L3 and L5 and to the pelvis at frequencies above about 7 Hz. Most vertical transmissibilities, apart from some to the head, show a peak in the frequency region of the principal resonance frequency of the apparent mass of each subject ($\pm$ 0.5

Table 7.3 Principal peak frequencies in the apparent masses of the eight subjects in the sitting posture.

Subject	1	2	3	4	5	6	7	8
Frequency [Hz]	5.25	5.00	5.75	5.25	5.00	5.75	5.25	4.75

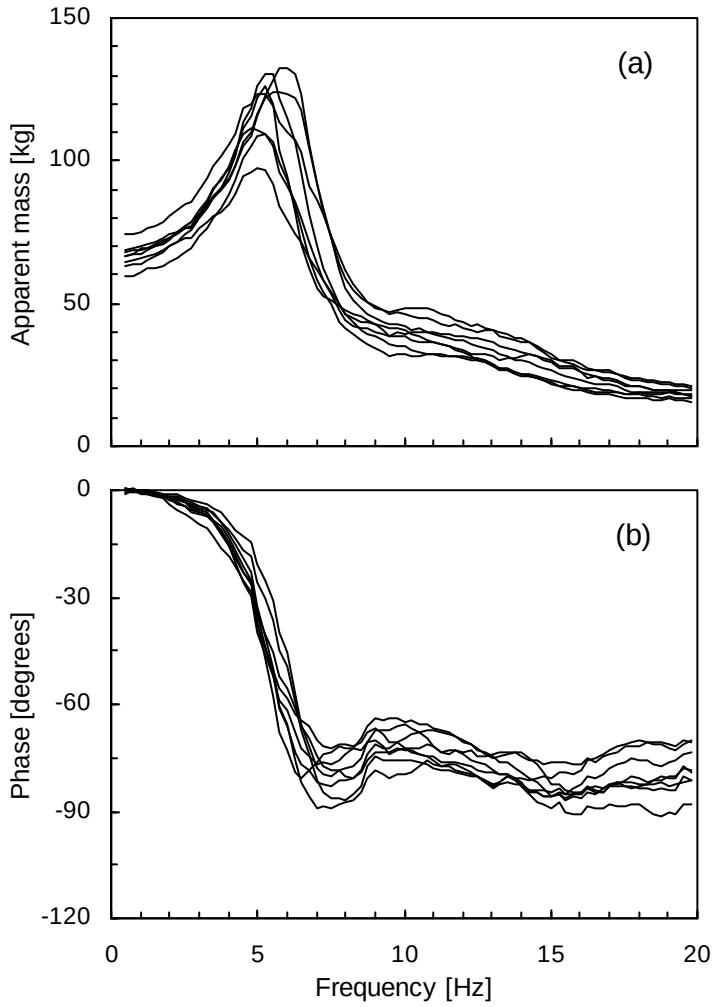

Figure 7.1 Apparent masses and phases of the eight subjects in the sitting posture.

Hz). The vertical transmissibility at the principal resonance frequency tended to decrease at higher measurement locations, although this was not the case for those to T1 for which the head motion might have had an effect. The maximum transmissibility to the lumbar spine was found at the resonance frequency for six of the eight subjects. The vertical transmissibilities to L5 and to the pelvis of seven subjects show another peak between 7 and about 10 Hz, which had a greater magnitude than that at about 5 Hz for some subjects. This second peak was also visible in the vertical transmissibilities to the upper locations over the lumbar spine, although this was not as clear as in those to L5 and to the pelvis.

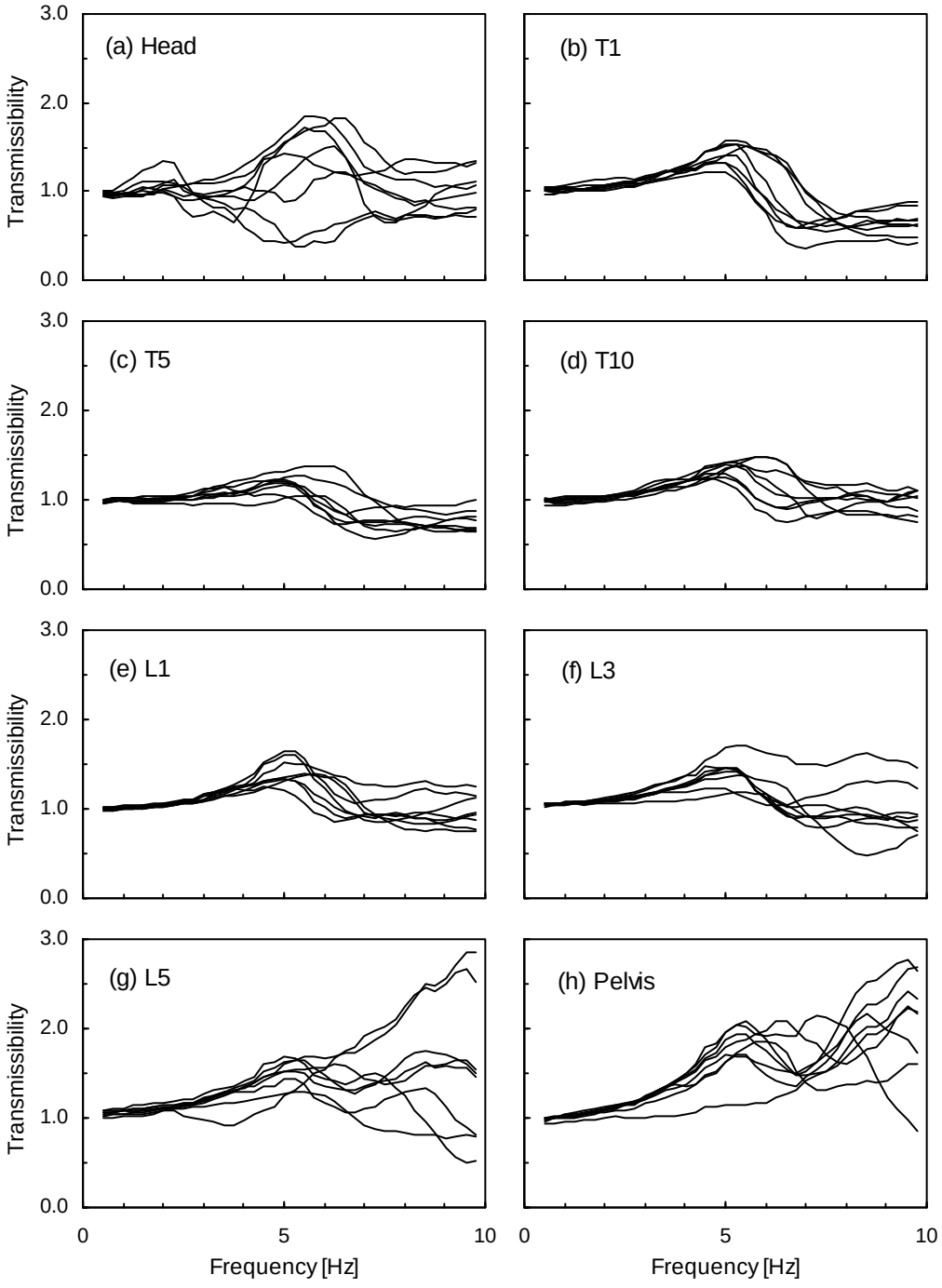

Figure 7.2 Vertical transmissibilities to each measurement location for the eight subjects in the sitting posture.

Figure 7.3 shows the fore-and-aft transmissibilities to each location for eight subjects. It was clear that the fore-and-aft transmissibilities to all locations, except to the head and T1, were much smaller than those in the vertical direction, as expected. The fore-and-aft transmissibilities to the head and T1 showed a peak between 6 and 7 Hz for most subjects, which was slightly higher than the principal resonance frequency of the apparent mass. The peak at this frequency range was not clear at the other locations. The fore-and-aft transmissibilities to T5 and L5 tended to be smaller than to the other locations over the spine. The fore-and-aft transmissibility at the principal resonance frequency tended to increase as the measurement location was higher: the modulus was a maximum at T1 and a minimum at L5 for seven subjects. However, the modulus at T5 was smaller than at T10, the next lower point, for seven of the eight subjects.

The transmissibilities from the vertical seat vibration to the pitch motion at each location are shown in Figure 7.4. Although inter-subject variability was large at some locations, it was possible to find overall trends for the subjects. Most pitch transmissibilities to locations over the spine were very small below 4 Hz and increased with an increase in the frequency above 4 Hz. The pitch transmissibilities to T1 and to the heads of all subjects showed a clear peak between 5 and 7 Hz. The magnitudes of the peaks seen at the head were greater than those at T1 for seven subjects ($p < 0.05$). The pitch transmissibilities to the locations over the spine were smaller than those to the head and T1 at frequencies below 10 Hz. At the principal resonance frequency of the apparent mass, the greatest pitch transmissibility was to the head for seven of the subjects, while pitch transmissibility to T1 tended to be greater than that to the other locations over the spine. In the region of the spine between T10 and L3, the pitch transmissibility was less than at other measurement points.

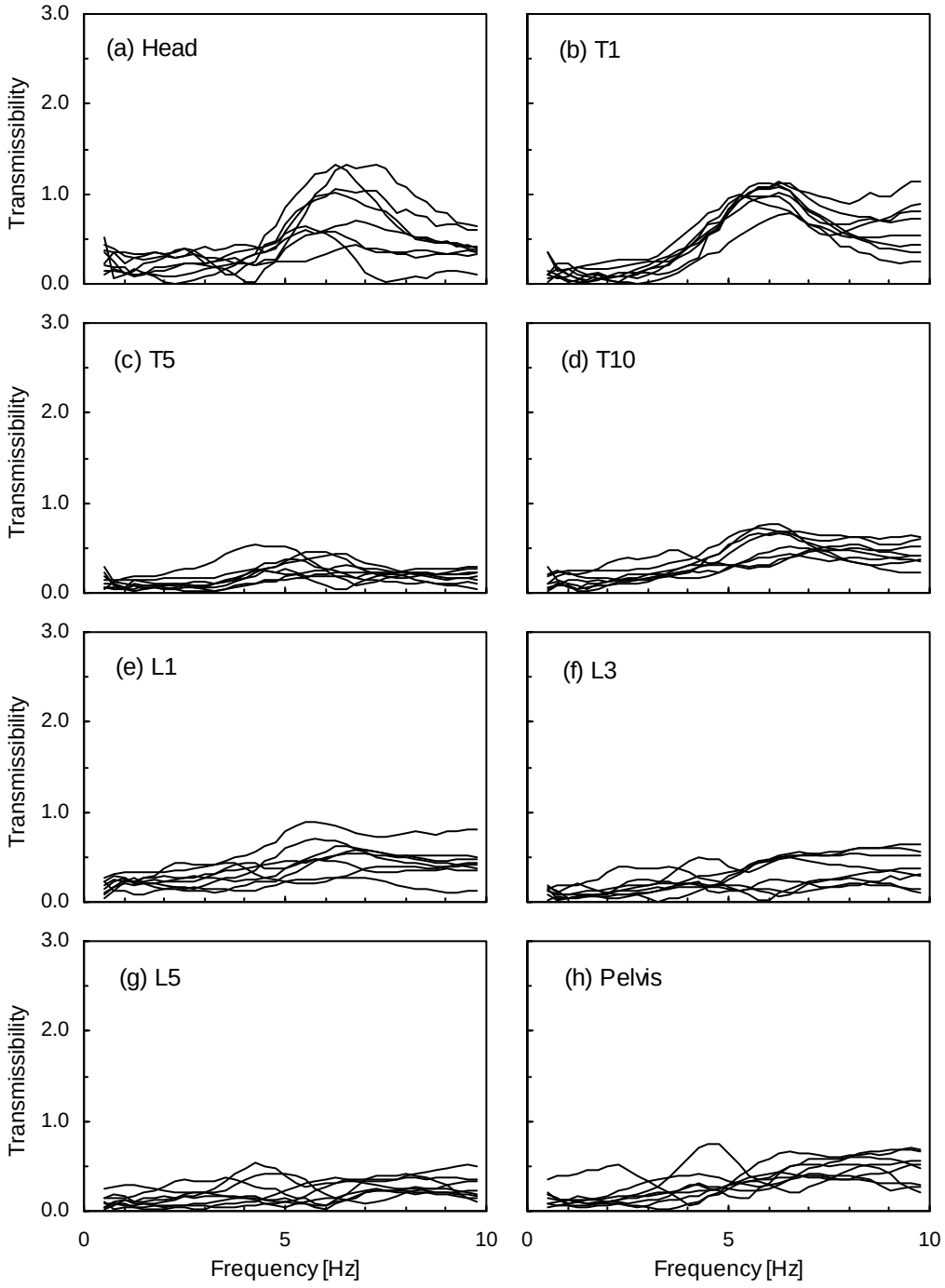

Figure 7.3 Fore-and-aft transmissibilities to each measurement location for the eight subjects in the sitting posture.

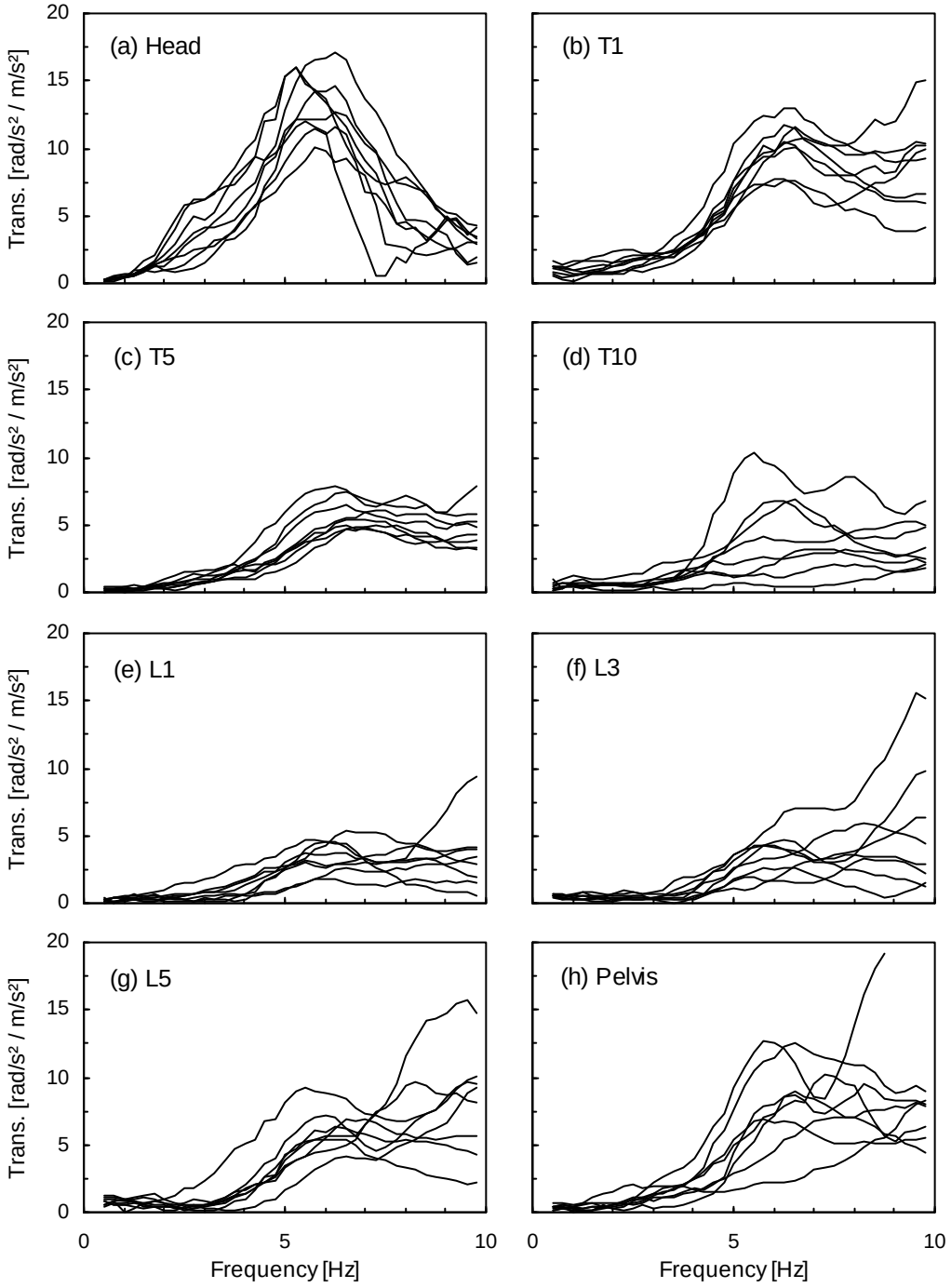

Figure 7.4 Pitch transmissibilities to each measurement location for the eight subjects in the sitting posture.

The vertical and fore-and-aft transmissibilities were used to illustrate the movement of the upper-body at the principal resonance frequency of the apparent mass for each subject, using Equations (7.1) and (7.2). The moduli and phases of the transmissibilities at the resonance frequencies of all subjects that were used to illustrate the movement are tabulated in Table 7.4. The vertical transmissibility was greatest at the pelvis at the

Table 7.4 Modulus and phase of the transmissibilities to all measurement points in vertical and fore-and-aft axes at the principal resonance frequency of the apparent mass in the sitting posture at 1.0 ms^{-2} r.m.s.

	Subject 1, 5.25 Hz		Subject 2, 5.0 Hz		Subject 3, 5.75 Hz		Subject 4, 5.25 Hz	
	Vertical		Vertical		Vertical		Vertical	
	Modulus	Phase	Modulus	Phase	Modulus	Phase	Modulus	Phase
Head	1.743	-18.89	0.413	-38.05	1.124	-29.51	1.628	-7.24
T1	1.141	-39.23	1.315	-41.39	1.466	-43.32	1.404	-39.28
T5	1.176	-19.83	1.046	-31.99	1.375	-33.60	1.194	-24.55
T10	1.223	-24.42	1.197	-25.59	1.479	-30.36	1.427	-19.25
L1	1.315	-21.71	1.206	-23.93	1.368	-27.30	1.599	-25.13
L3	1.415	-24.66	1.224	-22.78	1.342	-33.62	1.449	-26.50
L5	1.636	-26.06	1.242	5.30	1.563	-29.09	1.430	-27.19
Pelvis	2.037	-32.11	1.155	-11.11	1.931	-41.16	1.704	-30.04
	Fore-and-aft		Fore-and-aft		Fore-and-aft		Fore-and-aft	
	Modulus	Phase	Modulus	Phase	Modulus	Phase	Modulus	Phase
Head	0.549	54.10	0.662	76.82	0.561	38.63	0.615	71.70
T1	0.968	53.25	0.947	116.22	0.980	90.91	0.833	28.07
T5	0.415	38.09	0.511	140.45	0.284	95.22	0.352	6.91
T10	0.612	-48.21	0.320	-127.96	0.285	-106.54	0.524	-97.89
L1	0.335	-103.88	0.235	-133.65	0.471	-75.29	0.426	-83.89
L3	0.346	-107.66	0.165	164.75	0.134	-153.55	0.349	-141.17
L5	0.401	176.99	0.191	154.69	0.041	-134.41	0.317	-142.16
Pelvis	0.238	-144.93	0.280	52.32	0.330	-173.27	0.516	174.93
	Subject 5, 5.0 Hz		Subject 6, 5.75 Hz		Subject 7, 5.25 Hz		Subject 8, 4.75 Hz	
	Vertical		Vertical		Vertical		Vertical	
	Modulus	Phase	Modulus	Phase	Modulus	Phase	Modulus	Phase
Head	0.473	-62.91	1.422	-15.57	1.415	-31.56	1.447	-2.67
T1	1.315	-34.85	1.493	-33.38	1.526	-38.40	1.497	-16.84
T5	1.203	-26.38	1.047	-11.84	1.137	-18.23	1.213	-6.22
T10	1.240	-20.46	1.471	-19.24	1.376	-20.48	1.295	-7.04
L1	1.337	-24.47	1.392	-21.31	1.643	-30.30	1.440	-10.85
L3	1.454	-30.10	1.173	-14.69	1.448	-28.59	1.601	-14.72
L5	1.681	-27.39	1.274	-19.76	1.526	-23.10	1.557	-10.29
Pelvis	1.954	-34.96	1.849	-31.86	1.936	-34.78	1.624	-15.70
	Fore-and-aft		Fore-and-aft		Fore-and-aft		Fore-and-aft	
	Modulus	Phase	Modulus	Phase	Modulus	Phase	Modulus	Phase
Head	0.574	42.91	0.284	20.65	0.618	55.52	0.631	87.82
T1	0.822	103.45	0.670	79.78	0.926	95.18	0.634	112.86
T5	0.264	129.83	0.131	116.57	0.170	13.06	0.131	90.13
T10	0.278	-105.95	0.432	-71.45	0.681	-54.67	0.440	-47.27
L1	0.370	-76.58	0.257	-37.87	0.851	-53.19	0.504	-39.32
L3	0.118	-151.72	0.150	173.89	0.303	-79.82	0.203	-51.83
L5	0.042	11.42	0.053	-38.01	0.122	-75.03	0.185	-5.70
Pelvis	0.338	150.26	0.357	-41.88	0.139	-144.36	0.248	-9.41

resonance frequency for seven subjects, of whom six showed the maximum transmissibility within the spine in the lumbar region. The phase difference of the vertical motion with respect to the seat motion tended to increase at T1 compared to those at other locations on the spine. The fore-and-aft motion at T1, where the motion was the greatest in this direction, was almost out of phase with the fore-and-aft motions at T10, L1 and L3. The fore-and-aft transmissibility to T5 tended to be smaller than at the adjacent measurement points, T1 and T10. At L5, the fore-and-aft transmissibility was the smallest for five subjects.

Figures 7.5 and 7.6 show a cycle of the movement of the all measurement points on the upper-body, using Subjects 5 and 7 as examples, at the principal resonance frequencies of 5.0 Hz and 5.25 Hz, respectively. The body was viewed from the right hand side. In the figures, a cycle is divided into eight equal intervals such that: (a) $t = 0$, the seat surface is at the initial position; (c) $t = T/4$ (where T is the period of the seat vibration), the seat is at the highest position; (e) $t = T/2$, the seat has returned to the initial position; (g) $t = 3T/4$, the seat is at the lowest position. For illustration, the displacement of the seat surface vibration, A in equations (7.1) and (7.2), was 0.05 m: i.e. the movements shown in Figure 7.5 and 7.6 are exaggerated. At their principal resonance frequency, the movements of the upper-bodies of the other subjects, except subject 2, demonstrated consistent trends with those shown in Figures 7.5 and 7.6.

It was clear that relative motion occurred between locations over the spine at the principal resonance frequency: all measurement points did not move in the same manner. Bending or rocking motions of the spine appeared to be dominant at frequencies around the resonance of the apparent mass. The upper thoracic spine, between T1 and T10, tended to rock about a point on the lower thoracic spine in the sagittal plane, with some slight bending. In the lower thoracic spine and the lumbar spine region, bending motion along the spine was more significant than in the upper thoracic spine. It seems that some pitch motion of the pelvis occurred at this frequency, although the pitch resonance of the pelvis is at a higher frequency. There was also pitch motion of the head at the principal resonance of the body.

To visualise the motions mentioned above, consider the movement of the upper-body when the seat moved upward (see Figures 7.5 and 7.6). The upper thoracic spine rocked backward, with a slight extension along the full length of the upper part of thoracic spine, while the head pitched forward. This combined movement was delayed compared to the upward seat motion, although the backward rocking was almost in phase with the extension. The pitch motion of the head was delayed compared to the rocking motion of the upper thoracic spine. The lower spine extended with upward seat

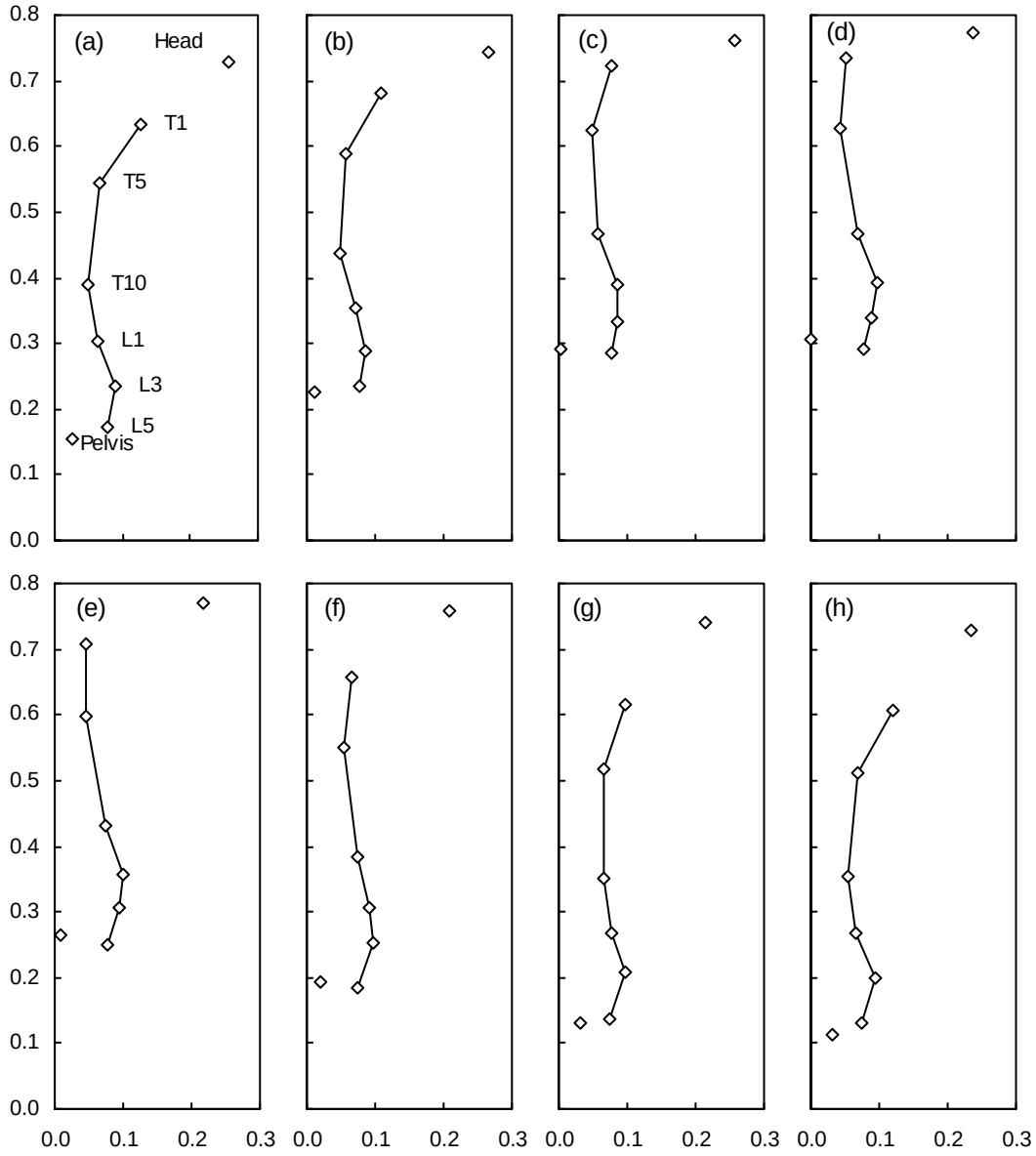

Figure 7.5 Movement of the upper-body at the principal resonance frequency of the apparent mass of Subject 5 in the sitting posture at 5.0 Hz: (a) $t = 0$, (b) $t = T/8$, (c) $t = T/4$, (d) $t = 3T/8$, (e) $t = T/2$, (f) $t = 5T/8$, (g) $t = 3T/4$, (h) $t = 7T/8$ (T: period of the seat vibration). (The units of body axes are metres [m]. The scale of the movement is exaggerated for clarity.)

motion, with a slightly smaller delay than that of the motion in the upper thoracic region. The extension of the lumbar spine possibly caused the forward motion of the upper lumbar spine and the lower thoracic spine, which may have contributed to the backward rocking motion of the upper thoracic spine. The pelvis pitched forward as the seat moved upward, although there appeared to be a delay with respect to the upward seat motion.

Computer program sources to animate the movements of the upper-body of all the

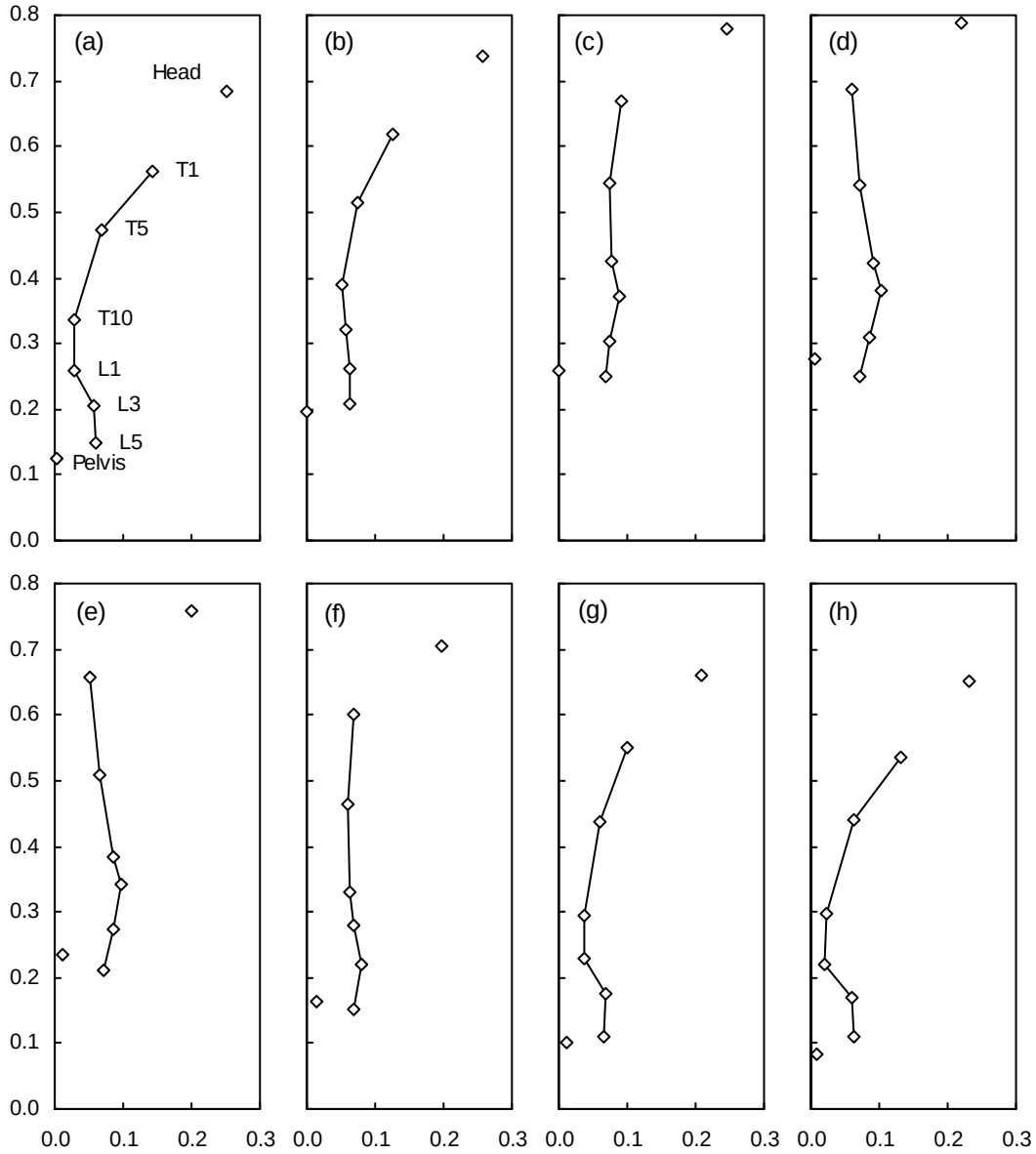

Figure 7.6 Movement of the upper-body at the principal resonance frequency of the apparent mass of Subject 7 in the sitting posture at 5.25 Hz: (a) $t = 0$, (b) $t = T/8$, (c) $t = T/4$, (d) $t = 3T/8$, (e) $t = T/2$, (f) $t = 5T/8$, (g) $t = 3T/4$, (h) $t = 7T/8$ (T: period of the seat vibration). (The units of both axes are metres [m]. The scale of the movement is exaggerated for clarity.)

subjects in the sitting posture, including those shown above, at the principal resonance frequency of the apparent mass are provided in Appendix E. Two M-file sources presented in Appendix E have been written for MATLAB for Windows version 4.2b.

7.3.2 Standing position

In the normal standing posture with a vibration magnitude of 1.0 ms^{-2} r.m.s., the apparent masses of the eight subjects showed a main peak in the frequency range between 5.25 and 6.5 Hz (Figure 7.7). Table 7.5 shows the frequencies at which the apparent masses were maximum in the frequency range below 20 Hz. These frequencies were regarded as the principal resonance frequencies of subjects in the standing posture at 1.0 ms^{-2} r.m.s. A broad peak can be seen in the apparent masses for most subjects in the frequency range between 10 and 13 Hz.

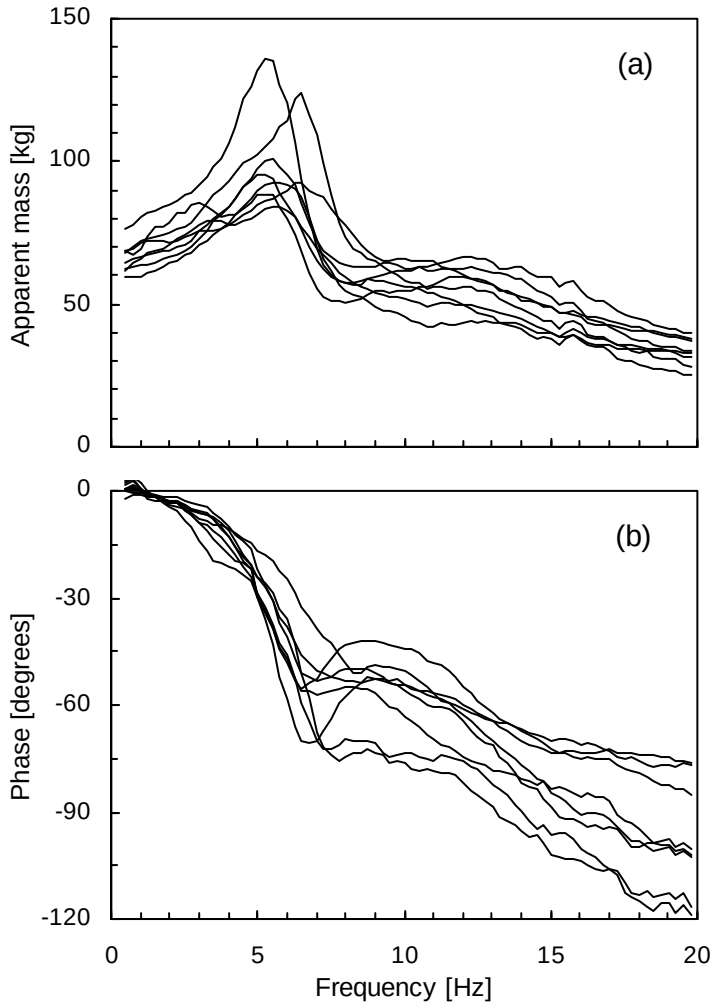

Figure 7.7 Apparent masses and phases of the eight subjects in the standing posture.

Table 7.5 Principal peak frequencies in the apparent masses of the eight subjects in the standing posture.

Subject	1	2	3	4	5	6	7	8
Frequency [Hz]	5.50	5.50	6.25	5.25	5.50	6.50	5.25	5.50

Figure 7.8 shows the transmissibilities from the vertical floor vibration to the vertical motion at each measurement location, except at the knee, in the standing posture with a vibration magnitude of 1.0 ms^{-2} r.m.s.

Variability in the vertical transmissibilities between subjects when standing was large for the head, the locations over the lumbar spine and the pelvis, which was a similar trend to when sitting (see Figures 7.2 and 7.8). Most vertical transmissibilities to the thoracic spine have a peak in the frequency region of the principal resonance frequency of the apparent mass (± 0.25 Hz), while peak frequencies of the transmissibilities to the lumbar spine tend to be higher than the principal resonance frequency of the apparent mass for some subjects. For six subjects whose principal resonance frequency of the apparent mass was lower than 6 Hz, the transmissibility was maximum at L5 at the principal resonance frequency of the apparent mass. For the other two subjects whose principal resonance frequency was higher than 6 Hz, the transmissibility was maximum at the pelvis. In the frequency range around the principal resonance, the vertical transmissibilities to the lumbar spine, in particular to L5, and to the pelvis in the standing posture were much greater than those in the sitting posture, while those to T5 and T10 were similar in both postures (Figures 7.2 and 7.8). The vertical transmissibility at the principal resonance frequency of the apparent mass was found to reduce over the region from L5 to T10 by between about 30% and 65% for each eight subjects. A second peak in the vertical transmissibility to L5 and the pelvis in the frequency range between 7 and 10 Hz was clearly seen for five subjects.

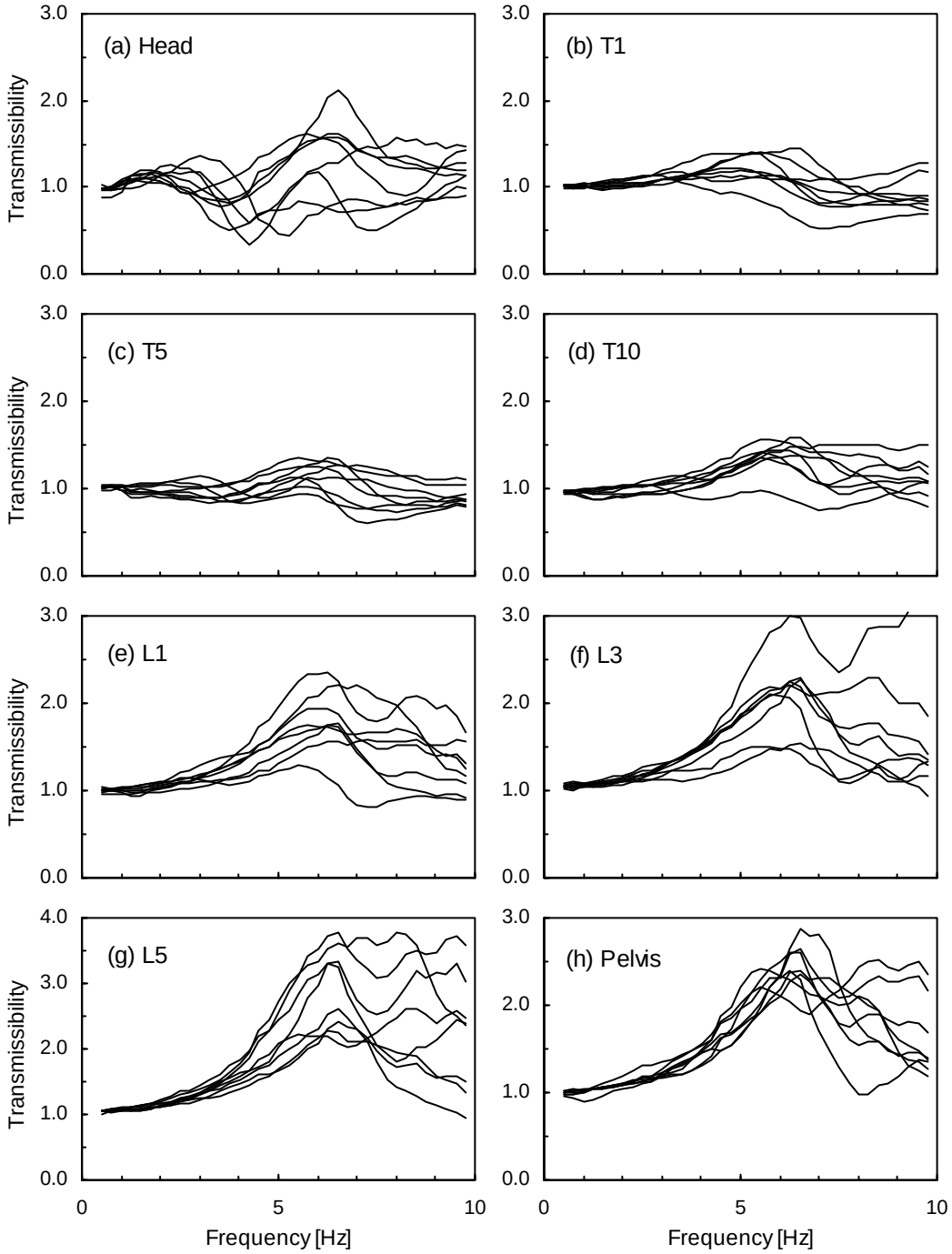

Figure 7.8 Vertical transmissibilities to each measurement location for the eight subjects in the standing posture.

The transmissibilities from the vertical floor vibration to the fore-and-aft motion at each measurement location, except at the knee, in the standing posture are shown in Figure 7.9. The fore-and-aft transmissibilities to all locations, except to the head and T1, were smaller than the vertical transmissibilities in the standing posture, as expected. The fore-and-aft transmissibilities to the head and T1 had a peak between 4.5 and 6.5 Hz for most subjects. These frequencies were within ± 0.25 Hz of the principal resonance frequency of the apparent mass for four subjects. The peak frequency of the fore-and-aft transmissibility to T1 in the standing posture was found to be less than that in the sitting posture for seven subjects ($p < 0.05$). The peak frequency of the fore-and-aft transmissibility to T1 also appeared to be less than the peak frequency of the fore-and-aft transmissibility to the head ($p < 0.05$). It seemed that the fore-and-aft transmissibilities to L3 in the standing posture were greater than those to the other locations over the spine, except to T1.

Figure 7.10 shows the transmissibilities from the vertical floor vibration to the pitch motion at each measurement location in the standing posture. Inter-subject variability in the pitch transmissibilities was large at some locations, in particular, at the lower lumbar spine in the standing posture: some subjects showed a great peak at about 6.5 Hz while others did not. Most pitch transmissibilities to locations over the spine increased with increasing frequency above 3 or 4 Hz with some local peaks. The pitch transmissibilities to the head in the standing posture had a clear peak at between 4.5 and 5.5 Hz, lower frequencies than for the corresponding motions in the sitting posture ($p < 0.05$). The first peak frequencies of the pitch transmissibilities to T1 in the standing posture ranged between 5.25 and 6.5 Hz for the eight subjects, which were also lower than those in the sitting posture ($p < 0.05$). The first peak frequencies of the pitch transmissibilities to the head tended to be lower than those to T1 ($p < 0.05$). The magnitudes of the peaks seen at the head were greater than those at T1 for six subjects in the standing posture ($p < 0.05$). The magnitudes of the peaks seen both at the head and at T1 were greater in the sitting posture than in the standing posture ($p < 0.05$). The pitch transmissibilities to other locations showed similar trends in the standing and sitting postures, except for those to L5 (Figures 7.4 and 7.10). As mentioned above, there was much larger inter-subject variability in the standing posture and some subjects showed a much greater peak transmissibility when standing than when sitting.

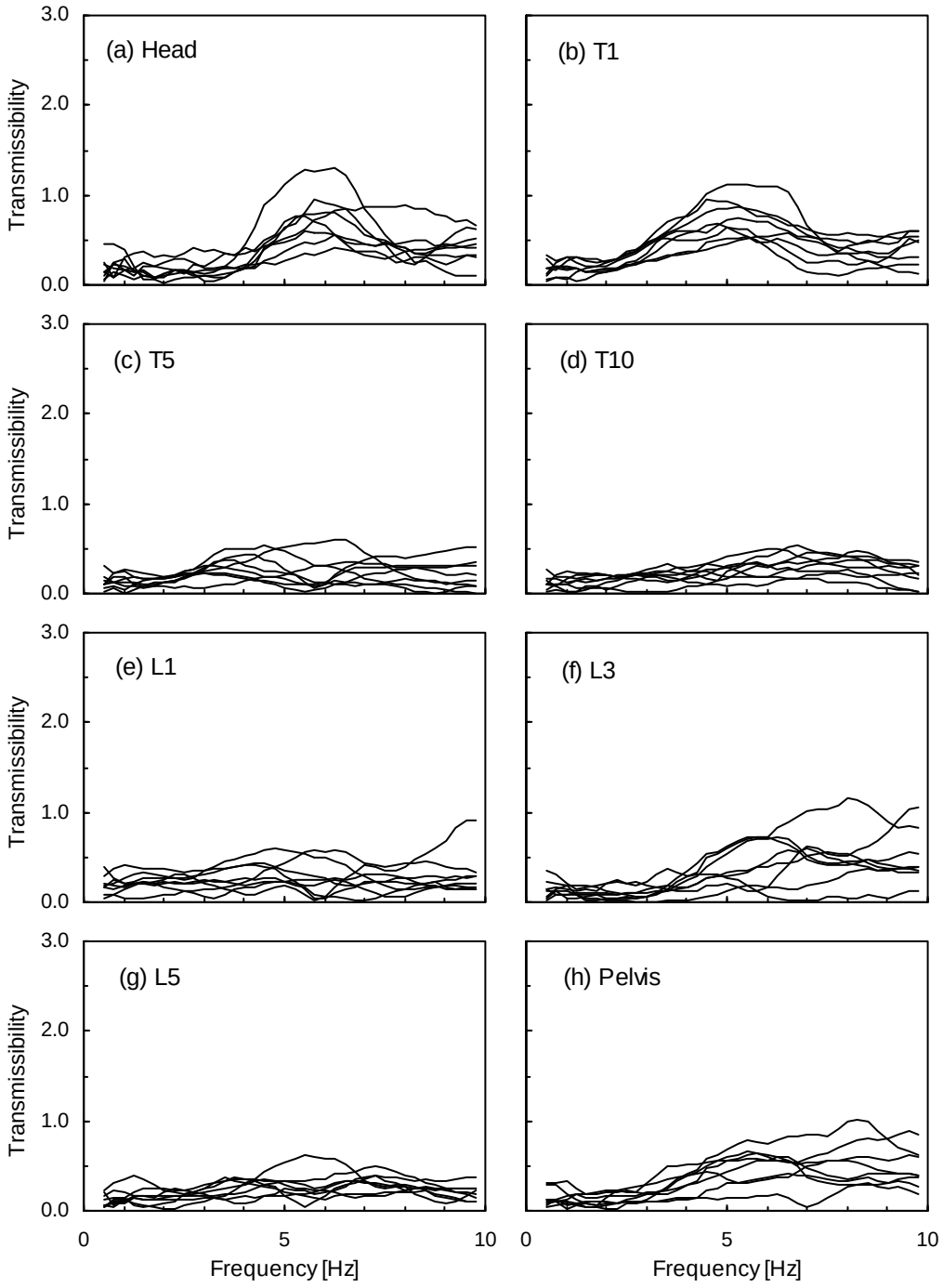

Figure 7.9 Fore-and-aft transmissibilities to each measurement location for the eight subjects in the standing posture.

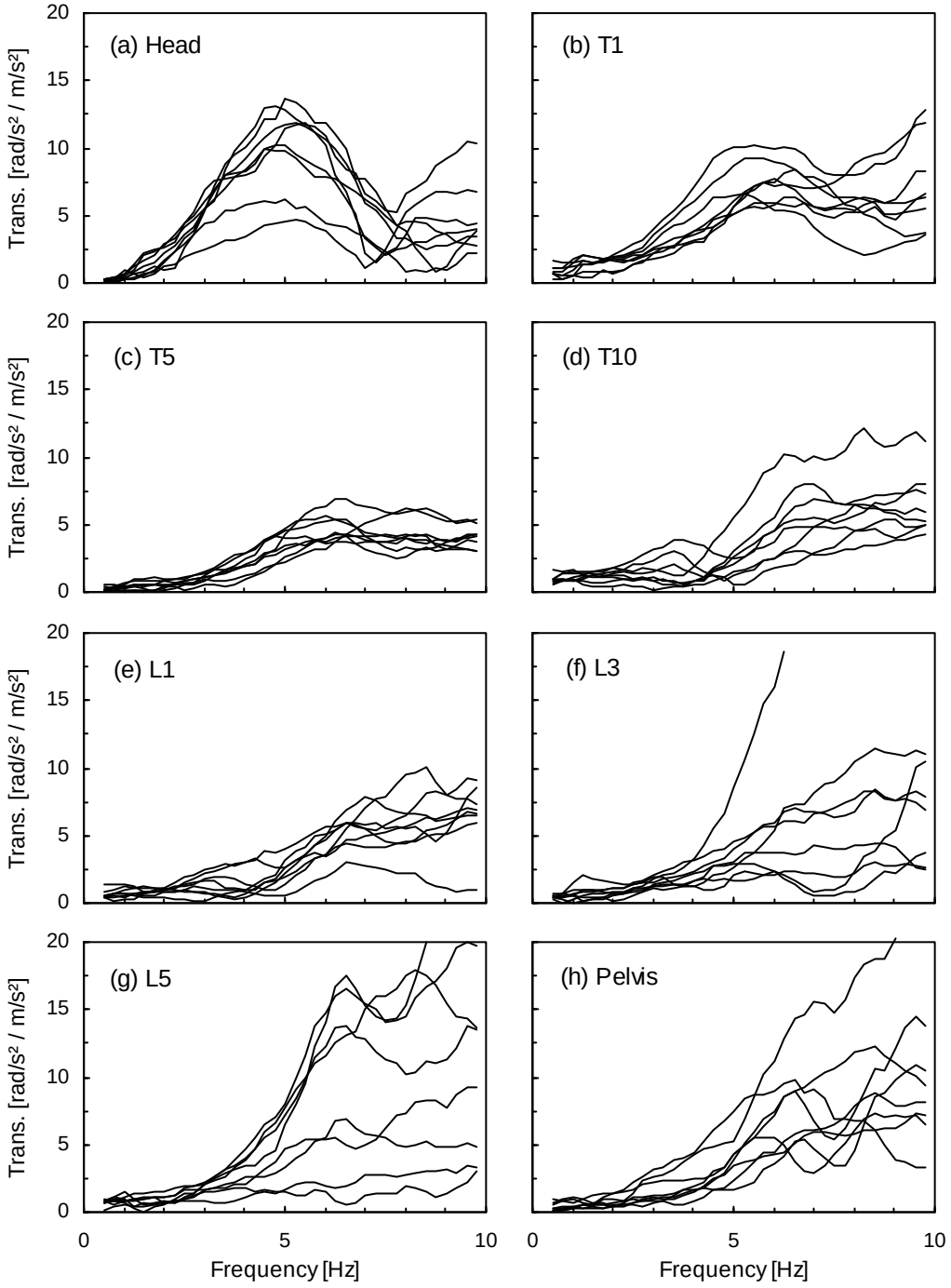

Figure 7.10 Pitch transmissibilities to each measurement location for the eight subjects in the standing posture.

The transmissibilities to the knee in the vertical and fore-and-aft axes in the standing posture are shown in Figure 7.11. In the vertical transmissibilities, six subjects showed a similar trend: the transmissibility increased slightly with increasing frequency. There was no clear peak in the vertical transmissibility to the knee at frequencies below 10 Hz. One subject shows a higher transmissibility, about 2.2, at about 10 Hz, compared to the other subjects, about 1.5. The transmissibilities from vertical floor vibration to the fore-and-aft motion at the knee showed a peak in the frequency range from 5.75 and 8.0 Hz, although large inter-subject variability can be seen. In the fore-and-aft direction, the transmissibilities to the knee tended to be greater than those at the other locations at the principal resonance frequency of the apparent mass.

Using the vertical and fore-and-aft transmissibilities obtained above, the movement of the body at the principal resonance frequency for each subject can be illustrated, as for seated subjects presented in the previous section. The moduli and phases of the transmissibilities at the resonance frequencies of all subjects used to illustrate the movement of the upper-body are tabulated in Table 7.6. In the standing posture, the vertical motion was found to be greatest at L5 for six subjects but greatest at the pelvis for the other two subjects, as stated above. The phase difference of the vertical motion with respect to the floor vibration was greatest in the lower upper body region (i.e. either at L3, at L5, or at the pelvis). The phase difference at T1 tended to be larger than that at other locations over the thoracic spine. The lowest transmissibility in the vertical axis in the upper-body was found either at the head, at T1, or at T5. The vertical transmissibilities at the knee tended to have almost the same magnitude as the lowest transmissibilities in the upper-body, although the data are not shown in Table 7.6. In the

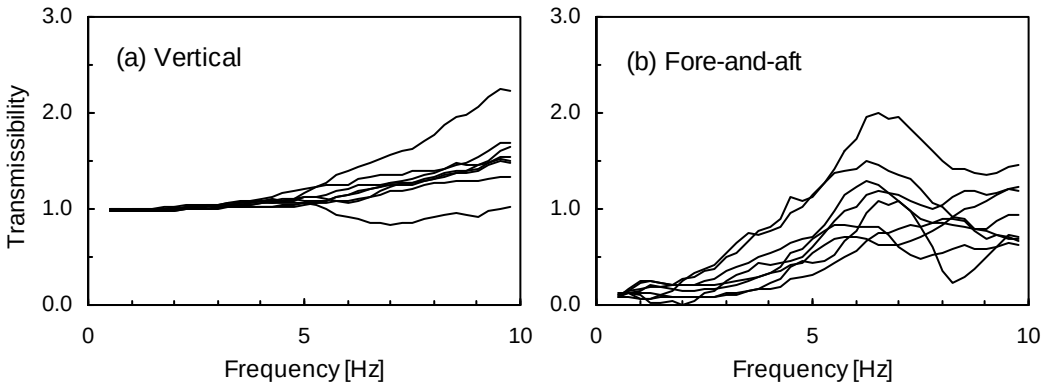

Figure 7.11 Vertical and fore-and-aft transmissibilities to the knee for the eight subjects in the standing posture.

fore-and-aft direction, the head motion tended to be greatest at the principal resonance frequency. The fore-and-aft motion at T1, which had a similar magnitude to that at the head, tended to be out of phase with the fore-and-aft motion at T10.

Figures 7.12 and 7.13 show a cycle of the movement of all measurement points on the upper-body in the standing posture, using Subjects 5 and 7 as examples, at the principal

Table 7.6 Modulus and phase of the transmissibilities to all measurement points in vertical and fore-and-aft axes at the principal resonance frequency of the apparent mass in the standing posture at 1.0 ms^{-2} r.m.s.

	Subject 1, 5.5 Hz		Subject 2, 5.5 Hz		Subject 3, 6.25 Hz		Subject 4, 5.25 Hz	
	Vertical		Vertical		Vertical		Vertical	
	Modulus	Phase	Modulus	Phase	Modulus	Phase	Modulus	Phase
Head	1.416	-14.77	0.539	-35.38	1.282	-7.42	0.976	-7.28
T1	1.168	-24.49	1.127	-22.38	1.100	-19.65	1.404	-26.52
T5	1.245	-17.35	1.069	-9.29	1.252	-9.38	1.116	-17.52
T10	1.418	-22.43	1.308	-18.65	1.475	-15.87	1.355	-16.10
L1	1.655	-30.87	1.946	-27.23	1.571	-20.57	2.132	-26.64
L3	2.012	-37.67	1.510	-24.15	1.526	-28.76	2.450	-27.78
L5	2.078	-34.86	3.136	-40.67	2.279	-48.31	2.879	-24.28
Pelvis	1.913	-35.49	2.421	-38.27	2.376	-50.80	2.153	-20.14
	Fore-and-aft		Fore-and-aft		Fore-and-aft		Fore-and-aft	
	Modulus	Phase	Modulus	Phase	Modulus	Phase	Modulus	Phase
Head	0.474	4.60	0.810	54.86	0.834	23.07	0.757	112.10
T1	0.528	39.83	0.541	96.35	0.734	79.92	0.626	111.63
T5	0.103	21.89	0.128	-178.88	0.295	84.85	0.132	-164.04
T10	0.340	-116.05	0.277	-145.67	0.188	-177.05	0.286	-90.30
L1	0.555	-152.19	0.162	-51.82	0.259	-123.88	0.143	-22.59
L3	0.680	-157.74	0.717	-41.52	0.435	-156.80	0.167	13.69
L5	0.623	-136.62	0.282	-9.65	0.404	-88.00	0.238	21.40
Pelvis	0.657	-108.71	0.777	-49.03	0.374	-147.14	0.136	4.00
	Subject 5, 5.5 Hz		Subject 6, 6.5 Hz		Subject 7, 5.25 Hz		Subject 8, 5.5 Hz	
	Vertical		Vertical		Vertical		Vertical	
	Modulus	Phase	Modulus	Phase	Modulus	Phase	Modulus	Phase
Head	0.830	-23.89	2.121	-35.73	1.373	-16.34	1.604	-19.36
T1	0.847	-32.28	1.457	-49.36	1.193	-28.09	1.402	-22.39
T5	0.943	-20.00	1.337	-24.25	1.007	-0.69	1.345	-13.69
T10	0.978	-17.06	1.590	-25.10	1.319	-11.67	1.565	-24.11
L1	1.282	-29.18	1.765	-40.21	1.788	-24.54	1.719	-24.55
L3	2.025	-44.35	2.267	-50.38	1.976	-29.83	2.156	-32.57
L5	2.832	-42.41	2.430	-53.30	2.233	-25.19	2.229	-35.63
Pelvis	2.185	-49.85	2.869	-58.89	1.821	-28.81	2.204	-38.32
	Fore-and-aft		Fore-and-aft		Fore-and-aft		Fore-and-aft	
	Modulus	Phase	Modulus	Phase	Modulus	Phase	Modulus	Phase
Head	0.591	30.24	1.221	-48.21	0.735	57.62	0.346	38.68
T1	0.728	65.94	1.024	-11.89	0.874	65.68	0.514	67.11
T5	0.163	72.52	0.607	-38.19	0.035	163.61	0.272	16.87
T10	0.459	-110.67	0.517	-92.61	0.255	-100.10	0.093	-66.52
L1	0.531	-76.87	0.194	-48.62	0.229	-106.42	0.194	-23.65
L3	0.186	-42.00	0.584	123.26	0.657	173.07	0.184	144.27
L5	0.161	-15.88	0.161	142.85	0.107	-121.40	0.188	-21.03
Pelvis	0.574	-43.11	0.410	-78.13	0.588	170.02	0.518	-58.54

resonance frequencies of 5.5 Hz and 5.25 Hz, respectively. The movement of the upper-body at the resonance frequencies in the sitting posture are shown in Figures 7.5 and 7.6 for the same two subjects. As in Figures 7.5 and 7.6, the body was viewed from the right hand side and a cycle is divided into eight equal intervals: (a) t = 0, the floor is at the initial position; (c) $t = T/4$ (where T is the period of the floor vibration), the floor is at the highest position; (e) t = T/2, the floor has returned to the initial position; (g) $t = 3T/4$, the floor is at the lowest position. For illustration, the displacement of the floor surface vibration was 0.05 m, as in Figures 7.5 and 7.6 (i.e. the movements shown in the figures are exaggerated). For the standing posture, inter-subject variability in the response of the lower spine at the principal resonance frequency was relatively large, compared to the variability for the sitting posture. In the sitting posture, the movements of the upper-bodies of all subjects, except Subject 2, demonstrated consistent trends with those shown in Figures 7.5 and 7.6. Figures 7.12 and 7.13 show two typical types of behaviour of the lower spine for the subjects when standing.

In the standing posture, bending or rocking motions of the spine appeared to be dominant at the principal frequency of the apparent mass, as in the sitting posture presented in the previous chapter. The movements of the upper thoracic spine, between T1 and T10, in the standing posture were almost identical to those in the sitting posture: rocking about a point on the lower thoracic spine in the sagittal plane, with slight bending along the spine. Bending motion along the spine in the lower thoracic spine and the lumbar spine region, was more significant than in the upper thoracic spine, which was also found in the sitting posture. In this region, much more significant axial relative motion was found to occur in the standing posture than in the sitting posture. In Figure 7.12, axial relative motion in the lumbar spine might be more dominant than bending motion along the spine for that subject (Subject 5). In Figure 7.13, however, axial relative motion in the lumbar and the lower thoracic spine seems to be as dominant as bending motion along the lumbar spine for that subject (Subject 7). Those two types of lower spine motion were found to be typical for the other subjects in the standing posture. Pitch motion of the pelvis and pitch motion of the head also seemed to occur at the principal resonance of the apparent mass.

To visualise the motions in the standing posture mentioned above, consider the movement of the upper-body when the floor moved upward (see Figures 7.12 and 7.13). Backward rocking motion of the upper thoracic spine in phase with a slight extension along the full length of the upper thoracic spine accompanied by forward pitch motion of the head was slightly behind the upward floor motion. The lower spine was compressed with the floor moving upward. Bending motion of the lower spine and movement of the lower part of the upper-body that contributed to the motion of the upper thoracic spine

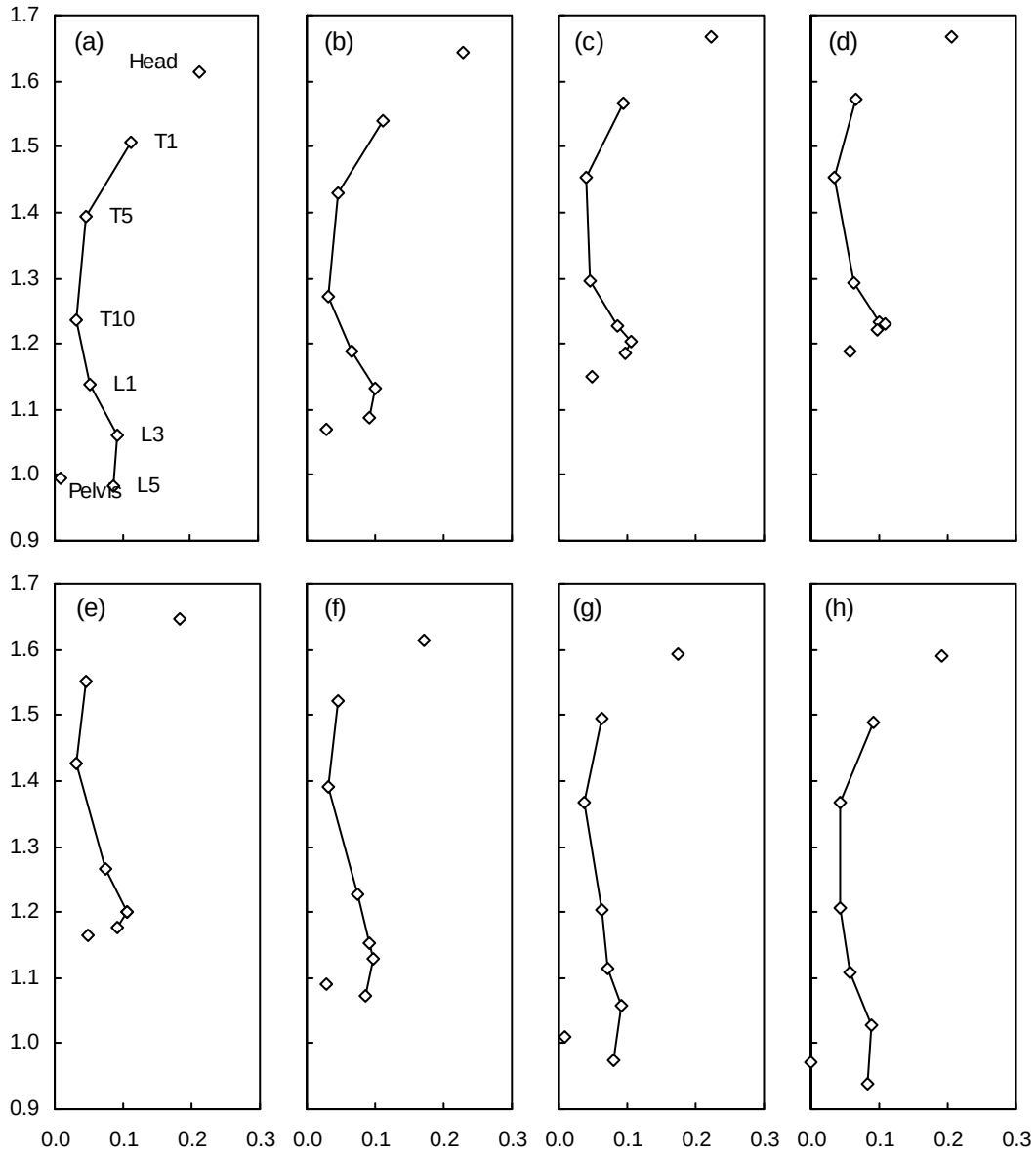

Figure 7.12 Movement of the upper-body at the principal resonance frequency of the apparent mass of Subject 5 in the standing posture at 5.5 Hz: (a) $t = 0$, (b) $t = T/8$, (c) $t = T/4$, (d) $t = 3T/8$, (e) $t = T/2$, (f) $t = 5T/8$, (g) $t = 3T/4$, (h) $t = 7T/8$ (T: period of the floor vibration). (The units of body axes are metres [m]. The scale of the movement is exaggerated for clarity.)

occurred, although it was difficult to characterise because of the variability in the movement among the subjects.

Computer program sources to animate the movements of the upper-body of all the subjects in the standing posture, including those shown above, at the principal resonance frequency of the apparent mass are provided in Appendix E.

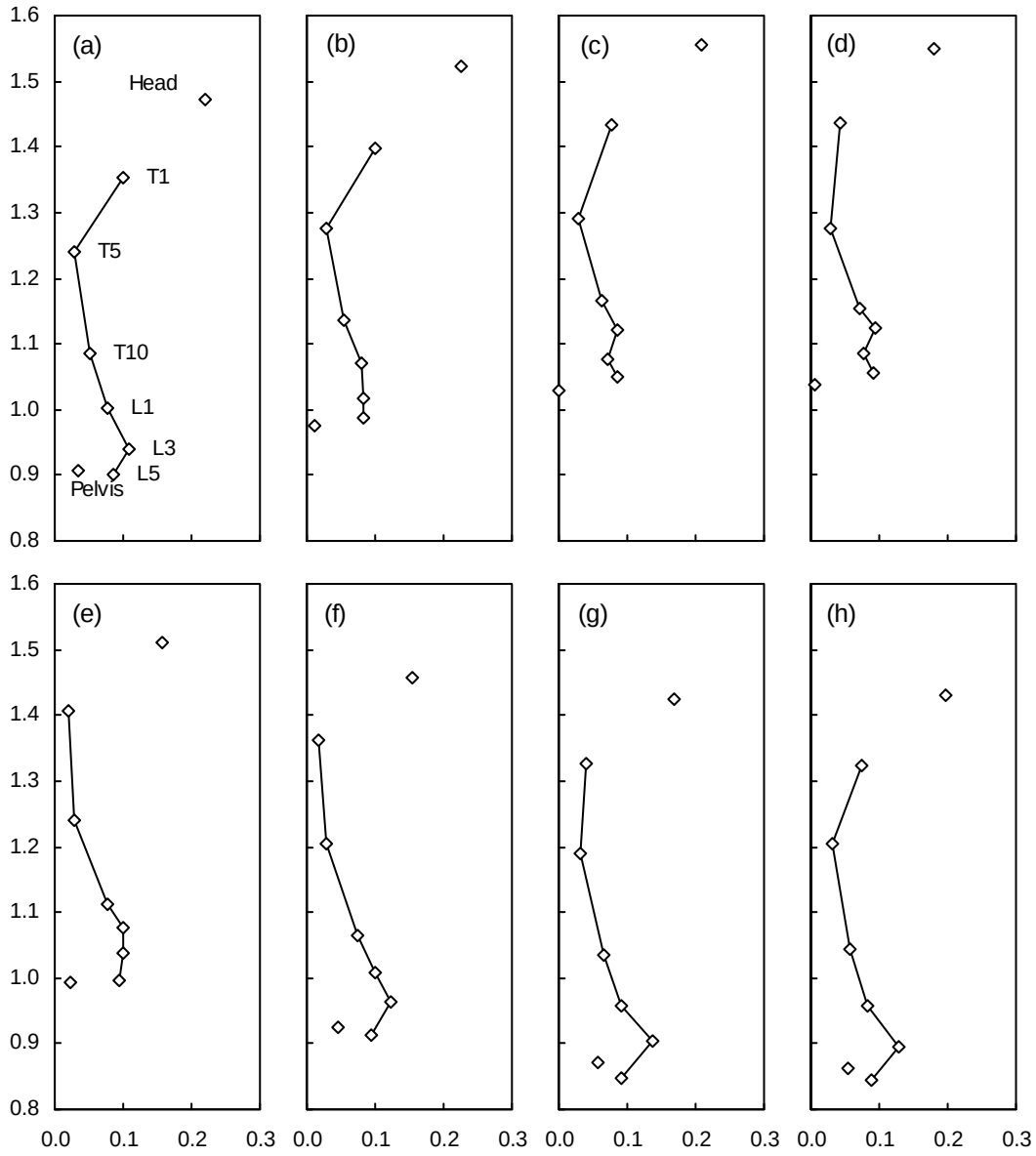

Figure 7.13 Movement of the upper-body at the principal resonance frequency of the apparent mass of Subject 7 in the standing posture at 5.25 Hz: (a) $t = 0$, (b) $t = T/8$, (c) $t = T/4$, (d) $t = 3T/8$, (e) $t = T/2$, (f) $t = 5T/8$, (g) $t = 3T/4$, (h) $t = 7T/8$ (T: period of the floor vibration). (The units of body axes are metres [m]. The scale of the movement is exaggerated for clarity.)

7.4 DISCUSSION

7.4.1 Discussion of seated position

This study indicates that a combination of bending and rocking motions of the spine are involved in the principal resonance of the apparent mass of seated people. Bending of the spine has been suggested in some previous studies. Sandover and Dupuis (1987) suggested that the resonances observed during human response to vibration were related to bending in the lumbar spine and possibly a rocking motion of the pelvis. The vertical, fore-and-aft, and angular (pitch) motions at the centroid of T12, L2 and L4 were resolved, and demonstrated resonant behaviour at about 4 Hz. However, the cinematographic technique was found to have insufficient accuracy to measure relative vertical motion between adjacent vertebrae at around the resonance frequency. The measured angular motion, and the calculated relative angular motion between adjacent vertebrae which were greatest at the lower lumbar spine, supported their hypothesis. This is consistent with the present study in which the transmissibility from the seat vertical vibration to pitch motion at L5 was the greatest in the lumbar region at the principal resonance frequency ($p < 0.05$, see Figure 7.4).

Bending motion of the lumbar spine at 4.5 Hz was also suggested by Hinz *et al*. (1988b), using measurements on the body surface over the spinous process of L3 and L4 in the vertical direction (parallel with the body surface) and in the fore-and-aft direction (orthogonal to the surface), together with measurements at the head and the acromion. It was stated that the relative vertical accelerations between L3 and L4 found at 4.5 Hz were mainly caused by bending of the spine, based on a relative angular motion between adjacent vertebrae of 0.6º peak-to-peak per 1 ms^{-2} r.m.s. seat vibration at 4.5 Hz as reported by Sandover and Dupuis (1987).

Assuming that between the measurement points the spine was straight, as in Figures 7.5 and 7.6, the relative angular motions between adjacent ‘straight’ spines at T5, T10, L1 and L3 were calculated using simulated time histories for the locations of the ends of each ‘straight’ spine where the motion was measured (Figure 7.14). Table 7.7 shows peak-to-peak relative angular displacements with the sinusoidal seat vibration at the resonance frequency of the apparent mass at a magnitude of 1.0 ms^{-2} r.m.s. The phases with respect to the seat vibration were also obtained from the time lag between

Table 7.7 Simulated peak-to-peak relative angular displacements between adjacent 'straight' spines at the resonance frequency of the apparent mass with sinusoidal seat acceleration of 1.0 ms^{-2} r.m.s. in the sitting posture. (The phases were obtained by the time lag between the maximum seat displacement and the relative angular motion; in degrees.)

	T5		T10		L1		L3	
Subject	angle	phase	angle	phase	angle	phase	angle	phase
1	0.49	-5	1.33	-134	0.81	18	1.16	-129
2	0.19	-28	0.79	-102	0.41	-96	0.59	98
3	0.27	-92	0.41	-28	1.80	-127	1.43	50
4	0.06	84	1.03	-42	1.23	-161	0.99	27
5	0.52	-83	0.34	-45	1.27	-131	0.89	37
6	0.53	-62	0.86	-95	0.75	170	1.15	21
7	0.55	-99	0.29	-76	2.01	-137	1.22	27
8	0.38	-114	0.52	-102	1.06	-156	0.90	3

maximum displacement in the seat vibration and the relative angular motion. The magnitude of the calculated relative angular motions agreed with those reported by Sandover and Dupuis (1987) but were slightly larger than those reported by Pope *et al*. (1991) who measured the intervertebral motion either between L3 and L4 or between L4 and L5 by means of a device with extensometers, called an intervertebral motion device, mounted skeletally. The values obtained in the lumbar region in this study could be considered as approximations to the relative angular motion between two vertebrae which are adjacent to the vertebra where the motion was measured: the calculated relative angular motion at L1 was that between T12 and L2 which may have mainly caused by bending of the spine. However, the values reported in the previous studies were obtained from two adjacent vertebrae and could include individual pitch motion of the vertebral bodies which did not result from bending of the spine. The relative angular motion tended to be greatest at L1, although variability between subjects was found. The relative angular motion at L1 was almost out of phase with that at L3, which implies that the spine in this region tended to move in an S-shape. This may be dependent on the initial curvature of the spine.

In Table 7.7, it is shown that the relative angular motion at T5 was smaller than at the other positions on the lower spine ($p < 0.05$), which implies that bending motion of the upper thoracic spine was less significant than that in the lower spine, as seen in Figures 7.5 and 7.6. It is likely that, at the resonance frequency, rocking about a point on the

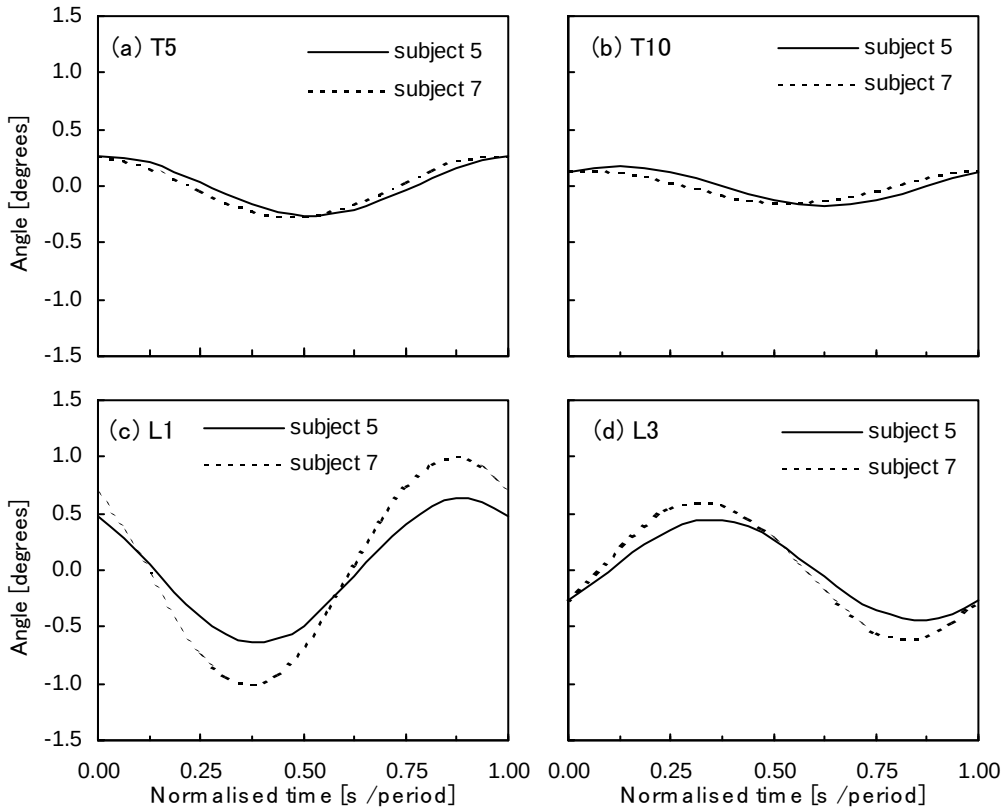

Figure 7.14 Simulated relative angular motions between adjacent 'straight' spines at T5, T10, L1 and L3 for Subjects 5 and 7 in the sitting posture whose movement of the upper-body is shown in Figures 7.5 and 7.6. (With sinusoidal seat vibration at the resonance frequency of the apparent mass at a magnitude of 1.0 ms^{-2} r.m.s.)

lower thoracic spine was dominant. The rib cage connected to the thoracic spine in this region may restrict bending motion. The rocking of the upper-thoracic spine coupled with the bending of the lumbar spine may cause the maximum fore-and-aft transmissibility at T1, at the resonance frequency for all subjects, as shown in Table 7.4.

Kitazaki (1994) and Kitazaki and Griffin (1997, 1998) found bending modes of the spine at frequencies close to the principal resonance frequency, although it was concluded that there was no main contribution of any bending motion of the spine to the principal resonance. In their experimental study (Kitazaki, 1994; Kitazaki and Griffin, 1998), it was found that a bending mode of the upper thoracic spine and the cervical spine was contained in the fourth mode at 4.9 Hz which was close to the principal resonance frequency. The fifth mode at 5.6 Hz was found to consist of a bending mode of the lumbar spine and lower thoracic spine and a pitching mode of the head. A bending mode of the entire spine was extracted in the fifth mode of their mathematical model at 5.77 Hz (1994, 1997). The fourth mode at 5.06 Hz also seemed to contain a bending

mode of the lower thoracic spine, although it was not stated. The nature of heavy damping of the human body makes it difficult to determine the extent of the contributions of each vibration mode to the principal resonance, especially when the modes are closely located as in the case of these studies: heavy damping tends to cause closely located modes couple with each other. In addition, it is usually difficult to determine the damping properties of mechanical systems and there is no reliable data on the damping properties of the human body segments. The bending modes of the spine which were found at frequencies close to the principal resonance in those studies may therefore have made some contribution to the principal resonance.

It seems that a pitching motion of the pelvis occurred together with bending of the lumbar spine at the resonance frequency. Pope *et al*. (1990) measured the vertical motion of L3 with an accelerometer attached to a *K*-wire threaded into the spinous process while controlling subjects' posture and muscle tension, together with a pelvis support. The transmissibility to L3 showed a marked peak at 5 Hz, coupled with an attenuation at about 8 Hz, in a reference posture (relaxed), which was altered by changes in the experimental conditions so as to affect 'the behaviour of the biological vertical spring and damper system between the pelvis and the seat'. This supported their suggestion that 'the first natural frequency was due to the biological subsystems between the L3 level and the seat'. They also reported that the rotational responses of the pelvis and of the head were likely to be more dominant at about 8 Hz.

Mansfield and Griffin (1997) and Mansfield (1998) measured the rotation of the pelvis in nine postures and demonstrated that the transmissibilities between seat vertical motion and pelvis pitch rotation were greatest in the frequency range from 10 to 18 Hz. No significant differences in the transmissibilities between the seat vertical vibration and the pelvis rotation were found in the 4 to 7 Hz frequency range among the different postures. It was concluded that the pelvis rotation did not contribute to previously reported changes in the 5 Hz apparent mass resonance frequency caused by postural changes.

In the present study, the transmissibility from the vertical seat vibration to the pelvis pitch vibration increased as the frequency increased: six subjects showed a local peak at frequencies between 5.75 and 7.25 Hz, which were higher than the principal resonance frequency of their apparent mass. The main peak might be located at higher frequencies as reported by Mansfield and Griffin (1997) and Mansfield (1998). The transmissibility from the seat vertical vibration to the pelvis pitch vibration at the principal resonance

frequency of the apparent mass tended to be greater than that to the pitch motion of L5; the difference was found to be statistically significant ($p < 0.05$) when excluding one subject who showed a different trend in the upper-body movement from the others. However, the difference in the phases of the pitch transmissibilities to the pelvis and to L5 at this frequency was not significant, although the pelvis pitch was expected to be ahead of the pitch of L5 if the pelvis pitch caused the bending of the lumbar spine. Therefore, it was not clear whether the pitch of the pelvis was a cause of the lumbar spine bending or a secondary effect, although the local resonance of the pelvis in pitch occurred at a consistently higher frequency than the resonance frequency of the apparent mass.

Kitazaki (1994) and Kitazaki and Griffin (1997, 1998) found a rotational mode of the pelvis with a second visceral mode in their sixth and seventh modes at about 8 Hz, which might have contributed to the second principal resonance in the driving point response. Possibly, a rotational mode of the pelvis may make a minor contribution to the principal resonance at about 5 Hz if there is heavy damping on the mode, as with bending modes of the spine as suggested above.

Kitazaki (1994) and Kitazaki and Griffin (1997, 1998) also pointed out the axial and shear deformation of the tissue beneath the pelvis may contribute to the resonance of the apparent mass at about 5 Hz, and this may explain the shift of the resonance frequency due to postural changes. The vertical transmissibilities to L5 and to the pelvis at the resonance frequency found in this study would be consistent with some local dynamic mechanism between the seat and the level of L5 and the posterior-superior iliac spine. Possibly, the tissue beneath the pelvis contributed the increased motion at the lower part of the upper body and, consequently, the resonance of the apparent mass. The fore-and-aft motion at L5 at this frequency was small in spite of the pitch of the pelvis, as seen in Figures 7.5 and 7.6. It might be hypothesised that at the resonance frequency the pelvis slides backward during forward pitch motion, with deformation of the tissue beneath, and moves forward during backward pitch motion, so as to leave the fore-and-aft motion at L5 small.

From Figures 7.5 and 7.6 and the results from the other subjects, it is concluded that any pure axial motions along the spine were not dominant at the resonance frequency, as stated by Kitazaki (1994) and Kitazaki and Griffin (1997, 1998), although slight compression and expansion between measurement points on the spine can be seen in Figures 7.5 and 7.6. Table 7.8 shows peak-to-peak relative motions between adjacent

measurement points on the spine, calculated using simulated time histories for the measurement locations. The measurements have been divided by the number of intervertebral discs between adjacent measurement points so as to indicate the approximate change in the distance between the centres of adjacent vertebral bodies. A sinusoidal seat vibration at the resonance frequency with a magnitude of 1.0 ms^{-2} r.m.s. was used in the calculation (i.e. a peak-to-peak displacement of approximately 2.9 mm at 5 Hz). All calculated values were below 0.4 mm peak-to-peak, except one which appeared to be much greater than the others. Although the variability between subjects and between measurement locations was large, the order of the simulated values was consistent with experimental data reported by Pope *et al*. (1991) which also show variability. Pure axial motions along the spine were found to be greater at higher frequencies, although the data are not shown here. It can be hypothesised that the dynamic response of the motion segments of the spine at the resonance frequency consisted of coupled translational and rotational motion in the sagittal plane, as Hinz *et al*. (1988b) and Pope *et al*. (1991) concluded. It is likely, however, that rotational motion is more dominant at this frequency such that coupled bending and rocking of the spine might be more significant as seen in Figures 7.5 and 7.6. The two initial curvatures of the spine, and the eccentricity of the weight of the upper-body with respect to the main vibration transmission path of the body in the vertical direction, may contribute to those dynamic mechanisms of the spine.

The movement of the upper-body of a seated subject at the principal resonance frequency in the apparent mass, as illustrated in this study, may be associated with more than one dynamic mechanism of the body. It might be hypothesised that, at the principal resonance frequency, a bending motion of the spine, a rocking motion of the thoracic spine, a motion involving axial and shear deformation of the tissue beneath the pelvis, and a pitch motion of the pelvis are coupled with each other due to the heavy damping properties of the human body. As Kitazaki (1994) and Kitazaki and Griffin (1997, 1998) found, the vibration mode of the viscera, which could be coupled with spinal motion, might also contribute to the resonance, although the motion of the viscera was not measured in this study.

Table 7.8 Simulated peak-to-peak relative displacements between adjacent measurement points on the spine divided by the number of intervertebral discs between adjacent measurement points. In the standing posture. (A sinusoidal seat vibration at the principal resonance frequency with an acceleration of 1.0 ms^{-2} r.m.s. was assumed; in millimetres [mm].)

	T1 - T5	T5 - T10	T10 - L1	L1 - L3	L3 - L5
Subject 1	0.114	0.006	0.170	0.159	0.148
Subject 2	0.097	0.112	0.021	0.064	0.859
Subject 3	0.039	0.059	0.134	0.192	0.277
Subject 4	0.188	0.155	0.205	0.126	0.026
Subject 5	0.026	0.081	0.092	0.336	0.379
Subject 6	0.245	0.179	0.096	0.230	0.187
Subject 7	0.237	0.148	0.308	0.130	0.220
Subject 8	0.215	0.063	0.166	0.377	0.239

7.4.2 Discussion of standing position

The results described in Section 7.3.2 implied that bending motion of the spine may be one of the dominant mechanisms contributing to the principal resonance of the apparent mass in the normal standing posture, as in the sitting posture. Assuming that the spine was straight between the measurement points, the relative angular motions between adjacent 'straight' spines at T5, T10, L1 and L3 were calculated using simulated time histories for the locations of the ends of each 'straight' spine for the standing posture. Peak-to-peak relative angular displacements in the standing posture with the sinusoidal floor vibration at the principal resonance frequency of the apparent mass at 1.0 ms^{-2} r.m.s. are shown in Table 7.9. Those calculated for the sitting posture were presented in Table 7.7.

The relative angular motion was greatest at L3 for six subjects in the standing posture ($p < 0.05$), while it tended to be greatest at L1 in the sitting posture. In the sitting posture, the relative angular motion at L1 was almost out of phase with that at L3, which implies that the spine in this region moved in an S-shape. However, this characteristic is not clear in the standing posture. The relative angular motions at T10 and at L1 tended to be less in the standing posture than in the sitting posture ($p = 0.123$ for T10 and $p = 0.050$ for L1). The relative angular motion at T5 was less than at the other positions on the

Table 7.9 Simulated peak-to-peak relative angular displacements between adjacent 'straight' spines at the resonance frequency of the apparent mass with sinusoidal seat acceleration of 1.0 ms^{-2} r.m.s. in the standing posture. (The phases were obtained by the time lag between the maximum seat displacement and the relative angular motion; in degrees.)

	T5		T10		L1		L3	
Subject	angle	phase	angle	phase	angle	phase	angle	phase
1	0.19	-14	0.45	-136	0.15	-8	0.79	29
2	0.42	-91	0.68	-7	0.54	77	2.37	-130
3	0.17	-94	0.26	29	0.88	-154	1.43	13
4	0.53	-94	0.69	-41	0.49	174	0.26	171
5	0.27	-44	0.74	-17	0.92	-114	0.49	162
6	0.37	-42	0.65	-46	0.86	-156	1.69	56
7	0.90	-63	0.26	-77	1.55	-156	2.98	21
8	0.52	-123	0.49	-15	0.94	-165	1.46	24

lumbar spine ($p < 0.05$), which was also found in the sitting posture. It may be implied that the rig cage connected to the thoracic spine restricts the relative motions between vertebrae in this region for both standing and seated bodies.

The most significant difference in the movement of the upper-body at the principal resonance frequency of the apparent mass between when standing and when sitting was the behaviour of the lower thoracic and lumbar spine, as seen in Figures 7.5 and 7.6 and in Figures 7.12 and 7.13. In the standing posture, a more significant axial motion can be seen in the lumbar region (Figures 7.12 and 7.13), while any pure axial motions along the spine were not dominant in the sitting posture (Figures 7.5 and 7.6). Table 7.10 shows peak-to-peak relative motions between adjacent measurement points on the spine in the standing posture, calculated from simulated time histories. Those in the sitting posture were shown in Table 7.8. The measurements have been divided by the number of intervertebral discs between adjacent measurement points so as to indicate the approximate change in the distance between the centres of adjacent vertebral bodies. A sinusoidal floor vibration at the resonance frequency with a magnitude of 1.0 ms^{-2} r.m.s. was used in the calculation (i.e. a peak-to-peak displacement of approximately 2.4 mm at 5.5 Hz).

In the standing posture, simulated peak-to-peak relative displacements at the principal resonance frequency reached as much as about 1.0 mm in the lower spine region,

Table 7.10 Simulated peak-to-peak relative displacements between adjacent measurement points on the spine divided by the number of intervertebral discs between adjacent measurement points. In the standing posture. (A sinusoidal seat vibration at the principal resonance frequency with an acceleration of 1.0 ms^{-2} r.m.s. was assumed; in millimetres [mm].)

	T1 - T5	T5 - T10	T10 - L1	L1 - L3	L3 - L5
Subject 1	0.007	0.093	0.280	0.495	0.180
Subject 2	0.028	0.142	0.503	0.673	2.008
Subject 3	0.073	0.099	0.068	0.194	0.923
Subject 4	0.110	0.119	0.719	0.419	0.597
Subject 5	0.056	0.037	0.257	1.070	0.921
Subject 6	0.195	0.096	0.314	0.601	0.236
Subject 7	0.240	0.205	0.505	0.443	0.463
Subject 8	0.081	0.164	0.104	0.663	0.204

below T10, except that between L3 and L5 for Subject 2 which appeared to be much greater than the others. In the sitting posture, however, all calculated values were below 0.4 mm, except that between L3 and L5 for Subject 2 which also appeared to be much greater than the others. The calculated relative displacements between two vertebrae in the region between T10 and L5 were greater in the standing posture than in the sitting posture ($p < 0.05$). There have not been found significant differences in the magnitude of the relative displacements in the upper thoracic region between the standing and sitting postures. It can be hypothesised that the movement of the motion segments of the spine at the resonance frequency consisted of coupled translational and rotational motion in the sagittal plane. It is likely that rotational motion is more dominant in the sitting posture such that coupled bending and rocking of the spine might be more significant as seen in Figures 7.5 and 7.6. However, axial motion as well as rotational motion are dominant in the standing posture, in particular, in the lower thoracic and lumbar regions as seen in Figures 7.12 and 7.13.

Nachemson and Morris (1964) and Nachemson (1981) showed from measurements of intradiscal pressure in the lumbar spine of living subjects that the load on L3 intervertebral disc was about 40% greater in a sitting upright posture than in a standing upright posture. The intervertebral discs in the lumbar region might, therefore, be less compressed and more flexible in the axial direction in the standing posture than in the sitting posture. This may be a possible cause of the observed difference in axial response of the lumbar spine between standing and sitting subjects.

The transmissibility of vertical floor vibration to pelvis pitch motion in the standing posture was found to increase with increasing frequency (Figure 7.10(h)). Pitching motions of the pelvis might, therefore, have occurred together with bending and axial motions of the lumbar spine at the resonance frequency at around 5 or 6 Hz, although the pelvis pitch motion might be more dominant at higher frequencies. As described in Section 6.5, differences in the phase of the pitch transmissibility to the pelvis between the standing and sitting postures were observed, while the phases of the vertical transmissibilities to the pelvis were similar for both postures (see Figure 6.29). It is likely that this difference in the phase of pelvis pitch motion made some contribution to different behaviour of the lower spine between the standing and sitting postures, as seen between Figures 7.5 and 7.6 and Figures 7.12 and 7.13.

The motion of the pelvis might be significantly affected by the motion of the legs. Table 7.11 shows the transmissibilities to the knee in the vertical and fore-and-aft directions at the principal resonance frequency in the apparent mass at 1.0 ms^{-2} r.m.s. for the eight subjects. The vertical transmissibilities to the knee were almost unity at the principal resonance frequency, which was much smaller than the vertical transmissibilities to the lower part of the upper-body. The phases of the vertical transmissibilities were close to zero. Therefore, there might not be any dynamic mechanisms in the lower legs in the vertical direction dominant at the principal resonance frequency. However, in the fore-and-aft axis, relatively large transmissibilities were found at the knee at the principal resonance frequency, compared to those at other locations: greatest fore-and-aft transmissibility was found at the knee for five subjects (see Tables 7.6 and 7.11). The knee tended to move forward when the floor moved upwards, although there was inter-

Table 7.11 Transmissibility to the knee in the vertical and fore-and-aft direction at the principal resonance frequency. (Phases are in degrees.)

	Subject 1, 5.5 Hz		Subject 2, 5.5 Hz		Subject 3, 6.25 Hz		Subject 4, 5.25 Hz	
	Modulus	Phase	Modulus	Phase	Modulus	Phase	Modulus	Phase
Vertical	0.990	-18.77	1.281	1.59	1.098	1.08	1.118	-5.27
Fore & aft	1.384	30.96	0.879	-96.44	0.658	-43.17	0.833	-42.19
	Subject 5, 5.5 Hz		Subject 6, 6.5 Hz		Subject 7, 5.25 Hz		Subject 8, 5.5 Hz	
	Modulus	Phase	Modulus	Phase	Modulus	Phase	Modulus	Phase
Vertical	1.080	-2.30	1.336	-9.68	1.078	-6.85	1.156	-0.15
Fore & aft	1.425	-105.66	1.077	-75.01	0.774	-26.67	0.696	-51.86

subject variability in the phase of the fore-and-aft transmissibility to the knee as in Table 7.11: as large as about 135 degrees for the eight subjects. Rocking motion of the legs about the ankle joints and shear deformation of the tissues beneath the feet may have contributed to the relatively great fore-and-aft transmissibilities to the knee. Bending motion of the legs at the knees might also have occurred, although the subjects were asked to maintain their legs locked.

It is likely, according to the results presented in this chapter, that some dynamic mechanisms contributing to the movement of the upper-body at the principal resonance of the apparent mass are common in standing and sitting positions: a bending motion of the spine, a rocking motion of the thoracic spine, and a pitch motion of the pelvis were observed for both positions. However, more significant axial motions in the lower spine were observed in the movement of the standing body than that in the sitting body at the principal resonance frequency. Rocking motion of the legs about the ankles, shear deformation of the tissues beneath the feet and slight bending motion of the legs at the knees, rather than any dynamic mechanisms of the legs in the vertical direction, might also make some contribution to the motion of the pelvis and, consequently, the movement of the upper-body at the resonance frequency.

7.5 CONCLUSIONS

Movements of the human body in seated and standing positions at the principal resonance frequency of the driving-point apparent mass during exposure to vertical whole-body vibration have been determined using multi-axis transmissibilities to eight locations on the upper-body. Two dimensional motion of the body was observed at the resonance frequency.

For the seated body, the body movements involved translation and rotation within the sagittal plane of the body. The lumbar spine, and probably the lower thoracic spine, tended to bend such that the maximum translational motion caused by the bending occurred in the region around L1, where the spine may deform in an S-shape. The thoracic spine tended to rock about the lower thoracic spine with slight bending along the full length of the thoracic spine; both of these motions were coupled with the bending motion of the lower spine. Pitch motion of the pelvis, which may be accompanied by axial and shear deformation of the tissue beneath the pelvis, also occurred at the resonance frequency, although the pitch resonance of the pelvis occurred at higher

frequencies. Any axial motions along the spine were not dominant at the principal resonance frequency near to 5 Hz.

For the standing body, a combination of appreciable bending and axial motions along the spine was found in the lumbar and lower thoracic region. The thoracic spine whose bending motion might be restricted significantly by the rib cage rocked about a point in the lower thoracic spine which was coupled with a combination of the bending and axial motions of the lower spine. Pitch motion of the pelvis which would have an effect on the response of the lower spine seemed to occur at the principal resonance frequency. Rocking motion of the legs about the ankle joints and slight bending motion at the knee joints were found to be more dominant than any dynamic response of the legs in the vertical direction at the resonance frequency of the apparent mass. It is, therefore, likely that a coupled motion between rotational motions at the ankle, knee and hip joints make some contribution to the upper-body movement of the standing body, although there were found to be a variability in the phase responses among the subjects.

Some dynamic mechanisms of the upper-body may make contributions to the principal resonance of the apparent mass both in the standing and sitting postures. It is hypothesised that more than one dynamic mechanism may contribute to the principal resonance in the apparent mass for the body observed at about 5 Hz. A bending motion of the spine, particularly the lumbar spine, a rocking motion of the thoracic spine and the rib cage, and a pitching motion of the pelvis, which may be coupled with each other due to the heavy damping of the human body, may be involved in the dynamic mechanisms causing the apparent mass resonance in both postures. For the seated body, a motion involving axial and shear deformation of the tissue beneath the pelvis may also contribute to the resonance. For the standing body, an appreciable axial motion in the lower spine may be coupled with the two dimensional motion of the spine and make some contribution to the resonance. A combination of rotational motions at the joints in the lower extremities and deformation of the tissue beneath the feet may be a major dynamic vibration transmission mechanism from the floor to the upper-body at the resonance frequency in the standing posture.

CHAPTER 8

MODELLING DYNAMIC RESPONSES OF THE HUMAN BODY IN STANDING AND SEATED POSITIONS TO VERTICAL WHOLE-BODY VIBRATION

8.1 INTRODUCTION

It was hypothesised from the experimental results presented in Chapter 7 that more than one dynamic mechanism in the upper-body may contribute to the principal resonance in the apparent mass at about 5 Hz for both seated and standing bodies. Bending of the spine, rocking of the thoracic spine and the rib cage, and pitching of the pelvis, which were coupled with each other, were involved in the body movement at the resonance frequency. For the seated body, deformation of the buttocks tissue may also make a contribution to the principal resonance. For the standing body, a combination of rotational motions at the joints in the legs and deformation of the foot tissue may be a major vibration transmission mechanism to the upper-body. This chapter documents an investigation of the dynamic mechanisms of the principal resonance by means of mathematical modelling.

The dynamic response of the human body in sitting and standing positions to vertical whole-body vibration has been investigated experimentally in previous studies. A principal resonance behaviour in the frequency region of 5 Hz has been consistently observed in the driving-point responses (i.e., the mechanical impedance and the apparent mass; e.g. Coermann, 1962; Fairley and Griffin, 1989). The transmissibilities of vertical motion to various body parts, for example, to the head or to the spine, also exhibit a peak at about 5 Hz (e.g. Panjabi *et al.*, 1986; Paddan and Griffin, 1988; Pope *et al*., 1990).

Understanding of the dynamic mechanisms involved in the resonances of the body is not clear even though this is important information when considering the effect of whole-body vibration on human comfort, performance and health. Several possible causes of the principal resonance at about 5 Hz have been suggested in previous experimental studies of the seated body: vertical motion of the pelvis and the entire body (Hagena *et al*., 1985;

Pope *et al*., 1990; Kitazaki and Griffin, 1998), bending motion of the lumbar spine (Sandover and Dupuis, 1987; Hinz *et al*., 1988), pitching motion of the pelvis (Sandover and Dupuis, 1987; Pope *et al*., 1990). The dynamic responses of the upper-body of seated and standing subjects during exposure to vertical whole-body vibration were measured at six locations along the spine, the head and the pelvis in the sagittal plane in the course of this study, as presented in previous chapters, Chapters 6 and 7. It was found that a dominant bending motion of the spine occurred at frequencies around 5 Hz for both seated and standing subjects.

Mathematical models can be used to seek theoretical insights into phenomena observed in real situations or in laboratory experiments. Various mathematical models claimed to represent the biodynamic responses of the seated body to vertical whole-body vibration have been developed in previous studies. Lumped parameter models with single or two degree-of-freedom were proposed in early studies (e.g. Latham, 1957; Payne, 1965). It is possible to take advantage of the simplicity of the calculation to model a particular aspect of the dynamic responses, such as the driving-point responses of the body by a few degrees of freedom (e.g. Fairley and Griffin, 1989; Wei and Griffin, 1998). A linear two degree-of-freedom lumped parameter model of the mechanical driving-point impedance has been proposed in ISO 5982 (1981). These simple models, however, cannot be used to explain the various aspects of the biodynamic responses simultaneously. It is also difficult to relate the masses of the model to the masses of the human body segments. Lumped parameter models, therefore, have been extended to several degrees of freedom. The model masses may be assumed to correspond to particular body parts, such as, the head, torso and abdomen (e.g. Payne and Band, 1971; Mertens and Vogt, 1978). Most lumped parameter models that have been proposed are one dimensional, in the vertical direction, so that it is impossible to represent the fore-and-aft and rotational motions of the body observed in experiments.

Lumped parameter models with two or three dimensions have been developed by Vulcan and King (1970) and Amirouche and Ider (1988) by using rotational connections between masses. Vulcan and King's four degree-of-freedom model had three masses (i.e., head, upper-torso and lower-torso masses) interconnected by a combination of translational (vertical) and rotational (pitch) linear springs and dampers. A nonlinearity due to the geometry of the model was also considered. The model was validated by comparing calculated time histories of the axial force and bending moment at the connection below the upper-torso mass to those measured in the lumbar spine of cadavers in an experiment. The effect of the head rotation on the force and moment in the lumbar spine

was discussed. Amirouche and Ider's model was similar to that of Vulcan and King but had more degrees of freedom: thirteen masses, including the head, neck, upper-, centre- and lower-torso, upper- and lower-arms, upper- and lower-legs masses, interconnected by vertical and rotational linear springs and dampers. The model was two dimensional for pure vertical input stimuli because of its symmetry about the mid-sagittal plane, although each rotational connection was assigned a three dimensional degree of freedom. Stiffness and damping parameters were determined by comparing the calculated vertical and pitch transmissibilities to the middle torso mass and the vertical transmissibility to the head mass using experimental data obtained elsewhere (Coermann, 1962; Pradko *et al*., 1965; Sandover, 1978; Griffin *et al*., 1978; Panjabi *et al*., 1986). Four natural frequencies in the frequency range below 20 Hz were obtained by modal analysis of the model.

In the present study, the capability of lumped parameter models to identify the dynamic mechanisms contributing to the seated and standing body resonances due to vertical whole-body vibration have been investigated. Rotational degrees of freedom have been incorporated in the models to represent the fore-and-aft and pitch motions of various body parts observed in previous experiments. Any fore-and-aft degrees of freedom have not been included in the model. The models have not been extended to more than six degree-of-freedom so as to retain an advantage in simplicity of formulation and calculation over finite element models (e.g. Belytschko and Privitzer, 1978; Kitazaki and Griffin, 1997). The validation of the models has been examined by comparing the apparent mass and transmissibilities calculated from the models to those obtained in the experiments presented in Chapters 6 and 7.

8.2 MODEL DESCRIPTION

Lumped parameter models with different degrees of freedom have been investigated so as to seek reasonable representations of the dynamic responses of seated and standing bodies exposed to vertical whole-body vibration in the mid-sagittal plane while representing the anatomical construction of the body. The elements used to construct the lumped parameter models were masses, linear translational springs and dampers, and linear rotational springs and dampers. The inclusion of rotational connective elements made the models two dimensional. An eccentricity of the centre of gravity of the mass elements supported by the rotational connective elements was taken into account such that vertical input motion yielded rotational responses of the masses. Each mass element can be assumed to represent some part of the body.

8.2.1 Equations of motion

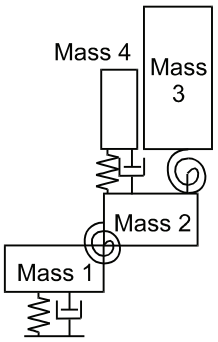

Figure 8.1 Example of seated body model. Four degree-of-freedom: two vertical and two pitch degrees of freedom (rotational dampers are not shown in the figure).

An example of the formulation of the equations of motion of a model with rotational degrees of freedom is presented in this section by using a four degree-of-freedom model of the seated body shown in Figure 8.1. Mass 1 is supported by the combination of a vertical translational spring and damper with its motion restricted to the vertical axis. A rotational spring and damper connects Mass 1 with Mass 2, which is placed on top of Mass 1. Mass 2 is, therefore, allowed to move in the vertical and pitch directions. Another rotational spring and damper connects Mass 2 and Mass 3, which is placed on top of Mass 2 in the same way as the connection between Mass 1 and Mass 2. Mass 4 is supported by a vertical translational spring and damper on top of Mass 2. The motion of Mass 4 is restricted to the vertical axis so as to simplify the problem. In this example model, Masses 1, 2, 3 and 4 could be assumed to represent the legs, the pelvis, the upper-body (except the pelvis and viscera), and the viscera, respectively, for the seated body. The connection between Masses 1 and 2 could be assumed to represent the ischial tuberosities. The connection between Masses 2 and 3 could be thought equivalent to a bending mode of the spine. The equations of motion of the model, by using the axes defined in ISO 2631-1 (1997), can be derived as follows:

$$m_1\ddot{z}_1 + c_1(\dot{z}_1 - \dot{z}_b) + k_1(z_1 - z_b) + c_4\left\{\dot{z}_1 + (e_1 + e_3)\dot{\theta}_2 - \dot{z}_4\right\} + k_4\left\{z_1 + (e_1 + e_3)\theta_2 - z_4\right\} + m_2\ddot{z}_1 + m_2e_1\ddot{\theta}_2 + m_3\ddot{z}_1 + m_3(e_1 + e_2)\ddot{\theta}_2 + m_3e_4\ddot{\theta}_3 = 0 \tag{8.1}$$

$$\left\{J_2 + m_3(e_1 + e_2)^2 + m_3(f_1 + f_2)^2 + m_4(f_1 + f_2)^2\right\}\ddot{\theta}_2 + c_{t2}\dot{\theta}_2 + c_{t3}(\dot{\theta}_2 - \dot{\theta}_3) + \left\{k_{t2} - m_2gf_1 - m_3g(f_1 + f_2)\right\}\theta_2 + (k_{t3} - m_3gf_4)(\theta_2 - \theta_3) + \left\{e_1m_2 + m_3(e_1 + e_2)\right\}\ddot{z}_1 + m_3\left\{(e_1 + e_2)e_4 + (f_1 + f_2)f_4\right\}\ddot{\theta}_3 + (e_1 + e_3)\left[c_4\left\{\dot{z}_1 + (e_1 + e_3)\dot{\theta}_2 - \dot{z}_4\right\} + k_4\left\{z_1 + (e_1 + e_3)\theta_2 - z_4\right\}\right] = 0 \tag{8.2}$$

$$J_3\ddot{\theta}_3 + c_{t3}(\dot{\theta}_3 - \dot{\theta}_2) + (k_{t3} - m_3gf_4)(\theta_3 - \theta_2) + m_3e_4\ddot{z}_1 + m_3\left\{(e_1 + e_2)e_4 + (f_1 + f_2)f_4\right\}\ddot{\theta}_2 = 0 \tag{8.3}$$

$$m_4\ddot{z}_4 + c_4\left\{\dot{z}_4 - \dot{z}_1 - (e_1 + e_3)\dot{\theta}_2\right\} + k_4\left\{z_4 - z_1 - (e_1 + e_3)\theta_2\right\} = 0 \tag{8.4}$$

where,

m_1, m_2, m_3, m_4	:	the masses of Masses 1, 2, 3, and 4, respectively
J_2, J_3	:	the moments of inertia of Mass 2 about the rotational connection between Masses 1 and 2, and of Mass 3 about the rotational connection between Masses 2 and 3, respectively
c_1, k_1	:	the damping and stiffness coefficients of the vertical damper and spring beneath Mass 1
c_{t2}, k_{t2}	:	the damping and stiffness coefficients of the rotational connection between Masses 1 and 2
c_{t3}, k_{t3}	:	the damping and stiffness coefficients of the rotational connection between Masses 2 and 3
c_4, k_4	:	the damping and stiffness coefficients of the vertical damper and spring beneath Mass 4
e_1, e_2, e_3, e_4	:	the horizontal distances from the rotational connection between Masses 1 and 2 to the central gravity of Mass 2, from the central gravity of Mass 2 to the rotational connection between Masses 2 and 3, from the central gravity of Mass 2 to the central gravity of Mass 4, and from the rotational connection between Masses 2 and 3 to the central gravity of Mass 3, respectively
f_1, f_2, f_3, f_4	:	the vertical distances from the rotational connection between Masses 1 and 2 to the central gravity of Mass 2, from the central gravity of Mass 2 to the rotational connection between Masses 2 and 3, from the central gravity of Mass 2 to the central gravity of Mass 4, and from the rotational connection between Masses 2 and 3 to the central gravity of Mass 3, respectively
z_b	:	the vertical displacement of the base
z_1, z_4	:	the vertical displacement of Masses 1 and 4, respectively
θ_2, θ_3	:	the pitch displacements of Masses 2 and 3, respectively
g	:	the gravitational acceleration

Equations (8.1), (8.2), (8.3) and (8.4) were derived from the vertical forces acting on Mass 1, the pitch moments about the connection point between Masses 1 and 2, the pitch moments about the connection point between Masses 2 and 3, and the vertical forces acting on Mass 4, respectively. It was assumed in the derivation of the equations that all the displacements are small such that the nonlinearity due to the geometry of the model would be neglected. It was also assumed that the vertical force acting between Masses 2 and 4 always acts in the vertical line through the central gravity of Mass 4. The horizontal

distance between a rotational connection and the centre of gravity of a mass, represented by e_1, e_2, e_3, and e_4, would be a negative value when a point mentioned first in the above nomenclature is located to the right of another point mentioned last in Figure 8.1. The equations of motion of other models used in this investigation were derived in a similar way, based on the same assumptions mentioned above.

8.2.2 Model parameters

The distributions of the masses, the locations of the centres of gravity of the masses and other geometrical properties of the models were determined from the model parameters used by Kitazaki and Griffin (1997) which was based on available literature, such as, Liu and Wickstrom (1973), Belytschko and Privitzer (1978), and National Aeronautics and Space Administration (1978). The moments of inertia of the masses were also determined from those used by Kitazaki and Griffin (1997), which provided the moments of inertia of the slices of the upper-body at each vertebral level. The moment of inertia of each model mass was calculated by assuming the slices of the body that corresponded to a model mass were all rigid and connected rigidly to each other. The inertial and geometrical properties which were not available in Kitazaki and Griffin, such as the mass of the legs and geometrical properties of the legs for the standing body, were determined from National Aeronautics and Space Administration (1978) and McConville *et al*. (1980).

The stiffness and damping parameters of the models were rather difficult to obtain directly from the literature because each combination of spring and damper did not necessarily represent a particular anatomical segment of the body, for some of which a stiffness and damping have been suggested in the literature. The values of stiffness and damping of most tissues in the living human body, such as those of the muscles, were not available. The stiffness and damping parameters of the models were, therefore, determined by comparing the calculated apparent mass and transmissibilities given for various masses by the model with those obtained at a vibration magnitude of 1.0 ms^{-2} r.m.s. in the experiment presented in Chapters 6 and 7. The apparent mass and the transmissibilities were analytically obtained from the equations of motion, such as Equations (8.1) to (8.4), using the Laplace transform. An error function between calculated values and measured values was defined as follows:

$$err = \sum_n \left| M_m(n\Delta f) - M_c(n\Delta f) \right|^2 + \sum_j A_j \sum_n \left| T_{jm}(n\Delta f) - T_{jc}(n\Delta f) \right|^2 \qquad (8.5)$$

where,

M_m, T_m : measured apparent mass and transmissibility in complex numbers

M_c, T_c : calculated apparent mass and transmissibility in complex numbers

Δf : frequency resolution of the measured data

$n\,\Delta f$: frequency (limited below 20 Hz for the apparent mass and below 10 Hz for the transmissibilities because of the limited experimental data)

j : location and direction (vertical, fore-and-aft or pitch) of transmissibility

A_j : weighting for transmissibility

Parameters which minimised the above error function were obtained by the Nelder-Meade simplex search provided by MATLAB (MathWorks Inc.) for both the individual and the median data from eight subjects used in the experiment presented in the corresponding chapters. The weightings for the transmissibilities, A_j, were determined arbitrarily such that the parameter search would converge and provide a good curve fit with both the apparent mass and the transmissibilities experimentally obtained. The transmissibility at an arbitrary location on the model mass was calculated by assuming the mass was rigid and the displacement was small. The locations for the transmissibilities used for the parameter identification depended on the way in which the model masses were separated. The closest locations to the centre of gravity of each model mass among those available in the experimental data were selected.

The masses and moments of inertia of the model masses and the lengths used in the model were adjusted so that the total mass of the model corresponded to the mass of the subject, m_s, by using scaling factors defined from the dimensional analysis. Assuming the density of the human body was constant, irrespective of the location, the mass of each portion of the body could be assumed to be proportional to its volume that was assumed to be proportional to the product of the three linear dimensions. The scaling factors used in the calculation of the model responses were therefore as follows: m_s/m_0 for the mass, $(m_s/m_0)^{5/3}$ for the moment of inertia, $(m_s/m_0)^{1/3}$ for the length, where m_0 is the initial total mass of the model. The total mass of the seated body model by Kitazaki and Griffin (1997) was 60.046 kg, which consisted of the head, neck, torso, the upper-arms, 30% of the hands and 30% of the thighs. The mass of the other part of the body (i.e., the fore-arms and the rest of the legs and hands) were determined based on the mass distribution of the total body mass provided by National Aeronautics and Space Administration (1978), shown in Table 8.1. The initial total mass of the model of 84.5 kg were consequently obtained.

Table 8.1 Percentage distribution of total body weight according to different segmentation plans. (After National Aeronautics and Space Administration, 1978).

Grouped Segments Percent of Total Body Weight		Individual Segments Percent of Grouped Segments Weight	
Head and Neck	= 8.4%	Head Neck	= 73.8% = 26.2%
Torso	= 50.0%	Thorax Lumbar Pelvis	= 43.8% = 29.4% = 26.8%
Total arm	= 5.1%	Upper arm Fore arm Hand	= 54.9% = 33.3% = 11.8%
Total leg	= 15.7%	Thigh Shank Foot	= 63.7% = 27.4% = 8.9%

8.3 RESULTS AND DISCUSSION

8.3.1 Seated body model

8.3.1.1 Effect of model structure for the pelvis region

Various lumped parameter models for the seated body were investigated first. Transmissibilities for vertical motion measured at the pelvis of seated subjects show a dominant peak at around the principal resonance frequency in the driving-point responses (see, e.g., Figure 7.2). This implies that some dynamic mechanism is required between the model mass representing the pelvis and the base representing the seat. The three models shown in Figure 8.2 were, therefore, examined. Masses 1, 2, 3, and 4 represented the legs, the pelvis, the upper-body (except the pelvis and the viscera), and the viscera, respectively. For Model 1, Masses 1 and 2 were assumed to be united as in Figure 8.2(a). A vertical connection, a rotational connection, and a combination of a vertical connection and a rotational connection were used for the mechanical structure beneath the pelvic mass in Models 1, 2 and 3, respectively.

The initial inertial properties, the locations of the centre of gravity of the masses and those of the connection beneath the masses, and the location of each point for the

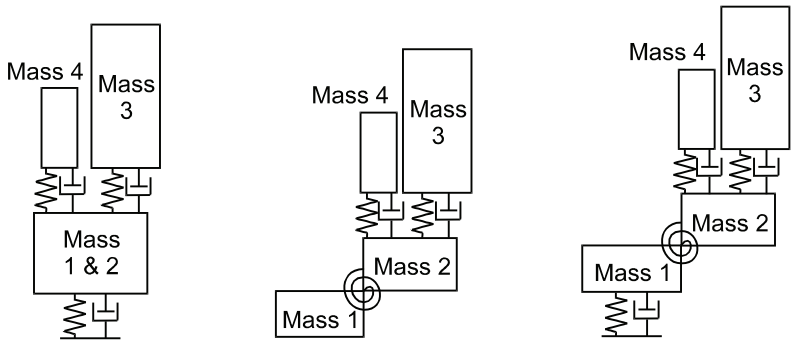

(a) Model 1 (b) Model 2 (c) Model 3

Figure 8.2 Lumped parameter models with different structure for the pelvis region.

transmissibility as calculated are tabulated in Table 8.2. The origin of the co-ordinate system was located at the ischial tuberosities. The values which are not shown in Table 8.2 were not required in the calculation of the model responses. The moment of inertia of Mass 3, upper-body mass, about the connection point between Masses 2 and 3 was used in an investigation mentioned in a later section. The apparent mass, the vertical and pitch transmissibilities to the pelvis and the vertical transmissibility to the fifth thoracic vertebra (T5) measured in the experiment (see Chapters 6 and 7) were used as target functions, to obtain the stiffness and damping parameters. The stiffness and damping coefficients obtained for each model by comparison with the median normalised apparent mass (as defined by Fairley and Griffin, 1989) and the median transmissibilities of the eight subjects are tabulated in Table 8.3. The values shown in Table 8.3 correspond to the inertial and geometric parameters shown in Table 8.2.

Table 8.2 Inertial and geometric parameters used in Models 1, 2, and 3. (Connection: point of connection between mass and mass below.)

Mass 1 - 4	Mass [kg]	Inertial Moment [kg·m^2]	Centre of gravity (x, z) [m]	Connection (x, z) [m]	Transmissibility (x, z) [m]
Legs	24.4	---	---	---	---
Pelvis	16.9	0.332	(-0.0244, 0.104)	(0,0)	(-0.100, 0.165)
Upper-body	30.4	7.49	(-0.0153, 0.593)	(-0.0949, 0.132)	(-0.0509, 0.551)
Viscera	12.8	---	(-0.0285, 0.254)	---	(-0.0285, 0.254)

Table 8.3 Stiffness and damping coefficients obtained for Models 1, 2 and 3.

Model	Buttocks, vertical		Pelvis, pitch		Upper-body, vertical		Viscera, vertical	
	Stiffness [N/m]	Damping [Ns/m]	Stiffness [Nm]	Damping [Nms]	Stiffness [N/m]	Damping [Ns/m]	Stiffness [N/m]	Damping [Ns/m]
1	1.51×10^{5}	3.00×10^{3}	---	---	7.37×10^{11}	1.14×10^{11}	2.39×10^{4}	1.84×10^{2}
2	---	---	1.27×10^{3}	2.91×10^{1}	7.05×10^{4}	6.43×10^{2}	1.89×10^{4}	1.44×10^{2}
3	2.03×10^{5}	2.68×10^{3}	9.56×10^{2}	2.98×10^{1}	1.12×10^{19}	2.61×10^{16}	2.62×10^{4}	2.75×10^{2}

Figure 8.3 compares the normalised apparent masses calculated from Models 1, 2, and 3 with the median normalised apparent mass obtained in the experiment. It was found to be difficult to obtain a reasonable representation of the apparent mass of the seated body using Model 2, which had only a rotational spring and a rotational damper beneath the pelvic mass. This was the case for other models which had only a rotational spring and damper beneath the pelvic mass, irrespective of the structure of the upper part of the model, although the details of these other models are not presented. The other two models, Models 1 and 3, with the pelvic mass supported by a vertical spring and damper were able to represent the apparent mass of each subject and the median apparent mass of the all subjects reasonably well. It is therefore implied that a vertical degree of freedom beneath the pelvis, which could be the buttocks tissues beneath the pelvis, makes some contribution to the apparent mass of the seated body in the frequency range below 20 Hz.

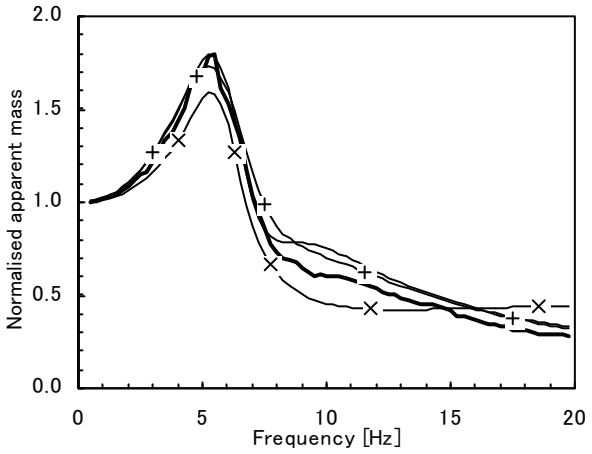

Figure 8.3 Apparent masses calculated from Models 1 ——— , 2 —×— , and 3 —+— , and obtained in the experiment ━━━ .

The transmissibilities calculated from the models and the median transmissibilities measured in the experiment are compared in Figure 8.4. The vertical transmissibility to the viscera was not measured in the experiment and is not included in Figure 8.4(d). For the vertical transmissibility to the pelvis, that calculated from Model 3 showed a peak at about 5 Hz with a similar magnitude to the measured value, while that calculated from Model 1 showed a peak in the same frequency range with a smaller magnitude. The pitch degree of freedom for the pelvic mass, Mass 2, in Model 3 contributed to an increase in the transmissibility at around 5 Hz to the same level as the measured value in this frequency range. This implies that the vertical transmissibility to the pelvis measured at the posterior-superior iliac spine (see Chapters 6 and 7) was affected by the pitch motion of the pelvis which occurred in this frequency range. The pitch degree of freedom of the pelvis is therefore required for an understanding of the dynamic mechanisms of the seated body.

The pitch motion of the pelvic mass also contributed to a decrease in the transmissibility at higher frequencies above the first peak frequency, which is not present in the

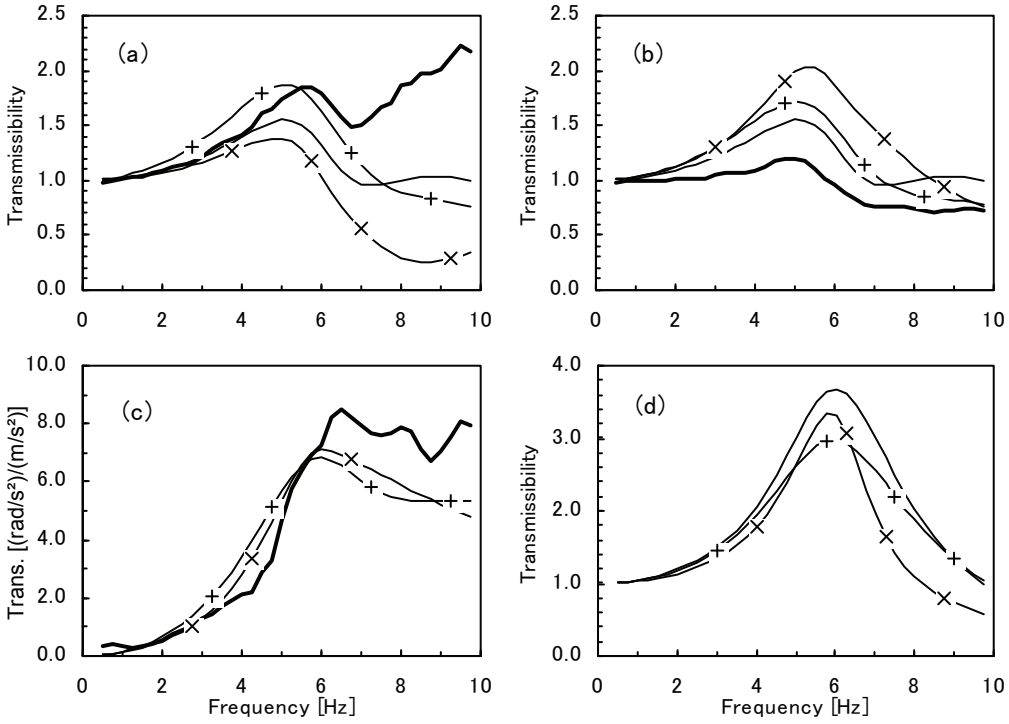

Figure 8.4 Transmissibilities calculated from the models and obtained in the experiment: (a) for the vertical motion at the pelvis and Mass 2, (b) for the vertical motion at T5 and Mass 3, (c) for the pitch motion of the pelvis and Mass 2. The calculated transmissibilities for the vertical motion of Mass 4 are also shown in (d). Model 1 ——— ; Model 2 —×— ; Model 3 —+— ; experiment ━━━ .

experimental data. This was attributed to too low stiffness obtained for the pitch of the pelvic mass, which was caused by a local peak in the pitch transmissibility to the pelvis at around 5 Hz, shown in Figure 8.4(c). It has been found that the pitch transmissibilities to the pelvis are greatest in the frequency range between 10 and 18 Hz (Mansfield and Griffin, 1997; Mansfield, 1998). The stiffness for the pelvis could, therefore, be higher than that shown here by using a set of experimental data with a wider frequency range, which would provide similar pitch transmissibilities at frequencies shown here and a peak in the frequency range between 10 and 18 Hz. This could improve the quality of the representation of the dynamic responses of the model.

As shown in Table 8.3, the stiffness and damping coefficients obtained for the vertical motion of the upper-body mass were too high (i.e., this system could be regarded as rigid and so did not contribute to the dynamic response in the frequency range investigated). The calculated vertical transmissibilities, therefore, were the same for all locations above the pelvis with these parameters. However, a tendency towards a decrease in the vertical transmissibilities has been observed as the measurement location along the spine is higher in this frequency range (see Chapters 6 and 7). This cannot be explained by vertical degrees of freedom of the upper-body structure, except with very low axial stiffness in the lower spine, giving a resonance frequency of below 1 Hz. However, such a low axial stiffness is not realistic according to the observation in previous studies (e.g. Kitazaki and Griffin, 1998) and the experimental results presented in the previous chapters.

8.3.1.2 Effect of visceral mass

A mass representing the viscera was used in the models presented in the previous section, as shown in Figure 8.2. It was found that when a mass or a series of masses with only vertical degrees of freedom were used for the upper-body structure, the transmissibilities to the locations on the upper-body calculated from the models always appeared to be higher than the experimental data for the spine when a reasonable apparent mass was obtained. Model 4 shown in Figure 8.5 was used to present the effect of the exclusion of the visceral mass: the visceral mass (Mass 4 in the models in Figure 8.2) was included in the upper-body mass (Mass 3). The mass of Mass 3, the locations of the centre of gravity and those of the connection beneath the mass, and the location of the point for the transmissibility as calculated for Mass 3 are tabulated in Table 8.4. The inertial and geometric parameters for Masses 1 and 2 were the same as those in Models

2 and 3 presented in Table 8.2. Stiffness and damping coefficients obtained for Model 4 by comparison with the median normalised apparent mass and the median transmissibilities are tabulated in Table 8.5. The apparent mass and the transmissibilities calculated from the model and the median apparent mass and the median transmissibilities measured in the experiment are compared in Figure 8.6.

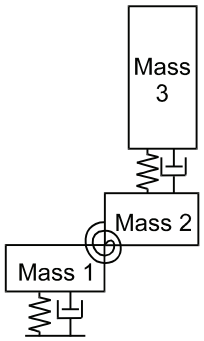

Figure 8.5 Lumped parameter model with united upper-body mass: Model 4.

The transmissibility to the vertical motion of the upper-body mass, Mass 3, calculated from Model 4 was much higher than the median vertical transmissibility to T5 measured in the experiment, as seen in Figure 8.6(c). The vertical transmissibility to the upper-body mass in Model 4 was also higher than those calculated from Models 1 and 3, by 30 to 40% at the peak, which had a visceral mass in parallel with the upper-body mass (Figure 8.4(b)).

When a mass to represent the viscera was used in parallel with those for the spinal column and other body structures, the calculated transmissibility to the viscera tended to be greater than the transmissibilities to other parts of the upper-body, as shown in Figure

Table 8.4 Inertial and geometric parameters used in Model 4. (Connection: point of connection between mass and mass below.)

Mass 3	Mass [kg]	Centre of gravity (x, z) [m]	Connection (x, z) [m]	Transmissibility (x, z) [m]
Upper-body	43.2	(-0.0192, 0.493)	(-0.0949, 0.132)	(-0.0509, 0.551)

Table 8.5 Stiffness and damping coefficients obtained for Model 4.

Buttocks, vertical		Pelvis, pitch		Upper-body, vertical	
Stiffness [N/m]	Damping [Ns/m]	Stiffness [Nm]	Damping [Nms]	Stiffness [N/m]	Damping [Ns/m]
2.67×10^{5}	3.54×10^{3}	1.79×10^{3}	3.62×10^{1}	1.40×10^{5}	2.15×10^{3}

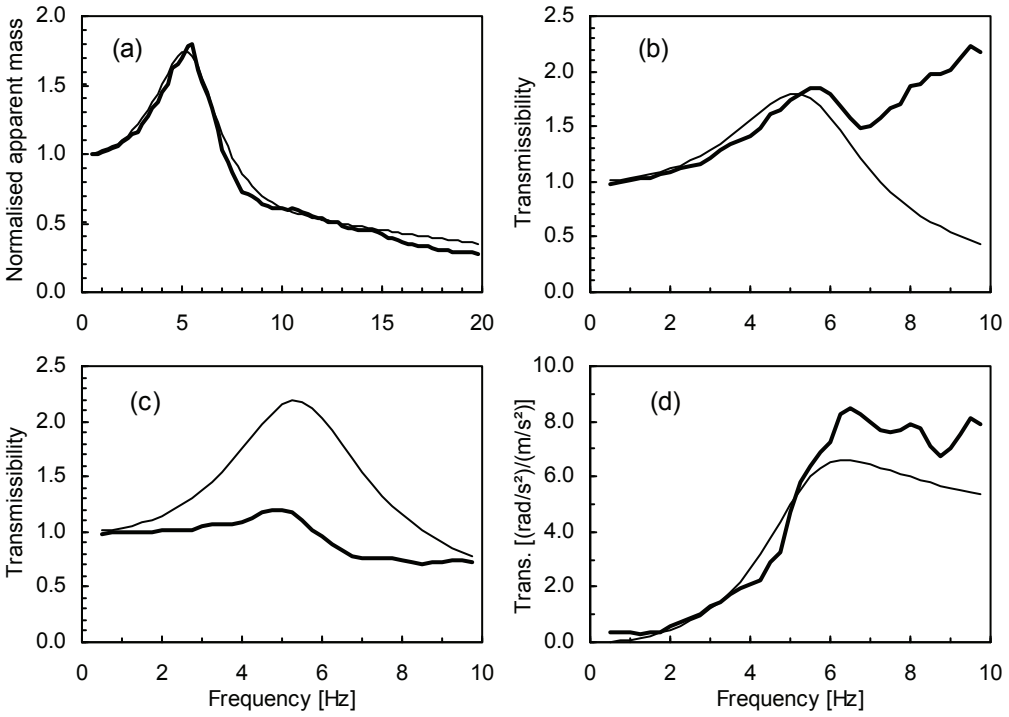

Figure 8.6 Apparent masses and transmissibilities calculated from Model 4 and obtained in the experiment: (a) normalised apparent mass, (b) vertical transmissibility to the pelvis and to Mass 2, (c) vertical transmissibility to T5 and to Mass 3, (d) pitch transmissibility to the pelvis and to Mass 2. Model 4 ——— ; experiment ━━━ .

8.4. This was consistent with the experimental results of Kitazaki and Griffin (1995), Mansfield (1998) and Mansfield and Griffin (1999) who showed that the vertical transmissibility measured on the abdominal wall was greater than that to the lumbar spine. Therefore, it might be reasonable to include a visceral mass into the models as shown in Figure 8.2 (i.e., Mass 4), although the dynamic interaction between the visceral mass and other masses might be improved.

8.3.1.3 Effect of model structure for the spine

From the experiment presented in Chapters 6 and 7, it has been found that a bending type of motion of the spine occurs at around the principal resonance frequency of the apparent mass when seated subjects are exposed to vertical whole-body vibration. The bending motion of the spine seems to be more dominant than any axial motion along the spine. Therefore, the possibility to represent the upper-body (except the pelvis and the viscera) by a rotational mass connected to the pelvic mass was investigated by using Models 5, 6, and 7 shown in Figure 8.7. The vertical, fore-and-aft and pitch

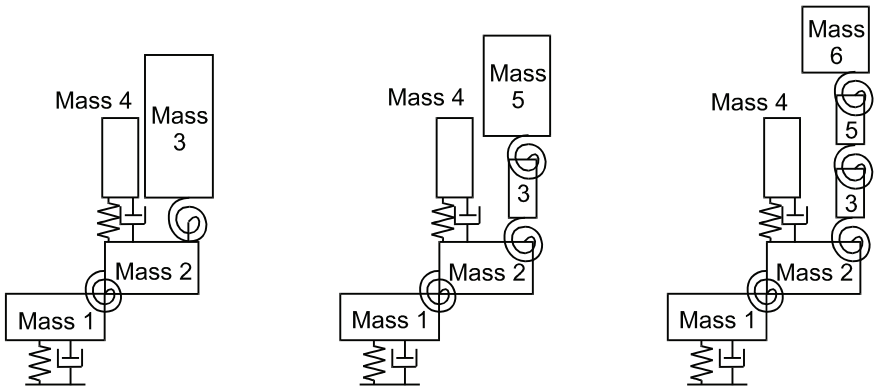

(a) Model 5 (b) Model 6 (c) Model 7

Figure 8.7 Lumped parameter models with different structure for the spine and upper-body.

transmissibilities and the apparent mass were used to obtain the stiffness and damping parameters of the model.

The inertial and geometric parameters initially assigned to Model 5 were the same as the parameters shown in Table 8.2. Stiffness and damping coefficients obtained by the parameter identification for Model 5 are shown in Table 8.6. The normalised apparent mass and transmissibilities calculated from Model 5 and those obtained in the experiment are shown in Figure 8.8.

The apparent mass calculated for Model 5 showed a good agreement with the measured apparent mass, as shown in Figure 8.8(a). The vertical transmissibility to the pelvic mass of Model 5 was lower than the measured transmissibility to the pelvis at frequencies above 5 Hz (Figure 8.8(b)). The second peak at about 10 Hz observed in the experimental result was not represented by the model. The calculated transmissibility from Model 5 was about 1.6 at its peak frequency of 5.0 Hz, while the measured transmissibility to T5 was about 1.2 at the same frequency. The transmissibilities calculated from Model 5 showed a decrease in the transmissibility in the principal

Table 8.6 Stiffness and damping coefficients obtained for Model 5.

Buttocks, vertical		Pelvis, pitch		Upper-body, pitch		Viscera, vertical	
Stiffness [N/m]	Damping [Ns/m]	Stiffness [Nm]	Damping [Nms]	Stiffness [Nm]	Damping [Nms]	Stiffness [N/m]	Damping [Ns/m]
1.53×10^5	3.15×10^3	4.77×10^2	6.72×10^0	1.59×10^3	5.27×10^1	2.67×10^4	1.85×10^2

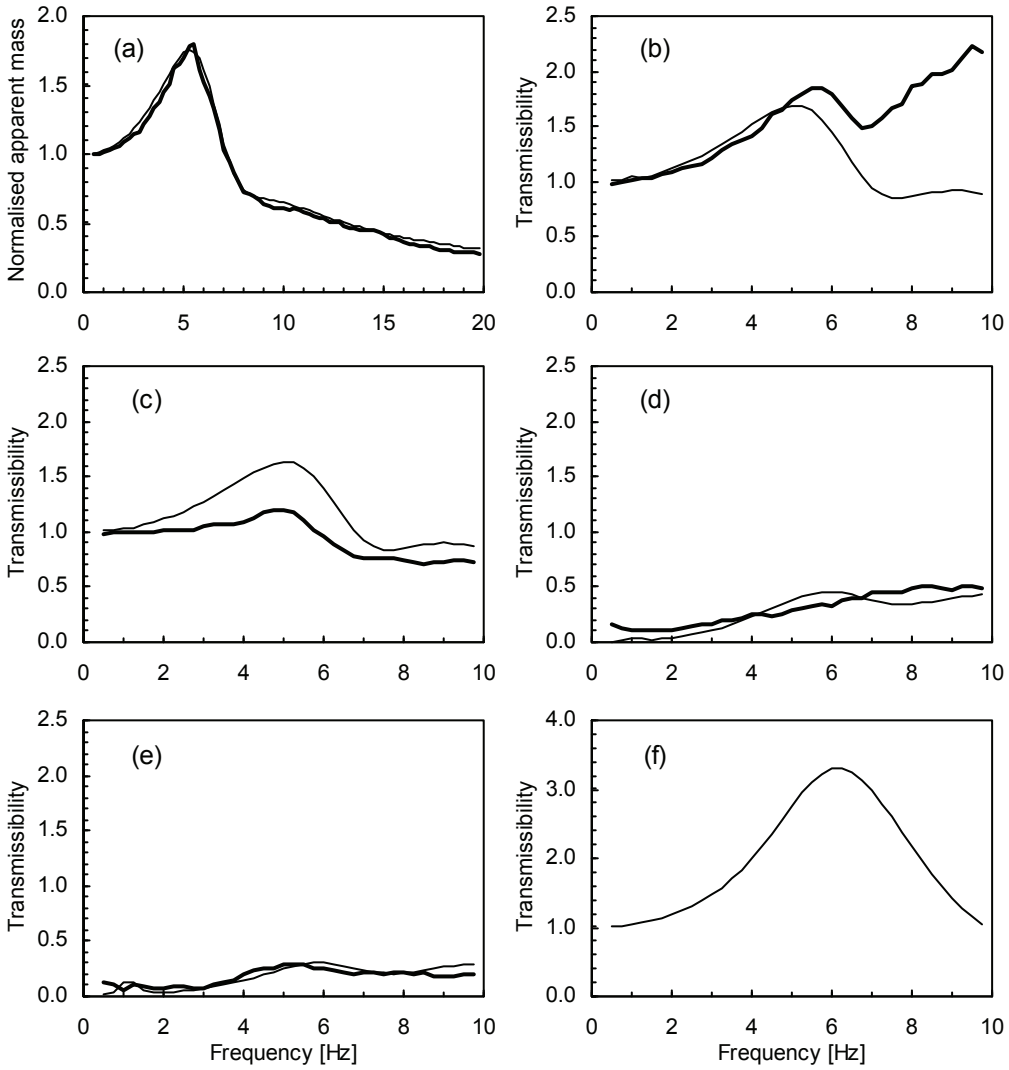

Figure 8.8 Apparent masses and transmissibilities calculated from Model 5 and obtained in the experiment: (a) normalised apparent mass, (b) vertical transmissibility to the pelvis and to Mass 2, (c) vertical transmissibility to T5 and to Mass 3, (d) fore-and-aft transmissibility to the pelvis and to Mass 2, (e) fore-and-aft transmissibility to T5 and to Mass 3, and (f) vertical transmissibility to Mass 4. Model 5 ——— ; experiment ━━━ .

resonance region as the location along the spine was higher, 1.7 at the pelvis and 1.6 at the upper-body. However, the amount of the decrease was not as large as that observed in the experimental data. The fore-and-aft transmissibilities calculated from Model 5 generally showed good agreements with the measured data.

Modal analysis of Model 5 with no damping yielded four vibration modes in the frequency range below 20 Hz. The natural frequencies and modal vectors obtained are tabulated in Table 8.7. The principal peak at about 5 Hz was attributed to a combination of a vertical

Table 8.7 Natural frequencies and mode shapes of Model 5 with no damping. (Mode shapes were normalised to have a vector magnitude of unity.)

Mode	1	2	3	4
Frequency [Hz]	1.11	5.66	8.34	12.3
Legs [m]	0.000	0.203	0.083	0.081
Pelvis [rad]	0.613	0.794	0.934	-0.996
Upper-body [rad]	0.790	-0.053	-0.019	0.032
Viscera [m]	0.018	0.571	-0.346	-0.028

motion of the pelvic and leg masses, a pitch motion of the pelvic mass, a rotational motion at the joint below the upper-body mass and a vertical motion of the visceral mass, corresponding to the second mode of the model (Table 8.7). An upward motion of the pelvic and leg masses was in phase with an upward motion of the visceral mass and a forward pitch motion of the pelvic mass which caused an upward motion of the upper-body masses. Modal analysis of Model 5 yielded a vibration mode at a frequency of about 1 Hz, which was dominated by a pitch motion of the whole upper-body (i.e., the pelvis and upper-body masses). It was not certain that this mode also existed in the human body because the minimum frequency available in the experimental data was 0.5 Hz, close to the first natural frequency of the model. However, a similar vibration mode, 'fore-and-aft motion of the head and the entire spine with the pelvis still caused by a bending deformation of the spine', was found at 0.28 Hz by a study using a finite element model by Kitazaki and Griffin (1997).

For the models with higher degrees of freedom than Model 5, sets of parameters were obtained for Model 6 for both the individual and the median experimental data. For Model 7, however, the parameter search for the stiffness and damping, mentioned in Section 8.2.2, did not converge either for the individual data or for the median data, even when a number of combinations of inertial and geometric parameters, initial values for the search, and weightings for the error function were tested. The more degrees of freedom used in the model, the more vibration modes would be yielded. However, there were only two resonances clear in the experimental data over the frequency range used. This may be the main cause of the difficulty in obtaining model parameters for higher degree-of-freedom models, such as Model 7, by the method used in this study.

Table 8.8 Inertial and geometric parameters used in Model 6. (Connection: point of connection between mass and mass below.)

Mass 1 - 5	Mass [kg]	Inertial Moment [kg·m^2]	Central gravity (x, z) [m]	Connection (x, z) [m]	Transmissibility (x, z) [m]
Legs	24.4	---	---	---	---
L4 - Pelvis	17.9	0.388	(-0.0301, 0.108)	(0,0)	(-0.100, 0.165)
T11 - L3	1.71	0.0188	(-0.0752, 0.312)	(-0.0612, 0.245)	(-0.0612, 0.245)
Head - T10	27.6	1.80	(-0.00753, 0.626)	(-0.0607, 0.414)	(-0.0121, 0.655)
Viscera	12.8	---	(-0.0285, 0.254)	---	(-0.0285, 0.254)

Table 8.8 shows the inertial and geometric parameters initially assigned to Model 6. Stiffness and damping coefficients obtained by the parameter identification for Model 6 are shown in Table 8.9. The normalised apparent mass and transmissibilities calculated by Model 6 and those obtained in the experiment are shown in Figure 8.9.

The apparent mass calculated from Model 6 showed a good agreement with the measured apparent mass, as for Model 5 (Figure 8.9(a)). The representation of the vertical transmissibilities (i.e., to the pelvis, L1 and T1) seemed to be reasonable, except the transmissibilities to the pelvis at higher frequencies (Figures 8.9(b) to (d)). However, as in Model 5, the decrease in the vertical transmissibility at higher locations along the spine observed in Experiment 3 was not represented quantitatively: 1.63 at the pelvis and 1.56 at L1 for Model 6 at 5 Hz, while 1.74 at the pelvis and 1.34 at L1 for the median experimental data. General trends in the fore-and-aft transmissibilities were similar for the calculated and measured data, although some differences can be seen (Figures 8.9 (e) to (g)).

Table 8.9 Stiffness and damping coefficients obtained for Model 6.

Buttocks vertical		Pelvis pitch		Lower upper-body pitch		Upper upper-body pitch		Viscera vertical	
Stiffness [N/m]	Damping [Ns/m]	Stiffness [Nm]	Damping [Nms]	Stiffness [Nm]	Damping [Nms]	Stiffness [Nm]	Damping [Nms]	Stiffness [N/m]	Damping [Ns/m]
1.44×10^5	3.10×10^3	8.99×10^2	4.26×10^1	1.04×10^3	5.44×10^1	1.21×10^3	8.17×10^0	2.74×10^4	1.95×10^2

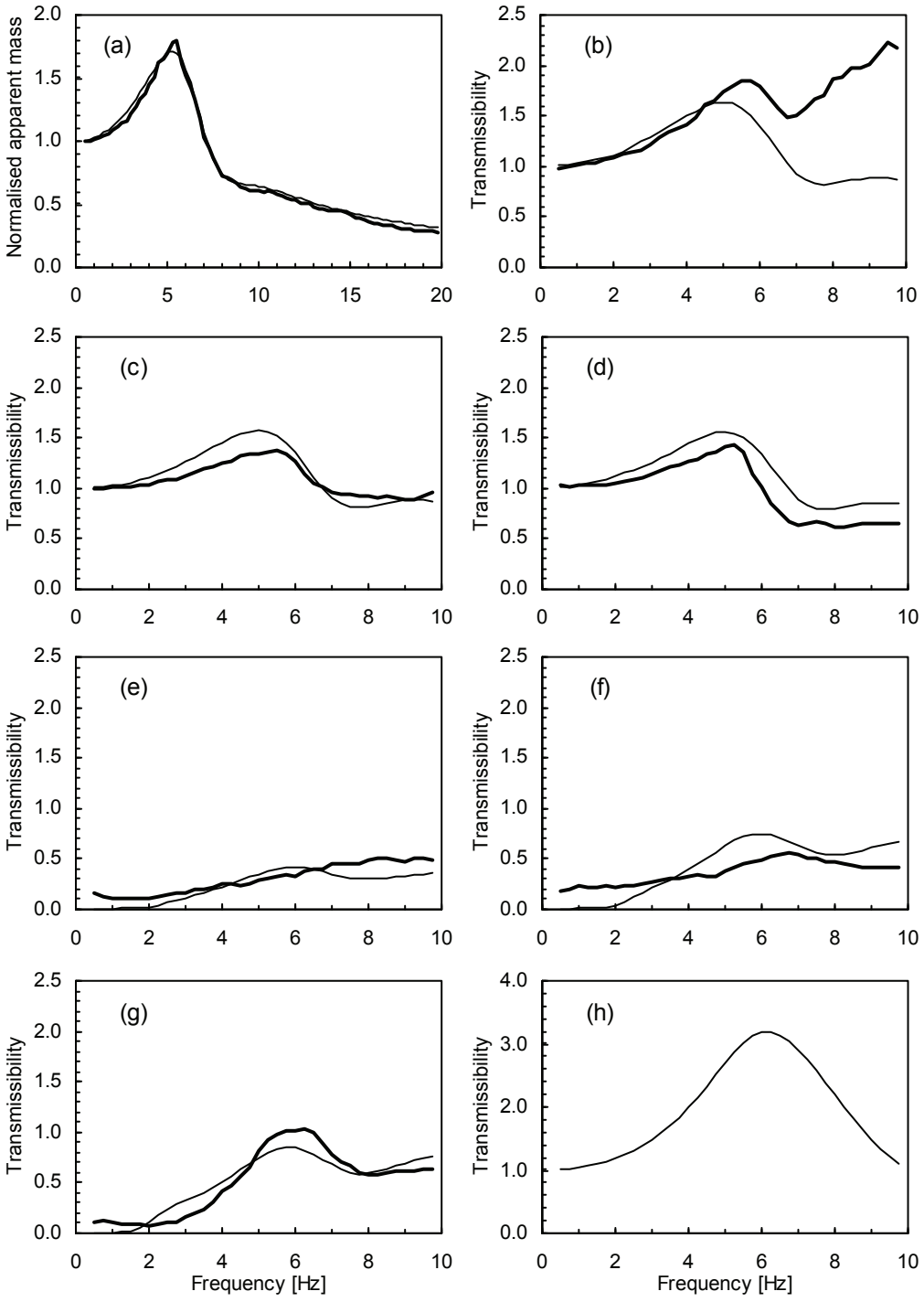

Figure 8.9 Apparent masses and transmissibilities calculated from Model 6 and obtained in the experiment: (a) normalised apparent mass, (b) vertical transmissibility to the pelvis and to Mass 2, (c) vertical transmissibility to L1 and to Mass 3, (d) vertical transmissibility to T1 and to Mass 5, (e) fore-and-aft transmissibility to the pelvis and to Mass 2, (f) fore-and-aft transmissibility to L1 and to Mass 3, (g) fore-and-aft transmissibility to T1 and to Mass 5, and (h) vertical transmissibility to Mass 4. Model 6 ——— ; experiment ━━━ .

Table 8.10 Natural frequencies and mode shapes of Model 6 with no damping. (Mode shapes were normalised to have a vector magnitude of unity. UB: upper-body.)

Mode	1	2	3	4
Frequency [Hz]	2.53	5.66	8.62	11.5
Legs [m]	-0.000	0.201	0.089	0.050
Pelvis [rad]	0.365	0.648	0.747	-0.787
Lower UB [rad]	0.463	0.497	0.590	-0.610
Upper UB [rad]	0.808	-0.058	-0.009	0.079
Viscera [m]	0.011	0.538	-0.294	-0.019

Four vibration modes were derived from Model 6 with no damping in the frequency range below 20 Hz. Table 8.10 shows the natural frequencies and modal vectors for the four modes. The mode shapes obtained from Model 6 were similar to those from Model 5 shown in Table 8.7. The first mode at a low frequency, 2.53 Hz for Model 6 and 1.11 Hz for Model 5, was a pitching motion of the pelvis in phase with a first bending mode of the spine. The second mode, at 5.66 Hz for both Models 5 and 6, which made main contribution to the principal resonance of the apparent mass of the model consisted of a deformation of the buttocks tissue and a vertical mode of the viscera which occurred in phase. The second mode also involved a second bending mode of the spine which might be observed in the experimental data shown in Chapter 7. In the third mode, at about 8.5 Hz, a deformation of the buttocks tissue was out of phase with a vertical visceral motion, which might correspond to the second broad peak observed in the apparent mass. A bending of the spine which was similar to that seen in the second mode was also involved in the third mode. The fourth mode, at about 12 Hz, was dominated by a rotational motion of the pelvis and a bending of the spine which was also similar to the bending in the second mode.

A rotational connection, or a series of rotational connections, for the upper-body model provided a decrease in the vertical transmissibilities at higher measurement locations along the spine, although the extent of the decrease was not as great as that observed in the experiment (Figures 8.8(b) and (c) and Figures 8.9(b), (c) and (d)). The fore-and-aft transmissibilities to the upper-body masses of Models 5 and 6 had similar magnitudes to those measured in the experiment (Figures 8.8(d) and (e) and Figures 8.9(e), (f) and (g)). One or two rotational masses for the whole upper-body structure, however, might not be

sufficient to represent complicated dynamic mechanisms of the spine. A series of rotational masses to represent the spinal column and other upper-body structures may be required when more detailed dynamic response of the spine are interested.

It appeared that the inclusion of rotational degrees of freedom in the upper-body model did improve the representation of the dynamic responses of the body, particularly the transmissibilities. However, a couple of different sets of rotational parameters which gave a similar quality of representation of the responses were obtained for Models 5 and 6, although general trends in the modal properties were similar. The parameter identification with different combinations of the inertial and geometric properties, the initial values for the parameter search and the error function in the parameter identification, might provide different sets of parameters. As mentioned above, this might be caused by the small number of resonances in the frequency range in the experimental data, which would have made it difficult to obtain the convergence of the parameter search for higher degree-of-freedom models.

The coherences of the measured transmissibilities were generally greater than 0.9 in the frequency range below 10 Hz. However, the coherences of the measured fore-and-aft transmissibilities at frequencies below 3.5 Hz from some subjects were lower than 0.9. This seemed to be mainly because of low transmissibilities at those frequencies. The low quality of the fore-and-aft transmissibilities might also have made the parameter identification difficult, especially for the pitch degrees of freedom.

The model structure for the upper-body shown in this thesis might have been too simple to represent a bending motion of the spine observed in the experiment. It was difficult, however, to increase the degrees of freedom of the model due to the difficulty in the parameter identification method used in this investigation for the reason mentioned above.

8.3.1.4 Parameter sensitivity in seated body models

The effect of changes in the model parameters on the model responses were examined with Models 5 and 6 for the seated body whose responses showed best agreements with the experimental data in this study. Ranges of the stiffness and damping parameters were determined. Initial errors between each measured frequency response function (i.e. the apparent mass or the transmissibility) and corresponding calculated response were

calculated by using the parameters shown in Tables 8.6 and 8.9 for Models 5 and 6, respectively. An error function for each frequency response function was defined as:

$$err = \left(\frac{\sum_{n} \left(T_m(n\Delta f) - T_c(n\Delta f) \right)^2}{\sum_{n} T_m(n\Delta f)^2} \right)^{1/2} \tag{8.6}$$

where,

T_m : measured frequency response function (modulus)

T_c : calculated frequency response function (modulus)

Δf : frequency resolution of the measured data

$n\,\Delta f$: frequency (limited below 20 Hz for the apparent mass and below 10 Hz for the transmissibilities because of the limited experimental data)

Parameter ranges for each stiffness and damping were determined so that a change in the parameter increased any error function for the apparent mass or the transmissibility defined in Equation (8.6) by 10%. A limit was not obtained if a change in the parameter reached 20% for a lower limit and 500% for a higher limit because the change was too large. The obtained lower and upper limits for each parameter with the corresponding initial values and ratios of the limits to the initial values are tabulated for Models 5 and 6 in Tables 8.11 and 8.12, respectively.

Table 8.11 Parameter ranges for Model 5. Stiffness in the vertical axis in [N/m], stiffness in the pitch axis in [Nm]. Damping in the vertical axis in [Ns/m], damping in the pitch axis in [Nms].

	Lower limit	Ratio [%]	Upper limit	Ratio [%]	Initial value
Stiffness					
Buttocks, vertical	$1.32\text{x}10^5$	86.6	$1.71\text{x}10^5$	112	$1.53\text{x}10^5$
Pelvis, pitch	$4.03\text{x}10^2$	84.4	$1.15\text{x}10^3$	242	$4.77\text{x}10^2$
Upper-body, pitch	$1.16\text{x}10^3$	73.2	$1.97\text{x}10^3$	124	$1.59\text{x}10^3$
Viscera, vertical	$2.16\text{x}10^4$	80.8	$3.28\text{x}10^4$	123	$2.67\text{x}10^4$
Damping					
Buttocks, vertical	$2.80\text{x}10^3$	89.0	$3.43\text{x}10^3$	109	$3.15\text{x}10^3$
Pelvis, pitch	$2.62\text{x}10^0$	39.0	$1.63\text{x}10^1$	242	$6.72\text{x}10^0$
Upper-body, pitch	$4.87\text{x}10^1$	92.4	$6.22\text{x}10^1$	118	$5.27\text{x}10^1$
Viscera, vertical	$1.26\text{x}10^2$	68.0	$2.79\text{x}10^2$	151	$1.85\text{x}10^2$

Table 8.12 Parameter ranges for Model 6. Stiffness in the vertical axis in [N/m], stiffness in the pitch axis in [Nm]. Damping in the vertical axis in [Ns/m], damping in the pitch axis in [Nms]. (UB: upper-body.)

	Lower limit	Ratio [%]	Upper limit	Ratio [%]	Initial value
Stiffness					
Buttocks, vertical	1.22×10^5	84.6	1.60×10^5	111	1.44×10^5
Pelvis, pitch	---	---	1.29×10^3	143	8.99×10^2
Lower UB, pitch	---	---	2.20×10^3	212	1.04×10^3
Upper UB, pitch	1.04×10^3	85.6	1.52×10^3	126	1.21×10^3
Viscera, vertical	2.46×10^4	89.8	3.51×10^4	128	2.74×10^4
Damping					
Buttocks, vertical	2.68×10^3	86.4	3.44×10^3	111	3.10×10^3
Pelvis, pitch	3.94×10^1	92.6	5.03×10^1	118	4.26×10^1
Lower UB, pitch	2.72×10^1	50.0	---	---	5.44×10^1
Upper UB, pitch	4.26×10^0	52.2	1.88×10^1	230	8.17×10^0
Viscera, vertical	1.22×10^2	62.8	3.40×10^2	175	1.94×10^2

The changes in the parameters for the vertical axis affected the apparent mass and the transmissibilities. The changes in the parameters for the pitch axis had effects on the transmissibilities but hardly affected the apparent mass. There were two rotational stiffness parameters in Model 6, the pelvis pitch and lower upper-body pitch, with which a lower limit was not able to be obtained in the 20 to 100% range (Table 8.12). An upper limit was not be determined for the damping parameter of lower upper-body pitch in Model 6 in the 100 to 500% range (Table 8.12). Those parameters mainly contributed to the first vibration mode at about 2.5 Hz, shown in Table 8.10, which had small effects on the apparent mass and transmissibilities. Large decreases in those two stiffnesses reduced the first natural frequency less than 0.5 Hz, the minimum frequency range in the experimental data. It was, therefore, difficult to obtain the lower limits for those stiffness parameters. Heavier damping on the lower upper-body pitch reduced the effect of the first mode on the responses which was initially small, so that the upper limit for that damping parameter was also difficult to determine.

The effect of each parameter on the principal resonance of the apparent mass was examined. The frequencies and magnitudes of calculated normalised apparent mass with ± 30% changes in each model parameter from the initial values shown in Tables 8.11 and 8.12 are tabulated for Models 5 and 6 in Table 8.13 and 8.14.

Table 8.13 Resonance frequencies and magnitudes of the calculated normalised apparent mass with ± 30% changes in each model parameter in Model 5. Initial values were 5.28 Hz and 1.75.

	Frequency [Hz]		Magnitude	
	- 30%	+ 30%	- 30%	+ 30%
Stiffness				
Buttocks, vertical	4.60	5.70	1.59	1.86
Pelvis, pitch	5.27	5.29	1.73	1.76
Upper-body, pitch	5.24	5.33	1.75	1.78
Viscera, vertical	4.83	5.47	1.73	1.73
Damping				
Buttocks, vertical	5.41	5.21	2.09	1.57
Pelvis, pitch	5.28	5.29	1.76	1.75
Upper-body, pitch	5.26	5.31	1.79	1.74
Viscera, vertical	5.40	5.20	1.81	1.71

Table 8.14 Resonance frequencies and magnitudes of the calculated normalised apparent mass with ± 30% changes in each model parameter in Model 6. Initial values were 5.24 Hz and 1.72. (UB: upper-body.)

	Frequency [Hz]		Magnitude	
	- 30%	+ 30%	- 30%	+ 30%
Stiffness				
Buttocks, vertical	4.52	5.69	1.55	1.83
Pelvis, pitch	5.22	5.26	1.70	1.73
Lower UB, pitch	5.25	5.24	1.71	1.72
Upper UB, pitch	5.22	5.26	1.70	1.72
Viscera, vertical	4.81	5.42	1.70	1.69
Damping				
Buttocks, vertical	5.37	5.17	2.06	1.53
Pelvis, pitch	5.23	5.26	1.74	1.70
Lower UB, pitch	5.23	5.25	1.71	1.72
Upper UB, pitch	5.24	5.24	1.72	1.71
Viscera, vertical	5.36	5.16	1.76	1.68

It was clear in Tables 8.13 and 8.14 that the stiffness and damping for the vertical buttocks elements had the most significant effects on the principal resonance of the

apparent mass. Contributions from the parameters for the vertical visceral elements were also observed, particularly in the resonance frequency. However, the pitch degrees of freedom in the models had little effects on the apparent mass resonance, although a bending mode of the series of rotational masses in Models 5 and 6 was involved in the vibration mode at about 5 Hz, as shown in Tables 8.7 and 8.10.

8.3.1.5 Discussion of model parameters in seated body models

Some mechanical parameters in Models 5 and 6 can be directly attributed to mechanical properties of particular body parts. However, those properties in the living human body were seldom available in the literature because of the difficulties in making measurements.

Vertical stiffness and damping for the buttocks tissue

The combination of vertical stiffness and damping at the bottom of each model can be considered to be the stiffness and damping properties of the buttocks tissue, as referred to in the above sections. Data provided by Robinovitch *et al*. (1991) who estimated effective stiffness and damping of the lateral aspect of the hip seemed to be the only available data giving mechanical properties of the buttocks tissue. In their study, the force acting on the hip when the subject's pelvis was released onto the force platform was modelled by a single degree-of-freedom system. Stiffness and damping parameters were estimated by curve-fitting. Significant variability was observed in both parameters estimated: 3.0×10^4 to 1.8×10^5 N/m for the stiffness and 2.5×10^2 to 1.3×10^3 Ns/m for the damping in their male subjects. The parameters for the buttocks tissue obtained in this study were 1.53×10^5 N/m and 3.15×10^3 Ns/m for Model 5 and 1.44×10^5 N/m and 3.10×10^3 Ns/m for Model 6, as in Tables 8.6 and 8.9. The stiffnesses for Models 5 and 6 were within the range reported by Robinovitch *et al*. (1991), although rather greater than the majority of their results around 9.0×10^4 N/m. The damping for both Model 5 and Model 6 was greater than that obtained by Robinovitch *et al*. (1991). These differences could be partly attributed to the difference in the portion of the hip involved in the motion. Nonlinear characteristics of the tissue due to the difference in loading condition might also cause different stiffness and damping properties.

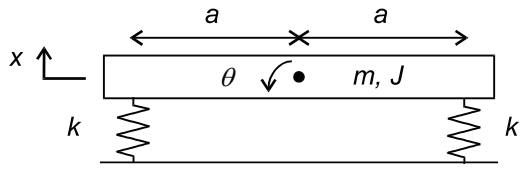

Figure 8.10 Model of rotational stiffness provided by two translational springs.

Pitch stiffness for the pelvis

Mechanical properties of the pelvis pitch elements in the models can be thought to be provided by the buttocks tissue. Figure 8.10 shows a model in which two identical translational springs in parallel provide rotational stiffness. Equations of motion of this two degree-of-freedom model were:

$$m\ddot{x} + k(x - a\theta) + k(x + a\theta) = m\ddot{x} + 2kx = 0 \tag{8.7}$$

$$J\ddot{\theta} - ak(x - a\theta) + ak(x + a\theta) = J\ddot{\theta} + 2a^2k\theta = 0 \tag{8.8}$$

where,

m, J : mass and inertial moment about the centre of gravity
k : stiffness of two identical springs
a : length between the centre of gravity and the connection point
x, θ : vertical and rotational displacement of the centre of gravity

The model was assumed to be symmetric about the vertical line passing through the centre of gravity. It is obvious from Equations (8.7) and (8.8) that the vertical stiffness coefficient of the model is given as $2k$ while the rotational stiffness coefficient is given as $2a^2k$. Therefore, the ratio of the rotational stiffness coefficient to the vertical stiffness coefficient was obtained as a^2. It was hypothesised that the vertical stiffness of the buttocks elements for Models 5 and 6 corresponded to $2k$ and the pitch stiffness of the buttocks corresponded to $2a^2k$ in the above model. The length between two springs, $2a$, in Figure 8.10 was then calculated for Models 5 and 6 by using parameters shown in Tables 8.6 and 8.9 respectively: 0.112 m for Model 5 and 0.158 m for Model 6. These results seemed to agree with the dimension of adult male buttocks, although they may be rather greater than the actual dimension. This may imply some contribution from the tissue beneath the thighs to the model parameters for the buttocks vertical element.

Vertical stiffness for the viscera

The parameters obtained for the visceral mass in the models can be compared with experimental results by Coermann *et al*. (1960). They measured the vertical motion of the abdominal wall of supine subjects caused by longitudinal vibrations (i.e., in *z*-axis for recumbent position in ISO 2631-1 (1997)). A distinct peak at 3 Hz was observed in the transmissibility from the input vibration to the vertical displacement of the abdominal wall. This peak may be attributed mainly to the behaviour of the organs in the abdominal cavity. Damped natural frequencies of only the visceral mass, spring and damper system in Models 5 and 6 were 7.18 and 7.26 Hz, respectively. These frequencies were more than twice as high as the peak frequency reported by Coermann *et al*. (1960). However, the calculated results here could be different from their experimental data. The difference in body position (i.e., between supine and seated) results in different loading condition on the visceral organs due to the gravity and the mass of other parts of the body so that mechanical properties of the soft tissues would be different in different body positions. The measurement axis used by Coermann *et al*. (1960) was not in line with the input vibration, which could also result in different mechanical properties observed in the results.

Pitch stiffness for the spine

The model parameters for the upper-body rotational elements could be thought equivalent to some lower modes of the spinal bending. Mechanical properties of bending motion of the spine are attributed to several body elements: main elements are the intervertebral discs, articular facets, ligaments, and muscles. It is clear that the measurement of the mechanical properties of those elements in living human body is very difficult. There have been studies in which stiffnesses of the vertebral column were measured *in vitro* by using spinal segments from cadavers (Markolf, 1970; Panjabi *et al*., 1977; Nachemson *et al*., 1979; Schultz *et al*., 1979; Berkson *et al*., 1979; Tencer *et al*., 1982; Miller *et al*., 1986, 1987; McGlashen *et al*., 1987). The static stiffnesses of a motion segment (i.e., two vertebrae interconnected by the intervertebral discs and other connective soft tissues except muscles) were usually measured in these studies. The results showed nonlinear behaviour of the spinal motion segments: the segments tended to become stiffer with increases in the deformation so that it was difficult to express the segment stiffness by a single number. Large variability was observed in the stiffnesses reported, probably due to difference between individuals, different stiffness depending on the level of the spine, different measurement methods and conditions, and difference in

the determination of the stiffness. Stiffnesses for flexion and extension varied between 50 and 320 Nm and between 120 and 440 Nm, respectively.

Results from *in vitro* measurements have been used in previous studies of finite element models of the body (Belytschko *et al*., 1976; Kitazaki and Griffin, 1997; Pankoke *et al*., 1998). However, it was still required in those studies to make assumptions or estimations of the model parameters because of the lack of other mechanical properties, such as effects of muscles and damping properties. Parameter identification for unknown properties was usually conducted by comparing the calculated model responses to the experimental data, as in the present study. There might be inherent difference in the properties in the living body and in the cadavers so that the parameters obtained from *in vitro* measurements might also require adjustment in some way. It was, therefore, difficult to conclude about the model parameters for rotational degrees of freedom in the upper-body with respect to comparison with the mechanical properties in a living body. However, it can be said that the parameters obtained were reasonable as long as the model responses represented the measured responses reasonably based on the discussion above.

8.3.2 Standing body model

8.3.2.1 Effect of model structure for the legs of the standing body

For the model of the dynamic response of the standing body, it is required to model the dynamic mechanism of the legs. It seems reasonable to model the movement of the joints at the ankle, knee and hip by a rotational connection in the sagittal plane, according to their anatomical structures and the experimental results shown in Chapters 6 and 7. The tissue at the soles of the feet could be represented by a vertical spring and damper. Four different models of the legs were used so as to investigate the effect of the model structure for the legs on the dynamic response of the body, Models 8 to 11 shown in Figure 8.11. The knee joint was assumed to be rigid in Models 8 and 9, because, in the experiment, the subjects were asked to keep their legs locked. The effect of the soles was not included in Models 8 and 10. The model structure for the upper-body for all standing body models presented here was the same as that for Model 5 shown in Figure 8.7(a).

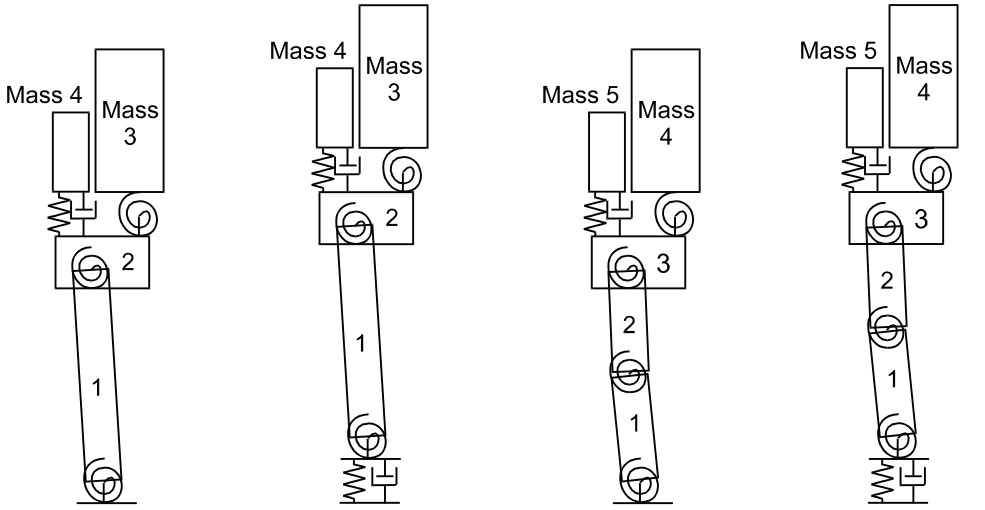

(a) Model 8 (b) Model 9 (c) Model 10 (d) Model 11

Figure 8.11 Lumped parameter models for the standing body.

Initial inertial and geometric properties are tabulated in Table 8.15. Stiffness and damping coefficients determined from the curve fitting for Models 8, 9, and 10 are shown in Tables 8.16 and 8.17, respectively. For Model 11, the parameter search did not converge, as in the case of Model 7 for the seated body, so that the stiffness and damping coefficients were not be able to be determined.

Table 8.15 Inertial and geometric parameters used in Model 8, 9, 10, and 11. (Connection: point of connection between mass and mass below.)

Model Mass	Mass [kg]	Inertial Moment [kg·m^2]	Centre of gravity (x, z) [m]	Connection (x, z) [m]	Transmissibility (x, z) [m]
Legs	24.4	10.6	(0.0600, 0.608)	(0, 0)	(0.0680, 0.488)
Calves	8.89	1.12	(0.0355, 0.335)	(0, 0)	(0.0680, 0.488)
Thighs	15.5	1.50	(0.0740, 0.765)	(0.0680, 0.488)	(0.0680, 0.488)
Pelvis	16.9	0.27	(0.0452, 1.036)	(0.0880, 0.962)	(-0.0304, 1.098)
Upper-body	30.4	7.49	(0.0543 1.526)	(-0.0253, 1.065)	(0.0187, 1.484)
Viscera	12.8	---	(0.0411, 1.187)	---	(0.0411, 1.187)

Table 8.16 Stiffness coefficients obtained for Models 8, 9 and 10.

Model	Sole, vertical [N/m]	Ankle, pitch [Nm]	Knee, pitch [Nm]	Hip, pitch [Nm]	Upper-body, pitch [Nm]	Viscera, vertical [N/m]
8	---	1.69×10^{4}	---	9.64×10^{2}	1.43×10^{1}	1.10×10^{5}
9	3.79×10^{5}	2.10×10^{4}	---	7.19×10^{2}	4.27×10^{2}	1.81×10^{4}
10	---	8.21×10^{3}	7.13×10^{2}	5.08×10^{2}	1.90×10^{3}	2.31×10^{4}

Table 8.17 Damping coefficients obtained for Models 8, 9 and 10.

Model	Sole, vertical [Ns/m]	Ankle, pitch [Nms]	Knee, pitch [Nms]	Hip, pitch [Nms]	Upper-body, pitch [Nms]	Viscera, vertical [Ns/m]
8	---	2.95×10^{2}	---	9.64×10^{0}	7.73×10^{0}	1.67×10^{2}
9	2.76×10^{3}	3.90×10^{2}	---	1.08×10^{1}	1.56×10^{1}	3.80×10^{2}
10	---	1.09×10^{2}	7.49×10^{0}	2.20×10^{1}	5.00×10^{0}	1.88×10^{2}

The apparent masses calculated from Models 8, 9 and 10 are compared with the median apparent mass obtained in the experiment, presented in Chapters 6 and 7, in Figure 8.12. The apparent mass calculated from Model 9 was close to that measured in the experiment, although a broad peak at about 9 Hz observed in the experimental data was not clear in the calculated apparent mass for Model 9. The apparent mass calculated from Model 10 also showed an agreement with the measured data, although the calculated principal resonance frequency was higher than the measured resonance frequency. The apparent mass calculated from Model 8, which included neither a vertical degree of freedom for the soles nor a rotational degree of freedom for the knee, showed a poor agreement with the measured apparent mass. The main resonance of the calculated values for Model 8 was smaller than the measured value. Some local resonances, which were not observed in the measured apparent mass, were clear in the apparent mass calculated from Model 8.

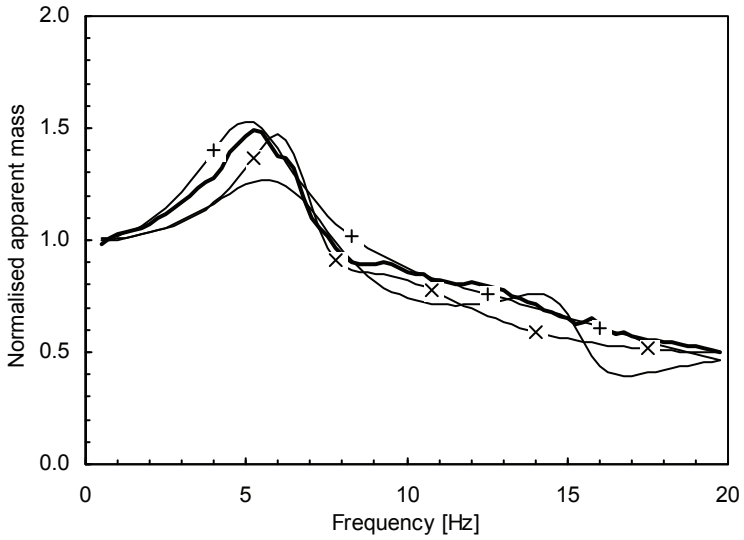

Figure 8.12 Apparent masses calculated from Models 8 ——— , 9 —+— and 10 —x— , and obtained in the experiment ━━━ .

The vertical transmissibilities calculated from the models and the median transmissibilities in the vertical axis obtained in the experiment are shown in Figure 8.13. Figure 8.14 compares the calculated and measured transmissibilities in the fore-and-aft direction. For the transmissibility to the vertical motion at the knee at frequencies below 6 Hz, those calculated from Models 8 and 10 were close to the measured values, which was almost unity in this frequency region (Figure 8.13(a)). The vertical degree of freedom for the sole included in Model 9 improved the representation of the apparent mass in this frequency range but made the representation of the vertical transmissibility to the knee worse. The transmissibility to the fore-and-aft knee motion was represented best by Model 10 which had a rotational degree of freedom for the knee (Figure 8.14(a)). A peak observed in the measured fore-and-aft transmissibility to the knee (see Figure 7.11(b)) might, therefore, be attributed to a bending motion of the legs at the knee, although the subjects were asked to lock their knee during the vibration exposure in the experiment presented in Chapters 6 and 7. It may be possible to improve the representation of the vertical transmissibilities to the lower upper-body of the standing body by incorporating a rotational degree of freedom for the knee joint in Model 9, as in Model 11.

The vertical transmissibilities to the pelvis calculated from Models 8 and 9 showed a better agreement with the experimental data than that from Model 10 in the frequency range between 2 and 7 Hz. However, the vertical transmissibility to the upper-body mass

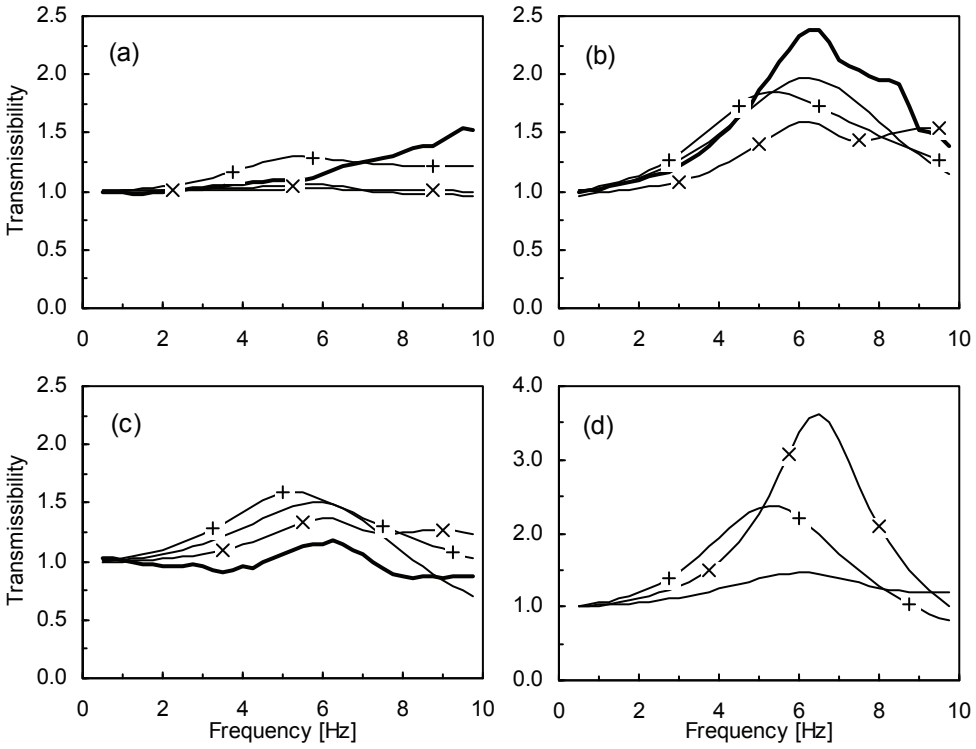

Figure 8.13 Vertical transmissibilities calculated from the models and obtained in the experiment: (a) for the knee, (b) for the pelvis, and (c) for T5. The calculated vertical transmissibilities for the visceral mass are also shown in (d). Model 8 ——— ; Model 9 —+— ; Model 10 —x— ; experiment ━━━ .

calculated from Model 10 was closer to the measured transmissibility to T5 than the transmissibilities obtained from Models 8 and 9. For the transmissibility to fore-and-aft motions at the pelvis and T5, those calculated from Models 9 and 10 showed similar magnitudes to the measured data in the frequency range below 10 Hz. Models 9 and 10 seemed to represent the upper-body responses generally with a similar quality.

Five vibration modes were obtained from Models 9 and 10 with no damping in the frequency range below 20 Hz. Tables 8.18 shows the natural frequencies and modal vectors for the five modes for Model 9. The first mode at 0.95 Hz was a combination of rocking and bending modes of the upper-body including the pelvis. The second mode at 5.43 Hz made a main contribution to the principal resonance of the apparent mass. A vertical motion of the viscera in phase with axial deformation of the sole tissues and a pitching of the pelvis out of phase with a pitching of the upper-body except the pelvis were involved in the second mode. The third mode at 7.07 Hz was dominated by a rocking of the legs in phase with a pitching of the pelvis. The fourth mode found at 7.40

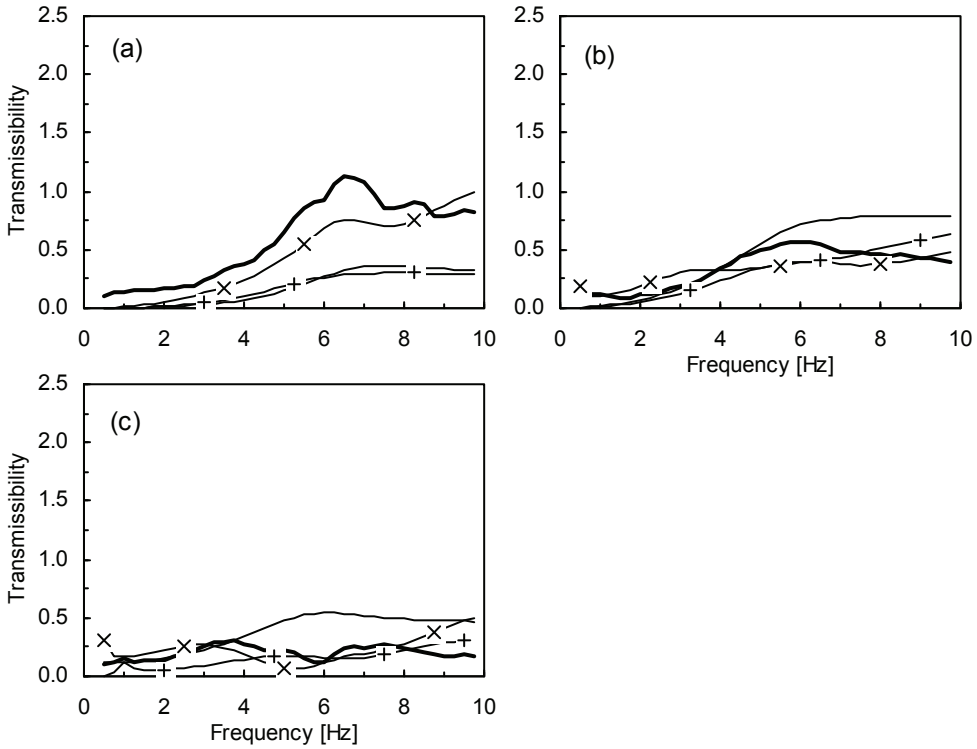

Figure 8.14 Fore-and-aft transmissibilities calculated from the models and obtained in the experiment: (a) for the knee, (b) for the pelvis, and (c) for T5. Model 8 ——; Model 9 —+—; Model 10 —x—; experiment ━━.

Hz contributed to the second broad peak in the apparent mass. The fourth mode shape was similar to the second mode shape except the visceral motion whose phase relation to the deformation of the sole tissues and pelvis pitch was opposite in the fourth mode compared to the second mode. The fifth mode at 15.8 Hz was dominated by an axial deformation of the sole tissues and a pitching of the pelvis. The directions of these two motions were opposite compared to the other four modes. The upper-body mass was isolated in the four higher modes (i.e., the second to fifth) by a rotational motion at the connection between the upper-body mass and the pelvis mass.

The natural frequencies and modal vectors for the five modes for Model 10 are tabulated in Table 8.19. The first mode at 0.42 Hz consisted of a bending motion at the knee. The model masses above the knee connection moved together with a slight bending in the upper-body in phase with the bending of the knee. The second mode at 3.02 Hz was dominated by a bending motion of the knee out of phase with a bending of the upper-body. The principal resonance of the apparent mass was caused by the third mode at 6.59 Hz. The mode shape involved a bending motion of the legs at the ankle, the knee

Table 8.18 Natural frequencies and mode shapes of Model 9 with no damping. (Mode shapes were normalised to have a vector magnitude of unity.)

Mode	1	2	3	4	5
Frequency [Hz]	0.95	5.43	7.07	7.40	15.8
Legs, vertical [m]	0.000	0.037	0.003	0.021	0.122
Legs, pitch [rad]	0.012	-0.061	0.513	-0.057	0.049
Pelvis [rad]	0.357	0.881	0.858	0.989	-0.991
Upper-body [rad]	0.934	-0.013	-0.016	0.004	0.012
Viscera [m]	0.016	0.467	0.006	-0.137	-0.012

Table 8.19 Natural frequencies and mode shapes of Model 10 with no damping. (Mode shapes were normalised to have a vector magnitude of unity.)

Mode	1	2	3	4	5
Frequency [Hz]	0.42	3.02	6.59	10.3	13.7
Calves [rad]	0.005	0.011	0.240	0.329	0.656
Thighs [rad]	0.529	0.982	-0.091	0.022	-0.034
Pelvis [rad]	0.592	0.066	-0.553	-0.942	0.754
Upper-body [rad]	0.608	-0.174	0.077	0.032	-0.020
Viscera [m]	0.017	-0.022	-0.789	0.051	0.003

and the hip joints and a visceral motion. The bending motion of the legs at the three joints seemed to transmit a vertical motion to the upper-body. The fourth and fifth modes were basically dominated by bending motions at three joints in the legs with different phase relations. As in Model 9, a rotational motion at the connection between the upper-body mass and the pelvis mass isolated the upper-body mass in the second to fifth modes.

It was expected that there were differences in modal properties between the two models due to different model structures. However, with respect to the vibration modes causing the principal resonance of the apparent mass, a vertical motion of the visceral mass and a pitching motion of the pelvis mass were involved in those modes in both models. An

upward motion of the visceral mass was in phase with a forward rotation of the pelvis mass. These two motions and their phase relation were consistent with those found in the vibration modes of the seated body models which caused the apparent mass resonance, as mentioned in Section 8.3.1.3 (i.e., Models 5 and 6). A vertical input motion to the pelvis and upper-body was transmitted through the legs with deformation of the sole tissues and bending motions at the joints in the legs for standing body models, as opposed to deformation of the buttocks tissues in the seated body models.

8.3.2.2 Parameter sensitivity in standing body models

The effect of changes in the parameters on the responses were investigated with Models 9 and 10 as for the seated body models described in Section 8.3.1.4. The error function given in Equation (8.6) was used in the investigation. Lower and upper limits for each parameters were determined in the same way as for the seated body model: parameter changes which increased any of error functions by 10%. The limits obtained for each parameters with the corresponding initial values and ratios of those limits to the initial values are tabulated for Models 9 and 10 in Tables 8.20 and 8.21, respectively.

General trends observed in the parameter sensitivity analysis were the same as those for the seated body models shown in 8.3.1.4: the parameters for the vertical axis affected the apparent mass and transmissibilities while the parameters for the pitch axis affected mainly the transmissibilities only. However, in the standing body models, particularly in Model 9, changes in the parameters of pitch degrees of freedom for the hip joint and upper-body showed effects on the apparent mass as well as the transmissibilities.

The principal resonance frequencies and magnitudes of the normalised apparent mass calculated from Models 9 and 10 with ± 30% changes in each parameter are tabulated in Tables 8.22 and 8.23, respectively. For both Models 9 and 10, the vertical degree of freedom for the visceral mass had the most significant effect on the apparent mass resonance. For Model 9, the vertical sole element, particularly its stiffness, showed a contribution to the resonance magnitude. The pitch stiffnesses for the pelvis and upper-body masses had a relatively large effect on the resonance frequency. The least effect of the pitch degrees of freedom for the ankle on the resonance was found in Model 9. For Model 10, the principal resonance of the apparent mass was dominated by the visceral element which was the only vertical degree of freedom in the model.

Table 8.20 Parameter ranges for Model 9. Stiffness in the vertical axis in [N/m], stiffness in the pitch axis in [Nm]. Damping in the vertical axis in [Ns/m], damping in the pitch axis in [Nms].

	Lower limit	Ratio [%]	Upper limit	Ratio [%]	Initial value
Stiffness					
Sole, vertical	$2.81x10^5$	74.2	$5.57x10^5$	147	$3.79x10^5$
Ankle, pitch	$1.88x10^4$	89.4	$3.05x10^4$	145	$2.10x10^4$
Hip, pitch	$5.03x10^2$	70.0	$8.92x10^2$	124	$7.19x10^2$
Upper-body, pitch	$1.90x10^2$	44.6	$4.83x10^2$	113	$4.27x10^2$
Viscera, vertical	$1.01x10^4$	55.6	$2.53x10^4$	140	$1.81x10^4$
Damping					
Sole, vertical	$1.59x10^3$	57.6	$5.41x10^3$	196	$2.76x10^3$
Ankle, pitch	$3.32x10^2$	85.0	$4.99x10^2$	128	$3.90x10^2$
Hip, pitch	$5.59x10^0$	51.8	$1.56x10^1$	144	$1.08x10^1$
Upper-body, pitch	$1.29x10^1$	83.0	$1.87x10^1$	120	$1.56x10^1$
Viscera, vertical	$2.39x10^2$	63.0	$1.07x10^3$	282	$3.80x10^2$

Table 8.21 Parameter ranges for Model 10. Stiffness in the vertical axis in [N/m], stiffness in the pitch axis in [Nm]. Damping in the vertical axis in [Ns/m], damping in the pitch axis in [Nms].

	Lower limit	Ratio [%]	Upper limit	Ratio [%]	Initial value
Stiffness					
Ankle, pitch	$7.70x10^3$	93.8	$9.11x10^3$	111	$8.21x10^3$
Knee, pitch	---	---	$1.01x10^2$	141	$7.13x10^1$
Hip, pitch	$1.92x10^2$	37.8	$6.05x10^2$	119	$5.08x10^2$
Upper-body, pitch	$1.81x10^3$	95.4	$2.05x10^3$	108	$1.90x10^3$
Viscera, vertical	$1.90x10^4$	82.2	$2.63x10^4$	114	$2.31x10^4$
Damping					
Ankle, pitch	$1.03x10^2$	94.6	$1.42x10^2$	130	$1.09x10^2$
Knee, pitch	$5.45x10^0$	72.8	$1.27x10^1$	169	$7.49x10^0$
Hip, pitch	$2.01x10^1$	91.2	$2.40x10^1$	109	$2.20x10^1$
Upper-body, pitch	---	---	$6.85x10^0$	137	$5.00x10^0$
Viscera, vertical	$1.36x10^2$	72.6	$2.48x10^2$	132	$1.88x10^2$

Table 8.22 Resonance frequencies and magnitudes of the calculated normalised apparent mass with ± 30% changes in each model parameter in Model 9. Initial values were 5.05 Hz and 1.53.

	Frequency [Hz]		Magnitude	
	- 30%	+ 30%	- 30%	+ 30%
Stiffness				
Sole, vertical	4.93	5.07	1.63	1.46
Ankle, pitch	5.01	5.07	1.52	1.53
Hip, pitch	4.83	5.24	1.47	1.56
Upper-body, pitch	4.94	5.15	1.51	1.55
Viscera, vertical	4.69	5.38	1.41	1.61
Damping				
Sole, vertical	5.13	4.98	1.56	1.50
Ankle, pitch	5.07	5.05	1.54	1.52
Hip, pitch	5.08	5.04	1.57	1.50
Upper-body, pitch	5.09	5.04	1.58	1.49
Viscera, vertical	4.99	5.22	1.60	1.50

Table 8.23 Resonance frequencies and magnitudes of the calculated normalised apparent mass with ± 30% changes in each model parameter in Model 10. Initial values were 6.01 Hz and 1.47.

	Frequency [Hz]		Magnitude	
	- 30%	+ 30%	- 30%	+ 30%
Stiffness				
Ankle, pitch	5.95	6.04	1.46	1.47
Knee, pitch	6.01	6.02	1.47	1.47
Hip, pitch	6.01	6.02	1.48	1.46
Upper-body, pitch	5.86	6.07	1.47	1.43
Viscera, vertical	5.03	6.78	1.34	1.56
Damping				
Ankle, pitch	6.04	6.00	1.49	1.45
Knee, pitch	6.01	6.01	1.47	1.47
Hip, pitch	6.05	5.98	1.49	1.45
Upper-body, pitch	6.03	6.00	1.48	1.46
Viscera, vertical	6.16	5.93	1.63	1.37

In the models for the standing body presented in this chapter, the geometrical properties for the upper-body were the same as those used for the models of the seated body. It is known, however, that the posture of the upper-body in a standing position is different from that in a sitting position: the curvature of the lumbar spine is more distinct in a standing position than in a sitting position, for example (e.g. Pheasant, 1996). The difference in the geometrical properties might affect the behaviour of the model, especially in the pitch direction, although this was not investigated in this study because reliable data for those geometrical properties were not available.

8.3.2.3 Discussion of model parameters in standing body models

Vertical stiffness for the sole tissue

The vertical stiffness at the bottom of Model 9 can be compared to the vertical stiffness of the soft tissue beneath the foot measured in previous studies. The behaviour of the heel pad during exposure to impacts, simulating walking and heel-strike running, has been measured by Nigg (1986), Jørgensen and Bojsen-Møller (1989) and Aerts and De Clercq (1993). In these studies, the stiffness of the heel pad was estimated from measurements of impact acceleration and force acting on the heel pad. Time integration of accelerations was usually involved in the analysis so as to determine displacement response. The heel pad stiffness varied between those studies: 1.5×10^5 to 4.5×10^5 by Nigg (1986) by assuming 15 cm^2 of the contact area between the heel pad and the ground, 1.9×10^5 N/m by Jørgensen and Bojsen-Møller (1989), 5.2×10^4 to 1.50×10^5 N/m by Aerts and De Clercq (1993). The vertical sole stiffness obtained for Model 9 was 3.79×10^5 N/m, 1.90×10^5 N/m for each leg by assuming two parallel springs. The order of the sole stiffness obtained for Model 9 was, therefore, comparable with these measurement results, although there should be some effect of the tissue beneath the foot other than the heel pad on the model stiffness.

Parameters for the leg joints

The rotational mechanical properties for the ankle, knee, and hip joints may be dependent on the muscle tension supporting the joints as well as the passive mechanical properties in the articulations. The dependency on the muscles in these leg joints may be more significant than that in the upper-body in a normally seated position. The muscle activity would differ for different types, magnitudes and directions of the motion exerted. It

is, therefore, difficult to obtain some sort of 'standard' data for those parameters with human subjects. The definition of stiffness and damping for those mechanical properties may also be difficult to determine. Therefore, there appear to be no such data available which can be compared with the obtained model parameters.

Parameters for the upper-body

The model structure of the upper-body in Models 9 and 10 was the same as the structure in Model 5 for the seated body, as mentioned above. The parameters for the upper-body and viscera in Models 9 and 10 can, therefore, be compared with those in Model 5. The pitch parameters for the upper-body mass for each model were: 4.27×10^{2} Nm for stiffness and 1.56×10^{1} Nms for damping in Model 9, 1.90×10^{3} Nm and 5.00×10^{0} Nms in Model 10, 1.59×10^{3} Nm and 5.27×10^{1} Nms in Model 5. These pitch parameters were affected by other pitch parameters in the parameter identification. The differences seen in those pitch parameters were, therefore, due to the different model structure in other parts. The vertical parameters for the visceral mass for each model were: 1.81×10^{4} N/m for stiffness and 3.80×10^{2} Ns/m for damping in Model 9, 2.31×10^{4} N/m and 1.88×10^{2} Ns/m in Model 10, 2.67×10^{4} Nm and 1.85×10^{2} Nms in Model 5. The parameters in Model 10 were similar to those in Model 5 and Model 6, another seated body model, although the parameters in Model 9 showed a different trend. The reason for the difference in the stiffness between Models 9 and 10 seemed to be that, in Model 9, the vertical visceral stiffness dominated the model responses at lower frequencies and the vertical sole stiffness dominated at higher frequencies, while, in Model 10, the vertical visceral stiffness covered the responses in all frequency region. It seemed that Model 10 was preferable to Model 9 because of the consistency in the visceral parameters with those in the seated body models. However, the principal resonance frequency of the apparent mass calculated from Model 10 was higher than the measured value as seen in Figure 8.12, while the apparent mass calculated from Model 9 showed a better agreement with the experimental data. It was, therefore, difficult to conclude which model was superior to another.

8.4 CONCLUSIONS

Alternative lumped parameter models with different structures to represent the dynamic response of the seated and standing body have been investigated. Rotational degrees of freedom with eccentricity of the centre of gravity of the masses have been included in the models to represent two dimensional motion of the body in the mid-sagittal plane observed in an experiment. Nonlinearities due to the geometry and material properties could be included in the models but were neglected in this investigation so as to retain simplicity.

It appeared that the inclusion of rotational degrees of freedom in the model improved the representation of the dynamic responses of the body, especially for the transmissibilities. In the seated body models, the principal resonance of the apparent mass at about 5 Hz was attributed to a vibration mode consisting of a vertical motion of the pelvis and legs and a pitch motion of the pelvis, both of which caused a vertical motion of the upper-body, a bending of the spine and a vertical motion of the viscera. The vertical motion due to deformation of the buttocks tissue and the vertical motion of the viscera made a dominant contribution to the apparent mass resonance. A vertical motion of the viscera and a pitching motion of the pelvis were also involved in vibration modes that made major contribution to the apparent mass resonance in standing body models. Vertical floor vibration may be transmitted to the pelvis and upper-body through the legs with deformation of the sole tissues and bending motions at the joints in the legs in the standing body, as opposed to deformation of the buttocks tissues in the seated body. The contribution of the bending motion of the spine seen in the experimental results to the principal resonance of the apparent mass may be relatively small, although the bending occurred at the resonance frequency. The apparent mass, or mechanical impedance, may not be suitable functions for the investigation on the spinal response to vertical whole-body vibration.

Models for the upper-body, particularly for the spine, shown in this report could be extended to a series of rotational masses which might give a more realistic representation of the spinal structure. It was, however, difficult to determine the stiffness and damping properties for models with more than six degree-of-freedom by using the parameter identification method used in this investigation. Possible reasons for the difficulty are: (1) the limited frequency range of the experimental data which restricts the number of resonances observed, (2) the nature of the human body with heavy damping which also

reduces the number of resonances seen in the experimental data, (3) the relatively low quality of the fore-and-aft transmissibilities at low frequencies measured in the experiment. Models developed in this chapter could be extended to nonlinear models so as to investigate the nonlinearity in the biodynamic responses observed in the experiments presented in the previous chapters. Nonlinear elements might be incorporated so as to investigate unknown mechanical properties of the soft tissues in the living human body. Geometrical nonlinearity due to the eccentricity of the centre of gravity of rotational masses might also be included in models.

CHAPTER 9

GENERAL DISCUSSION, GENERAL CONCLUSIONS, AND RECOMMENDATIONS

9.1 GENERAL DISCUSSION

9.1.1 Principal resonance of the apparent mass

The main objective of the study identified from the review of literature was to understand the dynamic mechanisms of the principal resonance observed in the driving-point apparent mass of the human body in standing and seated positions when exposed to vertical whole-body vibration. The principal resonance in the apparent mass of subjects in a normal standing posture was found in the frequency range around 5 Hz with a total of 32 male subjects in three experiments. The principal resonance frequency tended to be higher in a standing position than in a sitting position, although the difference was generally within 1 Hz, in 20 subjects for whom the apparent mass in a sitting posture was measured in Experiments 1 and 3. The principal resonance frequency decreased by about 1 Hz with a postural change from normal to slouched in the upper-bodies of standing subjects with straight legs. This postural change in the upper-body has shown a similar frequency shift in previous studies with seated subjects (e.g. Fairley and Griffin, 1989). A decrease in the principal resonance frequency by about 1.5 Hz due to an increase in the input vibration magnitude from 0.125 to 2.0 ms^{-2} r.m.s. was observed in the apparent masses with both standing and seated subjects. These findings (i.e., similarities in the apparent mass resonance characteristics for standing and seated subjects) implied that the causes of the principal resonance in the apparent mass were similar in standing and sitting positions. It was likely that some dynamic mechanisms in the upper-body caused the resonance.

9.1.2 Dynamic mechanisms of the seated body

Movements of the upper-bodies of seated subjects at the principal resonance frequency were illustrated, based on transmissibility measurements in three axes in the sagittal

plane at eight locations with eight subjects. The movement at the resonance consisted of bending of the lumbar spine and probably the thoracic spine below T10, rocking of the thoracic spine and rib cage about the lower thoracic spine, pitching of the pelvis, and deformation of the tissue beneath the pelvis. The lumbar spine seemed to bend in an S-shape at L1. Slight bending along the full length of the thoracic spine also occurred at the resonance, which might be restricted by the connections between the vertebrae and ribs (i.e., the costovertebral joints). The movement at the resonance described above may be considered a vibration mode shape which contributes to the resonance. In many mechanical structures, each vibration mode is usually well isolated from each other mode because of relatively low damping properties, so that the motion at a natural frequency may be almost identical to the corresponding vibration mode shape. The damping properties in the human body in the frequency range of interest may be attributed to the muscles, connective tissues, and other soft tissues in the body. However, there have been no available data on the damping properties of these soft tissues in the living human body. The damping ratio obtained for the local tissue-accelerometer system presented in Appendices C.3 and D.3, a minimum value of 0.2, indicates heavy damping properties of the body soft tissues. If there were more than one vibration mode at around the resonance frequency, as reported by Kitazaki (1994) and Kitazaki and Griffin (1997, 1998), the modes could be coupled with each other due to the heavy damping properties in the body. Therefore, the movement at the resonance observed was not necessarily the mode shape corresponding to the principal resonance.

The results obtained in the present study can be compared with those obtained by Kitazaki (1994) and Kitazaki and Griffin (1997, 1998) which have been the only other investigations of the dynamic mechanisms of the seated body based on a comprehensive set of measurement locations in the body. Experimental modal analysis was attempted on the transmissibilities obtained here, as in Kitazaki (1994) and Kitazaki and Griffin (1998), although the analysis details are not described in this thesis because of uncertainties in the results. One or two vibration modes were derived from the transmissibilities below 10 Hz, as opposed to eight modes by Kitazaki (1994) and Kitazaki and Griffin (1998). The first mode shape at about 5 Hz extracted in the present study was similar to the movements described above. The observed motions in different body parts involved in the movements at the resonance could be separate vibration modes at different natural frequencies, as in Kitazaki (1994) and Kitazaki and Griffin (1998). It seemed, however, that those motions were coupled with each other due to the heavy damping of the human body and appeared as one mode in the experimental

modal analysis performed here. There were one or two clear peaks observed in the measured transmissibilities at frequencies below 10 Hz, as presented in Chapters 6 and 7. This might have resulted in one or two vibration modes extracted from the experimental modal analysis in the present study. The smaller number of vibration modes derived in this study than in Kitazaki (1994) and Kitazaki and Griffin (1998) may be partly because of the lack of measurement of the visceral motion. It is, therefore, difficult to conclude about the discrepancy in vibration modes extracted from experimental modal analysis between this study and Kitazaki (1994) and Kitazaki and Griffin (1998).

The investigation of alternative lumped parameter models with different structures showed that two vertical degrees of freedom were required to represent the apparent mass for the seated body. The apparent mass and transmissibilities calculated from the model and the experimental data were compared. The tissues beneath the pelvis and the viscera, rather than any structures in the vertebral column, appeared to be reasonable body structures to incorporate in the model as those two vertical degrees of freedom. Two models, Models 5 and 6 (see Section 8.3.1.3), appeared to represent the seated body responses reasonably. The vibration mode of both models contributing to the principal resonance consisted of vertical motion of the pelvis and leg masses, pitch motion of both the pelvis mass and upper-body masses, and vertical motion of the viscera. This showed an agreement with the body movement at the resonance obtained from the measured transmissibilities described above. It was found that the principal resonance of the apparent mass was most affected by changes in mechanical parameters for the vertical degrees of freedom for the buttocks tissue and viscera. This implied that the principal resonance was dominated by those vertical degrees of freedom. Bending motion of the spine did not seem to make a main contribution to the principal resonance, although significant bending was observed in the experimental data as well as in the model response. The apparent mass in the vertical direction, therefore, is not the best objective measure to investigate the effect of vibration on the spine, even though bending motion occurred at the apparent mass resonance frequency.

Kitazaki (1994) and Kitazaki and Griffin (1997) concluded from their finite element model that ‘the driving point response at about 5 Hz consisted of an entire body mode, in which the head, spinal column and the pelvis move almost rigidly, with axial and shear deformation of tissue beneath the pelvis occurring in phase with a vertical visceral mode.’ It was also stated that ‘a bending mode of the lumbar spine was included in the next higher mode at 5.77 Hz which seemed to make a minor contribution to the principal

resonance, while a rotational mode of the pelvis was not found in either the principal mode nor in the next higher mode.' These findings about the principal resonance mechanisms from the finite element models are almost consistent with the findings from the lumped parameter models in the present study, except the contribution from pitch motion of the pelvis. It was recommended by Kitazaki (1994) that his model should be modified further to predict the transmissibilities quantitatively. The lumped parameter models developed in the present study seem to represent the transmissibilities quantitatively better than the model by Kitazaki (1994), although the model structure in this study was much simpler, so that the number of locations at which to calculate the transmissibility was limited. An advantage of the lumped parameter models developed in the present study may be the simplicity of the model structure. The effects of each model parameter on the model response were rather easily demonstrated so that the contributions of each part of the model to the response could be understood clearly. The lumped parameter models developed for the seated body in this study provided reasonable representations of the anatomical nature and the dynamic response of the body with some simplicity assisting the fundamental understanding of the body dynamic mechanisms at frequencies below 10 Hz.

9.1.3 Dynamic mechanisms of the standing body

Movements of the standing body at the principal resonance frequency were illustrated as for the seated body, by using transmissibilities in three axes in the sagittal plane at eight locations with eight subjects. Bending of the lumbar and lower thoracic spine, rocking of the thoracic spine and rib cage about the lower thoracic spine with slight bending along the full length of the thoracic spine, and pitching of the pelvis were involved in the movement at the resonance with both standing and seated bodies. For the standing body, axial motion along the spine in the lumbar and lower thoracic regions was combined with the bending motion. The difference in the axial spinal motion between standing and seated bodies might be attributed to lower intradiscal pressure in the lumbar spine in an upright standing position than in an upright sitting position (Nachemson and Morris, 1964; and Nachemson, 1981). A less compressed lumbar spine, probably due to more lordosis and less muscle activity involved to maintain the posture, might be more flexible in the axial direction. Rocking of the legs about the ankle joints, slight bending at the knee joints, and probably shear deformation of the foot sole tissue were found to be more dominant than any vertical dynamic response of the legs.

These motions seemed be major vibration transmission mechanisms from floor to the upper-body in a standing position.

In the investigation of lumped parameter models for the standing body, different model structures for the legs were examined. Two models with the same basic structure as for the upper-body in seated body Model 5, represented the measured apparent mass and transmissibilities reasonably well (Models 9 and 10, see Section 8.3.2.1). Model 9 had two rotational connections for the hip and ankle joints and a vertical degree of freedom for the tissue beneath the foot, while Model 10 had three rotational connections for the hip, knee and ankle joints. For the two models, the vibration modes which corresponded to the principal resonance of the apparent mass included vertical motion of the visceral mass, pitching motion of the pelvis mass and pitching motion of the upper-body mass. Vertical floor vibration seemed to be transmitted to the pelvis and the upper-body through the legs with deformation of the tissue beneath the foot and bending motions at three leg joints at the resonance. Changes in the model parameters for the vertical degrees of freedom, particularly for the viscera, most affected the principal resonance of the apparent mass. It was found that the pitch stiffness of the pelvis and upper-body masses had some effects on the resonance frequency. It is likely that the apparent mass resonance for the standing body is most dominated by the dynamic response of the viscera. There may be some minor contributions from the rotational responses in the upper-body, such as pitching of the pelvis and bending of the spine.

9.2 GENERAL CONCLUSIONS

It is concluded that the principal resonance in the apparent mass of the seated body at about 5 Hz is mainly caused by deformation of the tissue beneath the pelvis and vertical motion of the viscera in the abdominal cavity. These motions occur in phase with each other. Bending motion of the spine, particularly the lumbar spine, and pitching motion of the pelvis also occur at the principal resonance frequency, although they do not make major contributions to the resonance. Any appreciable axial motion in the spine is not involved in the dynamic response at frequencies below 10 Hz. Some other objective measurement, rather than the driving-point response, may be required to represent the dynamic response of the spine.

The principal resonance in the apparent mass of the standing body is most dominated by the dynamic response of the viscera. Rotational motions at the ankle, knee and hip

joints and deformation of the tissue of the foot sole are major vibration transmission mechanisms from the floor to the upper-body. Significant bending motion of the spine is involved in the body movement at the principal resonance frequency, although the contribution to the apparent mass resonance is relatively small, as in the seated body. Axial motion in the lower spine has been observed in the movement at the resonance in the standing body, although the cause of the different axial spinal response between standing and seated bodies has not been clear.

9.3 RECOMMENDATIONS

It was found that the dynamic response of the viscera made a major contribution to the principal resonance of the apparent mass for seated and standing bodies. However, the mechanisms of the visceral response have not been well understood. The word ‘viscera’ used in this study meant the organs held in the abdominal cavity and other surrounding tissues. The viscera were represented by a single degree of freedom system in the models developed in this study. It is obvious, however, that the dynamic response of the viscera is far more complicated than a simple single degree of freedom because of the mechanical properties of the soft tissues and the abdominal muscle activity. The dynamic interaction between the viscera and the spine and other upper parts of the body, which were ignored in this study, may have some effect on the measured transmissibilities and apparent mass. Knowledge of the dynamic behaviour of the visceral region is, therefore, important for an understanding of the body response.

The causes of the nonlinearity observed in the apparent mass and transmissibilities were not identified in this study. Mansfield (1998) concluded that ‘the nonlinearity observed in the apparent mass is likely to be caused by the geometry of the body’, after rejecting several possible factors: ‘involuntary changes in posture’, ‘stiffening of the skeleton’, ‘dynamics of the tissue beneath the ischial tuberosities’, ‘changes in muscle tone’, ‘nonlinear dynamics of system parameters’, and ‘active muscle control’. The modelling investigation in the present study indicated that bending, or buckling, of the vertebral column made a minor contribution to the principal resonance of the apparent mass, although nonlinear effects due to the geometry of rotational masses were neglected in the models. It may be, therefore, difficult to conclude that nonlinearity due to the geometry of the body is the only cause of the nonlinearity observed in the apparent mass. Nonlinear effects observed in the apparent mass caused by increasing vibration magnitude could be modelled by decreasing stiffnesses for both of the two

vertical springs for the viscera and buttocks tissue, for example, in Model 5, although the calculation results are not presented. It is likely, therefore, that some softening nature in the soft tissues in the body makes a contribution to the resonance frequency decreases due to increases in the vibration magnitude. It was found by Lakie *et al*. (1979, 1984), Hagbarth *et al*. (1985) and Lakie (1986) that relaxed human muscles in the fingers and wrists showed 'thixotropic' behaviour (stiffer in small movements than in large movements). Other soft tissues in the living human body, such as those in the viscera, might also have similar properties which contribute to the nonlinearity in the apparent mass and transmissibilities. Further investigations on the mechanical properties of soft tissues are required so as to identify the causes of nonlinearity.

It was found that the transmissibilities measured at the lower spine for standing subjects were significantly greater than those for seated subjects. The transmissibilities obtained for seated subjects showed good agreements with the transmissibilities determined in previous studies. However, the transmissibilities to the lower spine obtained for standing subjects tended to be greater than those reported in previous studies, although only two subjects were involved in the data from the previous studies. The previous data with two standing subjects were within the inter-subject variability in this study. The differences observed between the data in this thesis and those in the previous studies might, therefore, be caused by the differences between individuals. An appreciable axial motion of the lower spine was observed in the movement at the principal resonance for standing subjects, which was not found with seated subjects. Variability between subjects both in the transmissibilities to the lower spine and in the movement of the lower spine at the principal resonance frequency was larger for standing subjects than for the seated subjects (see Chapters 6 and 7). These differences in the variabilities between standing and seated positions within a subject might not be expected. It is, therefore, recommended to investigate the transmissibility to the lower spine with a group of several subjects by using other measurement methods, for example, the direct measurement so as to confirm the difference in the lower spine response between standing and seated positions.

In the investigation of lumped parameter models, the degrees of freedom in the models were restricted to five because of the difficulty in determining model stiffness and damping parameters by the parameter identification method used. Experimental data at higher frequencies above 10 Hz might increase the number of peaks in the transmissibilities so that it might be possible to increase the degrees of freedom in the models with the same parameter identification method. Some different methods of

determining model mechanical parameters might be required to increase the degrees of freedom in the models with the experimental data obtained so as to represent the dynamics of the spine better. The lumped parameter models can also be improved by incorporating the dynamic interaction between the viscera and parts of the body other than the pelvis. However, the dynamic interaction between the viscera and the surrounding body elements, which may be influenced by the intra-abdominal pressure and direct contact between the viscera and other body elements, has not been fully understood. A fore-and-aft degree of freedom to represent shear deformation of the tissue beneath the pelvis, which seemed to occur at the principal resonance frequency in seated subjects, might be incorporated in the models. Nonlinear system parameters, such as nonlinear stiffness, and geometrical nonlinearity can be included in such models so as to investigate the causes of the nonlinearity observed in the apparent mass and transmissibility.

The apparent masses of subjects when standing with the legs bent and when standing on one leg showed decreases in the principal resonance of the apparent mass compared to the apparent mass for the normal standing posture: reduced to about 3 Hz in the legs bent posture, and to about 4 Hz in the one leg posture. At higher frequencies above the main resonance, the apparent masses in these two postures were lower than the apparent mass in the normal standing posture. These dynamic behaviours were similar to those observed in mechanical structures with vibration isolators. It may be expected that these postural changes in the legs result in more flexible leg joints and lower stiffness in the legs. It seems that bending of the legs for the legs bent posture, and three dimensional rotational motions at the joints in the leg for the one leg posture, were responsible for the vibration isolation of the upper-body. When people are exposed to vertical vibration in a standing position, they may tend to bend the legs so as to reduce discomfort caused by vibration. The legs bent posture could provide useful information on the mechanical functions of the legs in terms of vibration isolation. The information from the one leg posture could be a basis of understanding the dynamic behaviour of the body when exposed to vibration during walking. Further investigation of these standing postures may, therefore, contribute to understanding of the dynamic response of the human body in a practical sense.

Investigations of the dynamic responses of the body to whole-body vibration in non-vertical axes are required so as to more fully understand the nature of the dynamic mechanisms inherent in the human body. This understanding is required to understand possible injury mechanisms of the body, particularly the spine, due to vibration and

shock. The dynamic responses will also have effects on subjective responses, such as discomfort due to vibration. Understanding of the relation between the dynamic and subjective responses may contribute to an objective basis for subjective responses.

APPENDIX A RELATION BETWEEN APPARENT MASS, NORMALISED APPARENT MASS AND TRANSMISSIBILITY IN LUMPED PARAMETER MODELS

The relation between apparent mass, normalised apparent mass and transmissibility was considered using lumped parameter models in a single axis (i.e., the vertical axis).

A.1 Single degree of freedom model

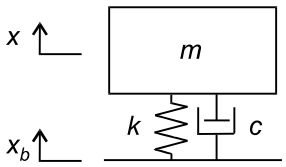

Figure A.1 Single degree of freedom model.

The equation of motion of the single degree of freedom model shown in Figure A.1 when exposed to input motion at the base is:

$$m\ddot{x}(t) + c(\dot{x}(t) - \dot{x}_b(t)) + k(x(t) - x_b(t)) = 0 \quad \text{(A.1)}$$

Using Laplace Transform with the initial conditions of $x(0) = 0$, $\dot{x}(0) = 0$, and $x_b(0) = 0$:

$$(ms^2 + cs + k)X(s) = (cs + k)X_b(s) \quad \text{(A.2)}$$

where $X(s)$ is the Laplace Transform of $x(t)$, the displacement of the mass, and $X_b(s)$ is the Laplace Transform of $x_b(t)$, the displacement of the base. The acceleration transmissibility, which is identical to the velocity and displacement transmissibility in the linear system, can be obtained from Equation (A.2) as:

$$T(s) = \frac{s^2 X(s)}{s^2 X_b(s)} = \frac{cs + k}{ms^2 + cs + k} \quad \text{(A.3)}$$

The force acting on the base, $f_b(t)$, is equal to the inertial force acting on the mass, $f(t)$:

$$f_b(t) = f(t) = m\ddot{x}(t) \quad \text{(A.4)}$$

Therefore, the Laplace Transform of the force acting on the base, $F_b(s)$, is:

$$F_b(s) = ms^2 X(s) \tag{A.5}$$

The apparent mass of the model, $M(s)$, can be obtained from Equations (A.3) and (A.5):

$$M(s) = \frac{F(s)}{s^2 X_b(s)} = \frac{ms^2 X(s)}{s^2 X_b(s)} = \frac{mX(s)}{X_b(s)} = \frac{m(cs+k)}{ms^2 + cs + k} = mT(s) \tag{A.6}$$

If the apparent mass is normalised by the mass of the model on the assumption that the spring and damping elements have no mass, the normalised apparent mass, $M_n(s)$, can be expressed as:

$$M_n(s) = \frac{M(s)}{m} = \frac{cs+k}{ms^2 + cs + k} = T(s) \tag{A.7}$$

As seen in the equations above, the apparent mass of the single degree of freedom model shown in Figure A.1 corresponds to the product of the total mass of the model and the transmissibility to the vertical motion of the mass. The normalised apparent mass of the model is identical to the transmissibility to the mass.

A.2 Two degrees of freedom model

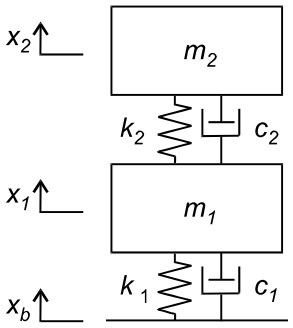

Figure A.2 Two degrees of freedom model.

The equation of motion of the two degrees of freedom model shown in Figure A.2 when exposed to input motion at the base are:

$$\begin{aligned} &m_1\ddot{x}_1(t) + c_1(\dot{x}_1(t) - \dot{x}_b(t)) + c_2(\dot{x}_1(t) - \dot{x}_2(t)) \\ &+k_1(x_1(t) - x_b(t)) + k_2(x_1(t) - x_2(t)) = 0 \\ &m_2\ddot{x}_2(t) + c_2(\dot{x}_2(t) - \dot{x}_1(t)) + k_2(x_2(t) - x_1(t)) = 0 \end{aligned} \tag{A.8a, b}$$

Using Laplace Transform with the initial conditions of $x_1(0) = 0$, $\dot{x}_1(0) = 0$, $x_2(0) = 0$, $\dot{x}_2(0) = 0$ and $x_b(0) = 0$:

$$\begin{aligned} &(m_1 s^2 + c_1 s + k_1 + c_2 s + k_2)X_1(s) - (c_2 s + k_2)X_2(s) = (c_1 s + k_1)X_b(s) \\ &-(c_2 s + k_2)X_1(s) + (m_2 s^2 + c_2 s + k_2)X_2(s) = 0 \end{aligned} \tag{A.9a, b}$$

Eliminate $X_2(s)$ in Equations (A.9a, b), the transmissibility to the bottom mass, m_1, is obtained as:

$$T_1(s) = \frac{X_1(s)}{X_b(s)} = \frac{(c_1 s + k_1)(m_2 s^2 + c_2 s + k_2)}{(m_1 s^2 + c_1 s + k_1)(m_2 s^2 + c_2 s + k_2) + m_2 s^2 (c_2 s + k_2)} \tag{A.10}$$

Substitute Equation (A.10) into Equation (A.9b), the transmissibility to the top mass, m_2, is:

$$T_2(s) = \frac{X_2(s)}{X_b(s)} = \frac{(c_1 s + k_1)(c_2 s + k_2)}{(m_1 s^2 + c_1 s + k_1)(m_2 s^2 + c_2 s + k_2) + m_2 s^2 (c_2 s + k_2)} \tag{A.11}$$

The force acting on the base is equal to the sum of the inertial forces acting on all the masses. Therefore, the apparent mass of the model, $M(s)$, can be obtained as:

$$\begin{aligned} M(s) &= \frac{F(s)}{s^2 X_b(s)} = \frac{m_1 s^2 X_1(s) + m_2 s^2 X_2(s)}{s^2 X_b(s)} \\ &= \frac{(c_1 s + k_1)\left\{m_1(m_2 s^2 + c_2 s + k_2) + m_2(c_2 s + k_2)\right\}}{(m_1 s^2 + c_1 s + k_1)(m_2 s^2 + c_2 s + k_2) + m_2 s^2 (c_2 s + k_2)} = m_1 T_1(s) + m_2 T_2(s) \end{aligned} \tag{A.12}$$

Thus the normalised apparent mass, $M_n(s)$, can be calculated by dividing the apparent mass by the total mass of the model, m_t ($m_t = m_1 + m_2$):

$$M_n(s) = \frac{m_1}{m_t} T_1(s) + \frac{m_2}{m_t} T_2(s) \tag{A.13}$$

The apparent mass of the two degree of freedom model shown in Figure A.2 corresponds to the sum of the products of the mass and the transmissibility to the vertical motion of the mass for each mass, as seen in Equation (A.12). The normalised apparent mass of the model can be obtained by a linear combination of the transmissibility to each mass, as seen in Equation (A.12). Each coefficient in the linear combination corresponds to the mass ratio to the total mass of the model. This should be true for any lumped parameter models with multi degrees of freedom in a single axis only.

$$M(s) = \sum_k m_k T_k(s) \tag{A.14}$$

$$M_n(s) = \sum_k \frac{m_k}{m_t} T_k(s) \tag{A.15}$$

APPENDIX B DATA FROM EXPERIMENT 1

B.1 Subjects in Experiment 1

Table B.1 Age, height and weight of the twelve subjects who participated in Experiment 1.

Subject		Age [yr]	Height [m]	Weight [kg]
1	J. V.	27	1.82	76
2	P. W.	25	1.84	67
3	M. T.	24	1.73	71
4	C. M.	21	1.68	75
5	Y. M.	25	1.79	72
6	E. H.	21	1.79	73
7	C. B.	25	1.86	88
8	C. L.	24	1.78	68
9	G. P.	28	1.77	77
10	L. R.	23	1.89	84
11	P. T.	20	1.88	92
12	D. G.	31	1.82	85

B.2 Instructions to subjects in Experiment 1

INSTRUCTIONS TO SUBJECTS

The aim of this experiment is to measure the motion of the body of standing and sitting persons during whole-body vertical vibration.

It is important that you maintain the required position and postures throughout the run. Please keep your upper-body and legs in the position shown. Seven postures will be required:

(1) **'normal (standing)'**
- upper-body: comfortable, upright posture with normal muscle tension
- legs: unlocked with normal muscle tension

(2) **'upper-body erected'**
- upper-body: erect posture (straight back and shoulders held back with normal muscle tension)
- legs: unlocked with normal muscle tension

(3) **'upper-body slouched'**
- upper-body: slouched posture (with a slight stoop and shoulders held forward with normal muscle tension)
- legs: unlocked with normal muscle tension

(4) **'body tensed'**
- as '(1) normal' but with all the muscles of the body tensed as much as possible

(5) **'legs bent'**
- upper-body: comfortable, upright posture with normal muscle tension
- legs: knees kept vertically above the toes

(6) **'one leg'**
- upper-body: comfortable, upright posture with normal muscle tension (To keep stable, you may lightly touch on the wall with finger tips)
- legs: one leg with unlocked knee

(7) **'normal (sitting)'**
- comfortable, upright posture with normal muscle tension

Only for the normal postures, for both standing and sitting, two magnitudes of stimuli are used so that a session is completed in nine runs. Measurements when barefoot are required so as to eliminate any effects of shoes. The experimenter will indicate the order in which these postures should be adopted.

You are free to terminate the experiment at any time by pressing the red STOP button.
Thank you for taking part in this experiment.

APPENDIX C DATA FROM EXPERIMENT 2

C.1 Subjects in Experiment 2

Table C.1 Age, height and weight of the twelve subjects who participated in Experiment 2.

Subject		Age [yr]	Height [m]	Weight [kg]
1	G. P.	28	1.77	77
2	P. W.	25	1.84	67
3	S. Y.	31	1.70	67
4	T. T.	29	1.78	66
5	D. G.	31	1.82	84
6	M. N.	35	1.71	65
7	J. V.	27	1.82	76
8	C. L.	24	1.78	68
9	J. M.	28	1.83	84
10	W. Y.	25	1.80	77
11	H. A.	31	1.70	71
12	C. B.	26	1.86	85

Table C.2 Dimensions of each subjects. Height of measurement locations (i.e., the knee, L3, T8 and T1), distance between two measurement locations on the pelvis in the transverse plane, and distance between L3 and the iliac crest in the sagittal plane. In metres [m].

Sub.	Knee	L3	T8	T1	Pelvis width	L3 - Pelvis
1	0.533	1.071	1.259	1.493	0.295	0.113
2	0.531	1.106	1.283	1.555	0.285	0.115
3	0.447	0.956	1.148	1.407	0.310	0.115
4	0.490	1.061	1.250	1.485	0.273	0.090
5	0.503	1.049	1.273	1.516	0.296	0.133
6	0.462	0.965	1.195	1.419	0.267	0.080
7	0.516	1.036	1.255	1.522	0.324	0.125
8	0.480	1.032	1.223	1.486	0.300	0.085
9	0.514	1.096	1.309	1.525	0.345	0.100
10	0.514	1.060	1.233	1.494	0.313	0.125
11	0.461	0.998	1.178	1.444	0.290	0.125
12	0.535	1.090	1.300	1.554	0.300	0.118

C.2 Instructions to subjects in Experiment 2

INSTRUCTIONS TO SUBJECTS

The aim of this experiment is to measure the motion of the human body in standing position during vertical whole-body vibration. The effect of posture and vibration magnitude on the vibration transmission through the body is to be investigated. The motions at the various parts of the body are measured with accelerometers attached to the skin.

It is important that you maintain the required postures throughout the run. Three postures will be required:

(1) **Normal**
: *Keep the legs straight and locked*.

(2) **Legs bent**
: *Hold the legs bent so that the knees kept vertically above the toes*.

(3) **One leg**
: *Stand on the left leg and keep it locked*.

Please *keep your upper-body comfortable, upright position* and *look forward* for all the above postures. *Any unnecessary body movements should be avoided*. Measurements when *barefoot* are required so as to eliminate any effects of shoes. The experimenter will indicate the order in which these postures should be adopted. For safety reason, you may lightly hold on to the rigid frame in front of you.

The experiment is completed by twelve runs which consist of combinations of above three postures and five vibration magnitudes. Local vibrations due to tissue-accelerometer systems are also required to be measured at each measurement point in order to identify the effect of the local vibration on measured vibration transmissibilities.

You are free to terminate the experiment at any time by pressing the STOP button attached to the frame.

Thank you for taking part in this experiment.

C.3 Local tissue-accelerometer system in Experiment 2

Table C.3 Natural frequencies and damping ratios of local tissue-accelerometer system in Experiment 2. -cont.

	T1		T8		L4	
	Vertical	Fore & aft	Vertical	Fore & aft	Vertical	Fore & aft
Subject 1						
Freq. [Hz]	19.0	37.1	33.6	28.6	23.0	31.1
Damping	0.310	0.381	0.511	0.507	0.441	0.303
Subject 2						
Freq. [Hz]	17.5	33.1	42.6	62.6	17.5	35.1
Damping	0.386	0.416	0.512	0.421	0.533	0.225
Subject 3						
Freq. [Hz]	33.1	43.1	50.6	32.6	18.5	33.6
Damping	0.494	0.547	0.583	0.425	0.465	0.340
Subject 4						
Freq. [Hz]	29.1	45.6	43.1	39.1	22.5	55.6
Damping	0.560	0.429	0.386	0.604	0.493	0.360
Subject 5						
Freq. [Hz]	28.0	36.1	34.1	30.6	20.5	39.1
Damping	0.627	0.440	0.501	0.408	0.471	0.376
Subject 6						
Freq. [Hz]	27.0	30.6	59.6	47.1	21.5	51.6
Damping	0.584	0.552	0.464	0.521	0.408	0.586
Subject 7						
Freq. [Hz]	19.0	48.1	50.6	33.1	43.0	18.0
Damping	0.475	0.566	0.490	0.324	0.332	0.417
Subject 8						
Freq. [Hz]	31.1	30.6	52.1	41.1	16.0	31.6
Damping	0.637	0.357	0.422	0.562	0.329	0.320
Subject 9						
Freq. [Hz]	17.5	33.1	21.5	37.6	17.5	25.0
Damping	0.432	0.551	0.354	0.335	0.650	0.334
Subject 10						
Freq. [Hz]	14.0	29.1	33.6	40.1	18.0	29.6
Damping	0.342	0.436	0.511	0.444	0.622	0.347
Subject 11						
Freq. [Hz]	17.5	36.1	46.1	31.1	17.0	28.0
Damping	0.386	0.352	0.558	0.673	0.449	0.243
Subject 12						
Freq. [Hz]	13.5	26.5	37.6	36.1	23.0	32.1
Damping	0.417	0.491	0.439	0.487	0.448	0.383

Table C.3 (continued) Natural frequencies and damping ratios of local tissue-accelerometer system in Experiment 2.

	Pelvis, left		Pelvis, right	Knee	
	Vertical	Lateral	Vertical	Vertical	Fore & aft
Subject 1					
Freq. [Hz]	21.0	30.1	24.5	30.1	69.6
Damping	0.498	0.533	0.725	0.503	0.461
Subject 2					
Freq. [Hz]	13.0	19.6	8.51	26.0	99.2
Damping	0.659	0.417	0.355	0.618	0.581
Subject 3					
Freq. [Hz]	30.1	40.1	25.0	22.5	35.6
Damping	0.671	0.582	0.613	0.348	0.523
Subject 4					
Freq. [Hz]	30.6	25.0	24.0	20.0	99.7
Damping	0.521	0.572	0.613	0.364	0.300
Subject 5					
Freq. [Hz]	21.0	28.6	31.1	23.5	94.7
Damping	0.692	0.729	0.882	0.288	0.669
Subject 6					
Freq. [Hz]	20.1	35.1	26.5	39.1	84.6
Damping	0.491	0.650	0.935	0.482	0.700
Subject 7					
Freq. [Hz]	28.0	17.0	53.6	19.0	29.1
Damping	0.796	0.556	0.786	0.414	0.630
Subject 8					
Freq. [Hz]	21.5	15.5	30.1	23.0	31.6
Damping	0.491	0.258	0.691	0.338	0.498
Subject 9					
Freq. [Hz]	15.5	20.5	10.0	17.5	93.2
Damping	0.711	0.720	0.634	0.589	0.383
Subject 10					
Freq. [Hz]	12.0	16.0	10.5	19.5	44.6
Damping	0.652	0.545	0.812	0.301	0.521
Subject 11					
Freq. [Hz]	16.5	16.5	11.0	18.5	22.0
Damping	0.713	0.467	0.750	0.321	0.430
Subject 12					
Freq. [Hz]	14.0	18.0	11.0	19.0	31.6
Damping	0.243	0.331	0.873	0.431	0.443

APPENDIX D DATA FROM EXPERIMENT 3

D.1 Subjects in Experiment 3

Table D.1 Age, height and weight of the twelve subjects who participated in Experiment 3.

Subject		Age [yr]	Height [m]	Weight [kg]
1	H. J.	33	1.67	63
2	N. W.	22	1.81	71
3	G. P.	29	1.77	75
4	D. G.	32	1.81	83
5	R. P.	23	1.75	73
6	T. K.	27	1.75	74
7	H. J.	29	1.69	65
8	Y. M.	27	1.79	70

D.2 Instructions to subjects in Experiment 3

INSTRUCTIONS TO SUBJECTS

The aim of this experiment is to measure the motion of the human body both in standing position and in seated position during vertical whole-body vibration. The effects of position and vibration magnitude on the vibration transmission through the body are to be investigated. The motions at the various parts of the body are measured with accelerometers attached to the skin. The head motion is also measured with a bite-bar.

It is important that you maintain the required postures throughout the run. *Any unnecessary voluntary body movements should be avoided*. Two postures will be required:

(1) **Standing normally**
: *Keep the legs straight and locked. Keep the upper-body comfortable, upright position and look forward.*

(2) **Sitting normally**
: *Keep the upper-body in the same position as that in standing normally posture, i.e., comfortable, upright position and look forward.*

Measurements when *barefoot* are required so as to eliminate any effects of shoes. For safety purposes, you may lightly hold on to the rigid frame in front of you when standing.

The experiment is completed by ten runs which consist of combinations of above two postures and five vibration magnitudes. Local vibrations due to tissue-accelerometer systems are also required to be measured at each measurement point in order to identify the effect of the local vibration on measured vibration transmissibilities.

You are free to terminate the experiment at any time. If you would like to terminate a vibration exposure, you can stop the shaker by pressing the STOP button either attached to the frame or held in your hand.

Thank you for taking part in this experiment.

D.3 Local tissue-accelerometer system in Experiment 3

Table D.2 Natural frequencies and damping ratios of local tissue-accelerometer system in Experiment 3. In the vertical axis.

	T1	T5	T10	L1	L3	L5	Pelvis	Knee
Subject 1								
Freq. [Hz]	15.0	24.0	25.4	27.4	26.4	23.4	14.5	14.5
Damping	0.607	0.324	0.307	0.287	0.340	0.313	0.429	0.454
Subject 2								
Freq. [Hz]	31.4	25.4	28.9	19.4	15.9	25.4	12.5	18.9
Damping	0.342	0.331	0.341	0.370	0.439	0.454	0.487	0.749
Subject 3								
Freq. [Hz]	15.0	39.9	51.3	32.4	23.4	26.4	24.4	22.4
Damping	0.639	0.286	0.300	0.295	0.409	0.252	0.589	0.409
Subject 4								
Freq. [Hz]	16.9	14.5	27.9	38.9	25.4	23.4	15.0	33.4
Damping	0.560	0.556	0.383	0.314	0.381	0.465	0.487	0.443
Subject 5								
Freq. [Hz]	16.9	40.0	33.9	21.9	25.4	28.9	17.9	33.4
Damping	0.583	0.228	0.356	0.497	0.316	0.376	0.396	0.297
Subject 6								
Freq. [Hz]	25.4	13.0	20.9	20.9	15.5	22.4	23.9	30.4
Damping	0.381	0.662	0.416	0.467	0.518	0.354	0.377	0.654
Subject 7								
Freq. [Hz]	16.4	10.0	12.5	50.3	30.9	22.4	25.4	26.4
Damping	0.492	0.589	0.514	0.394	0.523	0.524	0.362	0.464
Subject 8								
Freq. [Hz]	25.9	31.4	23.4	39.4	36.4	30.9	33.9	33.9
Damping	0.346	0.328	0.378	0.334	0.390	0.393	0.371	0.425

Table D.3 Natural frequencies and damping ratios of local tissue-accelerometer system in Experiment 3. In the fore-and-aft axis.

	T1	T5	T10	L1	L3	L5	Pelvis	Knee
Subject 1								
Freq. [Hz]	32.4	46.8	31.9	25.9	33.4	26.4	27.9	75.7
Damping	0.301	0.275	0.324	0.578	0.484	0.427	0.343	0.601
Subject 2								
Freq. [Hz]	23.4	24.9	45.3	20.9	25.9	40.4	20.4	76.7
Damping	0.502	0.334	0.281	0.436	0.388	0.325	0.425	0.305
Subject 3								
Freq. [Hz]	52.8	47.8	38.9	33.9	34.4	41.9	21.4	52.8
Damping	0.314	0.282	0.417	0.296	0.298	0.338	0.523	0.435
Subject 4								
Freq. [Hz]	34.4	27.9	41.4	41.4	32.9	37.4	36.4	48.8
Damping	0.320	0.406	0.231	0.231	0.306	0.283	0.365	0.477
Subject 5								
Freq. [Hz]	29.9	40.4	35.4	35.9	28.4	33.9	20.9	40.4
Damping	0.348	0.465	0.467	0.201	0.333	0.248	0.529	0.325
Subject 6								
Freq. [Hz]	53.8	41.9	47.8	23.9	46.8	33.9	40.9	46.3
Damping	0.172	0.198	0.350	0.482	0.188	0.401	0.265	0.231
Subject 7								
Freq. [Hz]	38.9	50.8	13.5	45.3	51.3	30.4	36.4	52.8
Damping	0.229	0.320	0.600	0.505	0.321	0.300	0.286	0.285
Subject 8								
Freq. [Hz]	55.3	56.8	42.4	50.8	66.8	28.4	50.8	35.4
Damping	0.200	0.264	0.516	0.556	0.237	0.592	0.556	0.228

Table D.4 Natural frequencies and damping ratios of local tissue-accelerometer system in Experiment 3. In the pitch axis.

	T1	T5	T10	L1	L3	L5	Pelvis
Subject 1							
Freq. [Hz]	21.4	25.9	27.4	31.9	29.9	23.9	19.9
Damping	0.446	0.401	0.533	0.336	0.305	0.355	0.472
Subject 2							
Freq. [Hz]	31.9	25.9	30.4	24.9	23.4	26.9	17.9
Damping	0.434	0.438	0.303	0.377	0.329	0.303	0.450
Subject 3							
Freq. [Hz]	38.9	44.3	41.4	34.9	31.9	27.9	23.9
Damping	0.322	0.319	0.283	0.254	0.323	0.291	0.429
Subject 4							
Freq. [Hz]	26.9	26.9	31.9	22.9	39.4	29.9	22.4
Damping	0.363	0.427	0.282	0.807	0.257	0.328	0.426
Subject 5							
Freq. [Hz]	25.9	22.4	41.4	33.9	34.9	29.9	27.4
Damping	0.371	0.623	0.235	0.291	0.275	0.270	0.340
Subject 6							
Freq. [Hz]	39.4	36.4	47.3	11.5	37.9	29.4	26.4
Damping	0.269	0.305	0.290	0.650	0.278	0.282	0.370
Subject 7							
Freq. [Hz]	34.4	43.9	58.8	59.3	41.4	35.4	25.9
Damping	0.319	0.358	0.279	0.389	0.442	0.321	0.362
Subject 8							
Freq. [Hz]	34.9	35.9	50.8	36.9	39.4	50.8	33.4
Damping	0.411	0.354	0.356	0.446	0.314	0.308	0.236

APPENDIX E M-FILES TO ANIMATE THE MOVEMENT OF THE UPPER-BODY OF STANDING AND SEATED SUBJECTS AT THE PRINCIPAL RESONANCE FREQUENCY

The following M-file sources, for MATLAB for Windows version 4.2b, can be used to animate the movement of the upper-body of standing and seated subjects caused by vertical floor or seat vibration at the principal resonance frequency, based on the data obtained in Experiment 3.

- **anmt_mv.m**: A function file to calculate and animate the movement of the upper-body based on the experimental results which can be recalled from expdata.m. The function can be called by:

  trs = anmt_mv(sb,k,mv);

  Here *sb* is subject number, chosen from 1 to 8, *k* specifies posture, 1 for seated and 2 for standing. Either an absolute movement of the body or a relative movement of the body with respect to the vibrating surface can be shown. *mv* = 1 for an absolute movement and *mv* = 2 for a relative movement to vibrating seat or floor. The function returns the transmissibilities and phases at each location in the vertical and fore-and-aft axes used in the animation as an answer, in a variable *trs* in this example.

- **expdata.m**: A function file to be called by anmt_mv.m to recall the experimental data obtained in Experiment 3. The co-ordinates of measurement locations and the transmissibilities to each measurement location in the vertical and fore-and-aft axes at the principal resonance frequency of the apparent mass are included.

---------- **anmt_mv.m** from here----------

```
function trs = anmt_mv(sb,k,mv);

%%%  DISPLAY MOVEMENT OF UPPER-BODY AT RESONANCE FREQUENCY  %%%
%%%       sb : subject number (1 - 8)                       %%%
%%%       k : condition                                     %%%
%%%         k = 1 : seated                                  %%%
%%%         k = 2 : standing                                %%%
%%%       mv : type of movement to animate                  %%%
%%%         mv = 1 : absolute motion                        %%%
%%%         mv = 2 : relative motion to base                %%%
%%%                                  3/12/1998, Y.Matsumoto %%%
```

```
%%  read experimental data                              %%
%%     fq : principal resonance frequency               %%
%%     lcm : co-ordinates of measurement locations      %%
%%     trs : transmissibilities and phases              %%

[fq,lcm,trs] = expdata(sb,k);

%%  calculate movement within a cycle  %%

nfpc = 20;                  % nfpc : number of frames per cycle
p2 = 2*pi;
ff = linspace(0,p2,(nfpc+1));
zv = [];
xf = [];
for n = 1:length(lcm)
%  vertical
  if mv == 2                %  relative motion
    zv1 = (trs(n,1) - 1) * sin(ff(1:nfpc) + trs(n,2));
  else                      %  absolute motion
    zv1 = trs(n,1) * sin(ff(1:nfpc) + trs(n,2));
  end
  zv = [zv; zv1];
%  fore-and-aft
  xf1 = trs(n,3) * sin(ff(1:nfpc) + trs(n,4));
  xf = [xf; xf1];
end

%%  scaling for clarity             %%
%%     scl : scaling factor         %%

scl = 0.02;                 %  arbitrary value for peak displacement
% rms = 1.0;                %  arbitrary value for rms acceleration
% scl = rms * sqrt(2) / (p2*fq)^2 ;
zv = scl * zv;
xf = scl * xf;

%%  create frames for animation  %%

M = moviein(nfpc);

for n = 1:nfpc
  zv1 = lcm(:,1) + zv(:,n);
  xf1 = lcm(:,2) + xf(:,n);

%  adjust vertical level of L5 for standing to that for seated for animation  %
  if k == 2
    zv1 = [zv1(1:8); zv1(7); zv1(9)];
    xf1 = [xf1(1:8); xf1(7); xf1(9)];
    vl5 = [ 0.15  0.15  0.18  0.23  0.21  0.20  0.18  0.20 ]; %  L5 level for seated (subject 1 - 8)
    zv1 = zv1 - (lcm(7,1) - vl5(sb));                        % for comparison with seated
  end

  plot(xf1(2:7),zv1(2:7),'w-',xf1,zv1,'wo')
  axis([ -0.4  0.9  0  1 ])
  M(:,n) = getframe;

end

%%  produce animation  %%
```

```
cycl = 5;                % cycl : number of cycles to animate
movie(M,cycl)
```

---------- **anmt_mv.m** ends----------

---------- **expdata.m** from here (called by anmt_mv.m) ----------

```
function [fq,lcm,trs] = expdata(sb,k);

%%%  GET EXPERIMENTAL DATA AT RESONANCE FREQUENCY    %%%
%%%       sb : subject number (1 - 8)                %%%
%%%       k : condition                              %%%
%%%         k = 1 : seated                           %%%
%%%         k = 2 : standing                         %%%
%%%       fq : principal resonance frequency [Hz]    %%%
%%%       lcm : locations of measurement points [m]  %%%
%%%       trs : transmissibilities and phases        %%%
%%%         1st column : vertical transmissibilities %%%
%%%         2nd column : vertical phases             %%%
%%%         3rd column : fore-and-aft transmissibilities %%%
%%%         4th column : fore-and-aft phases         %%%
%%%         1st to 8th (or 9th for standing) rows :  %%%
%%%           Head, T1, T5, T10, L1, L3, L5, Pelvis, (Knee)  %%%
%%%                                    3/12/98, Y.Matsumoto  %%%

fq = [  5.25  5.0   5.75  5.25  5.0   5.75  5.25  4.75      % for seated (subject 1 - 8)
        5.5   5.5   6.25  5.25  5.5   6.5   5.25  5.5   ];  % for standing (subject 1 - 8)
fq = fq(k,sb);

if k == 1   %  seated

%%  measurement location                                          %%
%%  vertical                                                      %%
%%  [  Head     T1      T5      T10     L1      L3      L5   Pelvis  ]   %%
lvm = [  0.72   0.60    0.49    0.34    0.26    0.21    0.15    0.15
         0.75   0.64    0.51    0.36    0.27    0.21    0.15    0.15
         0.70   0.62    0.50    0.35    0.28    0.24    0.18    0.18
         0.78   0.68    0.56    0.42    0.36    0.30    0.23    0.23
         0.75   0.67    0.57    0.41    0.33    0.27    0.21    0.21
         0.76   0.66    0.56    0.38    0.32    0.25    0.20    0.20
         0.72   0.61    0.49    0.36    0.30    0.24    0.18    0.18
         0.75   0.65    0.55    0.40    0.32    0.26    0.20    0.20 ];
%%  fore-and-aft                                                  %%
%%  [  Head     T1      T5      T10     L1      L3      L5   Pelvis  ]   %%
lfm =  [  0.22   0.09    0.05    0.07   0.085   0.085   0.07    0.01
          0.30   0.10    0.05   0.065   0.08   0.095   0.09    0.03
          0.26   0.10    0.06   0.065   0.08   0.085   0.08    0.02
          0.24   0.09    0.05    0.06  0.075   0.085   0.07    0.01
          0.23   0.08    0.05   0.055  0.075   0.085   0.07    0.01
          0.20   0.09    0.05   0.065   0.08    0.09   0.08    0.02
          0.23   0.10    0.07    0.06  0.065   0.075   0.07    0.01
          0.18   0.08    0.06   0.055   0.07    0.08   0.07    0.01 ];

%%  vertical transmissibilities                                   %%
%%  [  Head     T1      T5      T10     L1      L3      L5   Pelvis  ]   %%
trv =  [  1.743  1.141   1.176   1.223   1.315   1.415   1.636   2.037
```

```
          0.413   1.315   1.046   1.197   1.206   1.224   1.242   1.155
          1.124   1.466   1.375   1.479   1.368   1.342   1.563   1.931
          1.628   1.404   1.194   1.427   1.599   1.449   1.430   1.704
          0.473   1.315   1.203   1.240   1.337   1.454   1.681   1.954
          1.422   1.493   1.047   1.471   1.392   1.173   1.274   1.849
          1.415   1.526   1.137   1.376   1.643   1.448   1.526   1.936
          1.447   1.497   1.213   1.295   1.440   1.601   1.557   1.624 ];
%%   phase vertical                                                    %%
%%   [  Head      T1      T5     T10      L1      L3      L5   Pelvis  ]   %%
phv = [ -18.89  -39.23  -19.83  -24.42  -21.71  -24.66  -26.06  -32.11
        -38.05  -41.39  -31.99  -25.59  -23.93  -22.78    5.30  -11.11
        -29.51  -43.32  -33.60  -30.36  -27.30  -33.62  -29.09  -41.16
         -7.24  -39.28  -24.55  -19.25  -25.13  -26.50  -27.19  -30.04
        -62.91  -34.85  -26.38  -20.46  -24.47  -30.10  -27.39  -34.96
        -15.57  -33.38  -11.84  -19.24  -21.31  -14.69  -19.76  -31.86
        -31.56  -38.40  -18.23  -20.48  -30.30  -28.59  -23.10  -34.78
         -2.67  -16.84   -6.22   -7.04  -10.85  -14.72  -10.29  -15.70  ] * pi/180;

%%   fore-and-aft transmissibilities                                   %%
%%   [  Head      T1      T5     T10      L1      L3      L5   Pelvis  ]   %%
trf =   [ 0.549   0.968   0.415   0.612   0.335   0.346   0.401   0.238
          0.662   0.947   0.511   0.320   0.235   0.165   0.191   0.280
          0.561   0.980   0.284   0.285   0.471   0.134   0.041   0.330
          0.615   0.833   0.352   0.524   0.426   0.349   0.317   0.516
          0.574   0.822   0.264   0.278   0.370   0.118   0.042   0.338
          0.284   0.670   0.131   0.432   0.257   0.150   0.053   0.357
          0.618   0.926   0.170   0.681   0.851   0.303   0.122   0.139
          0.631   0.634   0.131   0.440   0.504   0.203   0.185   0.248 ];
%%   phase fore-and-aft                                                %%
%%   [  Head      T1      T5     T10      L1      L3      L5   Pelvis  ]   %%
phf =  [  54.10   53.25   38.09  -48.21 -103.88 -107.66  176.99 -144.93
          76.82  116.22  140.45 -127.96 -133.65  164.75  154.69   52.32
          38.63   90.91   95.22 -106.54  -75.29 -153.55 -134.41 -173.27
          71.70   28.07    6.91  -97.89  -83.89 -141.17 -142.16  174.93
          42.91  103.45  129.83 -105.95  -76.58 -115.72   11.42  150.26
          20.65   79.78  116.57  -71.45  -37.87  173.89  -38.01  -41.88
          55.52   95.18   13.06  -54.67  -53.19  -79.82  -75.03 -144.36
          87.82  112.86   90.13  -47.27  -39.32  -51.83   -5.70   -9.41  ] * pi/180;

else  %  standing

%%  measurement location                                                  %%
%%   vertical                                                           %%
%       [  Head      T1      T5     T10      L1      L3      L5   Pelvis    Knee  ]   %%
lvm = [    1.46    1.36    1.25    1.12    1.05    0.99    0.94    0.94    0.38
           1.59    1.50    1.35    1.22    1.15    1.11    1.05    1.05    0.46
           1.58    1.50    1.38    1.23    1.17    1.12    1.07    1.07    0.49
           1.62    1.52    1.40    1.25    1.18    1.13    1.08    1.08    0.45
           1.58    1.48    1.36    1.20    1.12    1.08    1.03    1.03    0.43
           1.57    1.47    1.36    1.21    1.13    1.07    1.02    1.02    0.43
           1.49    1.38    1.24    1.10    1.04    0.99    0.95    0.95    0.38
           1.59    1.46    1.34    1.19    1.11    1.06    1.01    1.01    0.42 ];
%%   fore-and-aft                                                       %%
%%   [  Head      T1      T5     T10      L1      L3      L5   Pelvis    Knee  ]   %%
lfm =  [   0.22    0.07    0.05   0.065    0.10    0.12    0.11    0.05    0.10
           0.26    0.09    0.06    0.11    0.13    0.14    0.12    0.06    0.13
           0.21    0.08    0.05    0.08    0.09    0.10    0.08    0.02    0.09
           0.23    0.07    0.05   0.075   0.095   0.105    0.10    0.04    0.12
           0.22    0.10    0.06   0.075    0.10    0.12    0.11    0.05    0.13
           0.24    0.10    0.06    0.06    0.09   0.105    0.09    0.03    0.11
```

```
          0.21    0.08    0.05   0.085    0.11   0.125    0.11    0.05    0.12
          0.20    0.10    0.06   0.095    0.12   0.135   0.125   0.065    0.12 ];

%%  vertical transmissibilities                                              %%
%%  [  Head      T1      T5     T10      L1      L3      L5   Pelvis    Knee  ]   %%
trv = [ 1.416   1.168   1.245   1.418   1.655   2.012   2.078   1.913   0.990
        0.539   1.127   1.069   1.308   1.946   1.510   3.136   2.421   1.281
        1.282   1.100   1.252   1.475   1.571   1.526   2.279   2.376   1.098
        0.976   1.404   1.116   1.355   2.132   2.450   2.879   2.153   1.118
        0.830   0.847   0.943   0.978   1.282   2.025   2.832   2.185   1.080
        2.121   1.457   1.337   1.590   1.765   2.267   2.430   2.869   1.336
        1.373   1.193   1.007   1.319   1.788   1.976   2.233   1.821   1.078
        1.604   1.402   1.345   1.565   1.719   2.156   2.229   2.204   1.156 ];
%%  phase vertical                                                           %%
%%  [  Head      T1      T5     T10      L1      L3      L5   Pelvis    Knee  ]   %%
phv = [-14.77  -24.49  -17.35  -22.43  -30.87  -37.67  -34.86  -35.49  -18.77
       -35.38  -22.38   -9.29  -18.65  -27.23  -24.15  -40.67  -38.27    1.59
        -7.42  -19.65   -9.38  -15.87  -20.57  -28.76  -48.31  -50.80    1.07
        -7.28  -26.52  -17.52  -16.10  -26.64  -27.78  -24.28  -20.14   -5.27
       -23.89  -32.28  -20.00  -17.06  -29.18  -44.35  -42.41  -49.85   -2.30
       -35.73  -49.36  -24.25  -25.10  -40.21  -50.38  -53.30  -58.89   -9.68
       -16.34  -28.09   -0.69  -11.67  -24.54  -29.83  -25.19  -28.81   -6.85
       -19.36  -22.39  -13.69  -24.11  -24.55  -32.57  -35.63  -38.32   -0.15 ] * pi/180;

%%  fore-and-aft transmissibilities                                          %%
%%  [  Head      T1      T5     T10      L1      L3      L5   Pelvis    Knee  ]   %%
trf = [ 0.474   0.528   0.103   0.340   0.555   0.680   0.623   0.657   1.384
        0.810   0.541   0.128   0.277   0.162   0.717   0.282   0.777   0.879
        0.834   0.734   0.295   0.188   0.259   0.435   0.404   0.374   0.658
        0.757   0.626   0.132   0.286   0.143   0.167   0.238   0.136   0.833
        0.591   0.728   0.163   0.459   0.531   0.186   0.161   0.574   1.425
        1.221   1.024   0.607   0.517   0.194   0.584   0.161   0.410   1.077
        0.735   0.874   0.035   0.255   0.229   0.657   0.107   0.588   0.774
        0.346   0.514   0.272   0.093   0.194   0.184   0.188   0.518   0.696 ];
%%  phase fore-and-aft                                                       %%
%%  [  Head      T1      T5     T10      L1      L3      L5   Pelvis    Knee  ]   %%
phf = [  4.60   39.83   21.89 -116.05 -152.19 -157.74 -136.62 -108.71   30.96
        54.86   96.35 -178.88 -145.67  -51.82  -41.52   -9.65  -49.03  -96.44
        23.07   79.92   84.85 -177.05 -123.88 -156.80  -88.00 -147.14  -43.17
       112.10  111.63 -164.04  -90.30  -22.59   13.69   21.40    4.00  -42.19
        30.24   65.94   72.52 -110.67  -76.87  -42.00  -15.88  -43.11 -105.66
       -48.21  -11.89  -38.19  -92.61  -48.62  123.26  142.85  -78.13  -75.10
        57.62   65.68  163.61 -100.10 -106.42  173.07 -121.40  170.02  -26.67
        38.68   67.11   16.87  -66.52  -23.65  144.27  -21.03  -58.54  -51.86 ] * pi/180;

end

lcm = [lvm(sb,:); lfm(sb,:)]';
trs = [trv(sb,:); phv(sb,:); trf(sb,:); phf(sb,:)]';
```

---------- **expdata.m** ends----------

REFERENCES

AERTS P. and DE CLERCQ D. 1993 *Journal of Sports Science*, 11, 449-461. Deformation characteristics of the heel region of the shod foot during a simulated heel strike: the effect of varying midsole hardness.

AMIROUCHE F. M. L. and IDER S. K. 1988 *Journal of Sound and Vibration*, 123 (2), 281-292. Simulation and analysis of a biodynamic human model subjected to low accelerations - a correlation study.

AMIROUCHE F. M. L., XIE M. and PATWARDHAN A. 1994 *Journal of Biomechanical Engineering - Transactions of the ASME*, 116 (4), 413-420. Optimization of the contact damping and stiffness coefficients to minimize human body vibration.

BELYTSCHKO T. and PRIVITZER E. 1978a *AGARD Conference Proceedings No. 253*, A9-1-15. A three dimensional discrete element dynamic model of the spine, head and torso.

BELYTSCHKO T. and PRIVITZER E. 1978b *Aerospace Medical Research Laboratory*, *Wright-Patterson Air Force Base*, *Ohio*, AMRL-TR-78-7. Refinement and validation of a three-dimensional head-spine model.

BELYTSCHKO T., RENCIS M. and WILLIAMS J. 1985 *Harry G. Armstrong Aerospace Medical Research Laboratory*, *Wright-Patterson Air Force Base*, *Ohio*, AAMRL-TR-85-019. Head-spine structure modeling: enhancements to secondary loading path model and validation of head-cervical spine model.

BELYTSCHKO T., SCHWER L. and PRIVITZER E. 1978 *Aviation, Space, and Environmental Medicine*, 49 (1), 158-165. Theory and application of a three-dimensional model of the human spine.

BELYTSCHKO T., SCHWER L. and SCHULTZ A. 1976 *Aerospace Medical Research Laboratory*, *Wright-Patterson Air Force Base*, *Ohio*, AMRL-TR-76-10. A model for analytic investigation of three dimensional spine-head dynamics.

BERKSON M. H., NACHEMSON A. and SCHULTZ A. B. 1979 *Journal of Biomechanical Engineering - Transactions of the ASME*, 101, 53-57. Mechanical

properties of human lumbar spine motion segments - part II: responses in compression and shear; influence of gross morphology.

BRITISH STANDARDS INSTITUTION 1989 *British Standard*, *BS 7085*. British Standard Guide to safety aspects of experiments in which people are exposed to mechanical vibration and shock.

BROMAN H., POPE M. H., BENDAT M., SVENSSON M., OTTOSSON C. and HANSSON T. 1991 *Journal of Orthopaedic Research*, 9, 150-154. The impact response of the seated subject.

CHRIST W. and DUPUIS H. 1966 *International Zeitschrift angewandte Physiologie einschliesslich Arbeitsphysiologie*, 22, 258-278. Uber die Beanspruchung der Wirbelsaule unter dem Einfluss sinusformiger und stochastischer Schwingungen.

COERMANN R. R. 1962 *Human Factors*, 4 (10), 227-253. The mechanical impedance of the human body in sitting and standing positions at low frequencies.

COERMANN R. R., ZIEGENRUECKER G. H., WITTWER A. L. and VON GIERKE H. E. 1960 *Aerospace Medicine*, 31, 443-455. The passive dynamic mechanical properties of the human thorax-abdomen system and of the whole body system.

COLLIER R. J. and DONARSKI R. J. 1987 *Journal of Biomedical Engineering*, 9, 321-328. Non-invasive method of measuring resonant frequency of a human tibia in vivo part 1.

CRAMER H. J., LIU Y. K. and VON ROSENBERG D. U. 1976 *Journal of Biomechanics*, 9, 115-130. A distributed parameter model of the inertially loaded human spine.

DEAN C. and PEGINGTON J. 1996a *Core anatomy for students*. *Volume 1: the limbs and vertebral column*. W.B. Saunders.

DEAN C. and PEGINGTON J. 1996b *Core anatomy for students*. *Volume 2: the thorax, abdomen, pelvis and perineum*. W.B. Saunders.

DONATI P. M. and BONTHOUX C. 1983 *Journal of Sound and Vibration*, 90 (3), 423-442. Biodynamic response of the human body in the sitting position when subjected to vertical vibration.

DUPUIS H. and ZERLETT G. 1987 *International Archieves of Occupational and Environmental Health*, 59, 323-336. Whole-body vibration and disorders of the spine.

EDWARDS R. G. and LANGE K. O. 1964 *Aerospace Medical Research Laboratories*, *Wright-Patterston Air Force Base*, *Ohio*. A mechanical impedance investigation of human response to vibration.

EL-KHATIB A., GUILLON F. and DÔMONT A. 1998 *Journal of Sound and Vibration*, 215 (4), 763-773. Vertical vibration transmission through the lumbar spine of the seated subject - first results.

EWINS D. J. 1984 *Modal testing: theory and practice*. John Wiley & Sons.

FAIRLEY T. E. 1981 *BSc project*, *University of Southampton*, *Southampton*. Measurement of the apparent mass of the human body.

FAIRLEY T. E. 1986 *PhD thesis*, *University of Southampton*, *Southampton*. Predicting the dynamic performance of seats.

FAIRLEY T. E. and GRIFFIN M. J. 1989 *Journal of Biomechanics*, 22 (2), 81-94. The apparent mass of the seated human body: vertical vibration.

GARG D. P. and ROSS M. A. 1976 *IEEE Transactions on Systems, Man, and Cybernetics*, SMC-6 (2), 102-112. Vertical mode human body vibration transmissibility.

GOLDMAN D. E. and VON GIERKE H. E. 1961 *Shock and vibration handbook*, Vol. 3, Ch 44, 1-51, McGraw-Hill, New York. Effects of shock and vibration on man.

GRIFFIN M. J. 1975 *Aviation, Space and Environmental Medicine*, 46 (3), 269-276. Vertical vibration of seated subjects: effects of posture, vibration level, and frequency.

GRIFFIN M. J. 1990 *Handbook of Human Vibration*, Academic Press.

GRIFFIN M. J., LEWIS C. H., PARSONS K. C. and WHITHAM E. M. 1978 *AGARD Conference Proceedings No. 253*, A28-1-18. The biodynamic response of the human body and its application to standards.

HAGBARTH K.-E., HÄGGLUND J. V., NORDIN M. and WALLIN E. U. 1985 *Journal of Physiology*. 368, 323-342. Thixotropic behaviour of human finger flexor muscles with accompanying changes in spindle and reflex responses to stretch.

HAGENA F. -W., PIEHLER J., WIRTH C. -J., HOFMANN G. O. and ZWINGERS Th. 1986 *Neuro-Orthopedics*, 2, 29-33. The dynamic response of the human spine to sinusoidal Gz-vibration. In vivo experiments.

HAGENA F. -W., WIRTH C. J., PIEHLER J., PLITZ W., HOFMANN G. O. and ZWINGERS Th. 1985 *AGARD Conference Proceedings*, 378 (16), 1-12. In-vivo experiments on the response of the human spine to sinusoidal Gz-vibration.

HERTERICH J. and SCHNAUBER H. 1992 *Journal of Low Frequency Noise and Vibration*, 11 (2), 52-61. The effect of vertical mechanical vibration on standing man.

HESS J. L. and LOMBARD C. F. 1958 *Aviation Medicine*, 29, 66-75. Theoretical investigations of dynamic response of man to high vertical acclerations.

HINZ B. and SEIDEL H. 1987 *Industrial Health*, 25, 169-181. The nonlinearity of the human body's dynamic response during sinusoidal whole body vibration.

HINZ B., SEIDEL H., BRÄUER D., MENZEL G., BLÜTHNER R. and ERDMANN U. 1988a *European Journal of Applied Physiology and Occupational Physiology*, 57, 707-713. Examination of spinal column vibrations: a non-invasive approach.

HINZ B., SEIDEL H., BRÄUER D., MENZEL G., BLÜTHNER R. and ERDMANN U. 1988b *Clinical Biomechanics*, 3, 241-248. Bidimensional accelerations of lumbar vertebrae and estimation of internal spinal load during sinusoidal vertical whole-body vibration: a pilot study.

HOPKINS G. R. 1971 *Symposium on Biodynamic Models and Their applications*, Wright-Patterson Air Force Base, Ohio, 649-669. Nonlinear lumped parameter mathematical model of dynamic response of the human body.

INTERNATIONAL ORGANIZATION FOR STANDARDIZATION 1981 *International Organisation for Standardization*, *Geneva*. Vibration and shock - mechanical driving point impedance of the human body, ISO 5982.

INTERNATIONAL ORGANIZATION FOR STANDARDIZATION 1987 *International Organisation for Standardization*, *Geneva*. Mechanical vibration and shock - mechanical transmissibility of the human body in the Z direction, ISO 7982.

INTERNATIONAL ORGANIZATION FOR STANDARDIZATION 1997 *International Organisation for Standardization*, *Geneva*. Mechanical vibration and shock - evaluation of human exposure to whole-body vibration - part 1: general requirements, ISO 2631-1.

JØRGENSEN U. AND BOJSEN-MØLLER F 1989 *Foot and Ankle*, 9 (11), 294-299. Shock absorbency of factors in the shoe/heel interaction - with special focus on role of the heel pad.

KAIGLE A. M., POPE M. H., FLEMING B. C. and HANSSON T. 1992 *Journal of Biomechanics*, 25 (4), 451-456. A method for the intravital measurement of interspinous kinematics.

KALEPS I., VON GIERKE H. E. and WEIS E. B. 1971 *Symposium on Biodynamic Models and Their applications*, Wright-Patterson Air Force Base, Ohio, 211-231. A five-degree-of-freedom mathematical model of the body.

KIM W., VOLOSHIN A. S., JOHNSON S. H. and SIMKIN A. 1993 *Journal of Biomechanical Engineering - Transactions of the ASME*, 115, 47-52. Measurement of the impulsive bone motion by skin-mounted accelerometers.

KITAZAKI S. 1994 *PhD thesis*, *University of Southampton*, *Southampton*. Modelling mechanical response to human whole-body vibration.

KITAZAKI S. and GRIFFIN M. J. 1995 *J. Biomechanics*, 28(7), 885-890. A data correction method for surface measurement of vibration on the human body.

KITAZAKI S. and GRIFFIN M. J. 1997 *Journal of Sound and Vibration*, 200 (1), 83-103. A modal analysis of whole-body vertical vibration, using a finite element model of the human body.

KITAZAKI S. and GRIFFIN M. J. 1998 *Journal of Biomechanics*, 31, 143-149. Resonance behaviour of the seated human body and effects of posture.

KOBAYASHI F., NAKAGAWA T., KANADA S., SAKAKIBARA H., MIYAO M., YAMANAKA K. and YAMADA S. 1981 *Industrial Health*, 19, 191-201. Measurement of human head vibration.

KRAUSE H. E. and LANGE L. O. 1967 *Biomechanics Monograph*, ASME, 57-66. The nonlinear behavior of biomechanical systems.

KRAUSE H. E. and SHIRAZI M. 1971 *Symposium on Biodynamic Models and Their applications*, Wright-Patterson Air Force Base, Ohio, 553-569. The transverse response of the lumbar spine under longitudinal loads.

LAKIE M. 1986 *Proceedings of the United Kingdom Informal Group Meeting on Human Response to Vibration*, Loughborough. Vibration causes stiffness changes (thixotropic behaviour) in relaxed human muscle.

LAKIE M., WALSH E. G. and WRIGHT G. W. 1979 *Proceedings of the Physiological Society*, 36-37. Passive wrist movements - a large thixotropic effect.

LAKIE M., WALSH E. G. and WRIGHT G. W. 1984 *Journal of Physiology*, 353, 265-285. Resonance at the wrist demonstrated by the use of a torque motor: an instrumental analysis of muscle tone in man.

LATHAM F. 1957 *Proceedings of the Royal Society*, B, 147, 121-139. A study in body ballistics: seat ejection.

LI T. F., ADVANI S. H. and LEE Y. -C. 1971 *Symposium on Biodynamic Models and Their applications*, Wright-Patterson Air Force Base, Ohio, 553-569. The effect of initial curvature on the dynamic response of the spine to axial acceleration.

LIU Y. K. and MURRAY J. D. 1966 *Proceedings of the Symposium on Biomechanics*, ASME, Ed. Fung, Y. C., New York, 167-186. A theoretical study of the effect of impulse on the human torso.

LIU Y. K. and VON ROSENBERG D. U. 1974 *Computers in Biology and Medicine*, 4, 85-106. The effect of caudocephalad ($+G_z$) acceleration on the initially curved human spine.

LIU, Y. K. and WICKSTROM J. K. 1973 *Perspectives in Biomedical Engineering*, *Proceedings of a Symposium organised in association with the Biological Engineering*

Society in Glasgow, 203-213. Estimation of the inertial property distribution of the human torso from segmented cadaveric data.

MAGNUSSON M., POPE M., ROSTEDT M. and HANSSON T. 1993 *Clinical Biomechanics*, 8, 5-12. Effect of backrest inclination on the transmission of vertical vibrations through the lumbar spine.

MANSFIELD N. J. 1998 *PhD thesis*, *University of Southampton*, *Southampton*. Non-linear dynamic response of the seated person to whole-body vibration.

MANSFIELD N. J. and GRIFFIN M. J. 1997 *Proceedings of Annual Conference of the Ergonomics Society*, 147-152. Effect of sitting posture on pelvis rotation during whole-body vertical vibration.

MANSFIELD N. J. and GRIFFIN M. J. 1999 *Awaiting publication*, *Journal of Biomechanics*. Non-linearities in biodynamic responses to whole-body vibration magnitude.

MARKOLF K. L. 1970 *Proceedings of Workshop on Bioengineering Approaches to Problems of the Spine*, 12 September, 87-143. Stiffness and damping characteristics of the thoracolumbar spine.

MCCONVILLE J. T., CHURCHILL T. D., KALEPS I., CLAUSER C. E. and CUZZL J. 1980 *Air Force Aerospace Medical Research Laboratory*, *Wright-Patterson Air Force Base*, *Ohio*, AFAMRL-TR-80-119. Anthropometric relationships of body and body segment moments of inertia.

MCGLASHEN K. M., MILLER J. A. A., SCHULTZ A. B. and ANDERSSON G. B. J. 1987 *Journal of Orthopaedic Research*, 5, 488-496. Load displacement behavior of the human lumbo-sacral joint.

MERTENS H. 1978 *Aviation, Space, and Environmental Medicine*, 49 (1), 287-298. Nonlinear behavior of sitting humans under increasing gravity.

MERTENS H. and VOGT L. 1978 *AGARD Conference Proceedings No. 253*, A26-1-17. The response of a realistic computer model for sitting humans to different types of shocks.

MESSENGER A. J. 1987 *Proceedings of the United Kingdom Informal Group Meeting on Human Response to Vibration*, Shrivenham. Effects of pelvic angle on the transmission of vertical vibration to the heads of seated subjects.

MESSENGER A. J. 1989 *Proceedings of the United Kingdom Informal Group Meeting on Human Response to Vibration*, Silsoe. Correlation of spinal posture and the transmission of vertical vibration to the heads of seated subjects.

MILLER J. A. A., SCHULTZ A. B. and ANDERSSON G. B. J. 1987 *Journal of Orthopaedic Research*, 5, 92-101. Load-displacement behavior of sacroiliac joints.

MILLER J. A. A., SCHULTZ, A. B., WARWICK D. N. and SPENCER D. L. 1986 *Journal of Biomechanics*, 19 (1), 79-84. Mechanical properties of lumbar spine motion segments under large loads.

MIWA T. 1975 *Industrial Health*, 13, 1-22. Mechanical impedance of human body in various postures.

MOFFATT C. A., ADVANI S. H. and LIN C. J. 1971 *American Society of Mechanical Engineers*, 71-WA/BHF-7, 1-12. Analytical and experimental investigations of human spine flexure.

MUKSIAN R. and NASH C. D. Jr. 1974 *Journal of Biomechanics*, 7, 209-215. A model for the response of seated humans to sinusoidal displacements of the seat.

MUKSIAN R. and NASH C. D. Jr. 1976 *Journal of Biomechanics*, 9, 339-342. On frequency-dependent damping coefficients in lumped-parameter models of human beings.

NACHEMSON A. L. 1981 *Spine*, 6 (1), 93-97. Disc pressure measurements.

NACHEMSON A. and MORRIS J. M. 1964 *Journal of Bone and Joint Surgery*, 46-A (5), 1077-1092. *In vivo* measurements of intradiscal pressure.

NACHEMSON A. L., SCHULTZ A. B. and BERKSON M. H. 1979 *Spine*, 4 (1), 1-8. Mechanical properties of human lumbar spine motion segments, influence of age, sex, disc level, and degeneration.

NATIONAL AERONAUTICS AND SPACE ADMINISTRATION 1978 *NASA Reference Publication 1024*. Anthropometric source book, volume I: anthropometry for designers.

NIGAM S. P. and MALIK M. 1987 *Journal of Biomechanical Engineering - Transactions of the ASME*, 109 (2), 148-153. A study on a vibratory model of a human body.

NIGG B. M. (ed.) 1986 *Biomechanics of Running Shoes*, Human Kinetics Publishers.

NOKES L., FAIRCLOUGH J. A., MINTOWT-CZYZ W. J., MACKIE I. and WILLIAMS J. 1984 *Journal of Biomedical Engineering*, 6, 223-226. Vibration analysis of human tibia: the effect of soft tissue on the output from skin-mounted accelerometers.

ORNE D. and LIU Y. K. 1971 *Journal of Biomechanics*, 4, 49-71. A mathemaical model of spinal response to impact.

PADDAN G. S. 1987 *Proceedings of the United Kingdom Informal Group Meeting on Human Response to Vibration*, *Shrivenham*. Transmission of vertical vibration from the floor to the head in standing subjects.

PADDAN G. S. 1988 *Proceedings of the United Kingdom and French Joint Meeting on Human Response to Vibration*, *Vandoeuvre*. Transmission of horizontal vibration from the floor to the head in standing subjects.

PADDAN G. S. 1991 *PhD thesis*, *University of Southampton*, *Southampton*. Transmission of vibration through the human body to the head.

PADDAN G. S. and GRIFFIN M. J. 1988 *Journal of Biomechanics*, 21 (3), 191-197. The transmission of translational seat vibration to the head - I. vertical seat vibration.

PADDAN G. S. and GRIFFIN M. J. 1992 *Proceedings of the Institution of Mechanical Engineers, Part H, Journal of Engineering in Medicine*, 206, 159-168. The transmission of translational seat vibration to the head: the effect of measurement position at the head.

PADDAN G. S. and GRIFFIN M. J. 1993 *Journal of Sound and Vibration*, 160 (3), 503-521. The transmission of translational floor vibration to the heads of standing subjects.

PANJABI M. M., ANDERSON G. B. J., JORNEUS L., HULT E. and MATTSSON L. 1986 *Journal of Bone and Joint Surgery, Incorporated*, 68A (5), 695-702. In vivo measurements of spinal column vibrations.

PANJABI M. M., KRAG M. H., WHITE A. A. III and SOUTHWICK W. O. 1977 *Orthopedic Clinics of North America*, 8 (1), 181-192. Effects of preload on load displacement curves of the lumbar spine.

PANKOKE S., BUCK B. and WOELFEL H. P. 1998 *Journal of Sound and Vibration*, 215 (4), 827-839. Dynamic FE model of sitting man adjustable to body height, body mass and posture used for calculating internal forces in the lumbar vertebral disks.

PAYNE P. R. 1965 *Aerospace Medical Research Laboratories*, *Wright-Patterson Air Force Base*, *Ohio*, AMRL-TR-65-127. Personnel restraint and support system dynamics.

PAYNE P. R. 1969 *Journal of Aircraft*, 6 (3), 273-278. Injury potential of ejection seat cushions.

PAYNE P. R. and BAND E. G. U. 1971 *Aerospace Medical Research Laboratory*, *Wright-Patterson Air Force Base*, *Ohio*, AMRL-TR-70-35. A four-degree-of-freedom lumped parameter model of the seated human body.

PHEASANT S. 1996 *Bodyspace - anthropometry, ergonomics and the design of work, Second edition*. Taylor & Francis.

POPE M. H., BROMAN H. and HANSSON T. 1989 *Clinical Biomechanics*, 4 (4), 195-200. Impact response of the standing subject - a feasibility study.

POPE M. H., BROMAN H. and HANSSON T. 1990 *Journal of Spinal Disorders*, 3 (2), 135-142. Factors affecting the dynamic response of the seated subject.

POPE M. H., KAIGLE A. M., MAGNUSSON M., BROMAN H. and HANSSON T. 1991 *Proceedings of the Institution of Mechanical Engineers, Part H, Journal of Engineering in Medicine*, 205 (1), 39-44. Intervertebral motion during vibration.

POPE M. H., SVENSSON M., BROMAN H. and ANDERSSON G. 1986 *Journal of Biomechanics*, 19 (8), 675-677. Mounting of the transducers in measurement of segmental motion of the spine.

POPE M. H., WILDER D. G., JORNEUS L., BROMAN H., SVENSSON M. and ANDERSSON G. 1987 *Journal of Biomechanical Engineering - Transactions of the ASME*, 109, 279-284. The response of the seated human to sinusoidal vibration and impact.

PRADKO F., LEE R. and KALUZA V. 1966 *ASME publication*, 66-WA/BHF-15. Theory of human vibration response.

PRADKO F., LEE R. A. and GREENE J. D. 1965 *ASME publication*, 65-WA/HUF-19. Human vibration-response theory.

PRADKO F., ORR T. R. and LEE R. A. 1965 *SAE paper 650426*, *Society of Automotive Engineers Mid-Year Meeting*, Chicago, III. Human vibration analysis.

PRASAD P. and KING A. I. 1974 *Journal of Applied Mechanics - Transactions of the ASME*, 41 (3), 546-550. An experimentally validated dynamic dynamic model of the spine.

PRIVITZER E. and BELYTSCHKO T. 1980 *Mathematical Modelling*, 1, 189-209. Impedance of a three-dimensional head-spine model.

PRIVITZER E., HOSEY R. R. and RYERSON J. E. 1982 *AGARD Conference Proceedings No. 322*, *Cologne*, 30-1-10. Validation of a biodynamic injury prediction model of the head-spine system.

RADONS S., BLACKKETTER D. O., JURIST J. and SNIDER R. 1979 *Proceedings of the Winter Annual Meetings of the ASME*, *Advances in Bioengineering*, *New York*, 57-60. Frequency response analysis of the in-vivo human spine.

RAO B. K. N. 1982 *Shock and Vibration Bulletin*, 52 (3), 89-99. Bio-dynamic response of human head during whole-body vibration conditions.

RAO B. K. N., ASHLEY C. and JONES B. 1975 *Journal of the Society of Environmental Engineers (March)*, 27-30. Effects of postural changes on the head response of standing subjects subjected to low frequency ‘constant velocity’ spectral inputs.

ROBINOVITCH S. N., HAYES W. C. and MCMAHON T. A. 1991 *Journal of Biomechanical Engineering - Transactions of the ASME*, 113, 366-374. Prediction of femoral impact forces in falls on the hip.

RYBICKI E. F. and HOPPER A. T. 1971 *Symposium on Biodynamic Models and Their applications*, *Wright-Patterson Air Force Base*, *Ohio*, 851-875. A dynamic model of the spine using a porous elastic material.

SAHA S. and LAKES R. S. 1977 *Journal of Biomechanics*, 10, 393-401. The effect of soft tissue on wave-propagation and vibration tests for determining the in vivo properties of bone.

SANDOVER J. 1978 *Aviation, Space and Environmental Medicine*, 49 (1), 335-339. Modelling human responses to vibration.

SANDOVER J. and DUPUIS H. 1987 *Ergonomics*, 30 (6), 975-985. A reanalysis of spinal motion during vibration.

SCHULTZ A. B., WARWICK D. N., BERKSON M. H. and NACHEMSON A. L. 1979 *Journal of Biomechanical Engineering - Transactions of the ASME*, 101, 46-52. Mechanical properties of human lumbar spine motion segments - part I: responses in flexion, extension, lateral bending, and torsion.

SEIGEL S. and CASTELLAN N. J. Jr. 1988 *Nonparametric statistics for the behavioral Sciences*, McGraw-Hill

SHIRAZI M. 1971 *Symposium on Biodynamic Models and Their applications*, *Wright-Patterson Air Force Base*, *Ohio*, 843-849. Response of the spine in biodynamic environments.

SMEATHERS J. E. 1989 *Clinical Biomechanics*, 4, 34-40. Measurement of transmissibility for the human spine during walking and running.

SUGGS C. W., ABRAMS C. F. and STIKELEATHER L. F. 1969 *Ergonomics*, 12 (1), 79-90. Application of a damped spring-mass human vibration simulator in vibration testing of vehicle seats.

TENCER A. F., AHMED A. M. and BURKE D. L. 1982 *Journal of Biomechanical Engineering - Transactions of the ASME*, 104, 193-201. Some static mechanical properties of the lumbar intervertebral joint, intact and injured.

TERRY C. T. and ROBERTS V. L. 1968 *Journal of Biomechanics*, 1, 161-168. A viscoelastic model of the human spine subjected to $+g_z$ accelerations.

TOTH R. 1966 *Proceedings of the 19th Annual Conference on Engineering in Medicine and Biology*, 102. Multiple degree-of-freedom, nonlinear spinal model.

VOGT H. L., COERMANN R. R. and FUST H. D. 1968 *Aerospace Medicine*, 39 (7), 675-679. Mechanical impedance of the sitting human under sustained acceleration.

VULCAN A. P. and KING A. I. 1970 *Dynamic Response of Biomechanical Systems*, *ASME*, *New York*, 84-100. Forces and moments sustained by the lower vertebral column of a seated human during seat-to-head acceleration.

VYKUKAL H. C. 1968 *Aerospace Medicine*, 39, 1163-1166. Dynamic response of the human body to vibration when combined with various magnitudes of linear acceleration.

WEI L. and GRIFFIN M. J. 1998 *Journal of Sound and Vibration*, 212 (5), 855-874. Mathematical models for the apparent mass of the seated human body exposed to vertical vibration.

WILDER D. G., FRYMOYER J. W. and POPE M. H. 1985 *Automedica*, 6, 5-35. The effect of vibration on the spine of the seated individual.

WILDER D. G. and POPE M. H. 1996 *Clinical Biomechanics*, 11 (2), 61-73. Epidemiological and aetiological aspects of low back pain in vibration environment - an update.

WILDER D. G., WOODWORTH B. B., FRYMOYER J. W. and POPE M. H. 1982 *Spine*, 7 (3), 243-254. Vibration and the human spine.

WILLIAMS J. and BELYTSCHKO T. 1981 *Air Force Aerospace Medical Research Laboratory*, *Wright-Patterson Air Force Base*, *Ohio*, AFAMRL-TR-81-5. A dynamic model of the cervical spine and head.

WILLIAMS J. L. and BELYTSCHKO T. B. 1983 *Journal of Biomechanical Engineering - Transactions of the ASME*, 105, 321-331. A three dimensional model of the human cervical spine for impact simulation.

WITTMANN T. J. and PHILLIPS N. S. 1969 *Journal of Biomechanics*, 2, 281-288. Human body nonlinearity and mechanical impedance analysis.

WOODMAN P. D. 1995 *Proceedings of the United Kingdom Informal Group Meeting on Human Response to Vibration*, Silsoe. The influence of skin tissue on the relative motion between the head and a helmet.

YOGANANDAN N., MYKLEBUST J. B., RAY G. and SANCES A. Jr. 1987 *CRC Critical Reviews in Biomedical Engineering*, 15 (1), 29-93. Mathematical and finite element analysis of spine injuries.

ZIEGERT J. C. and LEWIS J. L. 1979 *Journal of Biomechanical Engineering - Transactions of the ASME*, 101, 218-220. The effect of soft tissue on measurements of vibrational bone motion by skin-mounted accelerometers.